NAM

Groningen Dynamic Model Update 2017

NAM Reservoir Engineering Team: Henk van Oeveren, Per Valvatne and Leendert Geurtsen

Datum September 2017

Editors Jan van Elk & Dirk Doornhof

General Introduction

The subsurface model of the Groningen field was built and is used to model the first step in the causal chain from gas production to induced earthquake risk. It models the pressure in the gas bearing formations in response to the extraction of gas (and water).

The reservoir model of the Groningen field was built in 2011 and 2012 and has a very detailed model of the fault zone in the field to support studies into induced earthquakes in the field. The model was used to support Winningsplan 2013 (Ref. 1 to 3) and has since been continuously improved (Ref. 4). This report describes the improvements since winningsplan 2016 and in particular the effort to obtain the best possible history match.

The pressure in the field is an important driver for compaction and therefore subsidence. Compaction in turn affects stress and strain and is therefore of importance for mechanism inducing earthquakes. The model therefore has an important role in the optimization of the gas withdrawal from the reservoir to reduce seismicity.

For Winningsplan 2013 and Winningsplan 2016, the model was reviewed by an independent consultant SGS Horizon. An extensive assurance review (Ref. 5) with opinion letter have been prepared by SGS Horizon. All references are available at:

www.nam.nl/feiten-en-cijfers/onderzoeksrapporten

References

1. Winningsplan Groningen 2013, Nederlandse Aardolie Maatschappij BV, 29th November 2013.
2. Technical Addendum to the Winningsplan Groningen 2013; Subsidence, Induced Earthquakes and Seismic Hazard Analysis in the Groningen Field, Nederlandse Aardolie Maatschappij BV (Jan van Elk and Dirk Doornhof, eds), November 2013.
3. Supplementary Information to the Technical Addendum of the Winningsplan 2013, Nederlandse Aardolie Maatschappij BV (Jan van Elk and Dirk Doornhof, eds), December 2013.
4. Groningen Field Review 2015 Subsurface Dynamic Modelling Report, Burkitov, Ulan, Van Oeveren, Henk, Valvatne, Per, May 2016.
5. Independent Review of Groningen Subsurface Modelling Update for Winningsplan 2016, SGS Horizon, July 2016.

NAM

Title	**Groningen Dynamic Model Update 2017**			**Date**	September 2017
				Initiator	NAM
Autor(s)	NAM Reservoir Engineering Team: Henk van Oeveren, Per Valvatne and Leendert Geurtsen	**Editors**	Jan van Elk Dirk Doornhof		
Organisation	NAM	**Organisation**	NAM		
Place in the Study and Data Acquisition Plan	<u>Study Theme: Prediction Reservoir Pressure based on gas withdrawal</u> <u>Comment:</u> The subsurface model of the Groningen field was built and is used to model the first step in the causal chain from gas production to induced earthquake risk. It models the pressure in the gas bearing formations in response to the extraction of gas (and water). The reservoir model of the Groningen field was built in 2011 and 2012 and has a very detailed model of the fault zone in the field to support studies into induced earthquakes in the field. The model was used to support Winningsplan 2013 (Ref. 1 to 3) and has since been continuously improved (Ref. 4). This report describes the improvements since winningsplan 2016 and in particular the effort to obtain the best possible history match. The pressure in the field is an important driver for compaction and therefore subsidence. Compaction in turn affects stress and strain and is therefore of importance for mechanism inducing earthquakes. The model therefore has an important role in the optimization of the gas withdrawal from the reservoir to reduce seismicity. The model has been reviewed by an independent consultant SGS Horizon (Ref. 5). An extensive assurance review with opinion letter have been prepared by SGS Horizon.				
Directly linked research	1. Winningsplan Groningen 2013, Nederlandse Aardolie Maatschappij BV, 29th November 2013. 2. Technical Addendum to the Winningsplan Groningen 2013; Subsidence, Induced Earthquakes and Seismic Hazard Analysis in the Groningen Field, Nederlandse Aardolie Maatschappij BV (Jan van Elk and Dirk Doornhof, eds), November 2013. 3. Supplementary Information to the Technical Addendum of the Winningsplan 2013, Nederlandse Aardolie Maatschappij BV (Jan van Elk and Dirk Doornhof, eds), December 2013.				

	4. Groningen Field Review 2015 Subsurface Dynamic Modelling Report, Burkitov, Ulan, Van Oeveren, Henk, Valvatne, Per, May 2016. 5. Independent Review of Groningen Subsurface Modelling Update for Winningsplan 2016, SGS Horizon, July 2016.
Used data	Sub-surface data from the Groningen field; open-hole logs, core data, pressure data, production data etc.
Associated organisation	Independent consultant SGS Horizon
Assurance	For Winningsplan 2013 and Winningsplan 2016, the model was reviewed by an independent consultant SGS Horizon.

NAM

Groningen Dynamic Model Update 2017

NAM Reservoir Engineering Team: Henk van Oeveren, Per Valvatne and Leendert Geurtsen

Datum September 2017

Editors Jan van Elk & Dirk Doornhof

General Introduction

The subsurface model of the Groningen field was built and is used to model the first step in the causal chain from gas production to induced earthquake risk. It models the pressure response in the gas bearing formations to the extraction of gas and water.

The reservoir model of the Groningen field was built in 2011 and 2012 and has a very detailed model of the fault zone in the field to support studies into induced earthquakes in the field. The model has been used to support Winningsplan 2013 (Ref. 1 to 3) and has since then been continuously improved (Ref. 4). This report describes the improvements since winningsplan 2016 and in particular the effort to obtain the history match.

The pressure in the field is an important driver for compaction and therefore subsidence. Compaction in turn affects stress and strain and is therefore of importance for mechanism inducing earthquakes. The model therefore has an important role in the optimization of the gas withdrawal from the reservoir to reduce seismicity.

For Winningsplan 2013 and Winningsplan 2016, the model was reviewed by an independent consultant SGS Horizon. An extensive assurance review (Ref. 5) with opinion letter have been prepared by SGS Horizon. All references are available at:

www.nam.nl/feiten-en-cijfers/onderzoeksrapporten

References

1. Winningsplan Groningen 2013, Nederlandse Aardolie Maatschappij BV, 29th November 2013.
2. Technical Addendum to the Winningsplan Groningen 2013; Subsidence, Induced Earthquakes and Seismic Hazard Analysis in the Groningen Field, Nederlandse Aardolie Maatschappij BV (Jan van Elk and Dirk Doornhof, eds), November 2013.
3. Supplementary Information to the Technical Addendum of the Winningsplan 2013, Nederlandse Aardolie Maatschappij BV (Jan van Elk and Dirk Doornhof, eds), December 2013.
4. Groningen Field Review 2015 Subsurface Dynamic Modelling Report, Burkitov, Ulan, Van Oeveren, Henk, Valvatne, Per, May 2016.
5. Independent Review of Groningen Subsurface Modelling Update for Winningsplan 2016, SGS Horizon, July 2016.

NAM

Title	**Groningen Dynamic Model Update 2017**	**Date**	September 2017
		Initiator	NAM
Autor(s)	NAM Reservoir Engineering Team: Henk van Oeveren, Per Valvatne and Leendert Geurtsen	**Editors**	Jan van Elk Dirk Doornhof
Organisation	NAM	**Organisation**	NAM
Place in the Study and Data Acquisition Plan	<u>Study Theme: Prediction Reservoir Pressure based on gas withdrawl</u> <u>Comment:</u> The subsurface model of the Groningen field was built and is used to model the first step in the causal chain from gas production to induced earthquake risk. It models the pressure response in the gas bearing formations to the extraction of gas and water. The reservoir model of the Groningen field was built in 2011 and 2012 and has a very detailed model of the fault zone in the field to support studies into induced earthquakes in the field. The model has been used to support Winningsplan 2013 (Ref. 1 to 3) and has since then been continuously improved (Ref. 4). This report describes the improvements since winningsplan 2016 and in particular the effort to obtain the history match. The pressure in the field is an important driver for compaction and therefore subsidence. Compaction in turn affects stress and strain and is therefore of importance for mechanism inducing earthquakes. The model therefore has an important role in the optimization of the gas withdrawal from the reservoir to reduce seismicity. The model has been reviewed by an independent consultant SGS Horizon (Ref. 5). An extensive assurance review with opinion letter have been prepared by SGS Horizon.		
Directly linked research	1. Winningsplan Groningen 2013, Nederlandse Aardolie Maatschappij BV, 29th November 2013. 2. Technical Addendum to the Winningsplan Groningen 2013; Subsidence, Induced Earthquakes and Seismic Hazard Analysis in the Groningen Field, Nederlandse Aardolie Maatschappij BV (Jan van Elk and Dirk Doornhof, eds), November 2013. 3. Supplementary Information to the Technical Addendum of the Winningsplan 2013, Nederlandse Aardolie Maatschappij BV (Jan van Elk and Dirk Doornhof, eds), December 2013.		

	4. Groningen Field Review 2015 Subsurface Dynamic Modelling Report, Burkitov, Ulan, Van Oeveren, Henk, Valvatne, Per, May 2016. 5. Independent Review of Groningen Subsurface Modelling Update for Winningsplan 2016, SGS Horizon, July 2016.
Used data	Sub-surface data from the Groningen field; open-hole logs, core data, pressure data, production data etc.
Associated organisation	Independent consultant SGS Horizon
Assurance	For Winningsplan 2013 and Winningsplan 2016, the model was reviewed by an independent consultant SGS Horizon.

Nederlandse Aardolie Maatschappij B.V.

Shell UPO

Groningen Dynamic Model Updates 2017

Date: September 2017

Issued by: Henk van Oeveren, Per Valvatne, Leendert Geurtsen

EP number: EP201708205454

Name	Ref. Indicator	Role	Date	Signature
Hein de Groot	NAM-UPO/T/DL	Discipline Lead Reservoir Engineering	10/08/17	RE Request for QC Groningen V4 dynami
Clemens Visser	NAM-UPO/T/GD	Discipline Lead Production Geology	04/09/17	RE V4 document + SADP dynamic modell

1 Executive summary

This document describes the Groningen field dynamic subsurface V4 model and its main changes with respect to the V2.5 model. V4 is to be used in the June 2017 update of the Hazard and Risk Assessment. The model will also be used in the Production Optimisation study to investigate minimisation of tremors by redistributing the offtake. Furthermore, it will be used for the corporate forecasting (e.g. OP17, ARPR.31.12.2017).

NAM issued the dynamic model V2.5 of the Groningen field in May 2016 (1), as part of the Winningsplan 2016 submission. The updates introduced in the V4 model are in accordance with the Study and Data Acquisition Plan (2), which was issued as an addendum to the Winningsplan 2016 submission. Model V4 incorporates the following elements, to which NAM committed in the Study and Data Acquisition Plan:

- Static geological model with porosity based on inversion of seismic data
- Closed in tubing head pressures to constrain the model
- The use of rock compressibility based on inversion of subsidence data[1]
- Gravity survey results
- Effects of gas in the aquifer were tested for this model based on 3 scenarios
- High permeability area in Central part of the field
- In-situ compaction measurements

A new static geological model, with properties based on inversion of seismic data, was up-scaled and history-matched until 31 December 2016. The V4 model is matched to the following six historical data types;

- Static down-hole pressure measurements (SP(T)G),
- Repeat formation test pressures (RFT),
- Closed-in tubing-head pressures converted to bottom-hole pressures (CITHP2BHP),
- Interpreted rise in gas-water contact (PNL),
- Stable subsidence data from 2 levelling surveys (1972 and 2013)
- Time-lapse gravity data

The GIIP of the base-case case model increased from 2924.5 (V2.5) to 2934.8 billion Nm3 (V4). The overall match to observed data remains good; the average pressure match to SPG is±2.35 bar over the entire production history.

The following recommendations are made to improve the model further, including implementation of additional improvement steps as committed to in the Study and Data Acquisition Plan (1);

- Close-the-loop on the seismic inversion to improve the porosity and permeability distribution,
- Investigate the dynamic impact of depleting a gas bearing Carboniferous underneath the main Rotliegend reservoir,
- The incorporation in the dynamic model and improvement of the understanding of the gas presence in the aquifer.

These recommended improvements are expected to be included in the dynamic model due in May 2018.

[1] The methodology for the inversion was already explained in the V2.5 model report (3), but the inversion result had not yet been used in the V2.5 dynamic model.

Contents

2 Introduction

2.1 Background

Following the 2012 Huizinge earthquake, NAM has initiated numerous technical studies to better understand the induced seismicity in the Groningen field, its causes, consequences, and possible ways of mitigation. Within this scope, the Groningen subsurface team finished the Groningen dynamic subsurface model V2.5 in 2016, linking subsidence to dynamic subsurface behaviour (1). This model has formed the input to various studies, including the 2016 Hazard and Risk Assessment, and (a modified version of) this model was used to generate forecasts for the 2016 Operating Plan and the 2016 Annual Review of Petroleum Resources.

2.2 Study and Data Acquisition Plan

Together with the Winningsplan 2016 submission, an update of the Study and Data Acquisition Plan was issued (1); outlining future studies into subsurface issues, offtake optimisation, and possible further improvements to the suite of models, including the dynamic reservoir model. NAM has committed to complete these studies. Most of the suggested improvements to the subsurface model have been incorporated into the V4 model update as described in this document. There are three further elements in the Study and Data Acquisition plan that are planned to be studied as part of the subsequent V5 dynamic model update. If successful, they will be incorporated in the model update, which is currently scheduled for August 2017. These remaining elements will be discussed in chapter 8.

2.3 Model objective

The V4 dynamic model will be used for the June 2017 update of the Hazard Assessment. Furthermore, it will be used for the production optimisation study that is aiming to minimise tremor rate (and risk) by controlling the field offtake at the cluster level within constraints set by the ministry of economic affairs. Additionally, the model will be used for production forecasting, supporting the 2017 Operating Plan and 2017 Annual Review of Petroleum Resources.

3 Updates to the model

This section describes the changes in the V4 model with respect to the V2.5 model. For a full description of the V2.5 model please refer to the GFR2015 document (1).

3.1 Static model

An updated static model was used, which differs from the V2.5 model in two main aspects:

1. The top reservoir horizon has been updated.
2. The interpolation of porosity between well locations is steered by a first-pass inversion of seismic data to porosity.

Both the updated top_reservoir horizon and the inversion-derived porosity trends were derived from a newly reprocessed and reimaged seismic cube (3), showing improved imaging of the Rotliegend reservoir interval.

In the previous V2.5 model, the 3D distribution of reservoir properties was based on wireline log data only. This leads to a slight overestimation of the total pore volume in the reservoir, because wells are typically targeting for the better-quality rock in structurally higher parts of the reservoir. The V4 model uses porosity trend maps derived from the inversion to interpolate between well locations, thus avoiding the bias towards slightly higher porosities at the well locations. It should be noted that the differences between V4 and V2.5 models are small, because of the high density of wells in the field. The north and north west parts of the field and the aquifer areas outside of the Groningen closure, are affected most, because reservoir quality tends to be lower in these areas compared to the central crestal part of the field.

Permeability is generated based on the new porosity grid and the existing porosity-permeability relationship derived from core measurements. This methodology is the same as used for the previous V2.5 static model. The differences in permeability are caused by the change in the underlying porosity.

3.2 Closed-in tubing-head pressures converted to bottom-hole conditions

The primary data used for history matching is a set of roughly 1800 reservoir pressure measurements obtained from Static Pressure and Temperature Gradient (SPTG) surveys. Until 2014, the offtake from production clusters was managed in such a way as to keep the reservoir pressure balanced across the field, resulting in stable pressure decline trends across the field. Consequently, over the last 20 years, the SPTG survey frequency has been reduced to about 1 survey per 5 years for each production cluster. Following the production restrictions in the LOPPZ clusters, the offtake distribution and regional flow patterns of gas have drastically changed (Figure 1). With the reduced offtake in the north and west, a pressure difference across the field has been established. This pressure difference is currently about 25 bars from north to south. This differential is causing gas to flow from the north towards the south. The speed and pattern of this flow is affected by the sealing behaviour of some faults.

To capture the dynamic response of the field to this change in reservoir management, additional sources for constraining pressure data have been sought. Since 2011, all production wells in Groningen are equipped with tubing head flow and pressure sensors that are continuously recording data. Empirical correlations have been developed for all production clusters to convert pressure at surface to reservoir conditions during periods of no flow. The accuracy of this conversion is typically very good (within 1 bar of actual downhole SPG measurements). Since most clusters are typically closed in at least a few times every year (for more than 1 day), this has created an abundant source of additional reservoir pressure data.

This CITHP-CIBHP dataset from 2011 onwards is now included in the history matching process for all production wells. This addresses the recommendation from the SGS Horizon external review of the V2.5 model, where it was suggested to add more calibration points for reservoir pressure matching at the clusters for the period from 2010 onwards (4).

In order to constrain the dynamic model to this new data type, the model resolution has been increased both temporally and spatially. Simulation time steps were refined from monthly to daily from 2011 onwards to explicitly model relatively short shut-ins that can be in the order of days. Additionally, local grid refinement (LGR) is applied to production clusters to better capture the pressure build-ups during these periods and avoid having multiple wells in a single grid block. Daily time steps and local grid refinement double the simulation time to about 5½ hours with respect to the original V2.5 grid and time step size.

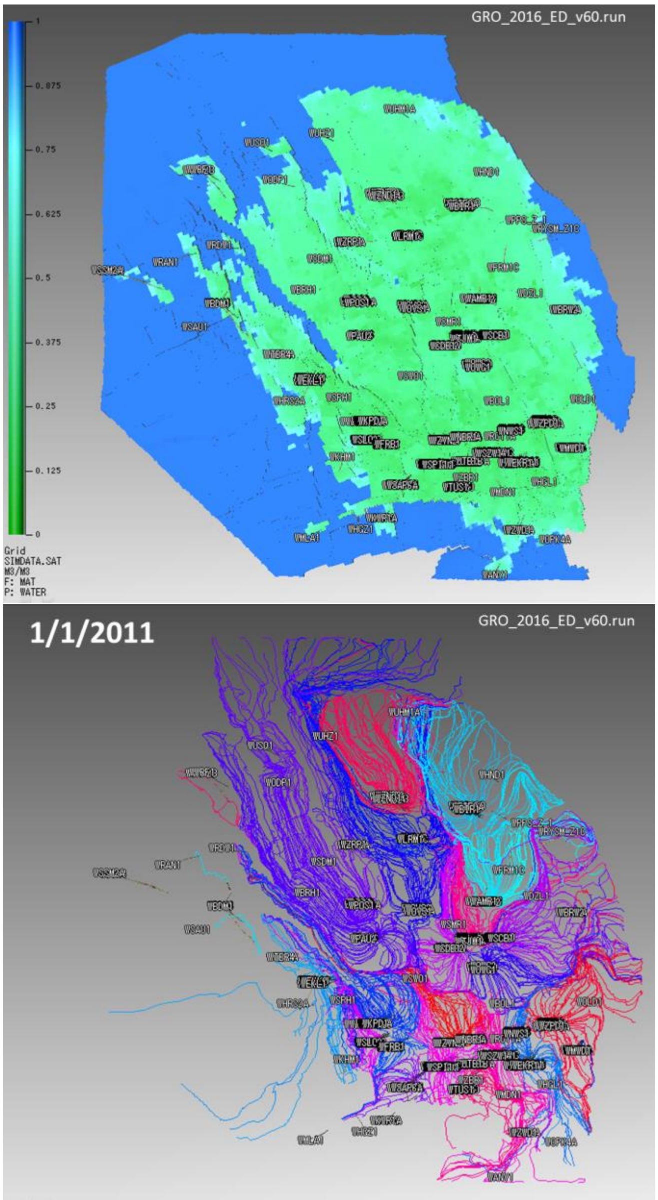

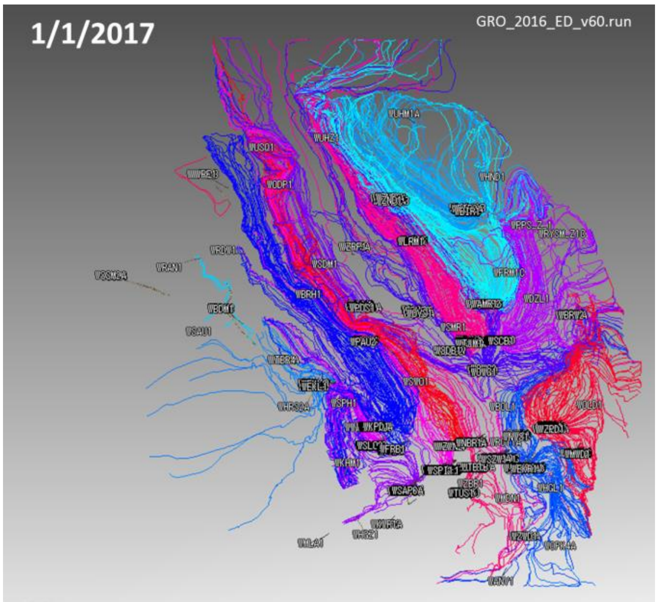

Figure 1: Change in flow pattern due to production restrictions (streamlines coloured by arriving producer)

3.3 Compressibility grid

Compaction is thought to be a key driving force for production induced seismicity, and thus of primary interest for the optimisation work that is aiming to minimise the tremor rate. The matrix compressibility directly impacts the (calculation of) compaction. Because rock compaction hardly contributes to the energy balance (Figure **4**), its impact on the pressure match is negligible, and it can be treated as an independent parameter for matching subsidence.

For previous models, a polynomial line-fit through core experiment data was used to generate the matrix compressibility (c_m) grid as a function of porosity. For GFR2012 and GFR2015, the polynomial fit through the data was multiplied by a constant factor (0.58), which resulted in an improved history match to pressure, as explained in the GFR2012 report (5). Compressibility calculated as a function of porosity for the V2.5 model is shown by the blue line in Figure 2.

The matrix compressibility in the V4 model is a grid resulting from model-based inversion of subsidence data and calculated reservoir pressure. This inversion method had already been used and assured for the Winningsplan 2016 subsidence prediction and was used in the dedicated subsidence model maintained by the NAM geomechanics team, see Reference (6). Because the forward prediction of compaction and subsidence was not an intended purpose for the V2.5 model, the final compressibility resulting from inversion had not been included into the V2.5 dynamic model. Using this geomechanical output in the dynamic reservoir model was, however, identified as an improvement opportunity for the V2.5 model, as the polynomial-fit does not capture areal trends in the compressibility-porosity relationship (1). Because the V4 model is intended to be used for tremor rate modelling, accurate areal prediction of compaction within the dynamic model is of significant importance. Consequently, the NAM geomechanics' subsidence inversion has now been applied to the V4 model and the resulting compressibility grid is used in the dynamic reservoir model instead of the polynomial function. This improves the subsidence match and the predictive capability of the model for compaction.

The resulting compressibility as a function of porosity is shown in Figure 2 and the areal distribution is shown in Figure 3.

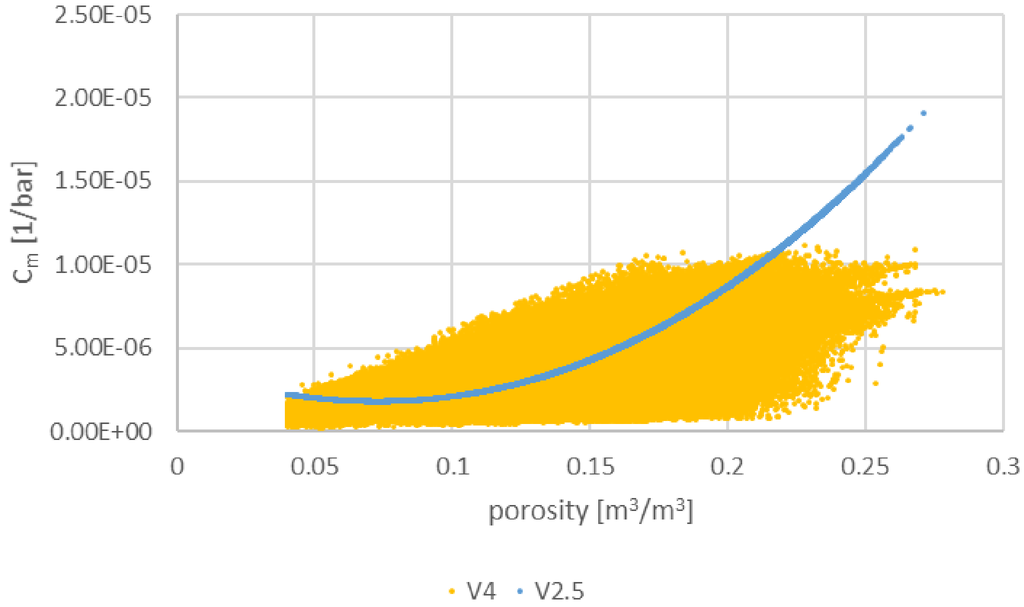

Figure 2 Matrix compressibility as function of porosity, as used in the V4 and the V2.5 dynamic reservoir model

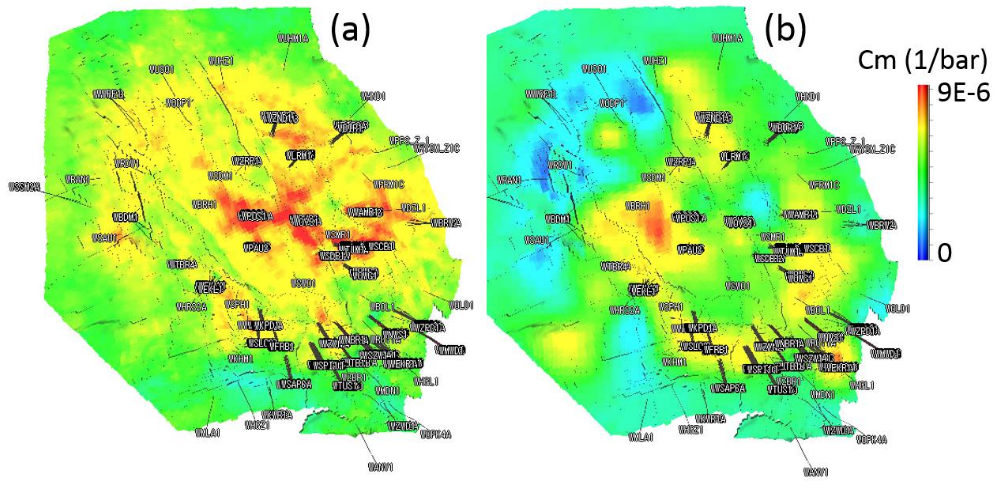

Figure 3: Areal distribution of compressibility when using a polynomial fit (a) versus direct use of inversion based compressibility grid (b).

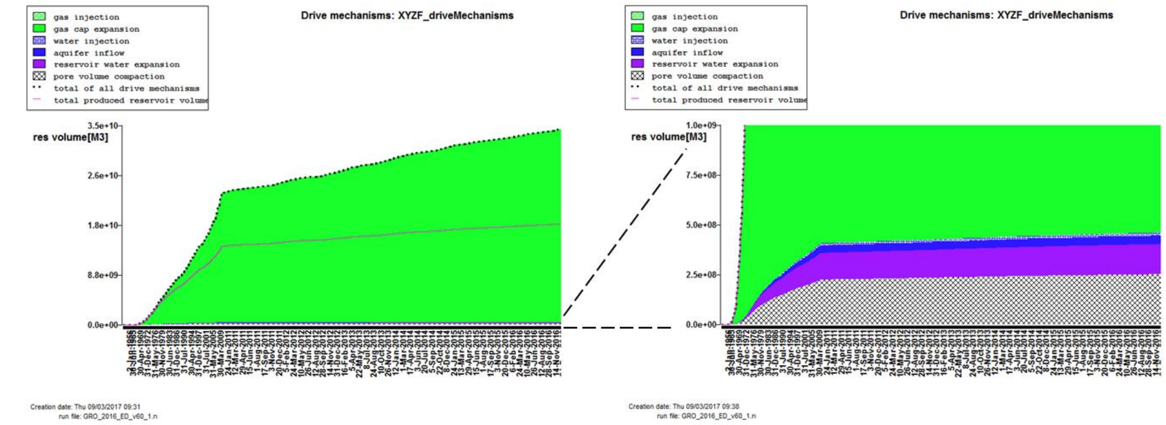

Figure 4 **Drive mechanism of the V4 model overview (left): the drive mechanism is fully dominated by gas expansion. The zoom in (right) shows that the contribution of reservoir compaction is 2 orders of magnitude smaller.**

3.4 Relative water permeability

Special core analysis on the Zeerijp-3 core was performed by CoreLab Aberdeen between 2016 and early 2017. Preliminary results suggest a water end-point relative permeability estimate of about 0.5 (7), which is significantly higher than the maximum of 0.12 used for the V2.5 model. A k_{rw} of 0.4 had already been reported in the Kooijpolder-2 core analysis report in 1992 (8), but was deemed an outlier and therefore not used in the uncertainty range (9). With the new study results indicating that the 1992 result was not an outlier, the upper limit of the uncertainty range for relative water permeability was adjusted from 0.12 for model V2.5 to 0.4 for model V4. The base case k_{rw} value that results in the best match for water influx against PNL surveys is now 0.4 (this was 0.12 in V2.5). Following finalisation of the core study by CoreLab and QC by NAM, the endpoint water relative permeability range might be increased further for the V5 model.

3.5 Lift table consolidation

In previous model updates, including V2.5, all wells in Groningen were represented by dedicated vertical lift performance (VLP) models. Maintenance of such a large set is a challenge. Starting in V2.5 the flowing performance (PQ) of production wells are matched to observed tubing head data prior to forecasting (10). PQ matching combined with the fact that most wells in Groningen are quite similar reduces the need for specific VLP curves for each well. The original set of about 300 well models has been reduced to 14 generic models (in terms of diameter, completion, deviation etc.) while 20 wells keep their dedicated model due to being sufficiently unique – mostly outstep wells from a production cluster (11; 12).

4 History matching methodology

For the V4 model update, a similar history matching method was applied as for the V2.5 model update. This method is described in detail in the GFR2015 report (1). However, one additional step was introduced in V4– model maturation using the gradients calculated by the Adjoint method. The methodology is outlined in the following six steps:

1. **Define local and field-wide mismatch functions.** These are defined as the root mean squared difference between a data point and model output. The following data are used for the mismatch functions;
   - Static reservoir pressure measurements (SPG) corrected to datum level,
   - Repeat formation tests (RFT),
   - Closed-in tubing-head pressure converted to bottom-hole conditions,
   - Gas water contact rise from pulsed neutron log measurements (PNL) interpreted by the petrophysicist
   - Stable subsidence data points averaged over a coarse grid (4×4 km). Stable means that data points which were impacted by slope instability, solution salt mining, or dyke works are omitted because they are deemed not representative for subsidence due to Groningen field compaction.

2. **Use the Adjoint functionality to calculate gradients of permeability and porosity with respect to the pressure mismatch.** The gradients can then be used to identify areas of under modelling. Under modelling means that variability required to improve a history match is not available in the variable parameter set-up according to Adjoint results. The results of the Adjoint calculations can indicate where reduction or increases in porosity and permeability could improve the match. These results are then translated in a set of variable model parameters, e.g. fault seal factors or permeability increases, and used in an experimental design workflow aimed to achieve an acceptable history match solution. This process is called model maturation and is used as a quick way to check if the set of variable parameters ensures the necessary control to achieve a history match (13). The process is adapted from the one proposed by T. Matsuura in 2015, Figure 5.

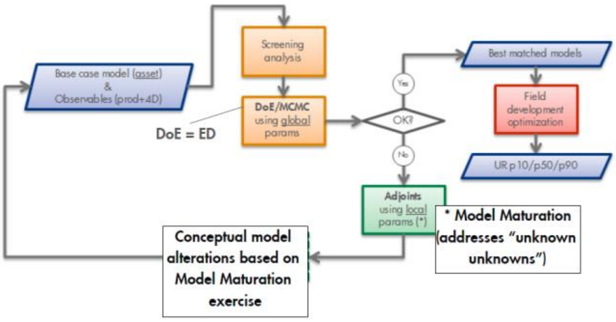

Figure 5 Two-stage AHM where DoE is used for matching global parameters and optimisation methods (Adjoint in this figure) are used to identify potential under modelling issues [figure and method by T. Matsuura - 2015]

A positive permeability gradient suggests a lower permeability is required to reduce the mismatch to pressures. An example of the interpretation of the Adjoint gradient map is a positive permeability gradient next to certain faults, see Figure 6 – left-hand picture, possibly indicating that these faults need to be less transmissible to improve the match to pressure. These faults are therefore added to the set of variable model parameters, see Appendix 2. A negative permeability gradient indicates where permeability should be increased, see Figure 6 – right-hand picture. More permeability increase is needed in the south than in the north. The Adjoint indicates a better history match might be achieved by a set of regional permeability multipliers for V4, contrary to the single permeability multiplier used for V2.5.

Permeability Gradient w.r.t. pressure mismatch

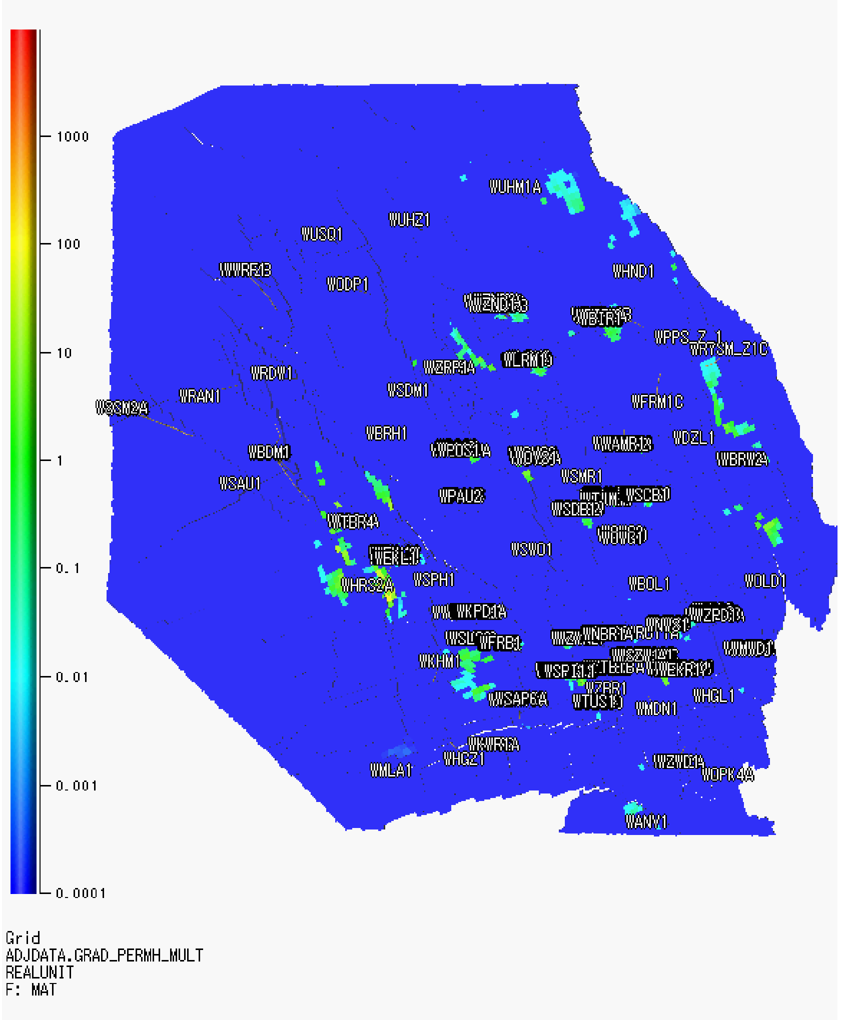

Negative Permeability Gradient w.r.t. pressure mismatch

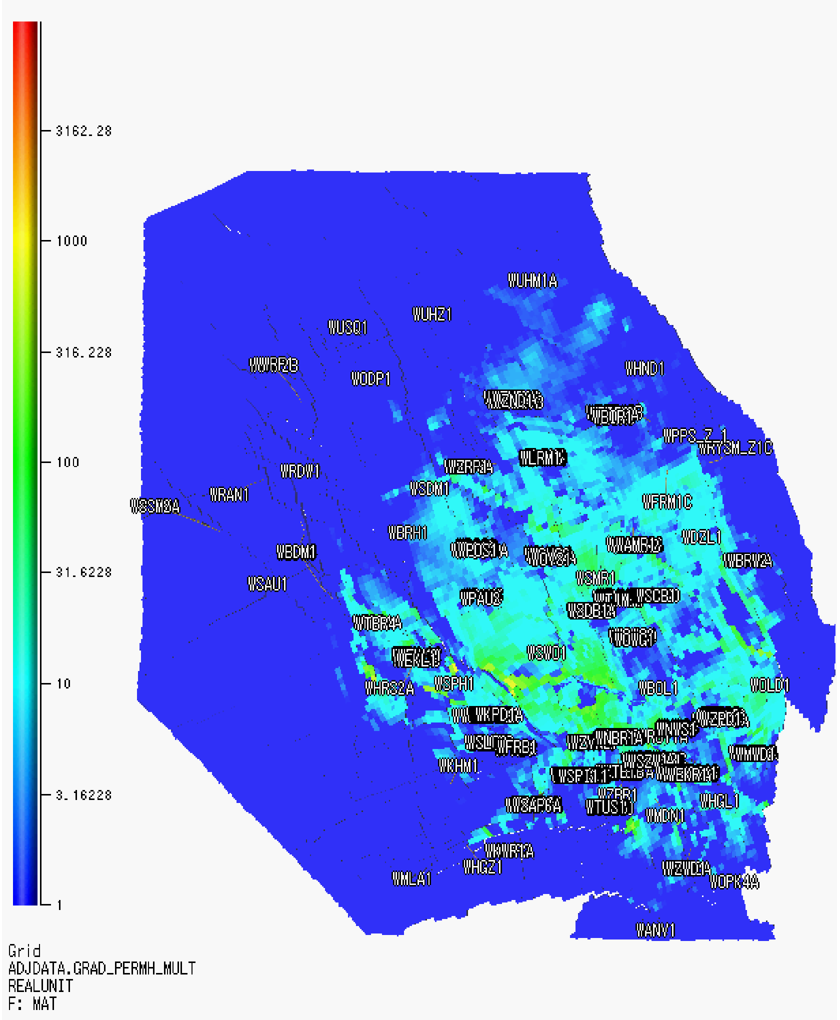

Figure 6: Permeability Gradient with respect to pressure mismatch. A positive gradient will indicate reductions necessary to reduce the mismatch, a negative gradient will indicate increases necessary to reduce the mismatch

3. **Define a set of variable model parameters.** Regional variable model parameters are defined for Gross Bulk Volume, Permeability, Fault Seal factors, Initial Free Water Level, Relative Permeability, Aquifer size and Skin (Skin only for those Land Asset wells which have been hydraulically fractured). The ranges of all parameters are based on measurements and studies – for details on the ranges see the GFR2015 report (1). The GFR2015 parameter set was expanded with the parameters identified by the model maturation, as described in step 2.

4. **History matching using space filling experimental design.** This design varies the identified variable model parameters within their allocated uniformly distributed ranges for every run in the ensemble of simulations, in this case, 1000 simulations.
   Then, a two-tier approach is followed to use the results of the space filling design to achieve a history match, identical to the approach used for V2.5:

   a) First, the *field-wide mismatch functions* are used to indicate which combination of variable model parameters result in the lowest overall mismatch to PNL, Subsidence and Pressure. The best-matched model is selected using a 3D cloud visualisation in Spotfire, Figure 7. In the 3D cloud, the history match errors decrease towards the origin. The models near the origin are therefore on average best matched to the three data types at field level. However, the space filling design of 1000 simulations will not be able to model all possible combinations of the variable parameters within their range. At certain locations, such as observation wells, the match could be further improved using local parameter variation.

   b) Second, *local mismatch parameters* are used to identify possible local improvements of the selected model. The purpose of the second step is to prevent the selection of a model that might have a low overall root mean squared error, but potentially high local mismatches. For example, the Kolham-1 observation well mismatch to pressure can be improved by constraining the fault seal factor separating Kolham-1 from the nearby Eemskanaal cluster to a value between $10^{-2.2}$ and $10^{-2.5}$, see Figure 8.

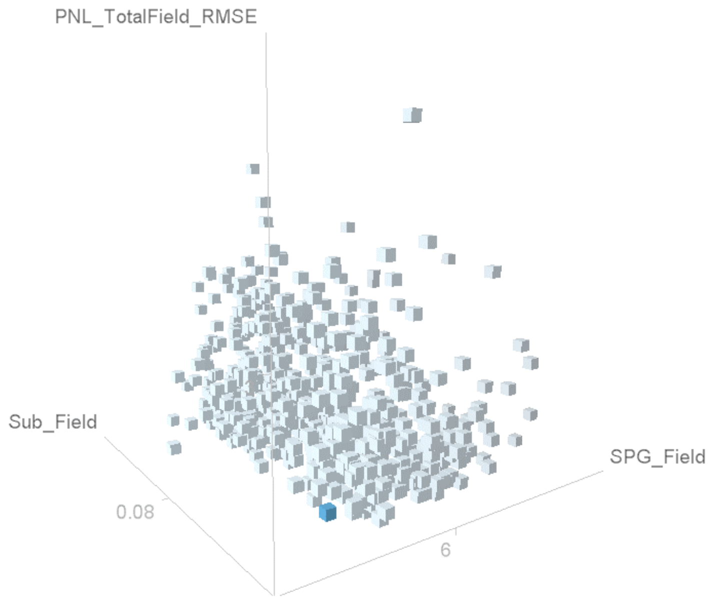

Figure 7 The mismatch to PNL, Subsidence and SPG for 1000 models, where the minimal mismatch to all is in the origin. An optimal model is indicated.

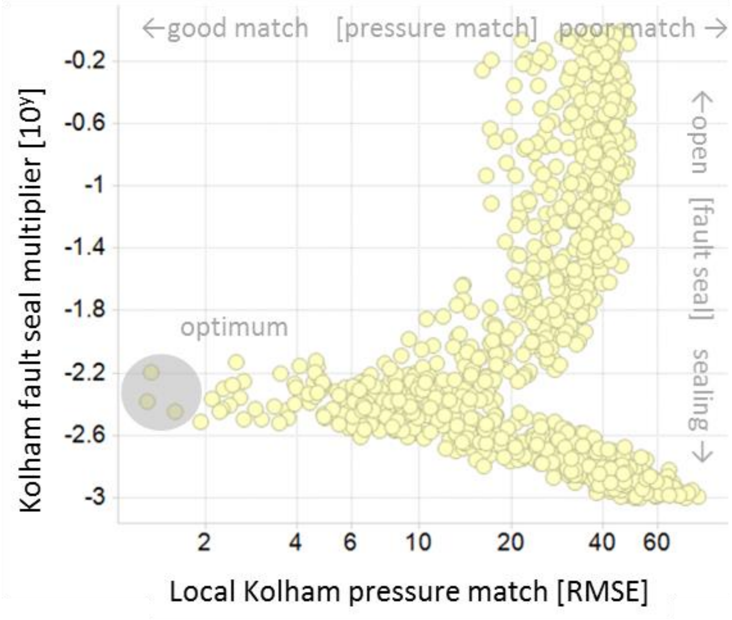

Figure 8 Mismatch of Kolham-1 model output to static pressure data for 1000 models for different fault seal settings. The X-axis gives the root mean squared error of the local pressure mismatch for the Kolham observation well. The Y-axis gives the fault sealing factor as a power of 10 for the fault separating Kolham from the nearby Eemskanaal cluster. The optimal setting is between $10^{-2.2}$ and $10^{-2.5}$.

5. **Improve the definition of variable model parameters.** The set of parameters is improved where an insufficient match was achieved in the field wide matching exercise. Some history matches result in inconsistent solutions. For example, an improvement in the match for a cluster might reduce the match for a nearby observation well. Another issue occurs when a variable parameter range has not been set wide enough in step 3. For example, in order to match a pressure lag observed in the data, a fault needs to be more sealing than is initially allowed for in the parameter range. To further improve the history match, the set of variable model parameters is updated. The updated definition of variable parameters, where most changes relate to fault sealing uncertainty, is subsequently checked with the geoscience team. With the new set-up, steps 4a and 4b are repeated until an acceptable match to all data, at all locations, is achieved.

6. **Geomechanical update.** When an acceptable history match is achieved, the associated model pressures and porosities are used by the NAM Geomechanics team for a subsidence inversion. This inversion step adjusts the compressibility grid in order to improve the subsidence match. The adjusted compressibility grid is then loaded back into the dynamic reservoir model. Since rock compressibility is a relatively modest energy source in the reservoir, the global pressure match is not significantly impacted by this step, see section 3.3. Only a repeat of the local match described in step 4b is required to obtain the final history match.

   Note that the importance of this compressibility iteration step is a result of the increased scope of the dynamic model. The model is envisaged to be used for optimisation of the regional distribution of field-offtake in order to minimise seismicity and/or seismic risk, and seismicity is believed to be a function of reservoir compaction. Although compaction itself is hard to measure, it is reflected at the surface as subsidence which is routinely monitored. Hence the subsidence inversion offers a way to reflect potential areal trends in the porosity-compressibility distribution, which the polynomial function (the prior to the inversion) did not capture.

5 Results

The main history match results from the best-matched V4 model are given in Appendix 1.

5.1 Permeability multipliers

History matching the dynamic model required a relatively consistent upward adjustment of the static model permeabilities by a factor of 2-3 throughout the field. This is within the uncertainty ranges from core data. However, in the "Central area" a larger increase in permeability was required (factor of 4). This requirement for relatively large permeability values in the Central has been consistent throughout the recent modelling updates, including GFR2012, and was investigated further.

Geologically the Central area is situated in a transition from conglomerates in the south (relatively lower permeability) to more sandy facies in the north. One hypothesis is that at this transition local high permeability streaks could provide a highly conductive connection from the Central area to the rest of the field. Such streaks would increase the lateral connectivity and could provide the pressure support during early field life which was matched in the dynamic model by the high permeability multipliers. Thin high-permeability streak in the fine-scale static model were smoothed away during the vertical upscaling process.

A detailed pressure transient analysis study was performed on a flowing build-up survey in the Zuiderpolder-12A well, within the Central area (Appendix 5). This study revealed that it is likely that permeabilities in the Central area are indeed affected by high permeability streaks.

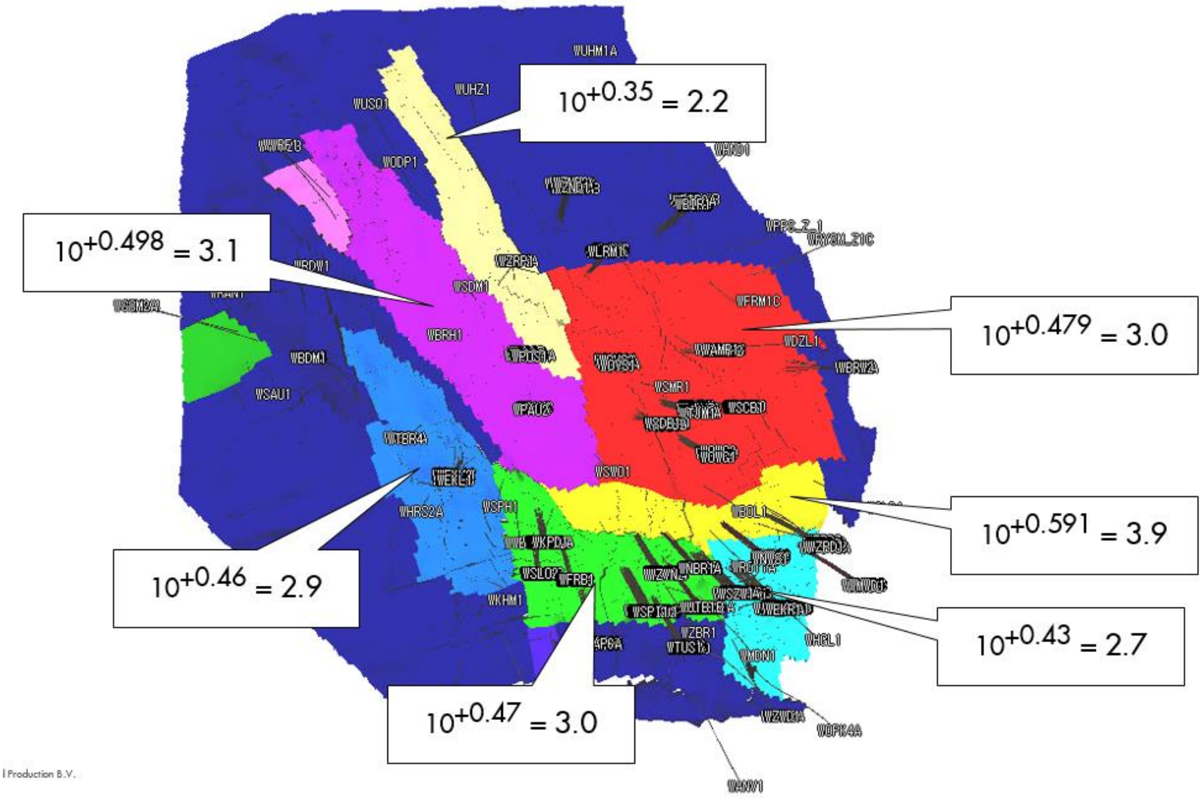

Figure 9: Permeability multipliers as applied in the final V4 model

5.2 In Place Volumes

The static GIIP of the upscaled V4 geological model is 2868.2 billion Nm3. The lower static GIIP volume of the V4 static model compared to the static model used for the V2.5 dynamic model can be attributed to the slightly lower average porosity, resulting from the implementation of seismic inversion results. History matching resulted in a dynamic GIIP of 2934.8 billion Nm3 (+2.3%). Within the Groningen closure, dedicated GBV multipliers were used for 9 regions (in alignment with the initialisation regions), varying between 1.005 and 1.024 for the main regions, see Figure 10.

The Harkstede fault block to the south-west is a special case (GBV multiplier 2.42). Based on history matching of the Harkstede-2A observation well and the Eemskanaal-13 production well, the dynamic GIIP was found to be 23.7 billion Nm3. This compares to a value of 16.9 billion Nm3 for the V2.5 dynamic model and 12.2 billion Nm3 for the V4 static model. The fault behaviour between this block and the main Eemskanaal region is complex, with a significant pressure lag observed. However, the final pressure match for the region is still good, as evident from Figure 11.

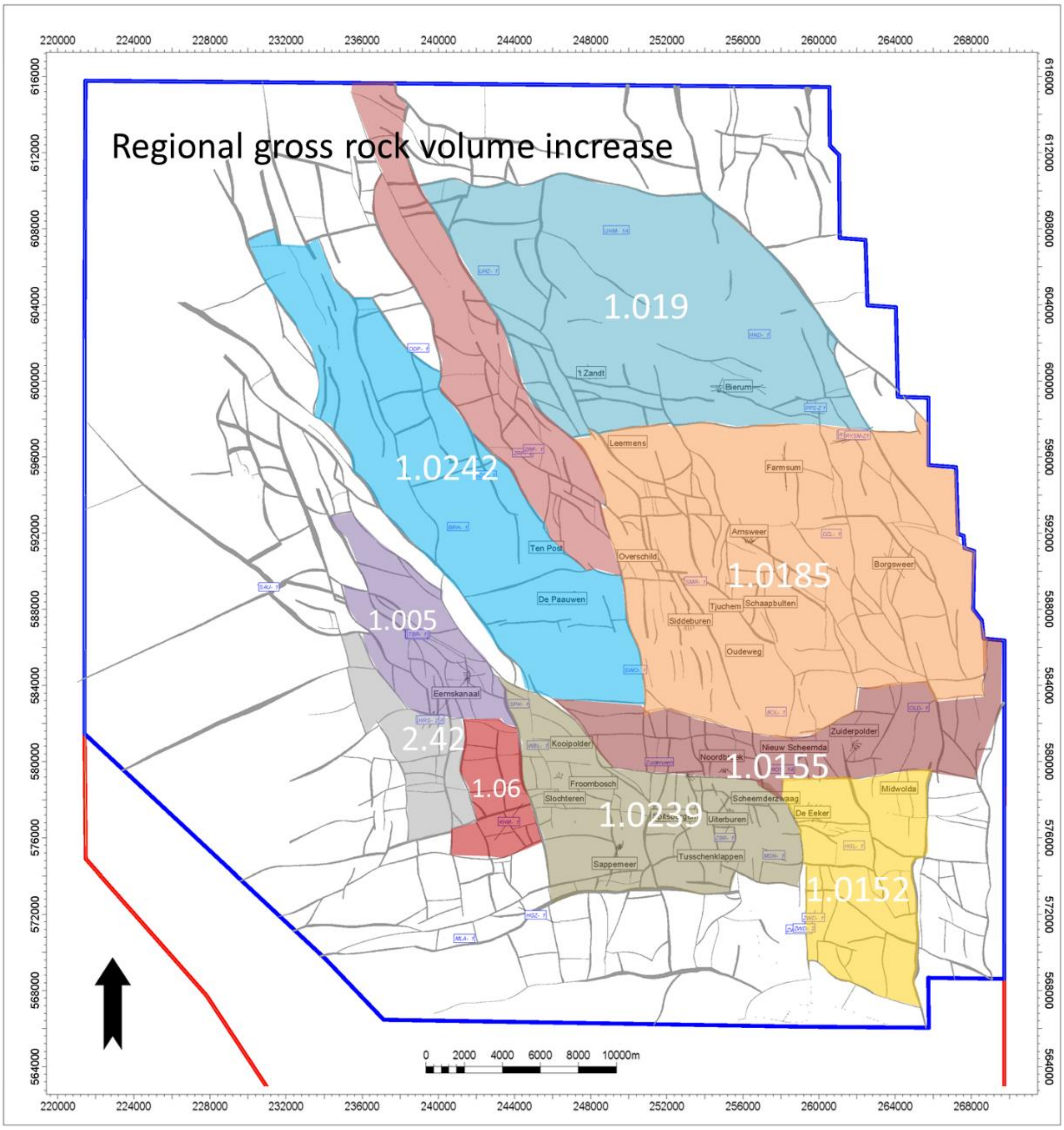

Figure 10 Regional gross bulk volume increases as applied in the final V4 model

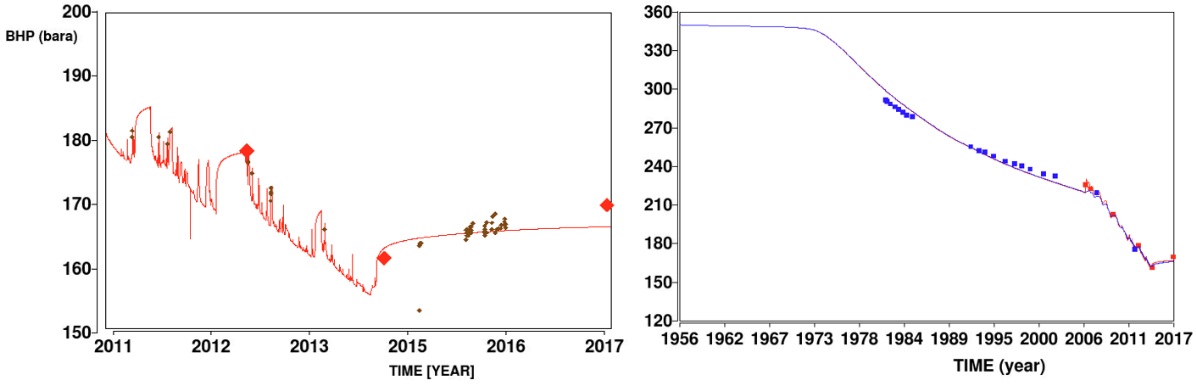

Figure 11: Pressure history match for well Emskanaal-13 and Harkstede-2A. Lines are model predictions (red EKL-13, blue HRS-2A), red and blue points are SPG measurements, while brown points are CITHP values converted to bottom hole conditions for EKL-13.

5.3 Reservoir pressure

The modelled reservoir pressure around the various production clusters is shown in Figure 12. The effect of the (LOPPZ) production caps on reservoir pressure is clearly evident, with a clear pressure lag developing towards the north of the field.

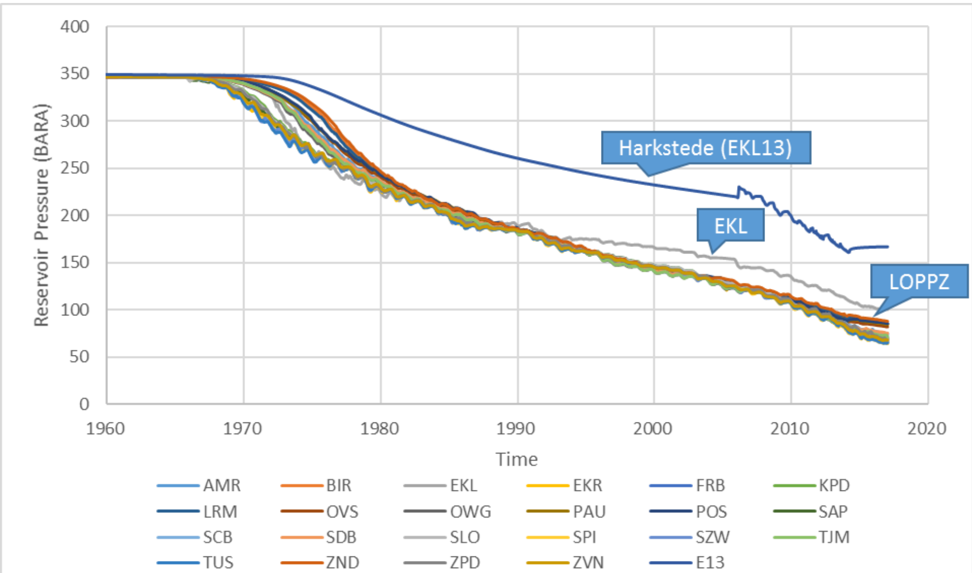

Figure 12: Modelled reservoir pressure around the various production clusters.

Overall, the V4 dynamic model properties have been constrained to more data types, and the pressure match in late field life is now constrained by additional pressure data from the high-resolution THP measurements. With the addition of the THP dataset from 2011 onwards, the focus on the late life pressure match has increased. The root mean squared error of the closed-in tubing-head pressure for the period 2011-2017 is ±1.41 bar. The root mean squared error of the overall field-wide pressure match to SPG data increased from ±2.17 bar for V2.5 to ±2.35 bar for V4. In their 2016 review of the V2.5 model, SGS Horizon classified a pressure mismatches less than ±5 bar as "good" (4).

Figure 13 shows the development of the SPG pressure mismatch over time, and Figure 14 shows the annual production volumes over time. It is clear the main pressure mismatch occurs during the early years of field production. During these early years, the shut-in times prior to measurement, which directly impacts the bottom-hole pressure, were not recorded. Potentially short shut-in times combined with high production rates will inevitably result in pressure mismatches since the build-up is poorly resolved in the model, this is graphically explained in Figure 15.

For the period 2011-2017 the match to pressures is shown to be diverging, although still relatively stable, for both SPG and THP pressures, this is shown in Figure 16. The divergence is mostly caused by the changes in the field off-take policy imposed by the ministry of economic affairs, which started early 2014.

Because of the switch from monthly to daily time-steps, after 2011 the model explicitly calculates short build-ups. This causes the calculated averaged pressures around each well (used to compare to SPG data) to overestimate the measured SPG pressure by roughly 1 bar, see Appendix 4. This means that for the last six years the difference between model and SPG data, shown in Figure 13 and Figure 16, is roughly 1 bar larger than it should be.

Note that the minor deterioration of the pressure match is also a consequence of the updated static model which is based on the first-pass inversion results (section 3.1). Especially in the North-East of the reservoir there is a need to close-the-loop between the inversion and the dynamic modelling work, see section 8.1

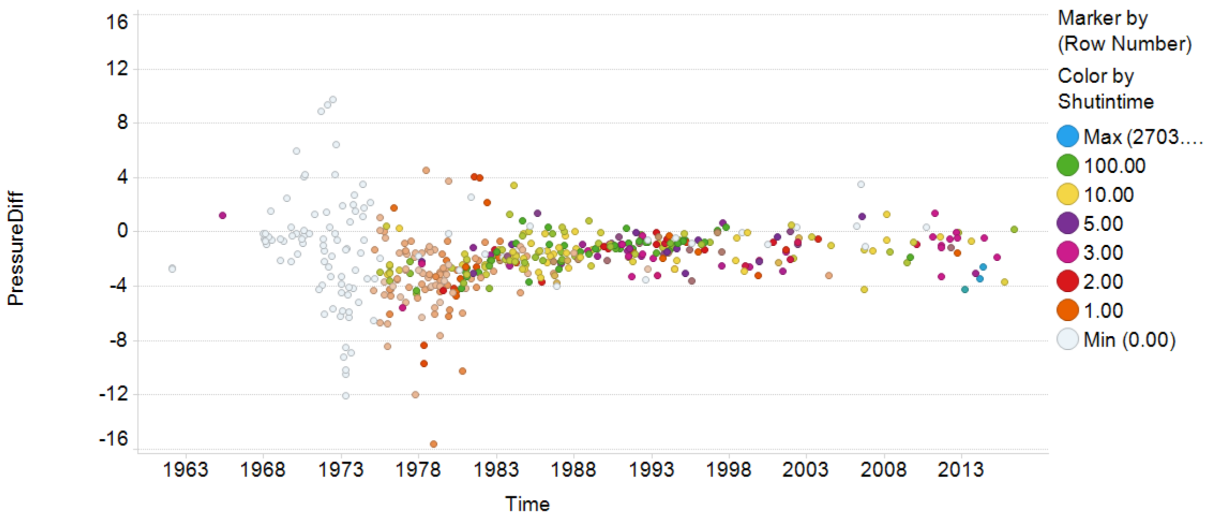

Figure 13 Difference of [SPG pressure - simulation] (a negative value means the model is over-predicting pressure), the colours indicate shut-in duration (no time indicated before 1975).

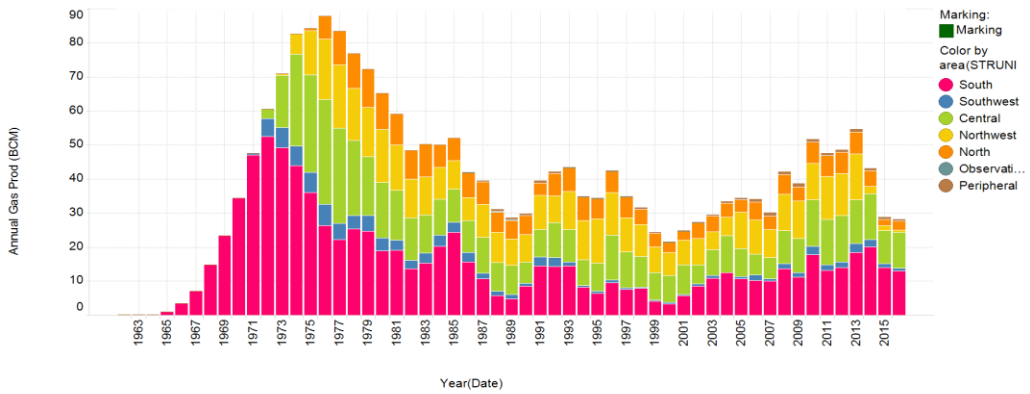

Figure 14: Annual production volume per geographical region over time.

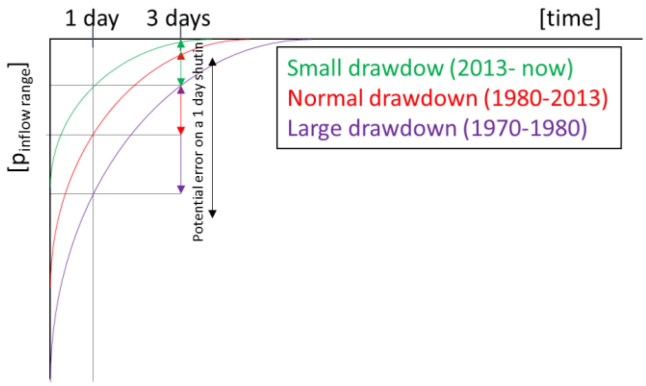

Figure 15: Schematic plot of the average pressure in a 3-day inflow range during a build-up. The potential error caused by assuming a 3-day shut-in for a 1-day shut-in occurs is illustrated to explain the large errors in Figure 13.

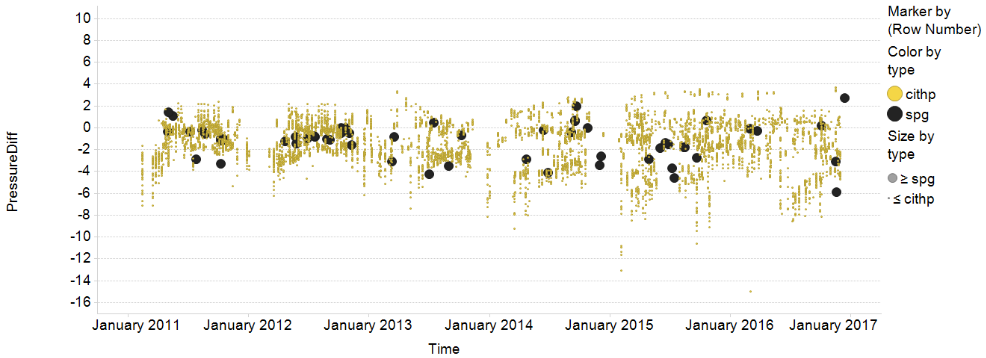

Figure 16 Difference between closed-in tubing head pressure and model output compared to the difference between SPG data and model output (a positive value means the model is under-predicting pressure).

5.4 Subsidence match

Subsidence is the surface imprint of reservoir compaction, which in turn is caused by pressure depletion due to gas production. Compaction is also believed to be the driving energy source for the seismicity observed in Groningen and therefore of special interest for this model update. Since direct measurements of compaction are sparse, only available from 5 wells in the reservoir, the compaction dataset is insufficient to constrain the full reservoir model. Subsidence data is, however, readily available from levelling and satellite surveys and can thus be used to constrain pressure depletion.

In model V2.5 subsidence data was first included in the history matching process. NAM's official subsidence predictions are made by the Geomechanics department using a high-fidelity model, which is an involved process. In order to include subsidence in the dynamic reservoir model history matching process (which involves hundreds of simulation runs), a proxy was setup in the dynamic reservoir model to calculate subsidence directly based on simplified overburden assumptions. Modelled subsidence is mainly the result of compressibility and pressure depletion. At well locations the pressure depletion is constrained relatively well by pressure measurements, and subsidence data mainly constrains the compressibility in the model. Away from well control, the subsidence can be used to constrain the reservoir pressure (if there is no subsidence, there is also no compaction, hence there should not be any depletion). As described in section 3.3, the best matched dynamic model realisation was used by the Geomechanics team for a subsidence inversion to fine-tune the compressibility grid in their high-fidelity model, in order to minimise the subsidence mismatch. The resulting compressibility grid was loaded back into the dynamic model. Figure 2 shows the prior and posterior matrix compressibility values as a function of porosity, and Figure 3 shows the associated compressibility grids. The comparison of the subsidence match in the dynamic model, when using the prior versus the posterior is shown in Figure 17. It can be observed that the modelled subsidence is significantly controlled by the compressibility; the subsidence match has changed in shape and magnitude.

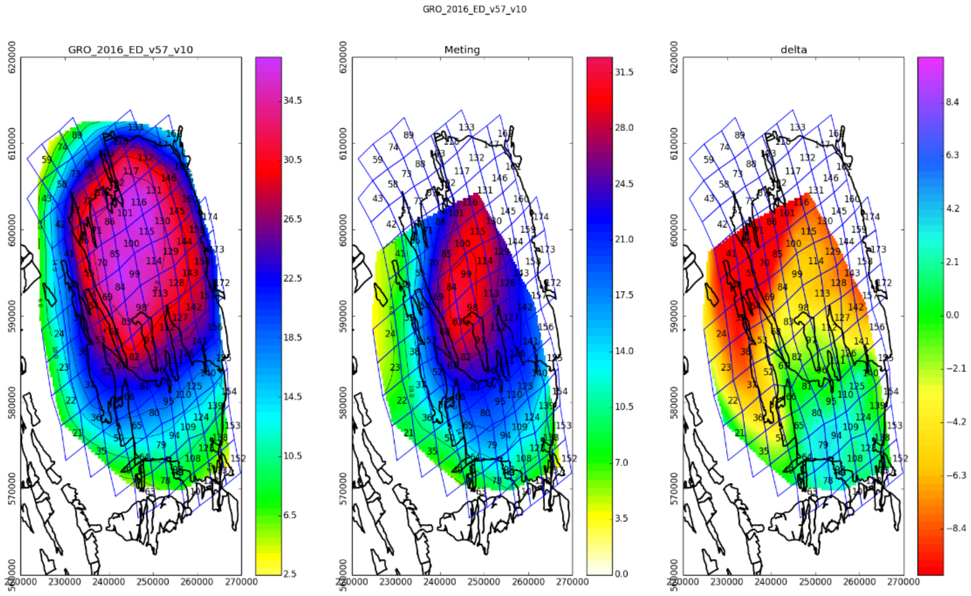

Initial compressibility estimate: Compressibility is polynomial function of porosity

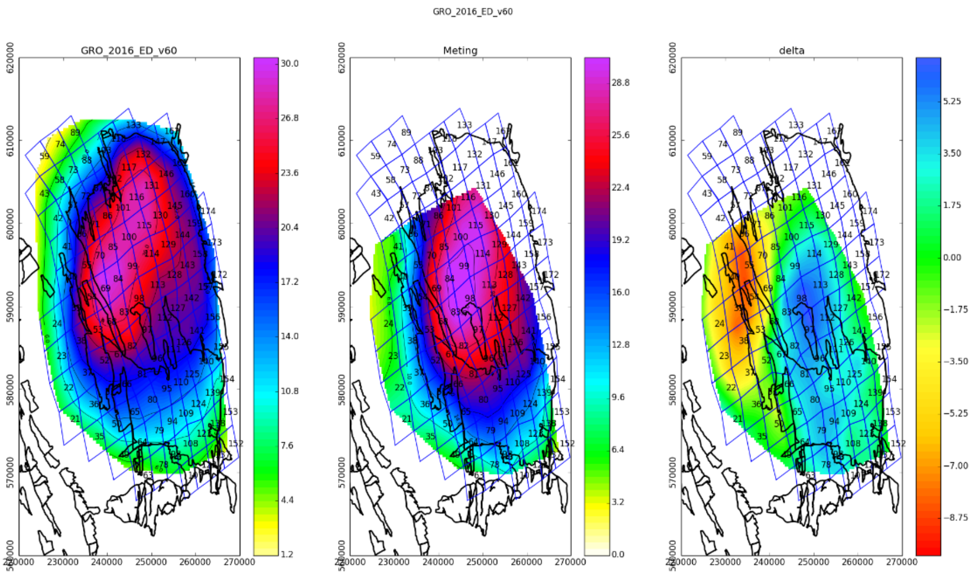

Final compressibility estimate: Compressibility grid based on subsidence inversion by geomechanics team

Figure 17 Subsidence match achieved by V4 model for two types of compressibility, the initial polynomial function and the final inversion based grid. The figures show the model output, the measurement and the delta. In the delta figure, warm colours indicate too much subsidence, cold colours indicate too little subsidence and a good match is green.

5.5 Compaction

In section 3.3 was explained how the c_m values in the V4 reservoir model are provided by the Geomechanics department, governing alignment of the calculated compaction between the dynamic reservoir model and the Geomechanics department. As a further QC step, the compaction as calculated by the reservoir model was compared to in-situ measurements.

In-situ measurements of compaction are routinely done in a selected set of observation wells throughout the field. Gamma ray markers bullets have been placed in those wells, at regular depth intervals. Periodic monitoring of the (change in the) distance between markers over time gives a measure for the compaction at locations along the wellbore (Figure 18). The markers were originally installed in eleven wells across the Groningen field, seven of which are still accessible for surveying. The marker interval data have been recorded over several decades. In the mid-nineties it was agreed with the regulator that three wells are to be logged regularly (HND-1, ROT-1A, SDM-1). Due to integrity issues, HND-1 was changed out with TBR-4. Note from Figure 18 that there are some duplications and trend breaks in the processed surveillance data, as a result of differences in surveillance contractors, inconsistencies in reporting and time-lapse comparison benchmarks. These issues will be addressed as per the "Compaction data integration" study that is outlined in the Study and Data Acquisition Plan, Reference (14). Meanwhile, Table 1 gives the interim estimate of compaction values for the time window 1972-2013, compared to the model results. As expected, there is generally a close comparison.

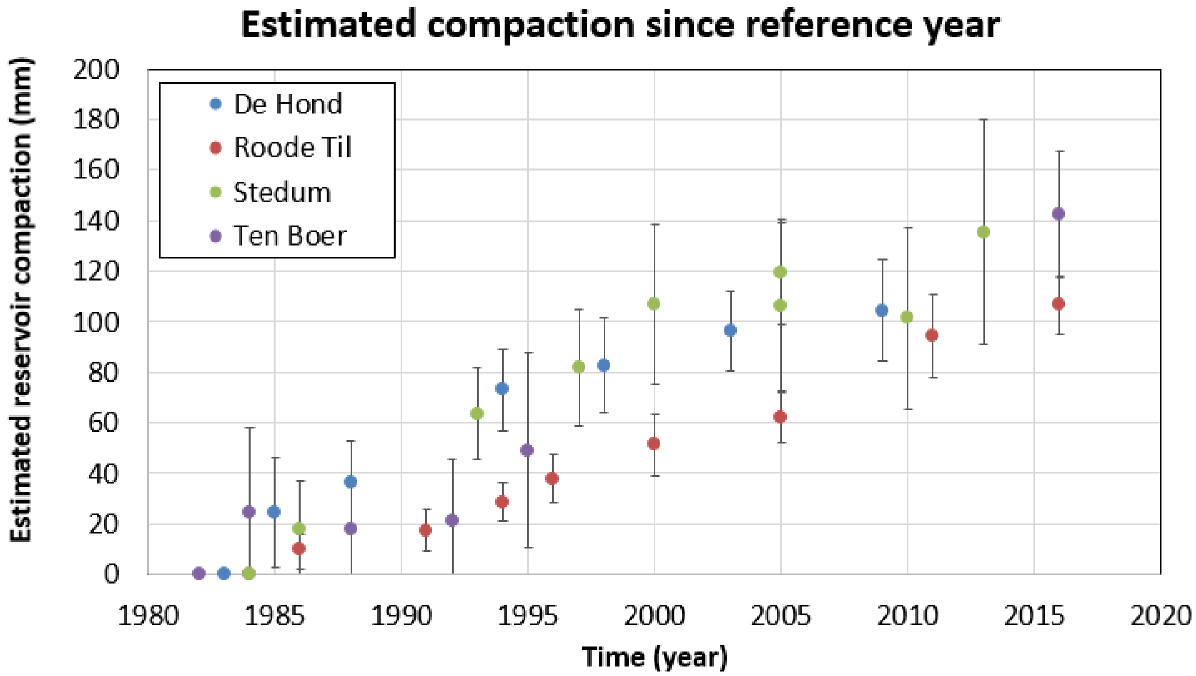

Figure 18: Estimated compaction since reference year, from surveillance of gamma ray marker bullets

Table 1: Comparison of V4 modelled compaction to the measurements (best estimate value)

Well	Compaction (cm)	
	1972.6 - 2013.3	
	Measurement	V4 model
De Hond-1	18	18
Delfzijl-1	21	21
Schildmeer-1	21	19
Roode Til-1A	15	13
Uithuizermeedem-1	21	21
Stedum-1	36	29
Ten Boer-4	29	26

6 Time-lapse gravity data

Time-lapse gravity measurements can detect mass changes in the field that are caused by density and saturation changes related to gas extraction (production) and aquifer influx.

6.1 Data availability

Four gravity surveys were acquired over the Groningen field in the past, first in 1978, then in 1984, 1988 and last in 1996. The number of observation points varied from 21 (1978) to 26 (1996), mostly at NAM sites.

In 2015 another gravity survey was done, covering a total of 98 stations, see Figure 19. Data was acquired at 21 pre-existing survey locations (4D points) and at 77 new locations. The survey was of excellent data quality.

Quad Geometrics (the survey contractor) re-processed and thoroughly evaluated the historical gravity data, including drift fitting, scale factor re-estimation, and improved tidal corrections, Reference (15). The quality of the historical gravity data slightly improved: the average station uncertainty reduced from 4-7 μGal down to 3-5 μGal. Some survey issues were detected for the 1984 and 1988 surveys, which are likely related to scale factor uncertainty. Because of the reduced confidence in these datasets, they were excluded from time-lapse analysis.

In Reference (16) additional sources of time-lapse signal uncertainties were analyzed, including groundwater variations, salt mining, and gas production from neighboring gas fields. These sources were found not to significantly affect an interpretation of historical data with respect to the reservoir induced signal. Due to the length of the time-span in between the surveys (and hence the change in cumulative gas production), the analyzed signals are much larger than the potential noise.

There is a relatively higher uncertainty for the time-lapse signal of the older surveys with respect to 2015:

- Some measurement sites were refurbished as part of the 1998-2009 Groningen Long Term project. The older surveys did not have good geodetic data, which makes it difficult to account for any potential changes in the vertical measurement height (e.g. new tarmac)
- Some new 2015 stations were established at close proximity to the original locations. The original gravity measurements were transferred to the new station locations with dedicated gradient measurements.
- Some stations were affected by significant near surface changes potentially leading to gravity changes and were judged unsuitable for interpretation.

Consequently, the 2015 survey mainly serves as a new baseline for future time-lapse surveys, only a limited number of points can be used for a time-lapse signal with the previous surveys.

The analysis is focused on 1996-1978 gravity signal because then no gravity stations were affected by any infrastructure changes. 2015-1978 gravity data is mainly analyzed for those stations which condition was not altered significantly.

Measured gravity changes range from approximately -50 μGal to 8 μGal for 1996-1978 and from -84 μGal to 13 μGal for 2015-1978 period. The average time-lapse signal uncertainty is estimated at approximately 10 μGal. The observed gravity changes are consistent with gas water contact (GWC) rise measurements, observed at certain wells for which saturation changes, interpreted from pulsed neutron logging (PNL) measurements, are available. The mismatch between the measured and modeled gravity shows certain patterns leading to scenario testing with using PNL measurements as additional constraints. The results show that observed gravity changes support more water influx than currently modelled in the North-East of the field nearby the Bierum cluster of producing wells. The opposite holds for the Stedum area, where gravity supports less water influx than currently modelled. Additional gas depletion in the South of the field in the Carboniferous formation, which is absent in the dynamic model, could also bring modeled gravity closer to the measured changes, however, not all of the mismatch could be explained with tested scenarios.

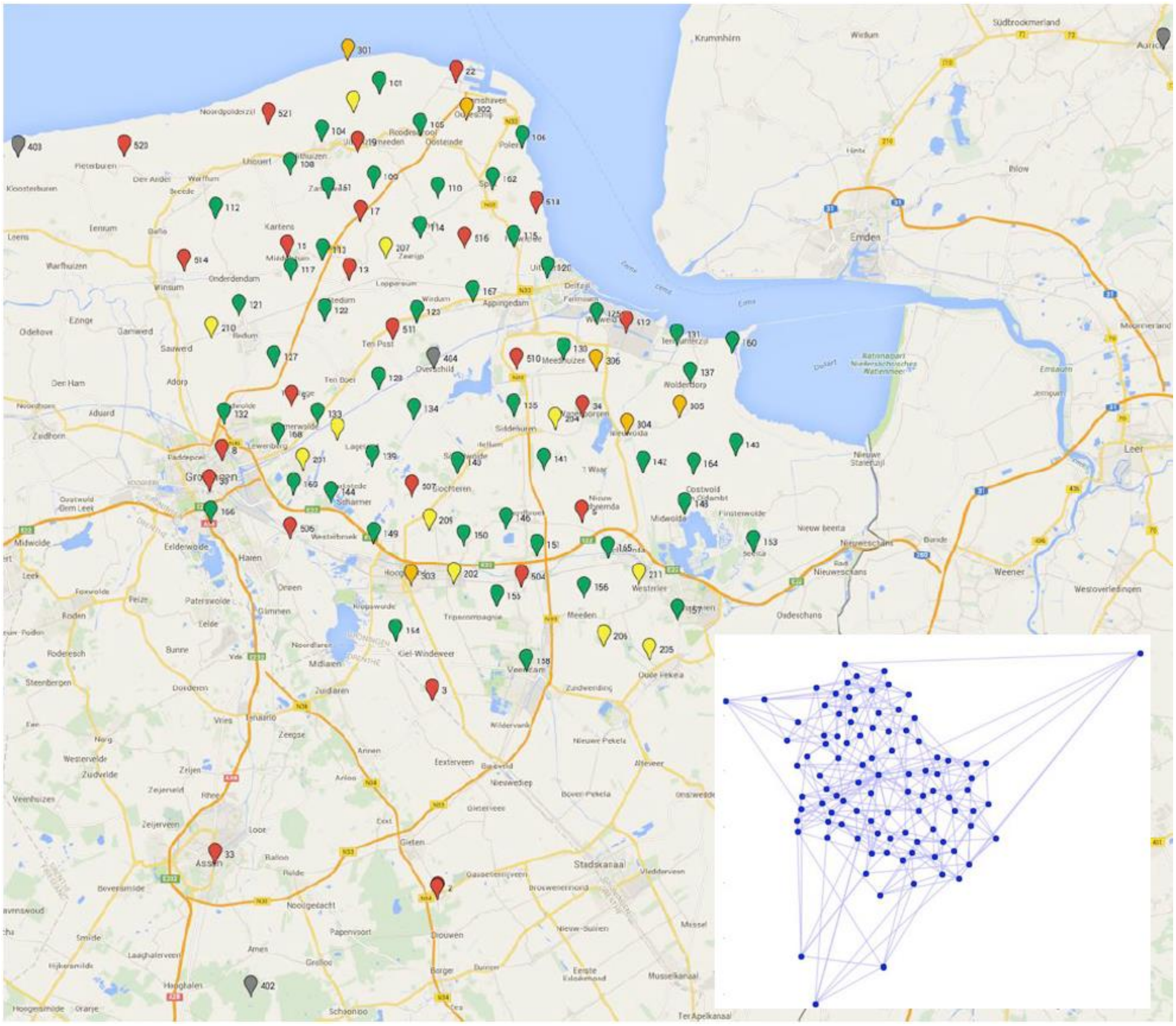

Figure 19: 2015 gravity survey stations, repeat locations in red

6.2 Model implementation

The Groningen dynamic reservoir model was upgraded to include calculation of gravity change at survey locations. The gravitational attraction is calculated from a point mass approximation: the mass change for a grid cell is represented as a point mass at the centre node. For each surface station the vertical component of the change in gravity can be calculated from a summation of the changes in the point mass at each grid block node as a function of its trigonometric reference to each respective grid block node (e.g. vertical distance, lateral distance, angle). A detailed derivation is given in the report by M. Glegola (17) and a detailed description of the implementation in the dynamic model explains the history matching approach (18).

6.3 Data interpretation

The total reservoir induced gravity change is the combined effect of gas extraction and (lateral) aquifer influx:

$$\Delta m_{total} = \Delta m_{gas} + \Delta m_{water}$$

The gas production signal is generally dominating the total gravity change. From static and dynamic reservoir modelling, there is a fairly good handle on the initial gas column weight (product of reservoir thickness, net-to-gross, porosity, gas saturation, gas density), and on the depletion of the gas column in time (governed by reservoir pressure decline, which is constrained by over 1800 SPG measurements and well matched). Therefore, time-lapse gravity measurements can help in constraining the uncertainty on water influx into the field.

Two examples are given for observations from the time-lapse gravity change. These examples compare dynamic model output to the measured gravity change signal and its respective uncertainty range. This time-lapse signal uncertainty does not account for large infrastructural changes, such as those occurred during the Groningen Long Term cluster renovation project.

6.3.1 Station 19

Station 19 is a stable measurement location (near a church) in the north-west of the field, near the Uiterhuizen-1 well. In Figure 20 the measured and modelled gravity change is given for 1996 and 2015 with respect to 1978. In 2015 the modelled gravity reduction is larger than what has been measured, and outside the uncertainty band of the measured signal. Given the high confidence in the model representation of the gas extraction (reservoir pressure match), the mismatch is thought to be driven by the modelled response of the aquifer. In the model the gas-water-contact is stable, however, no recent calibration measurements (PNL) are available. This mismatch in gravity data suggests that there is a net aquifer influx near station 19.

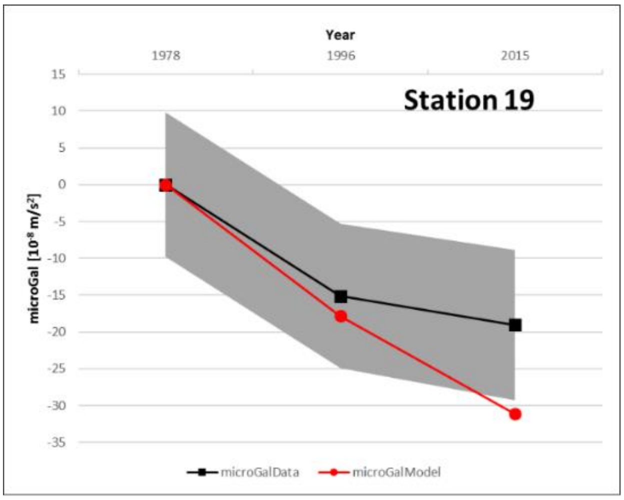

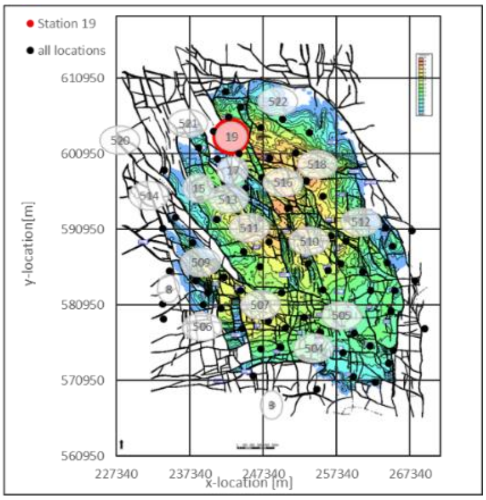

Figure 20 left: change in gravity at station 19 comparing the measurement and its uncertainty range to the model output. right: map showing the location of station 19

6.3.2 Station 504

Station 504 is located in the south of the field, near the Tussenklappen production cluster. This location has been altered between 1996 and 2015 for the Groningen Long Term project and the gravity station had to be transferred to the new, nearby location in 2015. The time-lapse gravity changes incorporating 2015 survey carry therefore high uncertainty, related to possible height changes (note that that the uncertainty band in Figure 20 reflects signal uncertainty but that it does not reflect these infrastructure changes). The pressure match for the Tussenklappen cluster is good and the density of the gas in the Slochteren is therefore expected to be captured well by the model at this location. However, the modelled gravity change is much smaller than the measured change in gravity. The Carboniferous basement underlying the Slochteren reservoir at the Tussenklappen location is gas bearing, and pressure measurements have demonstrated locally depletion of the Carboniferous (19). Potentially the depletion of the Carboniferous is more global in nature (e.g. by gas migrating upwards into the Rotliegend), and as such may present sufficient additional mass reduction of the system to explain the observed mismatch in the gravity data.

An alternative scenario was tested, whereby solution salt mining south of this station would cause the mismatch. However, the modelling results based on Nedmag salt production data (16), show that it is of an insignificant magnitude to explain the mismatch at this station.

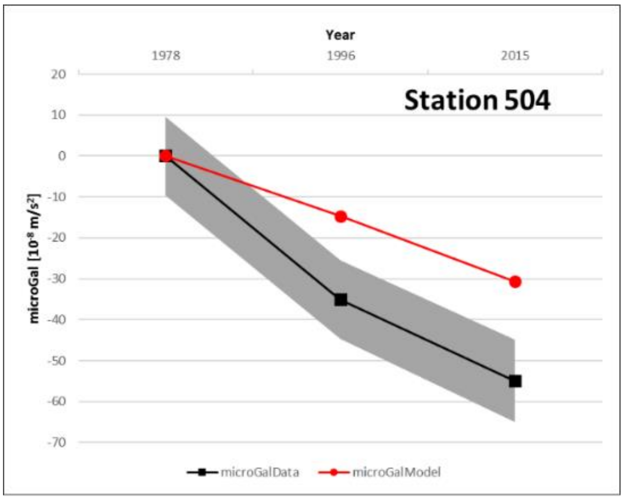

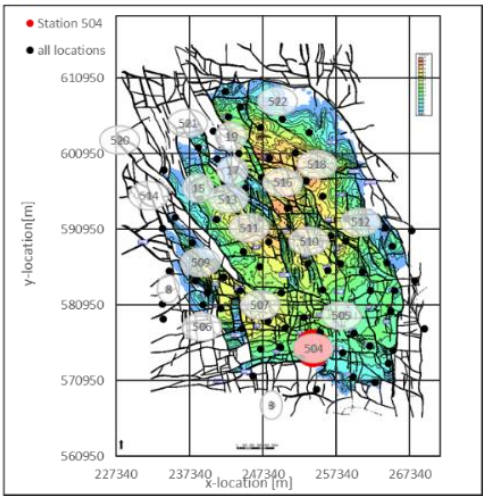

Figure 21 left: change in gravity at station 504 comparing the measurement and its uncertainty range to the model output. right: map showing the locatio0n of station 504

6.4 Conclusion

The proposed methodology of calculating gravity changes for the Groningen field dynamic model allows for a comparison of model output to time-lapse gravity changes, obtained from the 1978,1996 and 2015 surveys.

Significant mismatches between model output and measurements can be interpreted to reflect areas that require improvements in modelled mass changes.

- Shortages in the modelled mass reduction may indicate over-estimation of the aquifer influx, or a shortage in modelled mass extraction (e.g. depletion of the Carboniferous, which is not included in the current setup of the dynamic model).
- Over-estimation of the modelled mass change can be interpreted to be the result an under-estimation of aquifer influx.

In the V4 model examples, the measurements of the gravity change are interpreted as to indicate there could be more aquifer influx into the northern section of the model, and in the southern part of the model there should be more mass depletion (pressure measurements in the Carboniferous support this), Figure 22. For future modelling exercises the aquifer influx in the north is expected to increase with the introduction of gas below the contact (further explained in section 7.2). In the following models the gas bearing fraction of the Carboniferous underlying the Groningen field will be added to the dynamic model to incorporate its potential dynamical impacts.

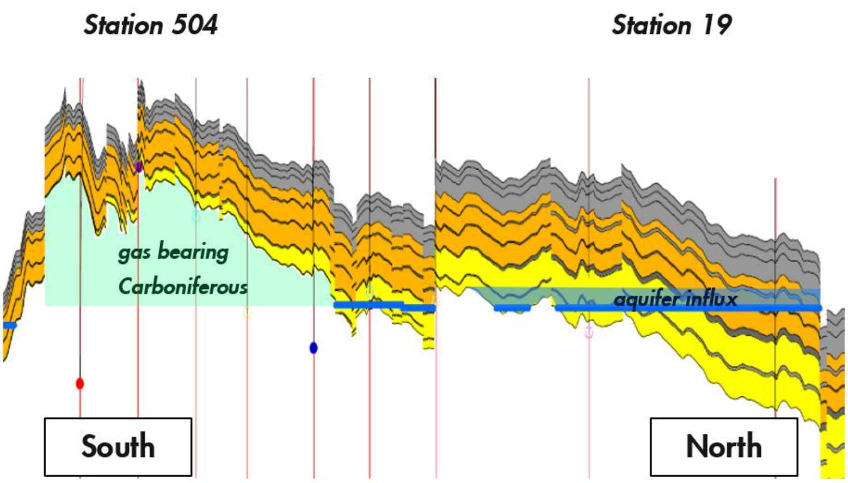

Figure 22: Reservoir cross-section indicating potential dynamic responses as suggested by the time-lapse gravity data

7 Gas in the aquifer

7.1 Indicators for gas in the aquifer

From the ongoing reservoir modelling work, various indications were found that suggest the possibility of gas saturation below the free water level (1):

- No Direct Hydrocarbon Indicator is observed from seismic. The static reservoir model is fairly well calibrated from 300-odd well penetrations in a layer-cake type reservoir. The static model was used to generate synthetic seismic. Only by introducing a gas saturation below the free water level was it possible to remove the DHI from the synthetic seismic and match the recorded seismic.
- Petrophysical interpretations indicate gas saturations below the Groningen free water levels. There are numerous measurements from Open Hole logs (which have a high uncertainty below the gas water contact), and there was a conclusive measurement of gas below the contact from a Cased Hole PNX log at Uithuizen-1 in April 2017.

More circumstantial indicators include:

- From RFT logging of infill wells the pore pressure depletion below the free water level has been observed to consistently lag with respect to the overlying gas column.
- Subsidence data suggests very limited depletion of the lateral aquifer to the north-west of the field
- The observed rise of the gas-water-contact in the north of the field (PNL data, gravity data) is difficult to match in the dynamic model. This impact on water rise is shown by an example in section 7.4.

7.2 Expected dynamic behaviour of gas in the aquifer

A potential presence of gas in the aquifer is expected to cause two distinct changes in the dynamic response of the aquifer.

Firstly, there is a massive increase in the compressibility of the (combined) pore fluid. As a result, the aquifer becomes a more significant factor in the overall drive mechanism, as compared to Figure 4. In those parts of the reservoir with bottom water, a potent energy source is introduced directly below the gas column. Figure 23 gives a schematic overview of the expected behavoir:

- In the initial situation prior to production, gas is trapped as individual bubbles within the pores. Gas is the non-continuous phase, and cannot travel through the pore throats.
- When the pressure in the aquifer starts to decrease through production of the gas reservoir, the gas bubbles expand. Depending on the initial saturation, at first it is expected that the expanding gas will push water up into the depleting gas reservoir.
- When the expanding gas exceeds the critical gas saturation, gas will become mobile and can migrate upwards (20).

From the compressibility equation:

$$c = -\frac{1}{V}\frac{\partial V}{\partial p}$$

it follows that for a small pressure reduction (without big change in the compressibility):

$$\Delta V \sim c\,\Delta p\,V$$

Hence a significant increase in the aquifer compressibility (due to the presence of gas) will enable a relatively small aquifer to provide a pressure response comparable to a much larger aquifer (without gas). The energy in such a “gas charged aquifer” is however in closer proximity to the depleting gas column, making the aquifer response more rapid.

As a second dynamic effect, the presence of gas changes the aquifer from a single-phase system to a two-phase system. The associated relative permeability effect will distinctly suppress the water permeability (at least down to the endpoint permeability at Sgr). The effective permeability reduction caused by the gas saturation in the aquifer will act as a pressure baffle, slowing down the depletion of the aquifer lateral to, and deeper below the field.

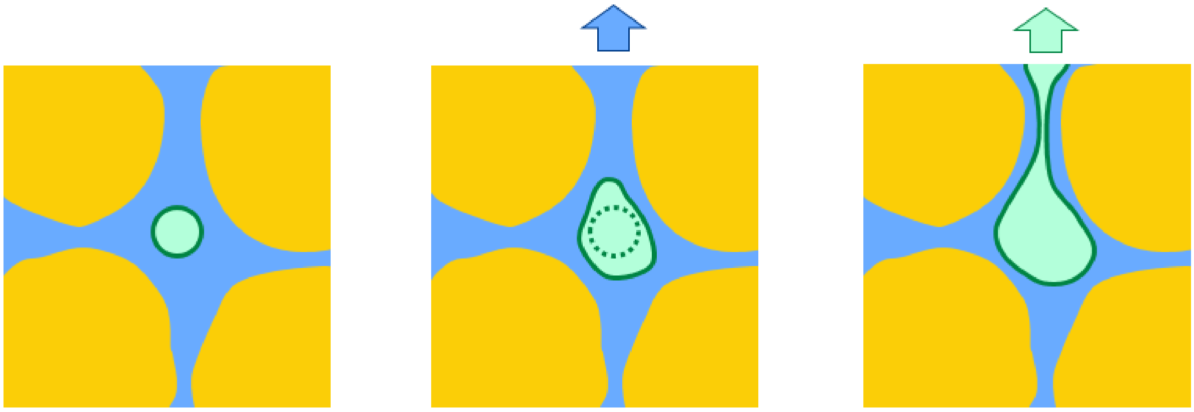

Figure 23 schematic of gas expansion in the aquifer due to pressure depletion.

7.3 Measurements

Conventional interpretation of saturation is done on the basis of Open Hole logs, interpreted with a focus on the gas column. Results are obtained using Waxman-Smit parameters that are calibrated to the gas bearing section of the field, and as such not necessarily representative for the water leg. Reassessment of these parameters for the water leg is required to obtain proper estimates for gas saturations below the free water level.

Only a limited number of wells in the Groningen field have significant penetration into the aquifer. None of the Groningen wells have a bare-foot completion (i.e. Open Hole). All existing wells have Cased Hole, or have been completed with uncemented liners. Schlumberger's PNXTM tool is a recent development in Cased Hole reservoir surveillance technology. It provides a novel type of measurement that can be interpreted to an actual saturation value. The Uithuizen-1 well (UHZ-1) was selected as a suitable candidate for PNX data acquisition, to complement the historic suite of Open Hole logs that were acquired when drilling the wells. UHZ-1 is an observation well located in the North of the field close to the earthquake-prone Loppersum area. Historically, the well has been periodically used to measure reservoir pressure and potential water encroachment. The presence of gas below the contact was already observed from the initial open hole log evaluation, however, gas saturation values were within the saturation measurement uncertainty.

In April 2017 PNX logging was carried out on UHZ-1. The survey conclusively confirmed the presence of gas in the aquifer (21). However, the interpretation of the measurements differs significantly with respect to the Open Hole analyses:

- The gas saturations interpreted from the PNX survey appeared to be significantly lower than those estimated based on Open Hole saturations. The interpreted results below the free water level show a maximum gas saturation of 10%. This is significantly lower than the 23 % gas saturation from the Open Hole interpretation at UHZ-1, although it should be realised that the Open Hole log gas saturation values in the water leg are uncalibrated. PNX measurements also require further calibration with detailed mineralogical data. A calibration project using core data and PNX measurements from the ZRP-3A well is scheduled for Q4 2017.

- The gas saturations interpreted from the PNX survey at UHZ-1 results appear to be limited to a depth of roughly 50 m below the current free water level, where the open-hole saturations appeared to be present throughout the entire logged Slochteren interval and there is no indication of a maximum depth to the open-hole interpreted saturations.

Further measurements are required to properly assess the uncertainty of these results. The PNX measurements suggest that the interpretation results are highly sensitive to the mineralogical content of the rock. A method is being established to incorporate knowledge of the reservoir mineralogy into the interpretation of the Open Hole logs, but this will need additional calibration to reduce associated uncertainties, Reference (21).

7.4 Scenario analysis of gas in the aquifer

The dynamic impact of gas in the aquifer on the pressure response and ultimately the subsidence match, was tested with the dynamic reservoir simulation model. These scenario analyses were carried out on the base case V4 model described in this report with the following two adjustments:

- No grid block volume multipliers were enabled, in other words the values shown in Figure 10 are all set to 1. This change to the V4 model was made because the aquifer gas has the potential to add energy and additional gas to the gas field. In the V4 model additional energy was added to the static volumes by increasing the grid block volumes.
- The compressibility grid as derived from the inversion of subsidence data (which compensates for areal trends in the compressibility) was not used. Instead the polynomial function of matrix compressibility to porosity was used, see Figure 2. This change was made because the compressibility grid resulting from subsidence data inversion, does not account for pressure lagging in the aquifer due to gas below the free water level. Not taking this pressure lag into account will result in a relatively low rock compressibility to achieve the same calculated subsidence as a model in which the aquifer is not lagging in pressure.

The two different interpretations, continuous and relatively high gas saturations based on open-hole measurements versus a lower gas saturation limited to a certain depth based on the PNX measurements are tested as scenarios on the adjusted V4 dynamic model. Three scenarios were used to test the sensitivity of gas below the free water level, varying only in the gas saturation below the free water level at the initialisation of the model (Figure 24)For all three scenarios, the full production history was simulated up to 31/12/2016. Due to :

Scenario 1 without gas in the aquifer

Scenario 2 10% gas saturation down to 50 m below the free water level (field wide),
based on the UHZ-1 PNX interpretation

Scenario 3 gas throughout the entire aquifer,
gas saturation values based on (uncalibrated) Open Hole logs, saturation field kriged between the wells.

For all three scenarios, the full production history was simulated up to 31/12/2016. Due to the relative permeability effect, the presence of gas results dampens the pressure depletion in the aquifer, Figure 25. Additionally, mobilisation of the gas beyond the critical gas saturation will result in an addition to the gas in the reservoir, resulting in a slower pressure decline for the same cumulative production, this is shown in the gas cap pressure difference between scenario 1 (~120 bar) and scenario 3 (~130 bar) in Figure 25.

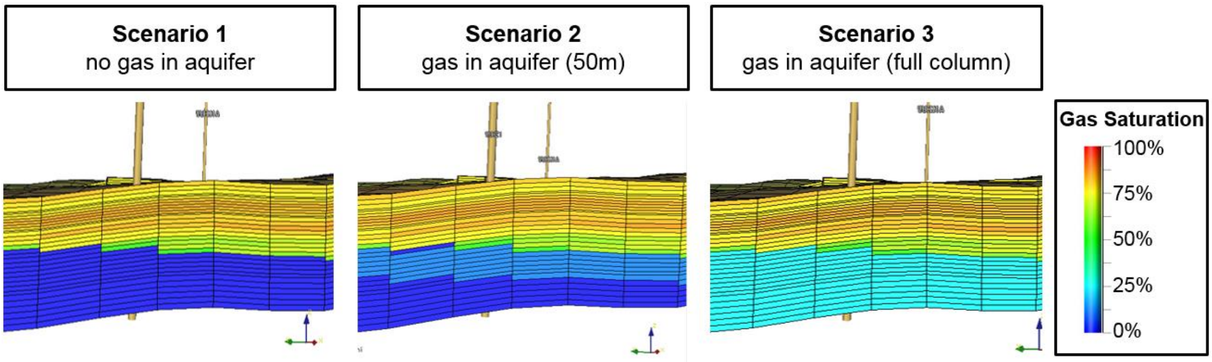

Figure 24: Initial gas saturation (1/1/1955) for a cross-section near the UHZ-1 well for three model realizations

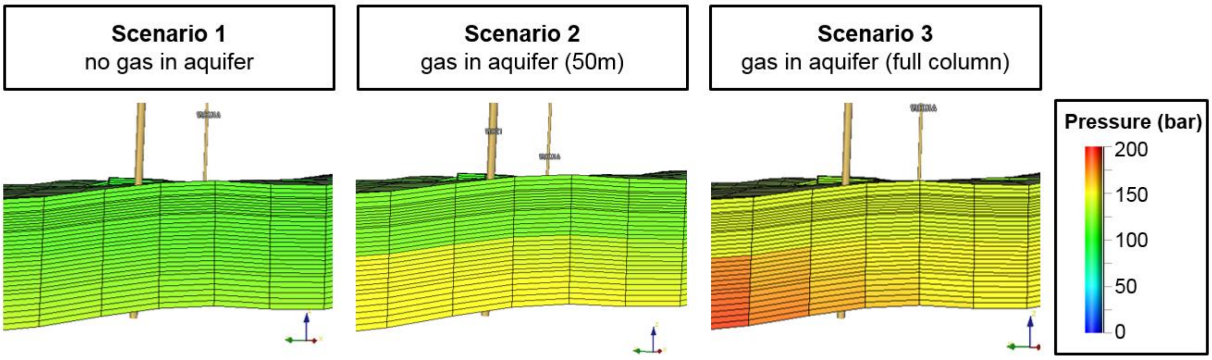

Figure 25: Reservoir pressure (31/12/2016), along cross-section at well UHZ-1.

Figure 26 shows the water rise at the Bierum-6 production well located in the north-east of the field. It is found that there is indeed a significant increase in the gas-water-contact rise. Note that Scenario 2 shows more water rise than Scenario 3. In Scenario 2 the gas saturation stays below the residual gas saturation in the model, which effectively acts as the critical gas saturation. In Scenario 3 the gas mobilises. The gas saturation in Scenario 3 has expanded to the residual gas saturation. In Scenario 3 the gas becomes mobile, for example for a porosity of 19%, at the residual gas saturation of 27% gas saturation (1), see Figure 27. Relatively higher saturations of gas in the water will result in a reduction in the relative permeability of water.

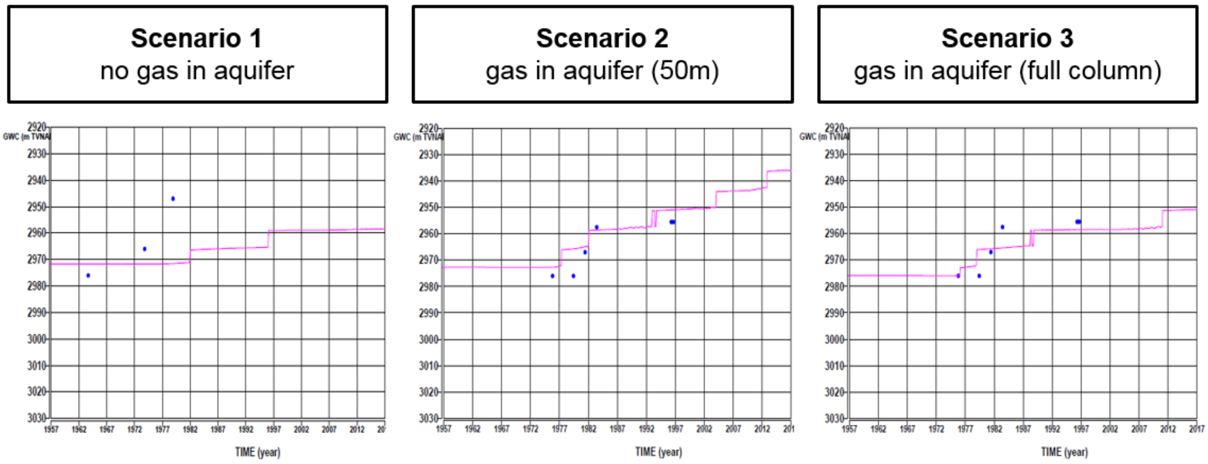

Figure 26: Modelled water influx (line) compared to interpreted water height from open-hole (dots).

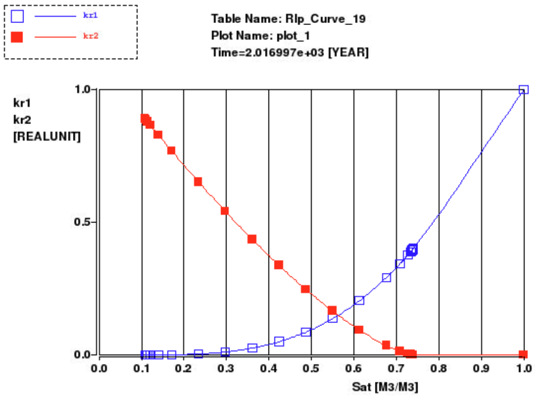

Figure 27: Gas (kr2-red) and water (kr1-blue) relative permeability curves for 19% porosity shown as a function of water saturation

Pressure depletion is directly related to compaction, which in turn is related to subsidence. The introduction of aquifer gas in the model results in less pressure depletion and also in less subsidence, which is shown for the respective scenarios in Figure 28, Figure 29 and Figure 30. In these figures the right-hand plot show the delta subsidence, which represents the mismatch between modelled and measured subsidence. In these figures green represents a good match, warm colours represent too much subsidence and cold colours represent too little subsidence.

Introducing gas in the aquifer dampens compaction caused by the depleting aquifer. An aquifer without gas saturation predicts too much (+8 cm) of subsidence in the north of the field. Increasing the gas saturation in the aquifer improves the match of modelled subsidence to data, reducing the error significantly (+3 cm).

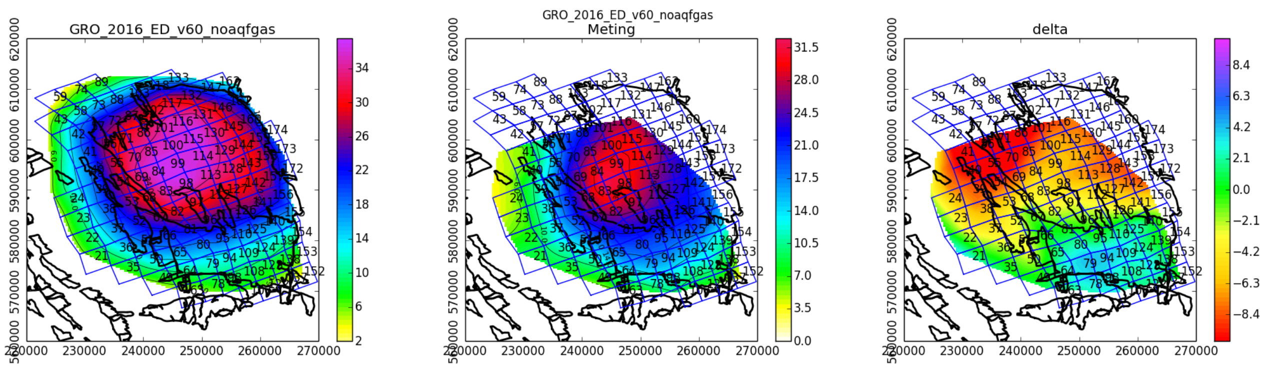

Figure 28: Scenario 1 – Subsidence proxy calculation for a model without gas in the aquifer

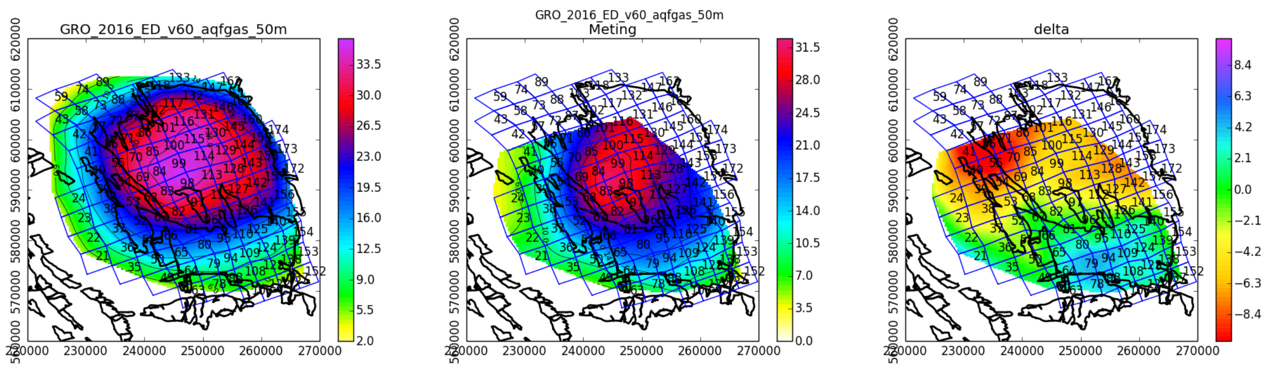

Figure 29: Scenario 2 – Subsidence proxy calculation for a model with 10% gas in the aquifer down to a depth of 50 m below the free water level

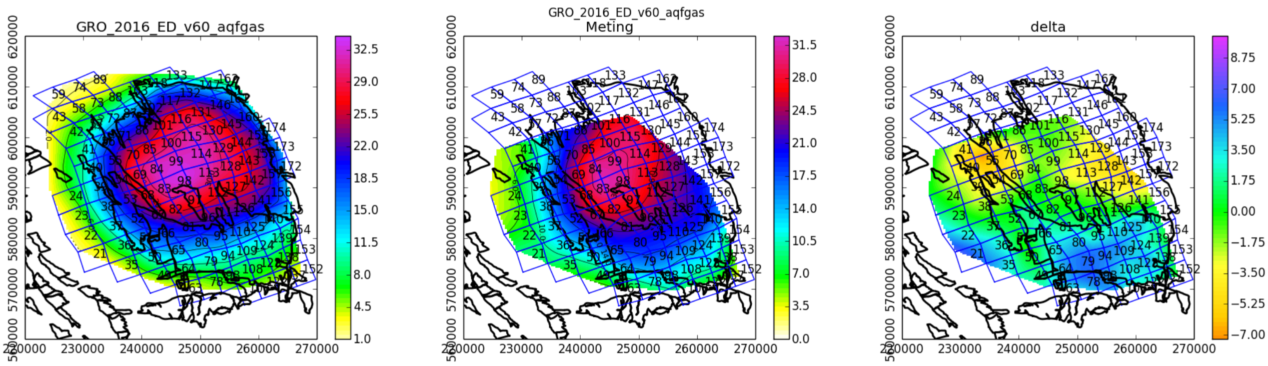

Figure 30: Scenario 3 –Subsidence proxy calculation for a model with average gas saturations below the free water level distributed based on open-hole measurements

7.5 Conclusion based on the sensitivity of gas in the aquifer

The following conclusions drawn from the modelling results.

- Gas in the aquifer results in a lower effective permeability due to a relative permeability effect, which results in a lower pressure depletion in the water leg caused by the pressure depletion in the gas cap, significantly dampening depletion, compared to an aquifer without gas. Thus, gas in the aquifer reduces compaction in the aquifer and consequently subsidence.
- Gas in the aquifer can increase the rise in gas-water-contact with respect to a model that does not have gas in the aquifer.
  Gas in the aquifer has the potential to deliver additional energy. Once the critical gas saturation is exceeded, the gas can migrate into the reservoir.

7.6 Gas in the aquifer: recommendations for future work

Currently the saturation and distribution of gas in the aquifer is uncertain. Furthermore, the interpretations of the open-hole and the PNX measurements show differences that are to be further reconciled.

It is recommended as a first step to investigate whether the presence of gas either extends to greater depth (as is suggested by the current open-hole interpretation), or is limited to a certain depth (50 m below the FWL as interpreted for UHZ-1 from the PNX). If the gas saturation depth is limited it is recommended to find out if it is at a same depth throughout the field, or showing significant variation from one location to the other. Hypothetically, a fixed maximum depth could represent a paleo-contact, suggesting thatover geological time the free water level moved upward to a shallower level. Alternatively, any gas saturation present throughout the logged interval and potentially extending to greater depths within the aquifer, could suggest that gas remained trapped in the pores when gas migration and charge was stopped.

From a geological perspective, a description of the origin of the gas in the aquifer is required to steer the modelling of the gas distribution in the aquifer away from the wells. If the distribution of gas in the aquifer is found, based on additional petrophysical work, to extend down to greater depths in the aquifer, this may be explained by migration of gas from a deep source underneath the Rotliegend reservoir.that got trapped on its way up to the reservoir. Available basin modelling studies (22) do report early gas charge from such a deep source rock, but also a second charge phase from a source located northwest of the Groningen field in the Lauwerszee Trough area.

From a reservoir engineering perspective, if additional petrophysical work confirms the presence of a paleo contact, it is recommended to investigate the critical gas saturation and whether the potential paleo gas can be described by a capillary pressure model. A hypothesis for a paleo-contact in Groningen could be a change in the reservoir temperature over geological time, after the field was charged. The temperature in the Groningen field is variable, with higher measured temperatures in the north than in the south (1). The temperature could have changed from a higher temperature to a lower temperature after the field was charged. Such a hypothetical reduction in temperature could have caused the gas to shrink and consequently in a rise of the free water level.

8 Recommendations for future work

Based on the V4 modelling exercise and the Study and Data Acquisition Plan, a number of recommendations can be made that are expected to further improve the workflow and the resulting model.

8.1 Seismic inversion to static properties

It is recommended to improve the process of property modelling in the static domain by considering the dynamic behaviour of the V4 model (model maturation). This recommendation is aimed at improving two issues identified in the dynamic model – a dynamic model with the same gas initially in place as the static model will decline faster in pressure than what was historically measured, in other words the model is lacking in energy, furthermore, the connectivity of certain wells should be improved.

1. The main sources for more energy are either additional gas or additional aquifer support. Aquifer support is largely constrained by the PNL measurements. The sources of additional gas can be several; additional gross volume, shorter gas-water transition zone, increased porosity or higher net to gross ratio. In the V4 dynamic model, these potential sources are all lumped into one variable model parameter per region: a Grid Block Volume (GBV) multiplier for each region. Based on several iterations, the seismic inversion to static properties (porosity) is not likely close the gap between static and dynamic GIIP, 2868 vs. 2935 BCM. Although this difference from static to dynamic GIIP is relatively modest (+2.3%), it is likely that better alignment between the static and dynamic domain can be achieved. One area of particular interest is the Harkstede block. Additional energy may originate from liberated gas from the aquifer or from gas extracted/released from the Carboniferous. The latter may well occur in the south of the field where part of the Carboniferous extends above the gas-water contact.

2. The up-scaled model, prior to history matching, has an inconsistency in the north of the field. In the northern part of the model, the initial set of permeability values (based on the inversion-derived porosity grid) is causing the observation wells to be lagging in pressure with respect to the nearby production clusters. An example of this is the connection between observation well De-Hond-1 and the nearby Bierum production cluster. Without any alteration, De-Hond-1 is lagging in pressure with respect to the Bierum cluster, see the left plot in Figure 31. However, no such pressure lag is actually measured by historical SPG surveys, see Figure 32. This means that De Hond-1 is not sufficiently connected in the model to the Bierum cluster or to other production clusters. A match was achieved by regionally increasing the permeability, see the right plot in Figure 31.

   After upscaling, the model permeability has been compared to available permeability interpretations from build-up tests, see Appendix 3. The well-test results suggest a reduction of permeability around the northern clusters. For instance, the build-up tests for Bierum cluster indicate that the local permeability in the model should be lower. This is inconsistent with the regional increase in connectivity required to achieve a pressure match in the northern observation wells. With the current modelling set-up a match in Bierum is mutually exclusive to a match in the northern observation wells.

   It is therefore recommended to improve the permeability distribution in the model, which is a direct function of the porosity in the north of the field. At a regional scale (e.g. north-east region) the permeability should be increased. Local features, e.g. imprints of floaters in the Zechstein, distort the seismic signal which translates into too low porosities and consequently too low permeability. These local features are not necessarily representative of the actual reservoir quality. At a well scale, the permeability should match with the permeability range derived from build-up interpretations. It is recommended to use information on Zechstein imprints to locally adjust the permeability distribution, such that a match in connectivity for both the observation wells and the production clusters in the north of the field becomes possible.

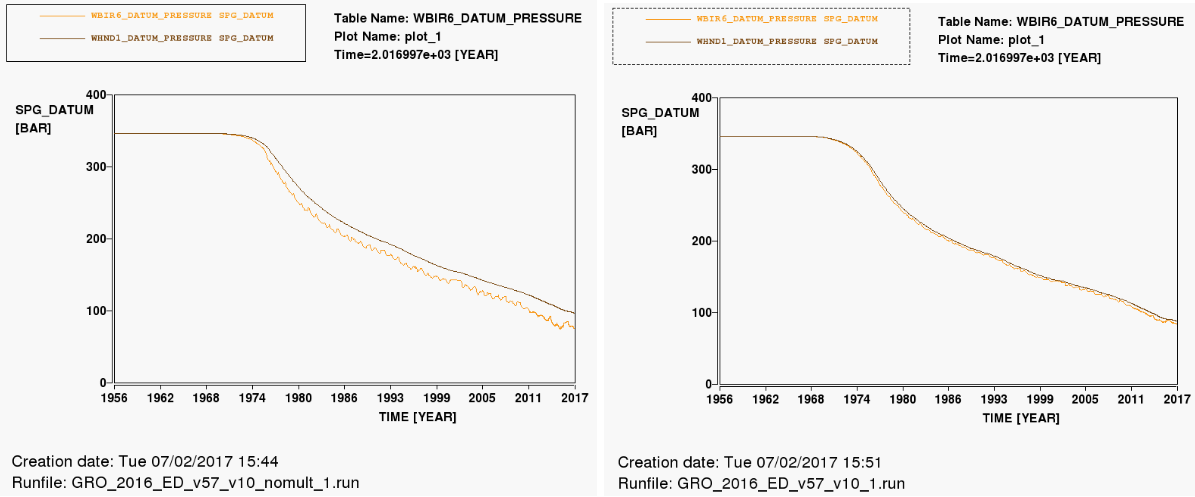

Figure 31 Both figures show the model output for BIR-6 and HND-1, without permeability increase in the north (left) and with permeability increase in the north (right).

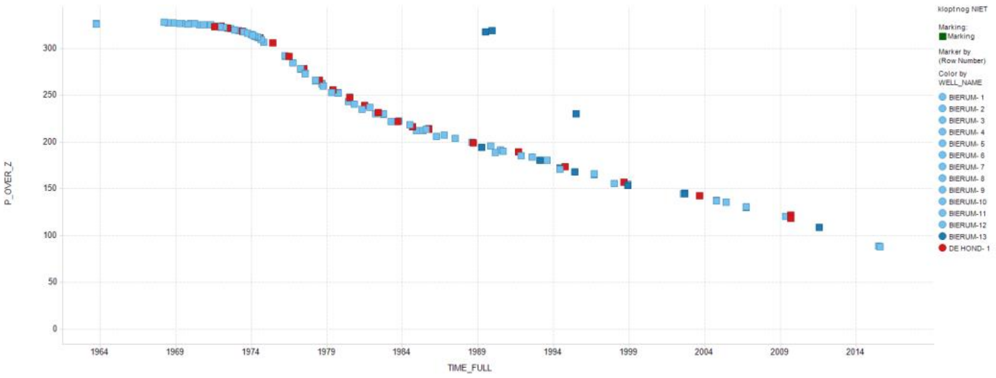

Figure 32 SPG data at datum depth 2875 m TVD NAP for all Bierum production wells and the nearby HND observation well, there is no pressure lag.

8.2 Carboniferous

It is recommended to explore the dynamic effect of a gas bearing Carboniferous formation in the south of the field, using the dynamic reservoir simulation model. The subsidence match in the south of the field indicates that the model is not subsiding as much as is observed. This could be caused by underestimation of the matrix compressibility or by a depleting gas bearing section of the Carboniferous. Although generally very low in permeability (23), the Carboniferous in the south of the field is gas bearing, and it is measured to be lagging only 50 bars behind the main field at the HGL-1 well. The Carboniferous top structure has been recently reinterpreted (24).To incorporate the gas bearing Carboniferous into the dynamic model a mechanism of depletion needs to be investigated. Available data (e.g. reservoir properties (23), pressure measurements in the Carboniferous (19)) can be used to populate and constrain this section of the model. Gas migration from the Carboniferous into the main reservoir can also explain some of the difference between static and dynamic GIIP and the difference between modelled and measured gravity change.

8.3 Gravity data

Upon implementation of a gas-bearing Carboniferous in the dynamic reservoir model, include gravity data as a field-wide matching function in the history matching methodology (17).

9 References

1. **Burkitov, U., van Oeveren, H.E.J. and Valvatne, P.** *Groningen Field Review 2015 Subsurface Dynamic Modelling Report.* Assen : NAM, 2016. EP201603238100.

2. **NAM.** *Study and Data Acquisition Plan Induced Seismicity in Groningen.* Assen : NAM, 2016. EP201604200072.

3. **Wervelman, R.** *Groningen Pre-SDM.* Rijswijk : Shell UI-Europe, 2015. EP201602210428.

4. **Horizon, SGS.** *Independent Review of Groningen Subsurface Modelling Update for Winningsplan 2016.* Voorburg : SGS Horizon, 2016. http://feitenencijfers.namplatform.nl/download/rapport/5820d1c5-d989-45f7-80b7-638156ee661e?open=true.

5. **van Jaarsveld, J.** *Groningen Field Review 2012 Dynamic Modelling and History Matching Results.* Assen : NAM, 2012. EP201202215894.

6. **van der Wal, O. and van Eijs, R.** *Subsidence inversion on Groningen using leveling data only.* Assen : NAM, 2016. EP201612206045.

7. **Craig, Alastair.** *Advanced Rock Properties Study for NAM BV, Well: Zeerijp-3A (Groningen).* Aberdeen : CORE LABORATORIES, 2017. ABZ160096.

8. ***Oil/water relative permeability measurements on three Groningen wells.* Assen : NAM, 1990. NAM 17533 RKER 89.211.**

9. Vermolen, E. *Groningen SCAL data review.* Assen : NAM, 2014.

10. Valvatne, P. *Groningen Model Update 2015: Surface Pressure and Flowrate Matching.* 2016. EP201603223496.

11. Garming, L. *Groningen generic lift curves.* 2016. EP201607217987.

12. Valvatne, P. *Groningen Model Update 2015: Use of Simplified Lift Models in MoReS.* 2017. EP201702245801.

13. Matsuura, T. *Example deck for Assisted History Matching using DYNAMO.* Rijswijk : UIO, 2015. 20150604.

14. NAM. *Study and Data Acquisition Plan Induced Seismicity in Groningen Update Post-Winningsplan 2016.* Assen : NAM, 2016. EP201604200072.

15. Eiken, O. *Gravity Monitoring of the Groningen gas field 2015.* Trondheim, Norway : Quad Geometrics, 2015. \\europe.shell.com\europe\E & P\NAM Assen\Department\Onshore_Dev\Groningen Asset\Disciplines\Reservoir Engineering\Gravity Study.

16. Glegola, M., et al. *Groningen 1978-2015 time-lapse gravity surveys results. Interpretation report.* Rijswijk : Shell, 2017.

17. Van Oeveren, Henk. *Implementation of time-lapse gravity data in the Groningen dynamic model.* Assen : s.n., April 2017. EP201704204007.

18. van Oeveren, H.E.J. *Implementation of time-lapse gravity data in the Groningen dynamic model.* Assen : NAM, 2017. EP201704204007.

19. Vos, L.L. *Groningen Field RFT and FIT Data & Information on Limburg Connectivity.* Assen : NAM, 2003. 200301000527.

20. Warrier, S. *Paleo gas.* Perth : Shell Australia, 2016. -.

21. Ishmukhametova, G. *Investigation of gas presence in the aquifer of the Groningen field.* Assen : NAM, 2017. EP201707201356.

22. Stevanovic, Snezana. *Updated Groningen Basin Model.* Rijswijk : SIEP, 2012.

23. Seubring, J. *Petrophysical Evaluation of the Groningen Field Carboniferous.* Assen : NAM, 1994. 26649.

24. van Assema, B. *Seismic interpretation and depth conversion of Top Carboniferous in the Groningen field, northeast Netherlands.* Assen : NAM, 2017. EP201706201191.

25. Miedema, W. *FBU Data Validation for the Groningen Field.* Assen : NAM, 2003. EP200301001671.

26. Geurtsen, E.L. and de Zeeuw, Q. *ZPD-12A Flowing Build-Up Test Interpretation - August 2014 Explaining the Groningen Central Area permeability multipliers.* Assen : NAM, 2017. EP201608201398.

27. de Zeeuw, Q. *CITHP to CIBHP conversion for the Groningen wells.* Assen : NAM, 2016. EP201612250703.

28. van Thienen-Visser, K. *Review Winningsplan Groningen.* Utrecht : TNO, 2013. http://nlog.nl/cmis/browser?id=workspace%3A//SpacesStore/7bcc6646-157d-4ef9-a580-06f4f00002fd.

29. Glegola, M, van den Beukel, A and Aasheim, O. *Ormen Lange 2014 Gravity survey.* Stavanger : Norske Shell, 2014. -\\europe.shell.com\europe\E & P\NAM Assen\Department\Onshore_Dev\Groningen Asset\Disciplines\Reservoir Engineering\Gravity Study.

30. Nagy, D., Papp, G. and Benedek, J. *The gravitational potential and its derivatives for the prism.* s.l. : Journal of Geodesy, 2000. 74, 552-560.

31. Vevatne, J.N., et al. *Use of Field-wide SEafloor Time-lapse Gravity in History Matching the Mikkel Gas Condensate Field.* Copenhagen : Statoil, 2012. F040 74th EAGE Conference & Exhibition incorporating SPE EUROPEC 2012.

Appendix 1 – V4 best match

SPG match	GRO_2016_ED_v60_SPTG_Match.pdf
RFT match	GRO_2016_ED_v60_RFT_Match.pdf
CITHP2BHP match	GRO_2016_ED_v60_CITHP2BHP.pdf
PNL match	GRO_2016_ED_v60_PNL_Match.pdf
Subsidence match	Figure 17 (bottom)

Appendix 2 – Variable model parameter range and optimal V4 setting

	V4	Minimum	Maximum
Gross bulk volume ranges			
NorthEast_gbv_Mult	1.019	1.015	1.025
NorthWest_gbv_Mult	1.0242	1.015	1.025
East_gbv_Mult	1.0185	1.015	1.025
Central_gbv_Mult	1.0155	1.015	1.025
SouthWest_gbv_Mult	1.0239	1.015	1.025
SouthEast_gbv_Mult	1.0152	1.015	1.025
Eemskanaal_gbv_Mult	1.005	1	1.02
Kolham_gbv_mult	1.06	1.01	1.1
Harkstede_gbv_mult	2.42	1.01	2.5
USQ_gbv_mult	1.26	1.2	1.5
OPK4_gbv_mult	1.05	0.95	1.1
BDM_gbv_mult	0.93	0.84	1
KWR_gbv_mult	1.05	1	1.1
FWD_gbv_mult	0.3	0.3	0.6
WRF_gbv_mult	1	0.99	1.01
ANV_gbv_mult	0.1	0.1	0.5
Permeability ranges 10^x			
NorthEast_k_Mult	0.631	0.45	0.65
NorthWest_k_Mult	0.498	0.45	0.65
East_k_Mult	0.479	0.45	0.65
Central_k_Mult	0.591	0.45	0.65
SouthWest_k_Mult	0.47	0.4	0.5
SouthEast_k_Mult	0.43	0.4	0.5
Eemskanaal_k_Mult	0.46	0.4	0.5
Ameland_k_Mult	-1.1	-3	0
Zeerijp_k_Mult	0.35	0	0.5
KWRLog_k_Mult	1	0	1
Feerwerd_k_Mult	-0.08	-1	1
Warffum_k_Mult	0.2	-1	1
OPK4_k_Mult	-1.27	-2	0
Fault transmissibility ranges 10^x			
LogFaultSeal_USQ	-2	-2	-1.5
LogFaultSeal_USQgas	-2.15	-3	-1
LogFaultSeal_ODP	-1.95	-2.1	-1.7
LogFaultSeal_BRH	-1.5	-3	0
LogFaultSeal_RDW	-0.4	-0.5	-0.3
LogFaultSeal_RDWN	-0.14	-0.3	0
LogFaultSeal_ZWD	0	-2	0
LogFaultSeal_ANV	-6	-6	0
LogFaultSeal_ANV_N	0	-1	0
LogFaultSeal_NE	-2.33	-4	-1
LogFaultSeal_NE_UHM	0	-0.5	0
LogFaultSeal_NE_UHZ	-1.7	-2	0
LogFaultSeal_NE_ZND	-1	-2	0
LogFaultSeal_ZRP	-1	-4	0
LogFaultSeal_BIRSouth	-0.4	-1	0
LogFaultSeal_BIR13	-0.4	-1	0
LogFaultSeal_RysAqf	-1.2	-2	-1
LogFaultSeal_RysAqfNorth	-2	-2	-1
LogFaultSeal_BRW5	-1.8	-3	-1
LogFaultSeal_AMR_LRM	-0.03	-1	0
LogFaultSeal_PopUps	0	-0.5	0
LogFaultSeal_TBR	-1.65	-2	-1
LogFaultSeal_TBR_ew	-2	-6	0
LogFaultSeal_TBR_ns	-2	-6	0
LogFaultSeal_SDBtoSZWtoEKR	0	-1	0
LogFaultSeal_SPHWest	-0.6	-1	-0.5
LogFaultSeal_KHMTrough	-1.85	-2	-1.3
LogFaultSeal_Harkstede	-1.25	-2	-1
LogFaultSeal_HarkstedeN	-0.3	-4	0
LogFaultSeal_HarkstedeNE	-4	-4	-1
LogFaultSeal_HRS_AQF	-0.4	-2	0
LogFaultSeal_LAU	0	-3.5	0
LogFaultSeal_HGZ	0	-0.1	0
LogFaultSeal_SAP15A	-0.25	-0.5	0
LogFaultSeal_PosPauTjm	-0.35	-0.4	0
LogFaultSeal_SDM	-2	-4	0
LogFaultSeal_OPK4	-0.08	0	0
LogFaultSeal_MLA	0	-2.4	0
LogFaultSeal_BDM	-7.5	-10	-5
LogFaultSeal_BDM3	-2.35	-2.6	-2
LogFaultSeal_BDM4	-1.2	-2	-1
LogFaultSeal_BDM5	0	-0.5	0
LogFaultSeal_RNM1	-1.9	-2	-1
LogFaultSeal_WRF1	-0.8	-2	0
Negative skin uncertainty (hydraulic fractures)			
Skin_KWR1A	-3	-4	-2

Skin_SSM2A	-3	-4	-2
Skin_SSM4	-3	-4	-2
Aquifer length uncertainty			
AqfLength_AnnerveenVeendam	0	0	6460
AqfLength_Lauwersee1	0	0	30397
AqfLength_Lauwersee2	1000	0	10721
AqfLength_Lauwersee3	3000	0	31384
AqfLength_Lauwersee4	3000	0	15898
AqfLength_Moewensteert	4505	0	37570
AqfLength_Rodewolt	8800	0	35715
AqfLength_Rysum	15321	0	15321
AqfLength_Usquert	49000	0	56757
AqfVsc	1.1	0.5	1.5
Relative permeability uncertainty			
Sw_unc	0.05	-0.05	0.05
density_gas	197	195	199
density_water	1172	1171	1173
Srg_slope	0	0	0.7
Krw_at_Srg	0.4	0.03	0.4
Krg_at_Swc	0.89	0.83	0.89
Nw	3	2.7	4
Ng	1.4	1.4	2
PhiMin	0.04	0.02	0.08
Min_Wat_Sat	0.45	0.26	0.6
Free water level uncertainty			
FWL_Groningen_Central	2992	2972	3012
FWL_Groningen_E	2972	2970	2972
FWL_Groningen_NE	2978	2970	2982
FWL_Groningen_NW	2984	2982	2984
FWL_Groningen_SE	3006	3003	3015
FWL_Groningen_SW	2995	2984	3006
FWL_Gron_Eemskanaal	2996	2993	2997
FWL_Gron_Ellerhuizen	2997	2970	3040
FWL_Gron_Harkstede	3016	3014	3018
FWL_Gron_Hoogezand	3030	3016	3030
FWL_Gron_Oldorp	2967	2966	2988
FWL_Gron_Zuidwending	3017	3006	3028
Compressibility and subsidence uncertainty			
Compress_rock_mult	1	0.9	1.1
PoissonRatio	0.25	0.24	0.26
TimeDecay	0.01	0.01	5

Appendix 3: Model audit trail

Software
Dynamo version 2016.1 was used for all dynamic modelling work. The static Petrel model was up-scaled using flow-based upscaling in Reduce++. MoReS was used for running the numerical 3D simulation. Multirun was used as the parent for the experimental space filling design.

Location
The model is stored in the following location:

\\europe.shell.com\tcs\ams\ui.nam\field\epe_re_08\groningen\GFR_Model_2015\20_HM\04_ExperimentalDesign_AHM\60_GRO_2016_ED_Version_60

Include files (historical data, PVT, Saturation functions etc.) used by the model can be found here:

\\europe.shell.com\tcs\ams\ui.nam\field\epe_re_08\groningen\GFR_Model_2015\Include\

Appendix 4: Permeability comparison of reservoir model versus build-up tests

After upscaling the static model, the permeability in the dynamic model was compared to the permeability obtained from build-up test interpretations. In 2003 an overview of all available build-up test analyses results was published (25), the distribution of permeability per cluster/location is given in Figure 33.

The mean permeability from Figure 33 is compared to the average permeability in a 3-day inflow range (ref. Appendix 4) in the dynamic model, Figure 34. Where the build-up test permeability is higher shows as a green circle, where it is lower in red. This comparison needs to be interpreted with some caution. Some differences between the model and build-up test permeabilities could be attributed to other dynamic effects, such as well bore impairment at 't-Zand cluster, close proximity to faults in the Zuiderveen pop-up structure or high perm streaks in the central region in the field.

This table has been used as an early check and was not used to constrain the posterior model permeability, which was constrained by pressure and PNL matches. As discussed in 8.1, permeability reduction in for instance the northern clusters might be required to match the model permeability to build-up permeability. However, this reduction might be in conflict with a history match to pressure data, for instance, a permeability increase is required to improve the connectivity of northern clusters to northern observation wells. This conflict is the main item addressed in the second seismic inversion by the geoscientists.

Cluster	Lognormal Distribution k [mD]				Normal Distribution k [mD]				No. Of tests
	Mean	P(15)	P(85)	Exp	Mean	P(15)	P(85)	Exp	
AMR	102	69	151	107	109	71	147	109	21
BIR	80	55	118	84	85	50	120	85	4
DZL									0
EKL	18	11	28	19	19	8	30	19	5
EKR	77	44	134	85	85	39	131	85	3
FRB	853				853				1
HND									0
HRS									0
KHM									0
KPD	65	23	182	90	91	37	145	91	13
LRM	134	115	156	135	135	114	157	135	7
MDN									0
MWD	173	138	216	176	177	141	212	177	8
NBR	377	292	486	385	383	287	479	383	2
NWS	138	121	158	139	139	122	157	139	8
OVS									0
OWG	562				562				1
PAU	349	210	579	379	384	211	556	384	5
POS	165	92	297	185	180	80	279	180	2
SAP	94	64	137	98	100	65	135	100	16
SCB	168	109	259	179	178	106	251	178	3
SDB	241				241				1
SDM	49				49				1
SLO	200				200				1
SPI	194				194				1
SZW	121	82	180	127	129	80	177	129	5
TBR									0
TJM	267	260	274	267	267	260	274	267	2
TUS	88	51	153	98	97	51	143	97	3
UTB	330	222	491	348	350	239	462	350	8
ZBR									0
ZND	79	47	133	86	88	48	127	88	7
ZPD	82				82				1
ZVN	32	11	88	44	52	0	108	53	9

Figure 33 Average permeability from build-up tests per cluster/location directly copied from an overview report [EP 200301001671]

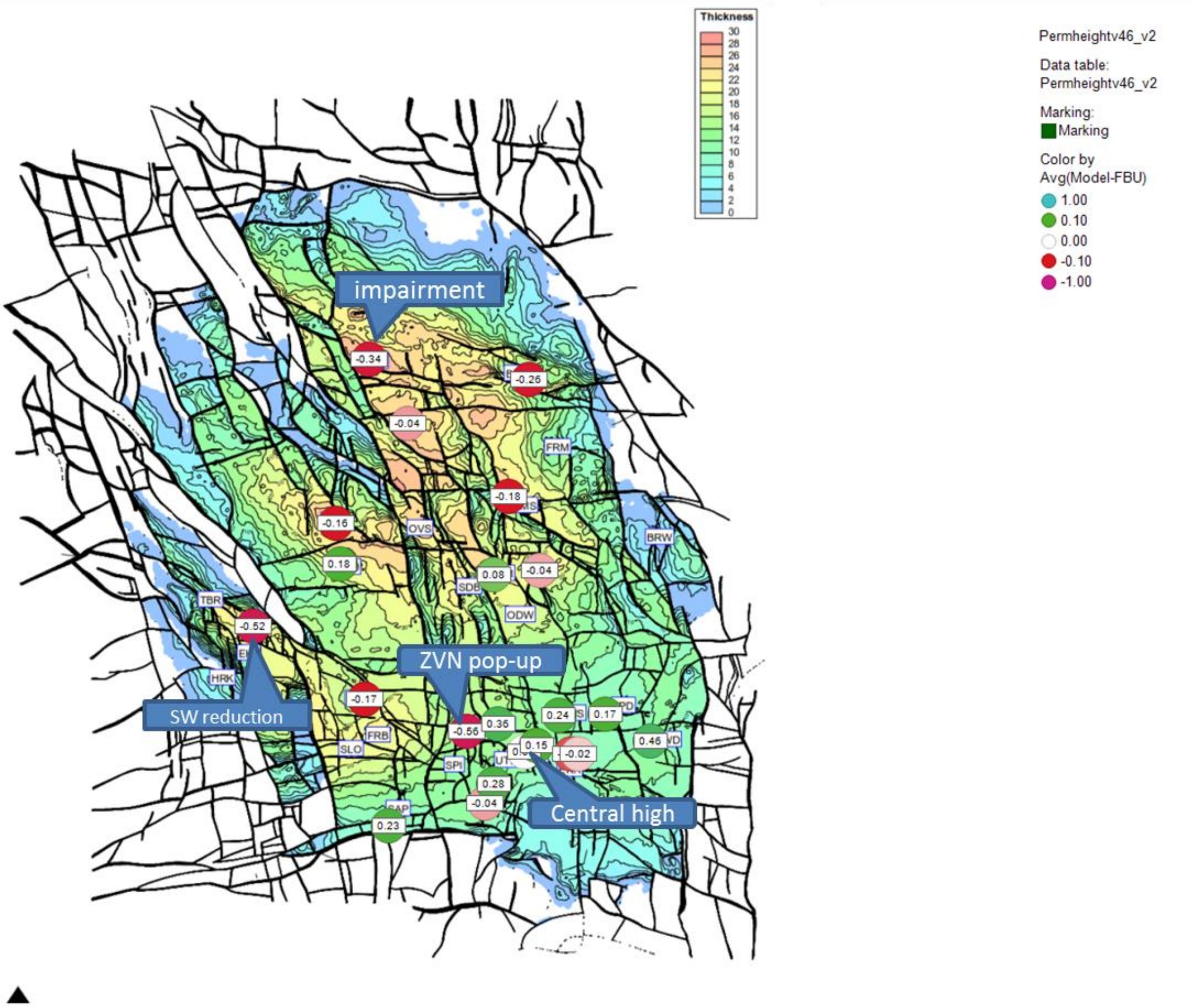

Figure 34 Areal overview of permeability mismatch between static model and permeability derived from build-up tests. Where the build-up test permeability is higher shows as a green circle, where it is lower in red. The permeability scaling factors are given as a power of 10 (e.g. -0.26 refers to $10^{-0.26} = 0.55$)

Appendix 5: Pressure matching

The evaluation of a history match on reservoir pressure is not entirely straightforward, because spot measurements of a continuous signal (reservoir pressure at a well location from an SPG measurement) are compared to the outcome of a discretized model (average pressure over a gridblock and over a simulator timestep). Prior to 2011, the V4 model is using monthly time steps (section 3.2). The shut-in of a production well and the associated pressure build-up is not reflected by the simulator if the shut-in is shorter than a calendar month. The calculated wellbore bottomhole pressure during that particular monthly timestep reflects the conditions of a flowing well.

To circumvent this issue, a reservoir pressure measurement is compared to the average pressure in a range of gridblocks around the well. The areal extent of the range is determined such that the average pressure in the range corresponds to the equivalent of the wellbore bottom hole pressure after 3 days of shut-in. Average pressures are calculated in this way for each well, for each timestep, to allow for a direct comparisson to the measurements without having to explicitly model each (short) buildup, which would require an impracticle number of simulation time-steps to capture all 1800 pressure measurements.

After 2011 the model takes daily timesteps (section 3.2) which, in combination with Local Gridblock Refinement, allows for explicit modeling of the shut-ins: the wellbore bottomhole pressure should match the SPG measurement directly. To check whether the approach based on the gridblock ranges is still valid, the difference between the bottom hole pressure and the average range pressure is determined. In Figure 35 the average pressure in the range is compared to the bottom hole pressure at the time an SPG measurement was taken (across all wells). This comparison shows that the output of the reservoir model to which SPG measurements are compared is roughly 1 bar higher than it should be for the period 2011-2017.

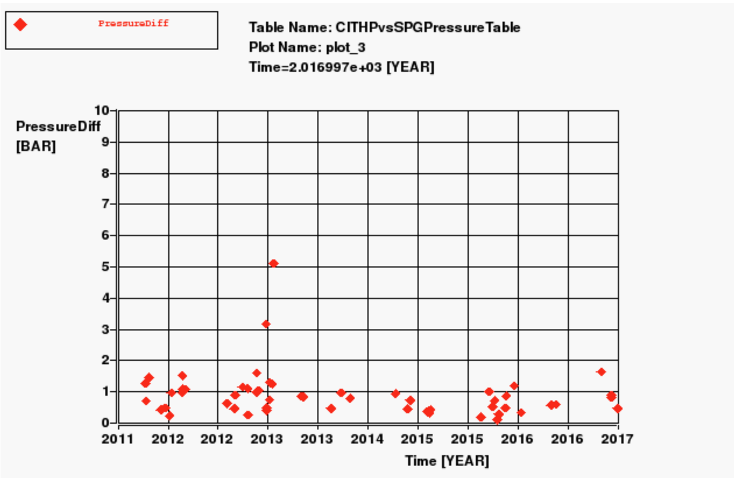

Figure 35 difference between model output for SPG and converted closed-in tubing head pressure (a positive value means the modelled SPG pressure is higher than the modelled closed-in tubing head pressure).

Appendix 6: Investigation of high permeabilities in the Central area

Over the period 1970-1980, the Zuiderpolder area exhibited a different pressure decline behaviour from the rest of the field, showing a slower decline in pressure than the nearby more southern clusters, see Figure 36. This behaviour was identified during GFR 2012, when Adjoint calculations indicated that the dynamic model needed higher permeability in the Groningen central area, see Figure 37. During the GFR 2015 work, again an increase in the central region permeability was required. To obtain a pressure match in the V4 model, the upscaled model permeability for this central area was increased 4-fold in the dynamic model, see Figure 38. This section describes the analysis of a well test performed in the Zuiderpolder (ZPD) production cluster located in the Central region, to support these modelling choices. The full analysis is documented in Reference (26).

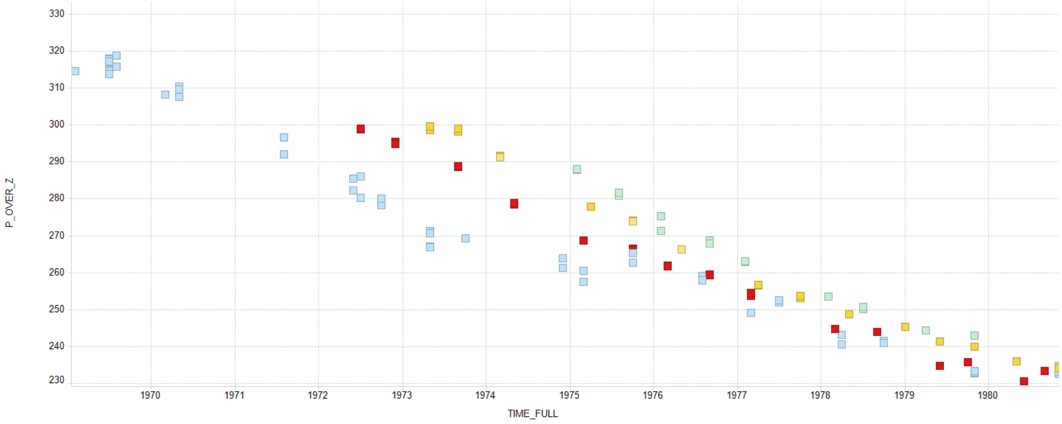

Figure 36 p/z over time for the Zuiderpolder cluster (red), the more southern Eeker cluster (blue) and the more northern Siddeburen (yellow) and Amsweer (green) clusters.

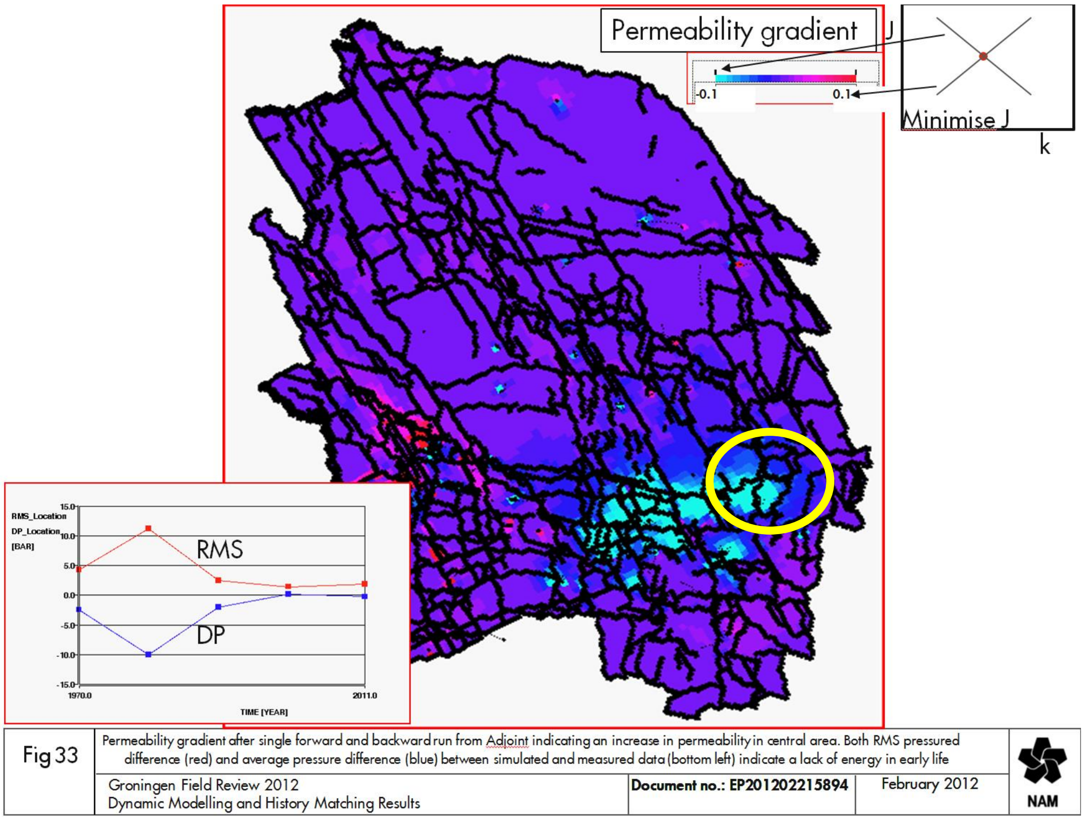

Figure 37 Permeability gradient resulting from Adjoint run on GFR 2012 Groningen MoReS model (top). The Central area clearly stands out (high permeability multipliers in red), with the ZPD location marked by the yellow circle.

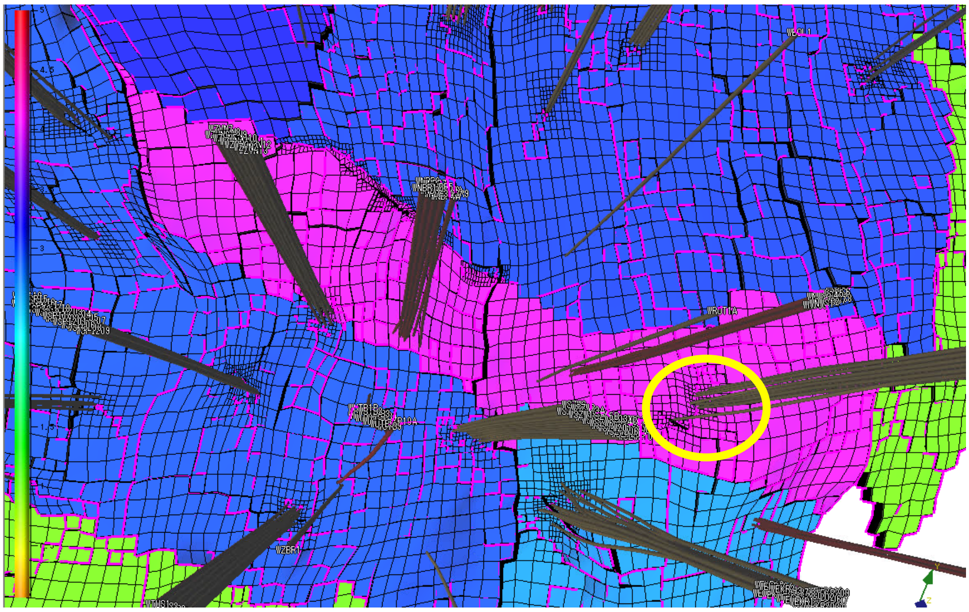

Figure 38 Permeability multipliers on the horizontal permeability from 0(yellow) to 5 (red), showing a 4 times increase in the central region compared to a 2.5-3 times increase in the nearby regions. ZPD cluster is indicated with a yellow circle.

Geologically the Central area is situated in a transition from conglomerates in the south (relatively lower permeability) to more sandy facies in the north but with increasing clay content and finer grain size. One hypothesis is that at this transition local high permeability streaks could provide a highly conductive connection from the Central area to the rest of the field. Such streaks would increase the lateral connectivity and could provide the pressure support during early field life which was matched in the dynamic model by the high permeability multipliers.

Due to upscaling steps in the static and dynamic model, these high permeability streaks may not get sufficiently captured in the model. The upscaling step in the static domain is illustrated in Figure 39, which shows a gamma ray and porosity log for ZPD-12A (left hand side) and for ZPD-10 (right hand side), along with the permeability layers in the static model. Actual core measurements are superimposed as white dots. Note that several intervals show core permeability around 1000 mD, where the permeability in the static model is around 100 mD. This implies that the permeability in the static model is locally underestimating the permeability measured in core samples. Figure 39 also shows that these high permeability intervals occur around the same stratigraphic depth in both ZPD-10 and ZPD-12A, suggesting lateral continuity.

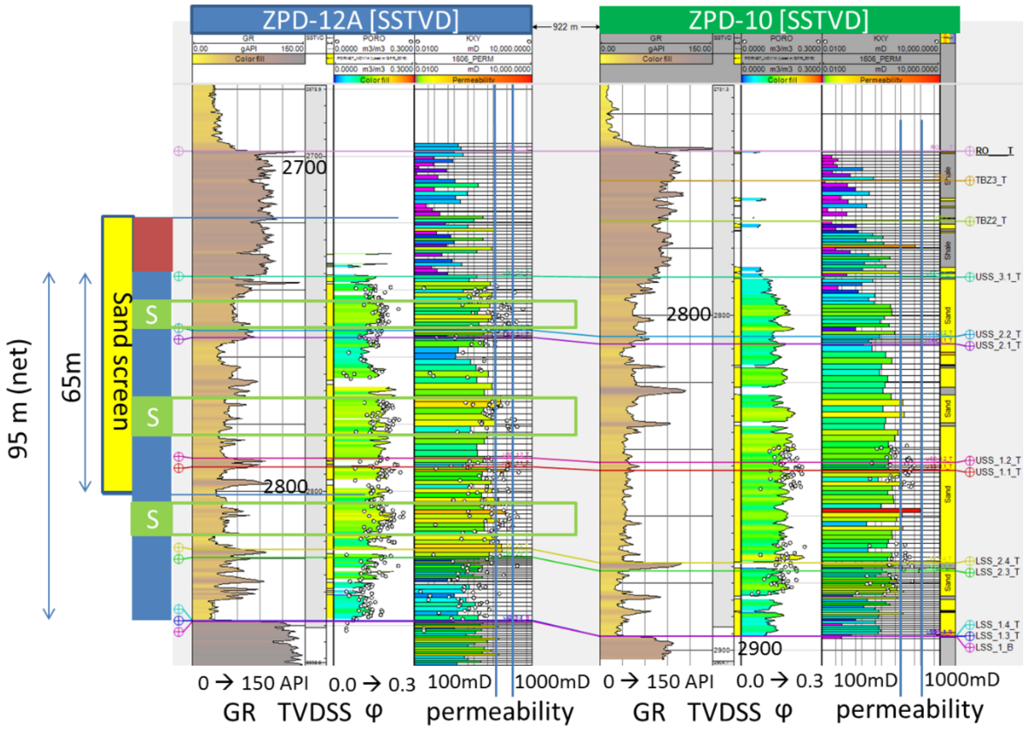

Figure 39: Well log of ZPD-12A and ZPD-10 showing both permeabilities as in the static model (colored bars in the rightmost logs) and core measurements (white dots in the rightmost logs).

In August 2014, a Flowing Build-Up (FBU) test was carried out on the Zuiderpolder-12A well. A downhole gauge was placed in the well for 61 days, covering a main build-up of 54 days. This well test was analysed with the use of dedicated well-testing software that relies on model based inversion. A variety of models is tested and when a model can reproduce the measured pressure it is considered, if it is geologically sound, to be representative of the subsurface.

Several hypotheses were tested with dedicated well test models, including high permeability streaks, a connected Carboniferous basement and conductive fractures. An acceptable match was obtained with a numerical model that has a single high permeability streak connected to the ZPD-12A well, as depicted in Figure 40. The late time mismatch is the result of the limited size of the numerical model, an extended model including additional faults could capture the pressure at the end of the test better. In this model, several faults surrounding the ZPD cluster needed to be partially sealed, see Figure 41. The connected Carboniferous basement and the conductive fracture models did not achieve acceptable matches.

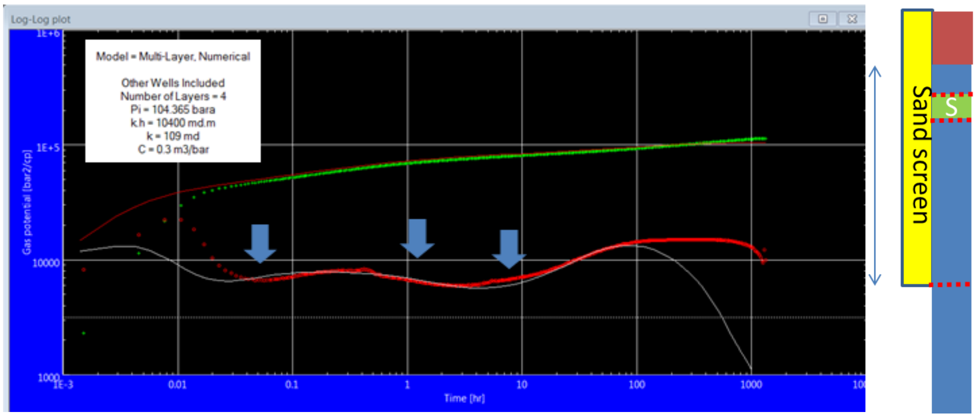

Figure 40: Numerical simulation with 1 high permeability streak in connection with the Sand Screen and a kv/kh of 0.1 and reservoir permeability of 100 mD. The fault model is depicted in Figure 41.

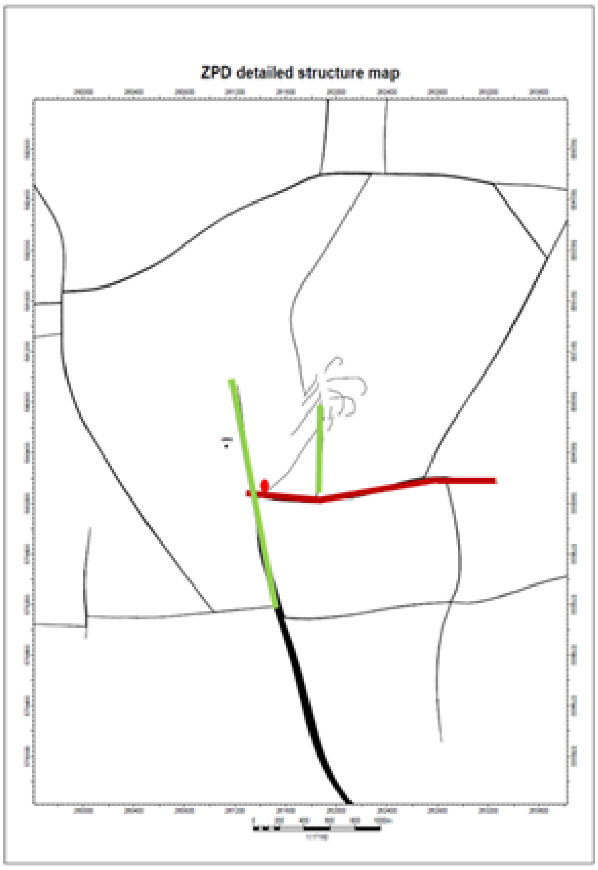

Figure 41: Fault representation around ZPD-12A in a high permeability streak model. The green line indicates a fully open fault (leak factor of 1.0), the red lines indicate a leak factor of 0.01 and the red dot marks the ZPD-12A well.

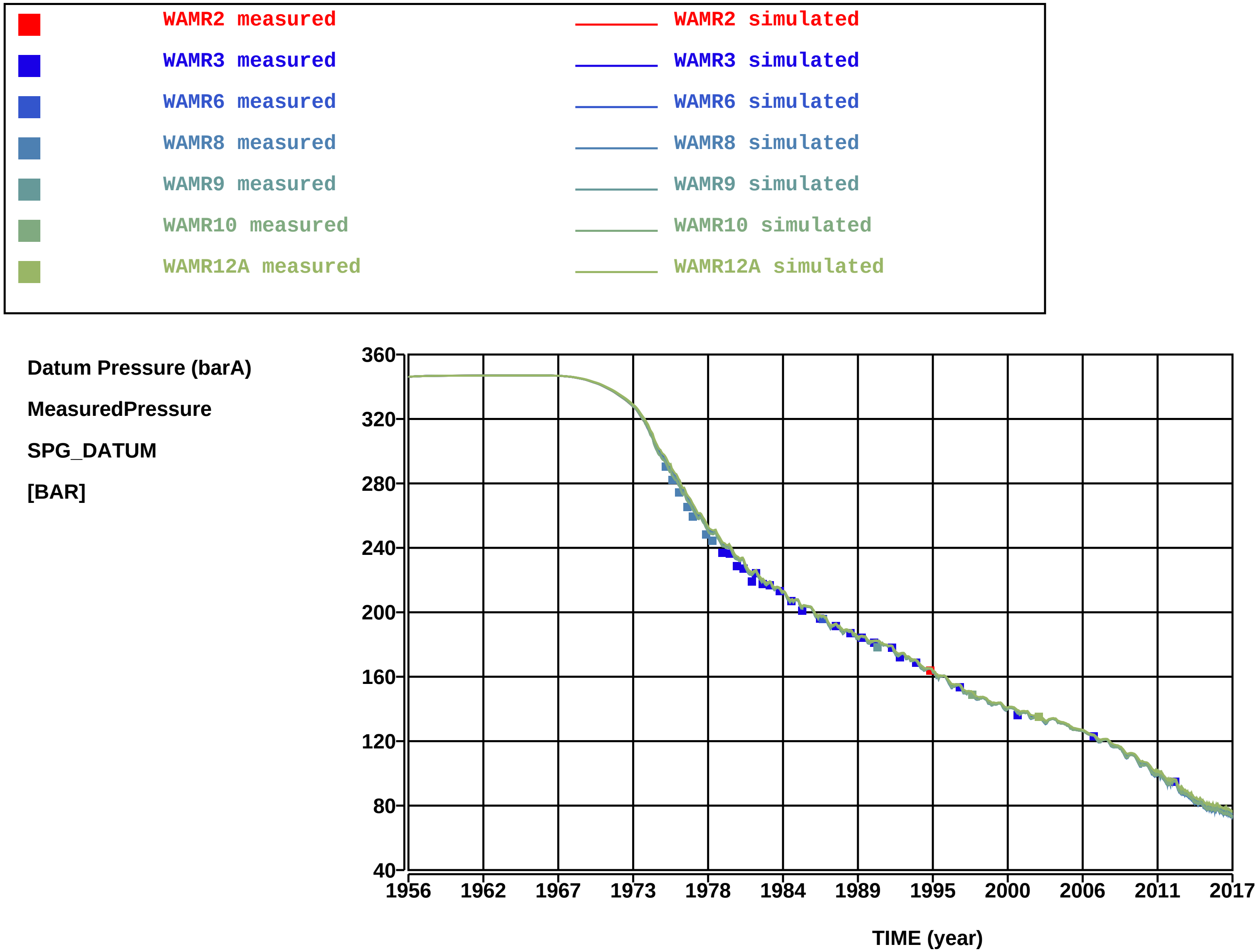

Table Name: WAMR2_PRES

Plot Name: SPTG_WAMR

Time=2.016997e+03 [YEAR]

Creation date: Thu 09/02/2017 16:08

Runfile: GRO_2016_ED_v60.run

Table Name: WBIR1_PRES

Plot Name: SPTG_WBIR

Time=2.016997e+03 [YEAR]

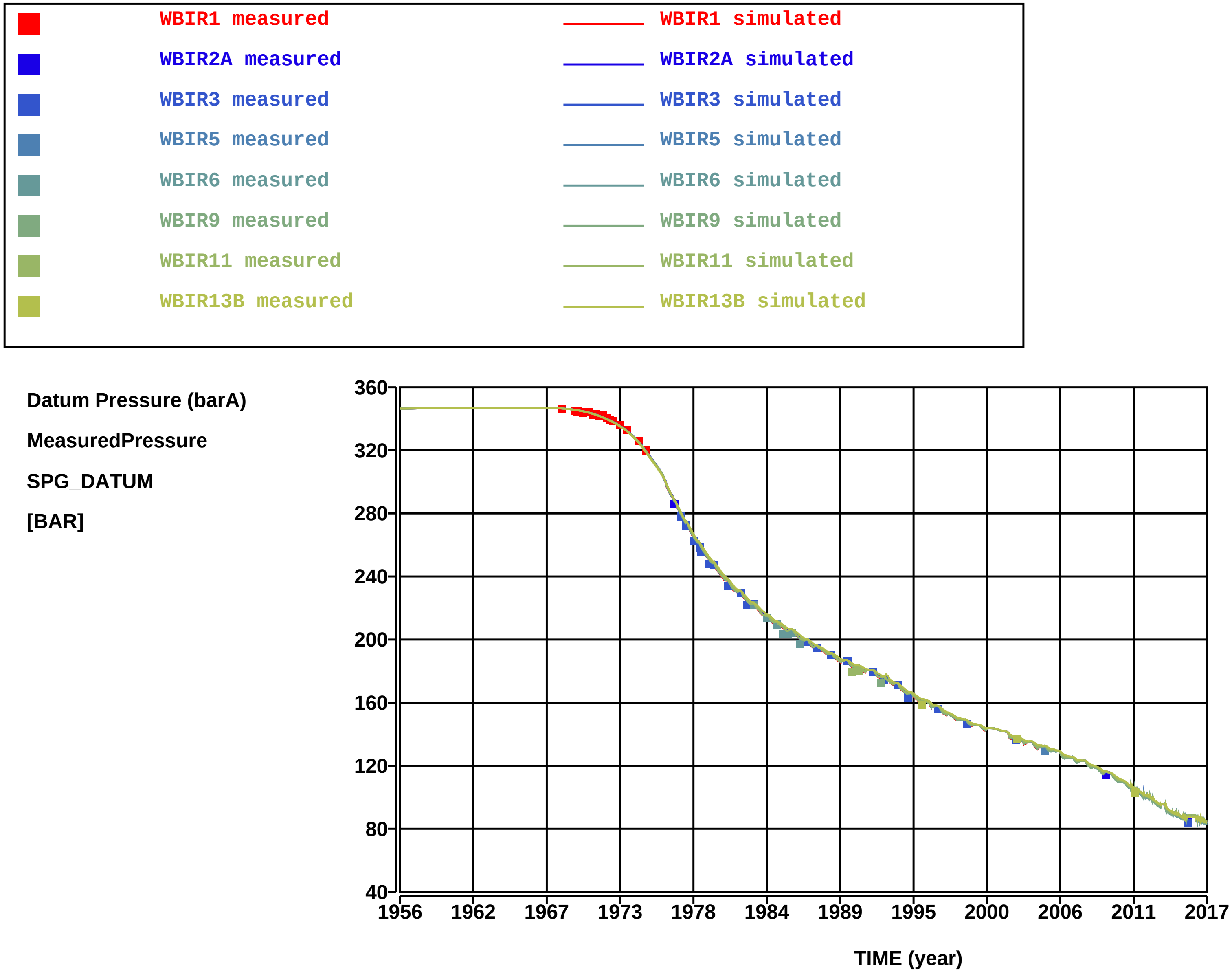

Creation date: Thu 09/02/2017 16:08

Runfile: GRO_2016_ED_v60.run

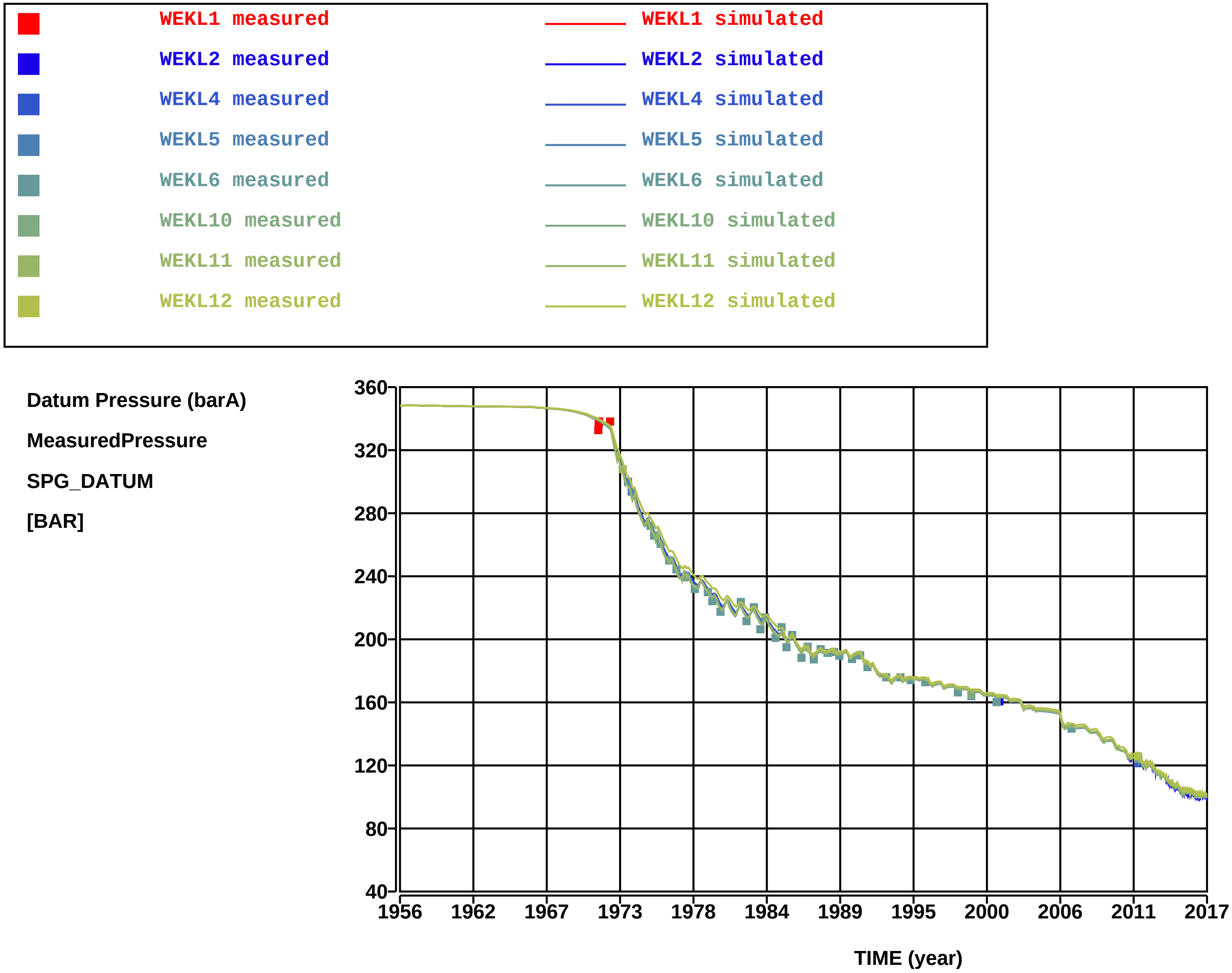

Table Name: WEKL1_PRES

Plot Name: SPTG_WEKL

Time=2.016997e+03 [YEAR]

Creation date: Thu 09/02/2017 16:08

Runfile: GRO_2016_ED_v60.run

Table Name: WEKR1_PRES

Plot Name: SPTG_WEKR

Time=2.016997e+03 [YEAR]

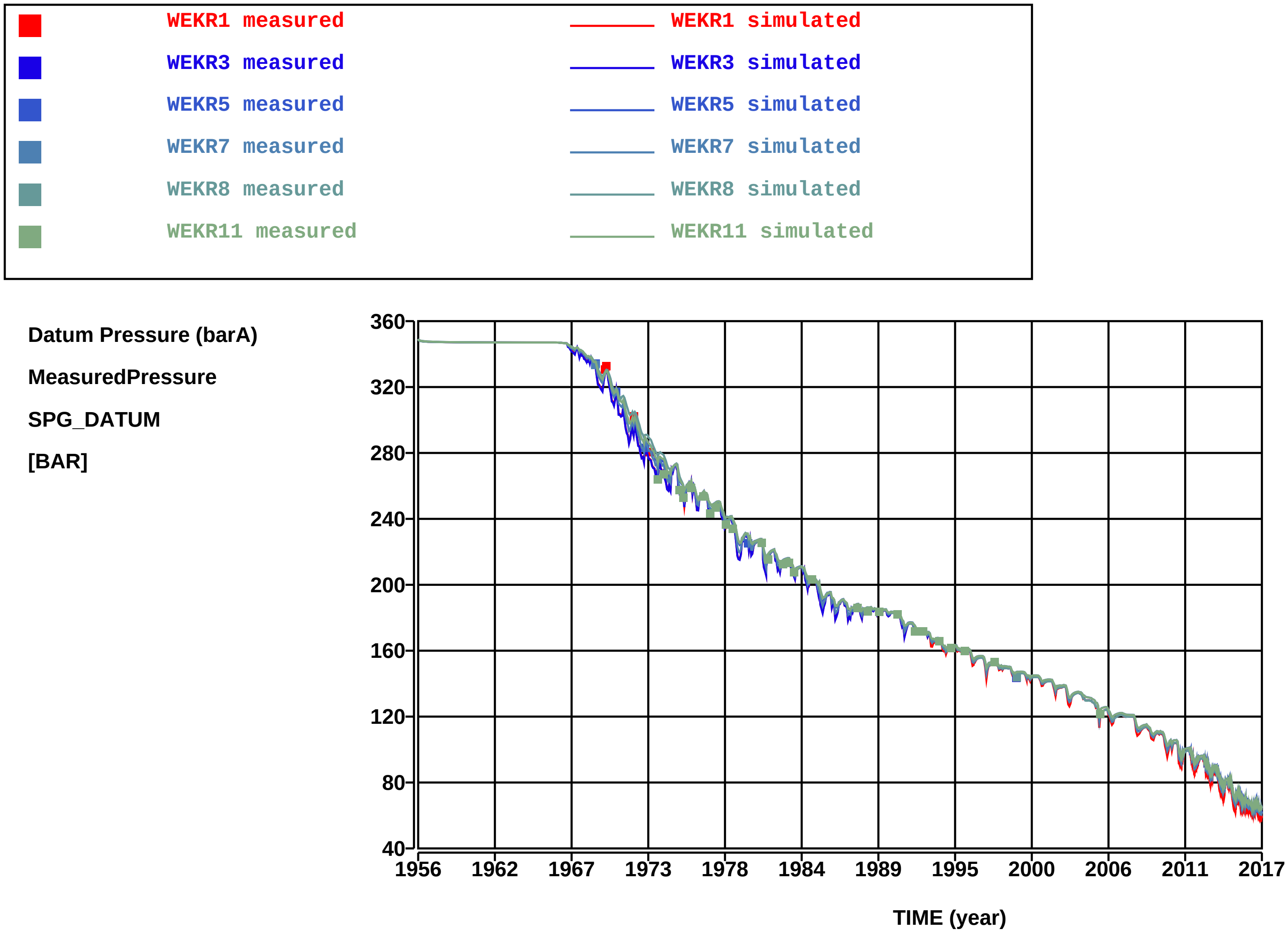

Creation date: Thu 09/02/2017 16:08

Runfile: GRO_2016_ED_v60.run

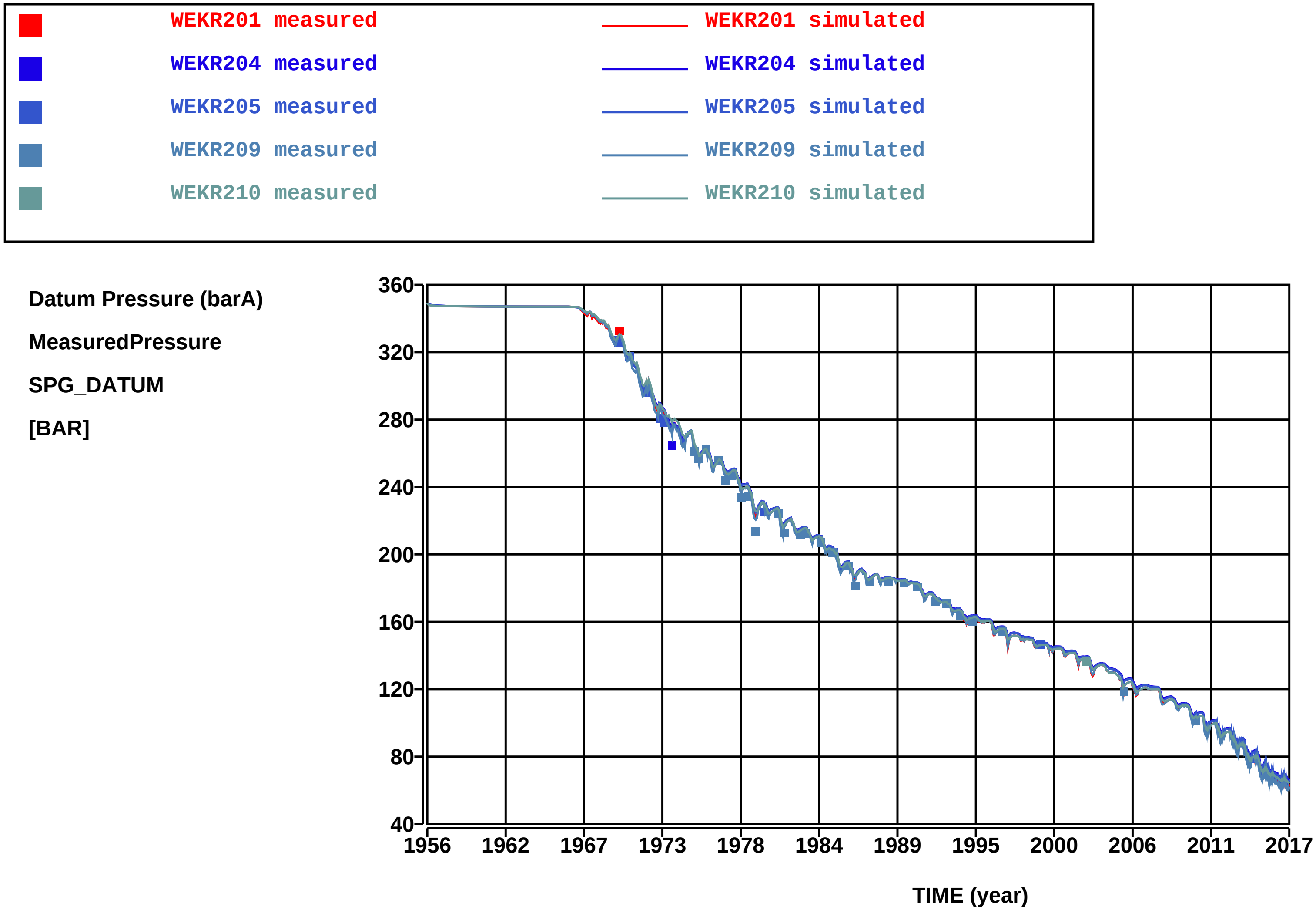

Table Name: WEKR201_PRES

Plot Name: SPTG_WEKR

Time=2.016997e+03 [YEAR]

Creation date: Thu 09/02/2017 16:08

Runfile: GRO_2016_ED_v60.run

■	WFRB1 measured	―	WFRB1 simulated
■	WFRB2 measured	―	WFRB2 simulated
■	WFRB3 measured	―	WFRB3 simulated
■	WFRB5 measured	―	WFRB5 simulated
■	WFRB7 measured	―	WFRB7 simulated

Table Name: WFRB1_PRES

Plot Name: SPTG_WFRB

Time=2.016997e+03 [YEAR]

Datum Pressure (barA)

MeasuredPressure

SPG_DATUM

[BAR]

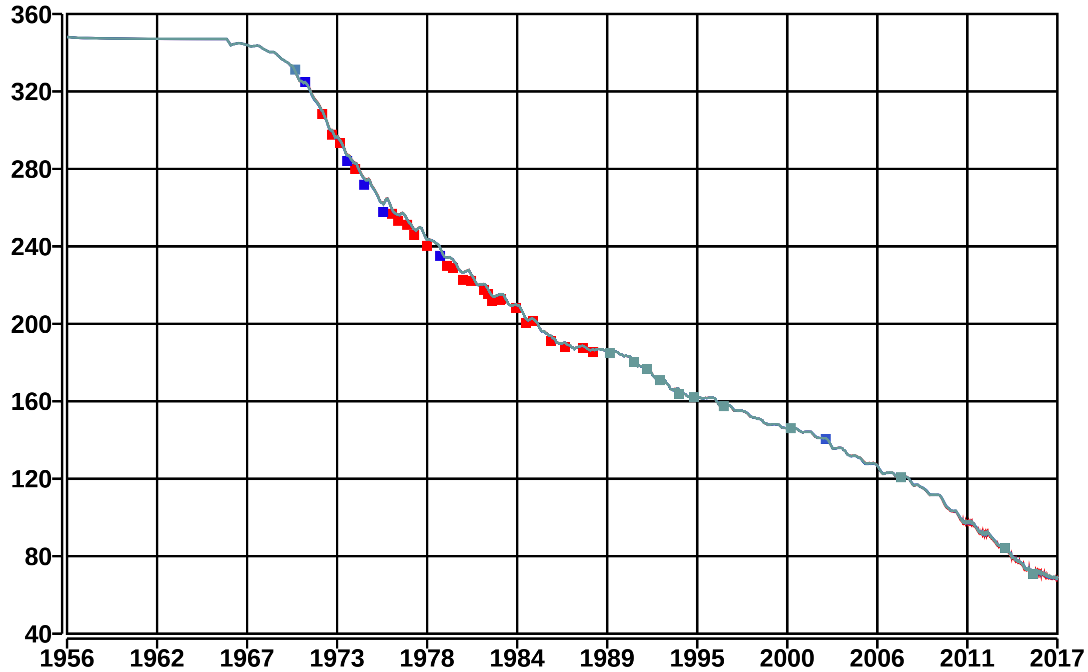

Creation date: Thu 09/02/2017 16:08

Runfile: GRO_2016_ED_v60.run

WKPD1 measured — WKPD1 simulated
WKPD4 measured — WKPD4 simulated
WKPD8 measured — WKPD8 simulated
WKPD11 measured — WKPD11 simulated
WKPD12 measured — WKPD12 simulated

Table Name: WKPD1_PRES

Plot Name: SPTG_WKPD

Time=2.016997e+03 [YEAR]

Datum Pressure (barA)

MeasuredPressure

SPG_DATUM

[BAR]

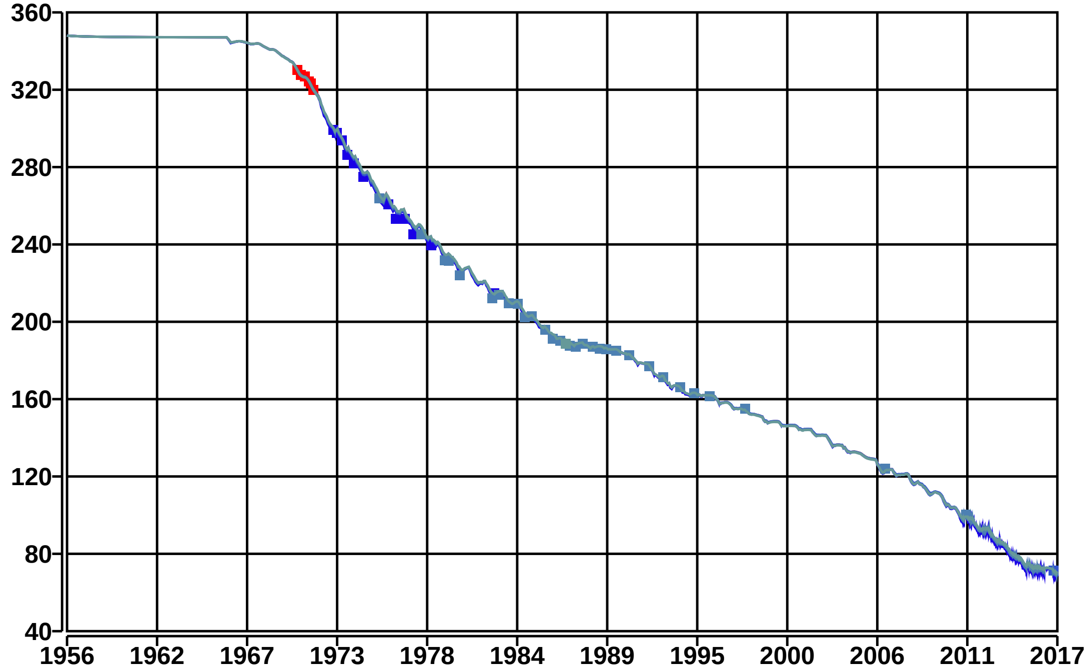

Creation date: Thu 09/02/2017 16:08
Runfile: GRO_2016_ED_v60.run

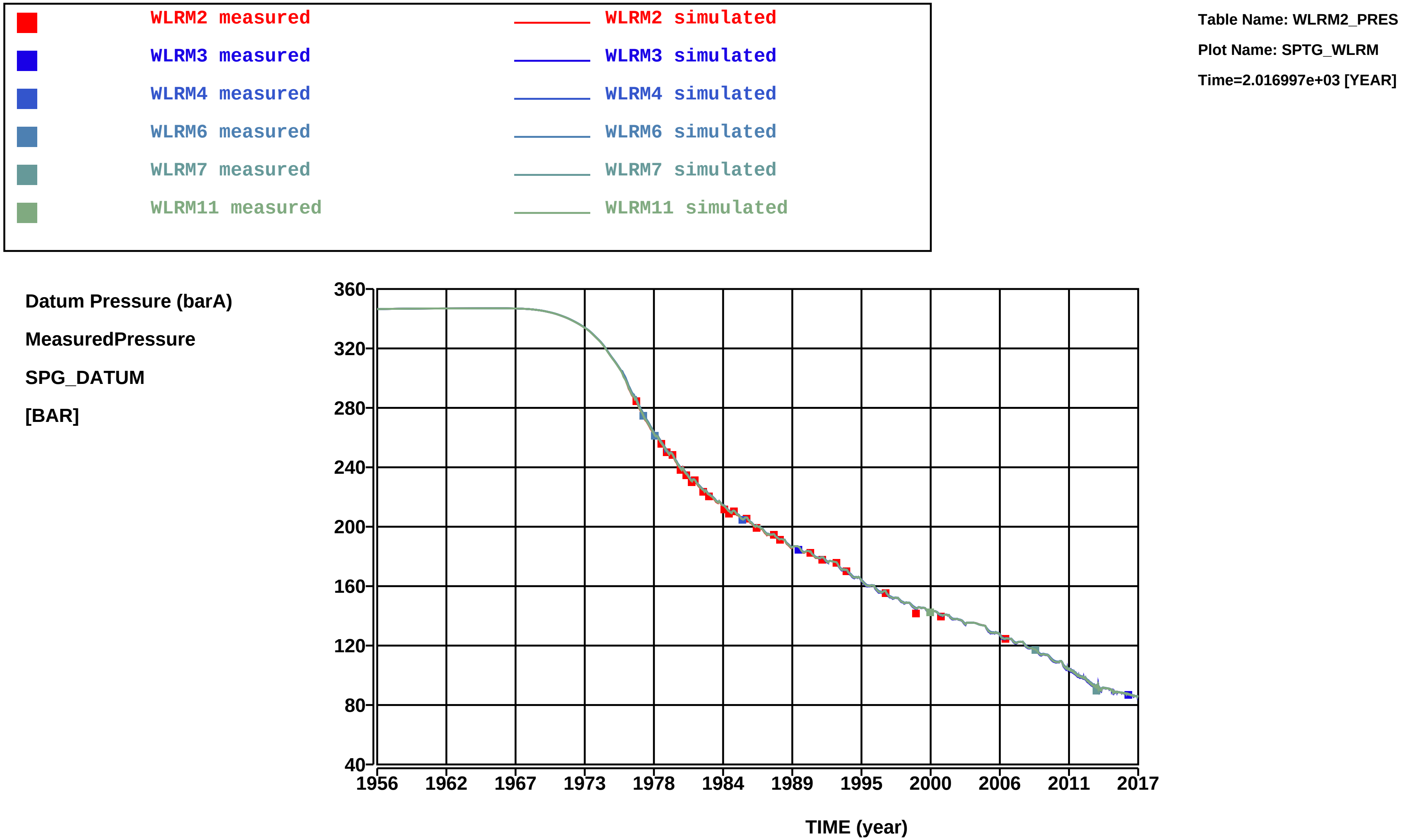

Creation date: Thu 09/02/2017 16:08
Runfile: GRO_2016_ED_v60.run

■	WMWD1 measured	———	WMWD1 simulated
■	WMWD3 measured	———	WMWD3 simulated
■	WMWD5 measured	———	WMWD5 simulated
■	WMWD6 measured	———	WMWD6 simulated

Table Name: WMWD1_PRES

Plot Name: SPTG_WMWD

Time=2.016997e+03 [YEAR]

Datum Pressure (barA)

MeasuredPressure

SPG_DATUM

[BAR]

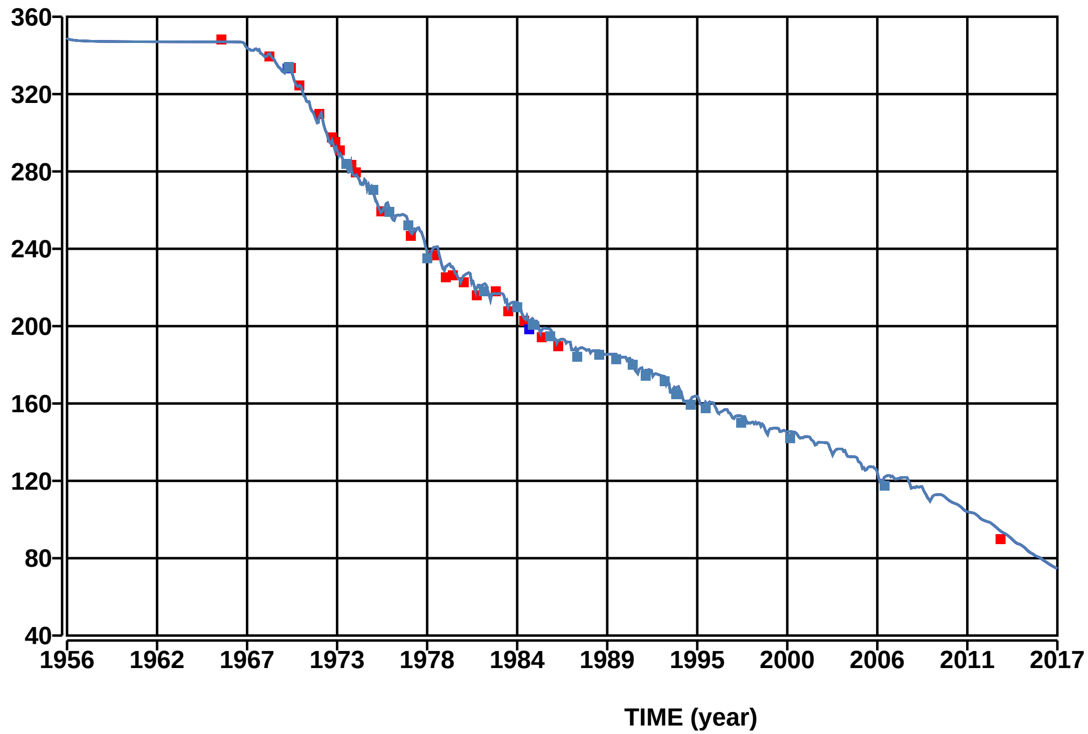

Creation date: Thu 09/02/2017 16:08
Runfile: GRO_2016_ED_v60.run

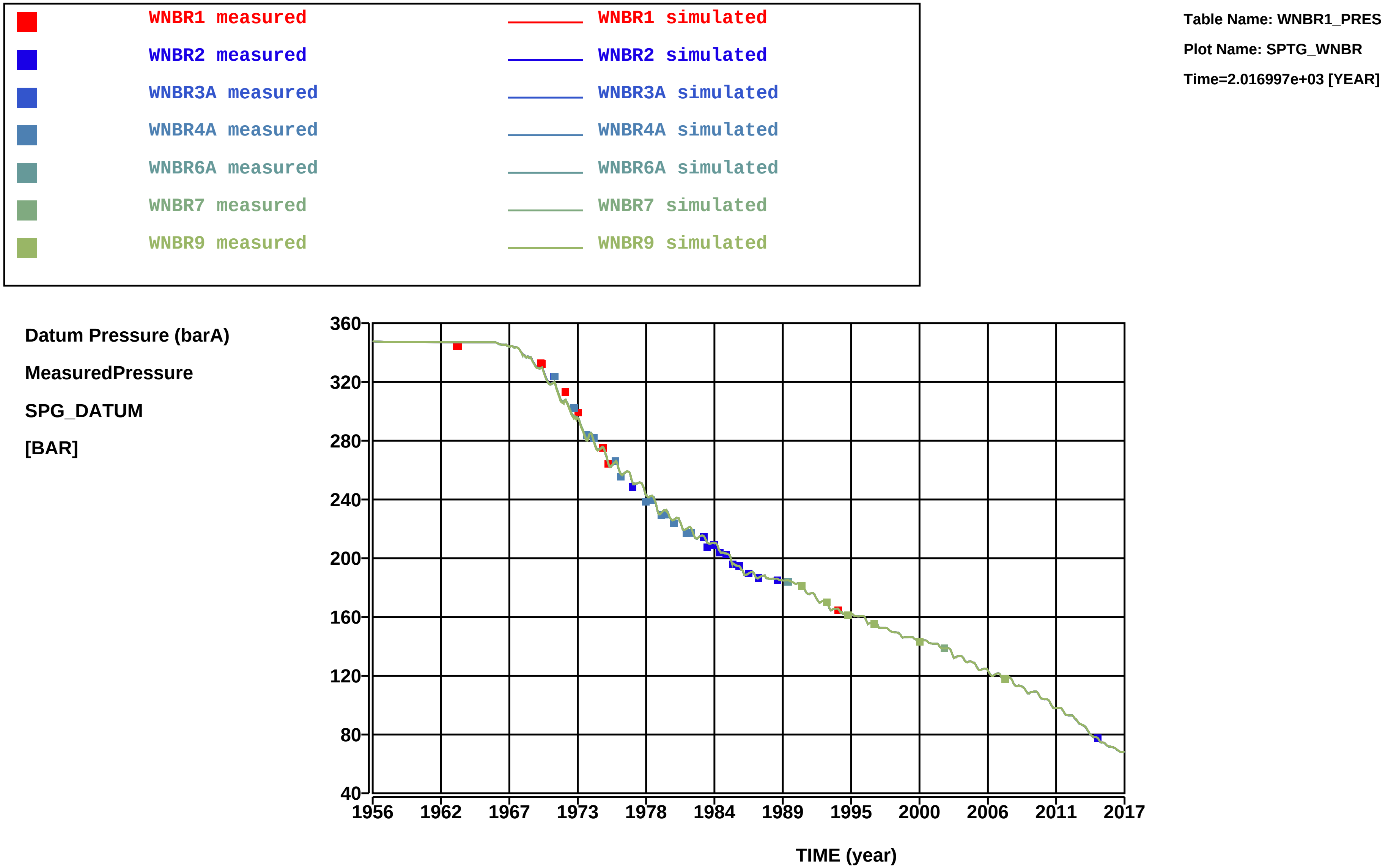

Creation date: Thu 09/02/2017 16:08
Runfile: GRO_2016_ED_v60.run

Table Name: WNWS1_PRES

Plot Name: SPTG_WNWS

Time=2.016997e+03 [YEAR]

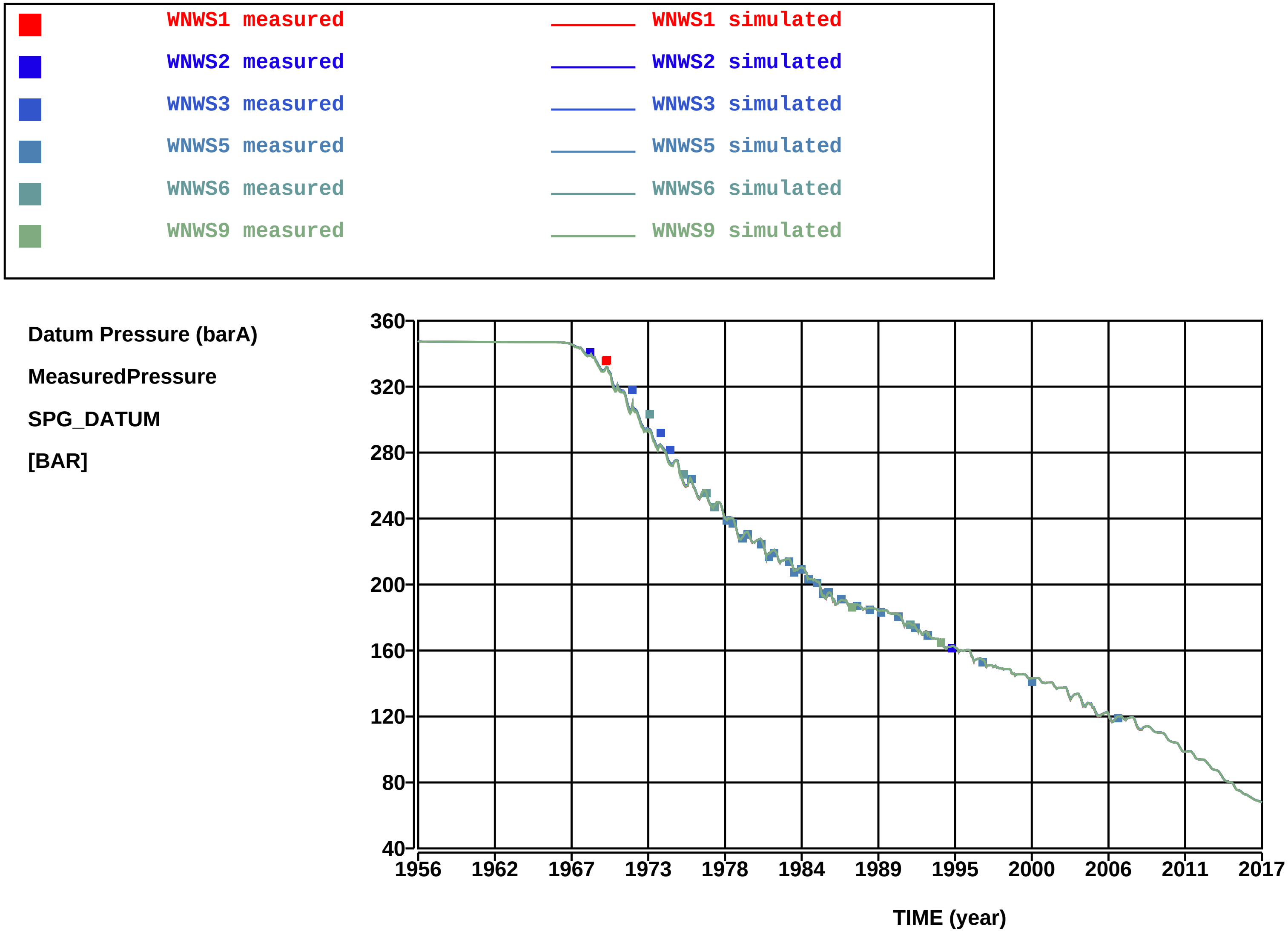

Creation date: Thu 09/02/2017 16:08

Runfile: GRO_2016_ED_v60.run

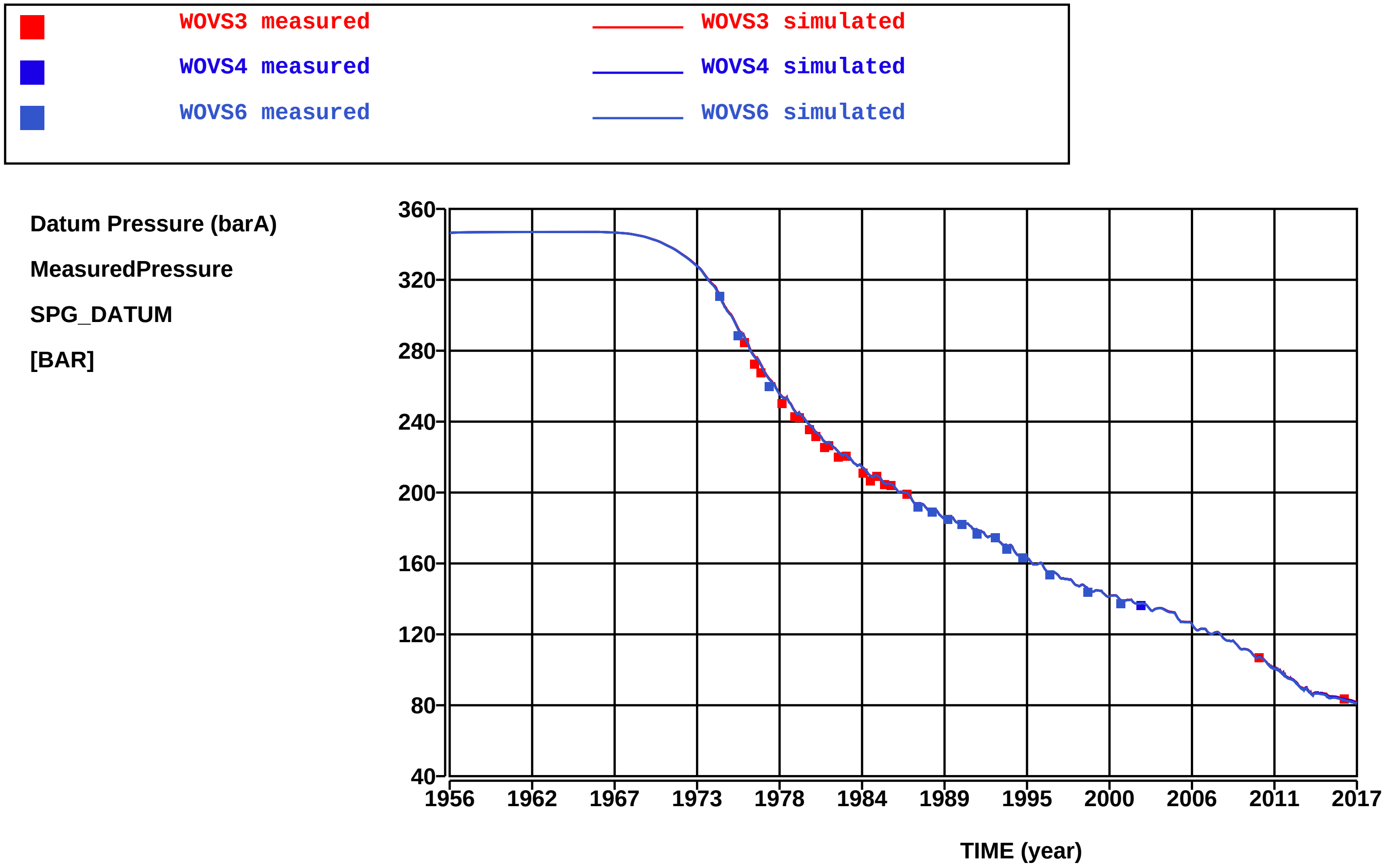

Table Name: WOVS3_PRES

Plot Name: SPTG_WOVS

Time=2.016997e+03 [YEAR]

Datum Pressure (barA)

MeasuredPressure

SPG_DATUM

[BAR]

Creation date: Thu 09/02/2017 16:08

Runfile: GRO_2016_ED_v60.run

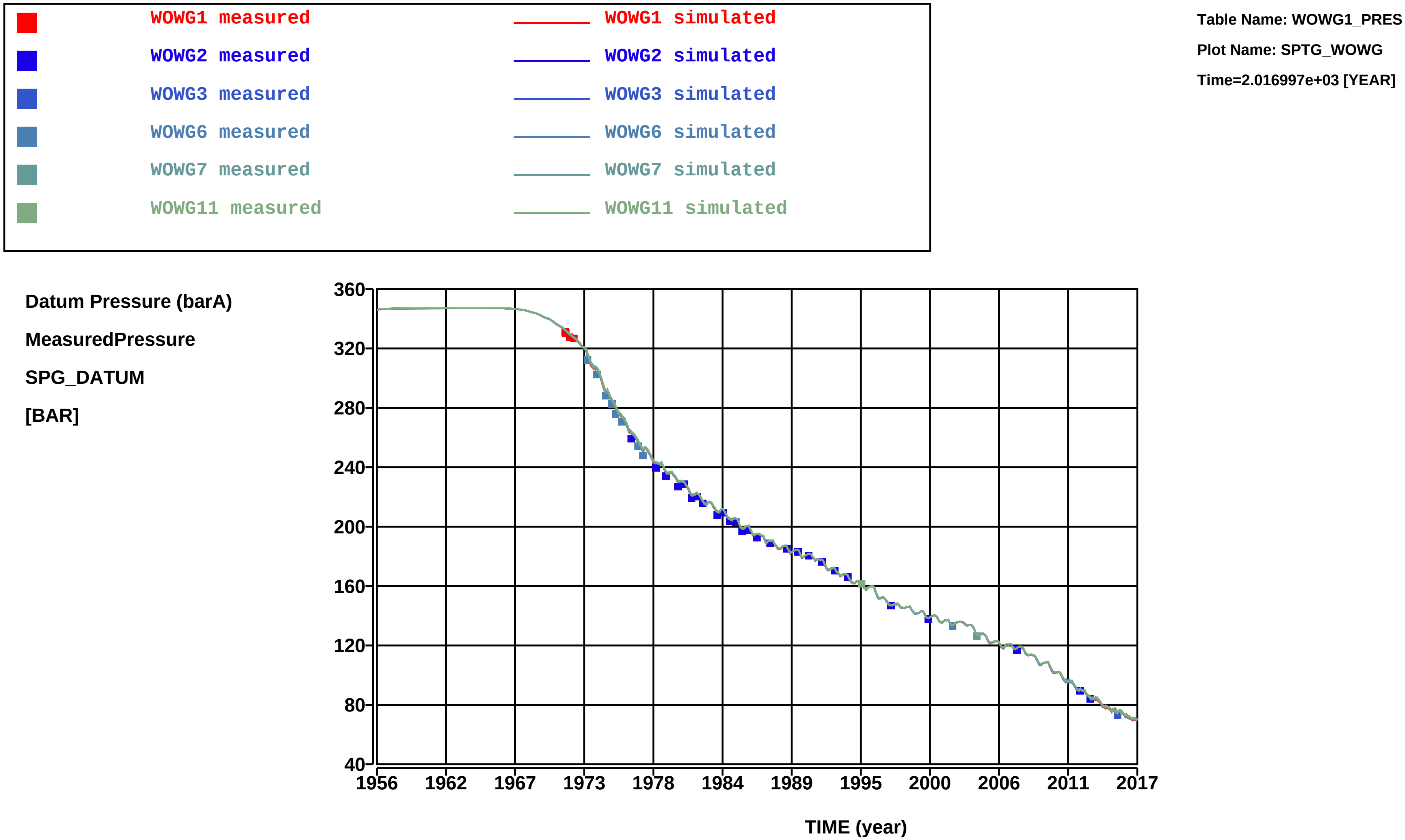

Creation date: Thu 09/02/2017 16:08
Runfile: GRO_2016_ED_v60.run

	WPAU2 measured		WPAU2 simulated
	WPAU3 measured		WPAU3 simulated
	WPAU6 measured		WPAU6 simulated

Table Name: WPAU2_PRES

Plot Name: SPTG_WPAU

Time=2.016997e+03 [YEAR]

Datum Pressure (barA)

MeasuredPressure

SPG_DATUM

[BAR]

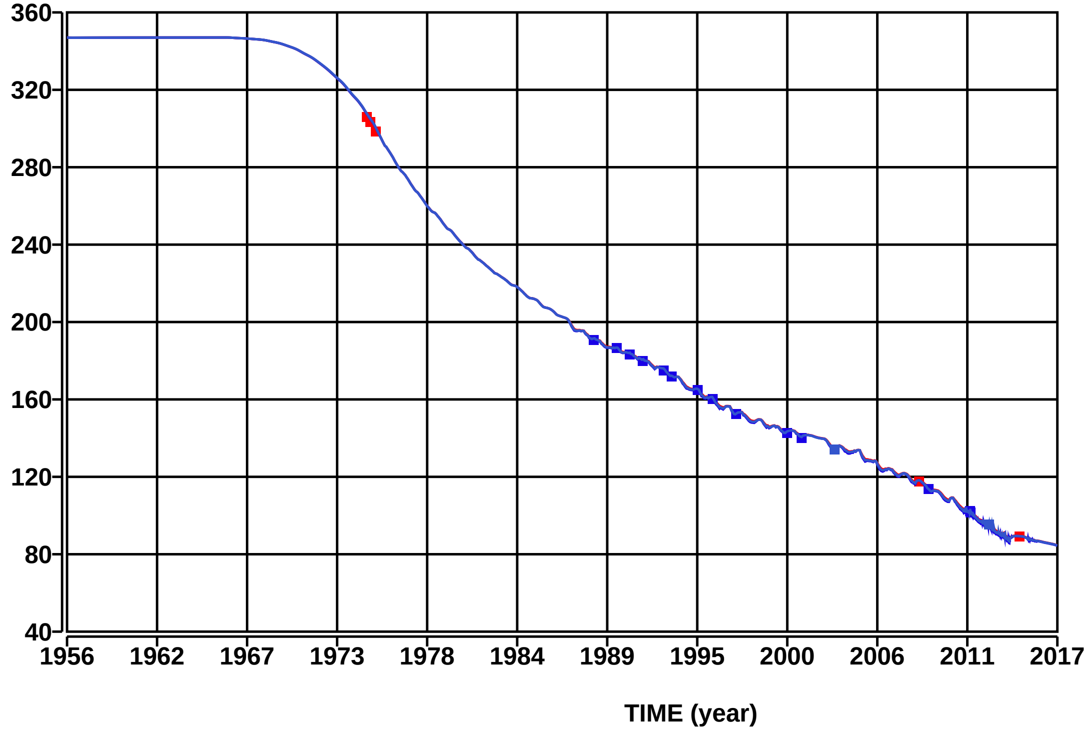

Creation date: Thu 09/02/2017 16:08
Runfile: GRO_2016_ED_v60.run

	WPOS1 measured		WPOS1 simulated
	WPOS2 measured		WPOS2 simulated
	WPOS3 measured		WPOS3 simulated
	WPOS4 measured		WPOS4 simulated
	WPOS9 measured		WPOS9 simulated

Table Name: WPOS1_PRES

Plot Name: SPTG_WPOS

Time=2.016997e+03 [YEAR]

Datum Pressure (barA)

MeasuredPressure

SPG_DATUM

[BAR]

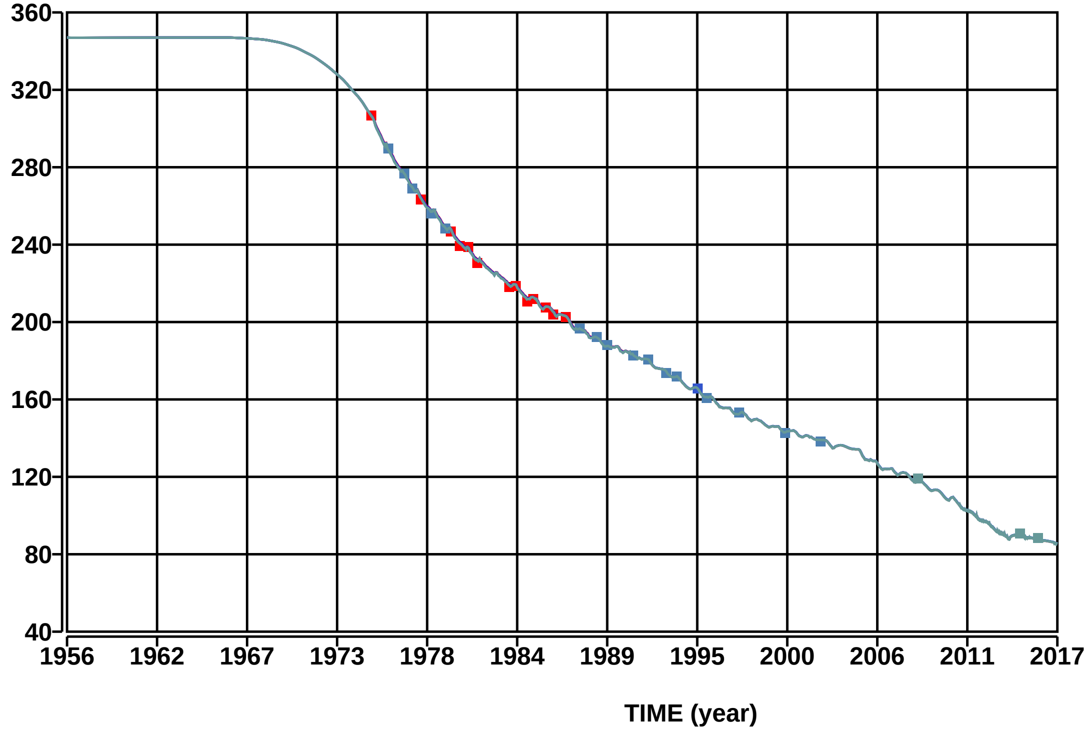

Creation date: Thu 09/02/2017 16:08

Runfile: GRO_2016_ED_v60.run

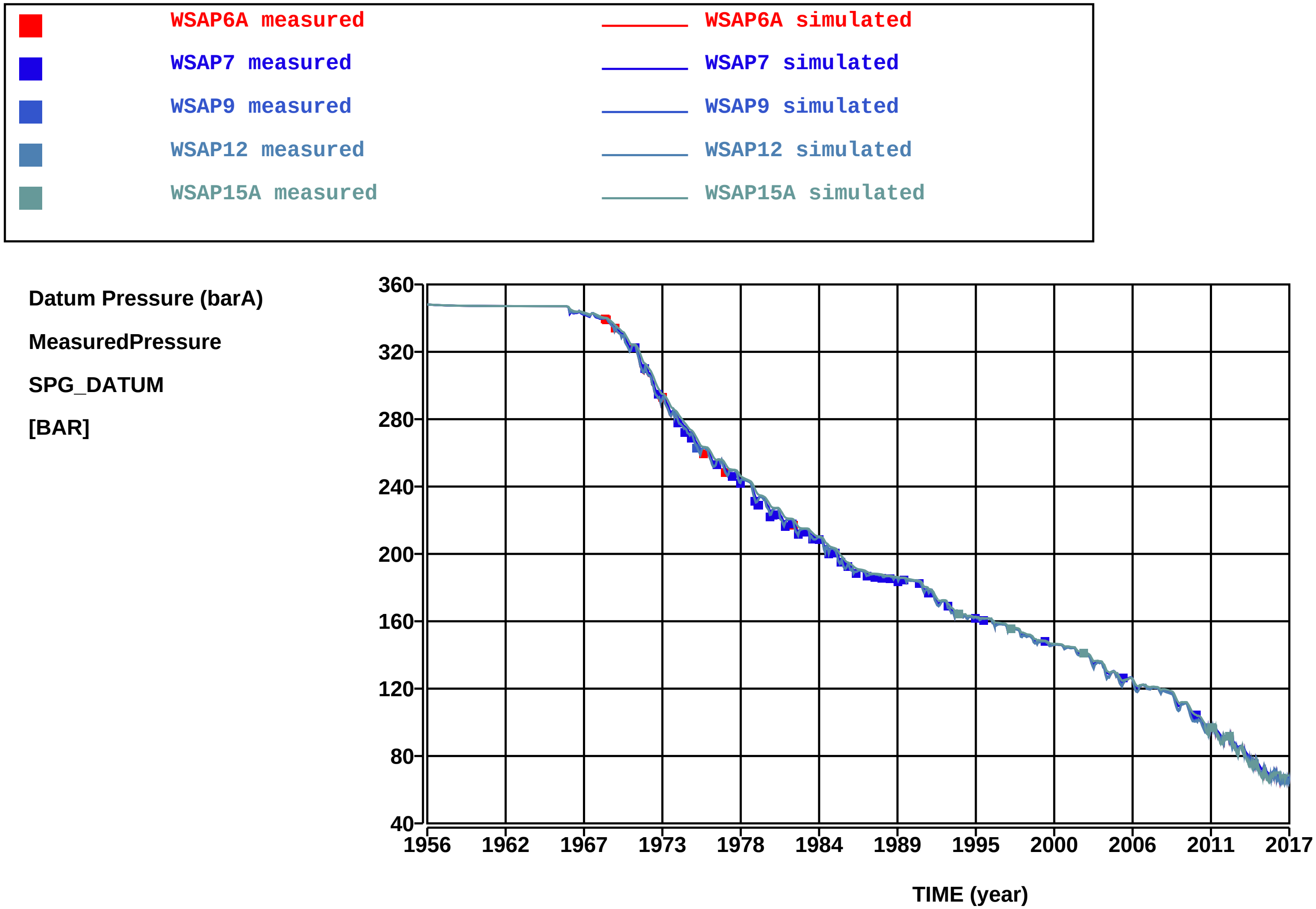

Table Name: WSAP6A_PRES

Plot Name: SPTG_WSAP

Time=2.016997e+03 [YEAR]

Creation date: Thu 09/02/2017 16:08

Runfile: GRO_2016_ED_v60.run

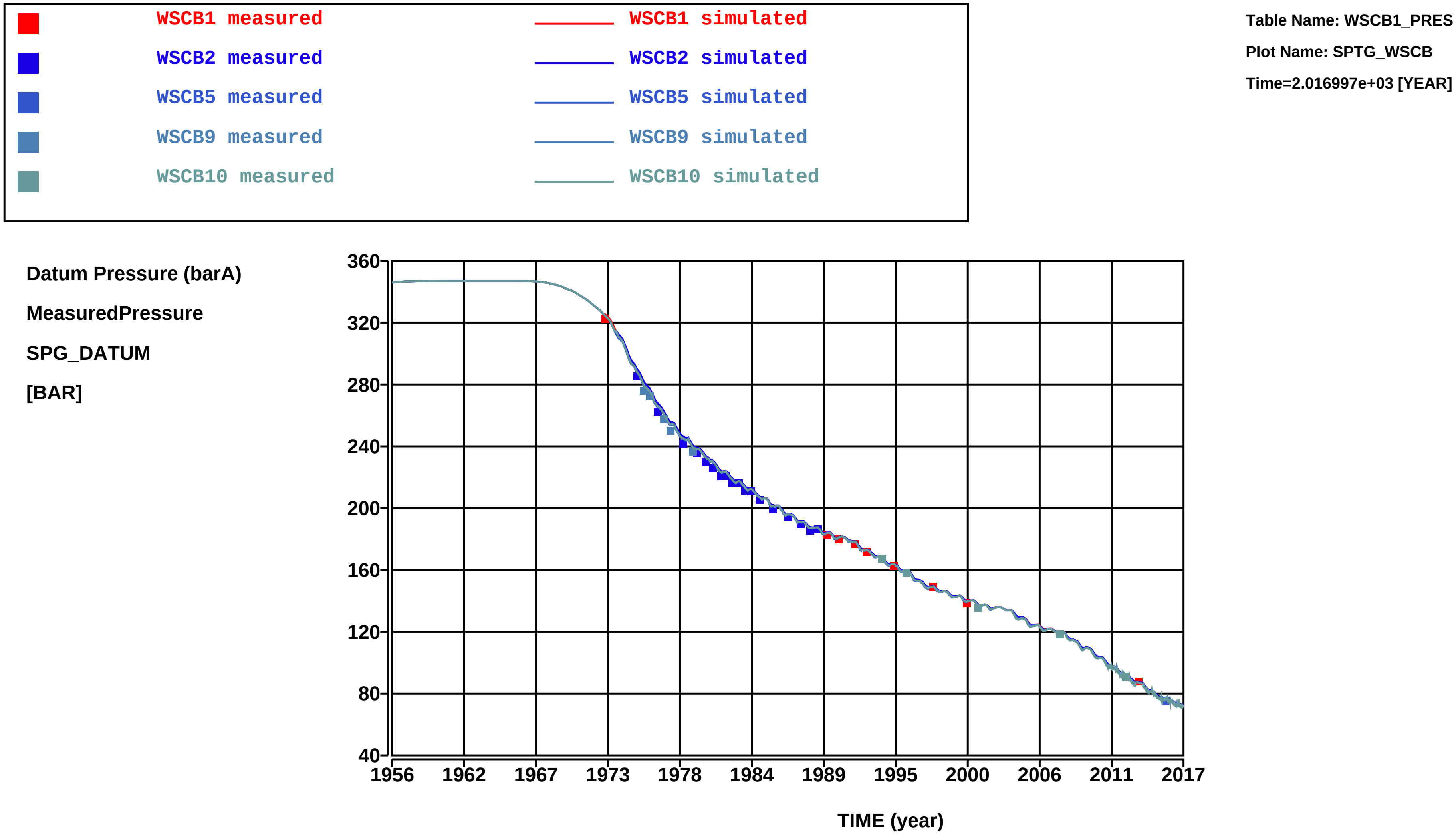

Creation date: Thu 09/02/2017 16:08
Runfile: GRO_2016_ED_v60.run

WSDB2 measured
WSDB3 measured
WSDB4 measured
WSDB7 measured
WSDB10 measured
WSDB11 measured

WSDB2 simulated
WSDB3 simulated
WSDB4 simulated
WSDB7 simulated
WSDB10 simulated
WSDB11 simulated

Table Name: WSDB2_PRES

Plot Name: SPTG_WSDB

Time=2.016997e+03 [YEAR]

Datum Pressure (barA)

MeasuredPressure

SPG_DATUM

[BAR]

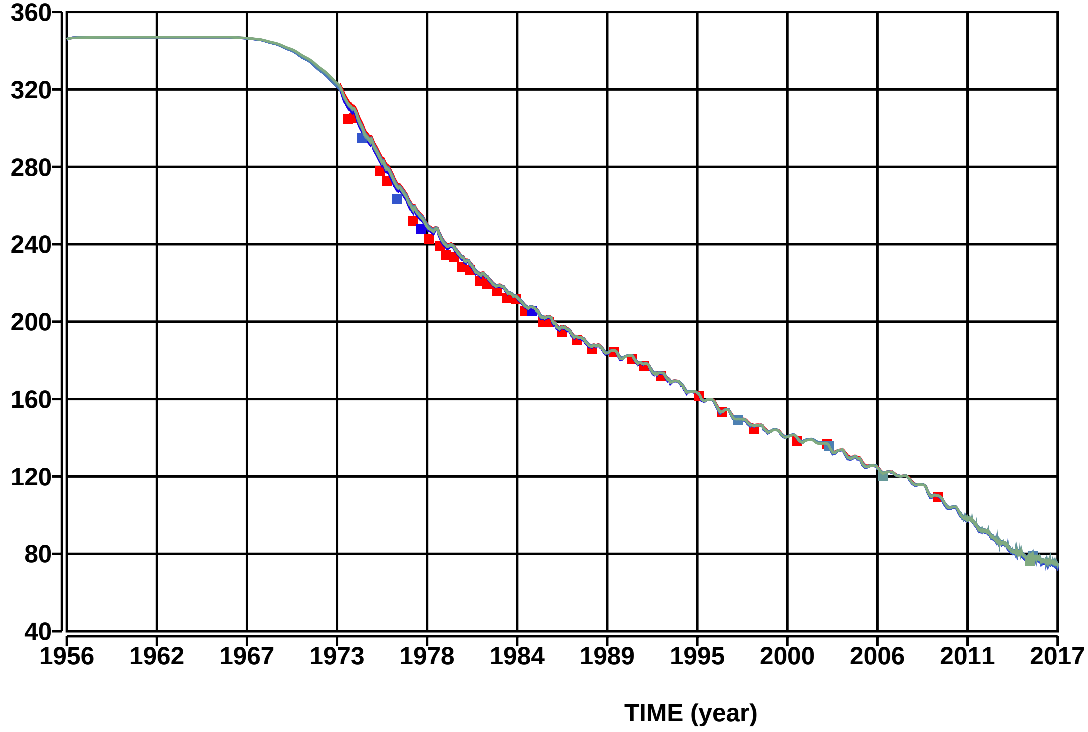

Creation date: Thu 09/02/2017 16:08
Runfile: GRO_2016_ED_v60.run

Table Name: WSLO2_PRES

Plot Name: SPTG_WSLO

Time=2.016997e+03 [YEAR]

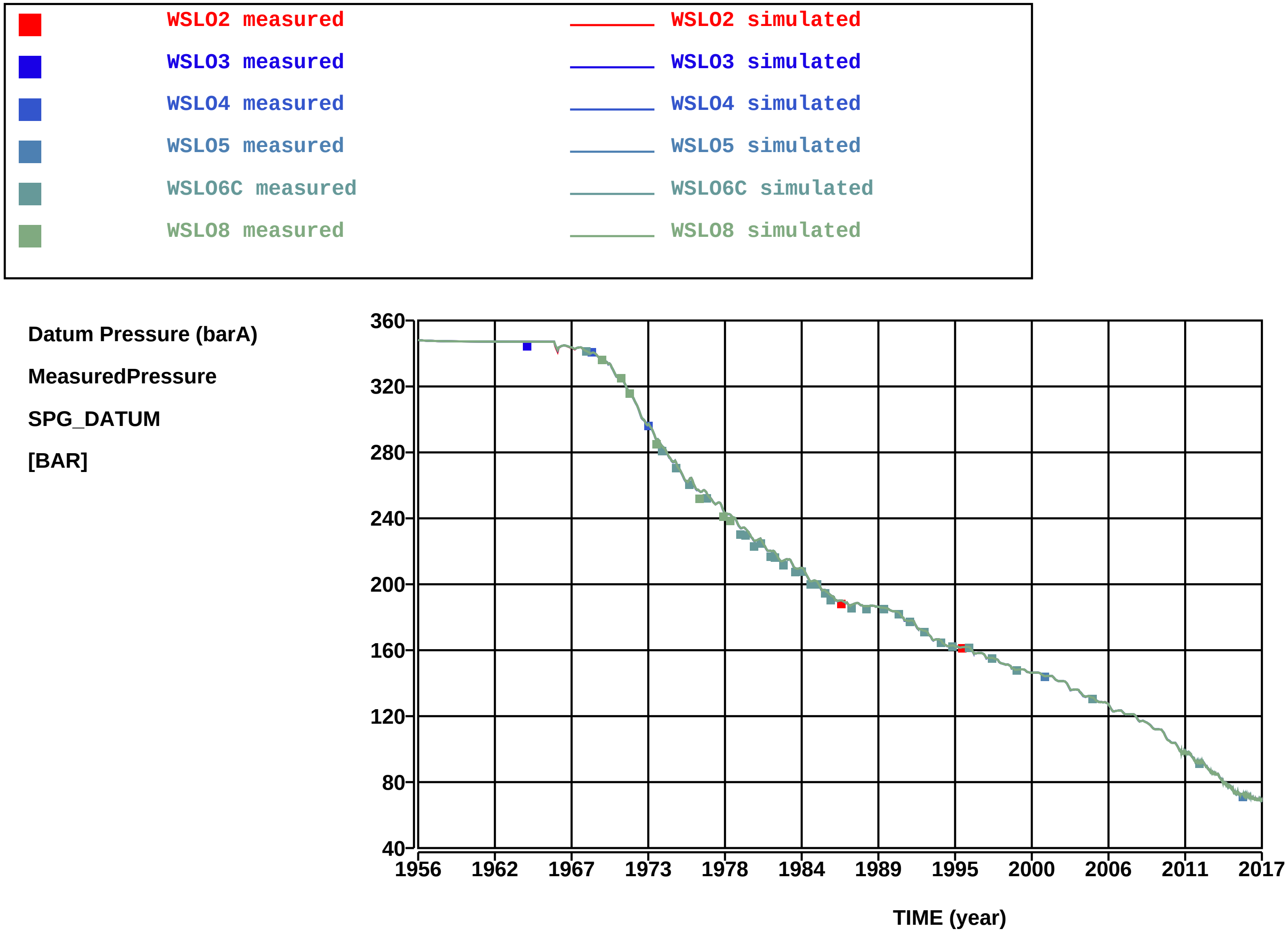

Creation date: Thu 09/02/2017 16:08

Runfile: GRO_2016_ED_v60.run

	WSPI1 measured		WSPI1 simulated
	WSPI2 measured		WSPI2 simulated
	WSPI3 measured		WSPI3 simulated
	WSPI4 measured		WSPI4 simulated
	WSPI6 measured		WSPI6 simulated

Table Name: WSPI1_PRES

Plot Name: SPTG_WSPI

Time=2.016997e+03 [YEAR]

Datum Pressure (barA)

MeasuredPressure

SPG_DATUM

[BAR]

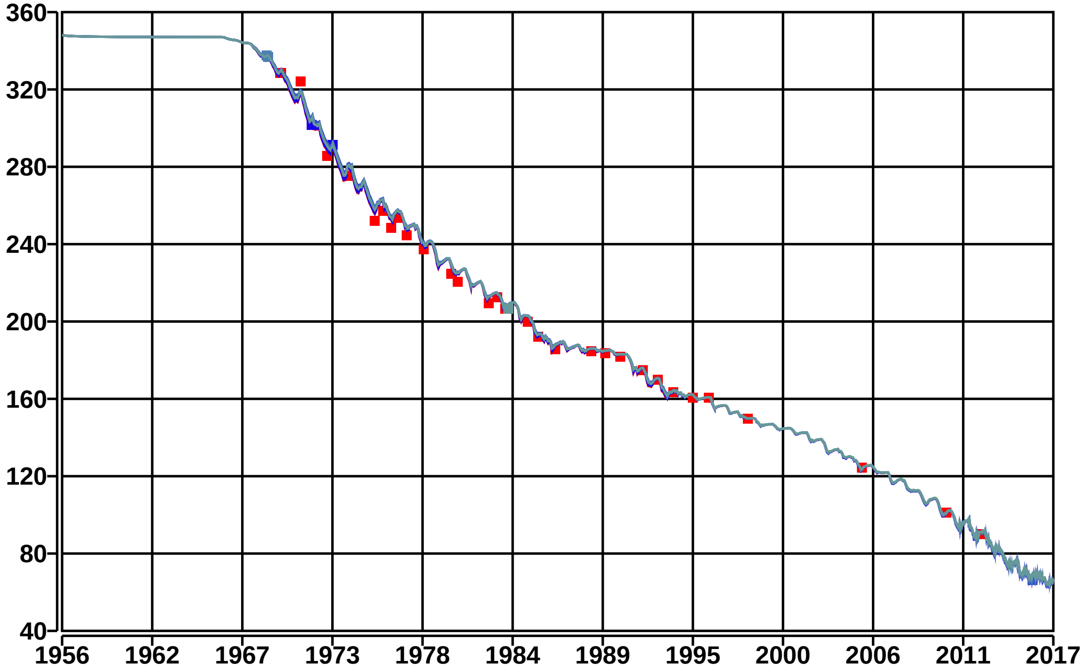

Creation date: Thu 09/02/2017 16:08
Runfile: GRO_2016_ED_v60.run

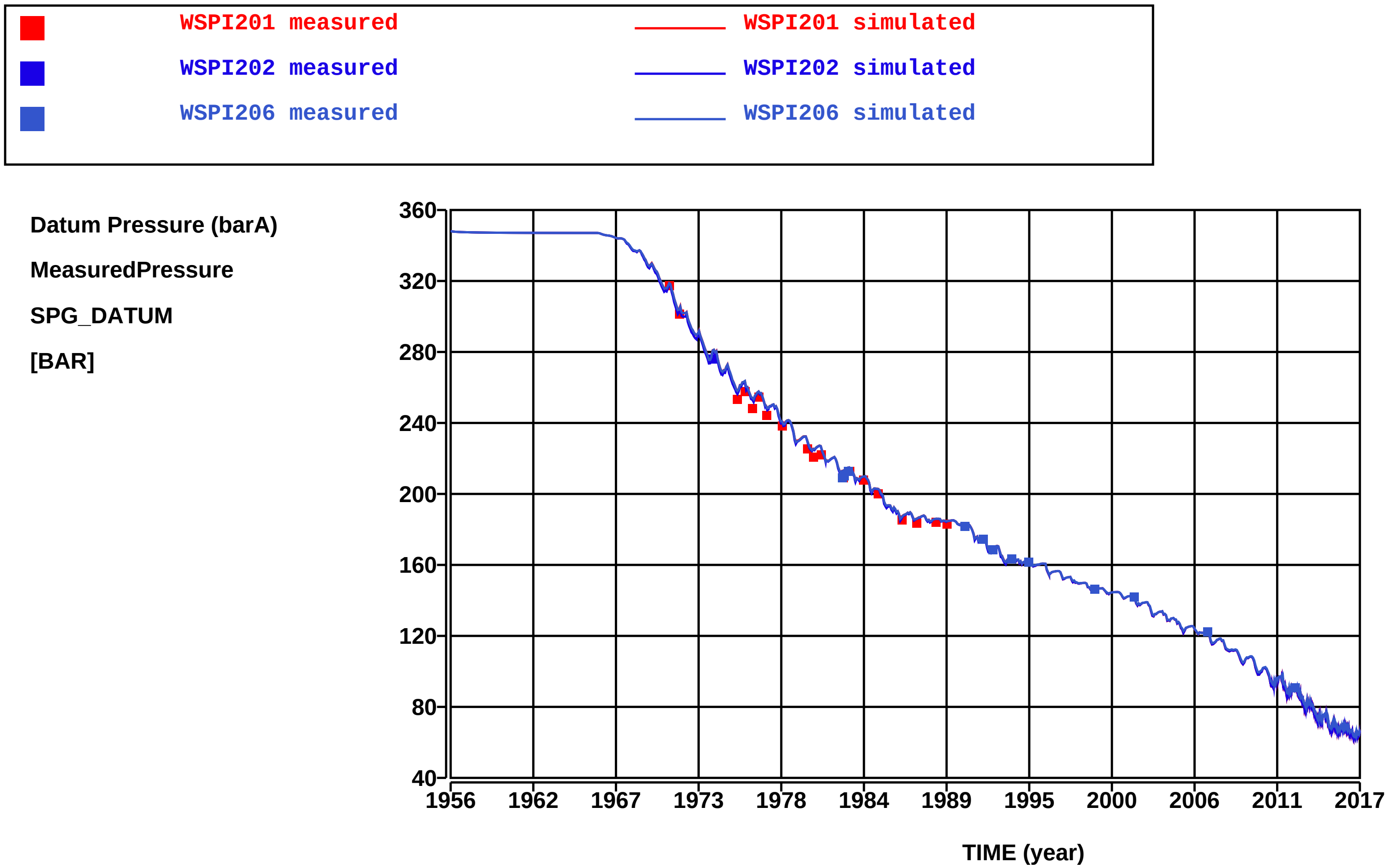

Table Name: WSPI201_PRES

Plot Name: SPTG_WSPI

Time=2.016997e+03 [YEAR]

Datum Pressure (barA)

MeasuredPressure

SPG_DATUM

[BAR]

Creation date: Thu 09/02/2017 16:08

Runfile: GRO_2016_ED_v60.run

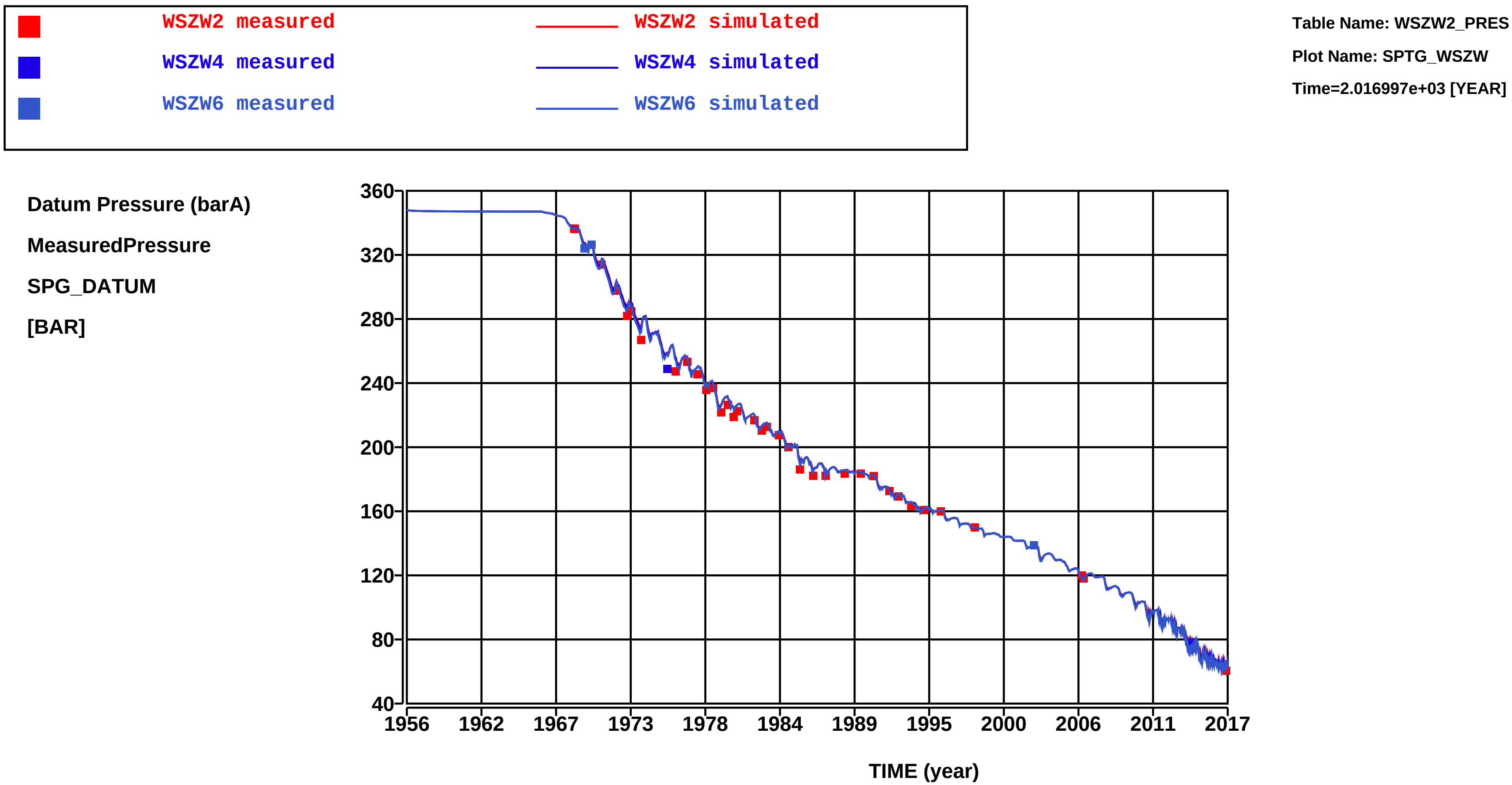

Creation date: Thu 09/02/2017 16:08
Runfile: GRO_2016_ED_v60.run

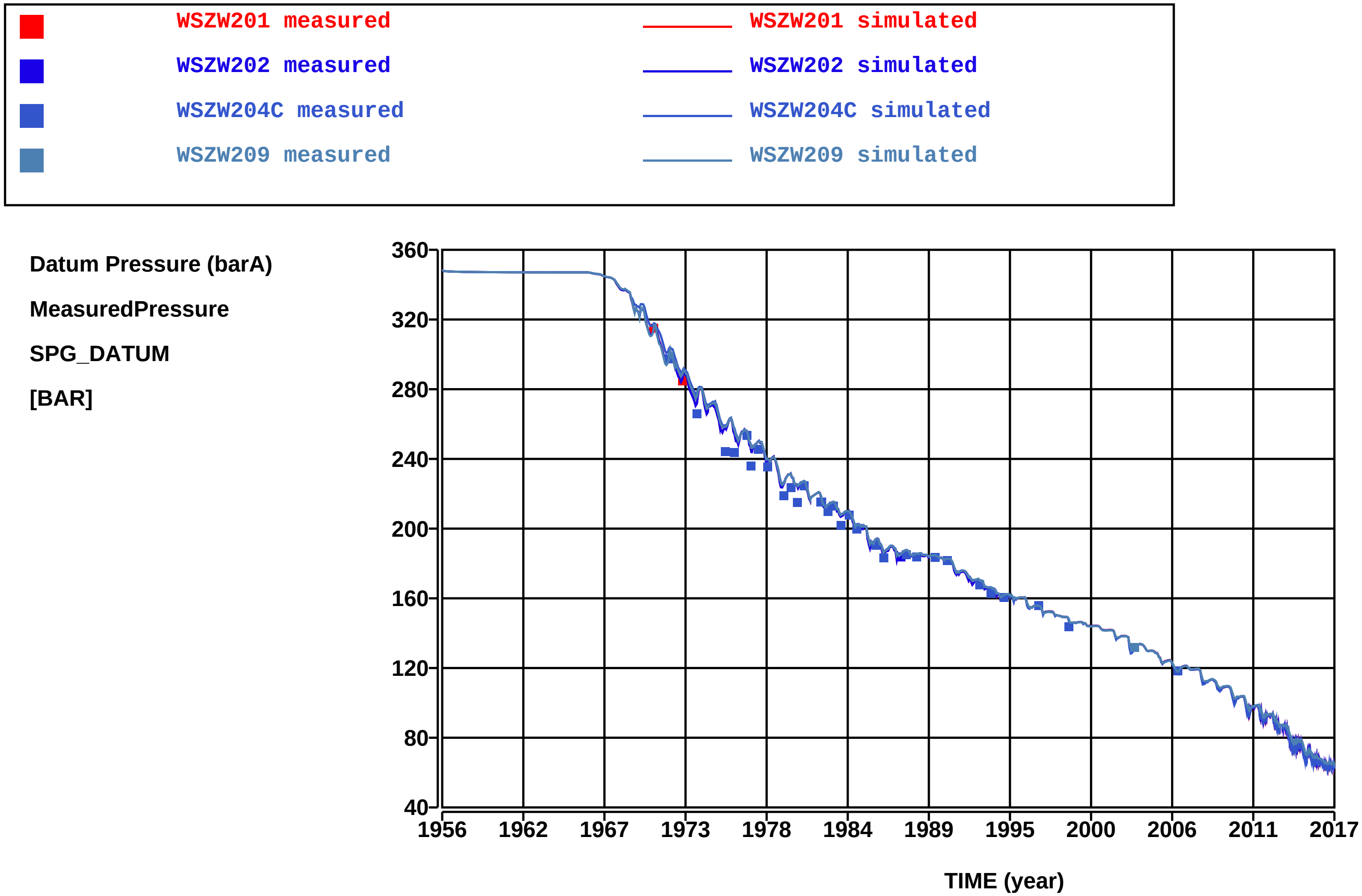

Table Name: WSZW201_PRES

Plot Name: SPTG_WSZW

Time=2.016997e+03 [YEAR]

Creation date: Thu 09/02/2017 16:08
Runfile: GRO_2016_ED_v60.run

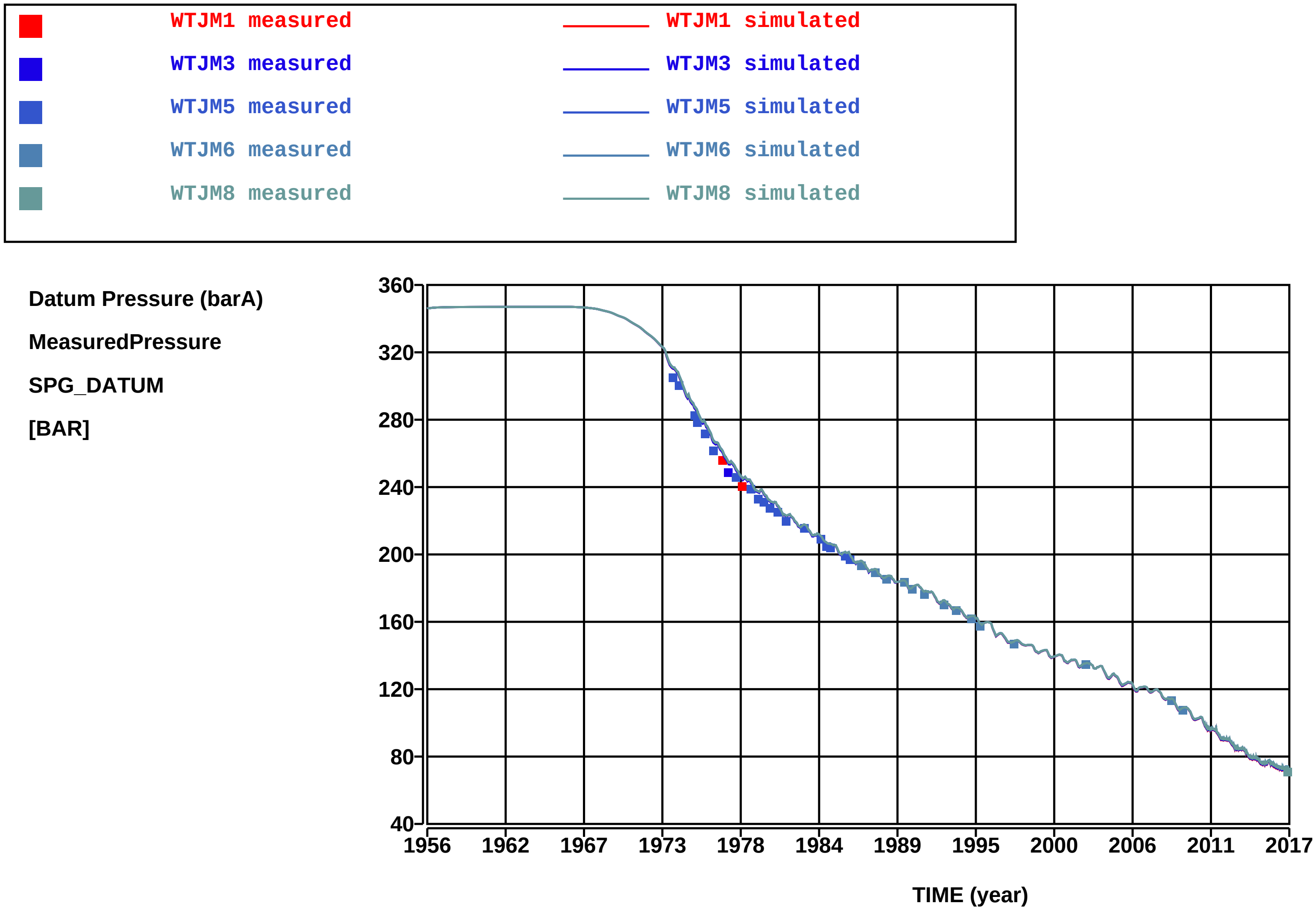

Table Name: WTJM1_PRES

Plot Name: SPTG_WTJM

Time=2.016997e+03 [YEAR]

Creation date: Thu 09/02/2017 16:08

Runfile: GRO_2016_ED_v60.run

Table Name: WTUS2_PRES

Plot Name: SPTG_WTUS

Time=2.016997e+03 [YEAR]

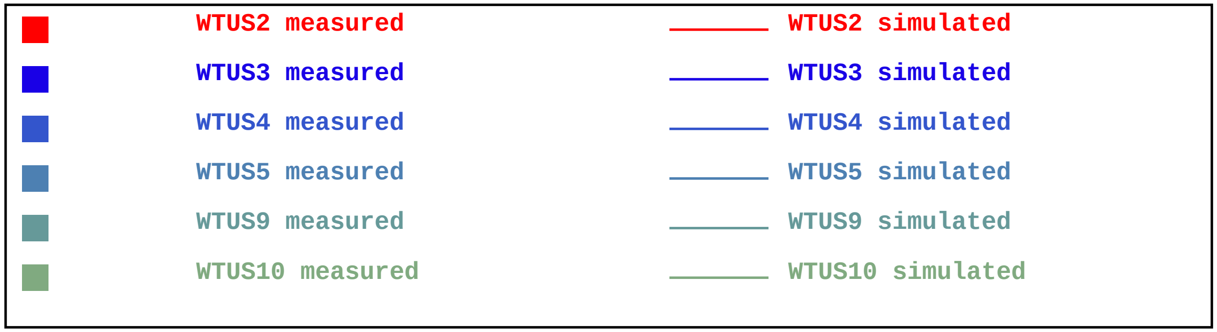

Datum Pressure (barA)

MeasuredPressure

SPG_DATUM

[BAR]

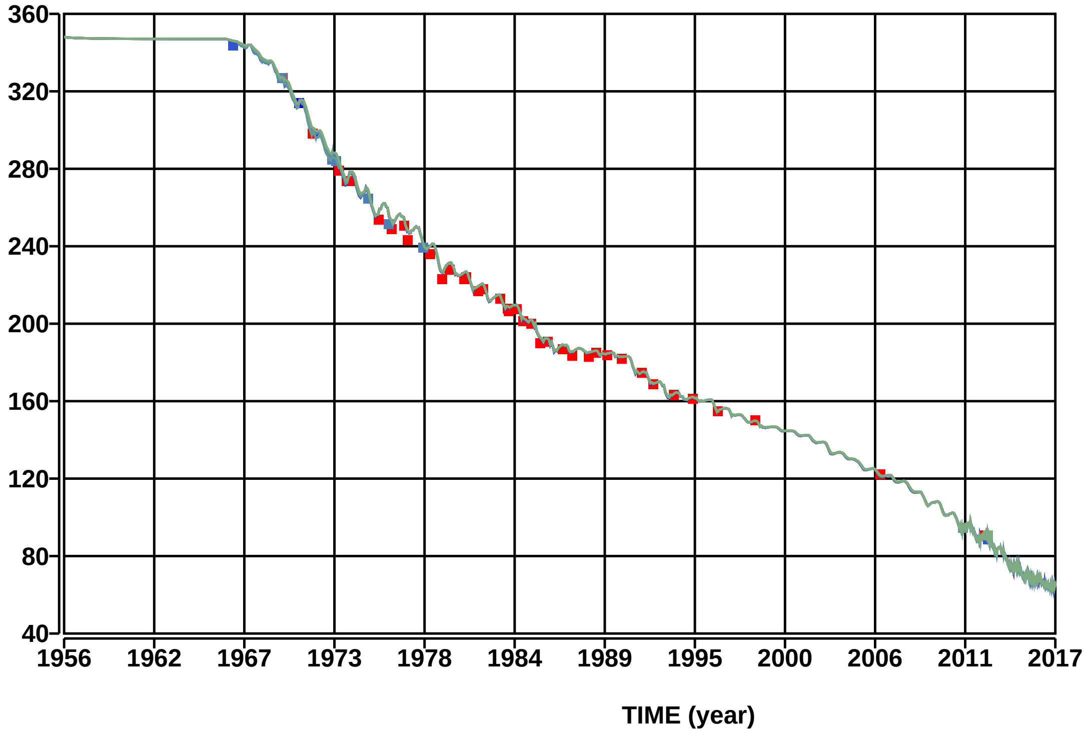

Creation date: Thu 09/02/2017 16:08

Runfile: GRO_2016_ED_v60.run

Table Name: WUTB2_PRES
Plot Name: SPTG_WUTB
Time=2.016997e+03 [YEAR]

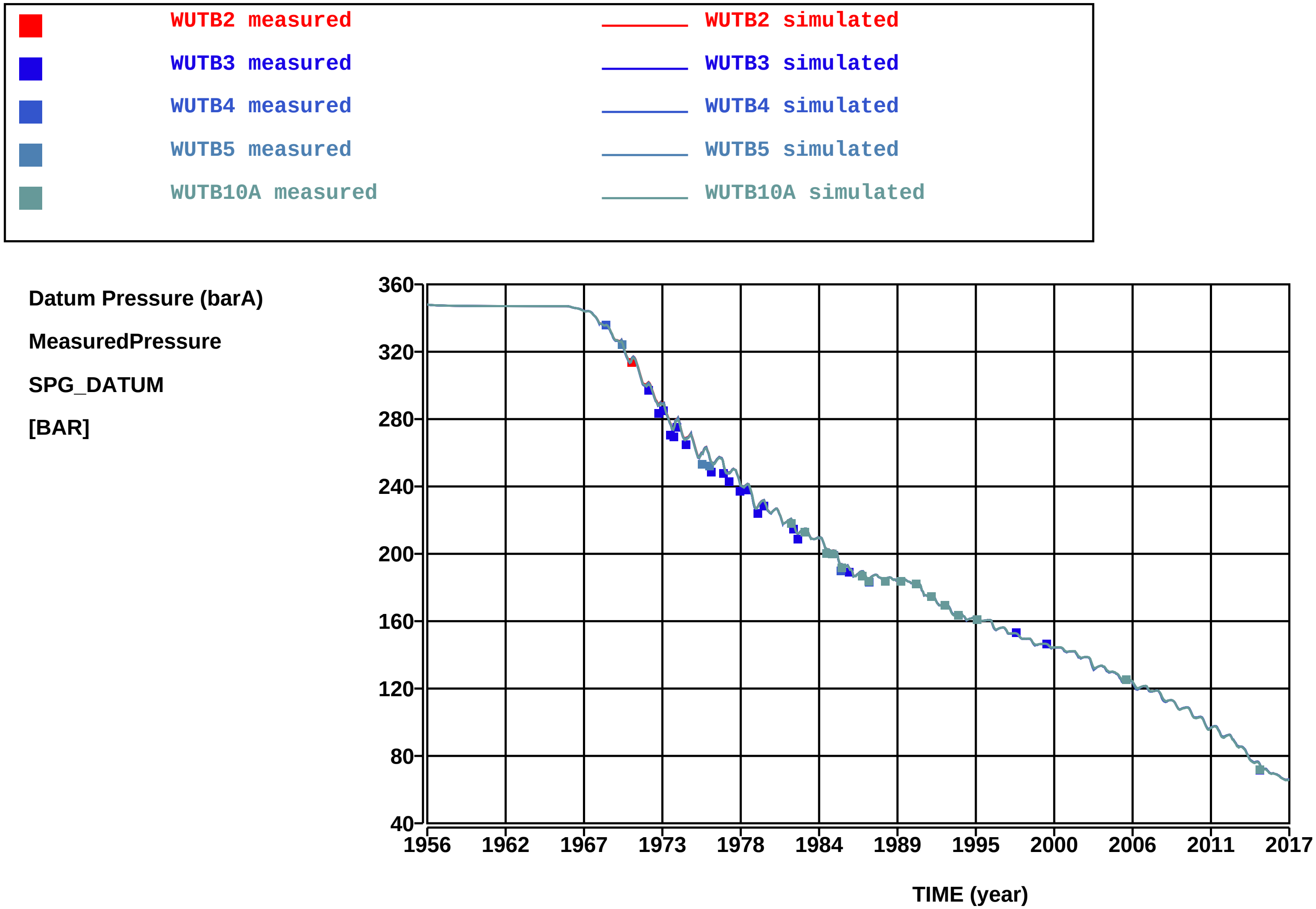

Creation date: Thu 09/02/2017 16:08
Runfile: GRO_2016_ED_v60.run

Table Name: WZND1_PRES

Plot Name: SPTG_WZND

Time=2.016997e+03 [YEAR]

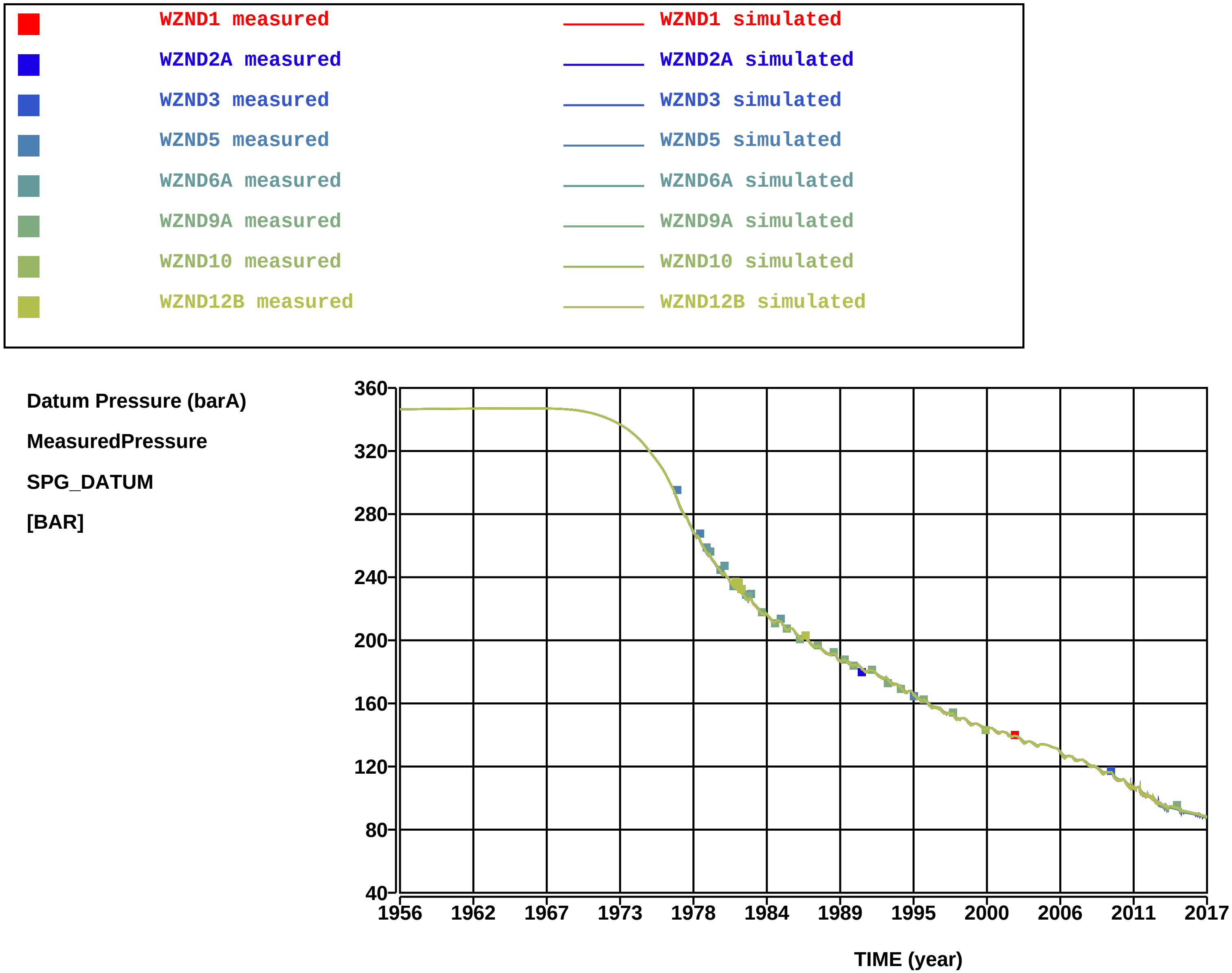

Creation date: Thu 09/02/2017 16:08

Runfile: GRO_2016_ED_v60.run

Table Name: WZPD1_PRES

Plot Name: SPTG_WZPD

Time=2.016997e+03 [YEAR]

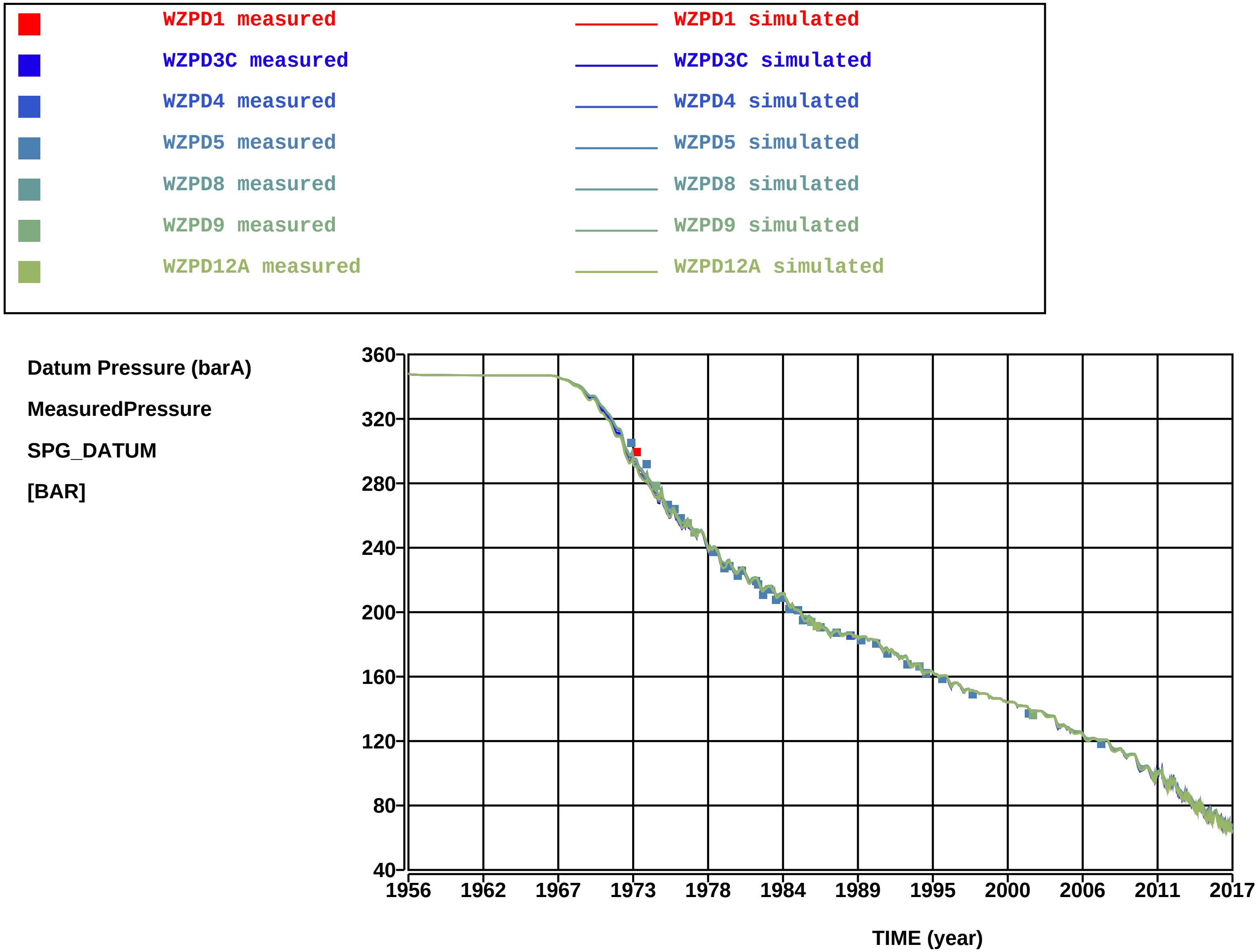

Creation date: Thu 09/02/2017 16:08

Runfile: GRO_2016_ED_v60.run

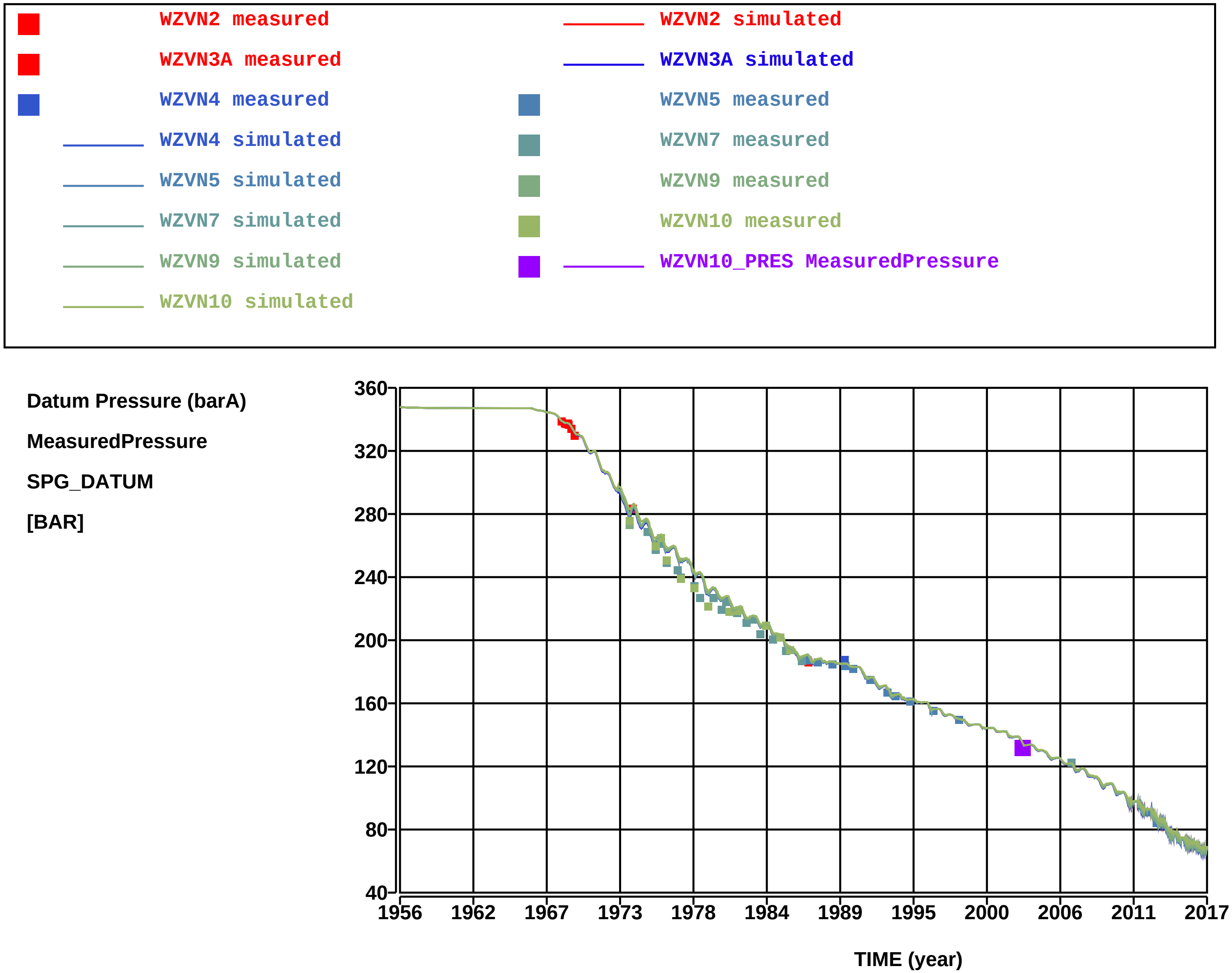

Table Name: WZVN2_PRES
Plot Name: SPTG_WZVN
Time=2.016997e+03 [YEAR]

Creation date: Thu 09/02/2017 16:08
Runfile: GRO_2016_ED_v60.run

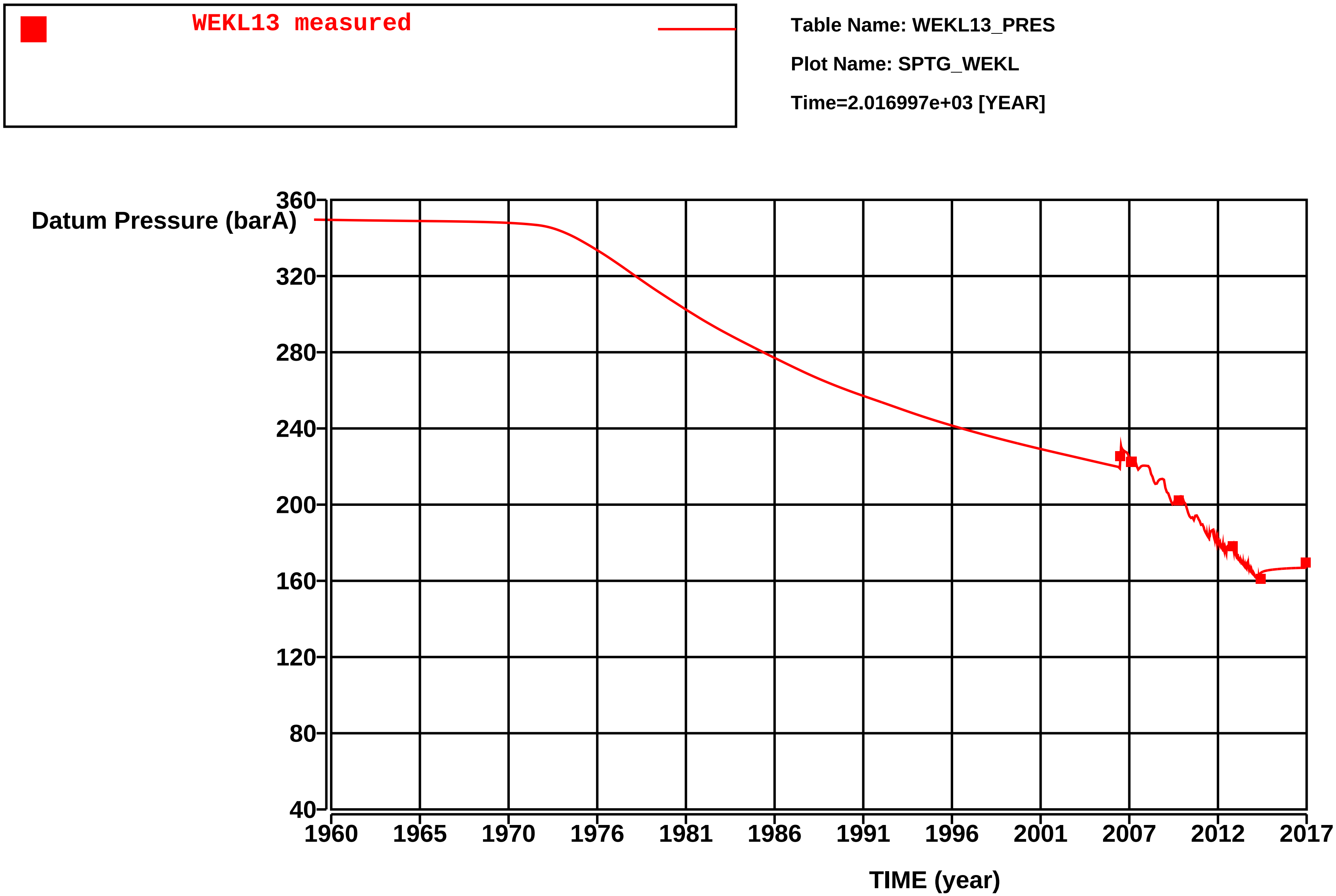

Table Name: WEKL13_PRES

Plot Name: SPTG_WEKL

Time=2.016997e+03 [YEAR]

Creation date: Thu 09/02/2017 16:08

Runfile: GRO_2016_ED_v60.run

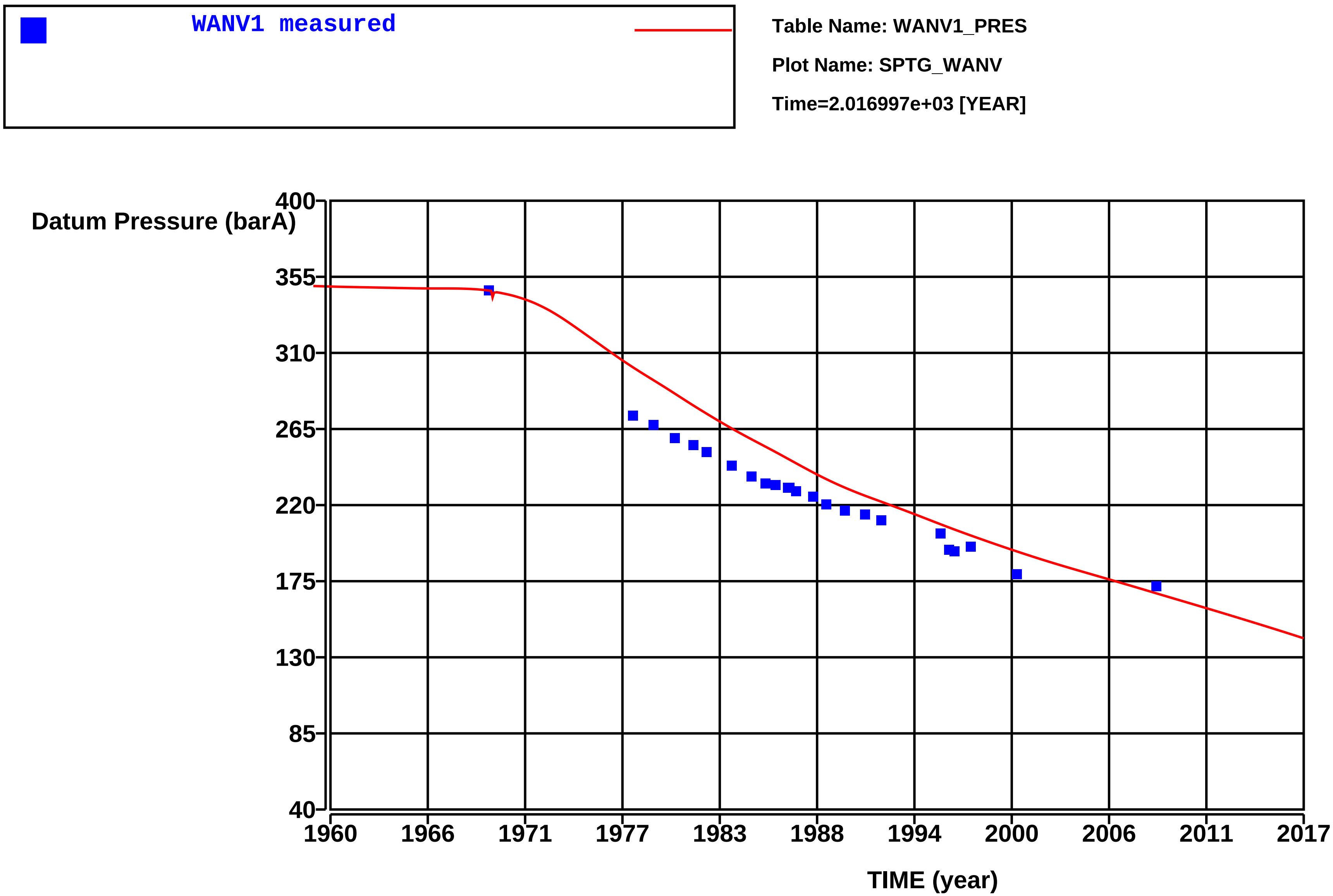

Creation date: Thu 09/02/2017 16:08
Runfile: GRO_2016_ED_v60.run

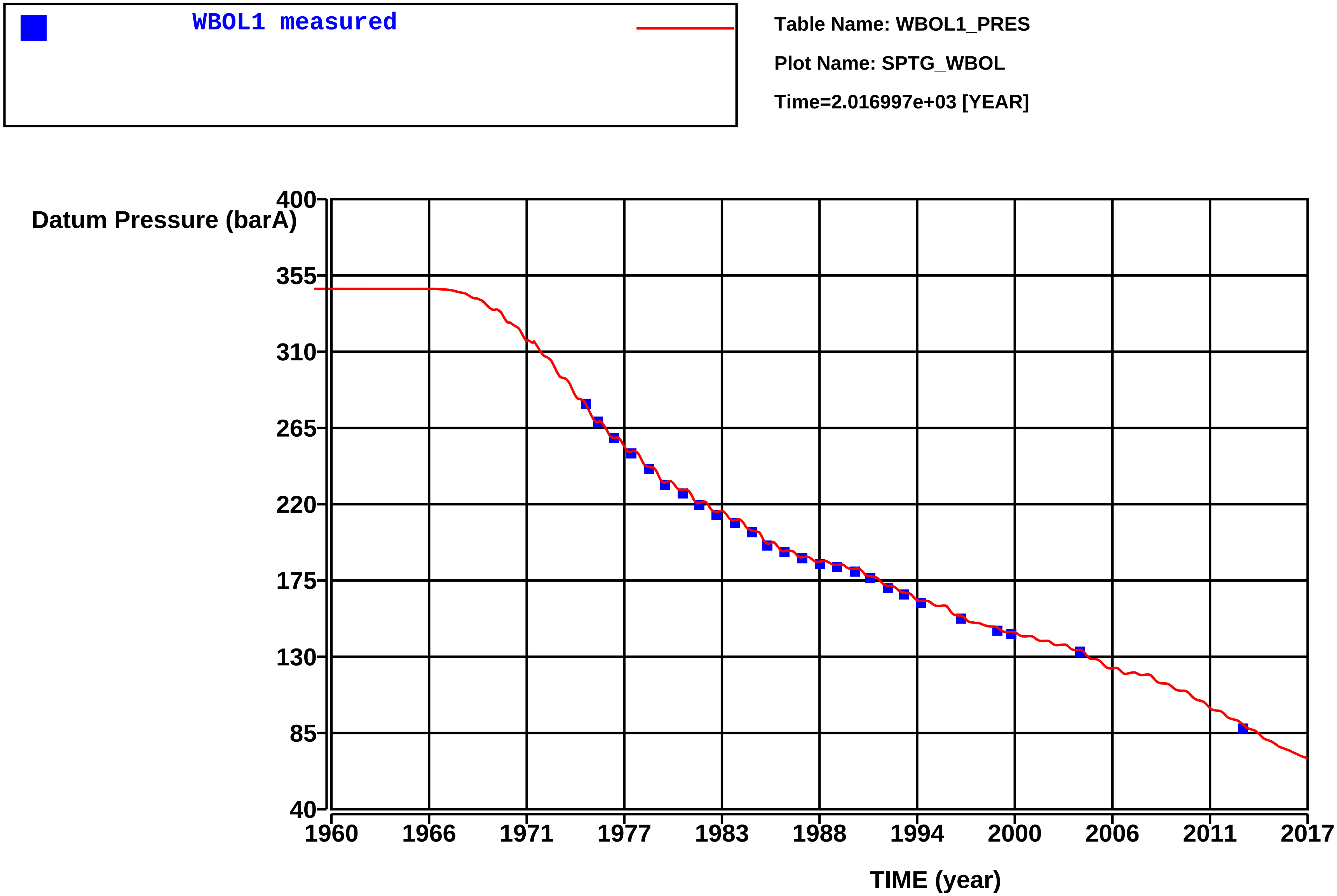

Table Name: WBOL1_PRES

Plot Name: SPTG_WBOL

Time=2.016997e+03 [YEAR]

Creation date: Thu 09/02/2017 16:08

Runfile: GRO_2016_ED_v60.run

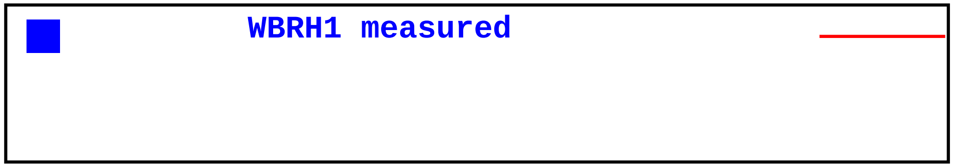

Table Name: WBRH1_PRES

Plot Name: SPTG_WBRH

Time=2.016997e+03 [YEAR]

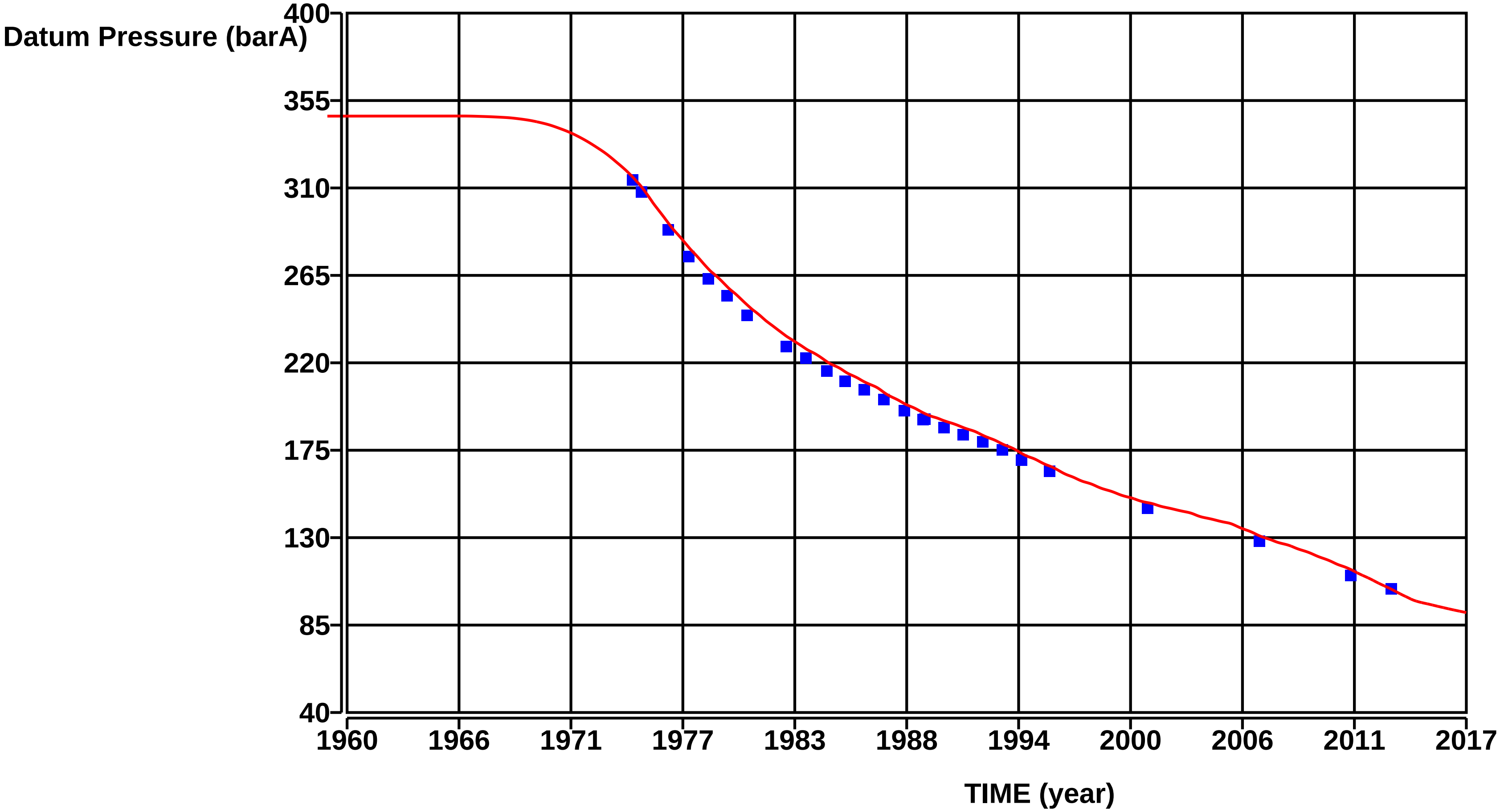

Creation date: Thu 09/02/2017 16:08
Runfile: GRO_2016_ED_v60.run

Table Name: WDZL1_PRES

Plot Name: SPTG_WDZL

Time=2.016997e+03 [YEAR]

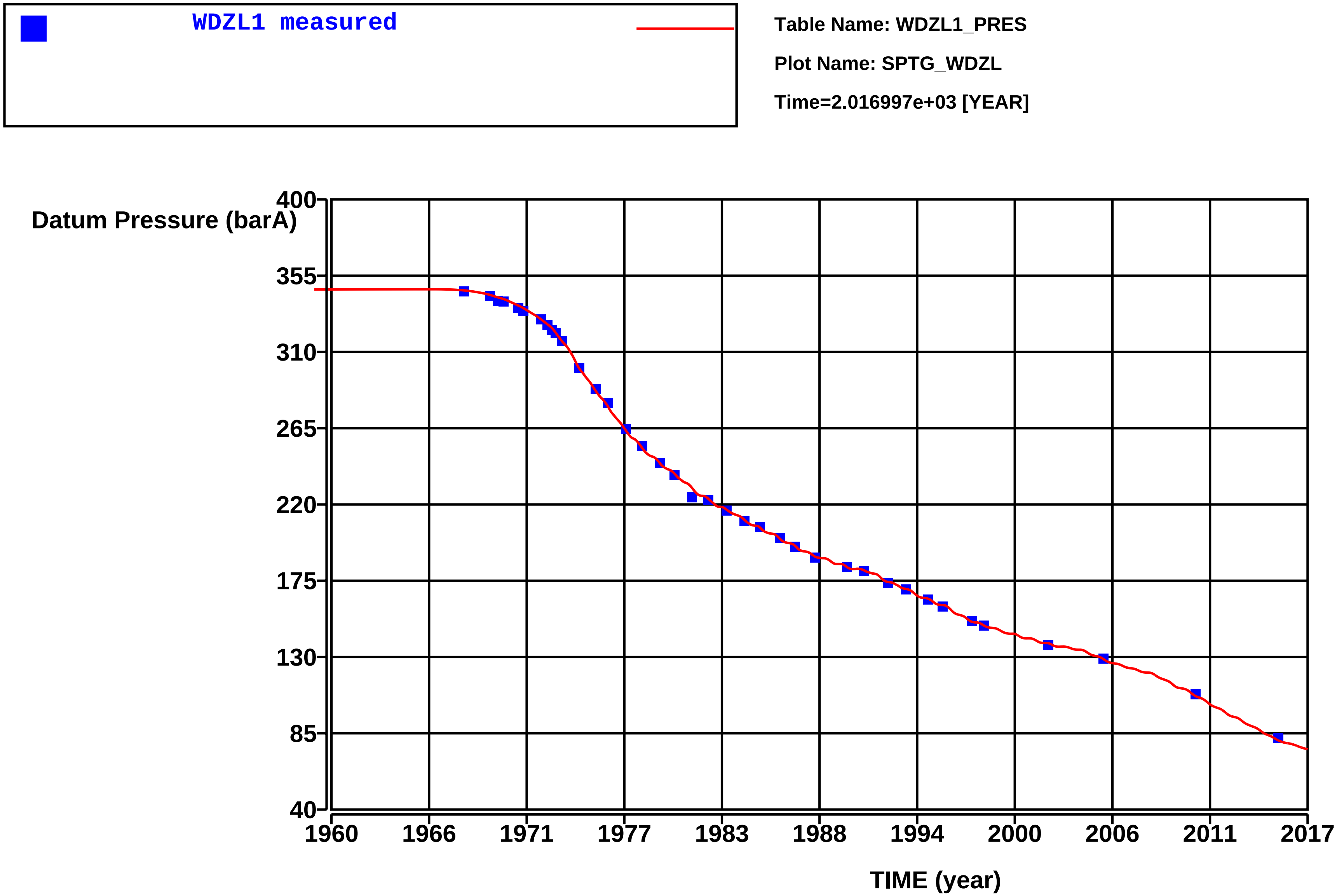

Creation date: Thu 09/02/2017 16:08

Runfile: GRO_2016_ED_v60.run

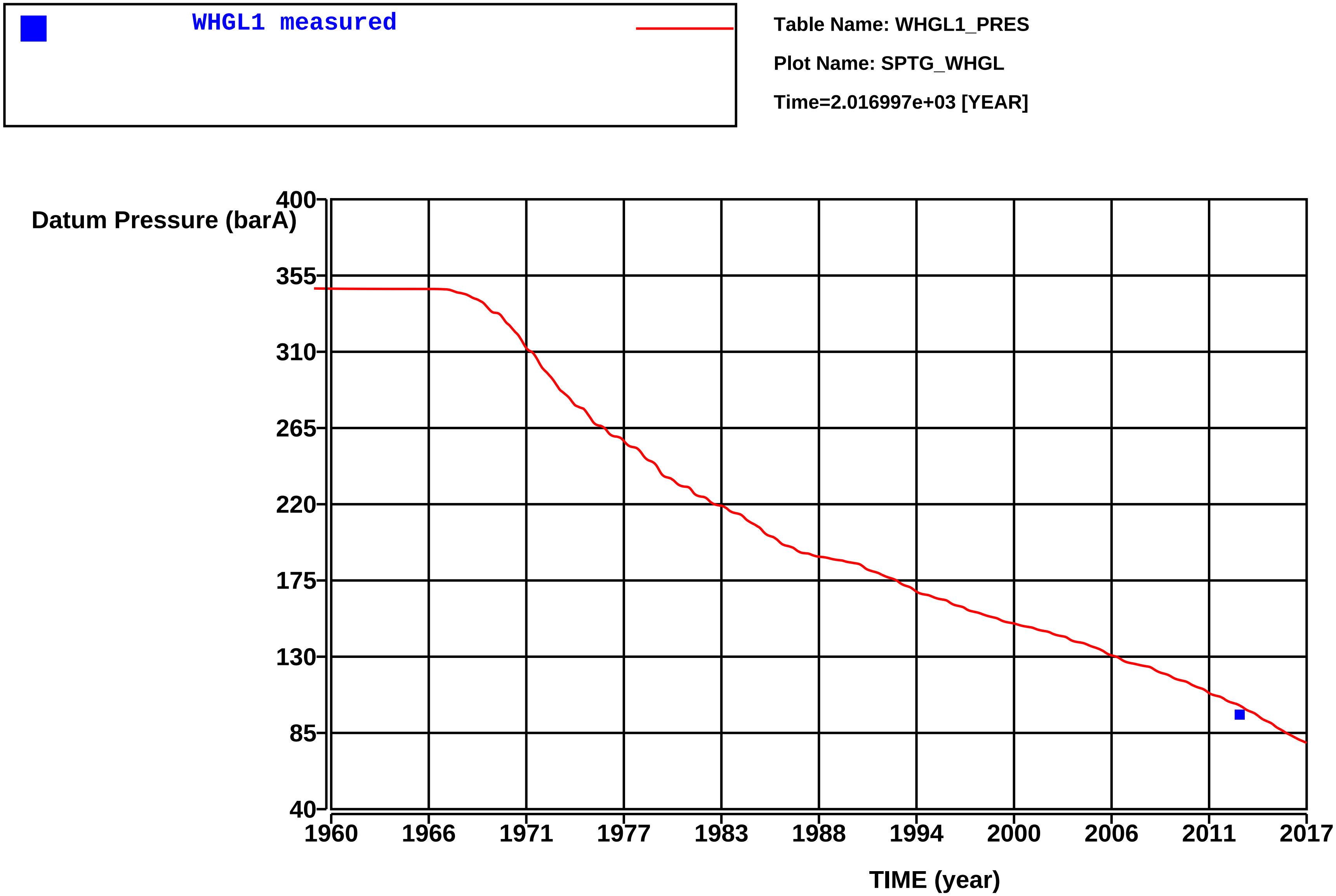

Table Name: WHGL1_PRES

Plot Name: SPTG_WHGL

Time=2.016997e+03 [YEAR]

Creation date: Thu 09/02/2017 16:08
Runfile: GRO_2016_ED_v60.run

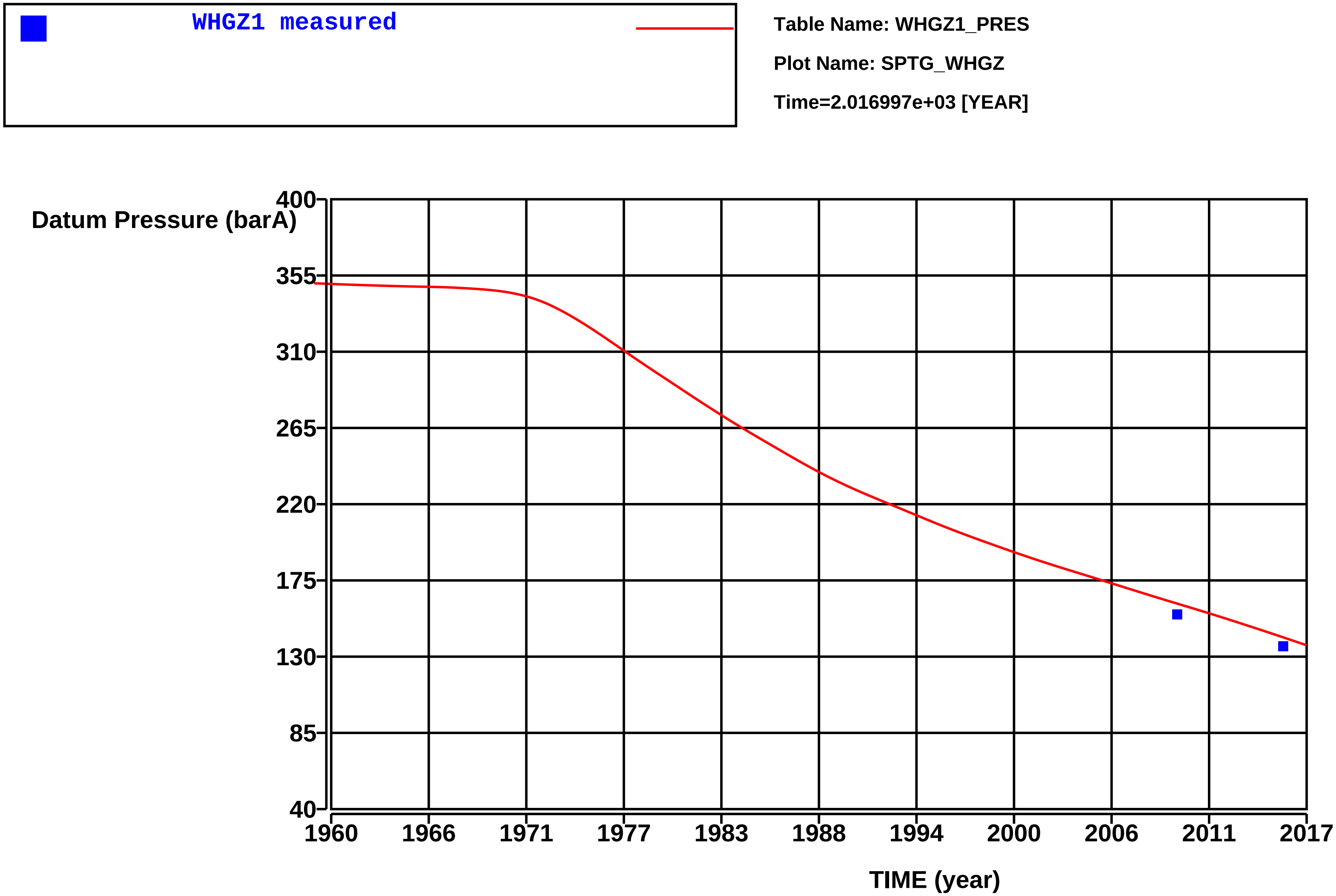

Creation date: Thu 09/02/2017 16:08
Runfile: GRO_2016_ED_v60.run

Table Name: WHND1_PRES

Plot Name: SPTG_WHND

Time=2.016997e+03 [YEAR]

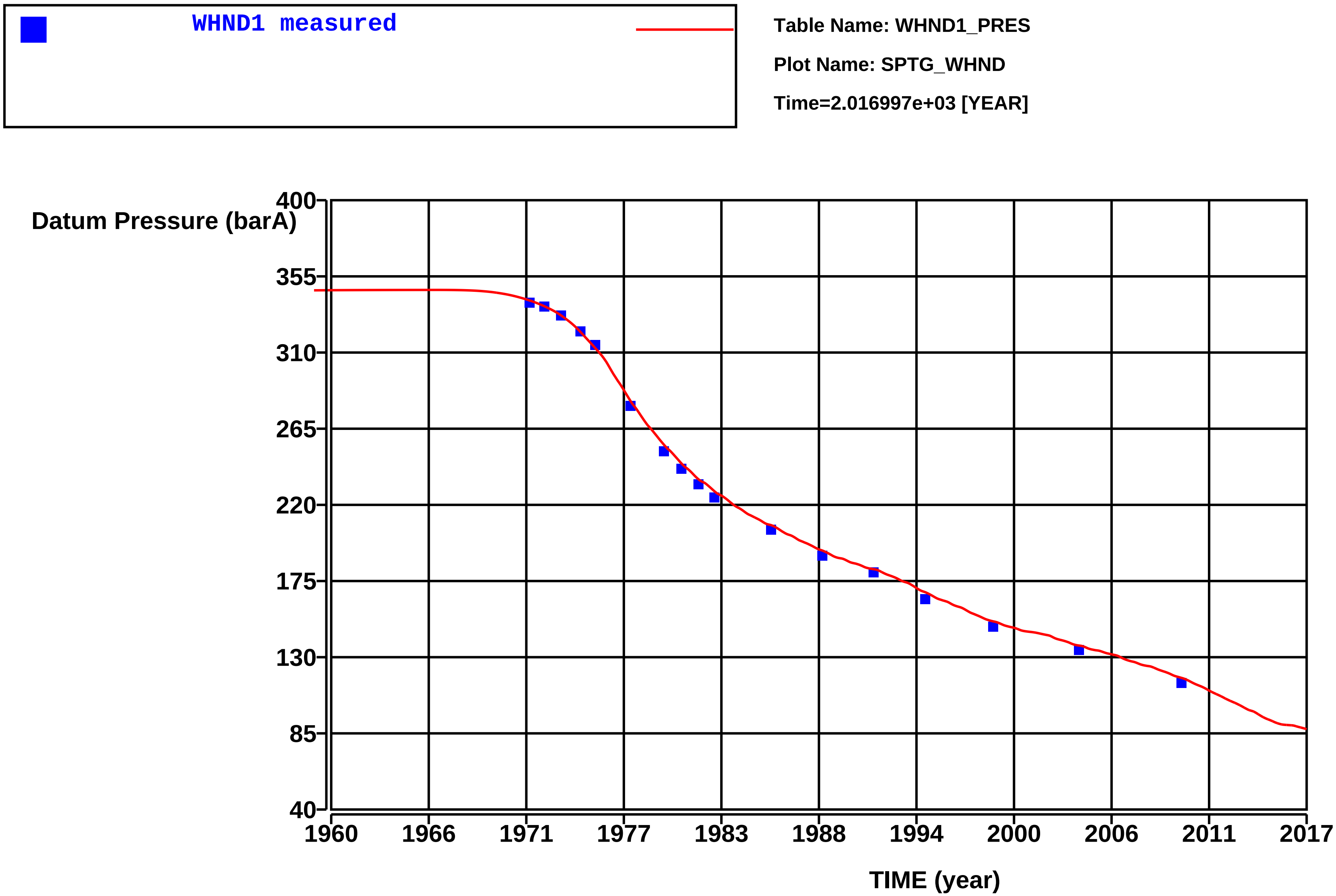

Creation date: Thu 09/02/2017 16:08

Runfile: GRO_2016_ED_v60.run

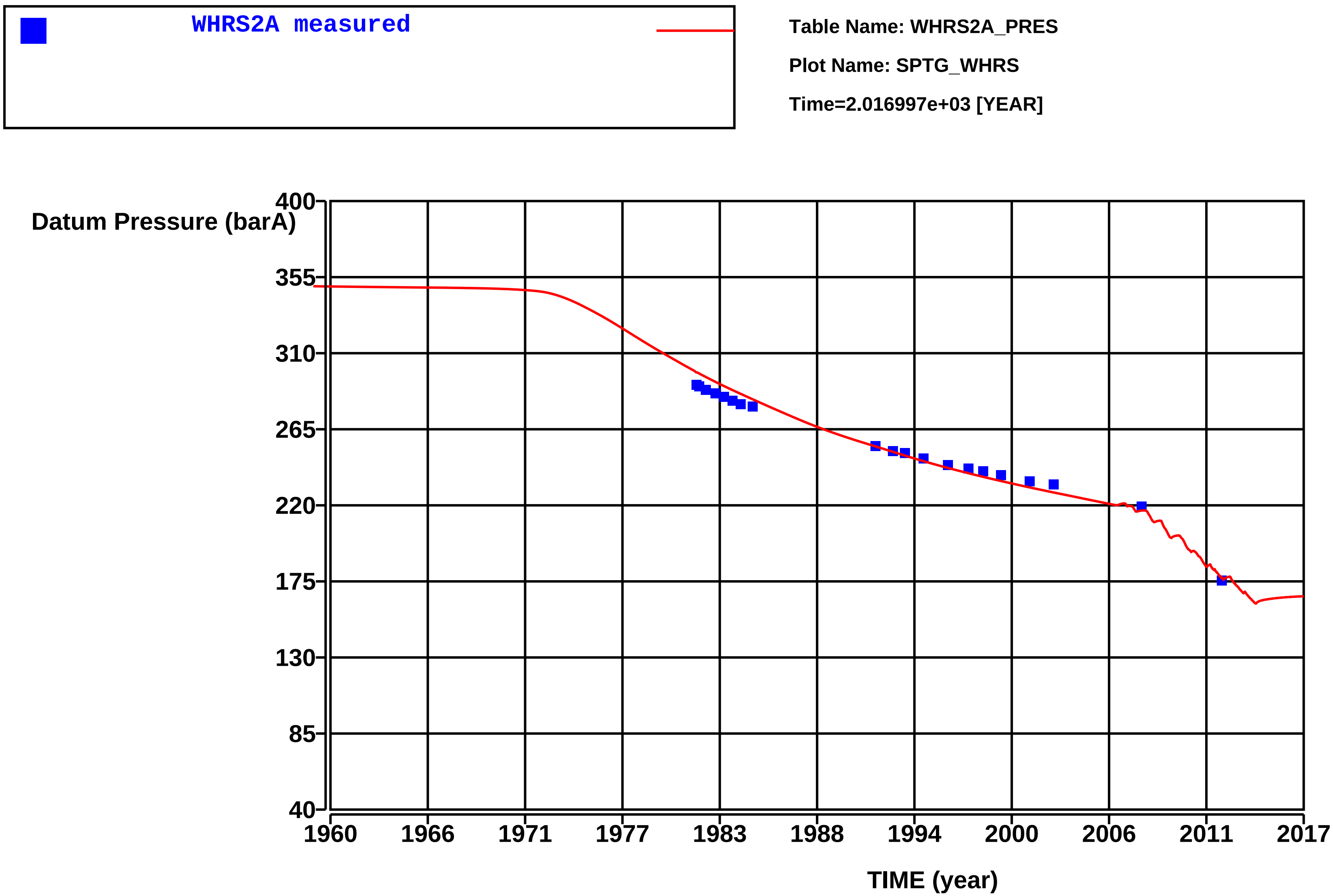

Creation date: Thu 09/02/2017 16:08

Runfile: GRO_2016_ED_v60.run

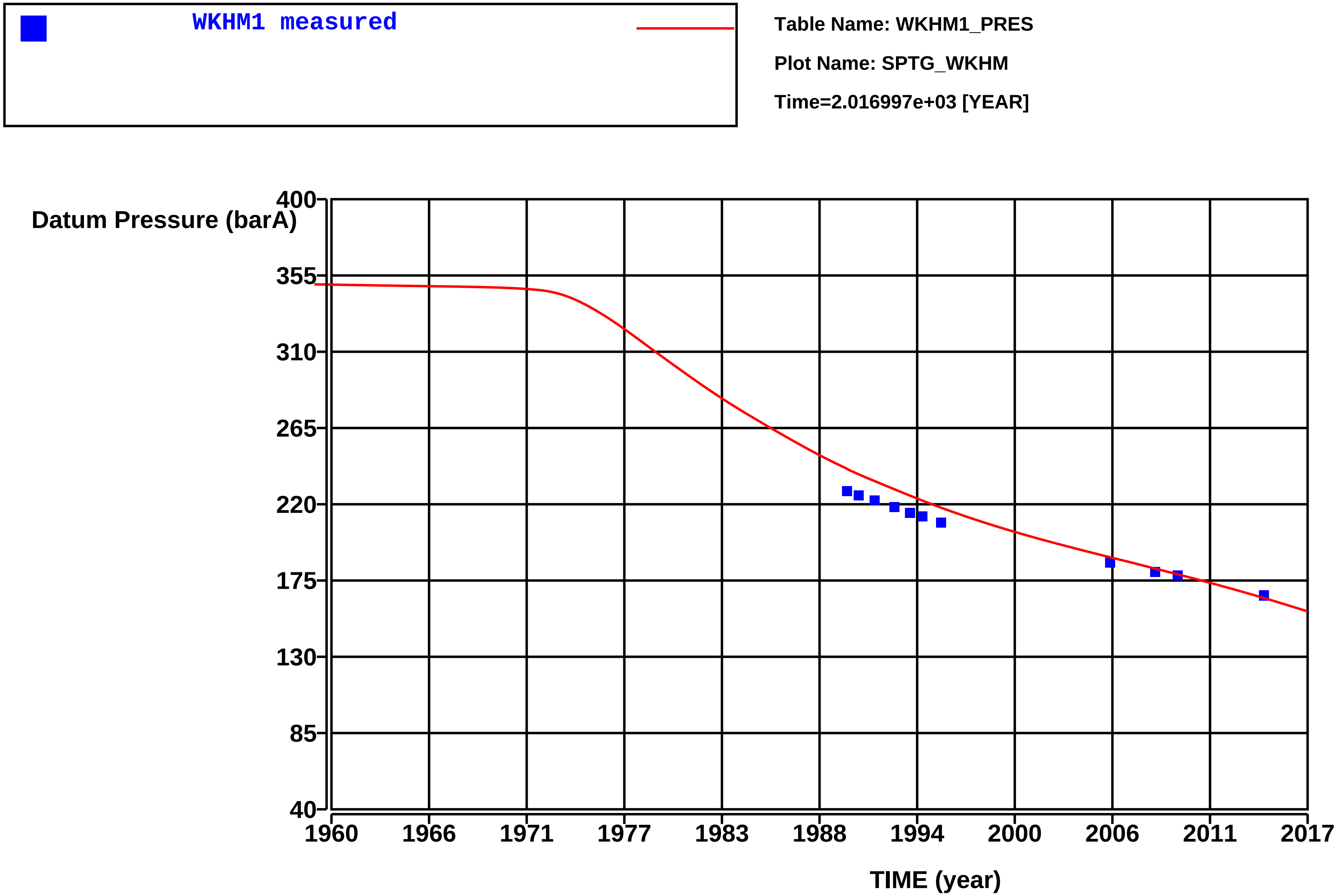

Creation date: Thu 09/02/2017 16:08
Runfile: GRO_2016_ED_v60.run

Table Name: WMDN1_PRES

Plot Name: SPTG_WMDN

Time=2.016997e+03 [YEAR]

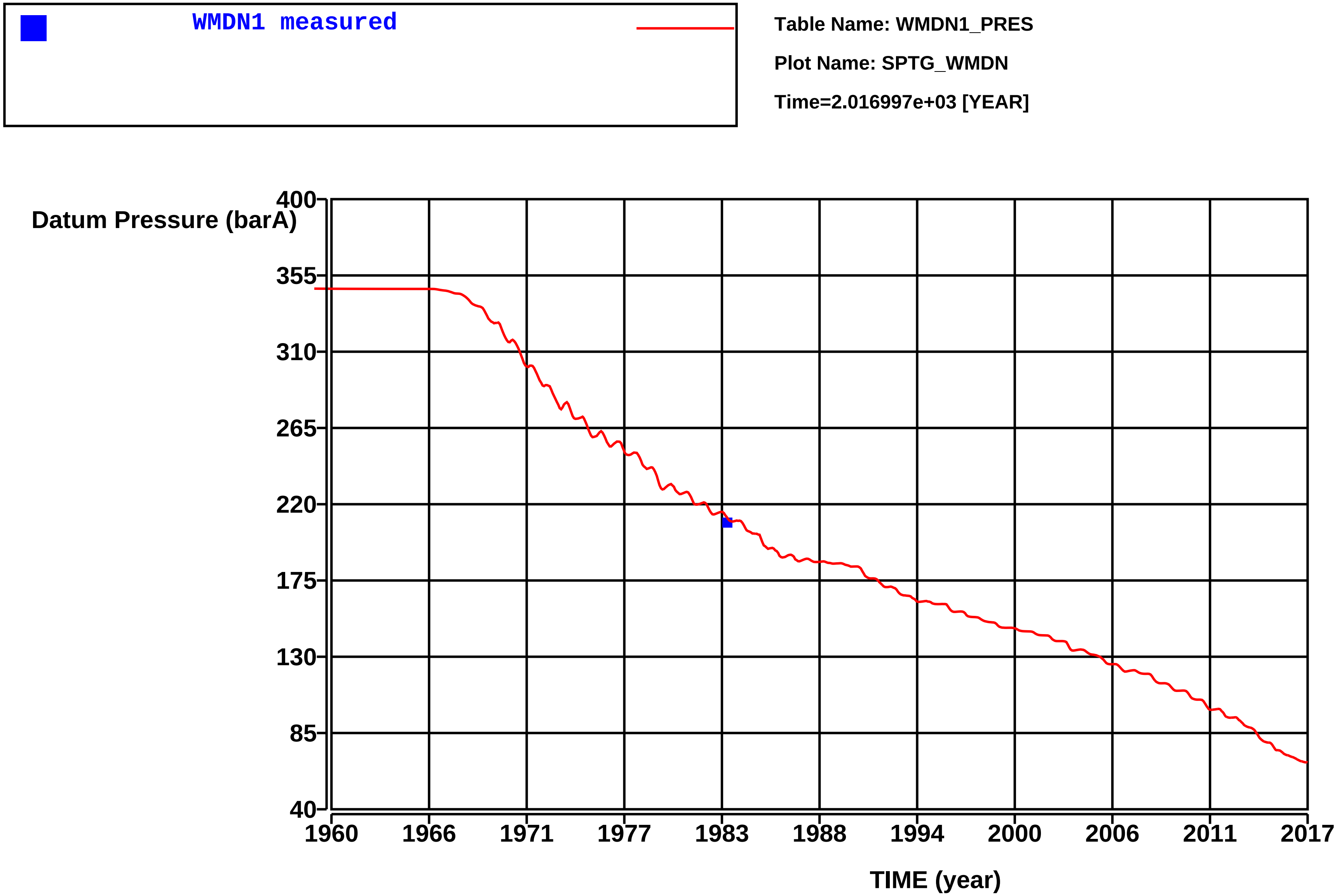

Creation date: Thu 09/02/2017 16:08

Runfile: GRO_2016_ED_v60.run

WODP1 measured

Table Name: WODP1_PRES

Plot Name: SPTG_WODP

Time=2.016997e+03 [YEAR]

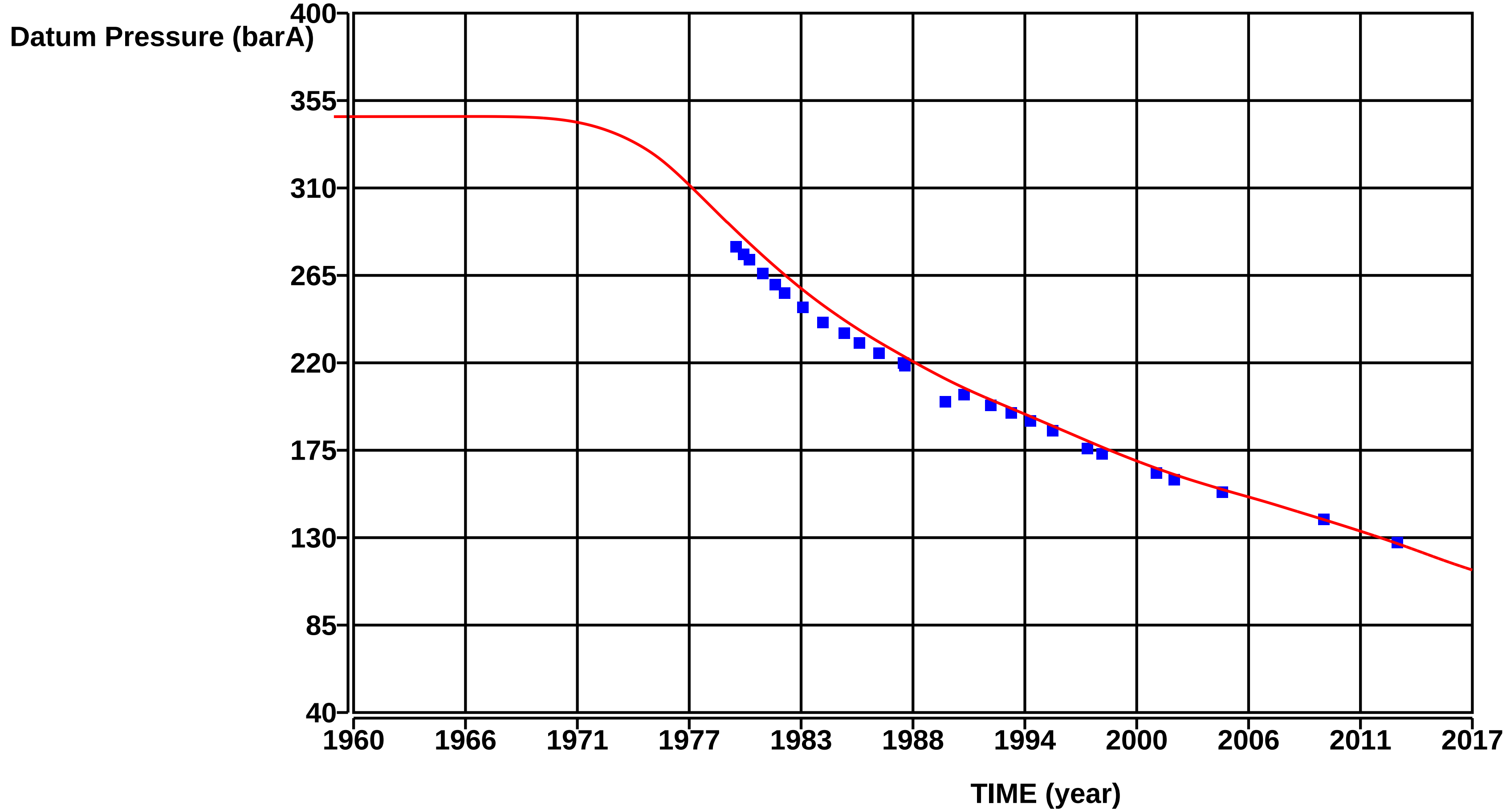

Creation date: Thu 09/02/2017 16:08

Runfile: GRO_2016_ED_v60.run

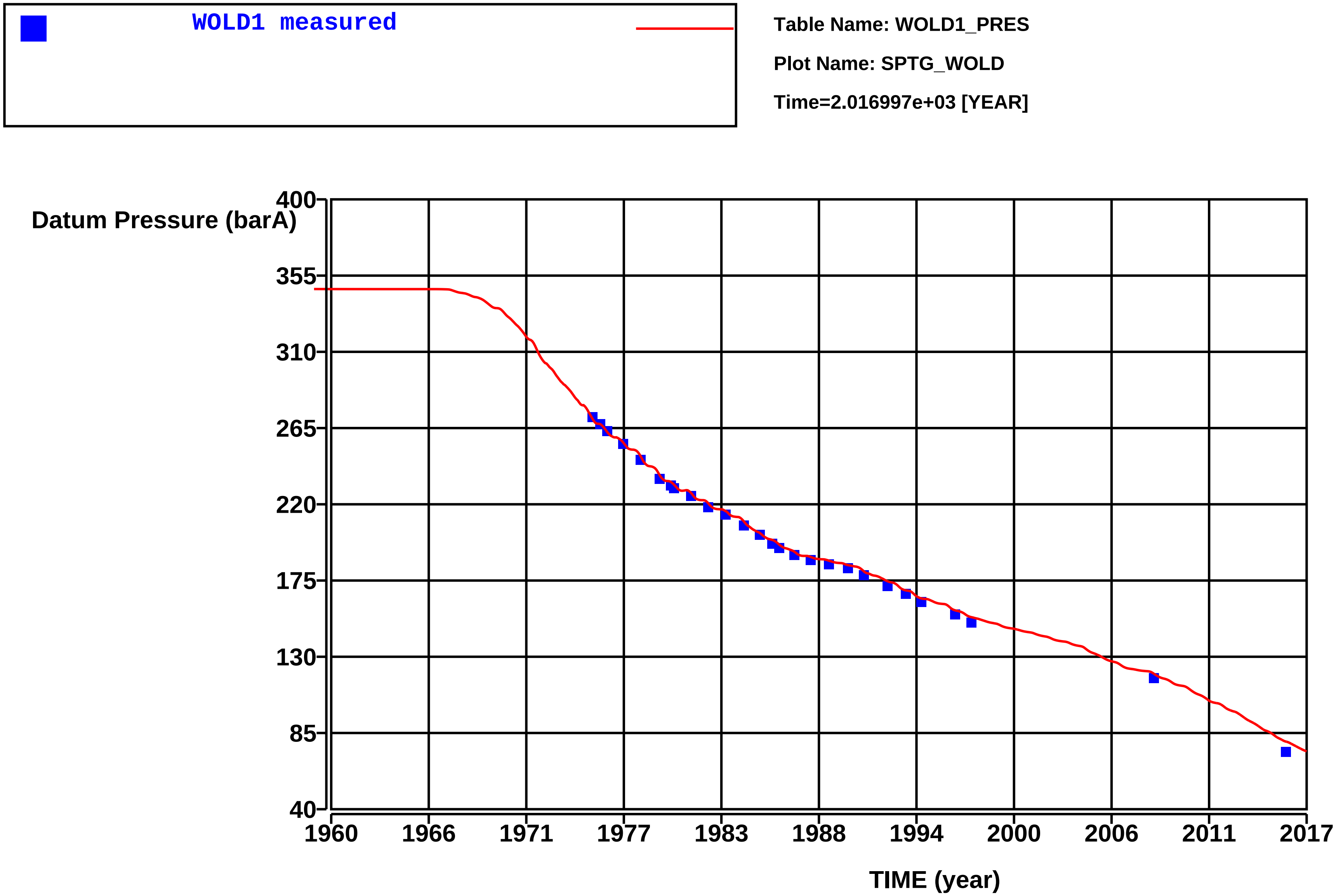

Creation date: Thu 09/02/2017 16:08
Runfile: GRO_2016_ED_v60.run

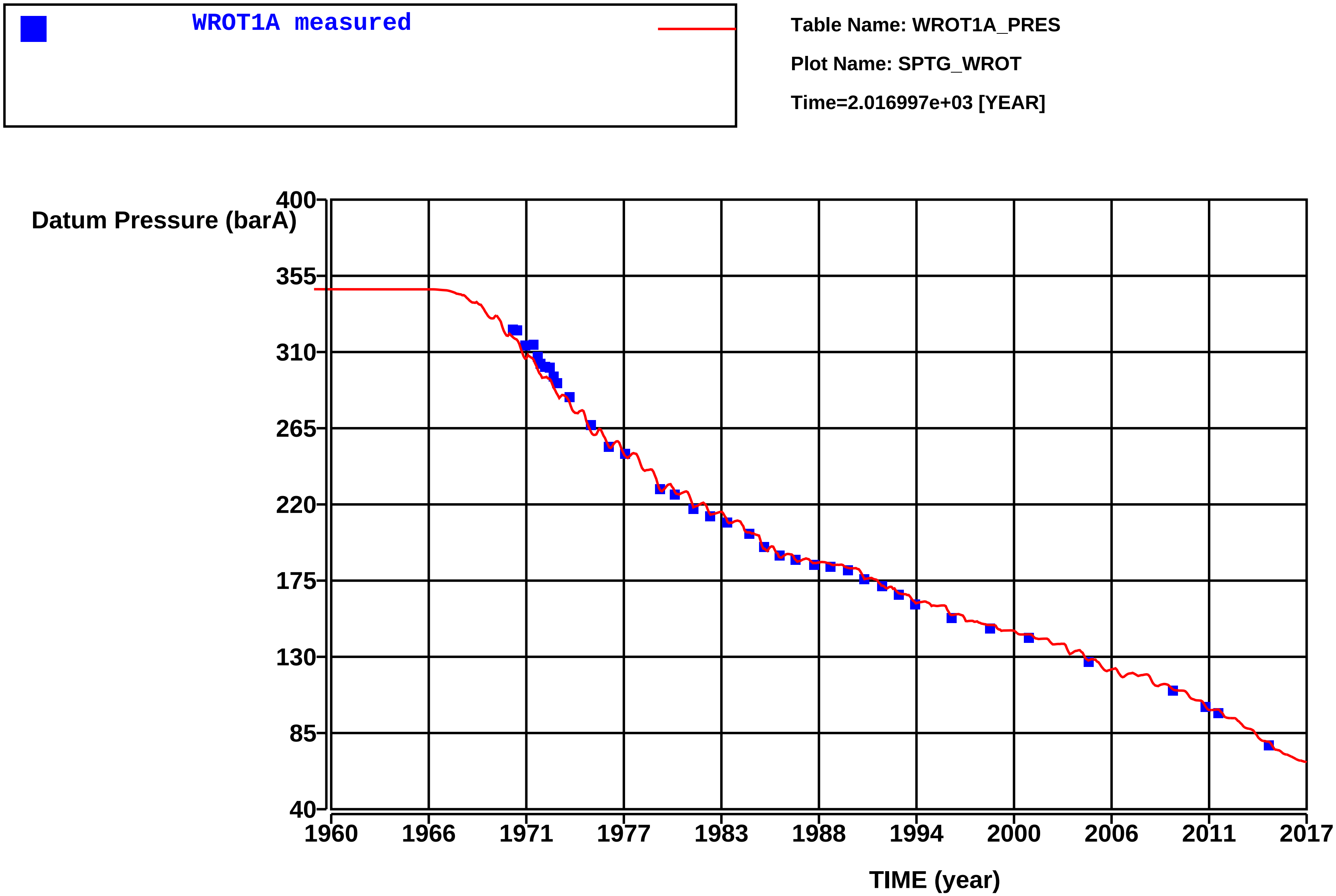

Creation date: Thu 09/02/2017 16:08
Runfile: GRO_2016_ED_v60.run

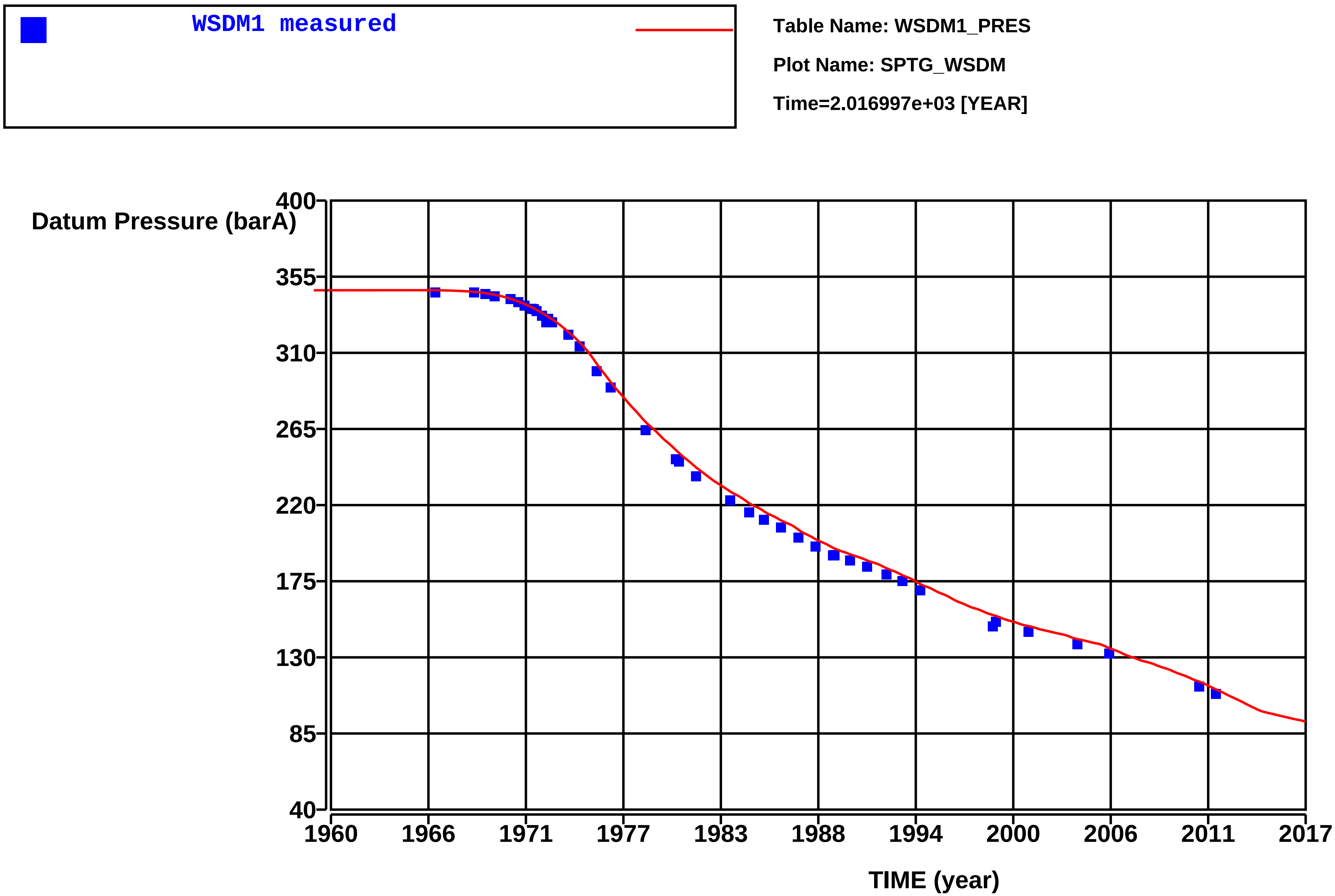

Creation date: Thu 09/02/2017 16:08
Runfile: GRO_2016_ED_v60.run

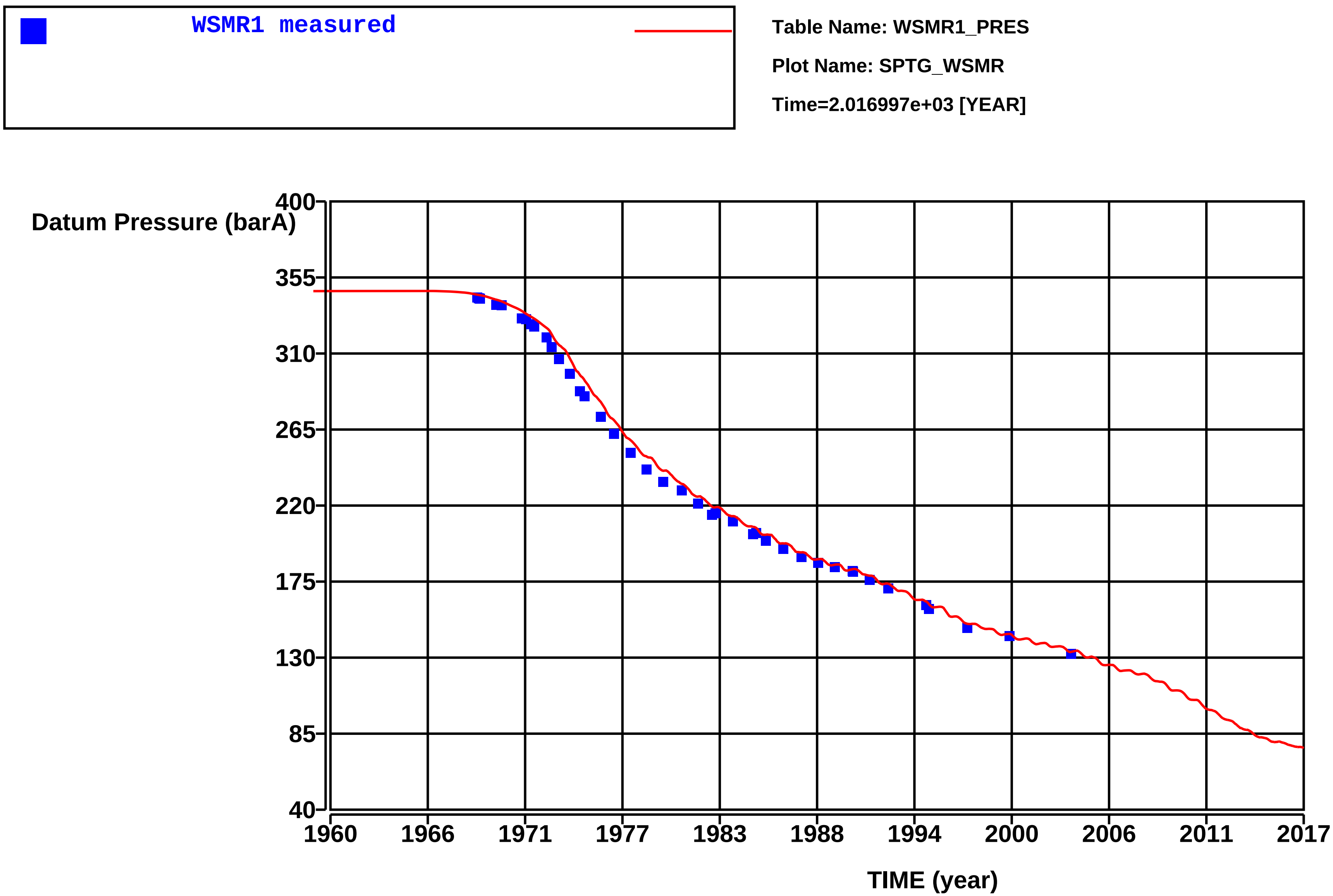

Creation date: Thu 09/02/2017 16:08
Runfile: GRO_2016_ED_v60.run

Table Name: WSPH1_PRES

Plot Name: SPTG_WSPH

Time=2.016997e+03 [YEAR]

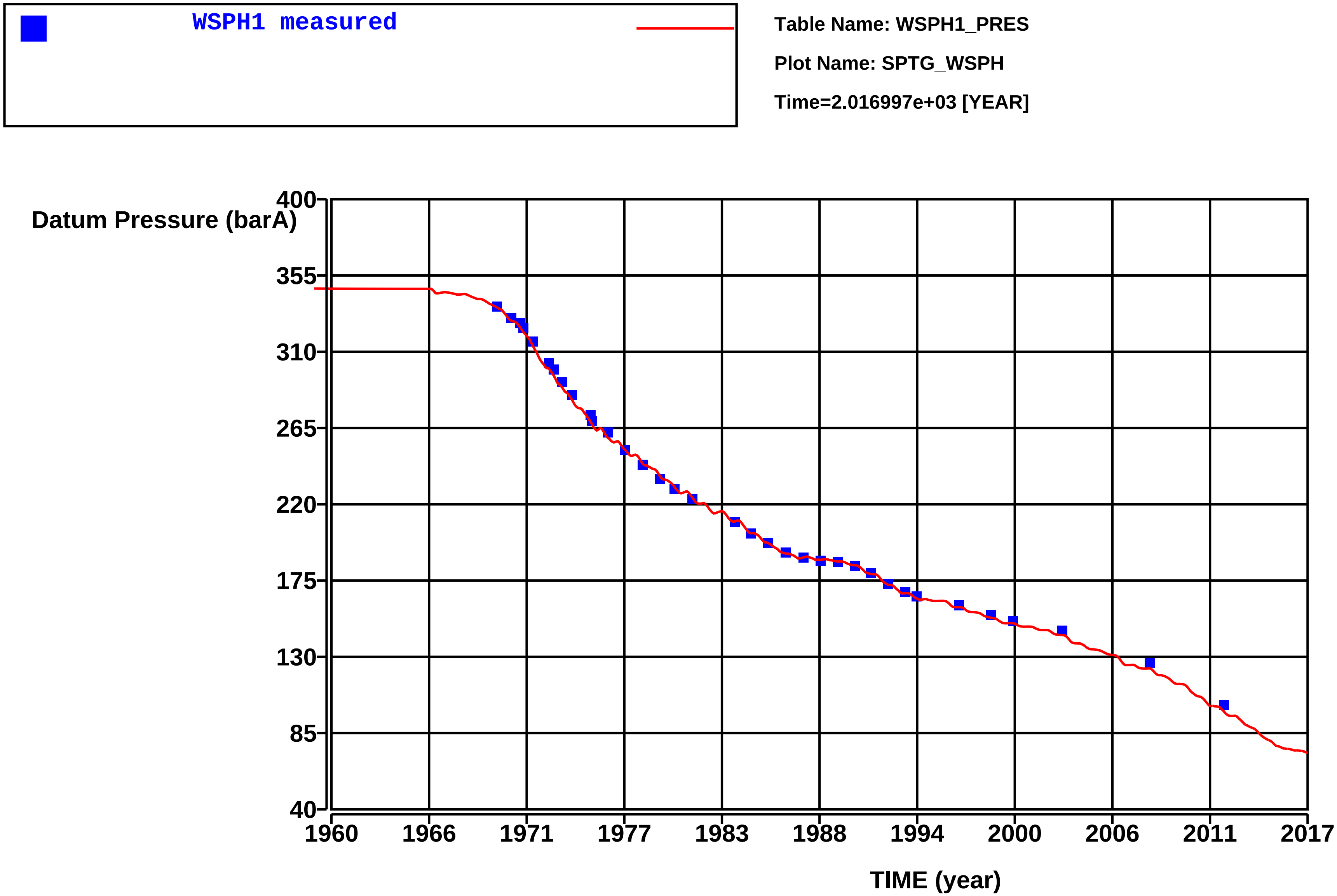

Creation date: Thu 09/02/2017 16:08

Runfile: GRO_2016_ED_v60.run

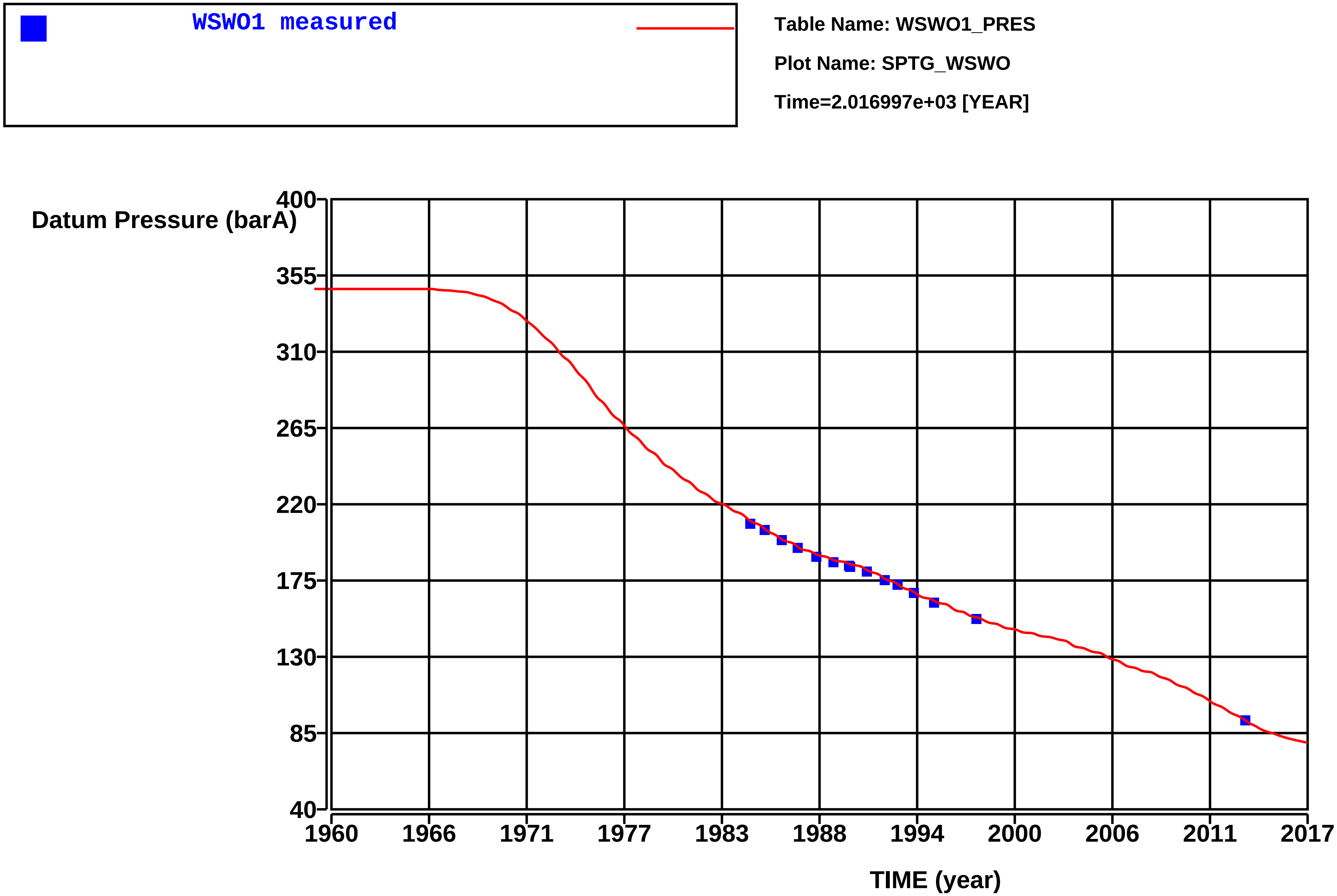

Table Name: WSWO1_PRES

Plot Name: SPTG_WSWO

Time=2.016997e+03 [YEAR]

Creation date: Thu 09/02/2017 16:08

Runfile: GRO_2016_ED_v60.run

Table Name: WTBR4_PRES

Plot Name: SPTG_WTBR

Time=2.016997e+03 [YEAR]

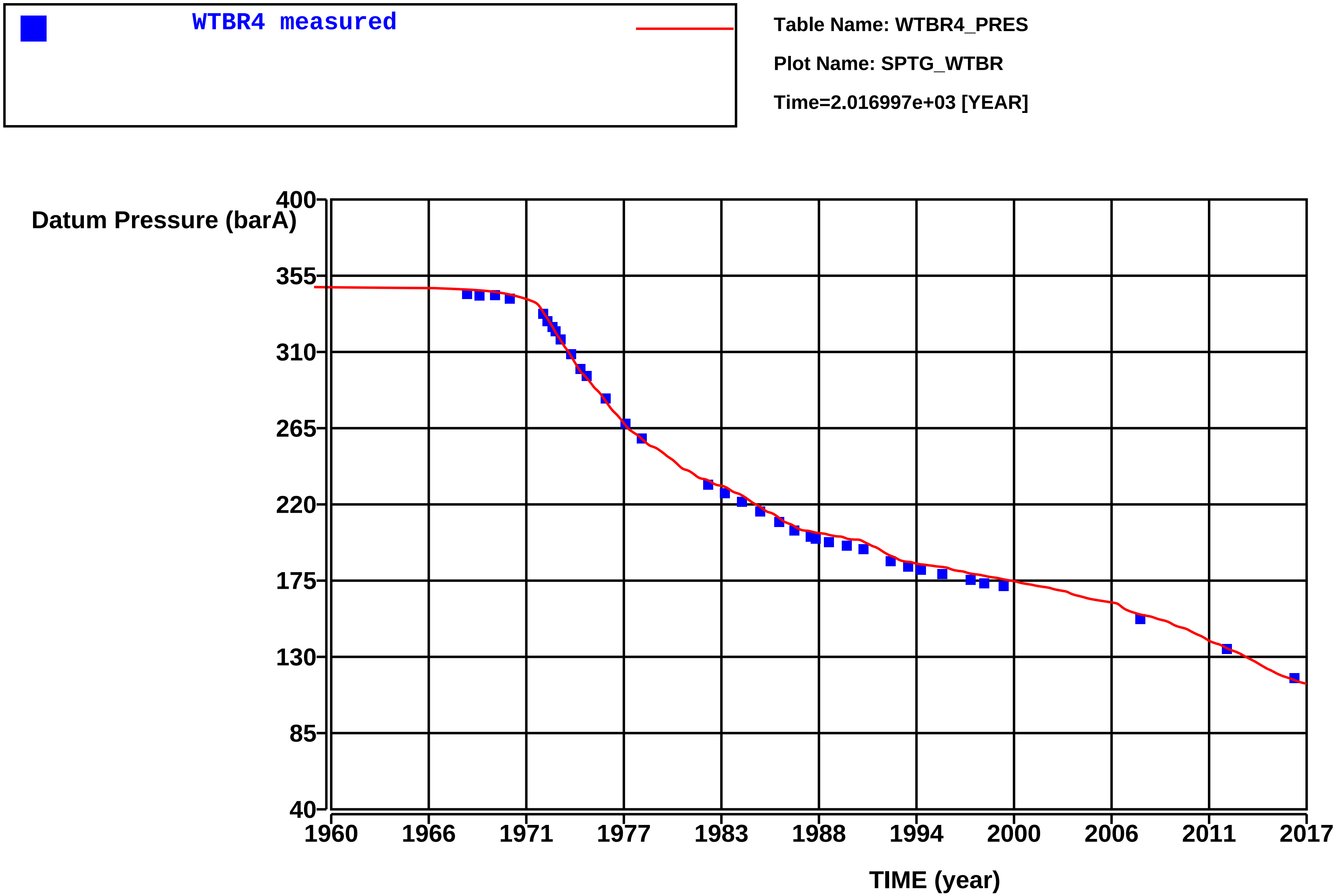

Creation date: Thu 09/02/2017 16:08

Runfile: GRO_2016_ED_v60.run

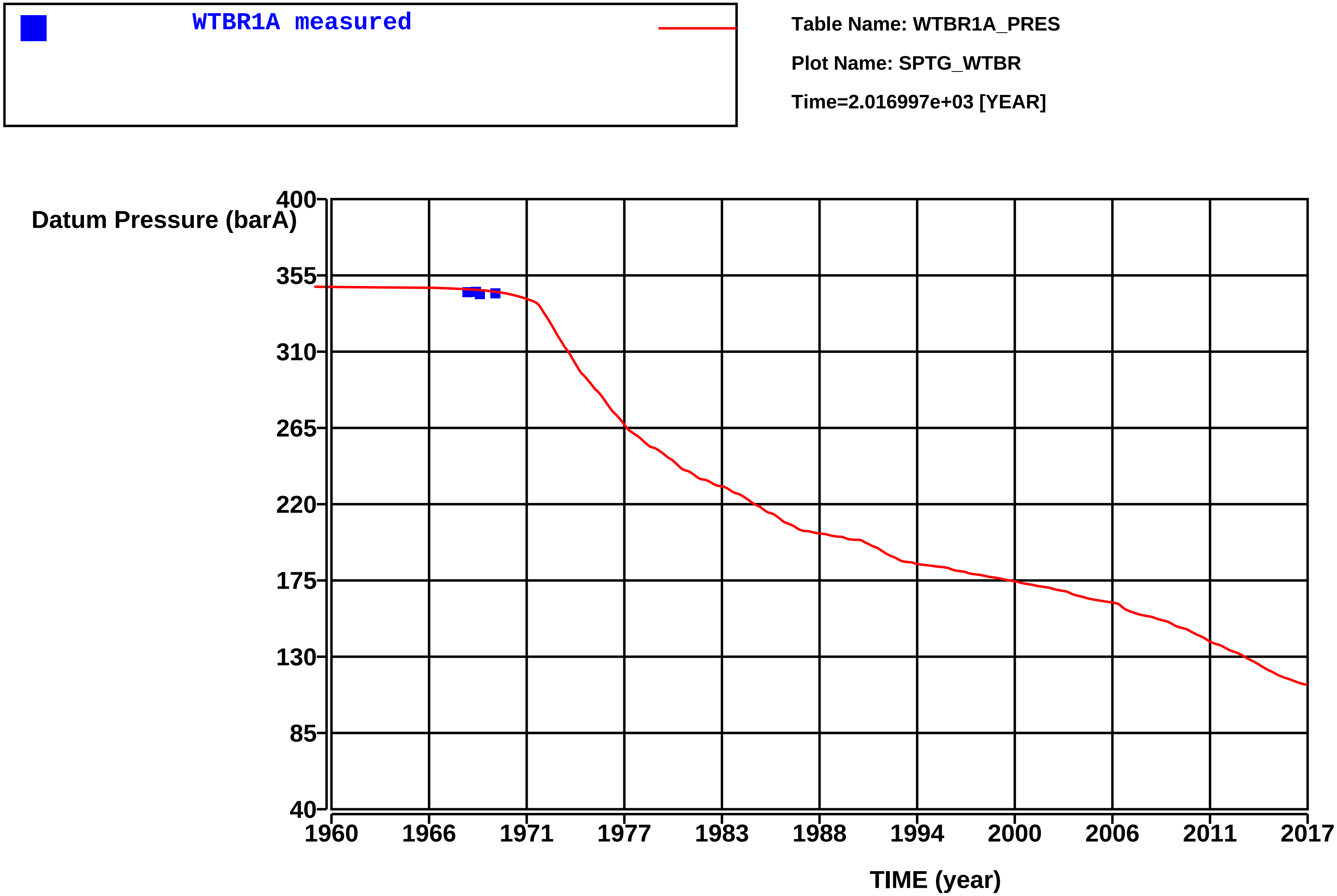

Creation date: Thu 09/02/2017 16:08
Runfile: GRO_2016_ED_v60.run

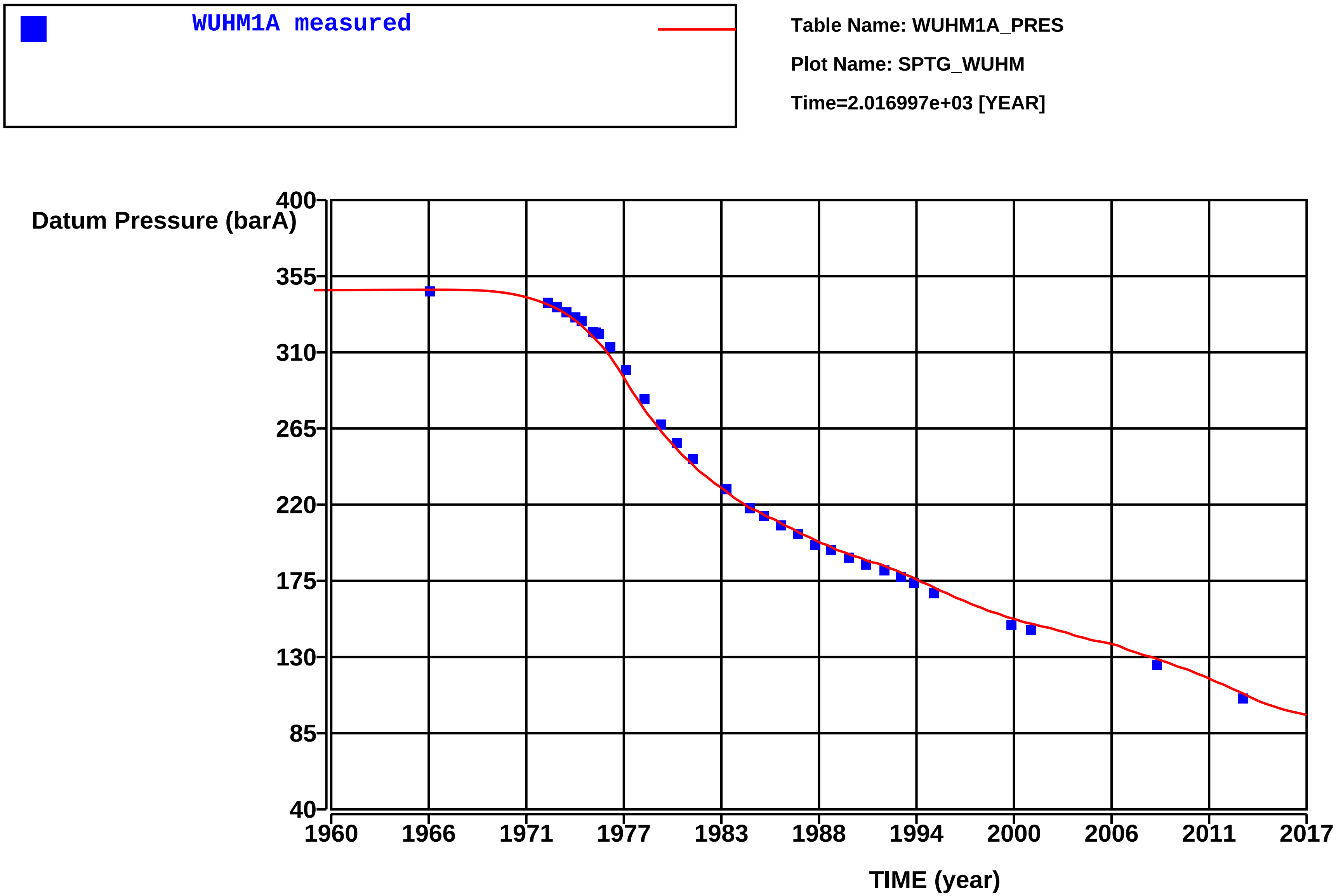

Creation date: Thu 09/02/2017 16:08
Runfile: GRO_2016_ED_v60.run

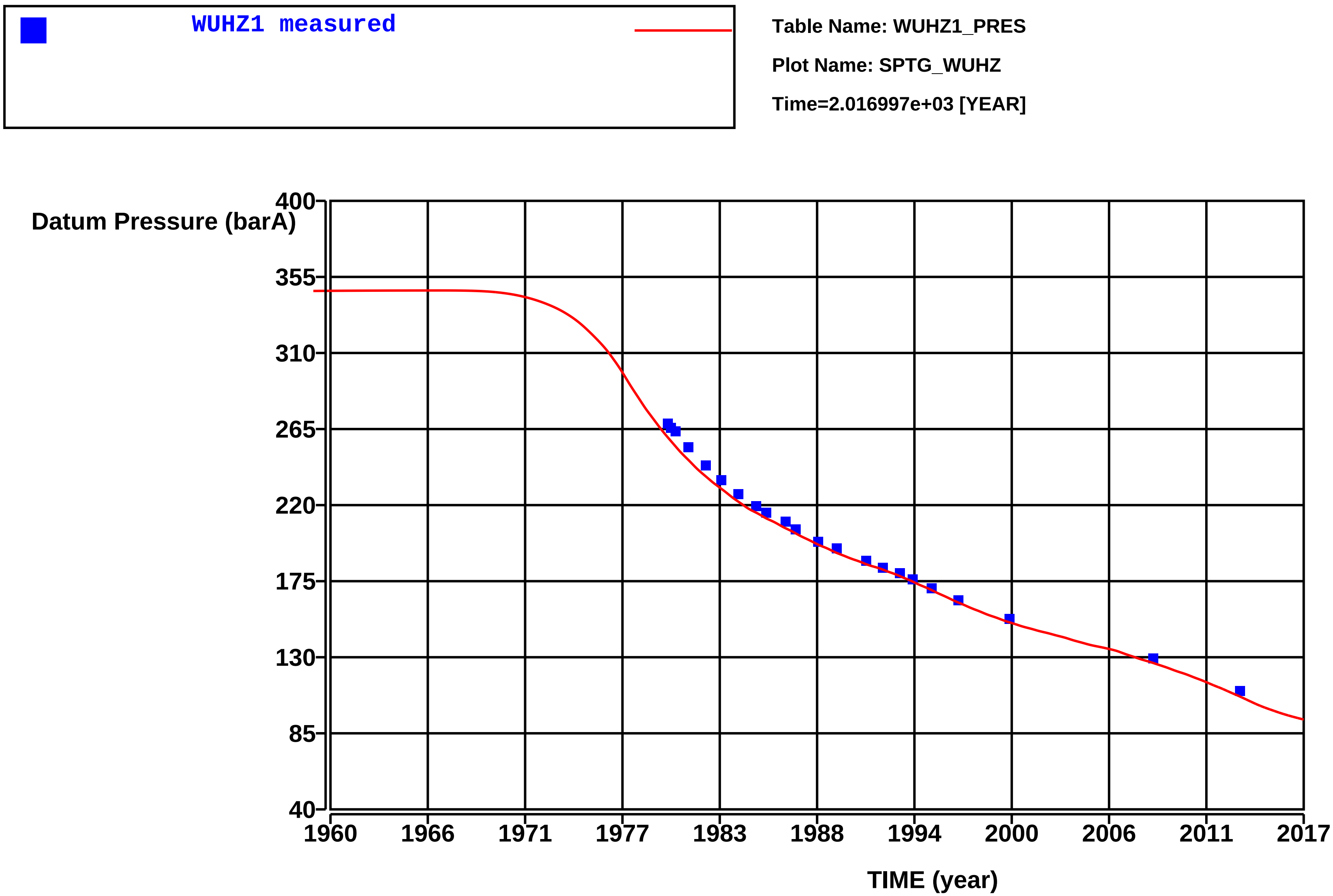

Table Name: WUHZ1_PRES

Plot Name: SPTG_WUHZ

Time=2.016997e+03 [YEAR]

Creation date: Thu 09/02/2017 16:08

Runfile: GRO_2016_ED_v60.run

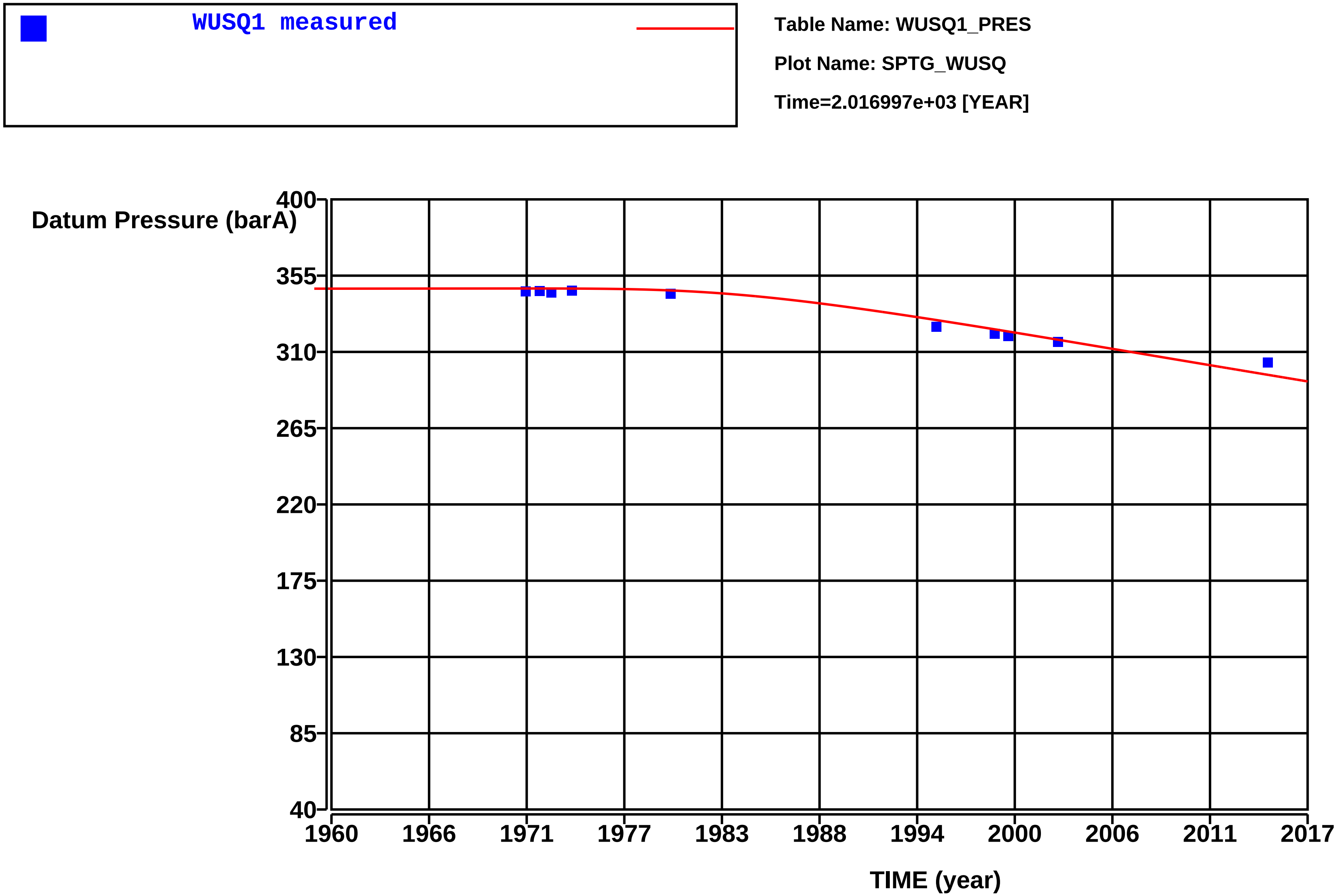

Table Name: WUSQ1_PRES

Plot Name: SPTG_WUSQ

Time=2.016997e+03 [YEAR]

Creation date: Thu 09/02/2017 16:08
Runfile: GRO_2016_ED_v60.run

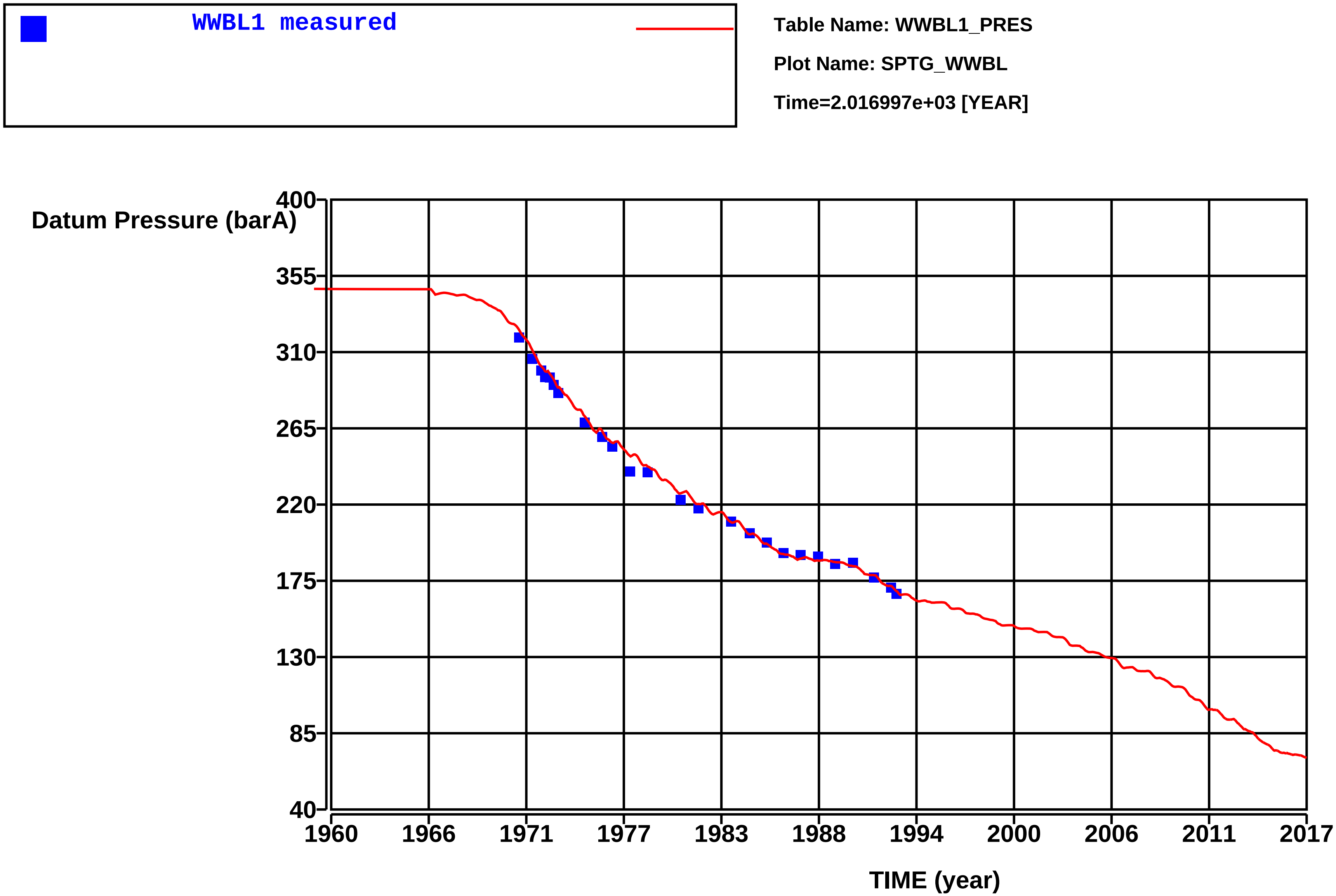

Creation date: Thu 09/02/2017 16:08
Runfile: GRO_2016_ED_v60.run

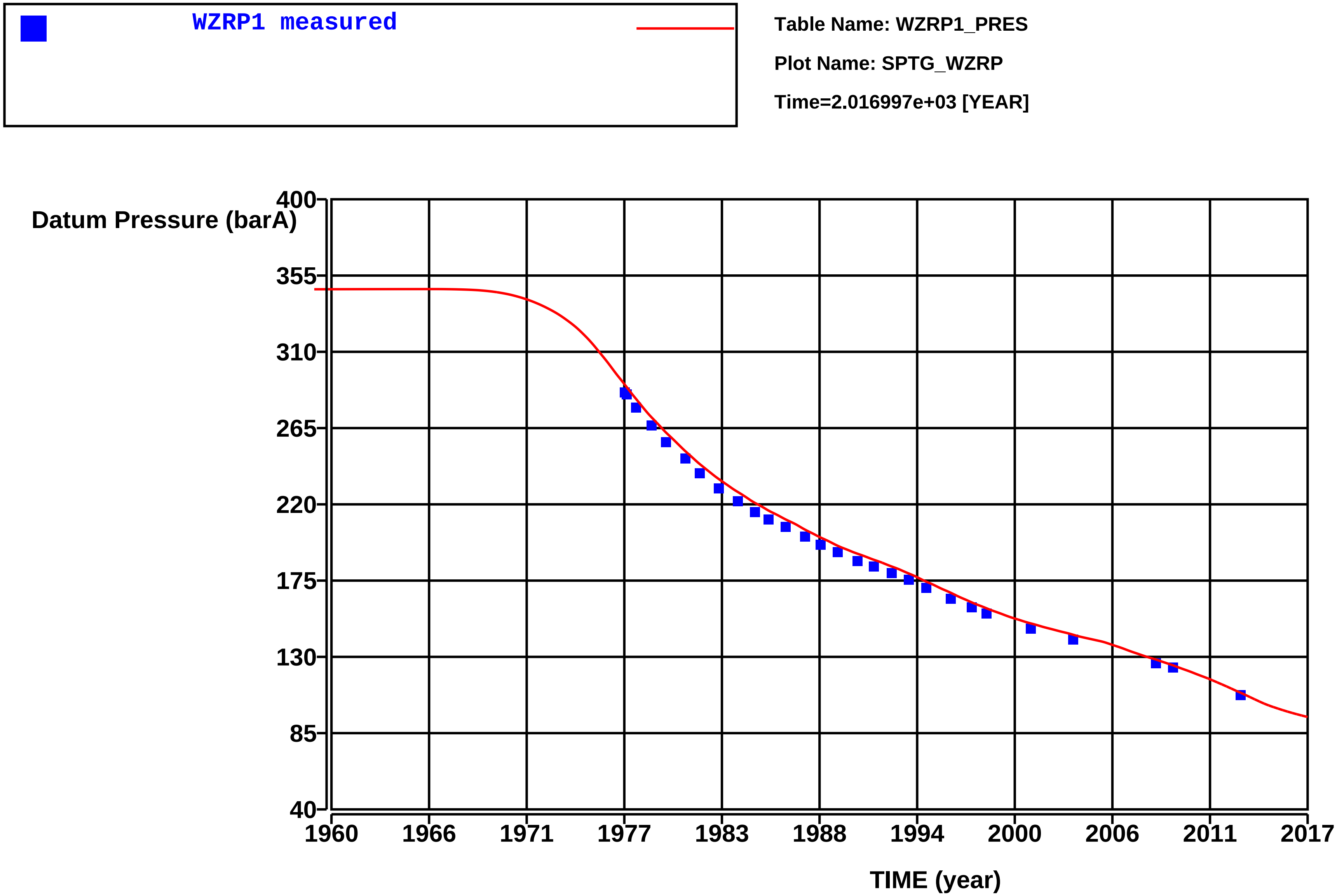

Table Name: WZRP1_PRES

Plot Name: SPTG_WZRP

Time=2.016997e+03 [YEAR]

Creation date: Thu 09/02/2017 16:08

Runfile: GRO_2016_ED_v60.run

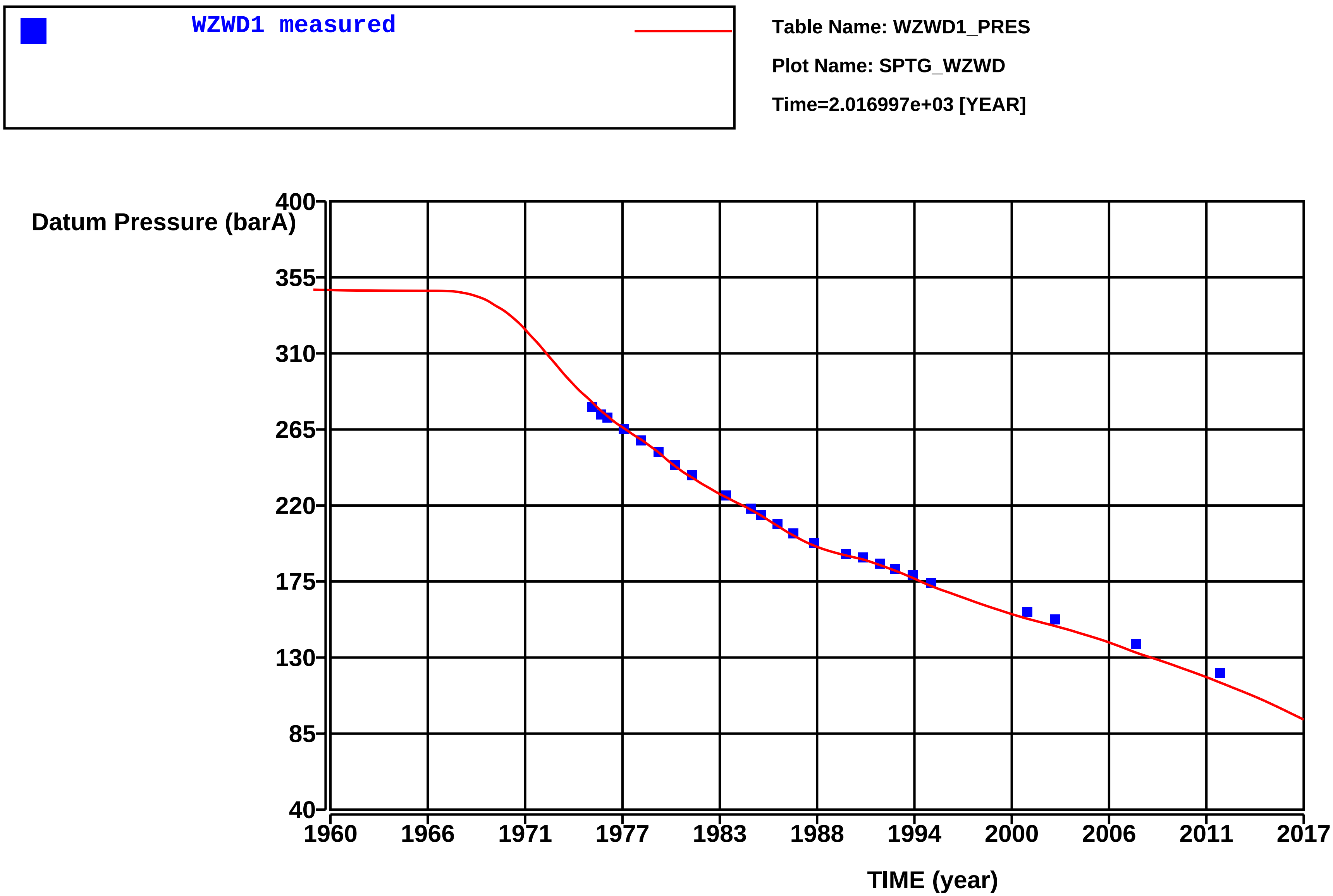

Creation date: Thu 09/02/2017 16:08
Runfile: GRO_2016_ED_v60.run

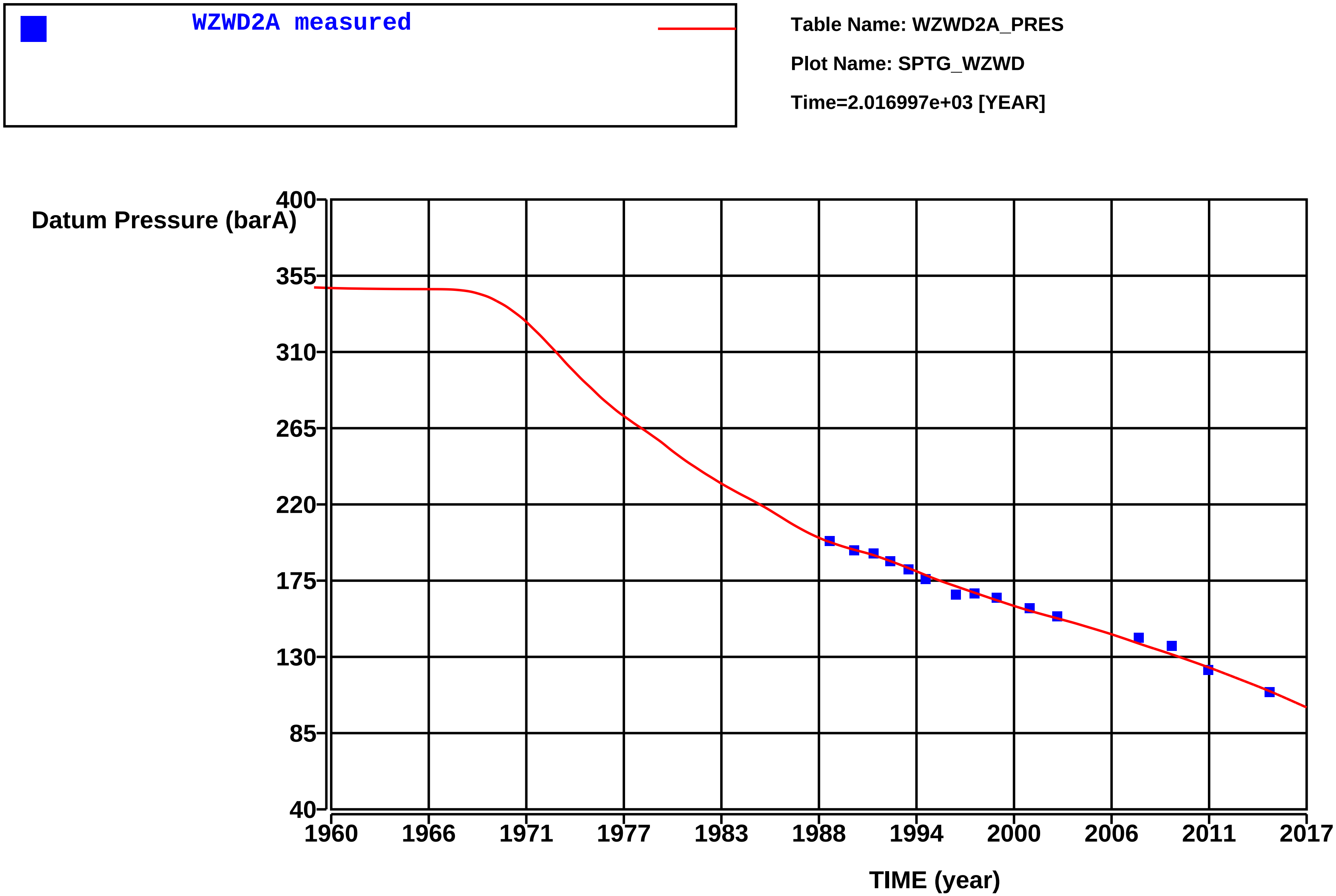

Table Name: WZWD2A_PRES
Plot Name: SPTG_WZWD
Time=2.016997e+03 [YEAR]

Creation date: Thu 09/02/2017 16:08
Runfile: GRO_2016_ED_v60.run

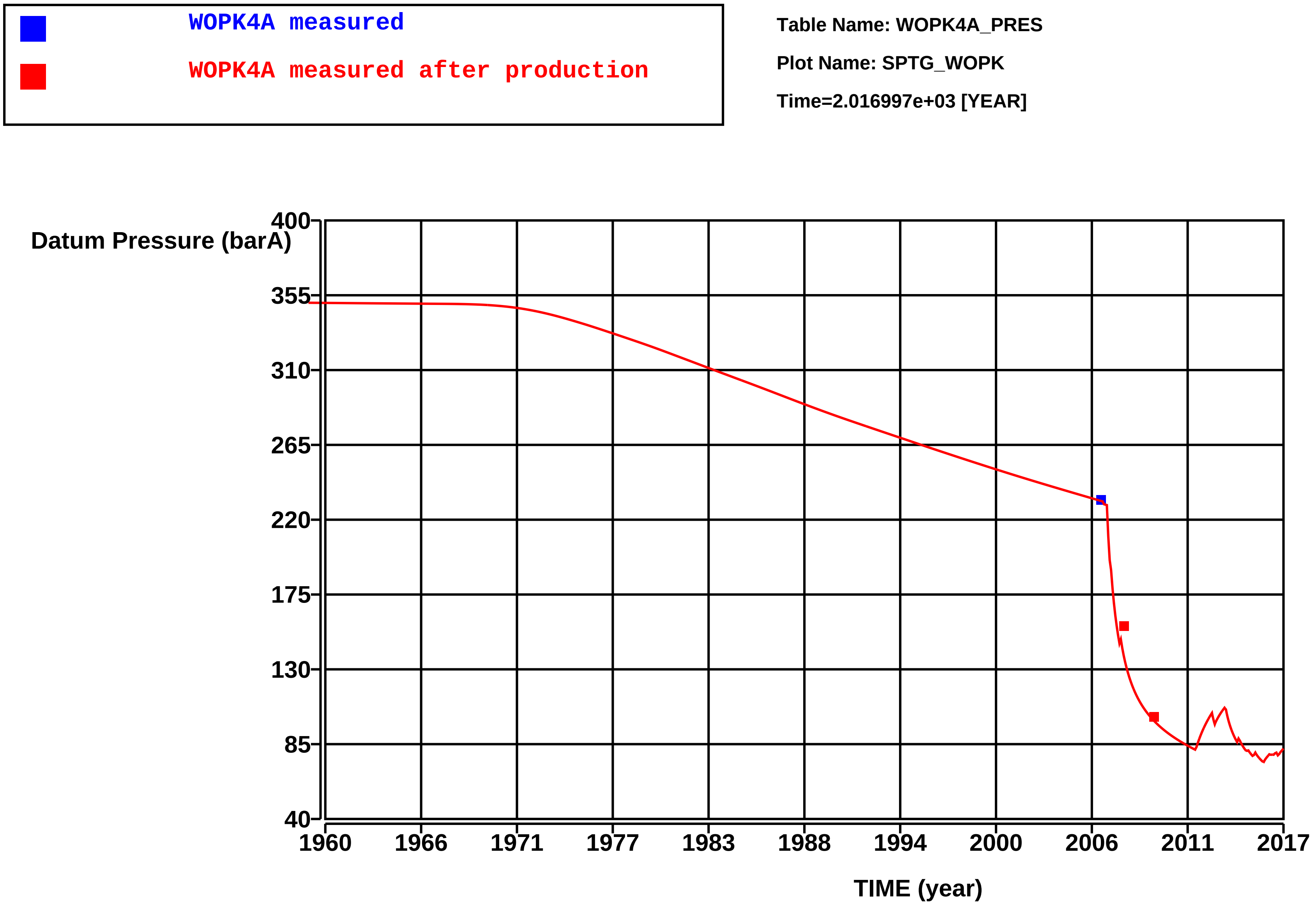

Creation date: Thu 09/02/2017 16:08
Runfile: GRO_2016_ED_v60.run

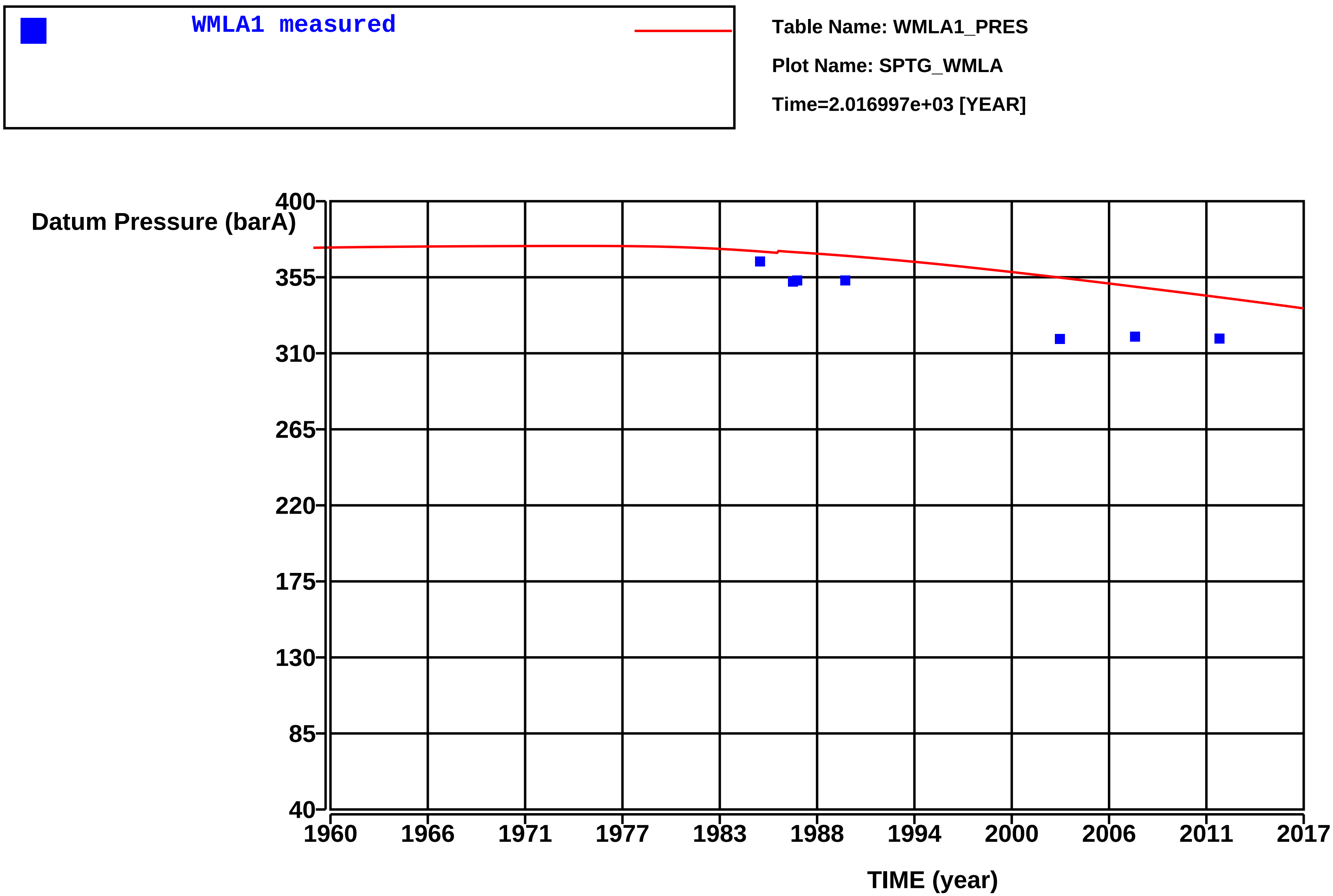

Table Name: WMLA1_PRES

Plot Name: SPTG_WMLA

Time=2.016997e+03 [YEAR]

Creation date: Thu 09/02/2017 16:08

Runfile: GRO_2016_ED_v60.run

Table Name: WBRW2_DATUM_PRESSURE

Plot Name: SPTG_WBRW

Time=2.016997e+03 [YEAR]

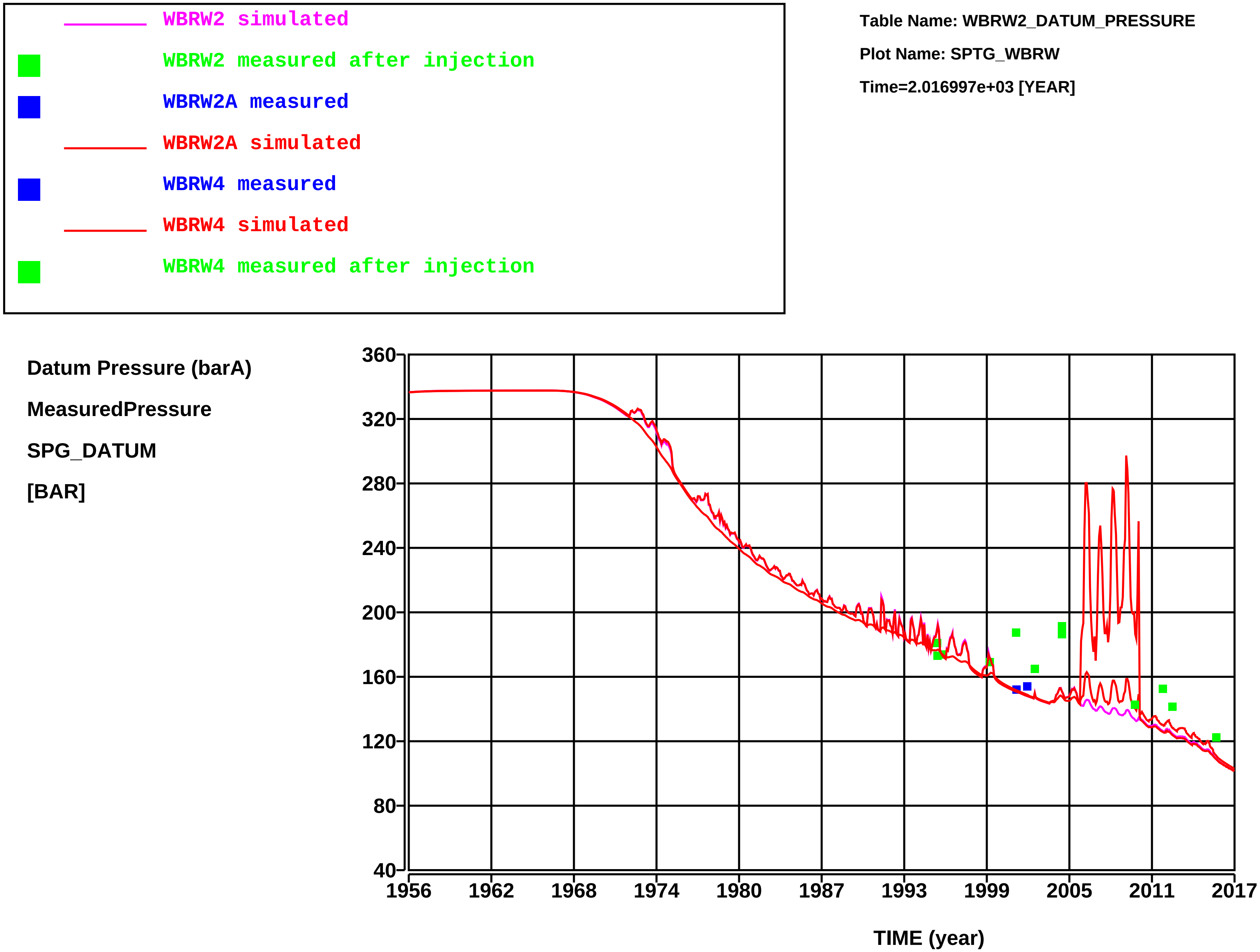

Creation date: Thu 09/02/2017 16:08

Runfile: GRO_2016_ED_v60.run

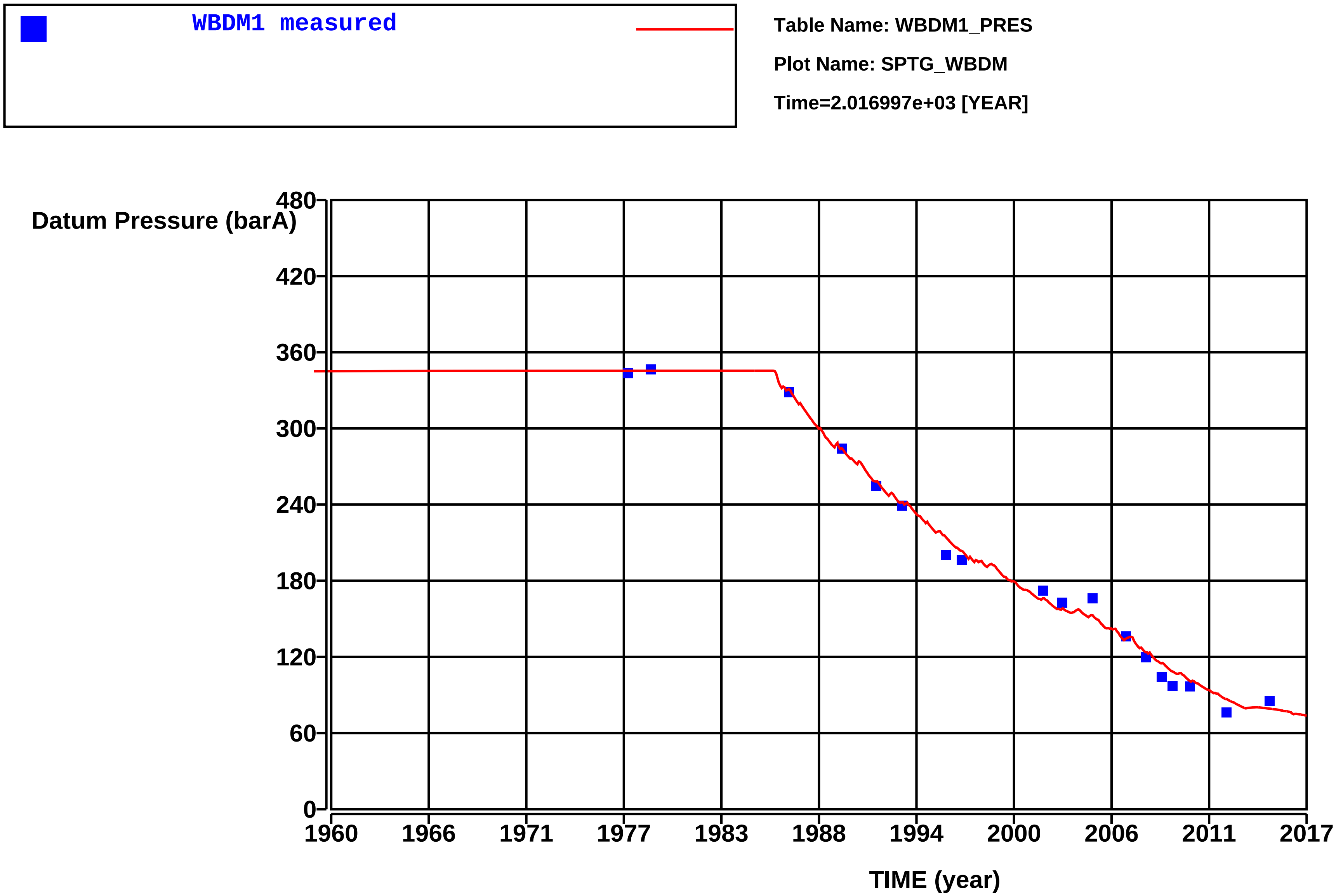

Creation date: Thu 09/02/2017 16:08
Runfile: GRO_2016_ED_v60.run

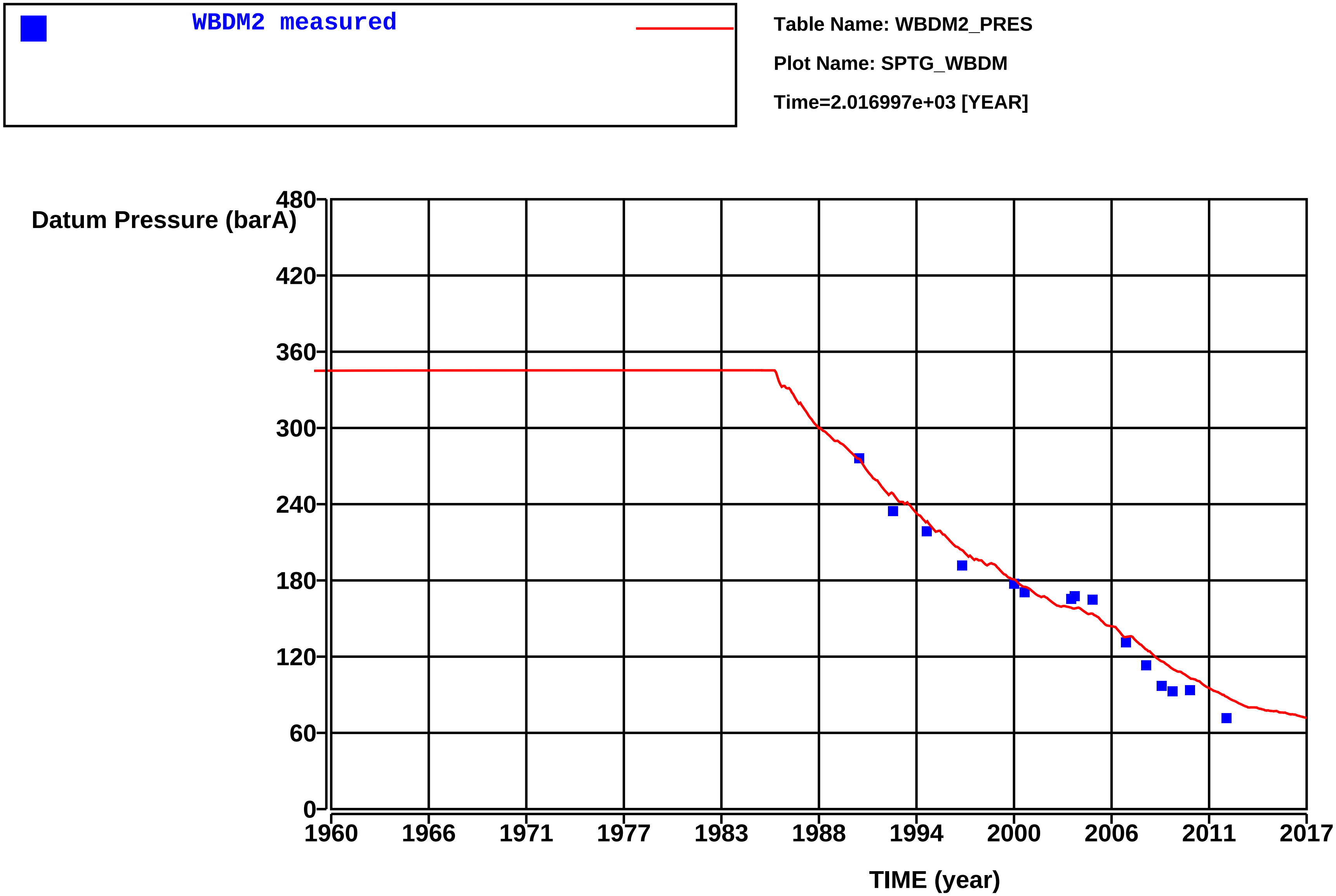

Table Name: WBDM2_PRES

Plot Name: SPTG_WBDM

Time=2.016997e+03 [YEAR]

Creation date: Thu 09/02/2017 16:08

Runfile: GRO_2016_ED_v60.run

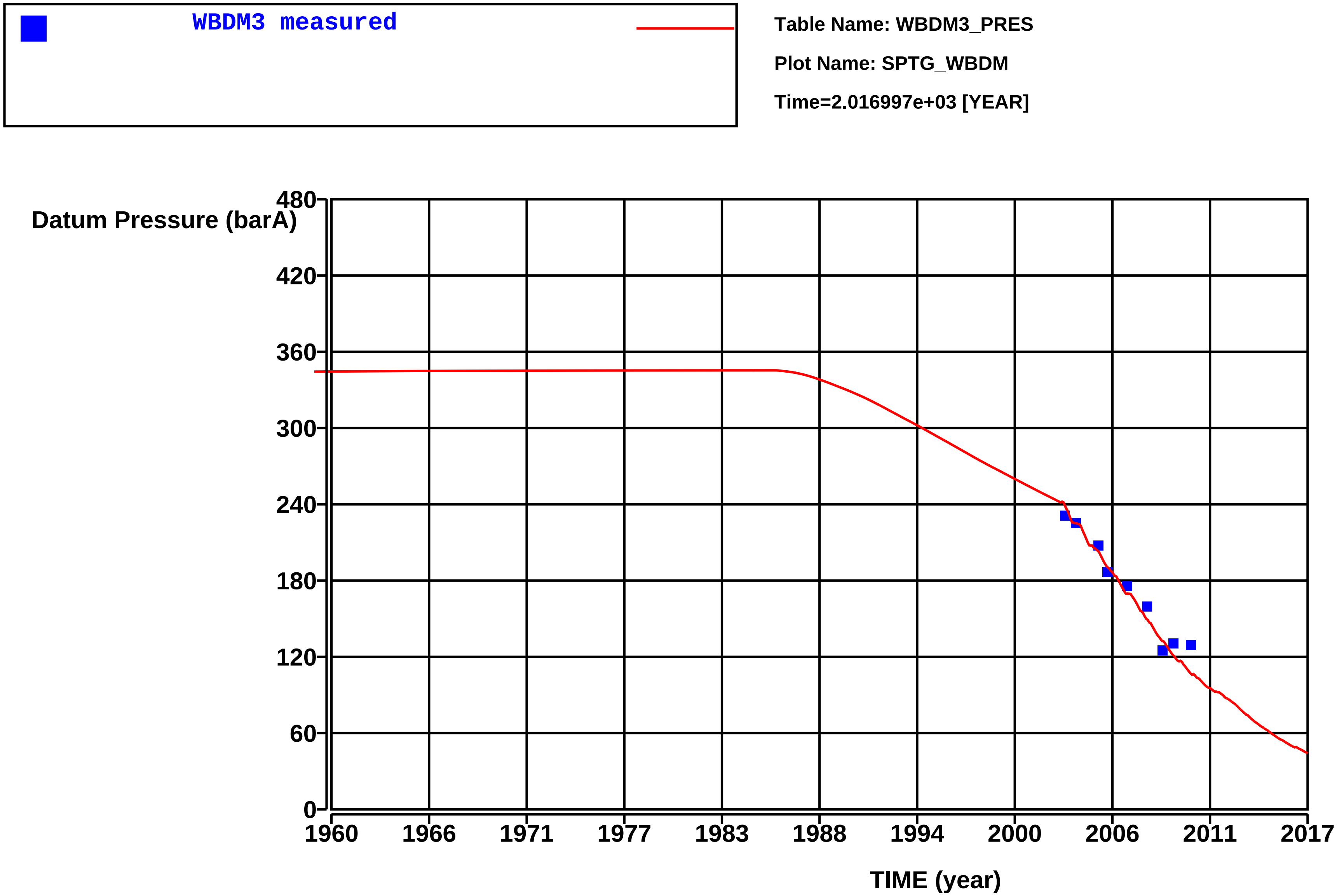

Table Name: WBDM3_PRES

Plot Name: SPTG_WBDM

Time=2.016997e+03 [YEAR]

Creation date: Thu 09/02/2017 16:08

Runfile: GRO_2016_ED_v60.run

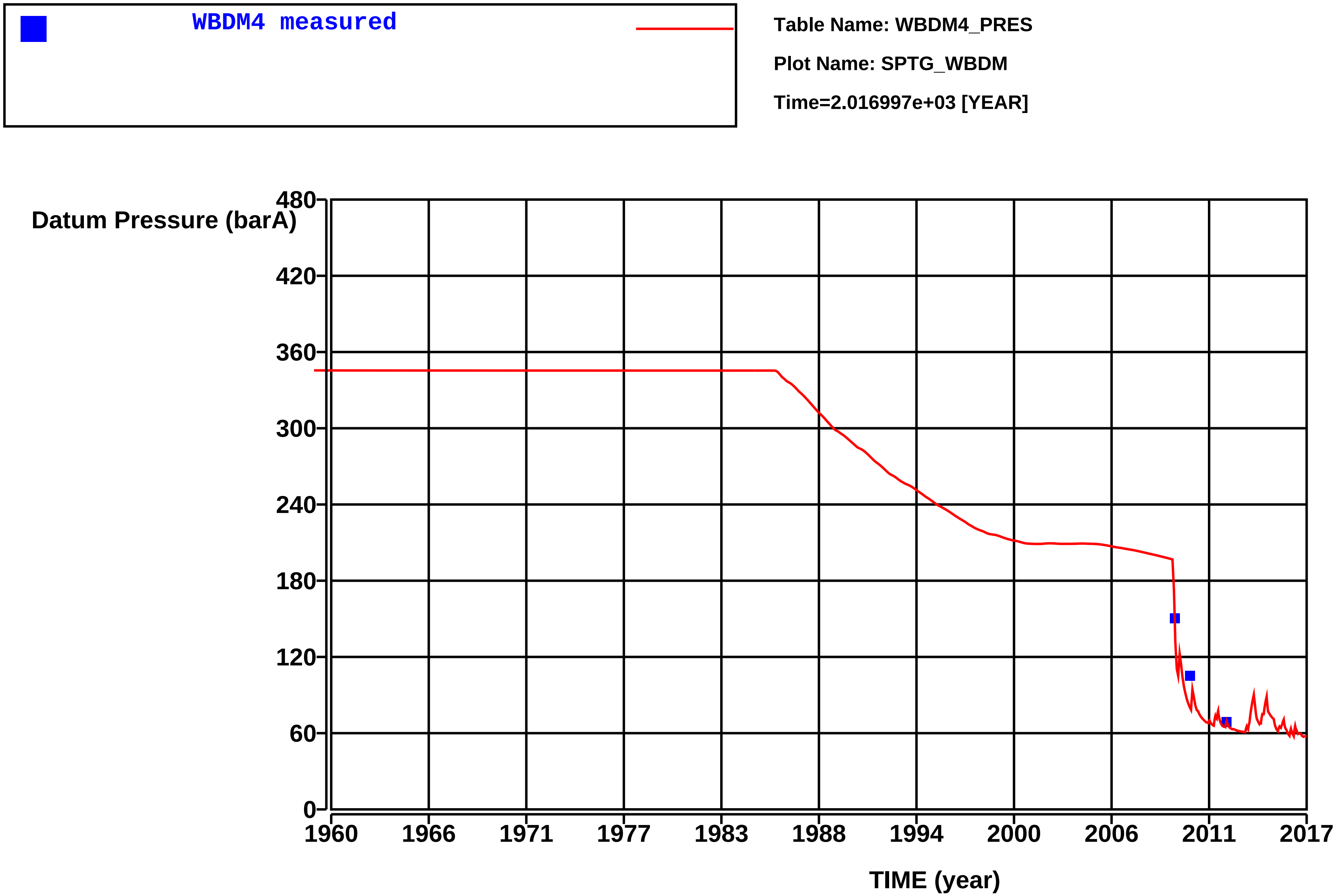

Creation date: Thu 09/02/2017 16:08
Runfile: GRO_2016_ED_v60.run

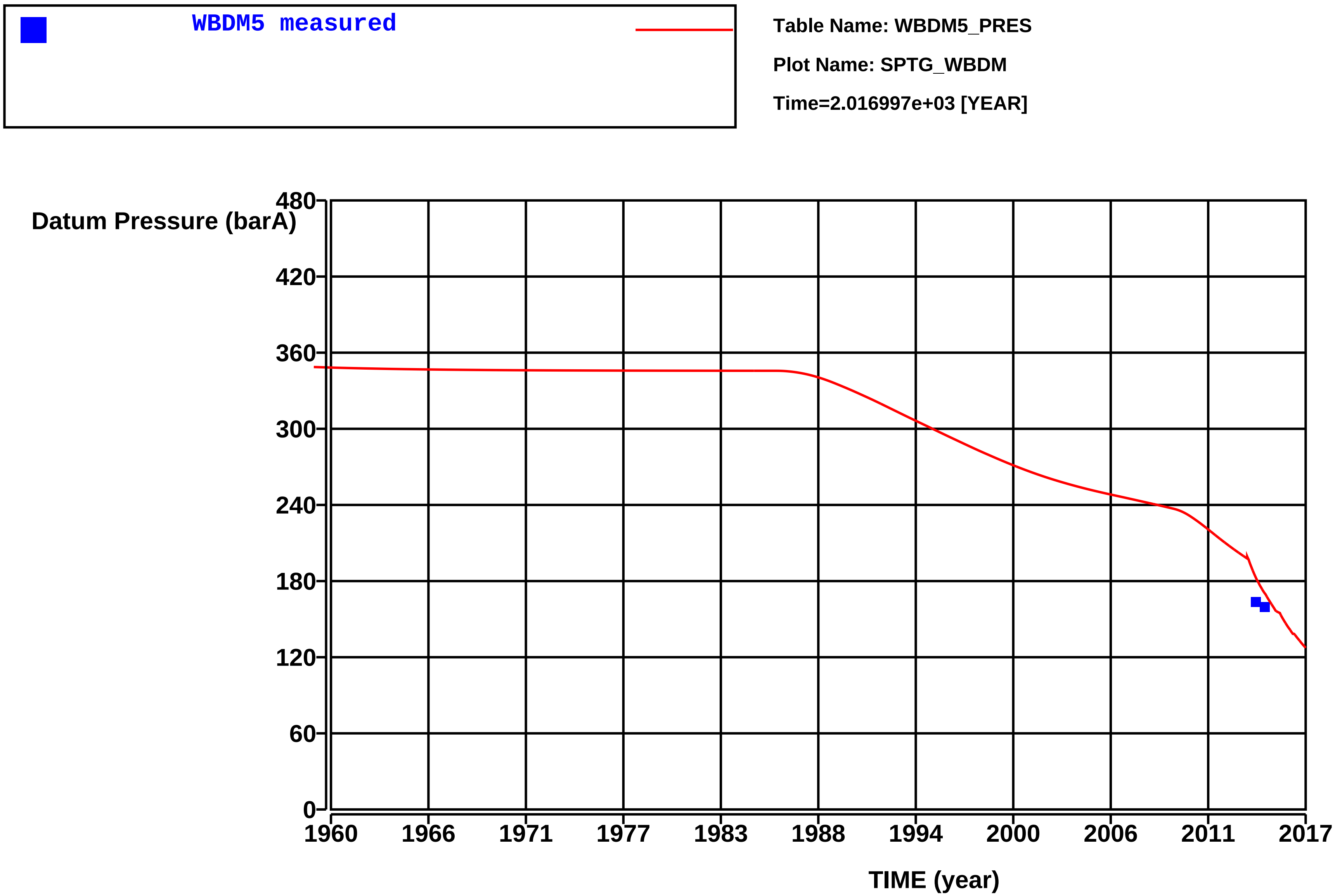

Creation date: Thu 09/02/2017 16:08
Runfile: GRO_2016_ED_v60.run

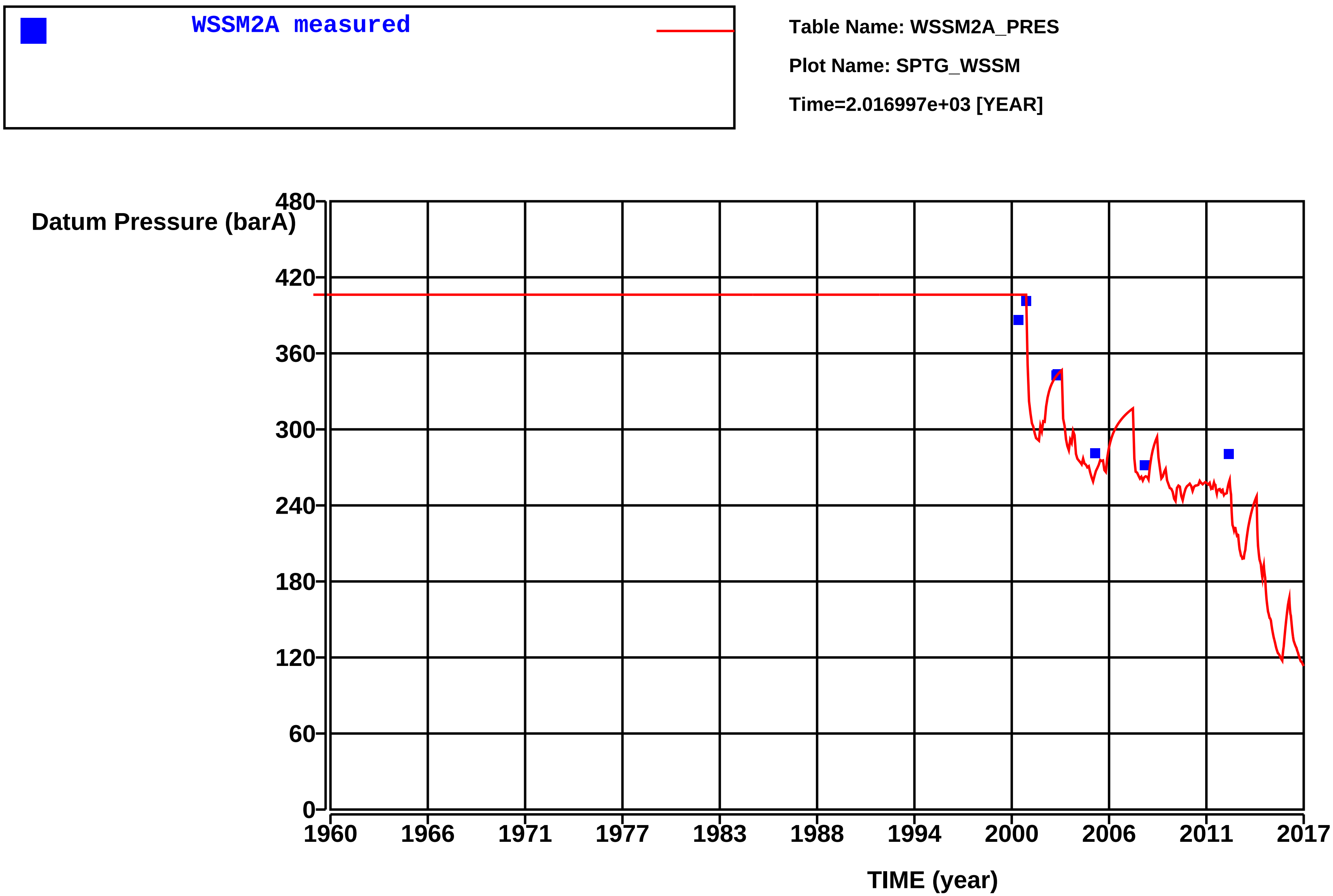

Creation date: Thu 09/02/2017 16:08

Runfile: GRO_2016_ED_v60.run

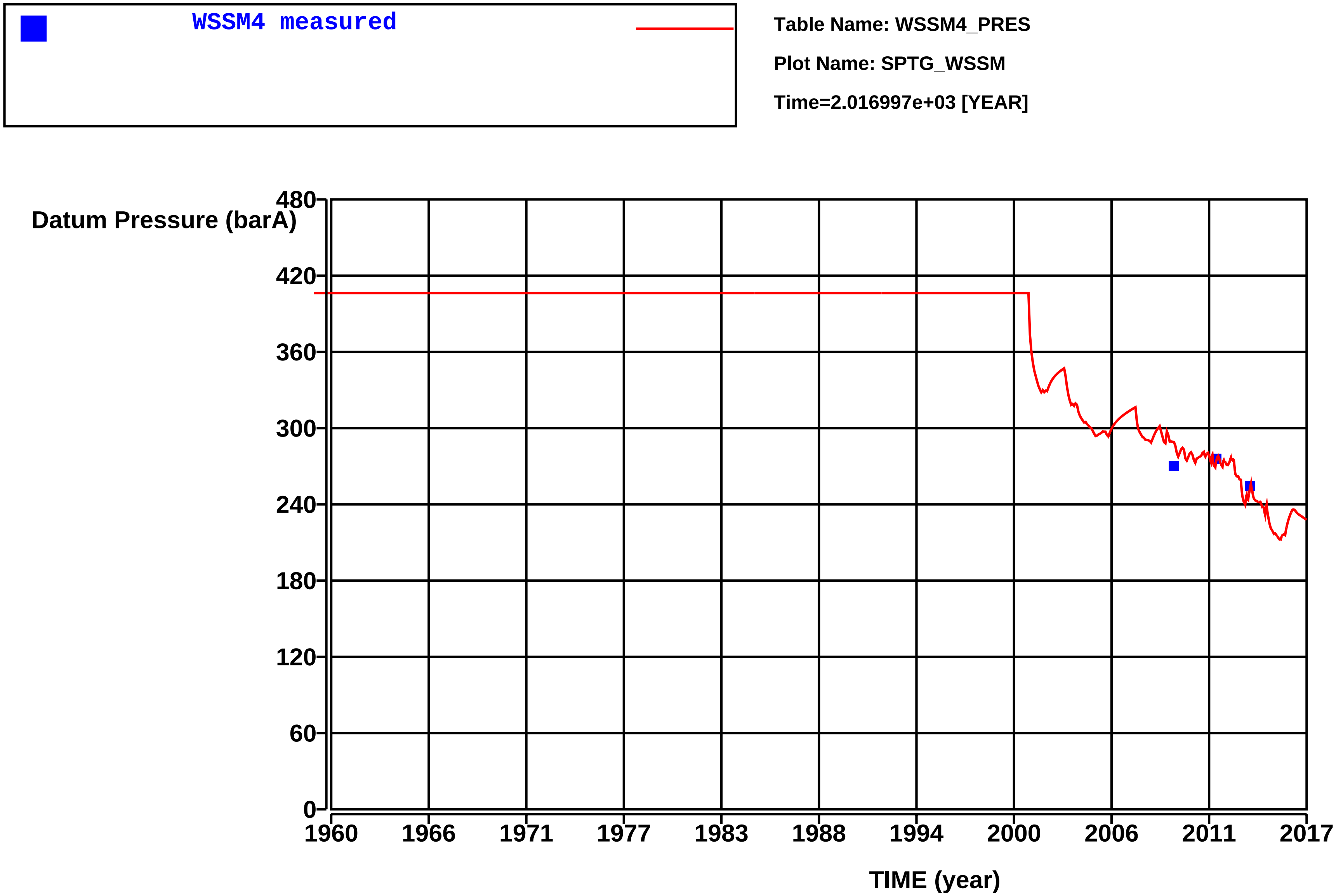

Creation date: Thu 09/02/2017 16:08
Runfile: GRO_2016_ED_v60.run

WKWR1A measured

Table Name: WKWR1A_PRES

Plot Name: SPTG_WKWR

Time=2.016997e+03 [YEAR]

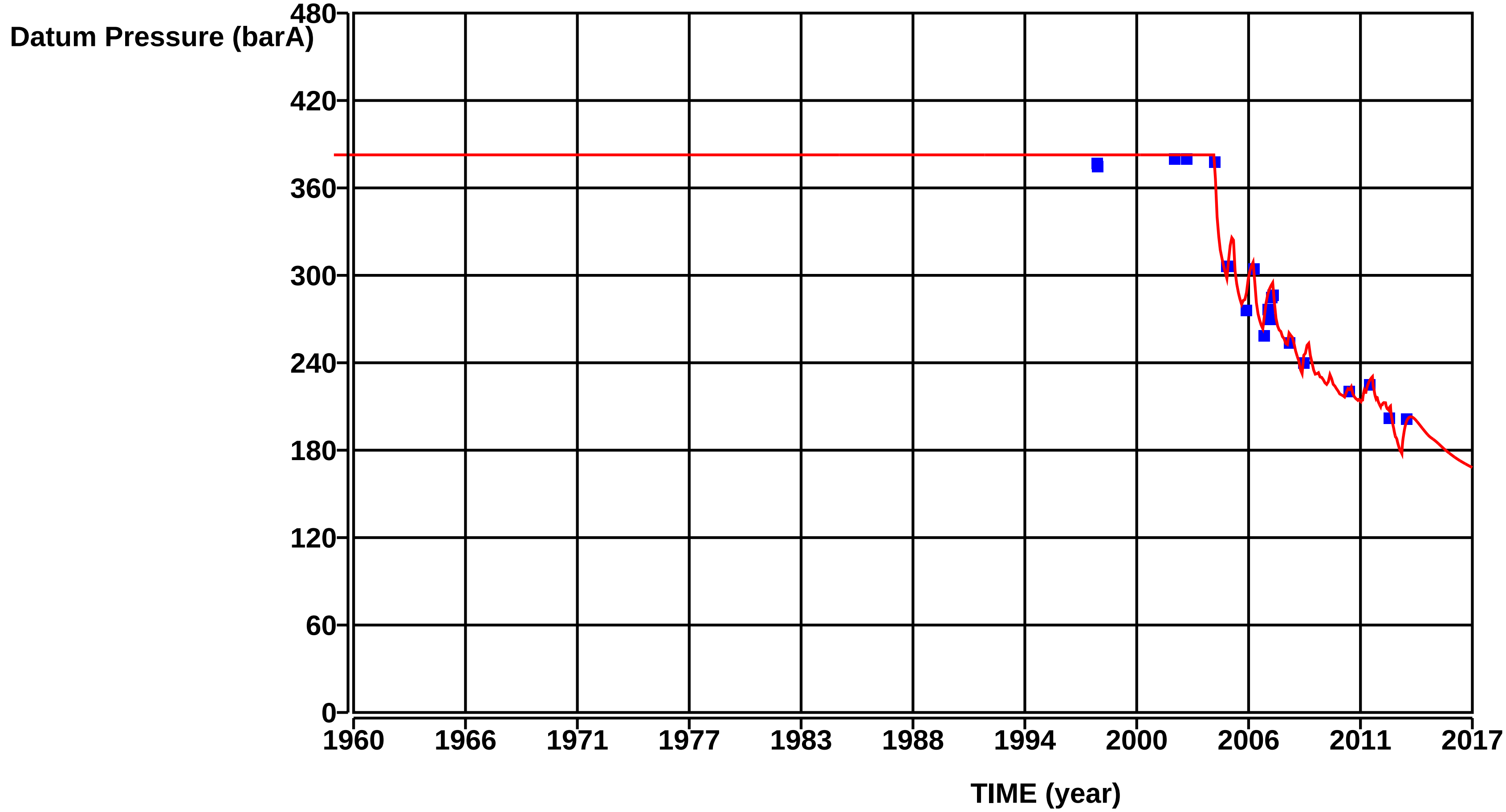

Creation date: Thu 09/02/2017 16:08

Runfile: GRO_2016_ED_v60.run

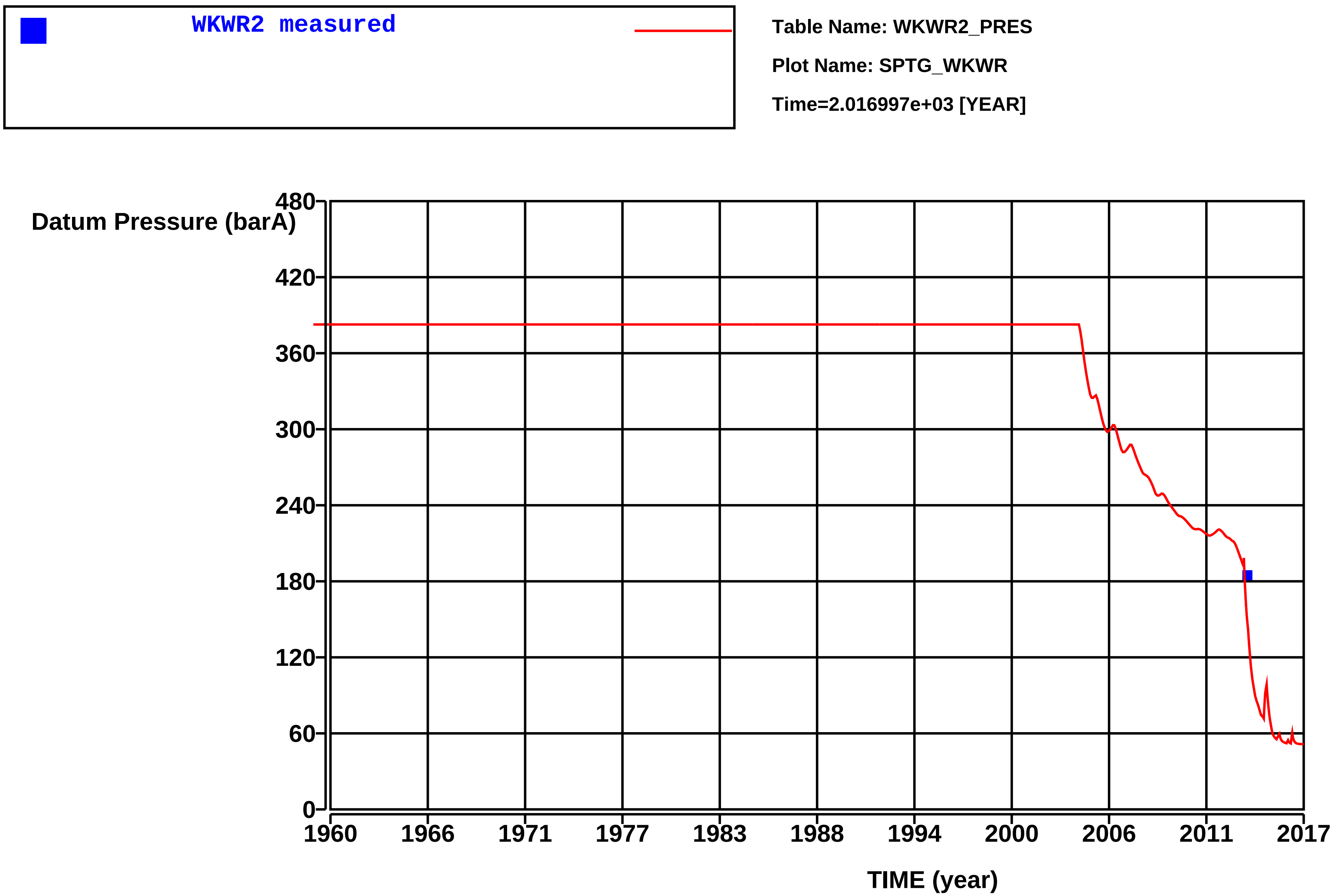

Creation date: Thu 09/02/2017 16:08

Runfile: GRO_2016_ED_v60.run

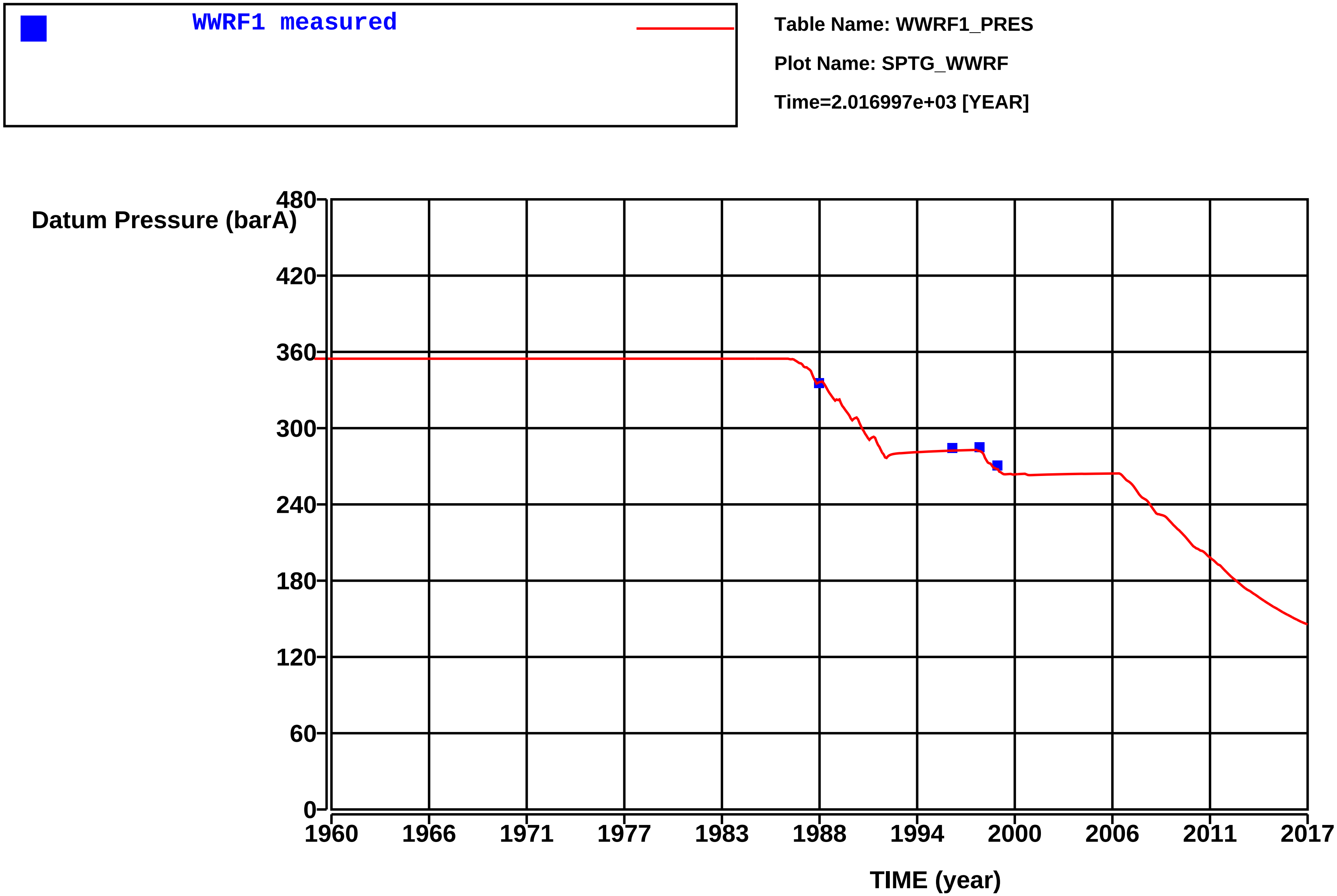

Creation date: Thu 09/02/2017 16:08
Runfile: GRO_2016_ED_v60.run

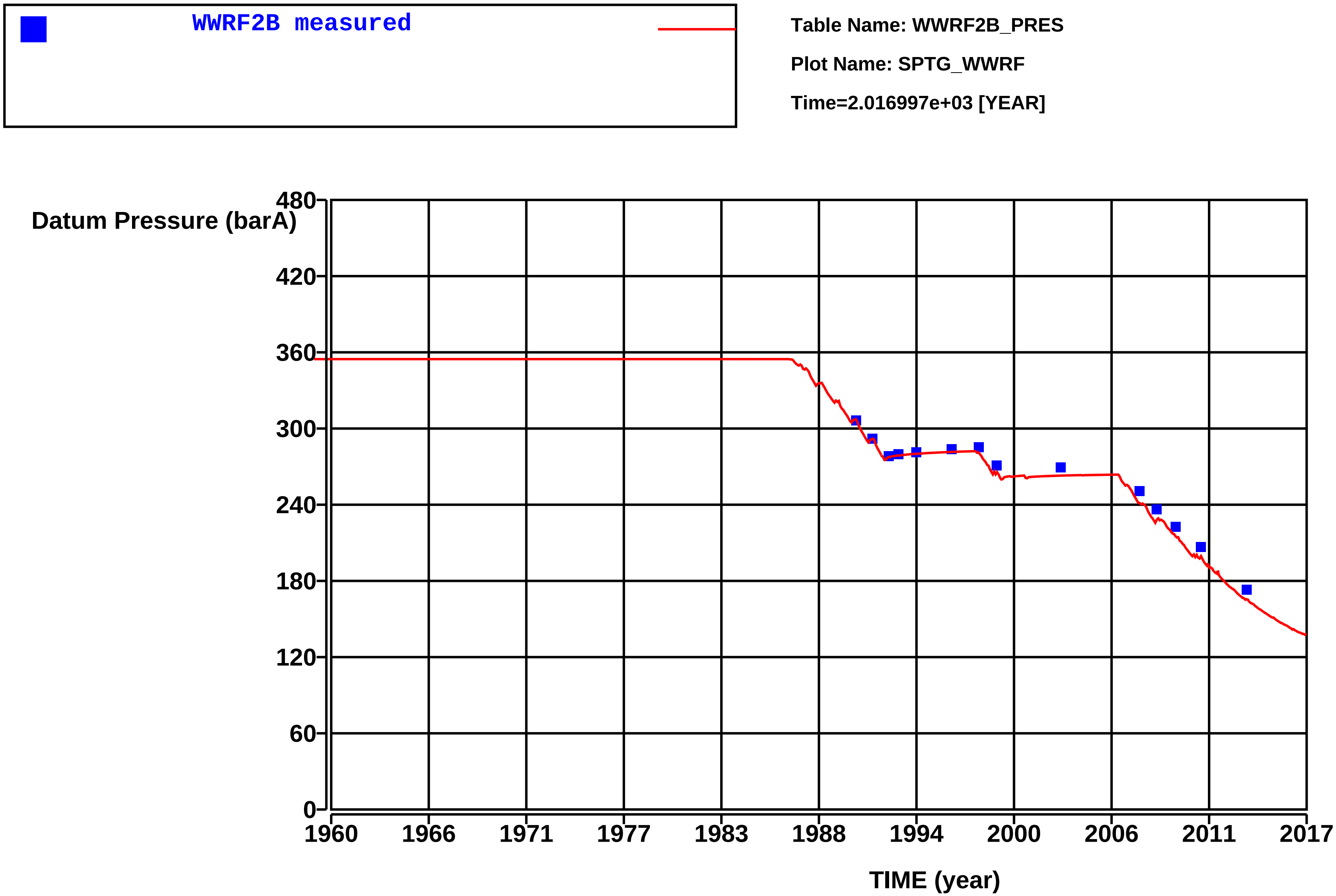

Creation date: Thu 09/02/2017 16:08
Runfile: GRO_2016_ED_v60.run

Table Name: WSAU1_RFT_Pseudo_Log

Plot Name: RFT_WSAU1

Time=2.016997e+03 [YEAR]

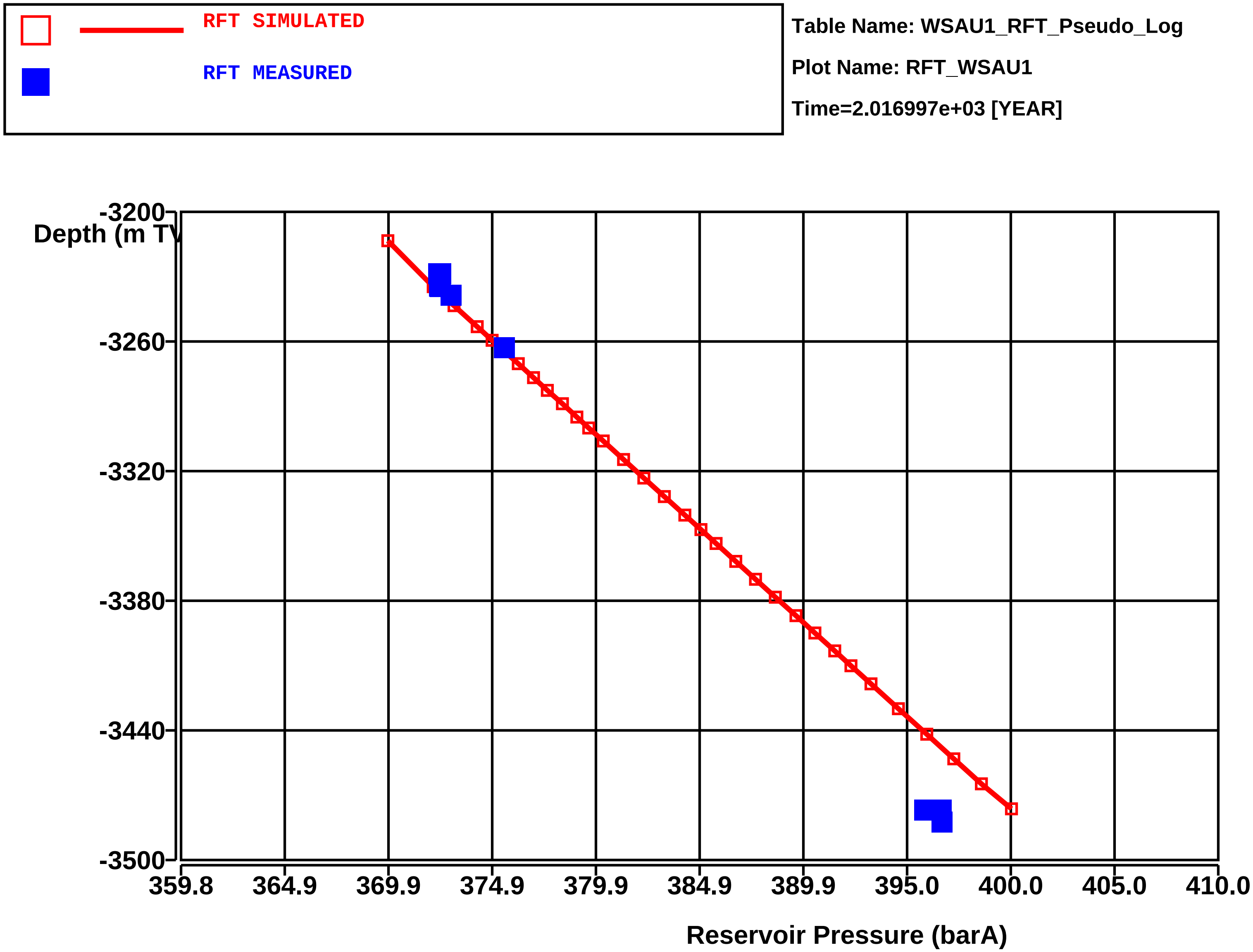

Creation date: Thu 09/02/2017 16:08

Runfile: GRO_2016_ED_v60.run

Table Name: WRAN1_RFT_Pseudo_Log

Plot Name: RFT_WRAN1

Time=2.016997e+03 [YEAR]

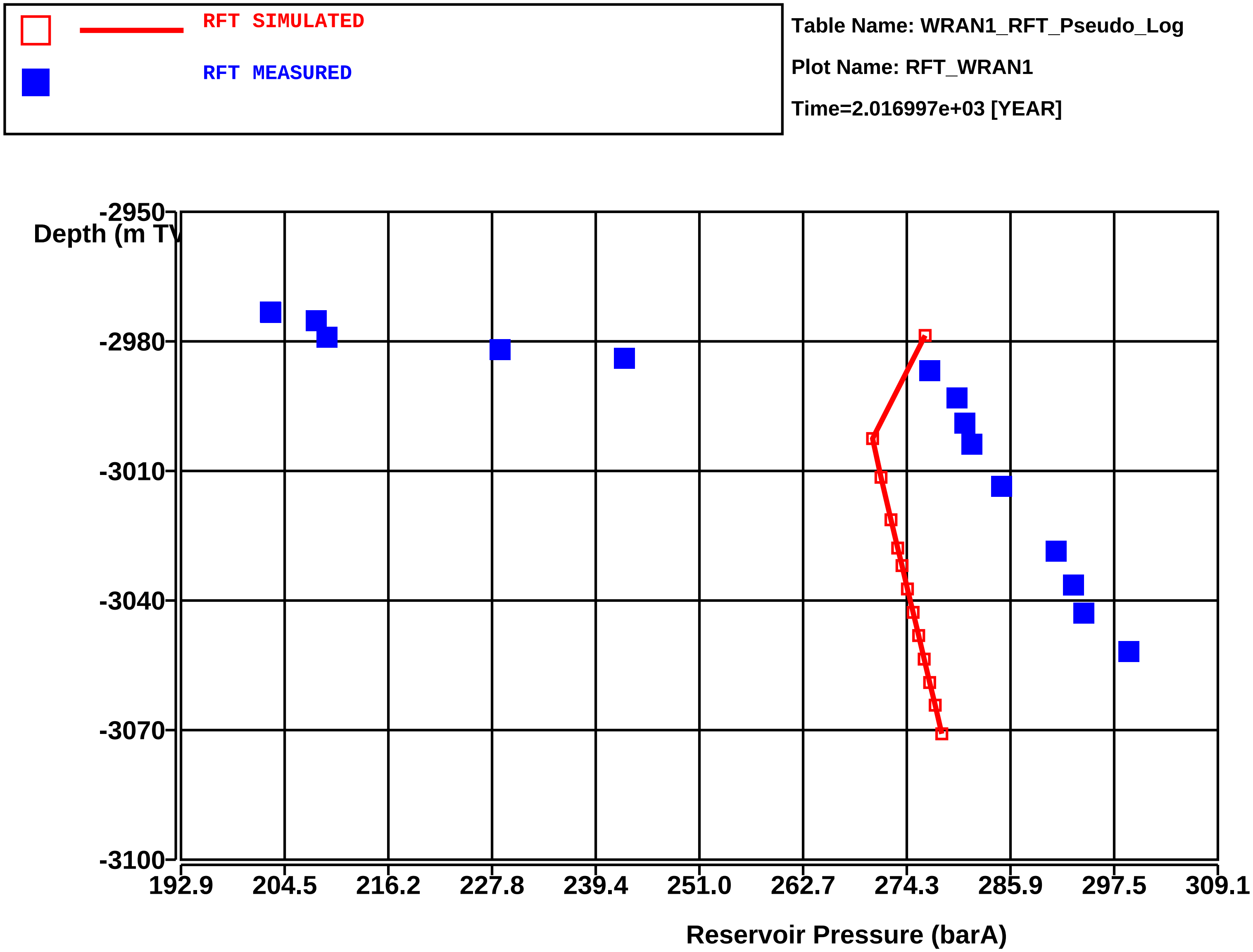

Creation date: Thu 09/02/2017 16:08

Runfile: GRO_2016_ED_v60.run

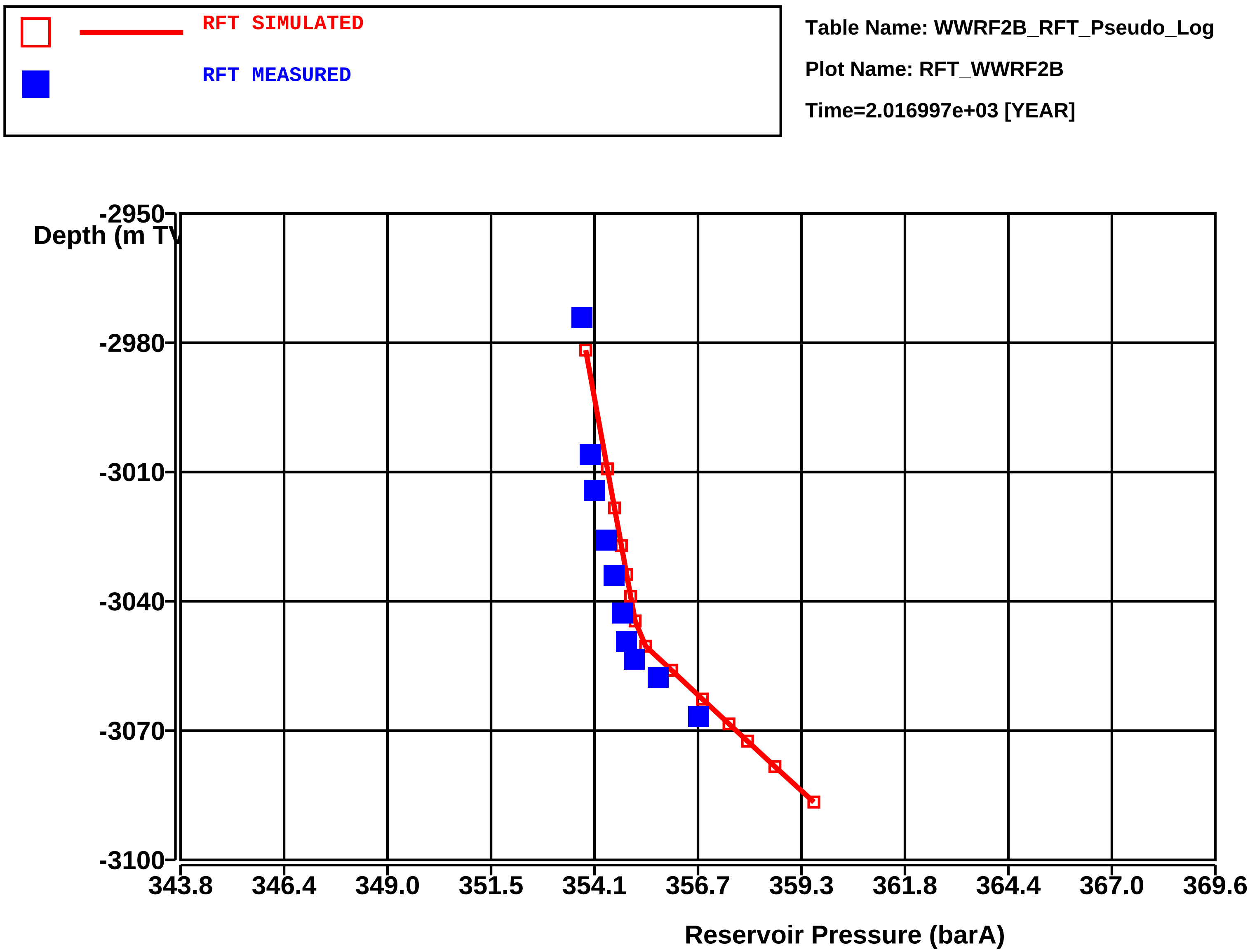

Creation date: Thu 09/02/2017 16:08
Runfile: GRO_2016_ED_v60.run

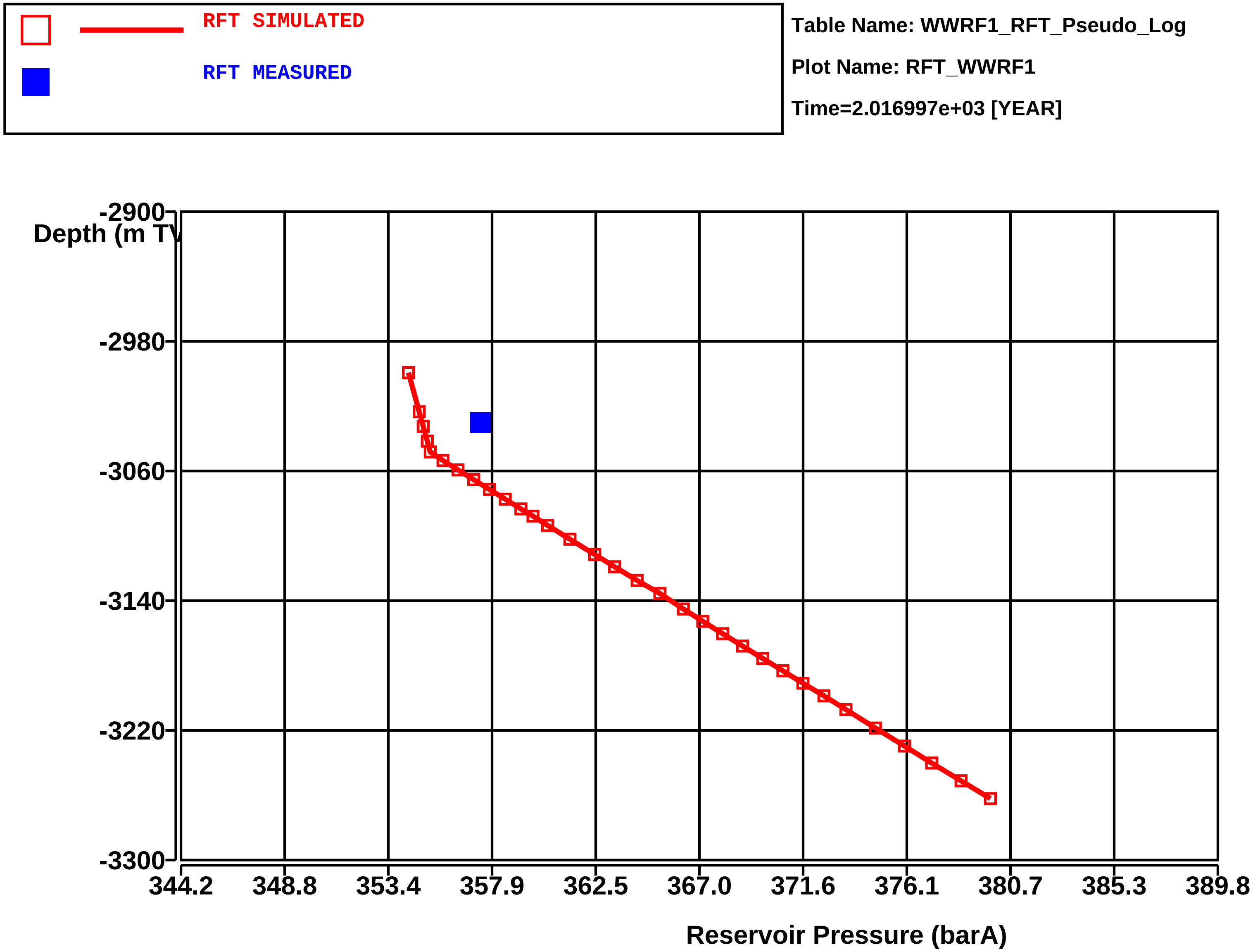

Table Name: WWRF1_RFT_Pseudo_Log

Plot Name: RFT_WWRF1

Time=2.016997e+03 [YEAR]

Creation date: Thu 09/02/2017 16:08

Runfile: GRO_2016_ED_v60.run

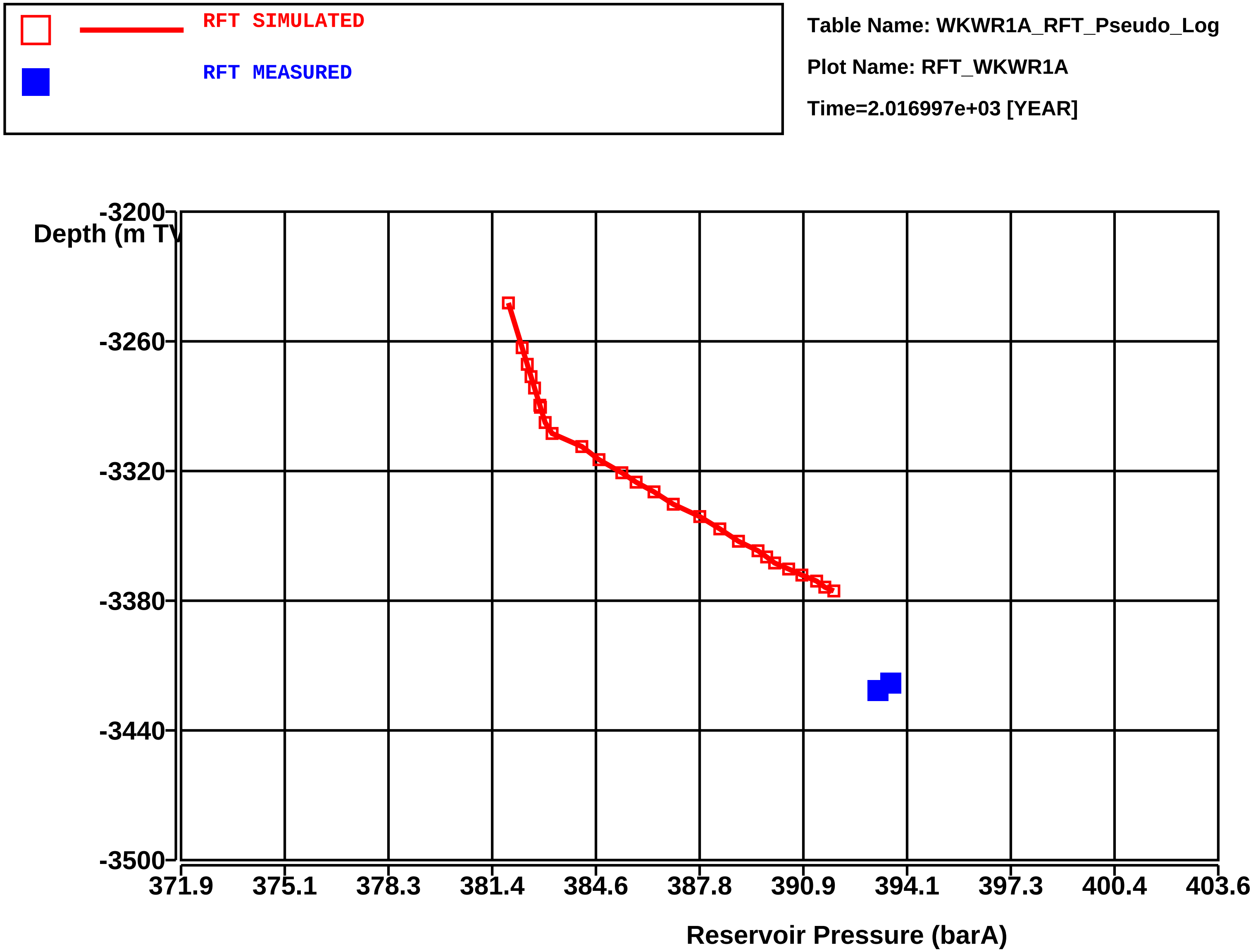

Creation date: Thu 09/02/2017 16:08
Runfile: GRO_2016_ED_v60.run

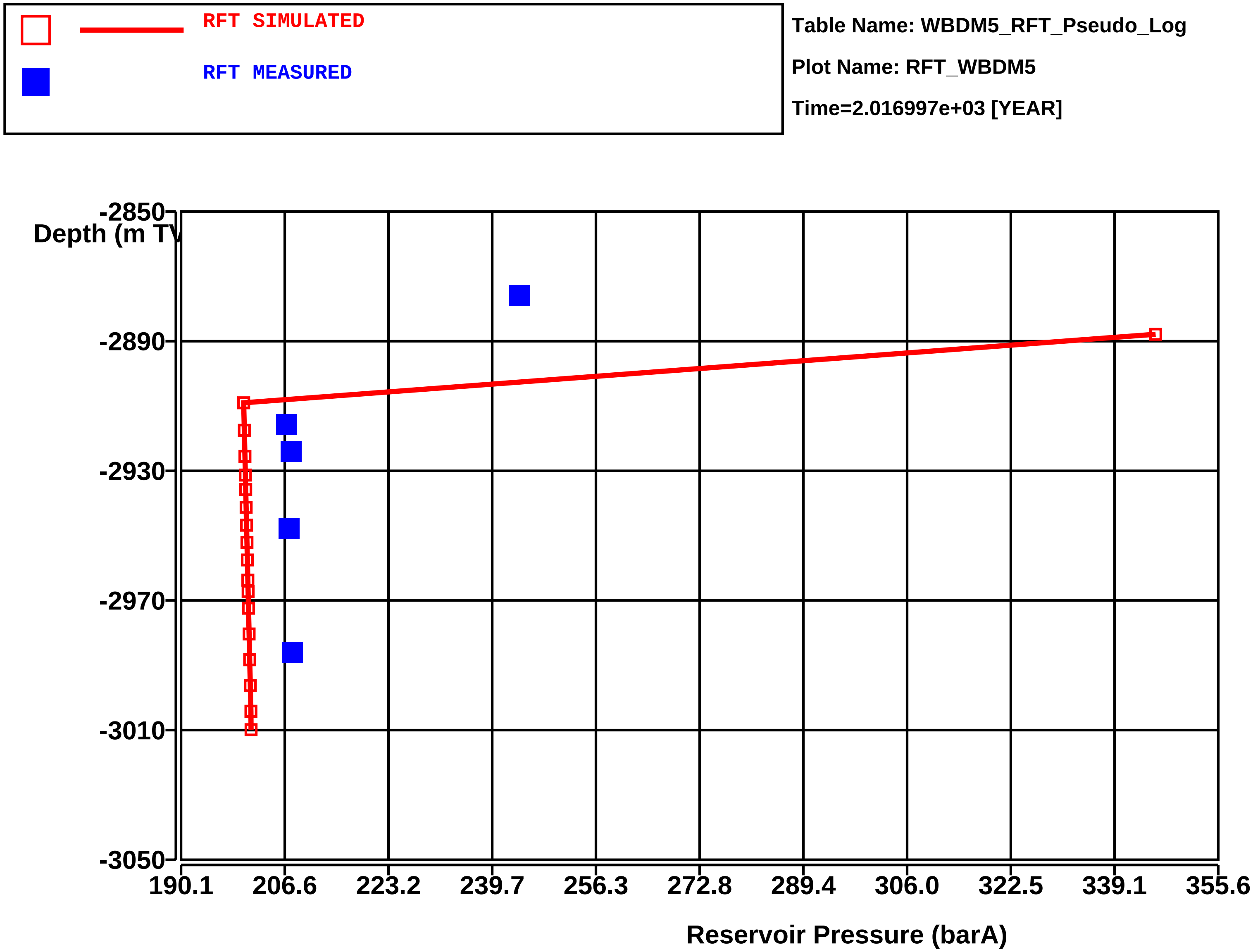

Table Name: WBDM5_RFT_Pseudo_Log

Plot Name: RFT_WBDM5

Time=2.016997e+03 [YEAR]

Creation date: Thu 09/02/2017 16:08

Runfile: GRO_2016_ED_v60.run

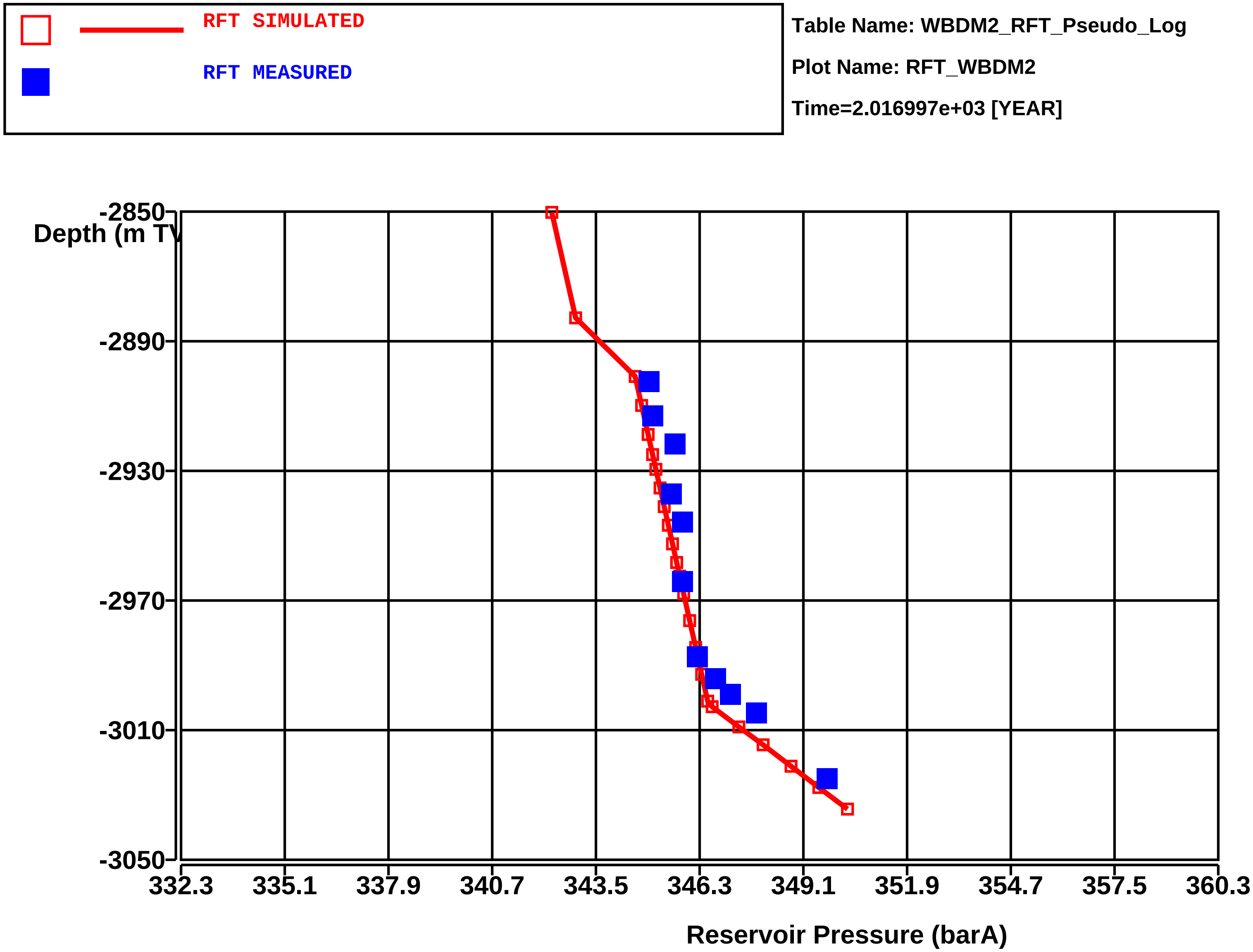

Table Name: WBDM2_RFT_Pseudo_Log

Plot Name: RFT_WBDM2

Time=2.016997e+03 [YEAR]

Creation date: Thu 09/02/2017 16:08

Runfile: GRO_2016_ED_v60.run

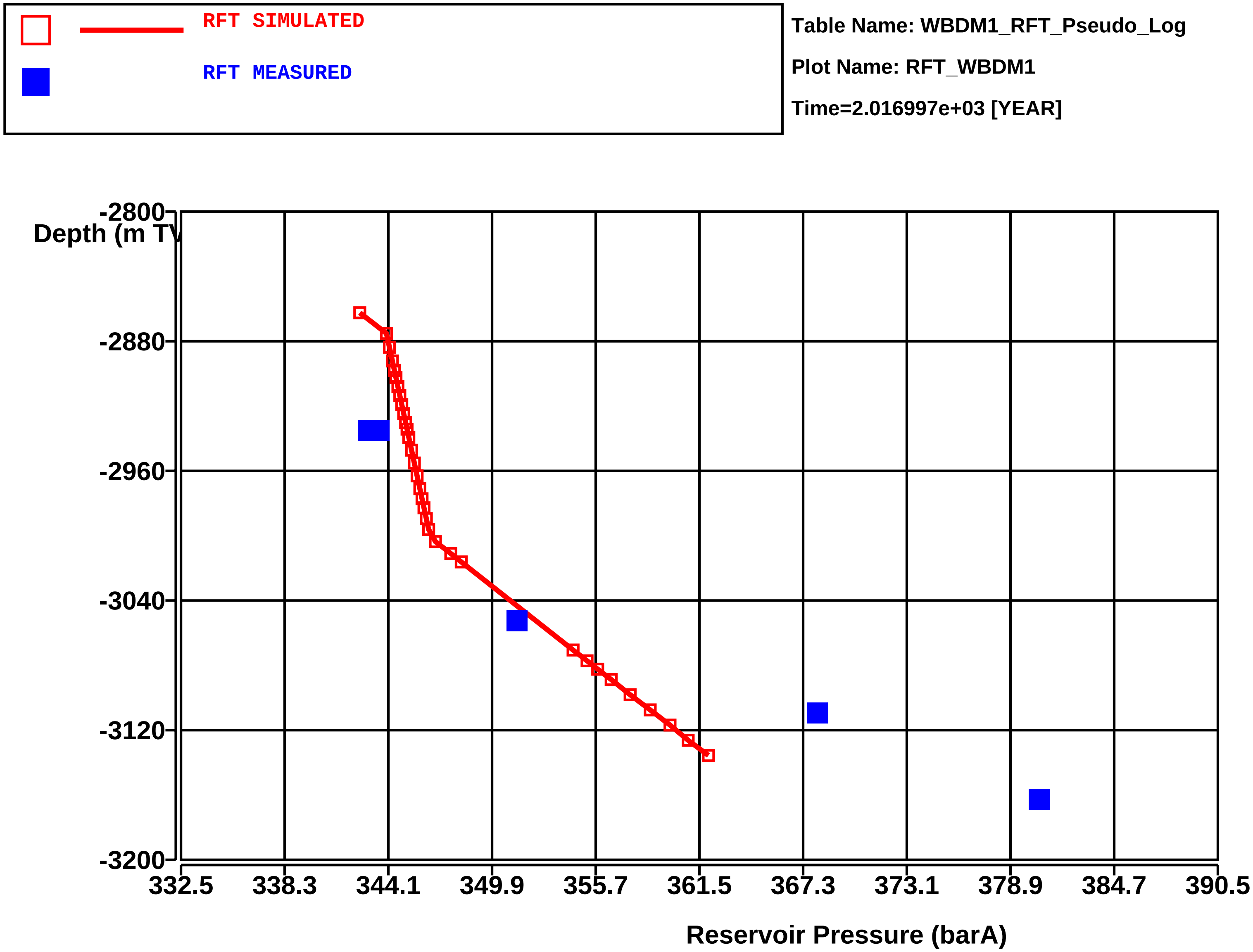

Creation date: Thu 09/02/2017 16:08
Runfile: GRO_2016_ED_v60.run

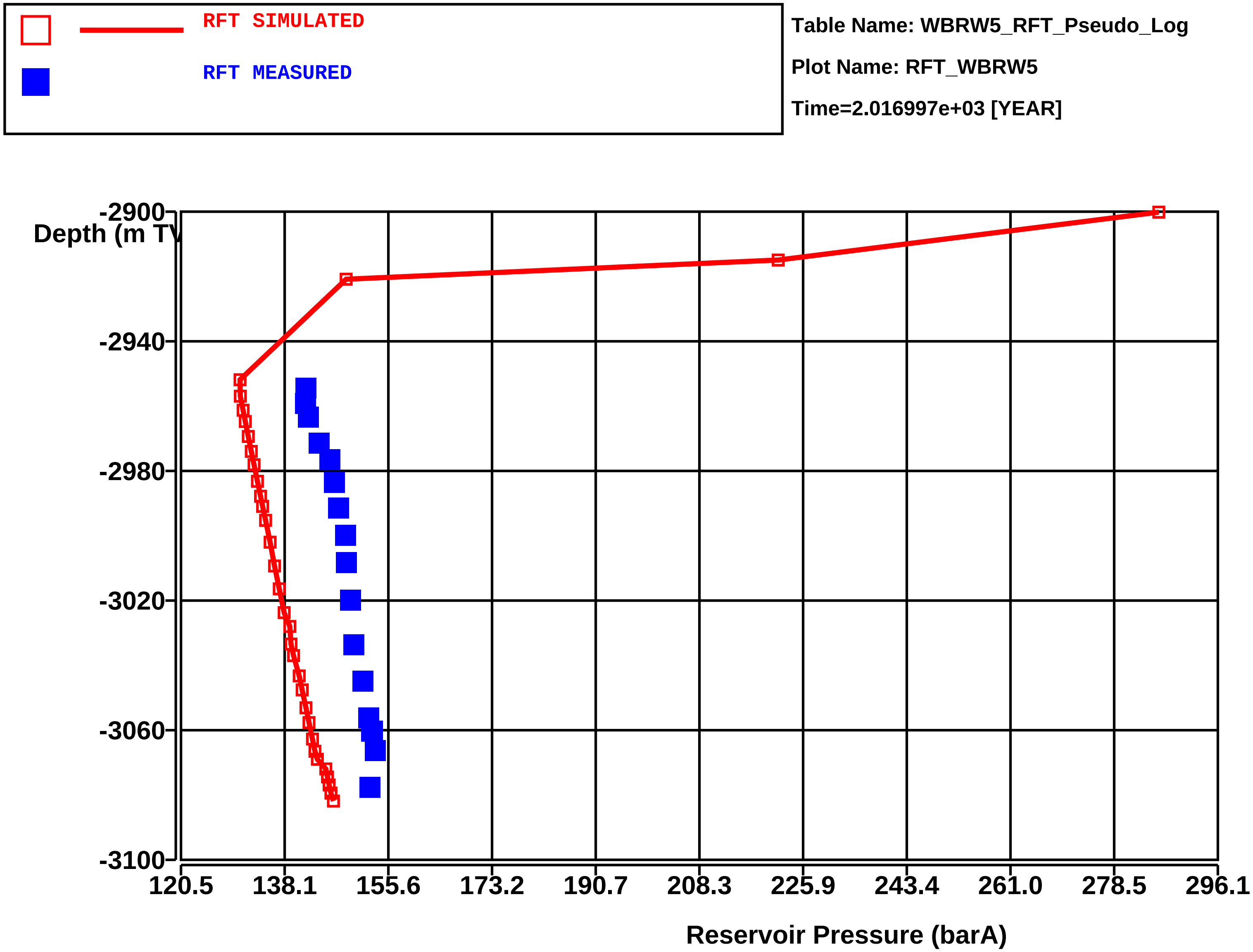

Creation date: Thu 09/02/2017 16:08
Runfile: GRO_2016_ED_v60.run

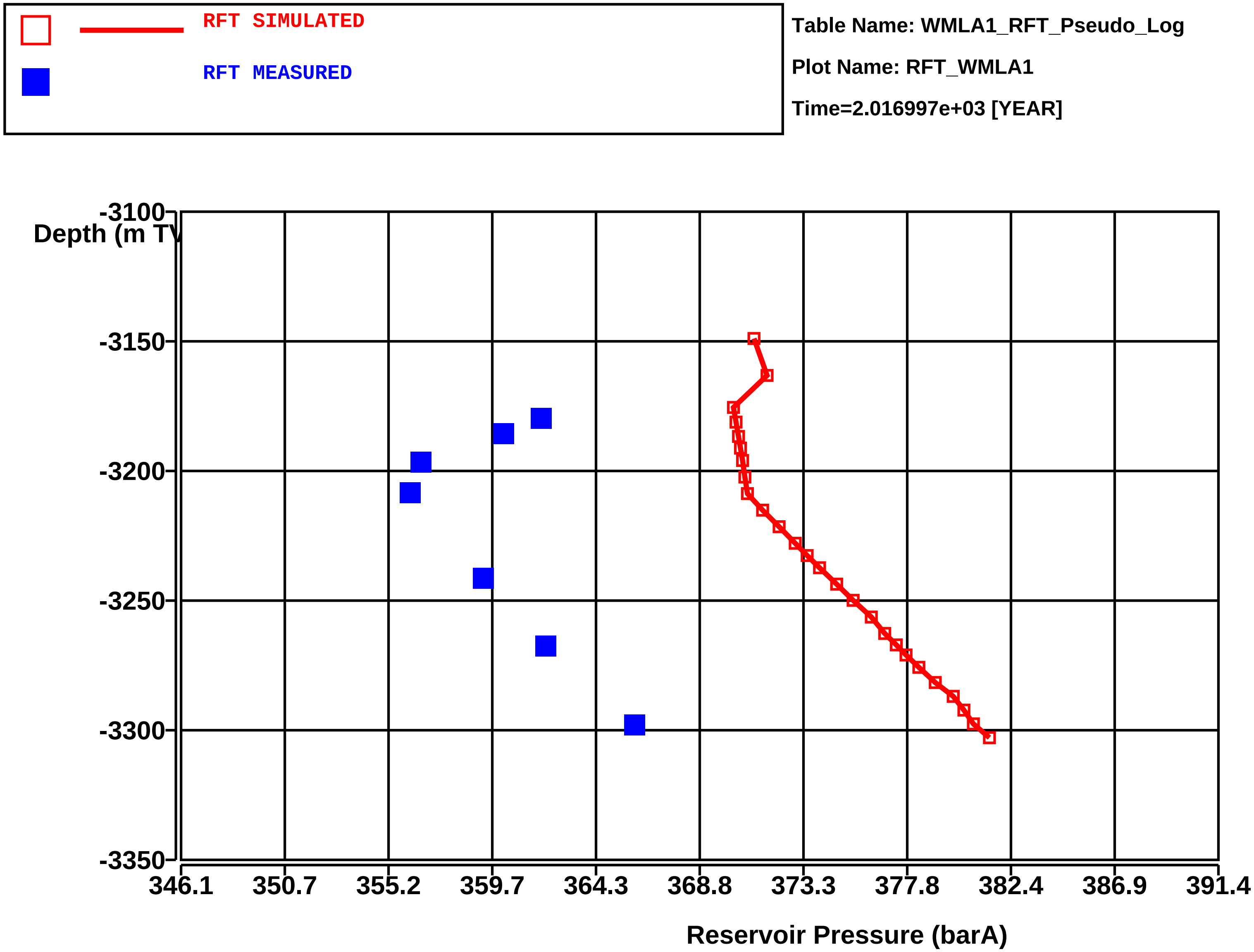

Creation date: Thu 09/02/2017 16:08
Runfile: GRO_2016_ED_v60.run

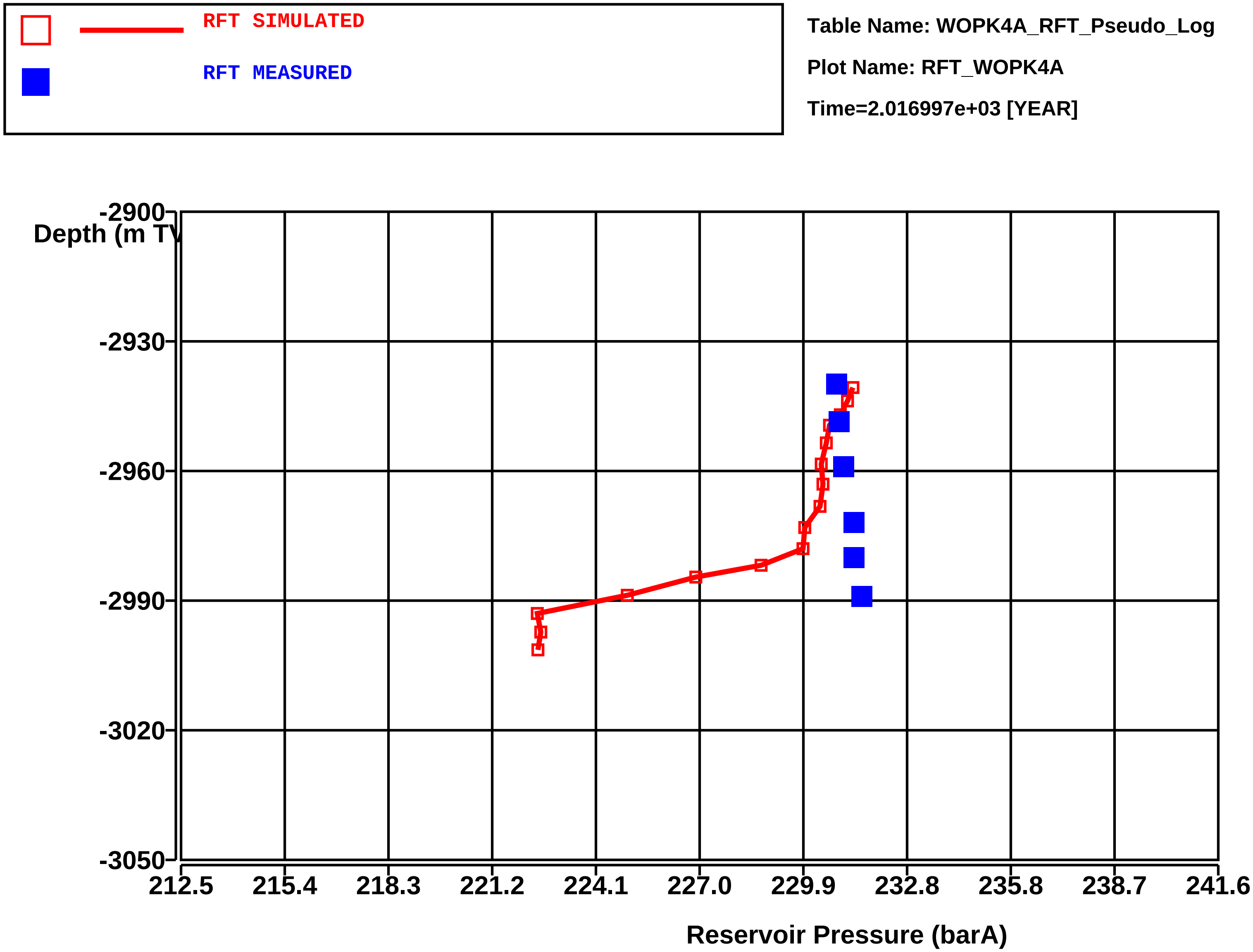

Table Name: WOPK4A_RFT_Pseudo_Log

Plot Name: RFT_WOPK4A

Time=2.016997e+03 [YEAR]

Creation date: Thu 09/02/2017 16:08

Runfile: GRO_2016_ED_v60.run

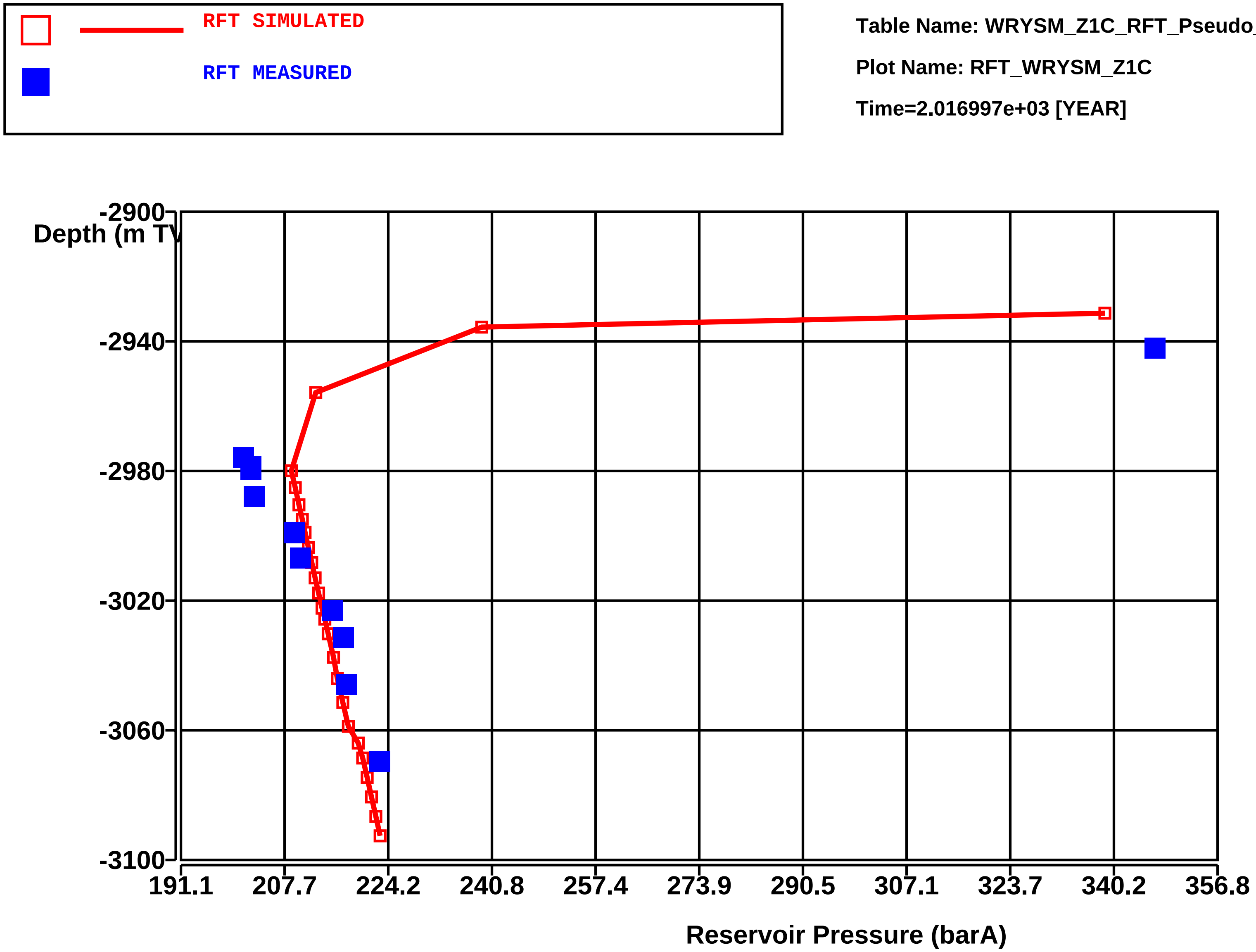

Table Name: WRYSM_Z1C_RFT_Pseudo_Log

Plot Name: RFT_WRYSM_Z1C

Time=2.016997e+03 [YEAR]

Creation date: Thu 09/02/2017 16:08

Runfile: GRO_2016_ED_v60.run

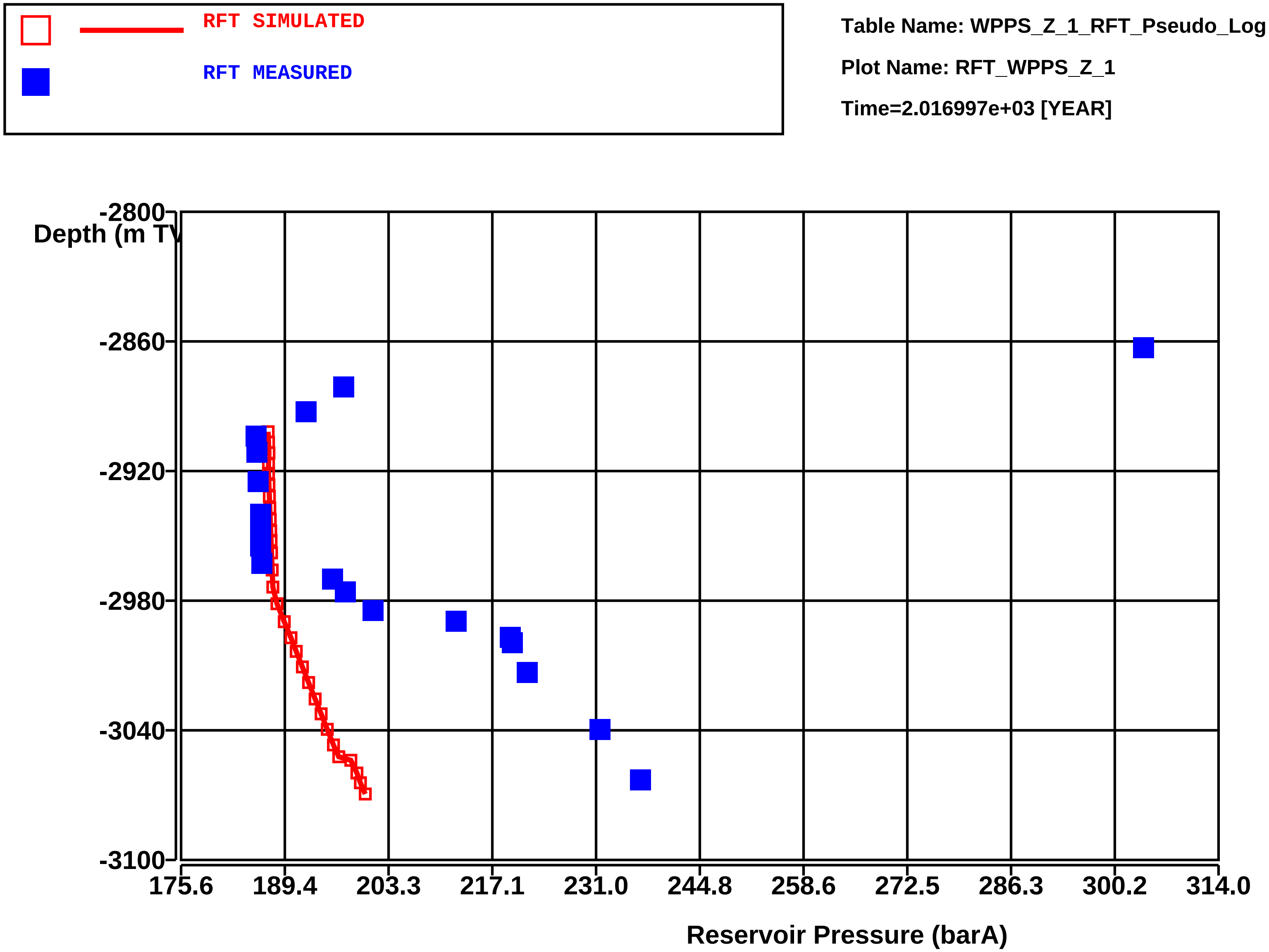

Creation date: Thu 09/02/2017 16:08
Runfile: GRO_2016_ED_v60.run

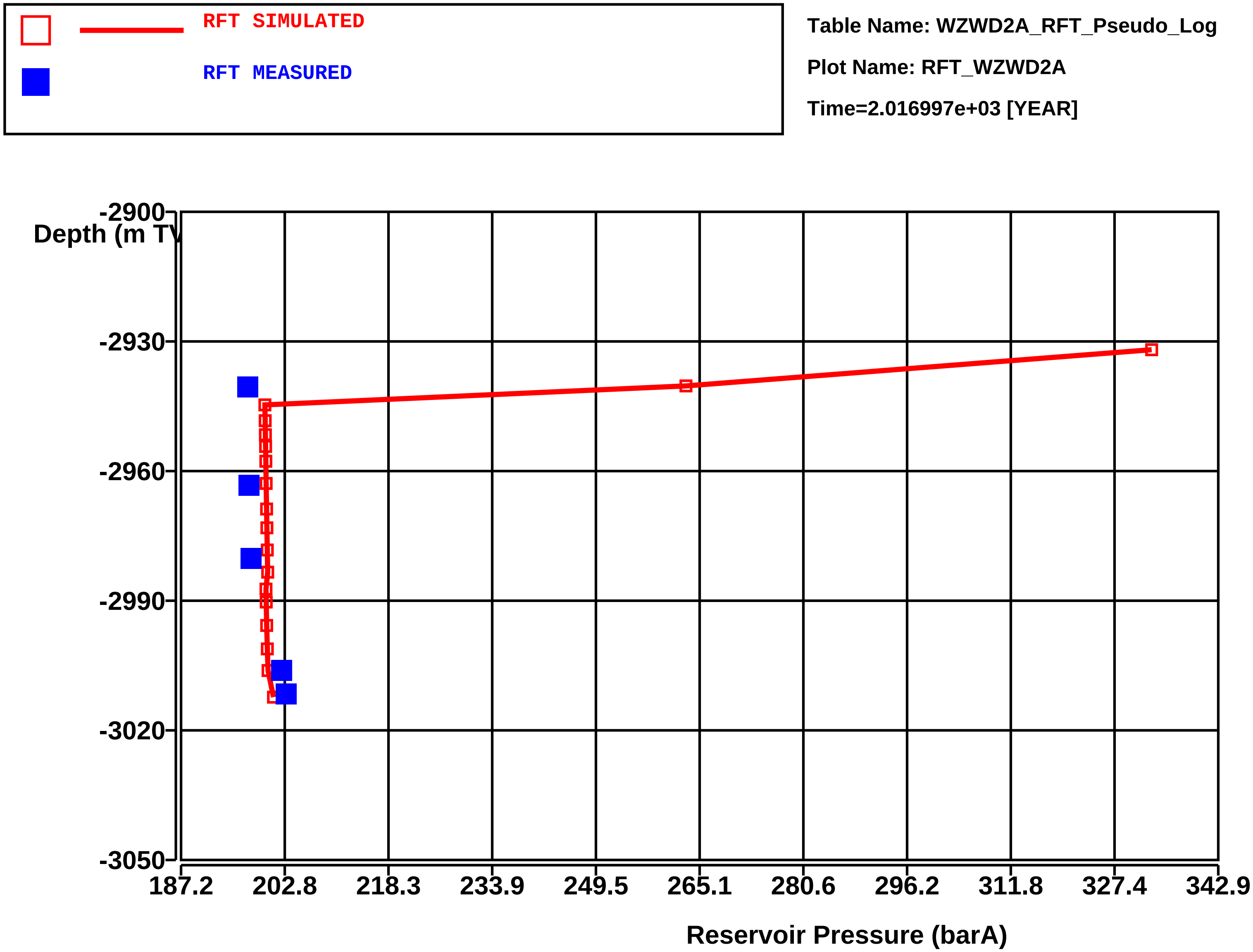

Creation date: Thu 09/02/2017 16:08
Runfile: GRO_2016_ED_v60.run

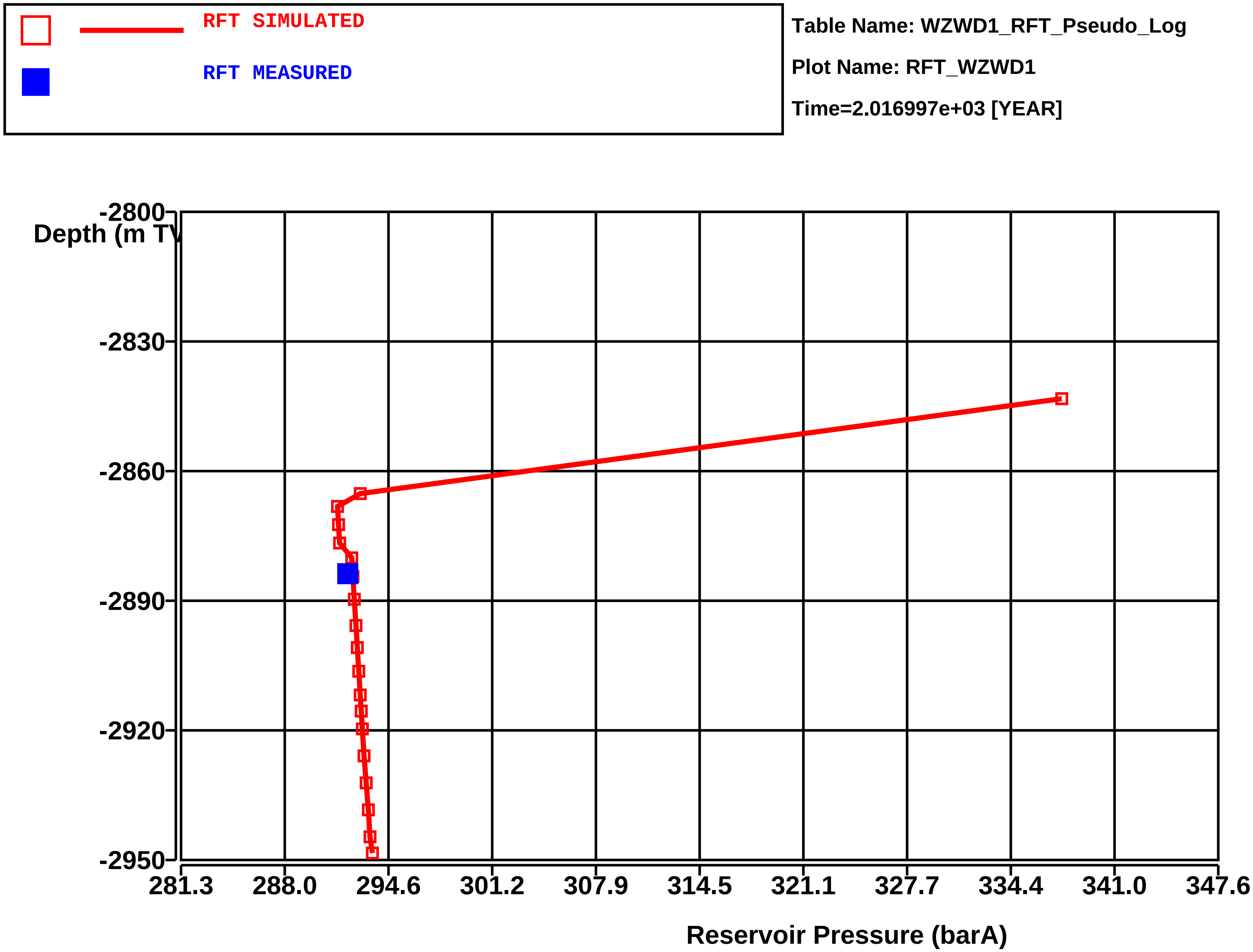

Creation date: Thu 09/02/2017 16:08
Runfile: GRO_2016_ED_v60.run

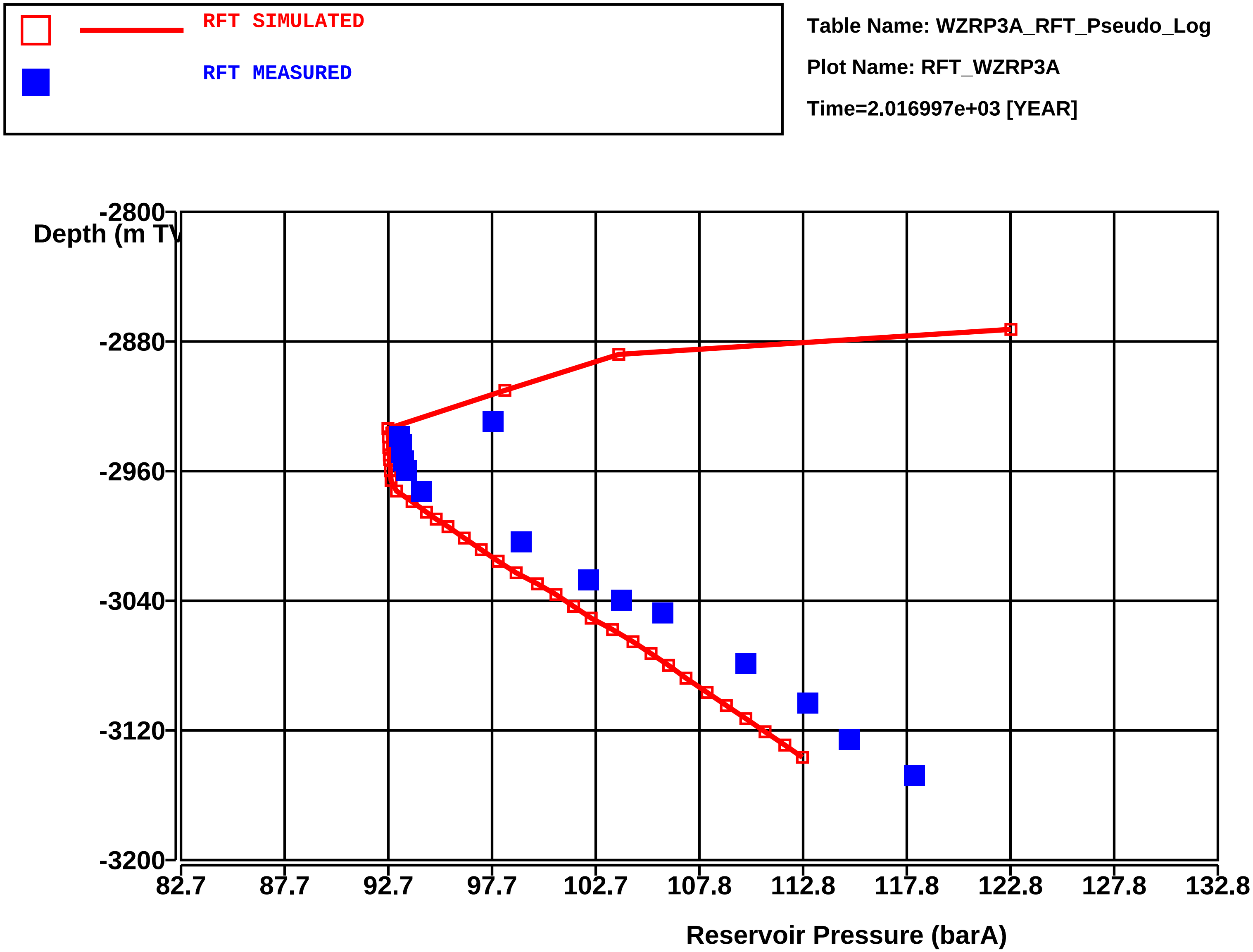

Table Name: WZRP3A_RFT_Pseudo_Log

Plot Name: RFT_WZRP3A

Time=2.016997e+03 [YEAR]

Creation date: Thu 09/02/2017 16:08

Runfile: GRO_2016_ED_v60.run

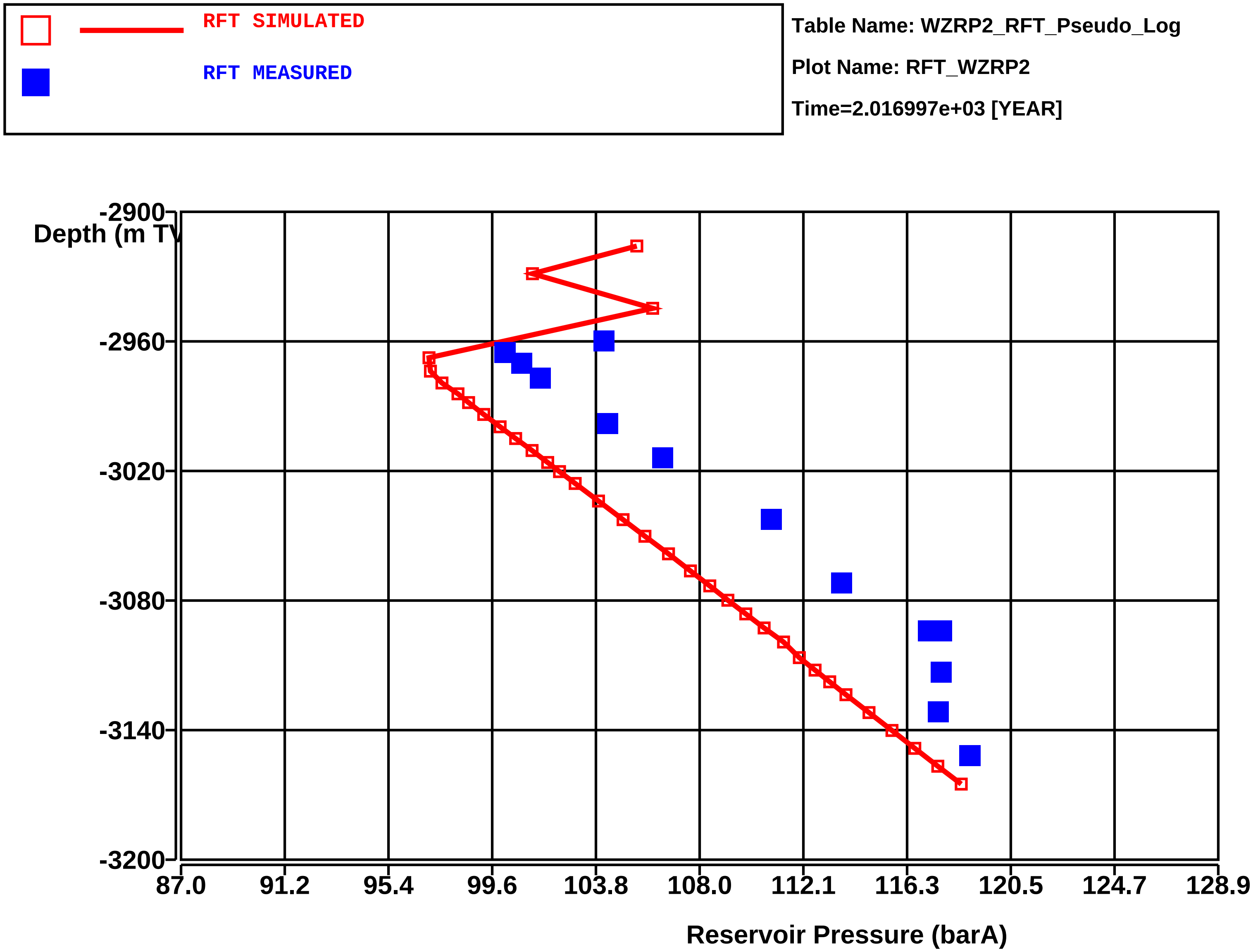

Creation date: Thu 09/02/2017 16:08

Runfile: GRO_2016_ED_v60.run

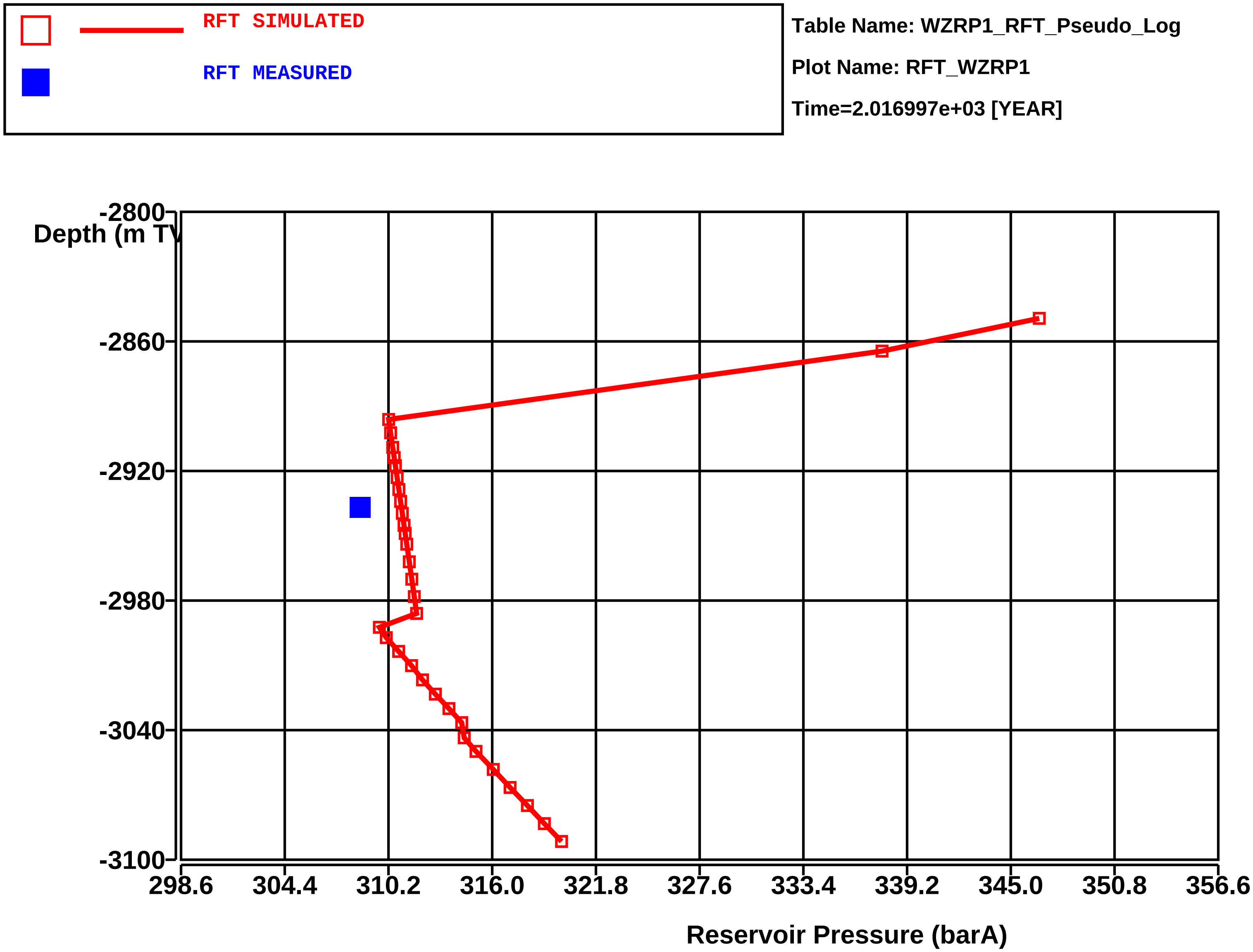

Creation date: Thu 09/02/2017 16:08

Runfile: GRO_2016_ED_v60.run

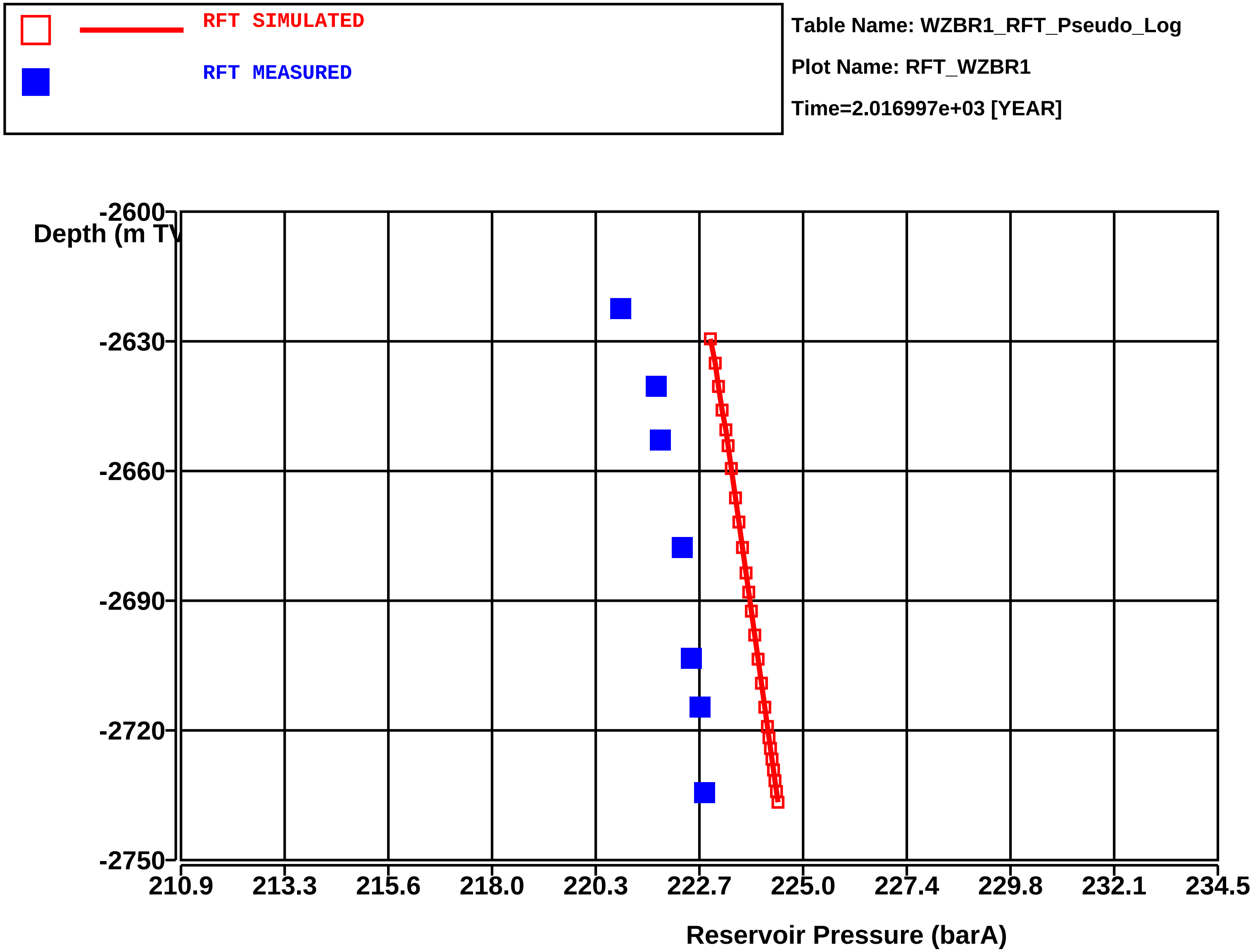

Table Name: WZBR1_RFT_Pseudo_Log

Plot Name: RFT_WZBR1

Time=2.016997e+03 [YEAR]

Creation date: Thu 09/02/2017 16:08

Runfile: GRO_2016_ED_v60.run

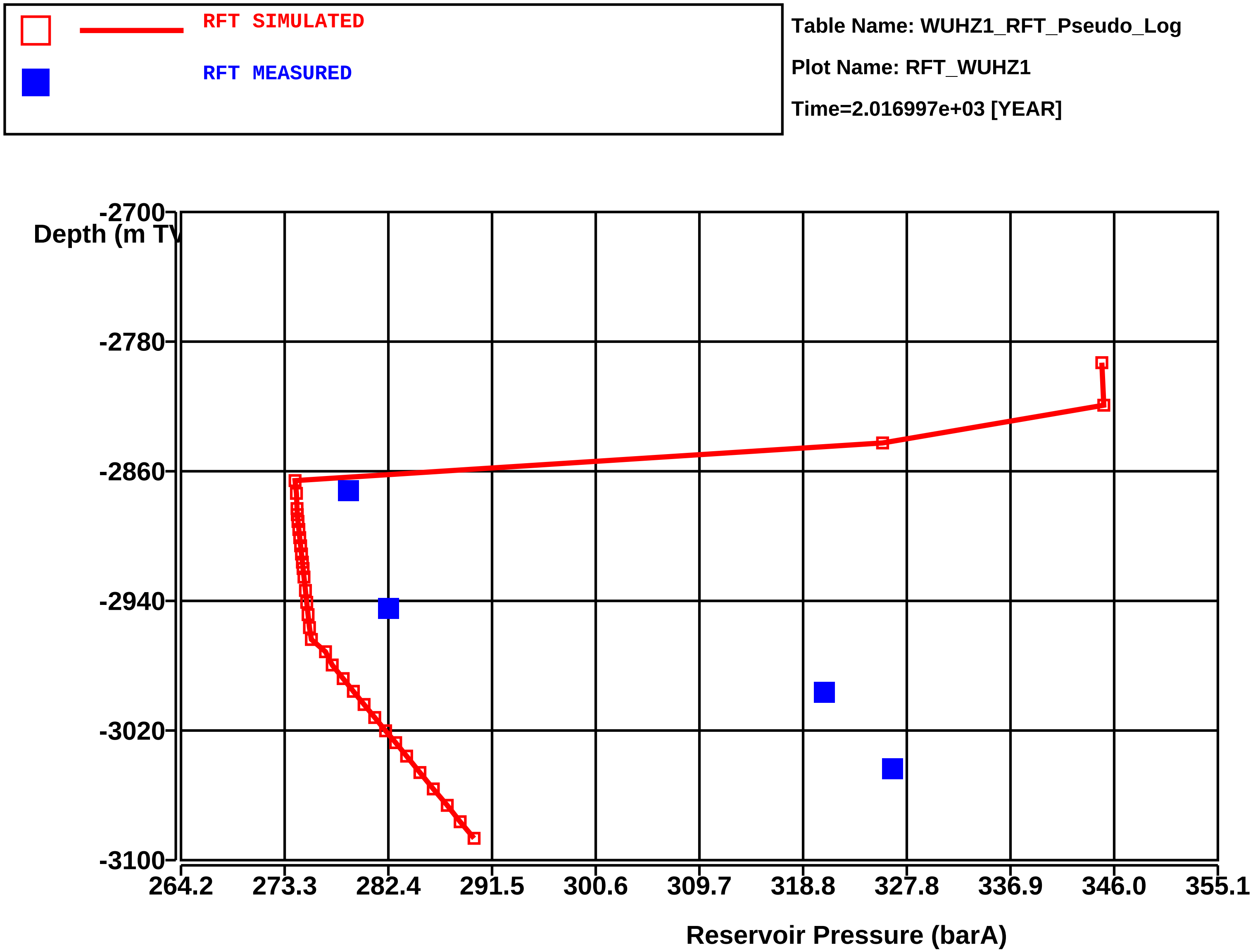

Creation date: Thu 09/02/2017 16:08

Runfile: GRO_2016_ED_v60.run

RFT SIMULATED

RFT MEASURED

Table Name: WSWO1_RFT_Pseudo_Log

Plot Name: RFT_WSWO1

Time=2.016997e+03 [YEAR]

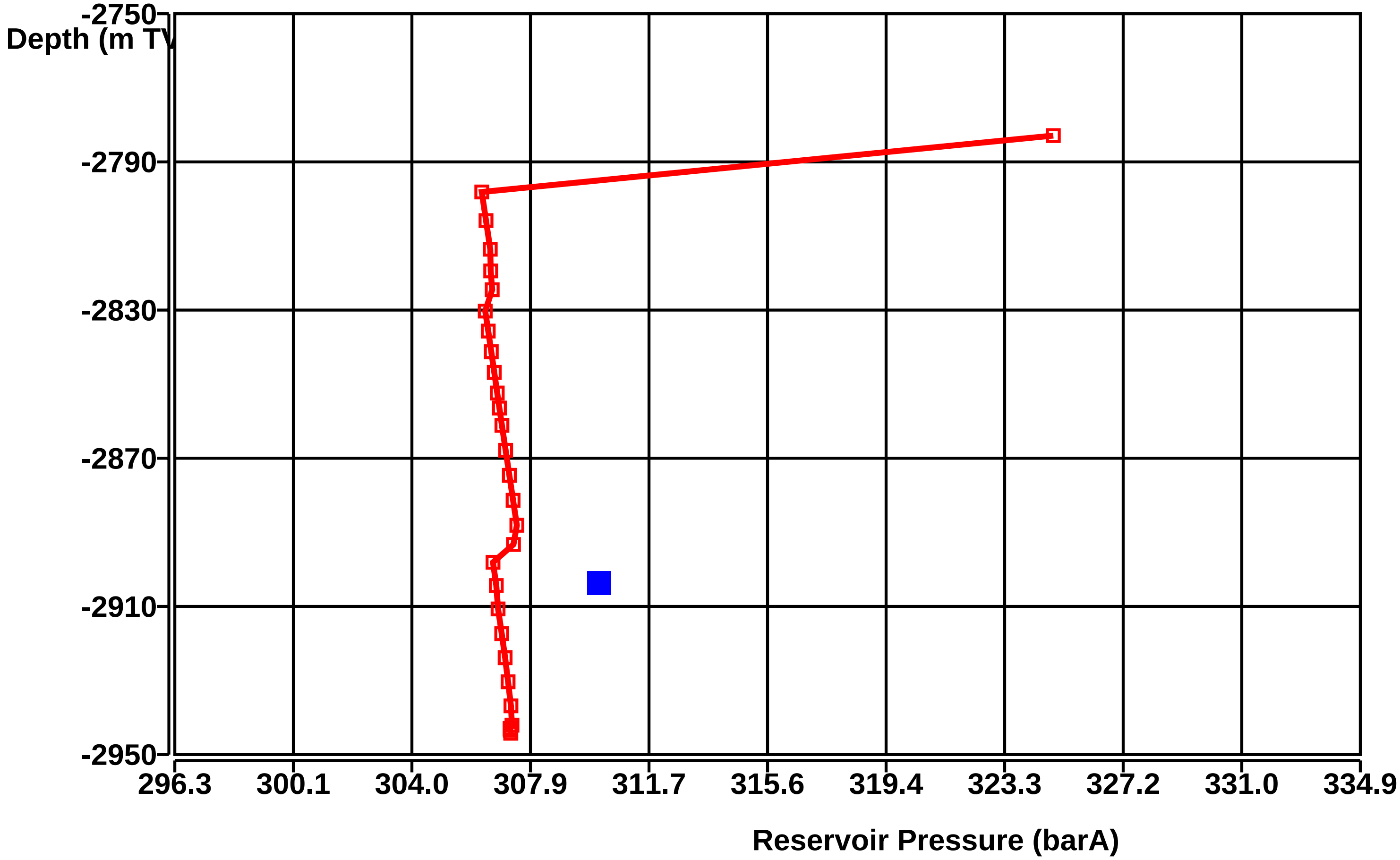

Creation date: Thu 09/02/2017 16:08

Runfile: GRO_2016_ED_v60.run

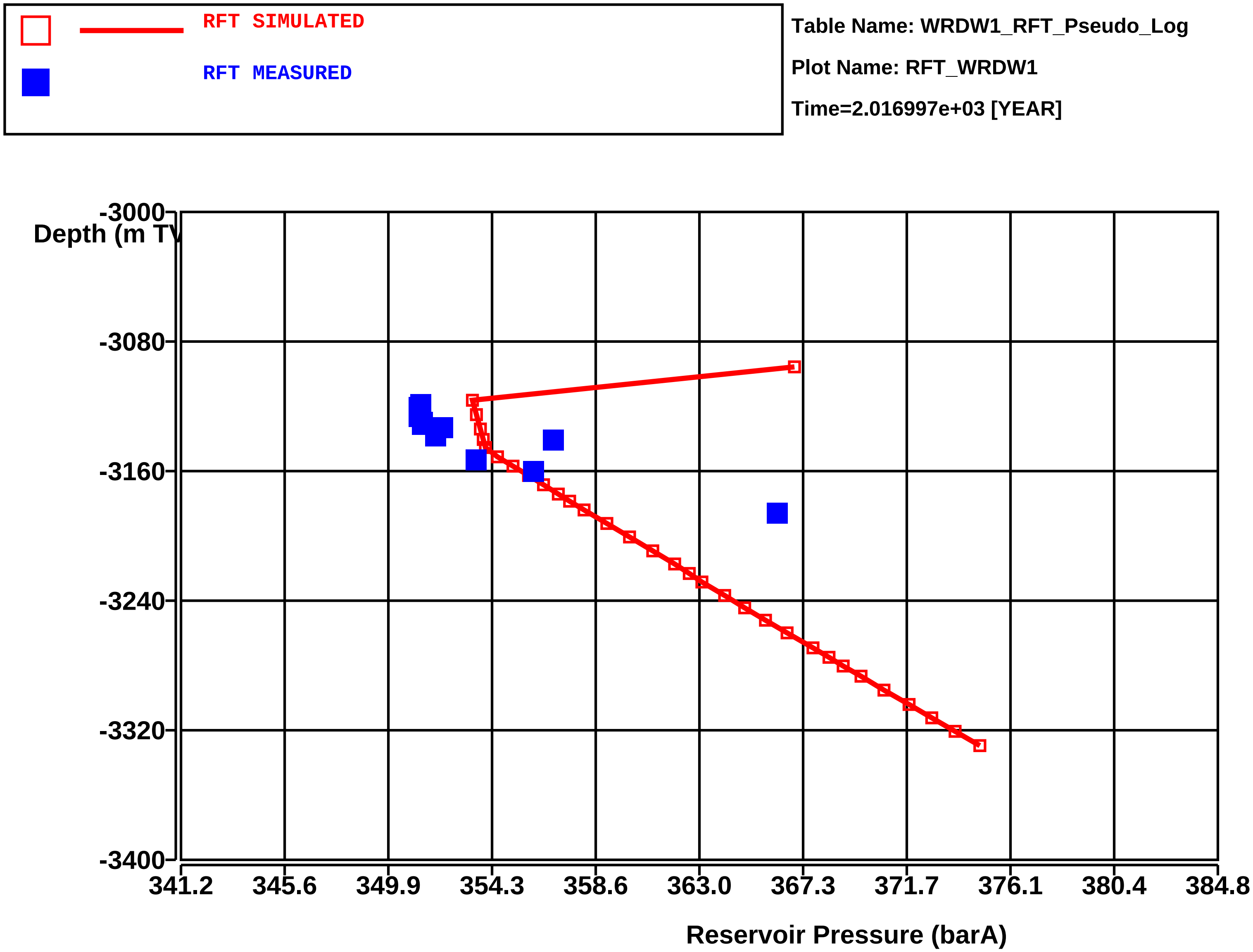

Creation date: Thu 09/02/2017 16:08
Runfile: GRO_2016_ED_v60.run

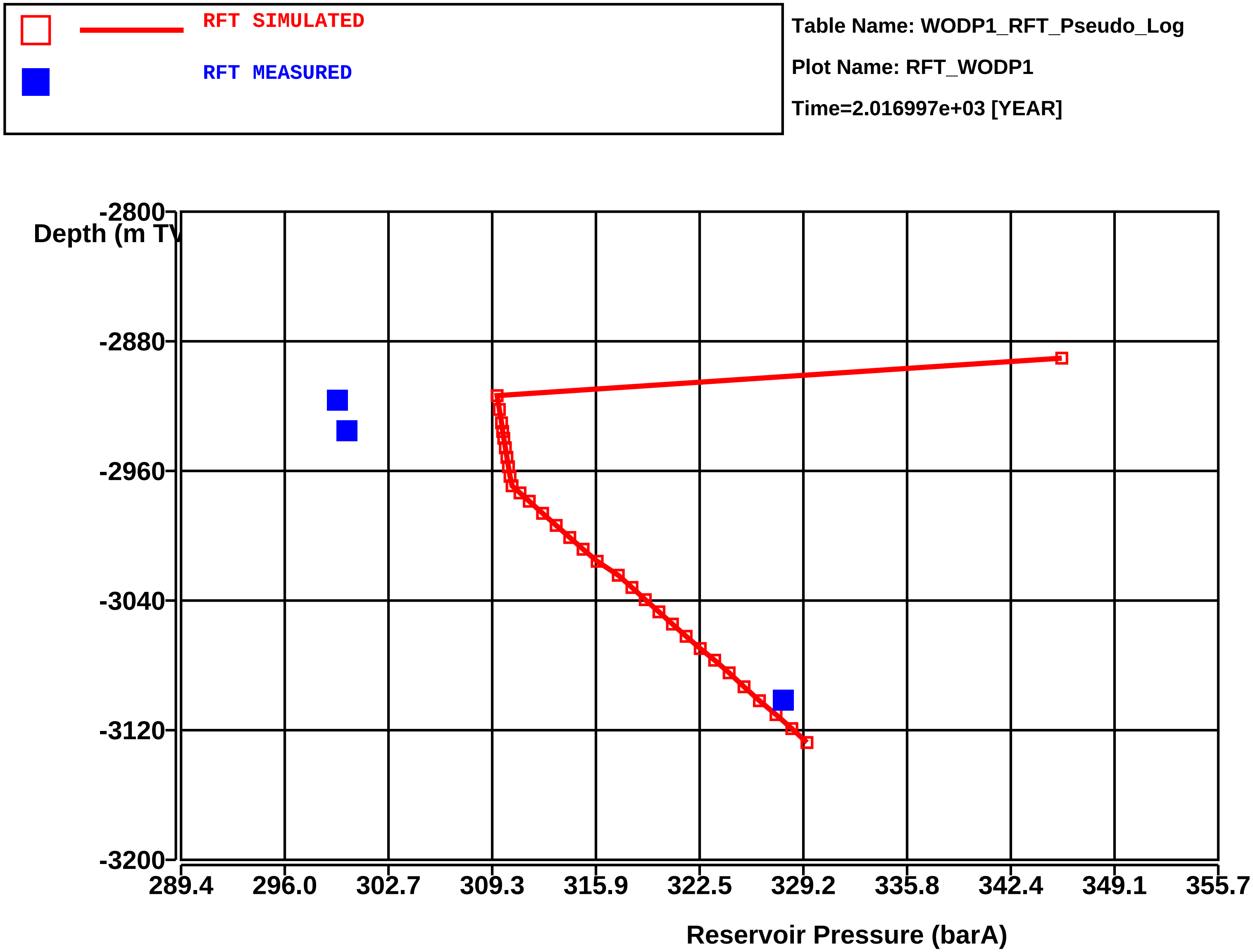

Table Name: WODP1_RFT_Pseudo_Log

Plot Name: RFT_WODP1

Time=2.016997e+03 [YEAR]

Creation date: Thu 09/02/2017 16:08
Runfile: GRO_2016_ED_v60.run

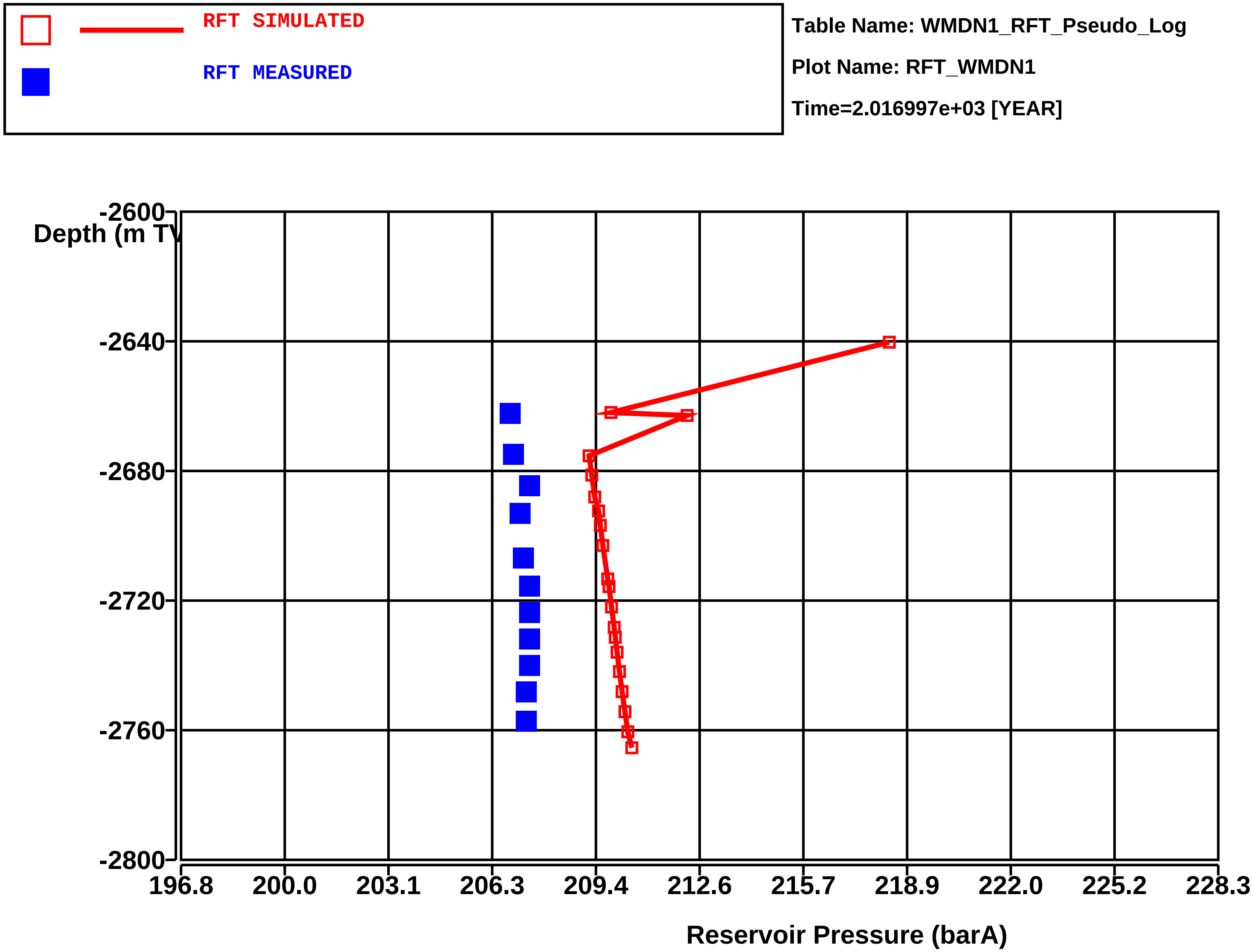

Table Name: WMDN1_RFT_Pseudo_Log

Plot Name: RFT_WMDN1

Time=2.016997e+03 [YEAR]

Creation date: Thu 09/02/2017 16:08

Runfile: GRO_2016_ED_v60.run

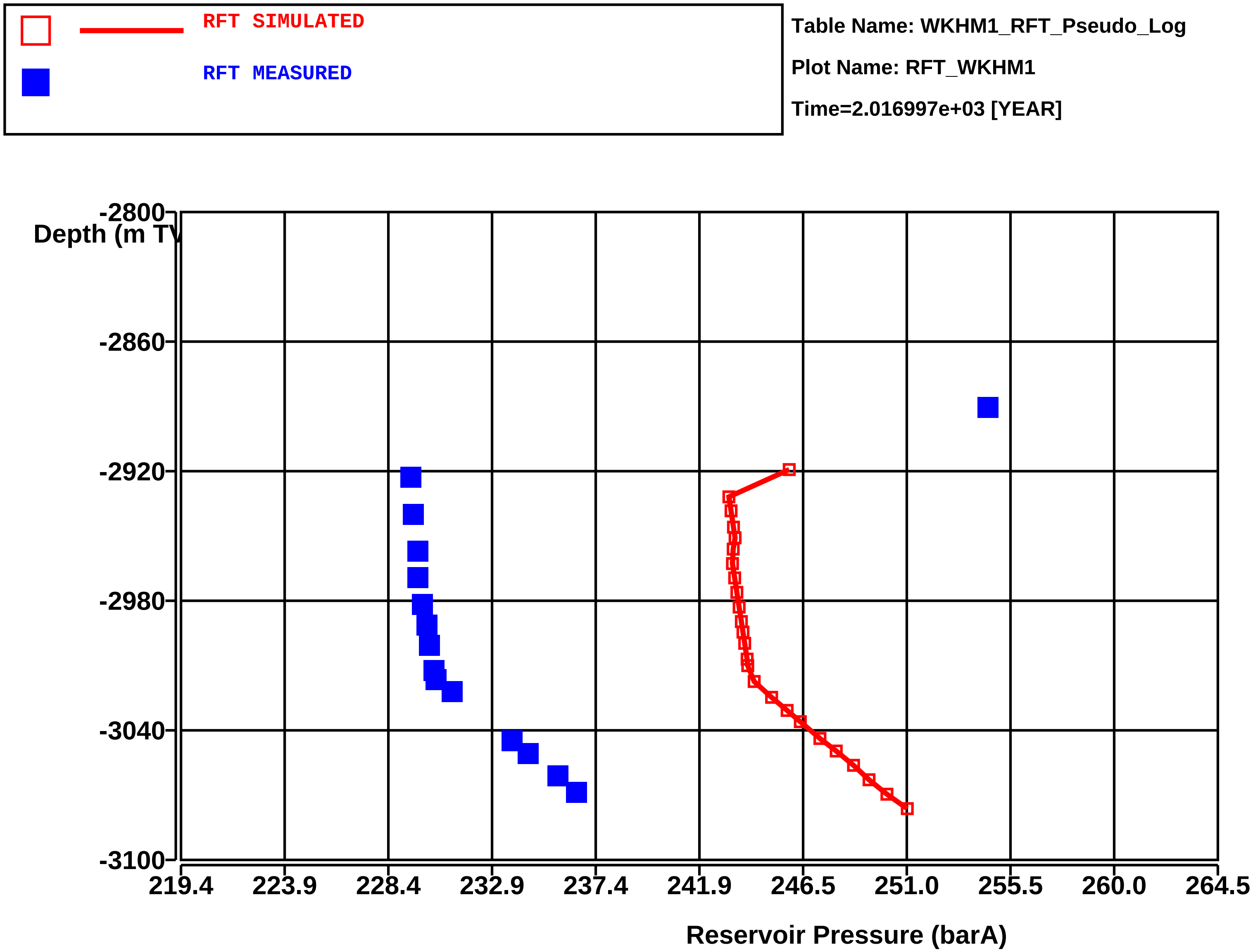

Creation date: Thu 09/02/2017 16:08

Runfile: GRO_2016_ED_v60.run

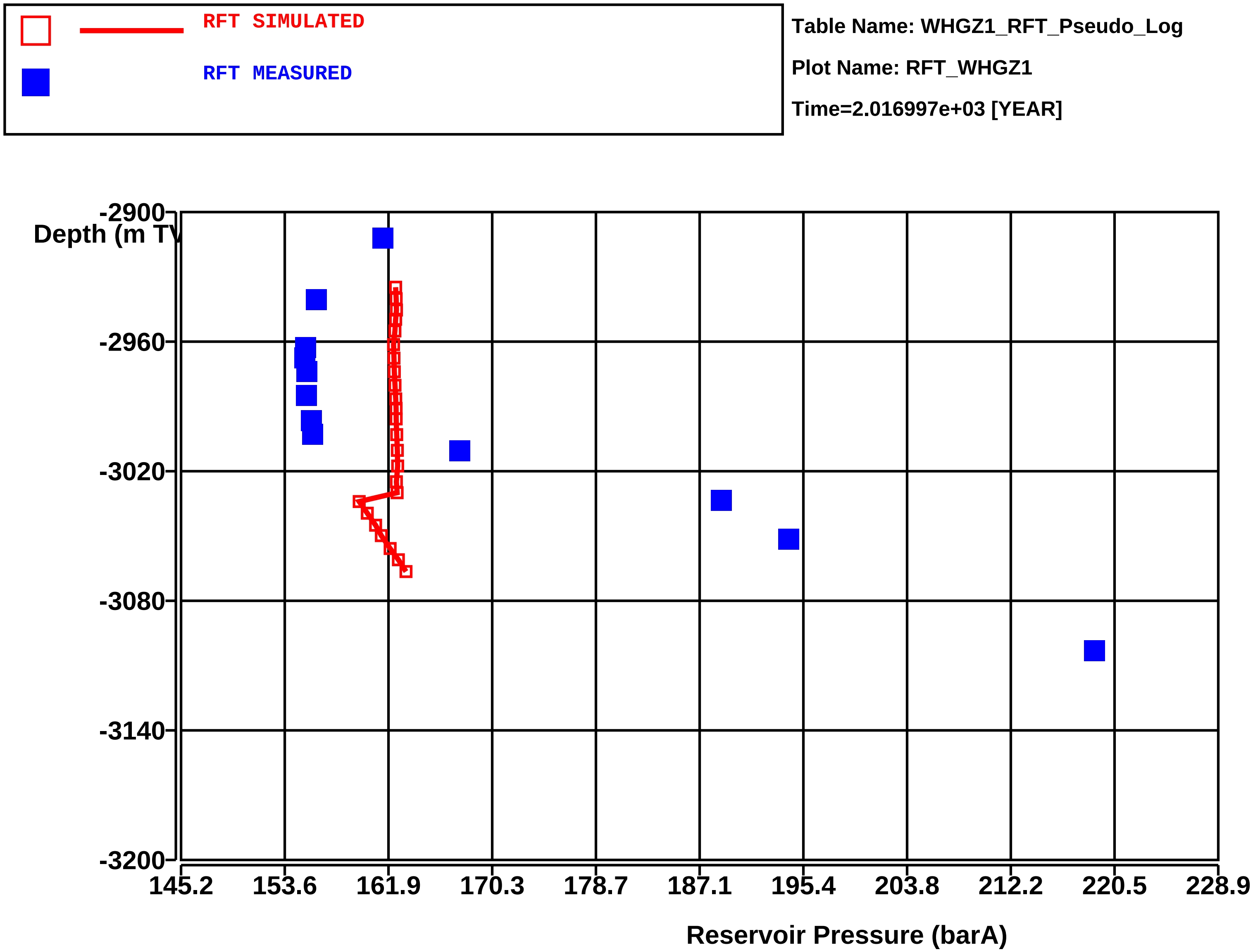

Creation date: Thu 09/02/2017 16:08
Runfile: GRO_2016_ED_v60.run

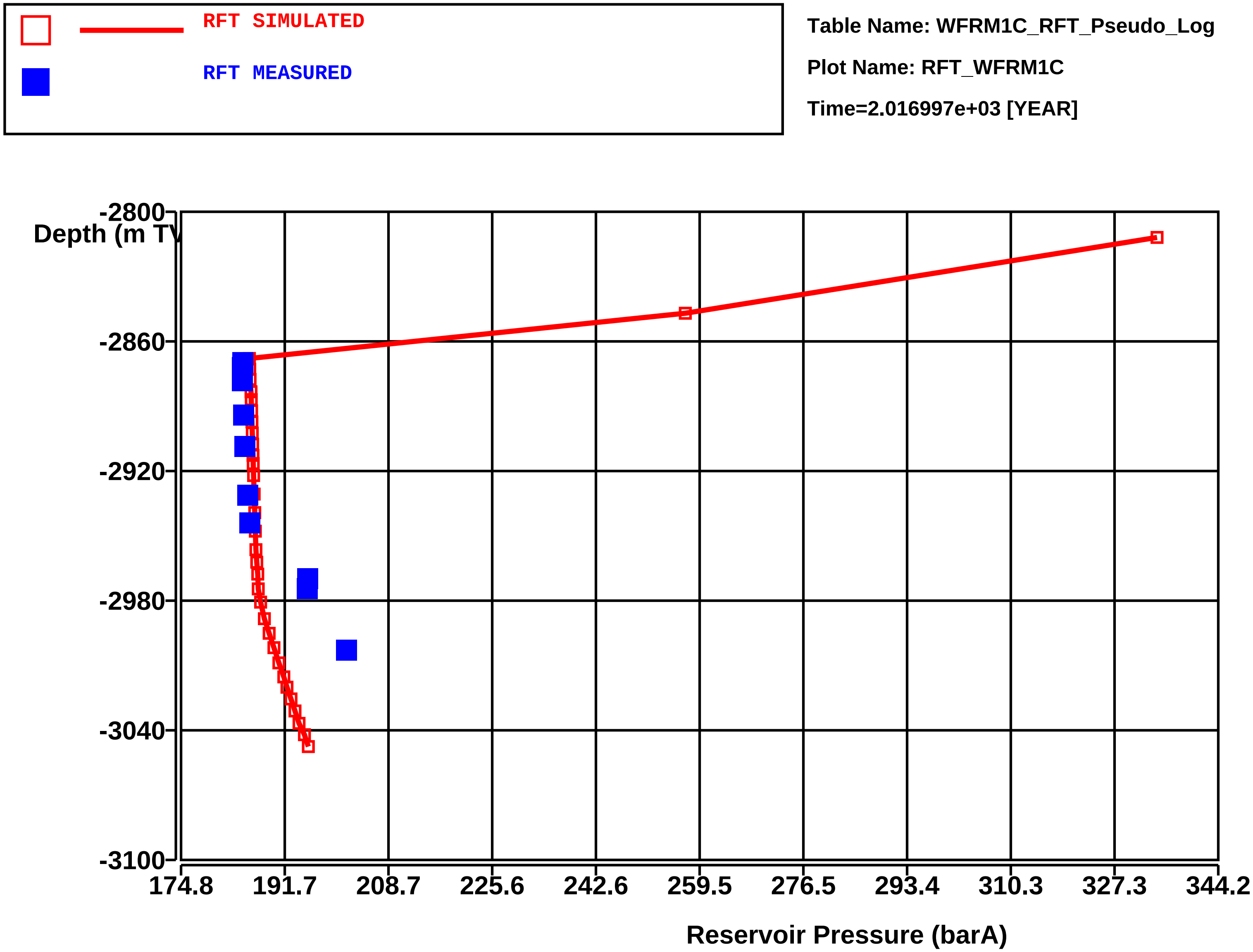

Table Name: WFRM1C_RFT_Pseudo_Log

Plot Name: RFT_WFRM1C

Time=2.016997e+03 [YEAR]

Creation date: Thu 09/02/2017 16:08

Runfile: GRO_2016_ED_v60.run

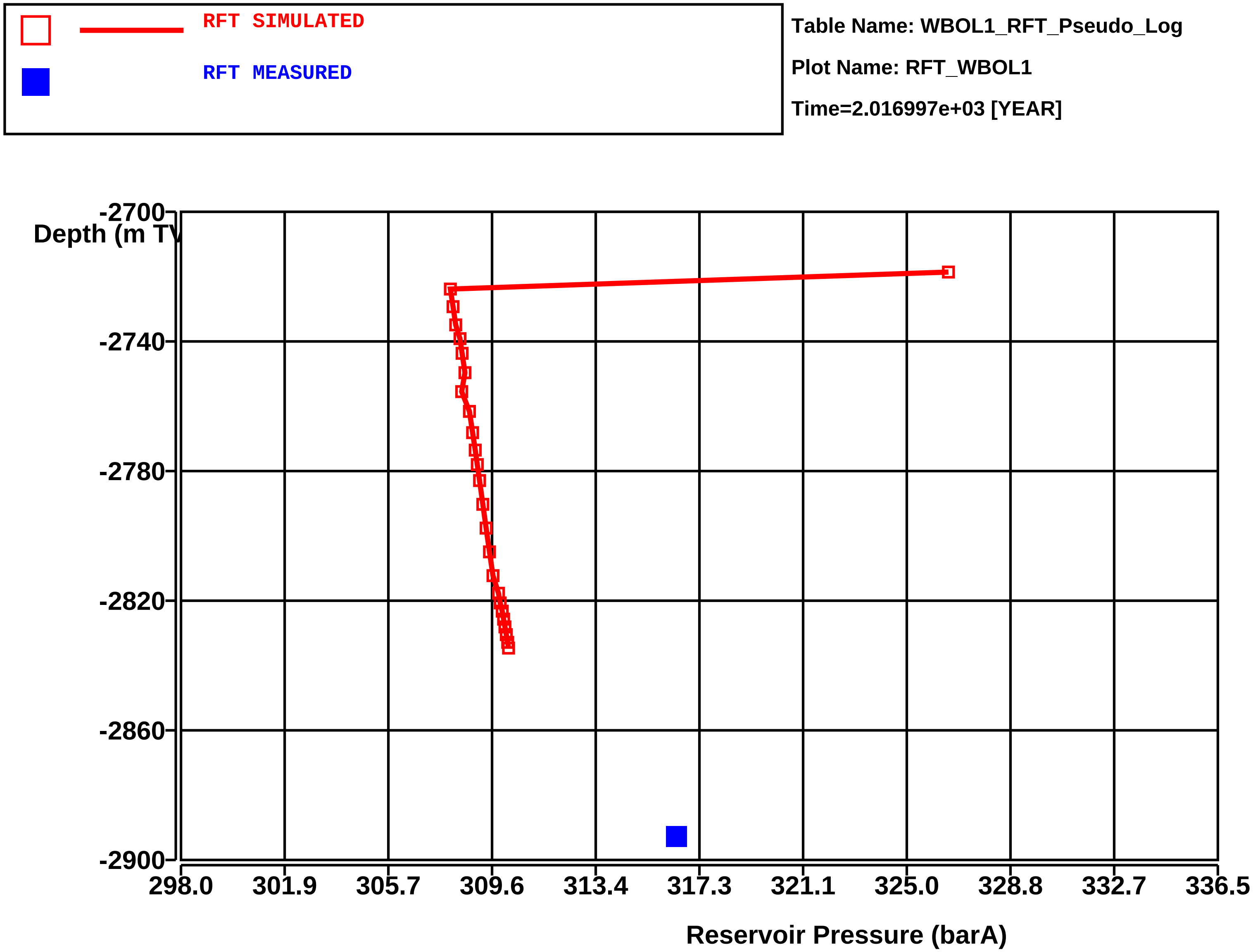

Creation date: Thu 09/02/2017 16:08
Runfile: GRO_2016_ED_v60.run

Table Name: WZVN13_RFT_Pseudo_Log

Plot Name: RFT_WZVN13

Time=2.016997e+03 [YEAR]

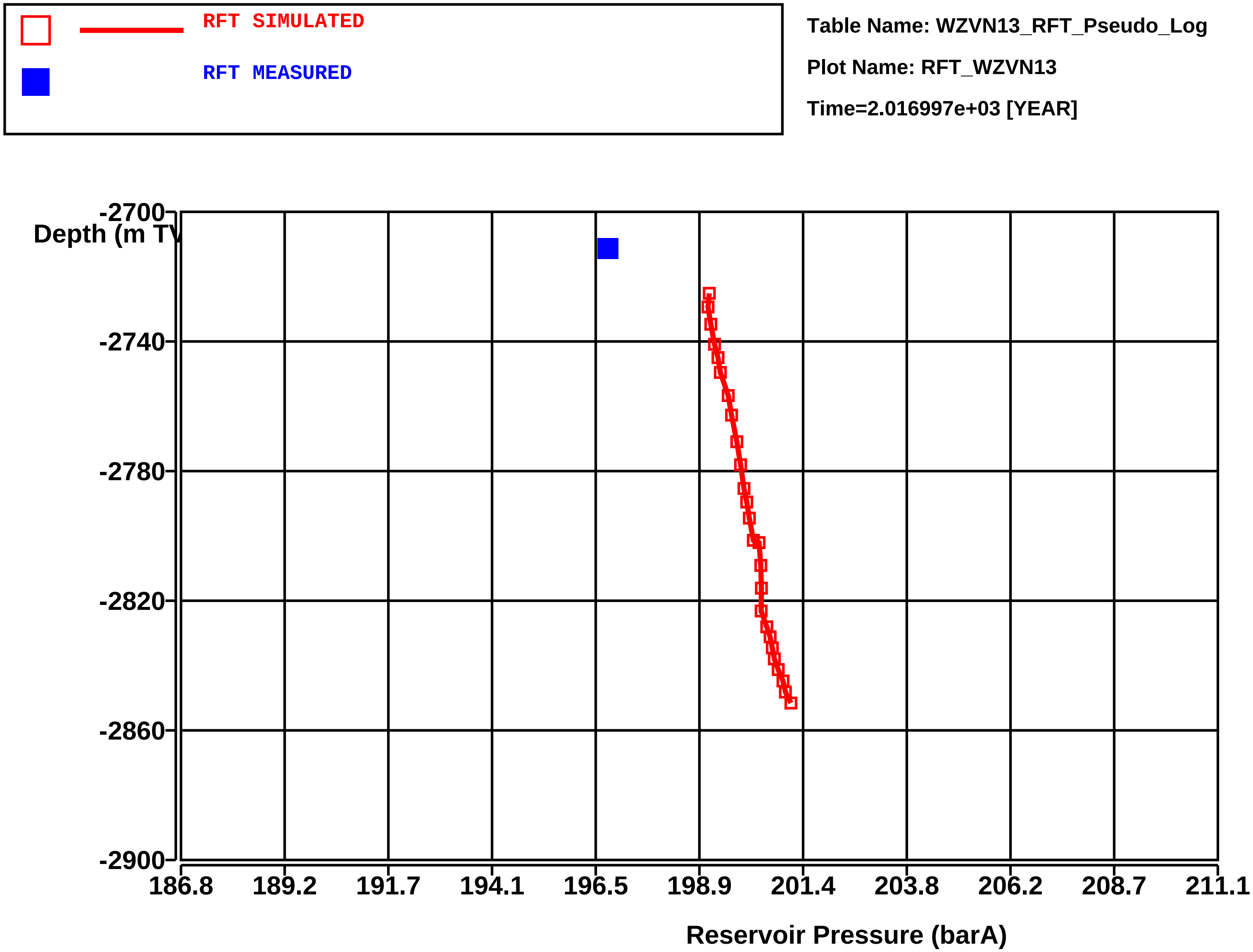

Creation date: Thu 09/02/2017 16:08

Runfile: GRO_2016_ED_v60.run

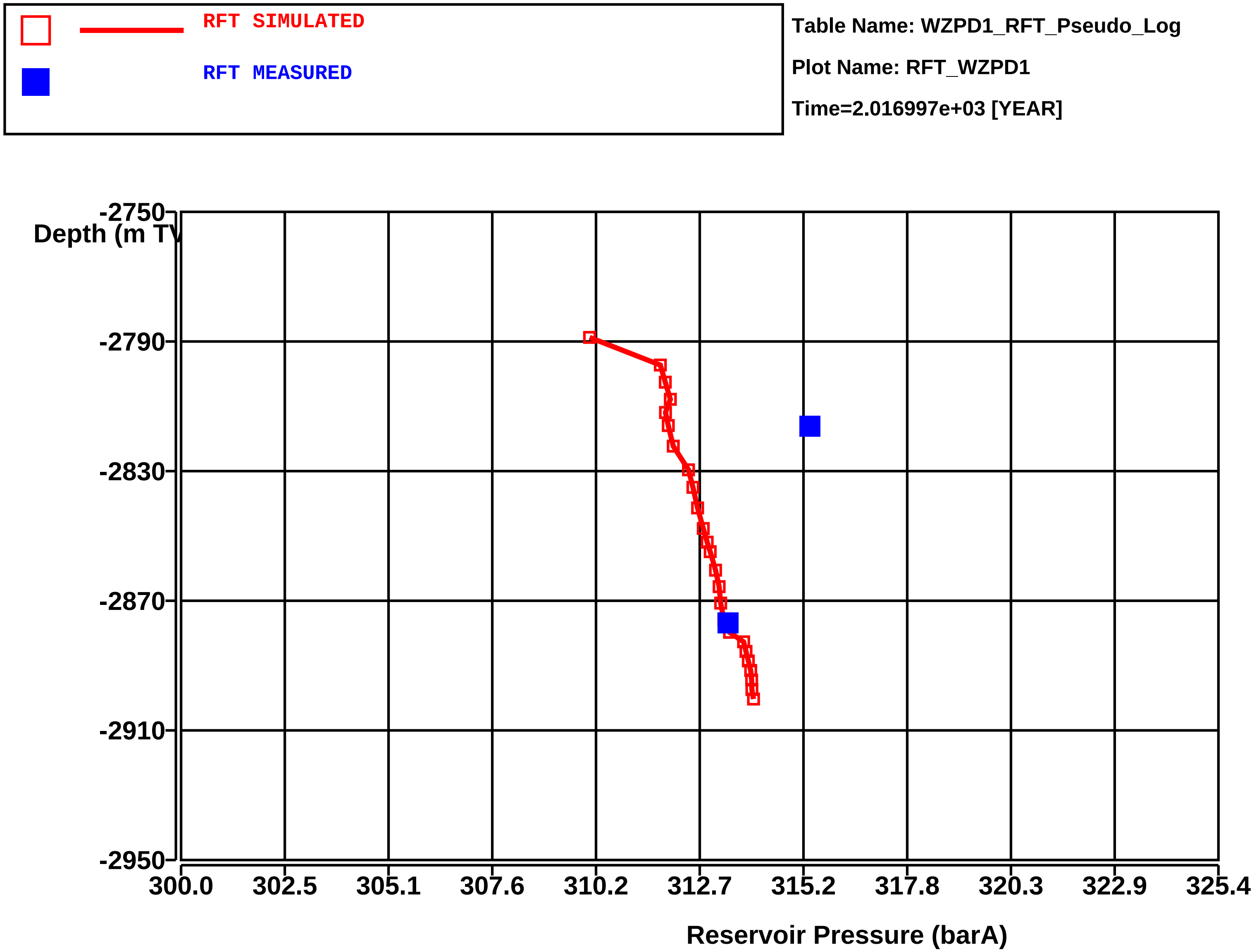

Creation date: Thu 09/02/2017 16:08

Runfile: GRO_2016_ED_v60.run

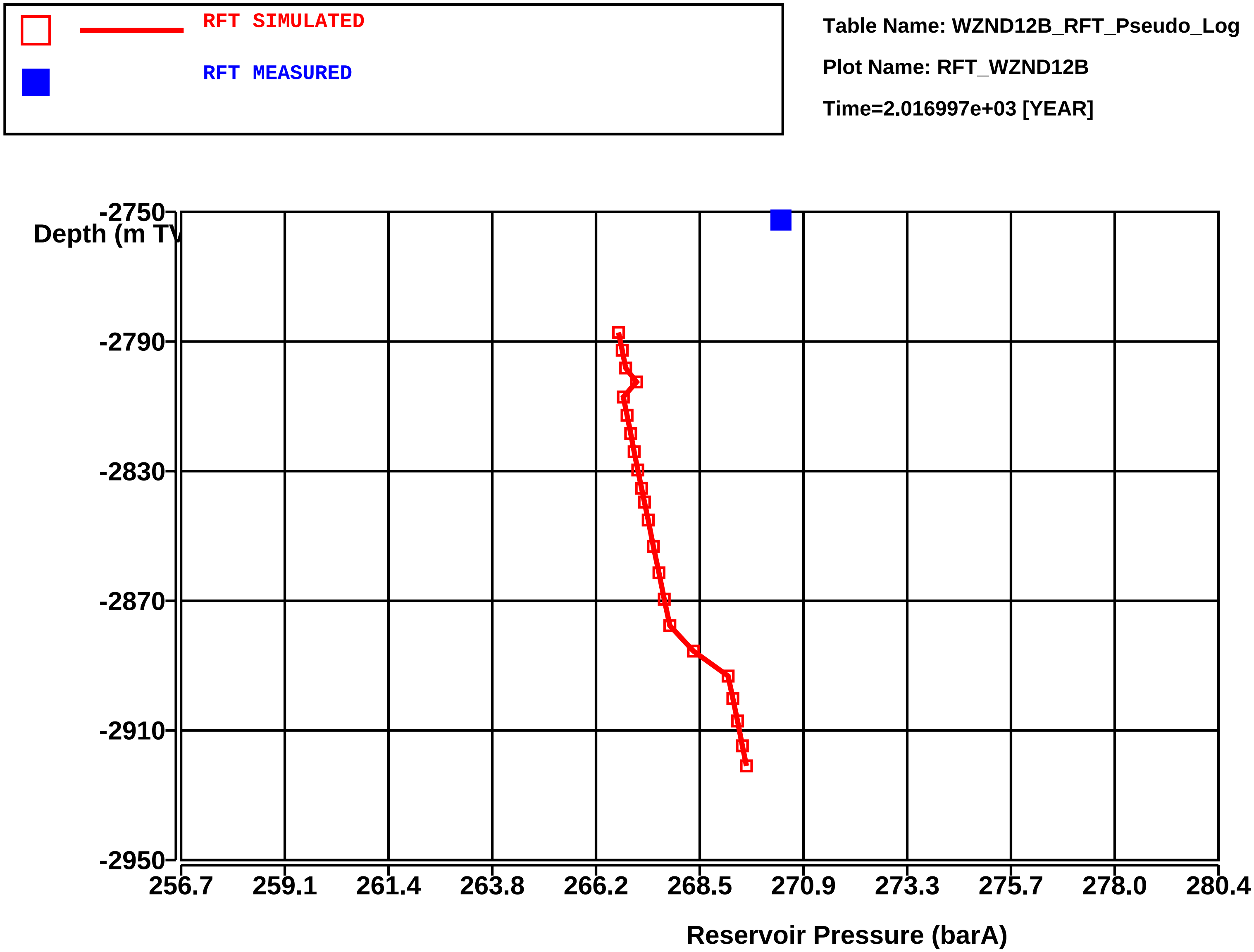

Table Name: WZND12B_RFT_Pseudo_Log

Plot Name: RFT_WZND12B

Time=2.016997e+03 [YEAR]

Creation date: Thu 09/02/2017 16:08

Runfile: GRO_2016_ED_v60.run

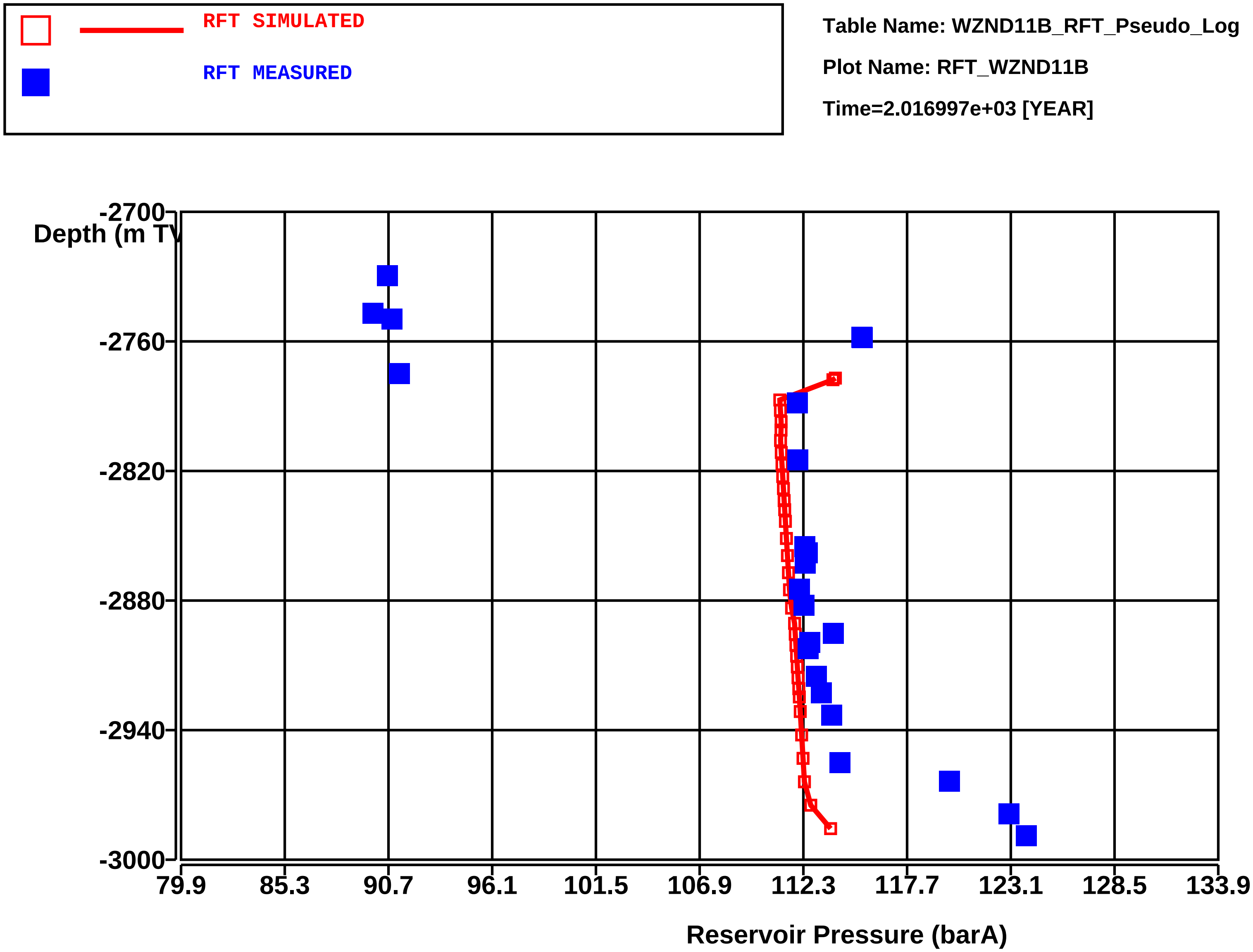

Table Name: WZND11B_RFT_Pseudo_Log

Plot Name: RFT_WZND11B

Time=2.016997e+03 [YEAR]

Creation date: Thu 09/02/2017 16:08

Runfile: GRO_2016_ED_v60.run

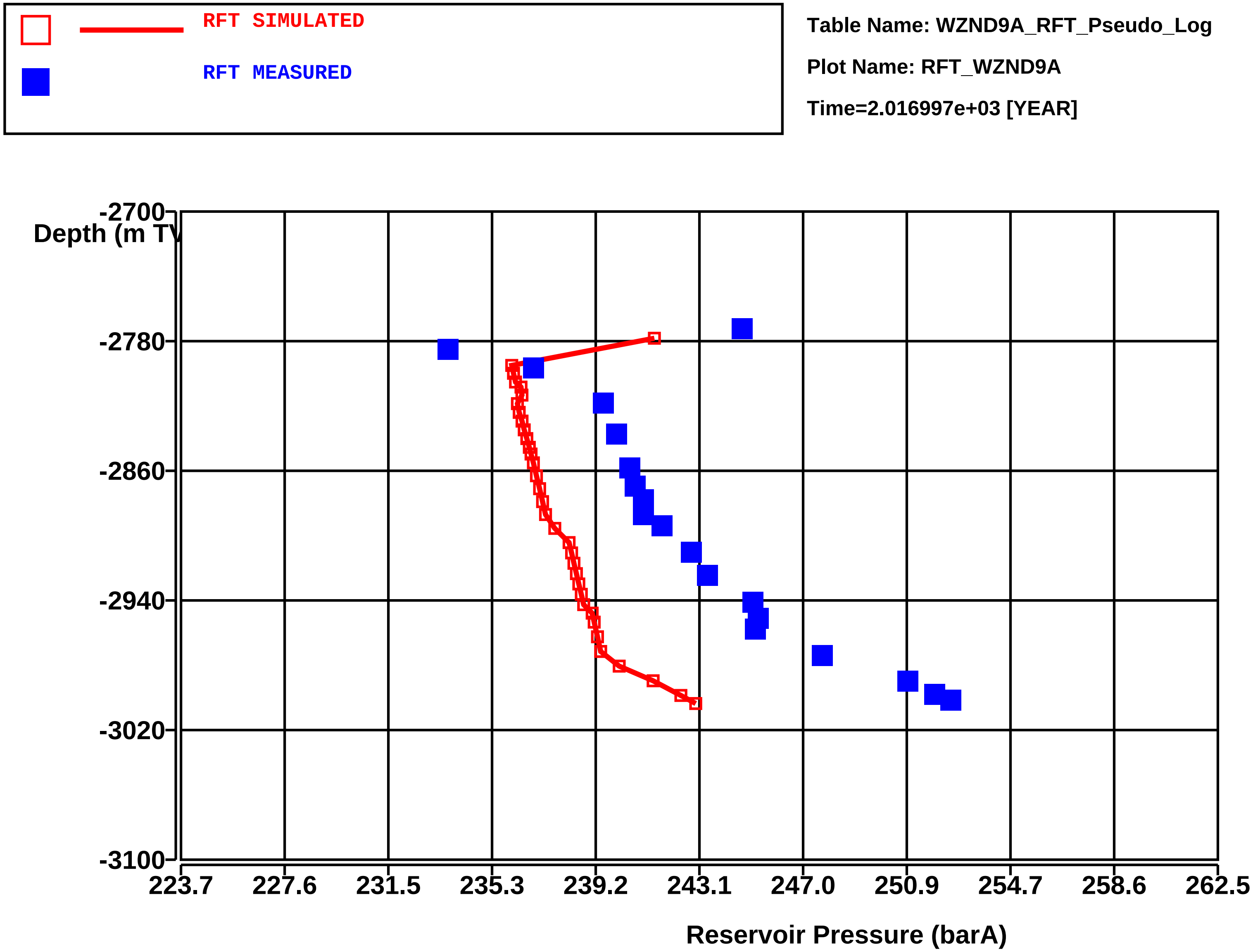

Creation date: Thu 09/02/2017 16:08

Runfile: GRO_2016_ED_v60.run

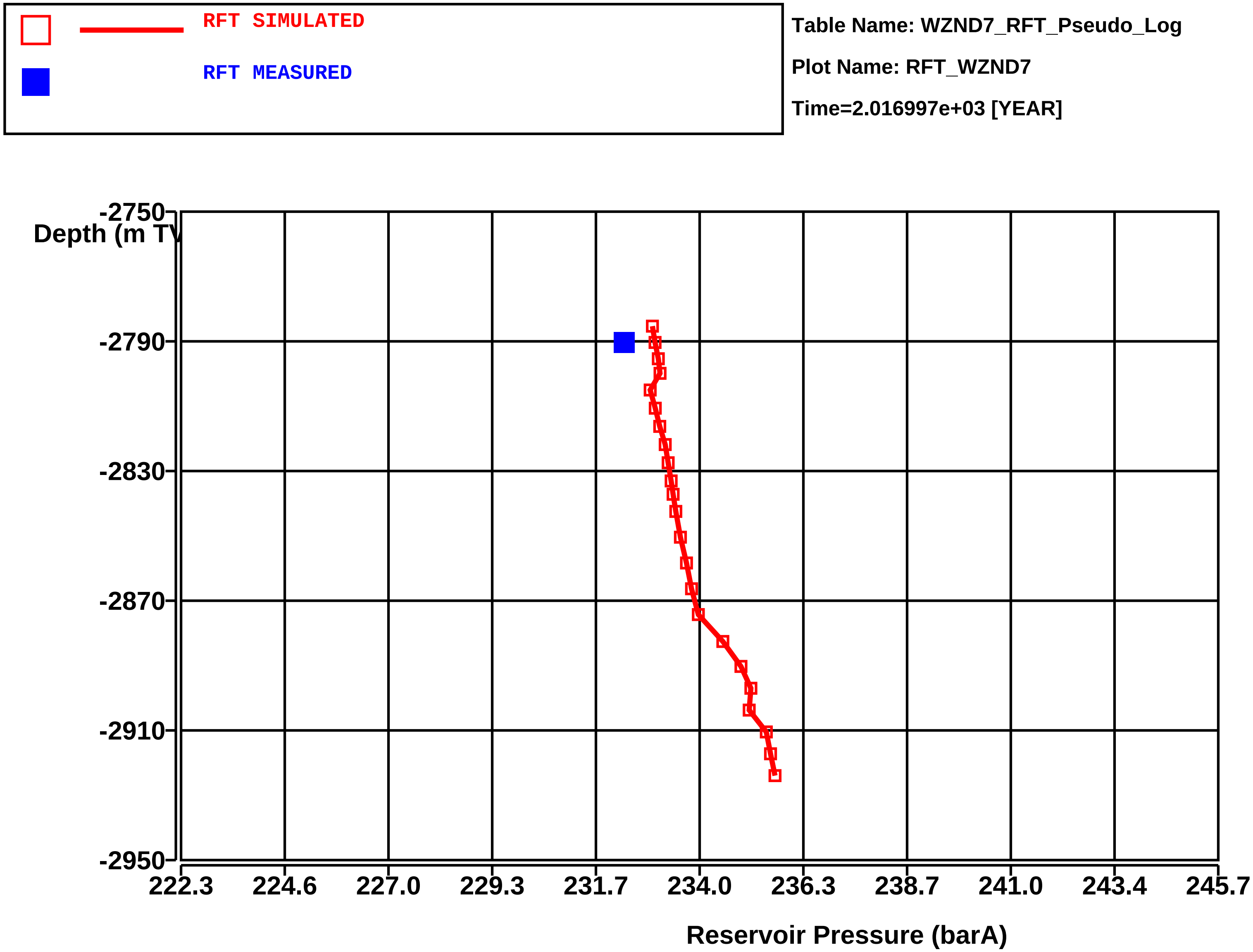

Creation date: Thu 09/02/2017 16:08
Runfile: GRO_2016_ED_v60.run

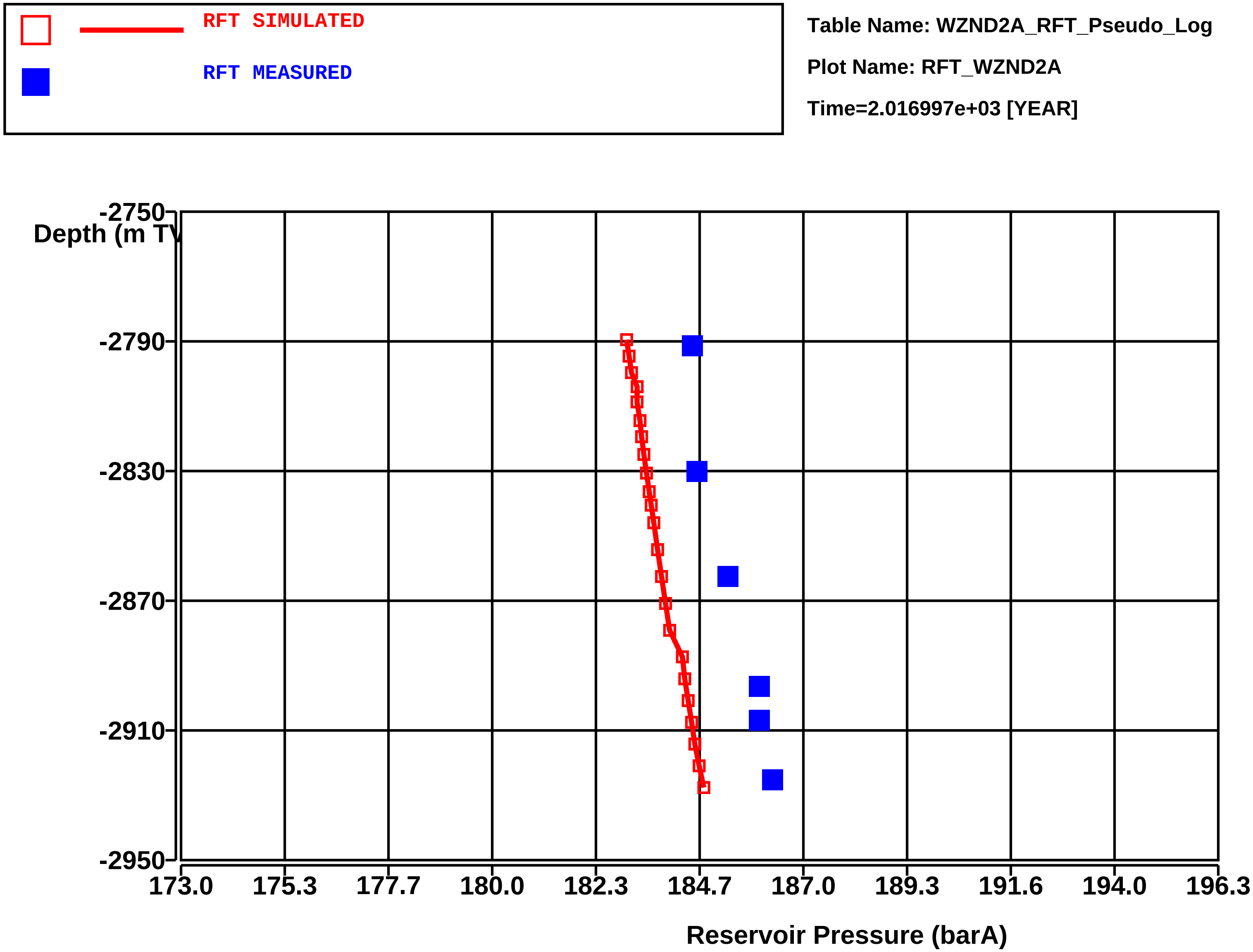

Table Name: WZND2A_RFT_Pseudo_Log

Plot Name: RFT_WZND2A

Time=2.016997e+03 [YEAR]

Creation date: Thu 09/02/2017 16:08

Runfile: GRO_2016_ED_v60.run

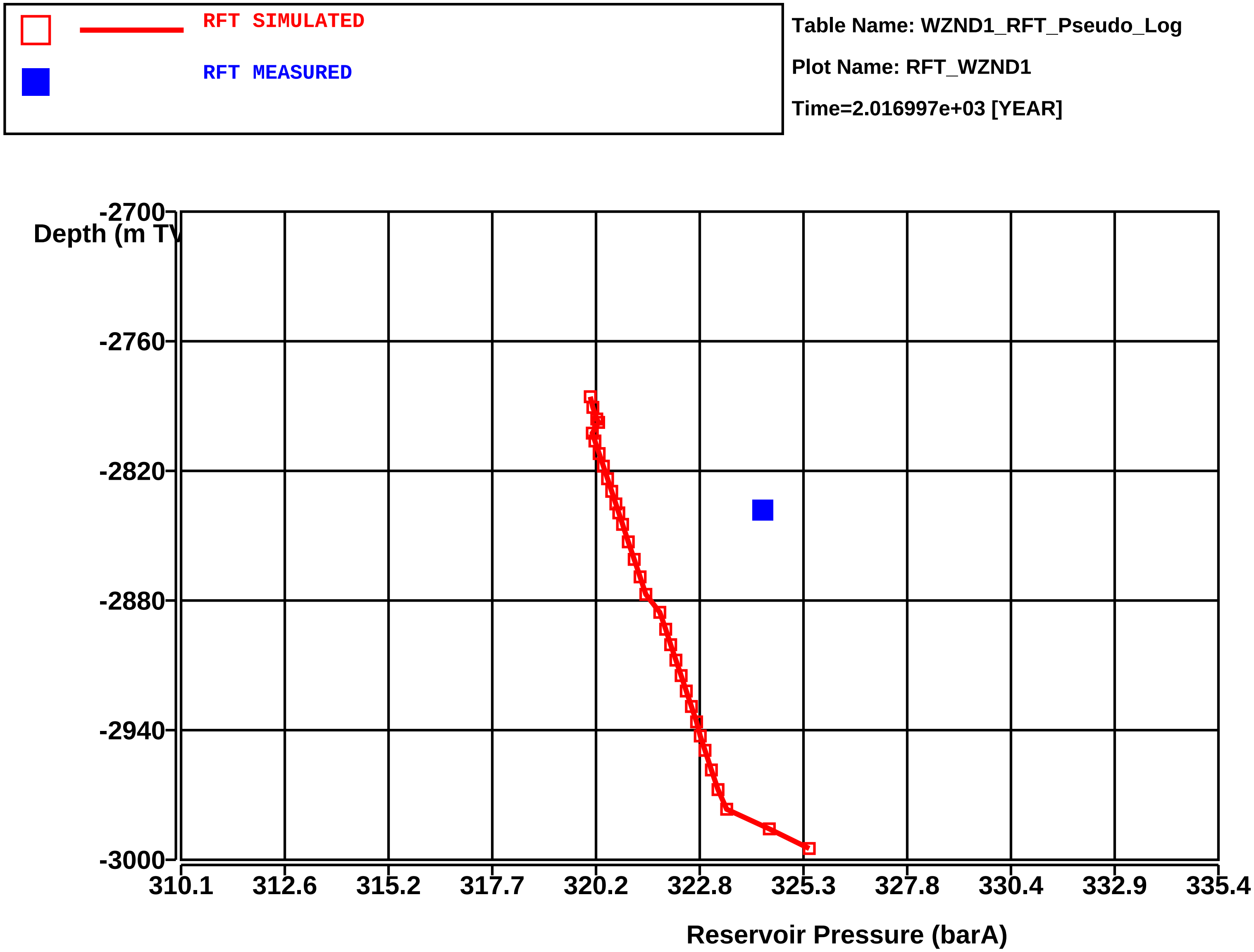

Creation date: Thu 09/02/2017 16:08
Runfile: GRO_2016_ED_v60.run

Table Name: WPAU3_RFT_Pseudo_Log

Plot Name: RFT_WPAU3

Time=2.016997e+03 [YEAR]

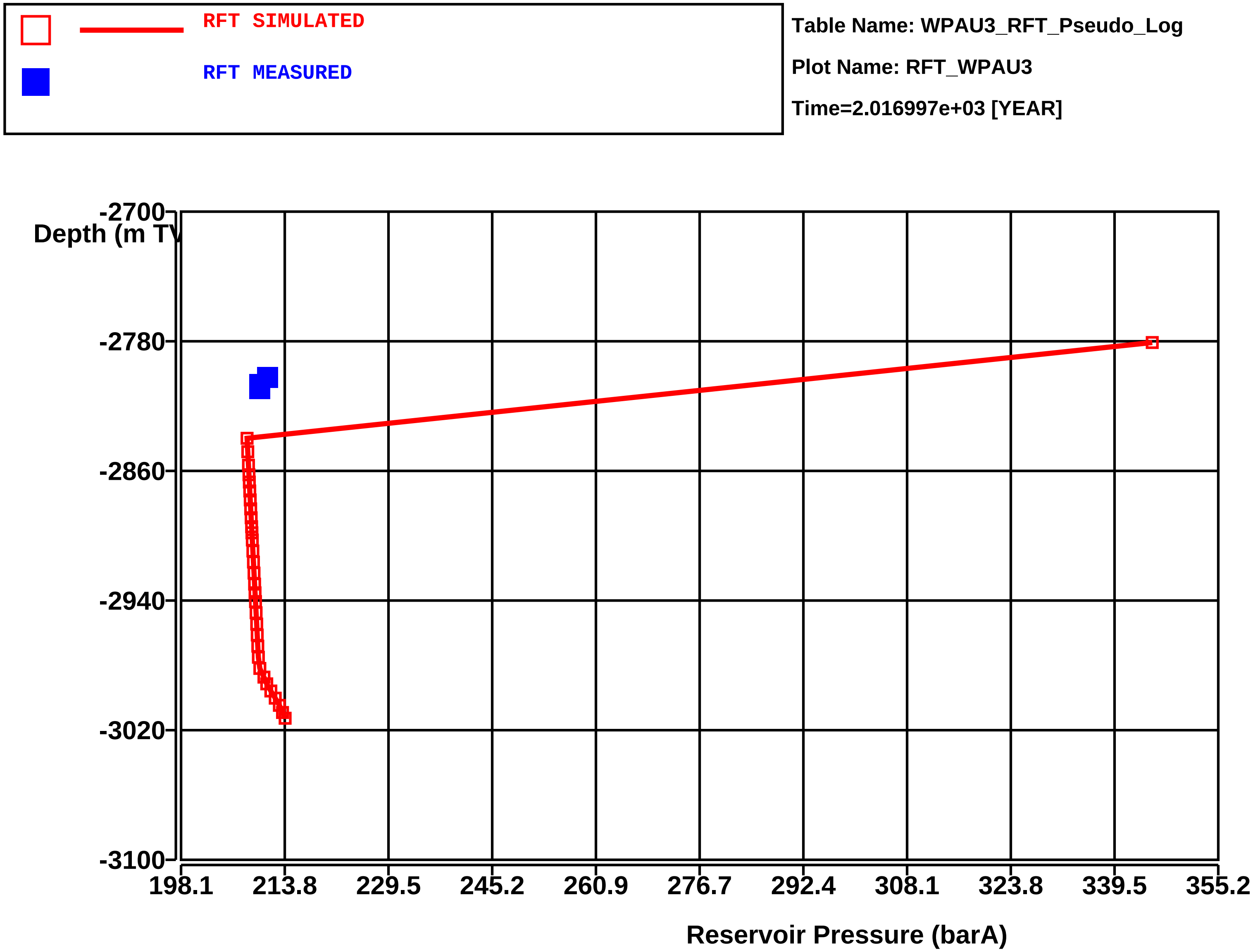

Creation date: Thu 09/02/2017 16:08

Runfile: GRO_2016_ED_v60.run

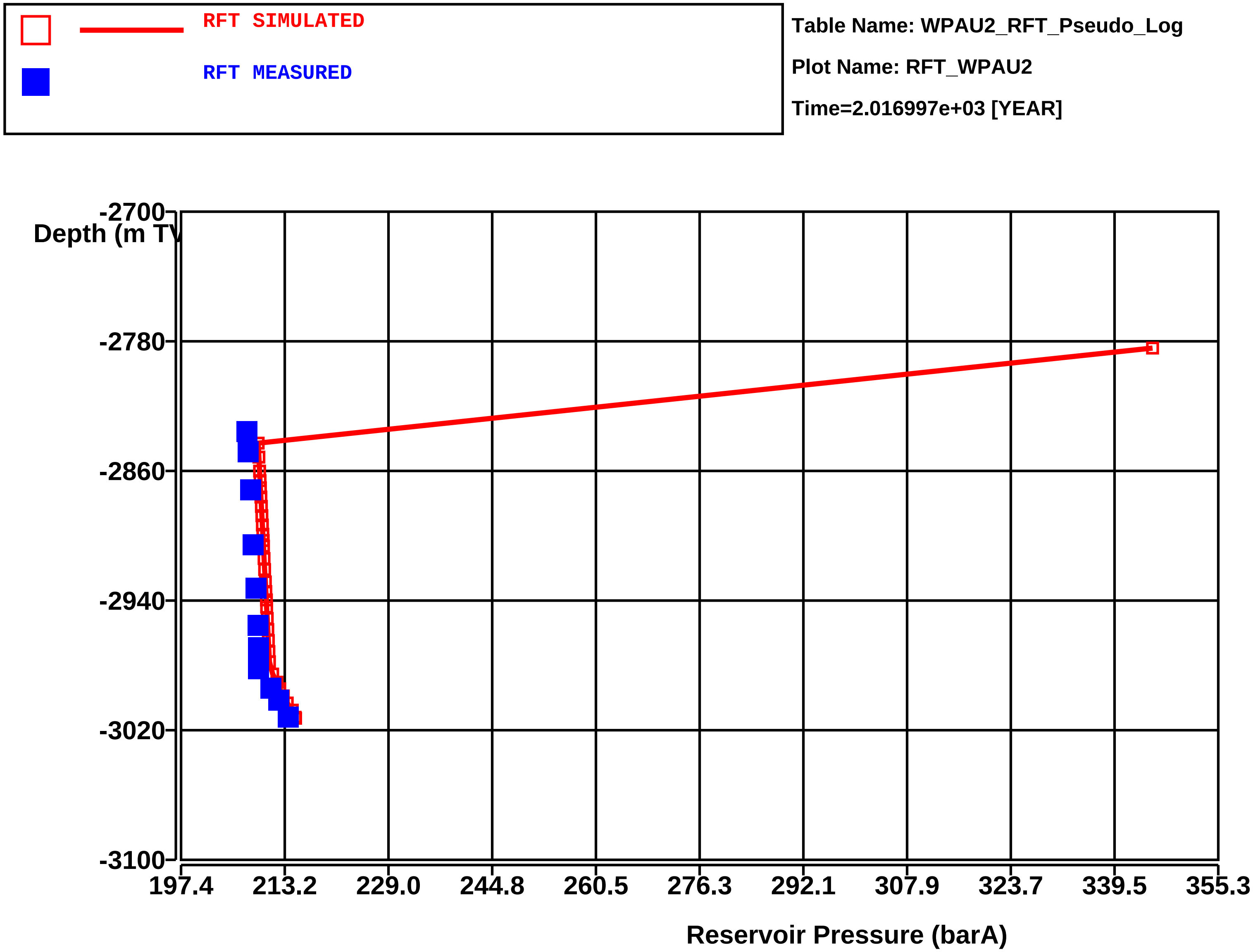

Table Name: WPAU2_RFT_Pseudo_Log

Plot Name: RFT_WPAU2

Time=2.016997e+03 [YEAR]

Creation date: Thu 09/02/2017 16:08

Runfile: GRO_2016_ED_v60.run

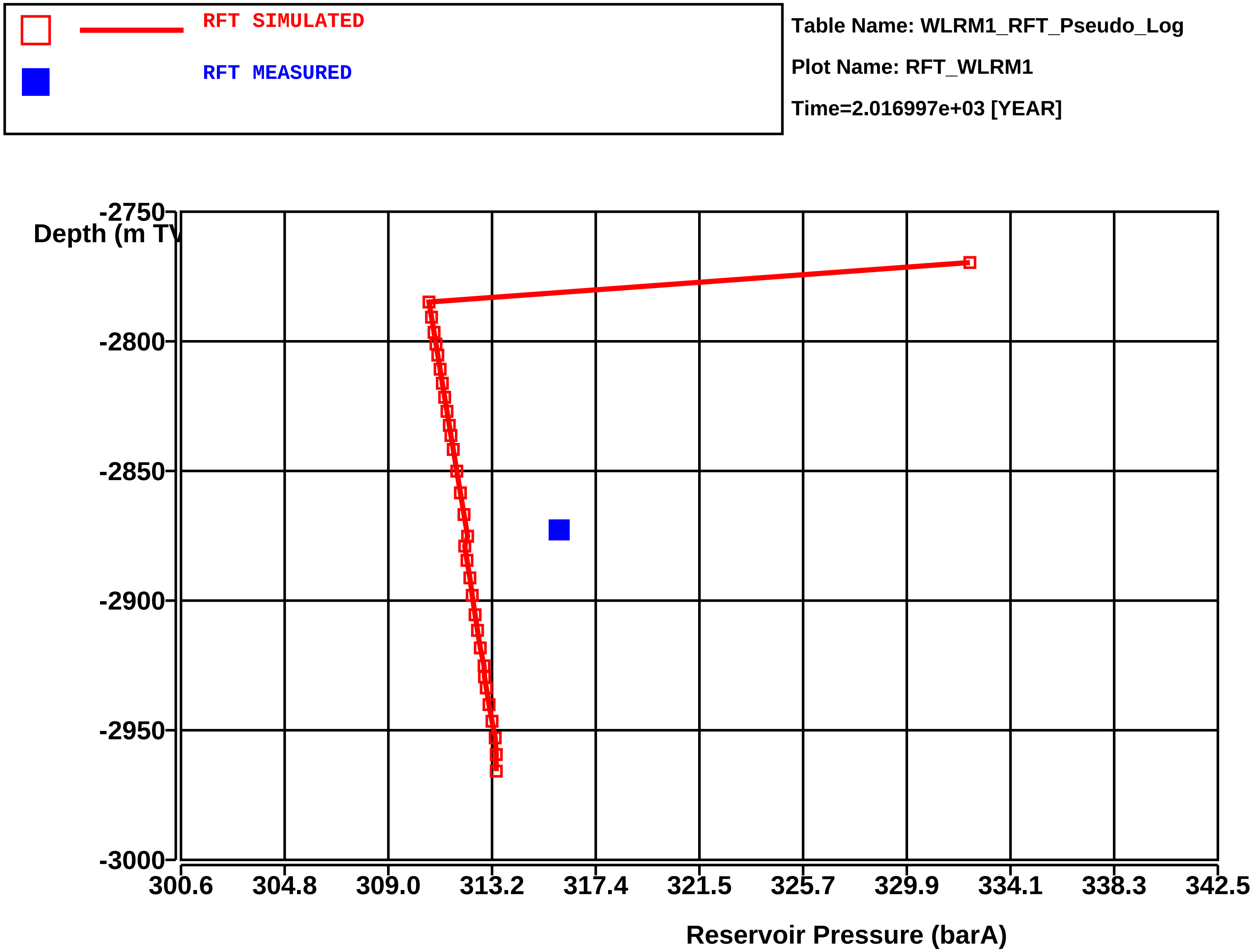

Creation date: Thu 09/02/2017 16:08

Runfile: GRO_2016_ED_v60.run

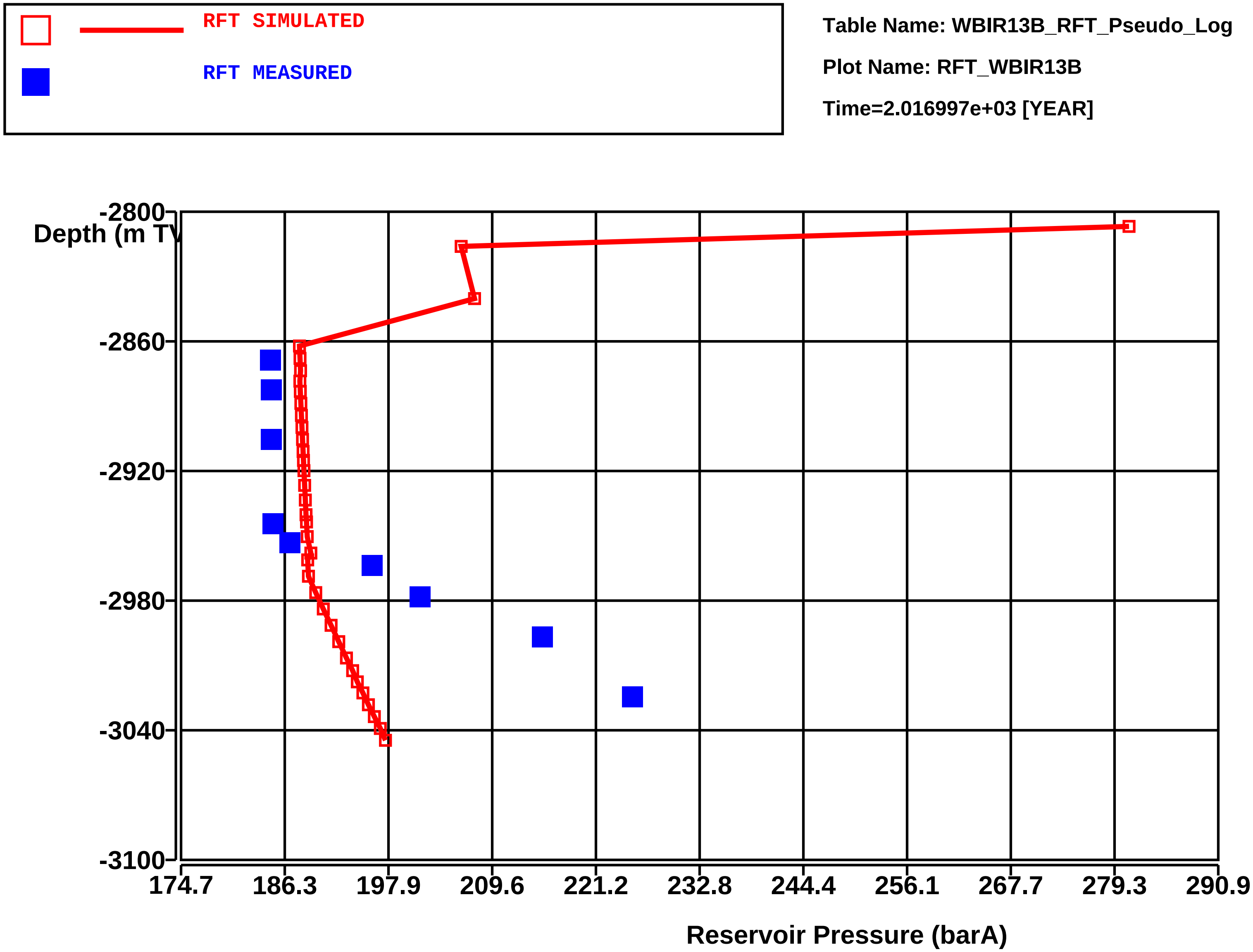

Creation date: Thu 09/02/2017 16:08
Runfile: GRO_2016_ED_v60.run

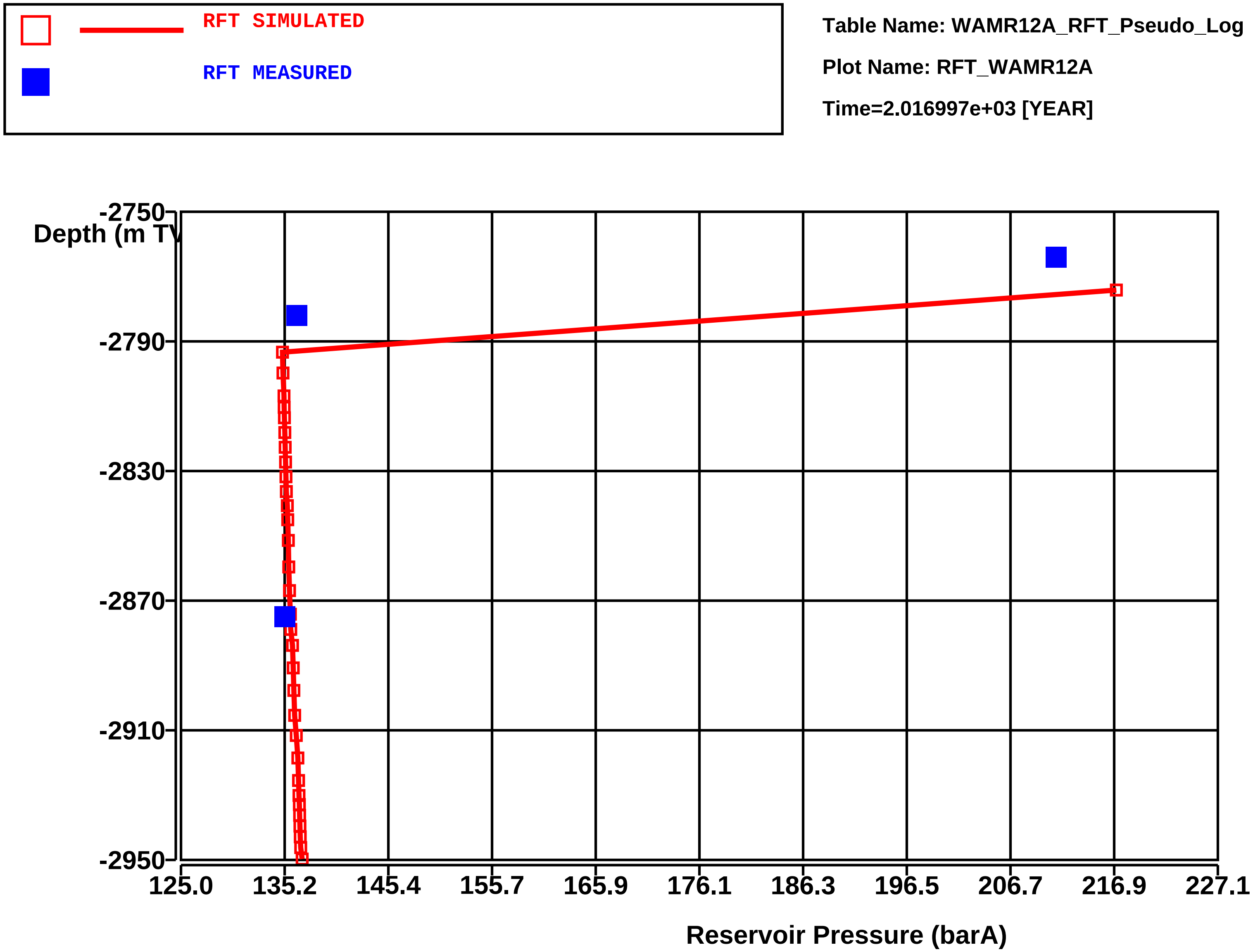

Table Name: WAMR12A_RFT_Pseudo_Log

Plot Name: RFT_WAMR12A

Time=2.016997e+03 [YEAR]

Creation date: Thu 09/02/2017 16:08

Runfile: GRO_2016_ED_v60.run

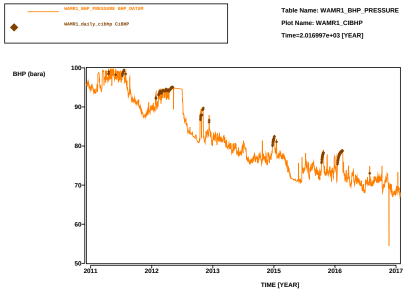

Creation date: Thu 09/02/2017 16:08
Runfile: GRO_2016_ED_v60.run

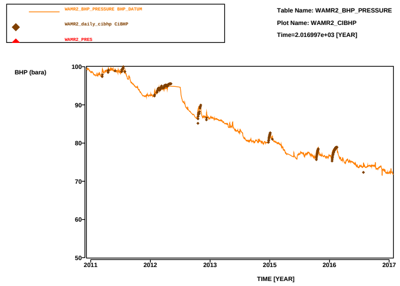

Creation date: Thu 09/02/2017 16:08
Runfile: GRO_2016_ED_v60.run

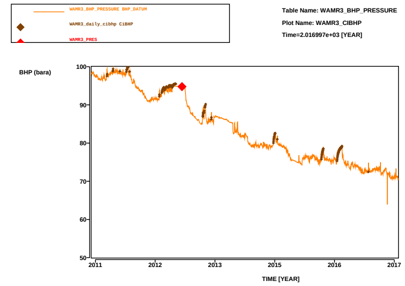

Creation date: Thu 09/02/2017 16:08
Runfile: GRO_2016_ED_v60.run

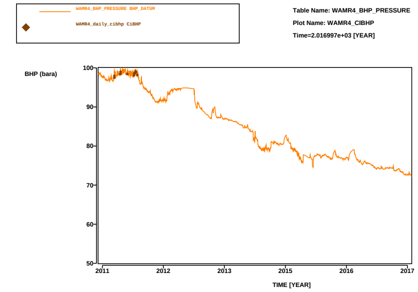

Creation date: Thu 09/02/2017 16:08
Runfile: GRO_2016_ED_v60.run

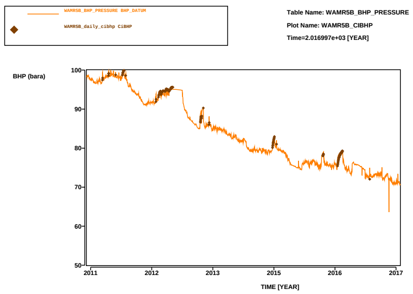

Creation date: Thu 09/02/2017 16:08
Runfile: GRO_2016_ED_v60.run

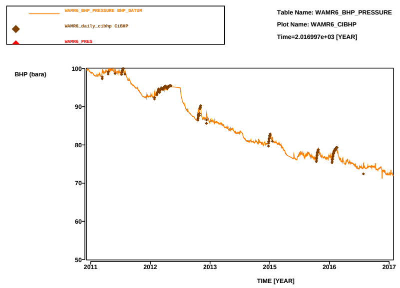

Creation date: Thu 09/02/2017 16:08
Runfile: GRO_2016_ED_v60.run

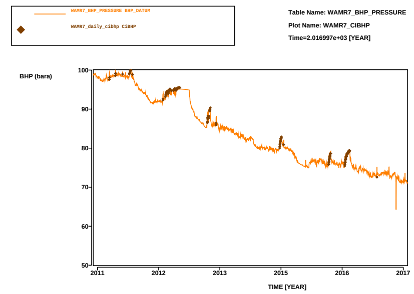

Creation date: Thu 09/02/2017 16:08
Runfile: GRO_2016_ED_v60.run

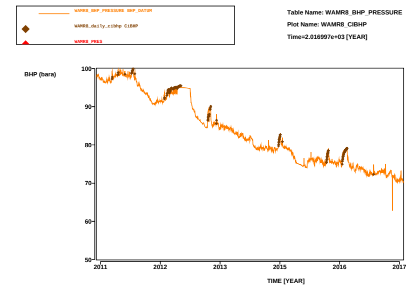

Creation date: Thu 09/02/2017 16:08
Runfile: GRO_2016_ED_v60.run

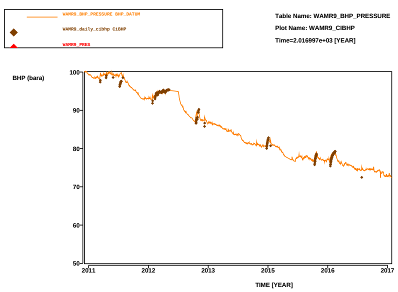

Creation date: Thu 09/02/2017 16:08
Runfile: GRO_2016_ED_v60.run

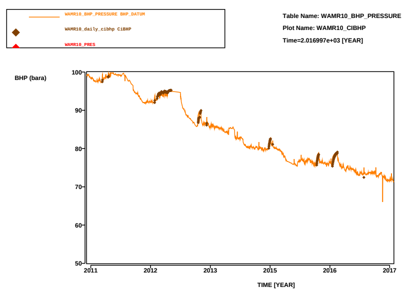

Creation date: Thu 09/02/2017 16:08
Runfile: GRO_2016_ED_v60.run

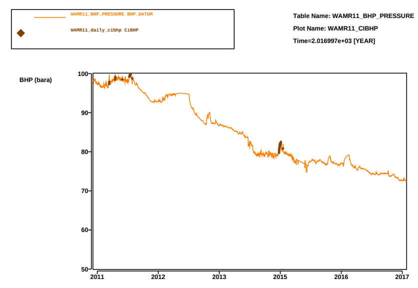

Creation date: Thu 09/02/2017 16:08
Runfile: GRO_2016_ED_v60.run

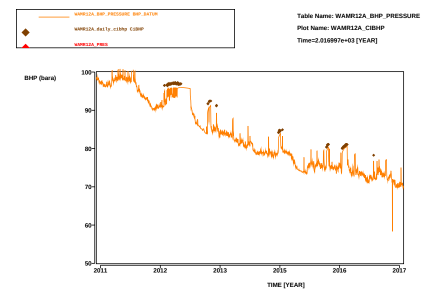

Creation date: Thu 09/02/2017 16:08
Runfile: GRO_2016_ED_v60.run

Table Name: WBIR1_BHP_PRESSURE
Plot Name: WBIR1_CIBHP
Time=2.016997e+03 [YEAR]

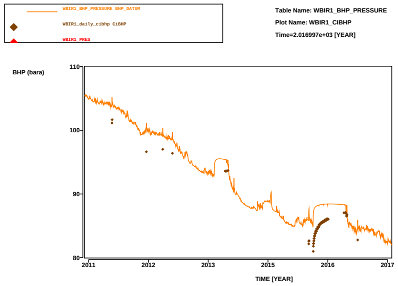

Creation date: Thu 09/02/2017 16:08
Runfile: GRO_2016_ED_v60.run

Table Name: WBIR2A_BHP_PRESSURE
Plot Name: WBIR2A_CIBHP
Time=2.016997e+03 [YEAR]

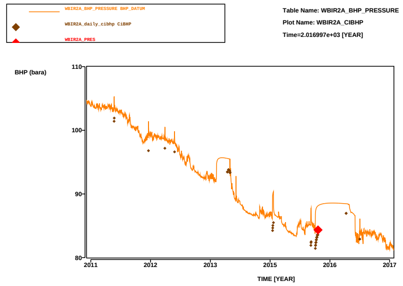

Creation date: Thu 09/02/2017 16:08
Runfile: GRO_2016_ED_v60.run

Table Name: WBIR3_BHP_PRESSURE
Plot Name: WBIR3_CIBHP
Time=2.016997e+03 [YEAR]

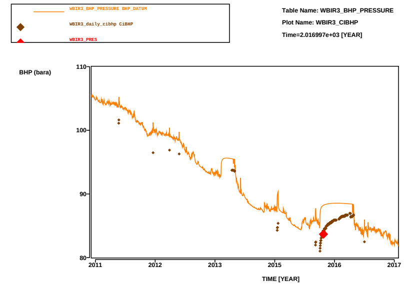

Creation date: Thu 09/02/2017 16:08
Runfile: GRO_2016_ED_v60.run

Table Name: WBIR4_BHP_PRESSURE
Plot Name: WBIR4_CIBHP
Time=2.016997e+03 [YEAR]

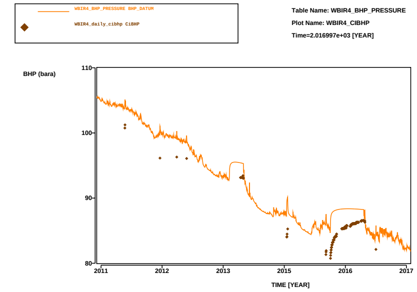

Creation date: Thu 09/02/2017 16:08
Runfile: GRO_2016_ED_v60.run

Table Name: WBIR5_BHP_PRESSURE
Plot Name: WBIR5_CIBHP
Time=2.016997e+03 [YEAR]

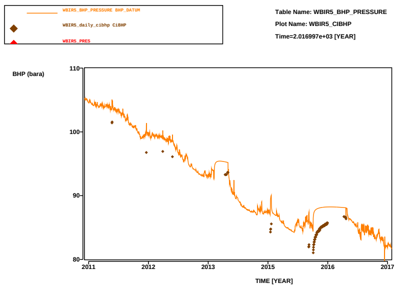

Creation date: Thu 09/02/2017 16:08
Runfile: GRO_2016_ED_v60.run

Table Name: WBIR6_BHP_PRESSURE
Plot Name: WBIR6_CIBHP
Time=2.016997e+03 [YEAR]

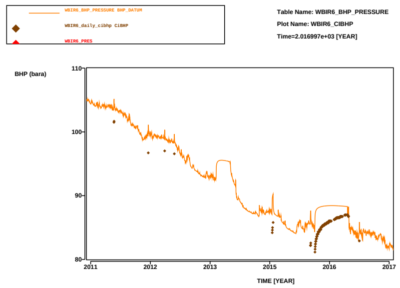

Creation date: Thu 09/02/2017 16:08
Runfile: GRO_2016_ED_v60.run

Table Name: WBIR7_BHP_PRESSURE
Plot Name: WBIR7_CIBHP
Time=2.016997e+03 [YEAR]

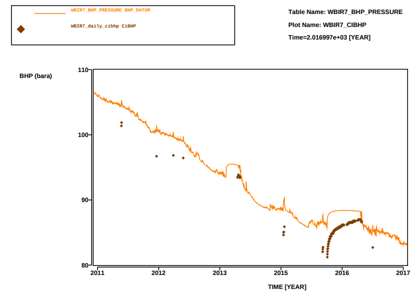

Creation date: Thu 09/02/2017 16:08
Runfile: GRO_2016_ED_v60.run

Table Name: WBIR8_BHP_PRESSURE
Plot Name: WBIR8_CIBHP
Time=2.016997e+03 [YEAR]

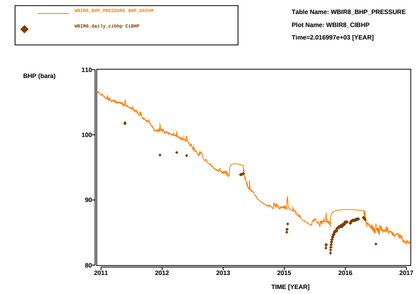

Creation date: Thu 09/02/2017 16:08
Runfile: GRO_2016_ED_v60.run

Table Name: WBIR9_BHP_PRESSURE
Plot Name: WBIR9_CIBHP
Time=2.016997e+03 [YEAR]

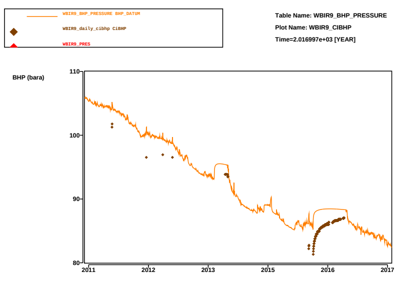

Creation date: Thu 09/02/2017 16:08
Runfile: GRO_2016_ED_v60.run

Table Name: WBIR10_BHP_PRESSURE
Plot Name: WBIR10_CIBHP
Time=2.016997e+03 [YEAR]

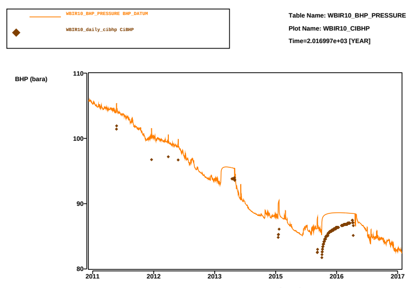

Creation date: Thu 09/02/2017 16:08
Runfile: GRO_2016_ED_v60.run

Table Name: WBIR11_BHP_PRESSURE
Plot Name: WBIR11_CIBHP
Time=2.016997e+03 [YEAR]

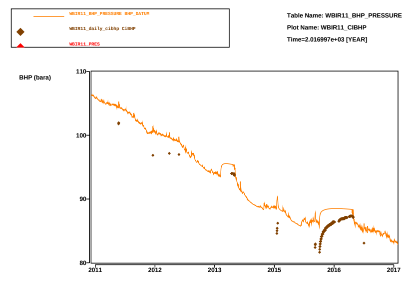

Creation date: Thu 09/02/2017 16:08
Runfile: GRO_2016_ED_v60.run

Table Name: WBIR12_BHP_PRESSURE
Plot Name: WBIR12_CIBHP
Time=2.016997e+03 [YEAR]

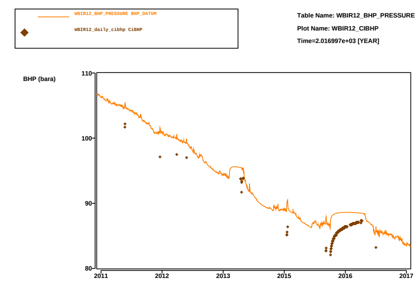

Creation date: Thu 09/02/2017 16:08
Runfile: GRO_2016_ED_v60.run

Table Name: WBIR13B_BHP_PRESSURE
Plot Name: WBIR13B_CIBHP
Time=2.016997e+03 [YEAR]

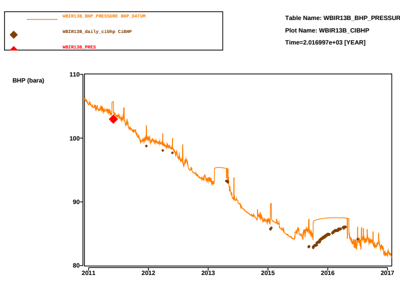

Creation date: Thu 09/02/2017 16:08
Runfile: GRO_2016_ED_v60.run

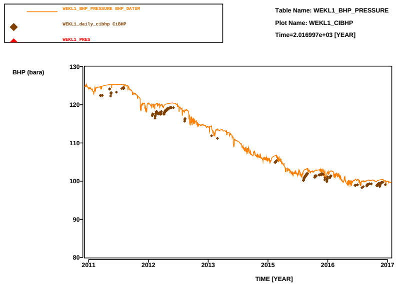

Creation date: Thu 09/02/2017 16:08
Runfile: GRO_2016_ED_v60.run

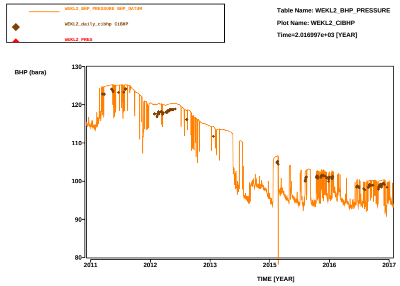

Creation date: Thu 09/02/2017 16:08
Runfile: GRO_2016_ED_v60.run

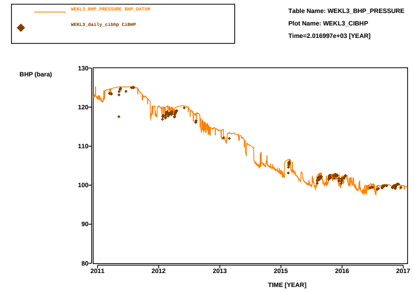

Creation date: Thu 09/02/2017 16:08
Runfile: GRO_2016_ED_v60.run

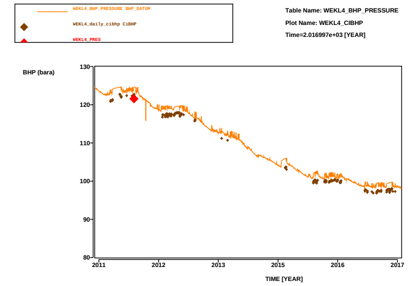

Creation date: Thu 09/02/2017 16:08
Runfile: GRO_2016_ED_v60.run

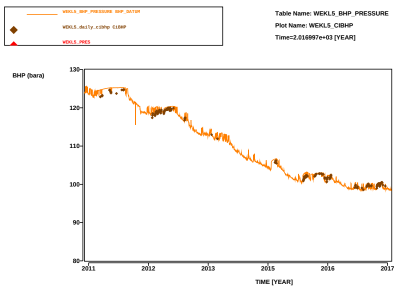

Creation date: Thu 09/02/2017 16:08
Runfile: GRO_2016_ED_v60.run

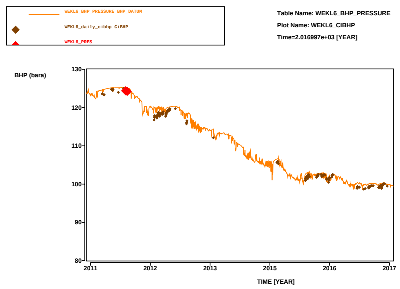

Creation date: Thu 09/02/2017 16:08
Runfile: GRO_2016_ED_v60.run

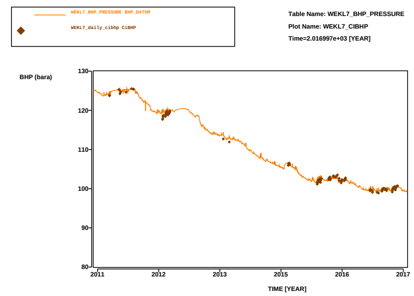

Creation date: Thu 09/02/2017 16:08
Runfile: GRO_2016_ED_v60.run

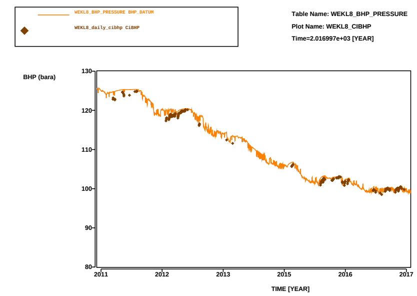

Creation date: Thu 09/02/2017 16:08
Runfile: GRO_2016_ED_v60.run

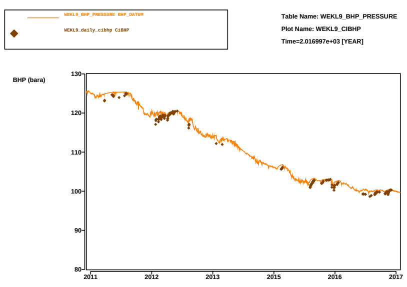

Creation date: Thu 09/02/2017 16:08
Runfile: GRO_2016_ED_v60.run

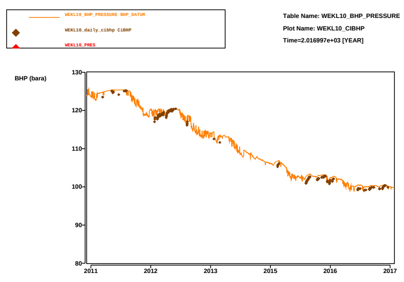

Creation date: Thu 09/02/2017 16:08
Runfile: GRO_2016_ED_v60.run

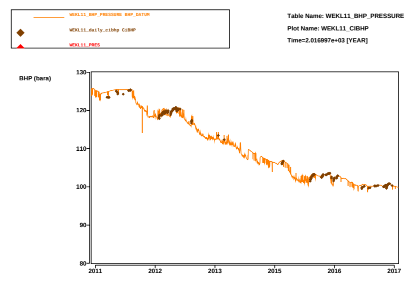

Creation date: Thu 09/02/2017 16:08
Runfile: GRO_2016_ED_v60.run

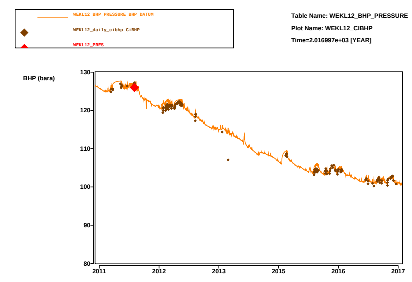

Creation date: Thu 09/02/2017 16:08
Runfile: GRO_2016_ED_v60.run

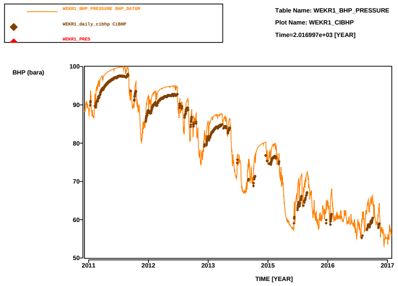

Creation date: Thu 09/02/2017 16:08
Runfile: GRO_2016_ED_v60.run

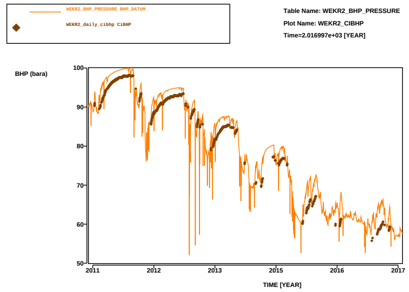

Creation date: Thu 09/02/2017 16:08
Runfile: GRO_2016_ED_v60.run

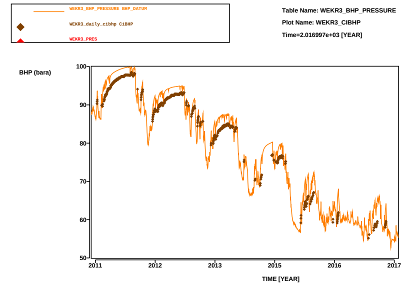

Creation date: Thu 09/02/2017 16:08
Runfile: GRO_2016_ED_v60.run

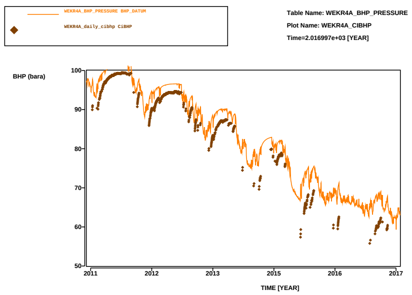

Creation date: Thu 09/02/2017 16:09
Runfile: GRO_2016_ED_v60.run

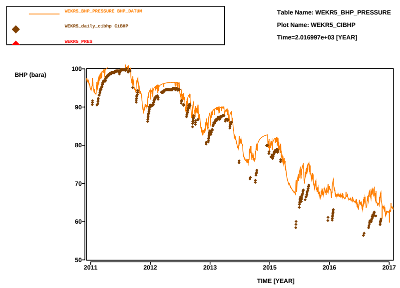

Creation date: Thu 09/02/2017 16:09
Runfile: GRO_2016_ED_v60.run

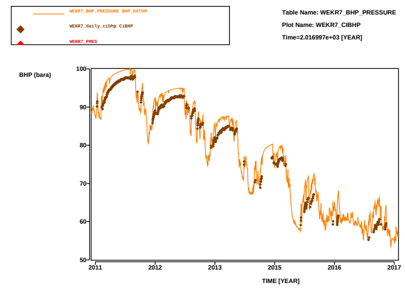

Creation date: Thu 09/02/2017 16:09
Runfile: GRO_2016_ED_v60.run

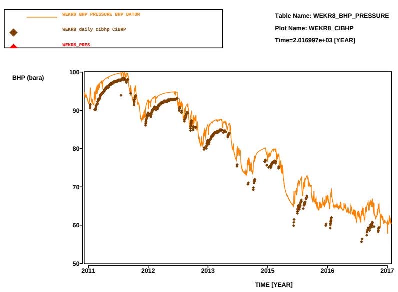

Creation date: Thu 09/02/2017 16:09
Runfile: GRO_2016_ED_v60.run

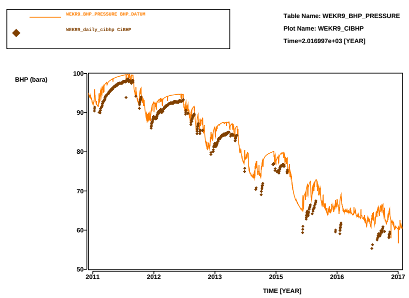

Creation date: Thu 09/02/2017 16:09
Runfile: GRO_2016_ED_v60.run

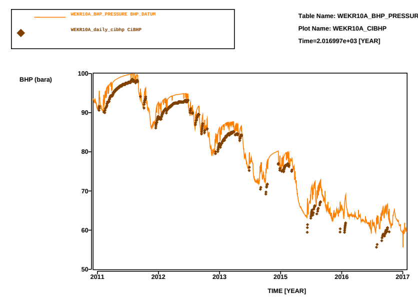

Creation date: Thu 09/02/2017 16:09
Runfile: GRO_2016_ED_v60.run

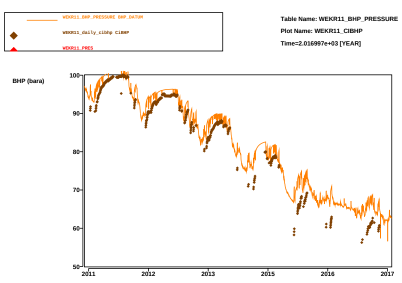

Creation date: Thu 09/02/2017 16:09
Runfile: GRO_2016_ED_v60.run

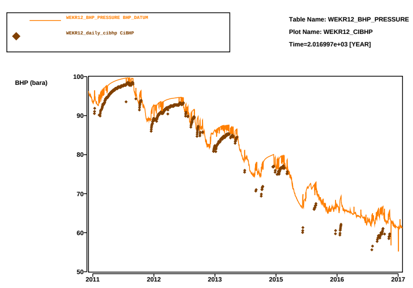

Creation date: Thu 09/02/2017 16:09
Runfile: GRO_2016_ED_v60.run

WEKR201_BHP_PRESSURE BHP_DATUM
WEKR201_daily_cibhp CiBHP
WEKR201_PRES

Table Name: WEKR201_BHP_PRESSURE
Plot Name: WEKR201_CIBHP
Time=2.016997e+03 [YEAR]

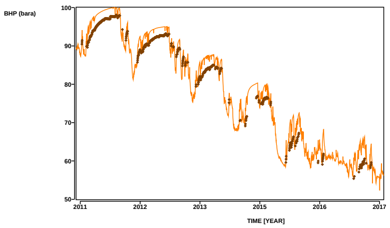

Creation date: Thu 09/02/2017 16:09
Runfile: GRO_2016_ED_v60.run

WEKR202_BHP_PRESSURE BHP_DATUM
WEKR202_daily_cibhp CiBHP

Table Name: WEKR202_BHP_PRESSURE
Plot Name: WEKR202_CIBHP
Time=2.016997e+03 [YEAR]

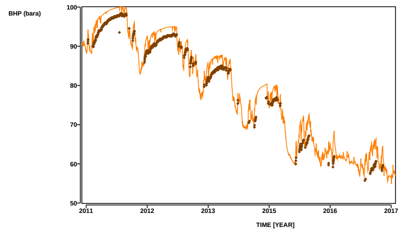

Creation date: Thu 09/02/2017 16:09
Runfile: GRO_2016_ED_v60.run

WEKR203_BHP_PRESSURE BHP_DATUM
WEKR203_daily_cibhp CiBHP

Table Name: WEKR203_BHP_PRESSURE
Plot Name: WEKR203_CIBHP
Time=2.016997e+03 [YEAR]

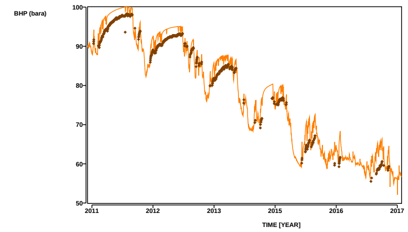

Creation date: Thu 09/02/2017 16:09
Runfile: GRO_2016_ED_v60.run

WEKR204_BHP_PRESSURE BHP_DATUM
WEKR204_daily_cibhp CiBHP
WEKR204_PRES

Table Name: WEKR204_BHP_PRESSURE
Plot Name: WEKR204_CIBHP
Time=2.016997e+03 [YEAR]

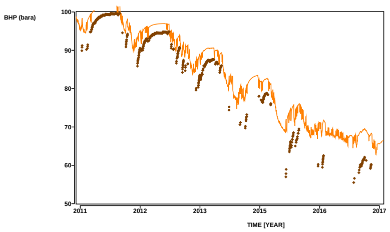

Creation date: Thu 09/02/2017 16:09
Runfile: GRO_2016_ED_v60.run

WEKR205_BHP_PRESSURE BHP_DATUM
WEKR205_daily_cibhp CiBHP
WEKR205_PRES

Table Name: WEKR205_BHP_PRESSURE
Plot Name: WEKR205_CIBHP
Time=2.016997e+03 [YEAR]

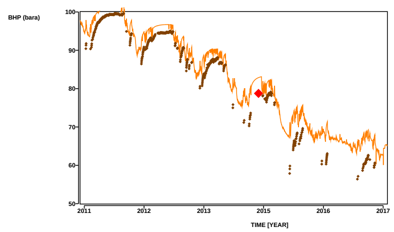

Creation date: Thu 09/02/2017 16:09
Runfile: GRO_2016_ED_v60.run

WEKR206_BHP_PRESSURE BHP_DATUM
WEKR206_daily_cibhp CiBHP

Table Name: WEKR206_BHP_PRESSURE
Plot Name: WEKR206_CIBHP
Time=2.016997e+03 [YEAR]

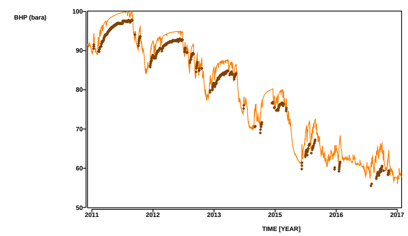

Creation date: Thu 09/02/2017 16:09
Runfile: GRO_2016_ED_v60.run

WEKR207_BHP_PRESSURE BHP_DATUM
WEKR207_daily_cibhp CiBHP

Table Name: WEKR207_BHP_PRESSURE
Plot Name: WEKR207_CIBHP
Time=2.016997e+03 [YEAR]

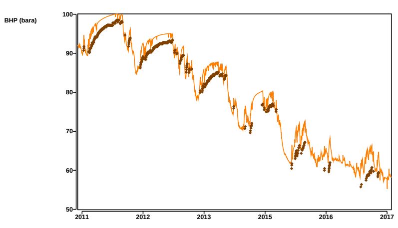

Creation date: Thu 09/02/2017 16:09
Runfile: GRO_2016_ED_v60.run

WEKR208_BHP_PRESSURE BHP_DATUM
WEKR208_daily_cibhp CiBHP

Table Name: WEKR208_BHP_PRESSURE
Plot Name: WEKR208_CIBHP
Time=2.016997e+03 [YEAR]

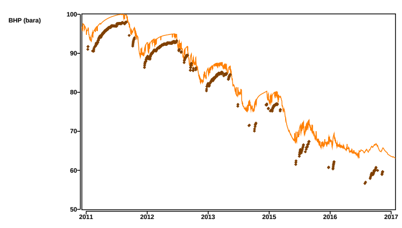

Creation date: Thu 09/02/2017 16:09
Runfile: GRO_2016_ED_v60.run

WEKR209_BHP_PRESSURE BHP_DATUM
WEKR209_daily_cibhp CiBHP
WEKR209_PRES

Table Name: WEKR209_BHP_PRESSURE
Plot Name: WEKR209_CIBHP
Time=2.016997e+03 [YEAR]

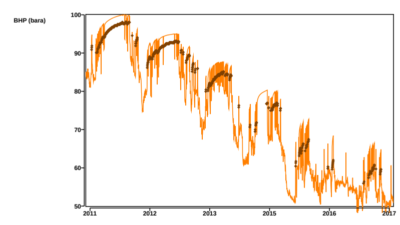

Creation date: Thu 09/02/2017 16:09
Runfile: GRO_2016_ED_v60.run

WEKR210_BHP_PRESSURE BHP_DATUM
WEKR210_daily_cibhp CiBHP
WEKR210_PRES

Table Name: WEKR210_BHP_PRESSURE
Plot Name: WEKR210_CIBHP
Time=2.016997e+03 [YEAR]

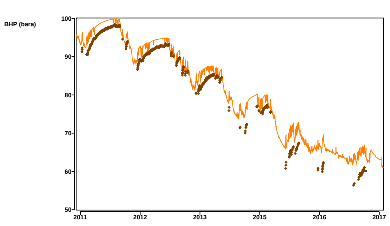

Creation date: Thu 09/02/2017 16:09
Runfile: GRO_2016_ED_v60.run

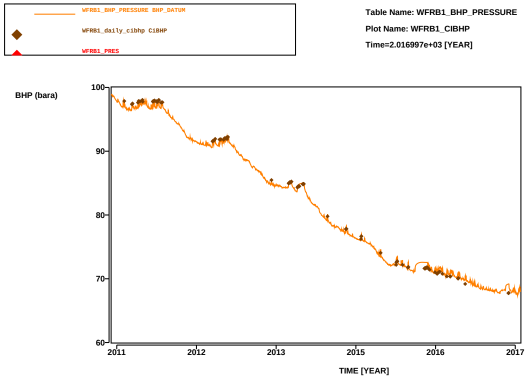

Creation date: Thu 09/02/2017 16:09
Runfile: GRO_2016_ED_v60.run

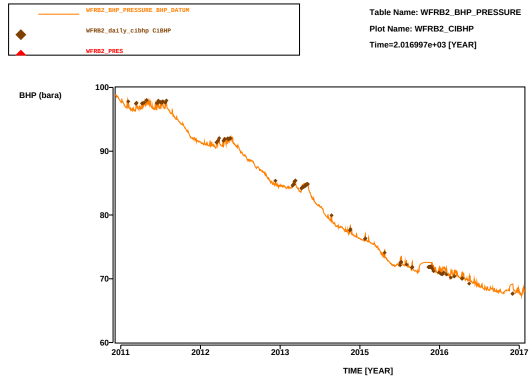

Creation date: Thu 09/02/2017 16:09
Runfile: GRO_2016_ED_v60.run

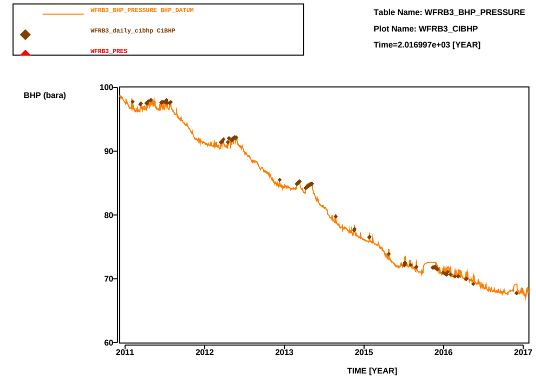

Creation date: Thu 09/02/2017 16:09
Runfile: GRO_2016_ED_v60.run

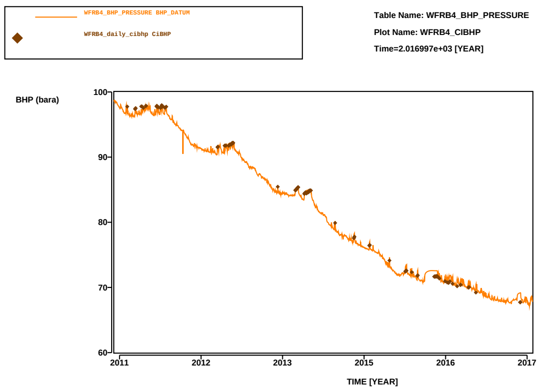

Creation date: Thu 09/02/2017 16:09
Runfile: GRO_2016_ED_v60.run

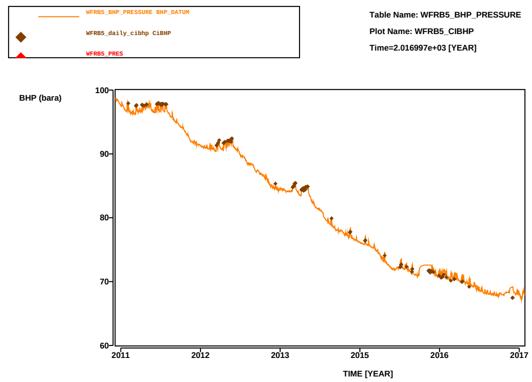

Creation date: Thu 09/02/2017 16:09
Runfile: GRO_2016_ED_v60.run

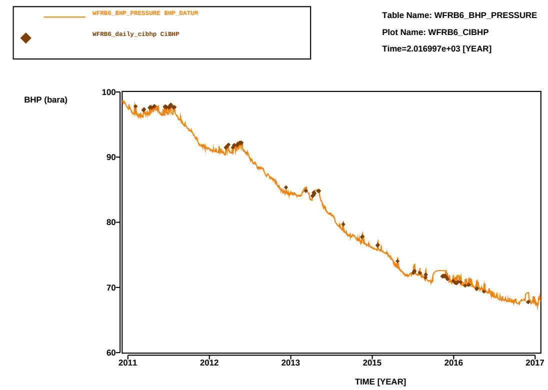

Creation date: Thu 09/02/2017 16:09
Runfile: GRO_2016_ED_v60.run

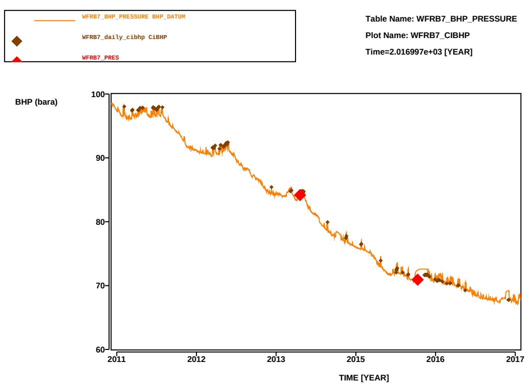

Creation date: Thu 09/02/2017 16:09
Runfile: GRO_2016_ED_v60.run

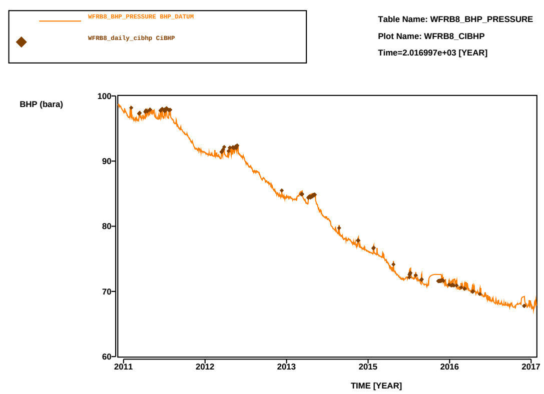

Creation date: Thu 09/02/2017 16:09
Runfile: GRO_2016_ED_v60.run

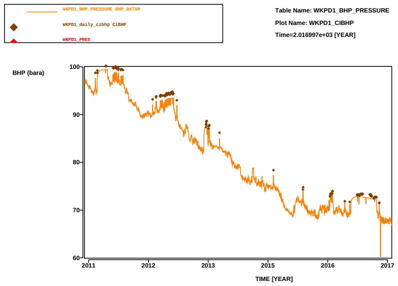

Creation date: Thu 09/02/2017 16:09
Runfile: GRO_2016_ED_v60.run

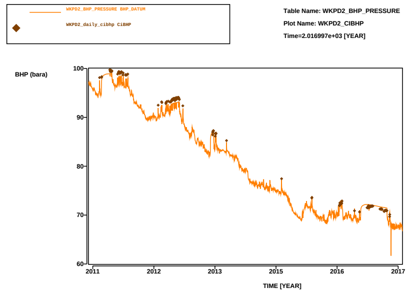

Creation date: Thu 09/02/2017 16:09
Runfile: GRO_2016_ED_v60.run

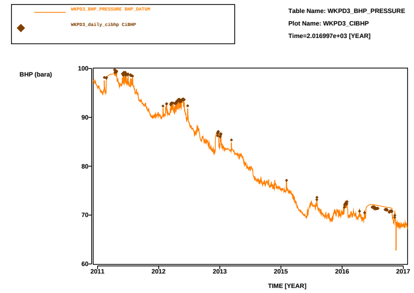

Creation date: Thu 09/02/2017 16:09
Runfile: GRO_2016_ED_v60.run

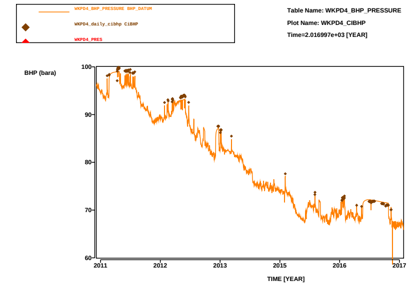

Creation date: Thu 09/02/2017 16:09
Runfile: GRO_2016_ED_v60.run

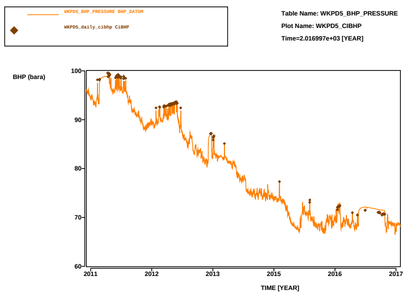

Creation date: Thu 09/02/2017 16:09
Runfile: GRO_2016_ED_v60.run

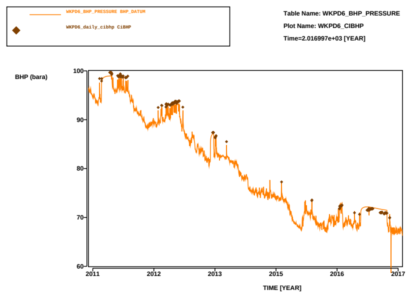

Creation date: Thu 09/02/2017 16:09
Runfile: GRO_2016_ED_v60.run

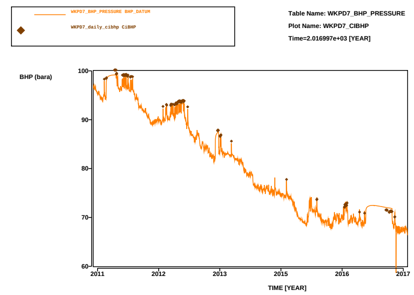

Creation date: Thu 09/02/2017 16:09
Runfile: GRO_2016_ED_v60.run

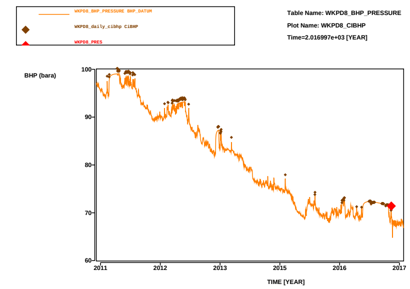

Creation date: Thu 09/02/2017 16:09
Runfile: GRO_2016_ED_v60.run

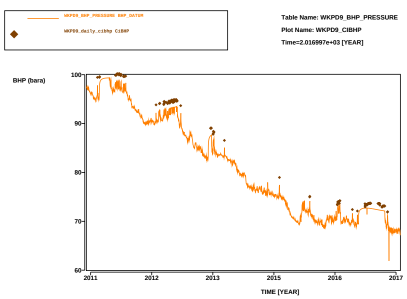

Creation date: Thu 09/02/2017 16:09
Runfile: GRO_2016_ED_v60.run

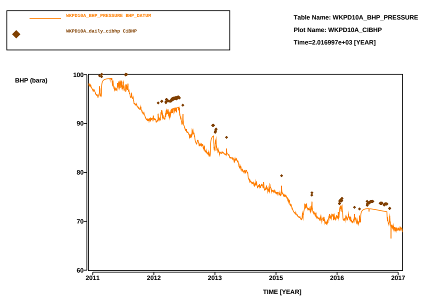

Creation date: Thu 09/02/2017 16:09
Runfile: GRO_2016_ED_v60.run

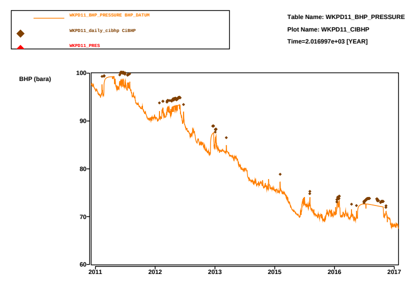

Creation date: Thu 09/02/2017 16:09
Runfile: GRO_2016_ED_v60.run

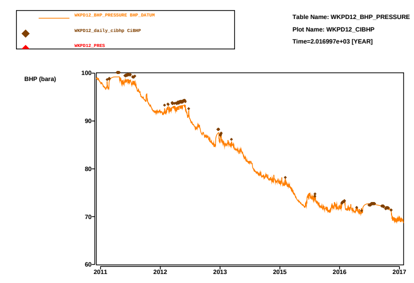

Creation date: Thu 09/02/2017 16:09
Runfile: GRO_2016_ED_v60.run

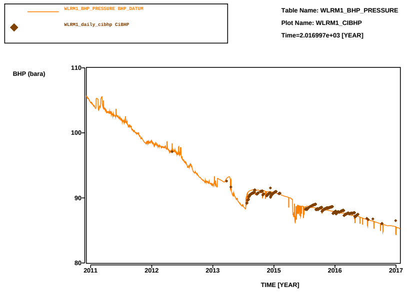

Creation date: Thu 09/02/2017 16:09
Runfile: GRO_2016_ED_v60.run

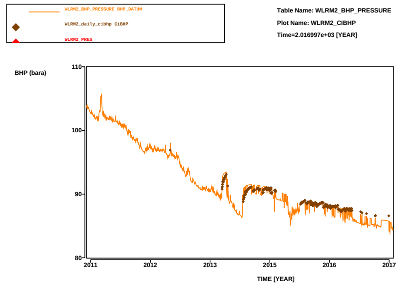

Creation date: Thu 09/02/2017 16:09
Runfile: GRO_2016_ED_v60.run

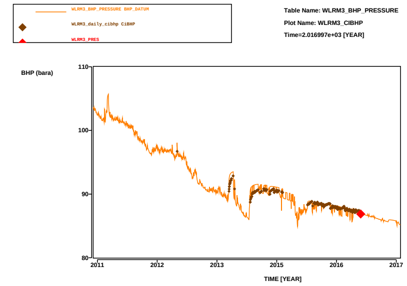

Creation date: Thu 09/02/2017 16:09
Runfile: GRO_2016_ED_v60.run

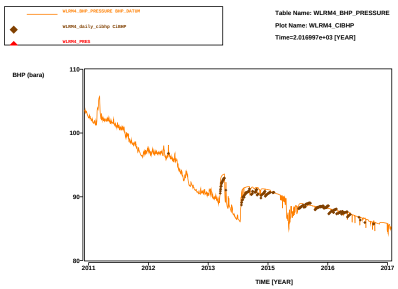

Creation date: Thu 09/02/2017 16:09
Runfile: GRO_2016_ED_v60.run

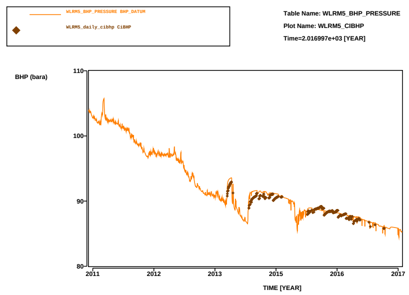

Creation date: Thu 09/02/2017 16:09
Runfile: GRO_2016_ED_v60.run

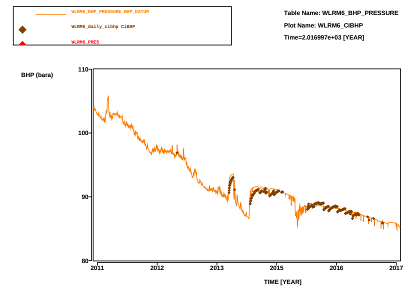

Creation date: Thu 09/02/2017 16:09
Runfile: GRO_2016_ED_v60.run

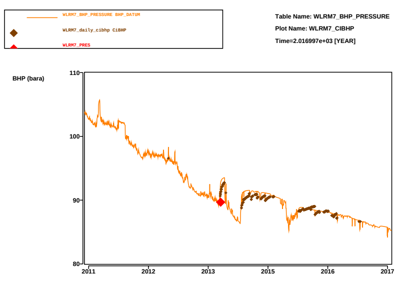

Creation date: Thu 09/02/2017 16:09
Runfile: GRO_2016_ED_v60.run

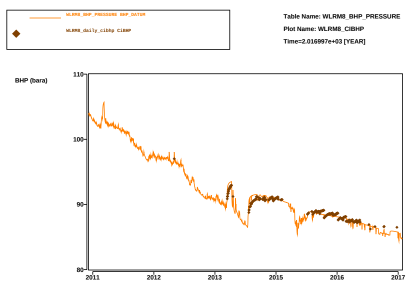

Creation date: Thu 09/02/2017 16:09
Runfile: GRO_2016_ED_v60.run

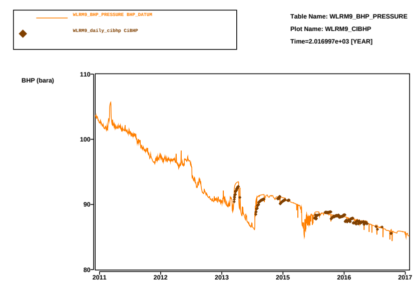

Creation date: Thu 09/02/2017 16:09
Runfile: GRO_2016_ED_v60.run

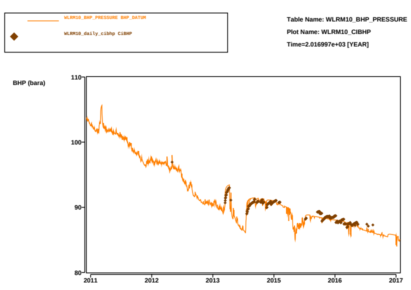

Creation date: Thu 09/02/2017 16:09
Runfile: GRO_2016_ED_v60.run

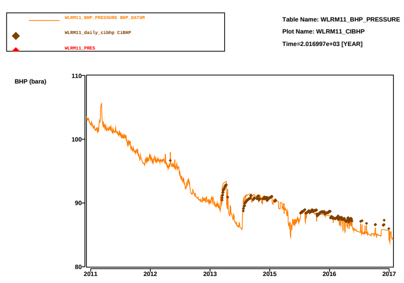

Creation date: Thu 09/02/2017 16:09
Runfile: GRO_2016_ED_v60.run

Table Name: WOVS1_BHP_PRESSURE
Plot Name: WOVS1_CIBHP
Time=2.016997e+03 [YEAR]

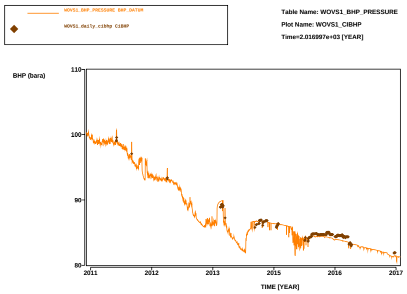

Creation date: Thu 09/02/2017 16:09
Runfile: GRO_2016_ED_v60.run

Table Name: WOVS2_BHP_PRESSURE
Plot Name: WOVS2_CIBHP
Time=2.016997e+03 [YEAR]

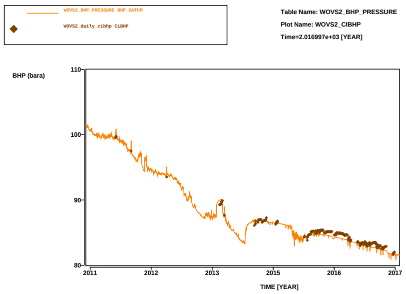

Creation date: Thu 09/02/2017 16:09
Runfile: GRO_2016_ED_v60.run

Table Name: WOVS3_BHP_PRESSURE
Plot Name: WOVS3_CIBHP
Time=2.016997e+03 [YEAR]

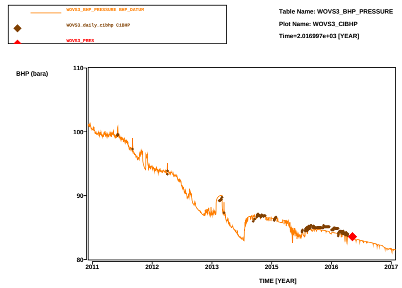

Creation date: Thu 09/02/2017 16:09
Runfile: GRO_2016_ED_v60.run

Table Name: WOVS4_BHP_PRESSURE
Plot Name: WOVS4_CIBHP
Time=2.016997e+03 [YEAR]

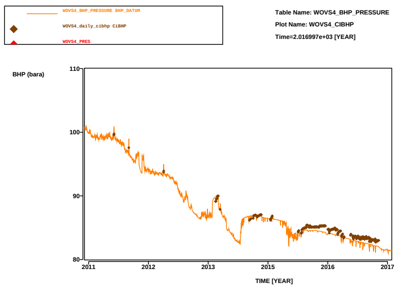

Creation date: Thu 09/02/2017 16:09
Runfile: GRO_2016_ED_v60.run

Table Name: WOVS5A_BHP_PRESSURE
Plot Name: WOVS5A_CIBHP
Time=2.016997e+03 [YEAR]

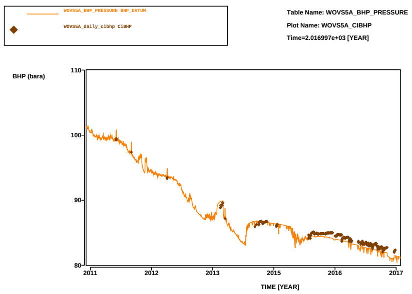

Creation date: Thu 09/02/2017 16:09
Runfile: GRO_2016_ED_v60.run

Table Name: WOVS6_BHP_PRESSURE
Plot Name: WOVS6_CIBHP
Time=2.016997e+03 [YEAR]

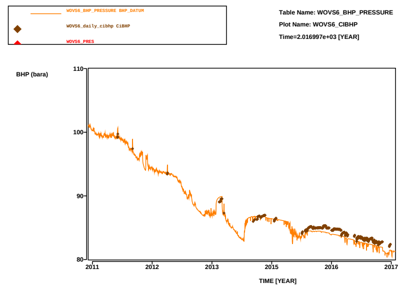

Creation date: Thu 09/02/2017 16:09
Runfile: GRO_2016_ED_v60.run

Table Name: WOVS7_BHP_PRESSURE
Plot Name: WOVS7_CIBHP
Time=2.016997e+03 [YEAR]

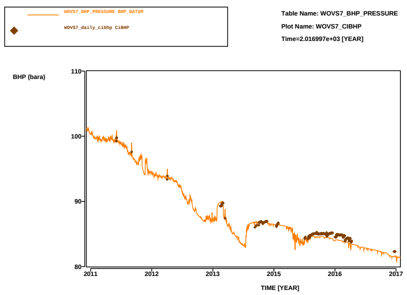

Creation date: Thu 09/02/2017 16:09
Runfile: GRO_2016_ED_v60.run

Table Name: WOVS8_BHP_PRESSURE
Plot Name: WOVS8_CIBHP
Time=2.016997e+03 [YEAR]

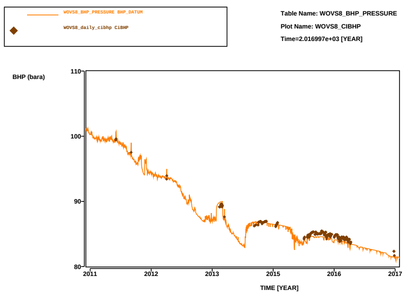

Creation date: Thu 09/02/2017 16:09
Runfile: GRO_2016_ED_v60.run

Table Name: WOVS9_BHP_PRESSURE
Plot Name: WOVS9_CIBHP
Time=2.016997e+03 [YEAR]

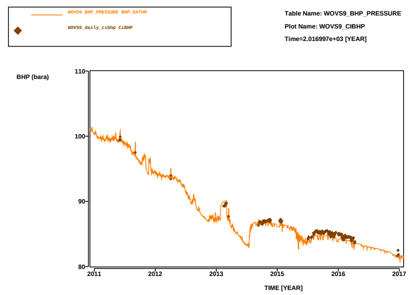

Creation date: Thu 09/02/2017 16:09
Runfile: GRO_2016_ED_v60.run

Table Name: WOVS10_BHP_PRESSURE
Plot Name: WOVS10_CIBHP
Time=2.016997e+03 [YEAR]

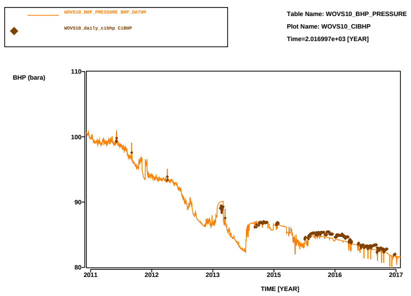

Creation date: Thu 09/02/2017 16:09
Runfile: GRO_2016_ED_v60.run

Table Name: WOVS11_BHP_PRESSURE
Plot Name: WOVS11_CIBHP
Time=2.016997e+03 [YEAR]

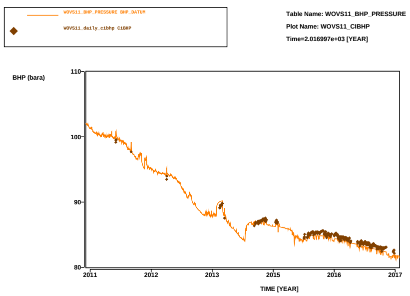

Creation date: Thu 09/02/2017 16:09
Runfile: GRO_2016_ED_v60.run

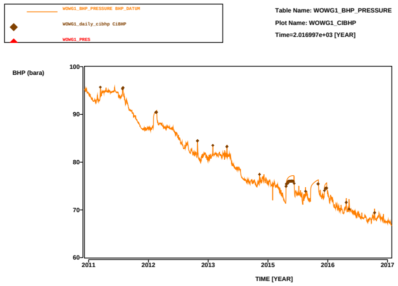

Creation date: Thu 09/02/2017 16:09
Runfile: GRO_2016_ED_v60.run

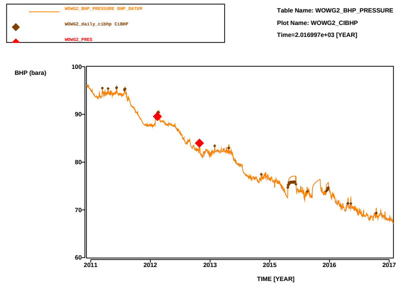

Creation date: Thu 09/02/2017 16:09
Runfile: GRO_2016_ED_v60.run

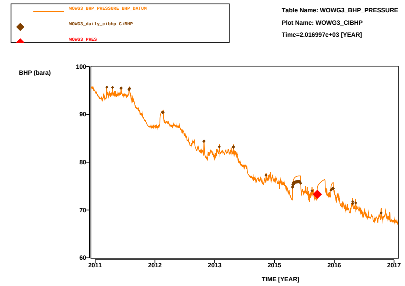

Creation date: Thu 09/02/2017 16:09
Runfile: GRO_2016_ED_v60.run

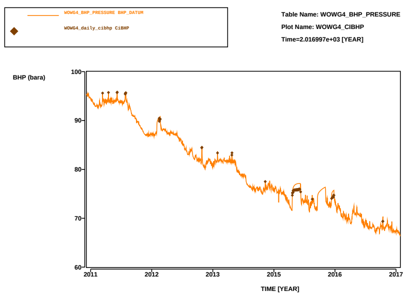

Creation date: Thu 09/02/2017 16:09
Runfile: GRO_2016_ED_v60.run

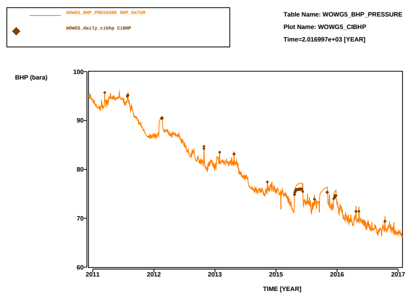

Creation date: Thu 09/02/2017 16:09
Runfile: GRO_2016_ED_v60.run

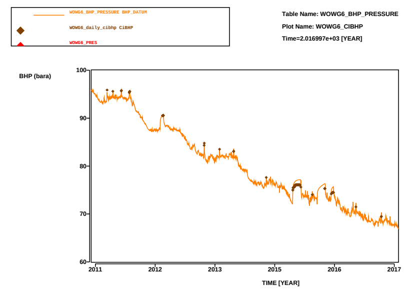

Creation date: Thu 09/02/2017 16:09
Runfile: GRO_2016_ED_v60.run

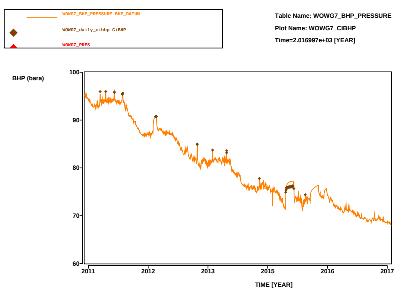

Creation date: Thu 09/02/2017 16:09
Runfile: GRO_2016_ED_v60.run

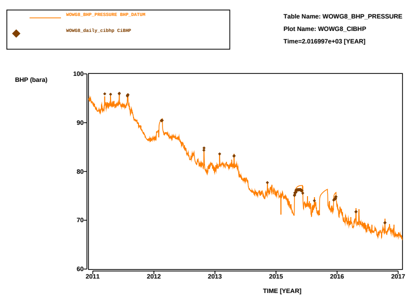

Creation date: Thu 09/02/2017 16:09
Runfile: GRO_2016_ED_v60.run

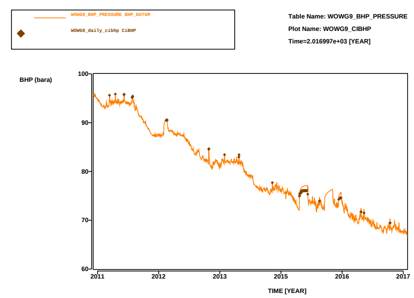

Creation date: Thu 09/02/2017 16:09
Runfile: GRO_2016_ED_v60.run

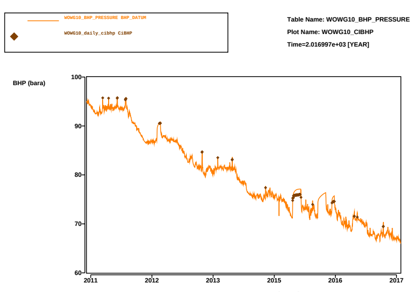

Creation date: Thu 09/02/2017 16:09
Runfile: GRO_2016_ED_v60.run

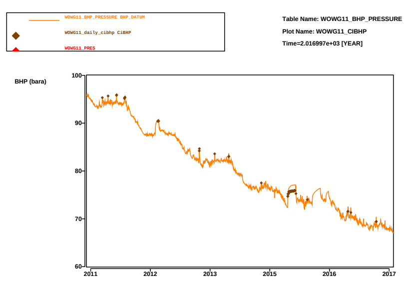

Creation date: Thu 09/02/2017 16:09
Runfile: GRO_2016_ED_v60.run

Table Name: WPAU2_BHP_PRESSURE
Plot Name: WPAU2_CIBHP
Time=2.016997e+03 [YEAR]

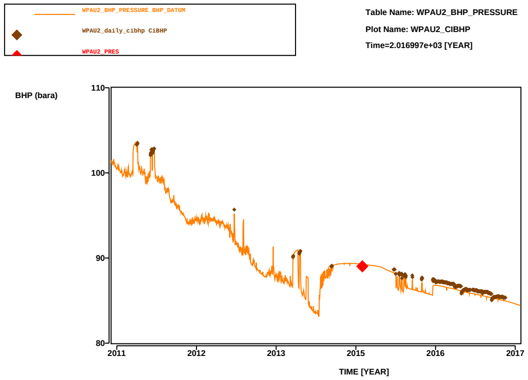

Creation date: Thu 09/02/2017 16:09
Runfile: GRO_2016_ED_v60.run

Table Name: WPAU3_BHP_PRESSURE
Plot Name: WPAU3_CIBHP
Time=2.016997e+03 [YEAR]

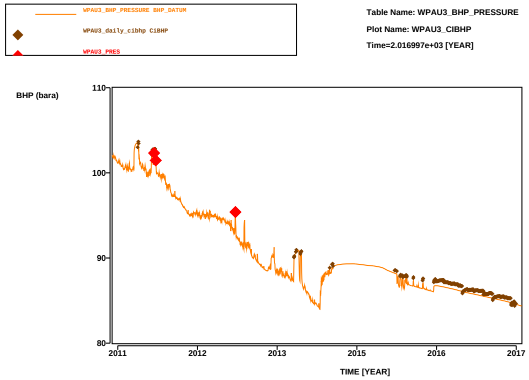

Creation date: Thu 09/02/2017 16:09
Runfile: GRO_2016_ED_v60.run

Table Name: WPAU4_BHP_PRESSURE
Plot Name: WPAU4_CIBHP
Time=2.016997e+03 [YEAR]

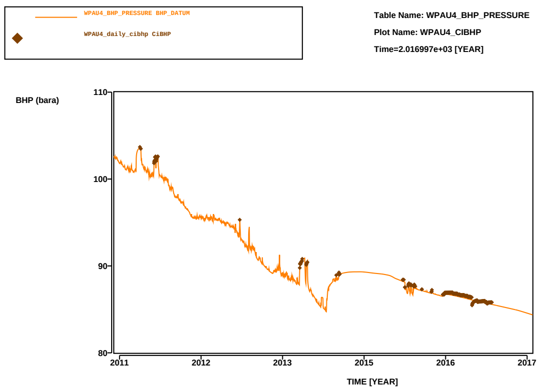

Creation date: Thu 09/02/2017 16:09
Runfile: GRO_2016_ED_v60.run

Table Name: WPAU5_BHP_PRESSURE
Plot Name: WPAU5_CIBHP
Time=2.016997e+03 [YEAR]

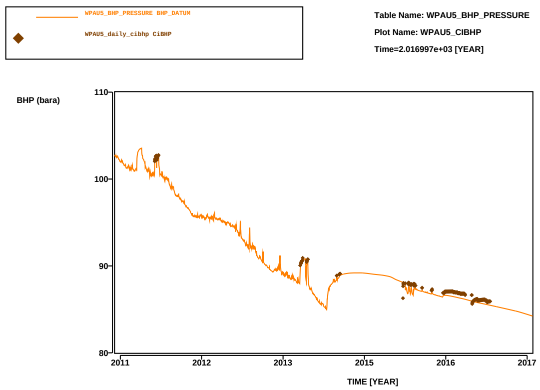

Creation date: Thu 09/02/2017 16:09
Runfile: GRO_2016_ED_v60.run

Table Name: WPAU6_BHP_PRESSURE
Plot Name: WPAU6_CIBHP
Time=2.016997e+03 [YEAR]

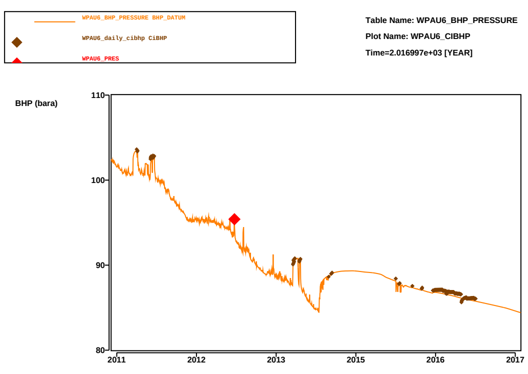

Creation date: Thu 09/02/2017 16:09
Runfile: GRO_2016_ED_v60.run

Table Name: WPOS1_BHP_PRESSURE
Plot Name: WPOS1_CIBHP
Time=2.016997e+03 [YEAR]

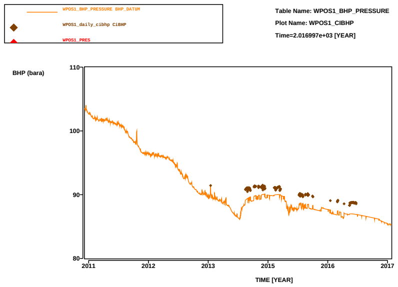

Creation date: Thu 09/02/2017 16:09
Runfile: GRO_2016_ED_v60.run

Table Name: WPOS2_BHP_PRESSURE
Plot Name: WPOS2_CIBHP
Time=2.016997e+03 [YEAR]

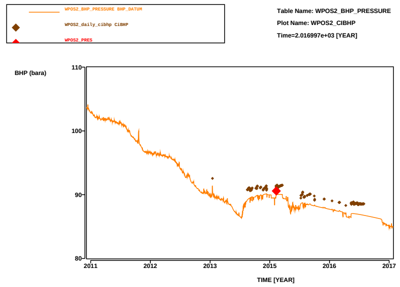

Creation date: Thu 09/02/2017 16:09
Runfile: GRO_2016_ED_v60.run

Table Name: WPOS3_BHP_PRESSURE
Plot Name: WPOS3_CIBHP
Time=2.016997e+03 [YEAR]

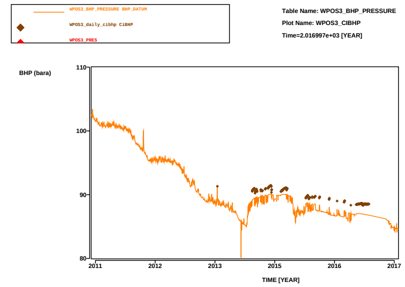

Creation date: Thu 09/02/2017 16:09
Runfile: GRO_2016_ED_v60.run

Table Name: WPOS4_BHP_PRESSURE
Plot Name: WPOS4_CIBHP
Time=2.016997e+03 [YEAR]

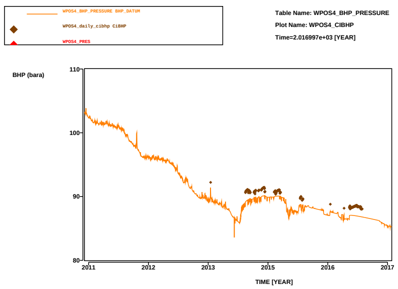

Creation date: Thu 09/02/2017 16:09
Runfile: GRO_2016_ED_v60.run

Table Name: WPOS5_BHP_PRESSURE
Plot Name: WPOS5_CIBHP
Time=2.016997e+03 [YEAR]

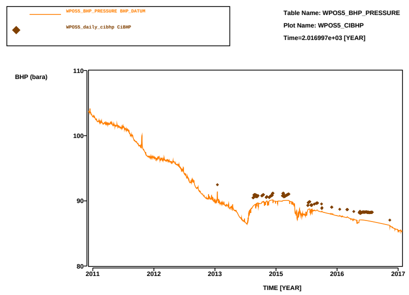

Creation date: Thu 09/02/2017 16:09
Runfile: GRO_2016_ED_v60.run

Table Name: WPOS6_BHP_PRESSURE
Plot Name: WPOS6_CIBHP
Time=2.016997e+03 [YEAR]

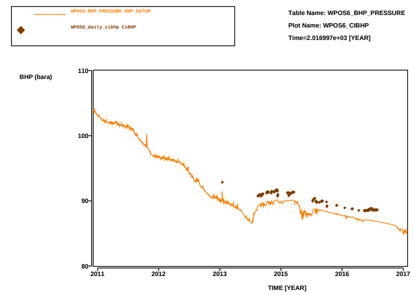

Creation date: Thu 09/02/2017 16:09
Runfile: GRO_2016_ED_v60.run

Table Name: WPOS7_BHP_PRESSURE
Plot Name: WPOS7_CIBHP
Time=2.016997e+03 [YEAR]

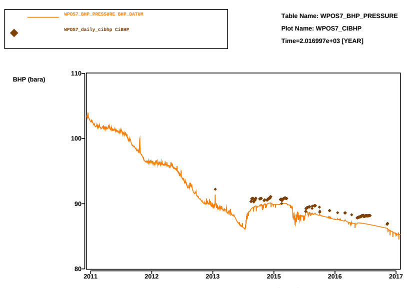

Creation date: Thu 09/02/2017 16:09
Runfile: GRO_2016_ED_v60.run

Table Name: WPOS8_BHP_PRESSURE
Plot Name: WPOS8_CIBHP
Time=2.016997e+03 [YEAR]

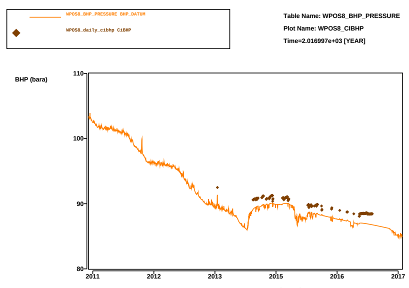

Creation date: Thu 09/02/2017 16:09
Runfile: GRO_2016_ED_v60.run

Table Name: WPOS9_BHP_PRESSURE
Plot Name: WPOS9_CIBHP
Time=2.016997e+03 [YEAR]

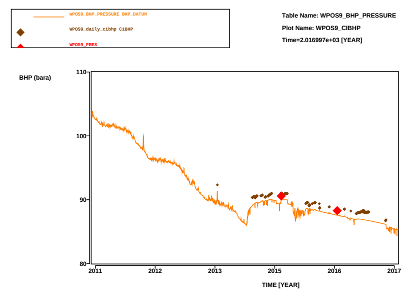

Creation date: Thu 09/02/2017 16:09
Runfile: GRO_2016_ED_v60.run

Table Name: WPOS10A_BHP_PRESSURE
Plot Name: WPOS10A_CIBHP
Time=2.016997e+03 [YEAR]

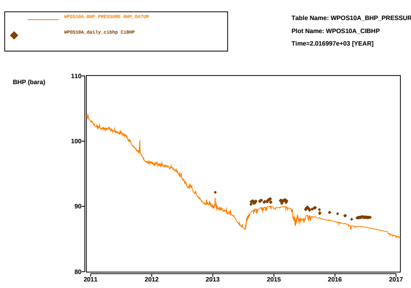

Creation date: Thu 09/02/2017 16:09
Runfile: GRO_2016_ED_v60.run

Table Name: WPOS11_BHP_PRESSURE
Plot Name: WPOS11_CIBHP
Time=2.016997e+03 [YEAR]

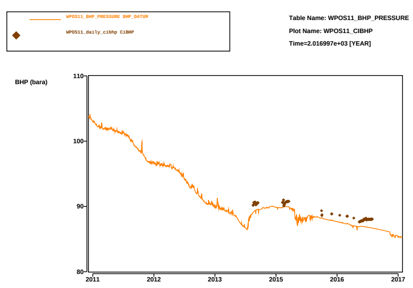

Creation date: Thu 09/02/2017 16:09
Runfile: GRO_2016_ED_v60.run

WSAP6A_BHP_PRESSURE BHP_DATUM
WSAP6A_daily_cibhp CIBHP
WSAP6A_PRES

Table Name: WSAP6A_BHP_PRESSURE
Plot Name: WSAP6A_CIBHP
Time=2.016997e+03 [YEAR]

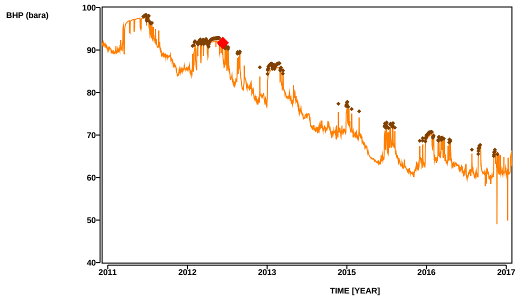

Creation date: Thu 09/02/2017 16:09
Runfile: GRO_2016_ED_v60.run

WSAP7_BHP_PRESSURE BHP_DATUM
WSAP7_daily_cibhp CIBHP
WSAP7_PRES

Table Name: WSAP7_BHP_PRESSURE
Plot Name: WSAP7_CIBHP
Time=2.016997e+03 [YEAR]

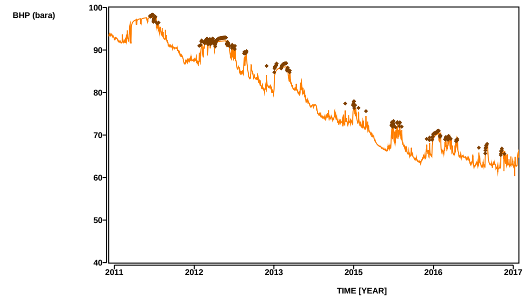

Creation date: Thu 09/02/2017 16:09
Runfile: GRO_2016_ED_v60.run

WSAP8_BHP_PRESSURE BHP_DATUM
WSAP8_daily_cibhp CIBHP

Table Name: WSAP8_BHP_PRESSURE
Plot Name: WSAP8_CIBHP
Time=2.016997e+03 [YEAR]

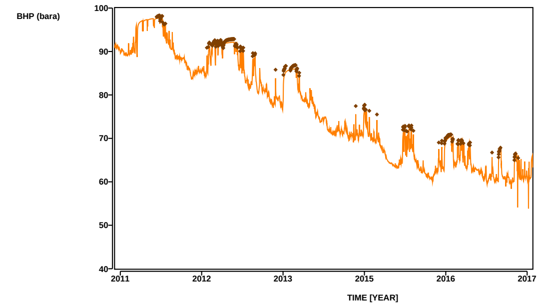

Creation date: Thu 09/02/2017 16:09
Runfile: GRO_2016_ED_v60.run

WSAP9_BHP_PRESSURE BHP_DATUM
WSAP9_daily_cibhp CIBHP
WSAP9_PRES

Table Name: WSAP9_BHP_PRESSURE
Plot Name: WSAP9_CIBHP
Time=2.016997e+03 [YEAR]

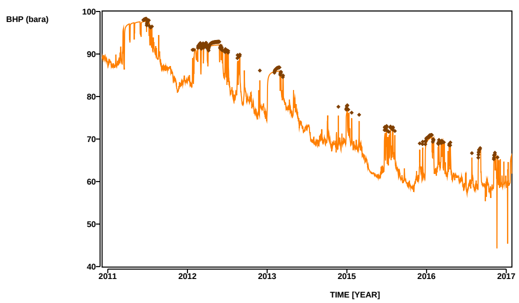

Creation date: Thu 09/02/2017 16:09
Runfile: GRO_2016_ED_v60.run

WSAP10_BHP_PRESSURE BHP_DATUM
WSAP10_daily_cibhp CIBHP

Table Name: WSAP10_BHP_PRESSURE
Plot Name: WSAP10_CIBHP
Time=2.016997e+03 [YEAR]

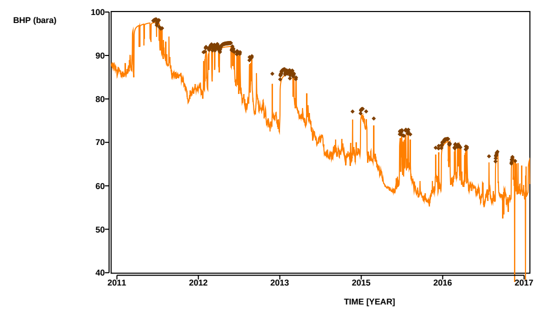

Creation date: Thu 09/02/2017 16:09
Runfile: GRO_2016_ED_v60.run

WSAP11_BHP_PRESSURE BHP_DATUM
WSAP11_daily_cibhp CIBHP

Table Name: WSAP11_BHP_PRESSURE
Plot Name: WSAP11_CIBHP
Time=2.016997e+03 [YEAR]

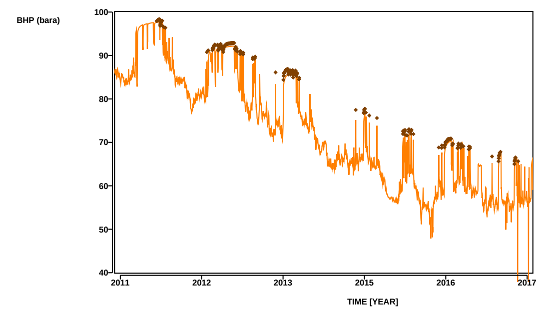

Creation date: Thu 09/02/2017 16:09
Runfile: GRO_2016_ED_v60.run

WSAP12_BHP_PRESSURE BHP_DATUM
WSAP12_daily_cibhp CIBHP
WSAP12_PRES

Table Name: WSAP12_BHP_PRESSURE
Plot Name: WSAP12_CIBHP
Time=2.016997e+03 [YEAR]

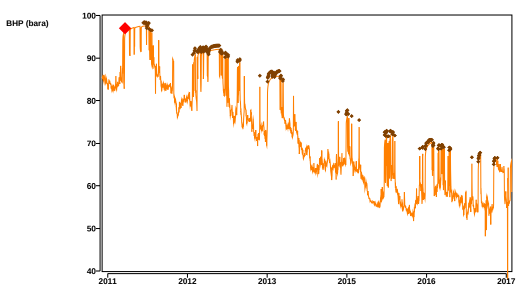

Creation date: Thu 09/02/2017 16:09
Runfile: GRO_2016_ED_v60.run

WSAP13_BHP_PRESSURE BHP_DATUM
WSAP13_daily_cibhp CIBHP

Table Name: WSAP13_BHP_PRESSURE
Plot Name: WSAP13_CIBHP
Time=2.016997e+03 [YEAR]

Creation date: Thu 09/02/2017 16:09
Runfile: GRO_2016_ED_v60.run

WSAP15A_BHP_PRESSURE BHP_DATUM
WSAP15A_daily_cibhp CIBHP
WSAP15A_PRES

Table Name: WSAP15A_BHP_PRESSURE
Plot Name: WSAP15A_CIBHP
Time=2.016997e+03 [YEAR]

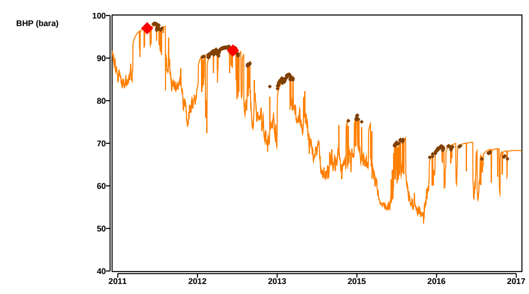

Creation date: Thu 09/02/2017 16:09
Runfile: GRO_2016_ED_v60.run

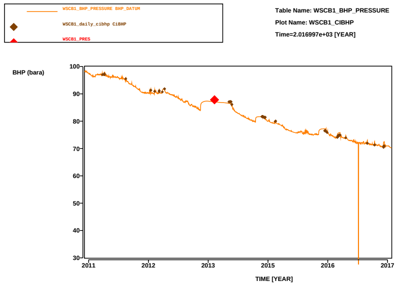

Creation date: Thu 09/02/2017 16:09
Runfile: GRO_2016_ED_v60.run

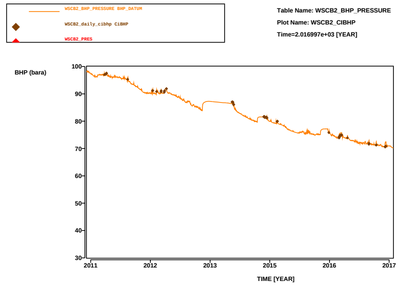

Creation date: Thu 09/02/2017 16:09
Runfile: GRO_2016_ED_v60.run

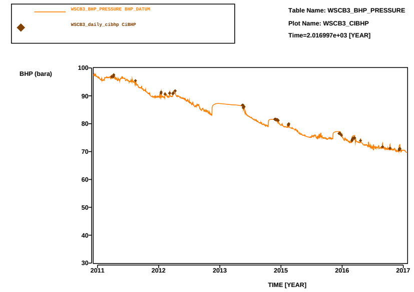

Creation date: Thu 09/02/2017 16:09
Runfile: GRO_2016_ED_v60.run

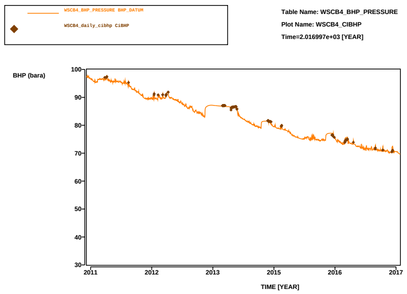

Creation date: Thu 09/02/2017 16:09
Runfile: GRO_2016_ED_v60.run

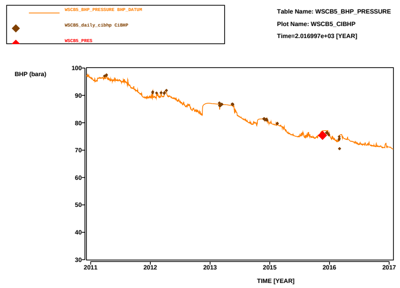

Creation date: Thu 09/02/2017 16:09
Runfile: GRO_2016_ED_v60.run

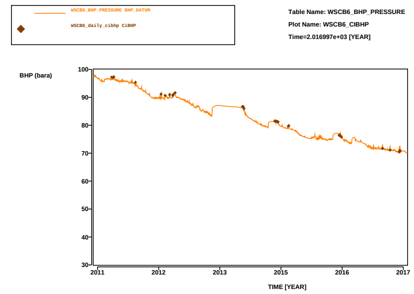

Creation date: Thu 09/02/2017 16:09
Runfile: GRO_2016_ED_v60.run

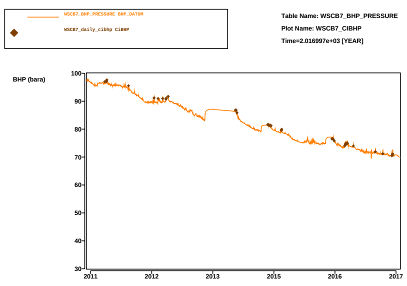

Creation date: Thu 09/02/2017 16:09
Runfile: GRO_2016_ED_v60.run

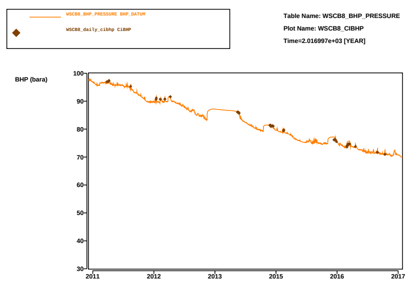

Creation date: Thu 09/02/2017 16:09
Runfile: GRO_2016_ED_v60.run

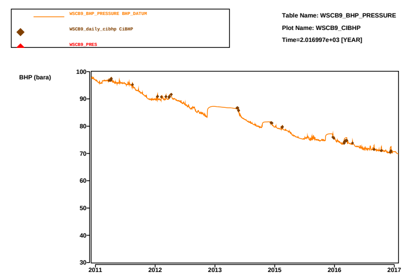

Creation date: Thu 09/02/2017 16:09
Runfile: GRO_2016_ED_v60.run

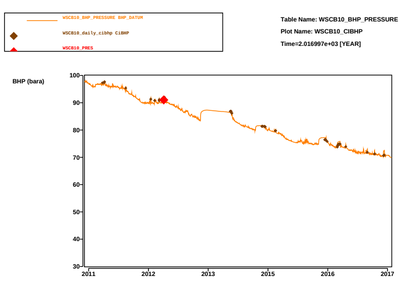

Creation date: Thu 09/02/2017 16:09
Runfile: GRO_2016_ED_v60.run

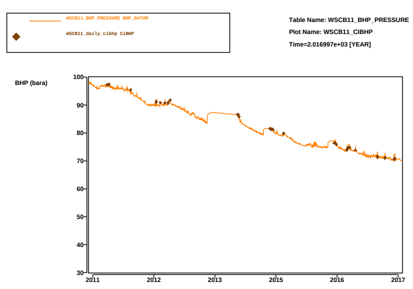

Creation date: Thu 09/02/2017 16:09
Runfile: GRO_2016_ED_v60.run

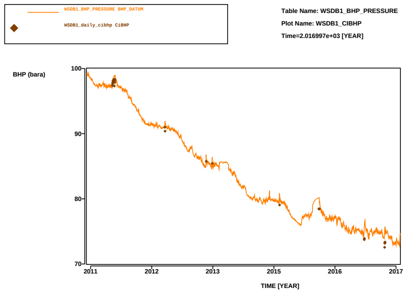

Creation date: Thu 09/02/2017 16:09
Runfile: GRO_2016_ED_v60.run

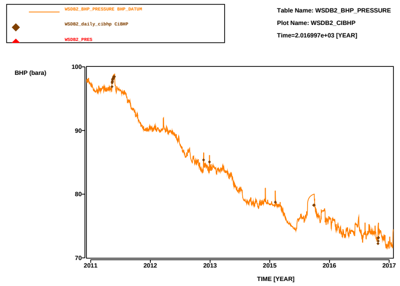

Creation date: Thu 09/02/2017 16:09
Runfile: GRO_2016_ED_v60.run

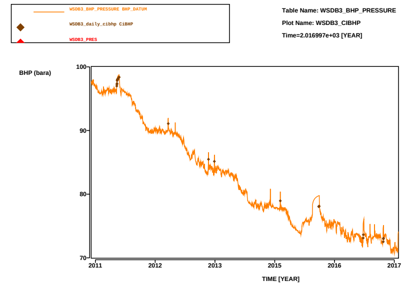

Creation date: Thu 09/02/2017 16:09
Runfile: GRO_2016_ED_v60.run

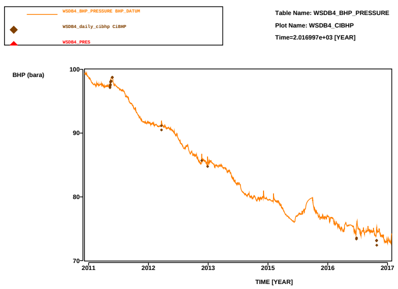

Creation date: Thu 09/02/2017 16:09
Runfile: GRO_2016_ED_v60.run

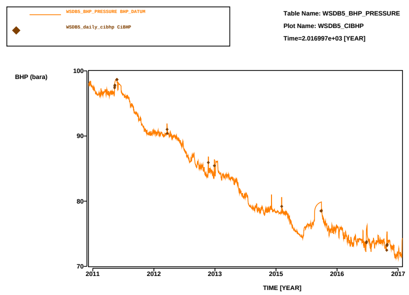

Creation date: Thu 09/02/2017 16:09
Runfile: GRO_2016_ED_v60.run

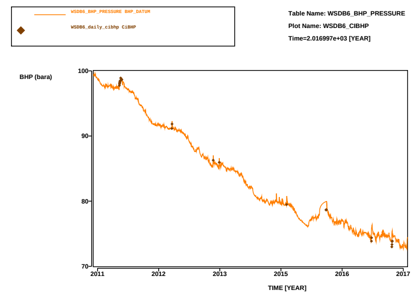

Creation date: Thu 09/02/2017 16:09
Runfile: GRO_2016_ED_v60.run

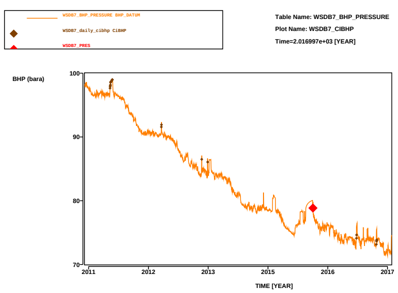

Creation date: Thu 09/02/2017 16:09
Runfile: GRO_2016_ED_v60.run

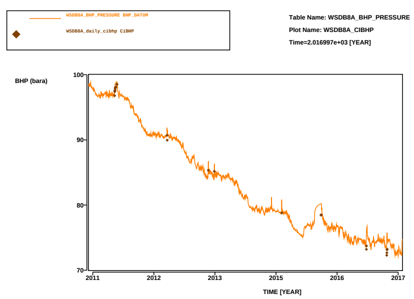

Creation date: Thu 09/02/2017 16:09
Runfile: GRO_2016_ED_v60.run

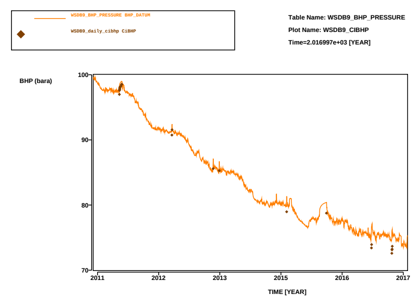

Creation date: Thu 09/02/2017 16:09
Runfile: GRO_2016_ED_v60.run

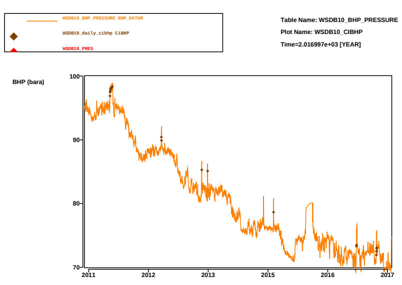

Creation date: Thu 09/02/2017 16:09
Runfile: GRO_2016_ED_v60.run

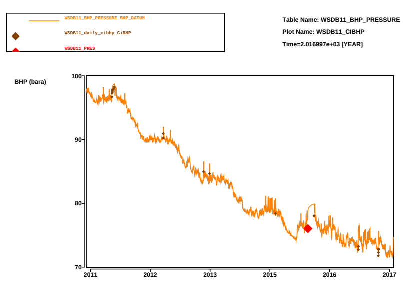

Creation date: Thu 09/02/2017 16:09
Runfile: GRO_2016_ED_v60.run

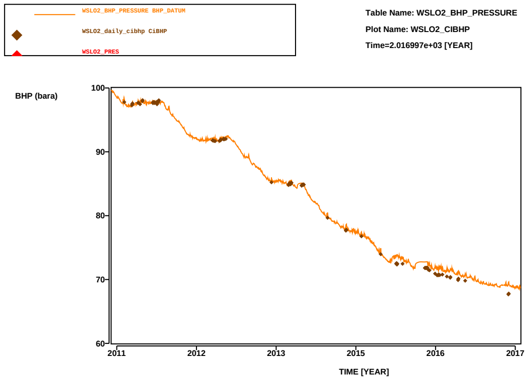

Creation date: Thu 09/02/2017 16:09
Runfile: GRO_2016_ED_v60.run

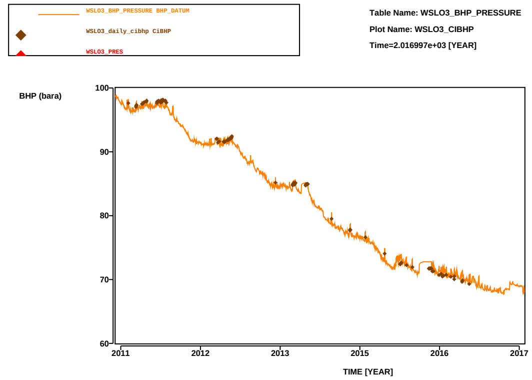

Creation date: Thu 09/02/2017 16:09
Runfile: GRO_2016_ED_v60.run

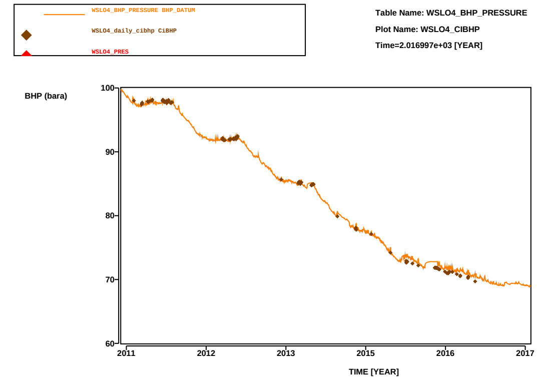

Creation date: Thu 09/02/2017 16:09
Runfile: GRO_2016_ED_v60.run

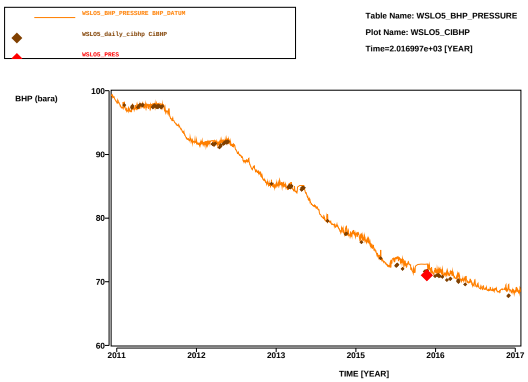

Creation date: Thu 09/02/2017 16:09
Runfile: GRO_2016_ED_v60.run

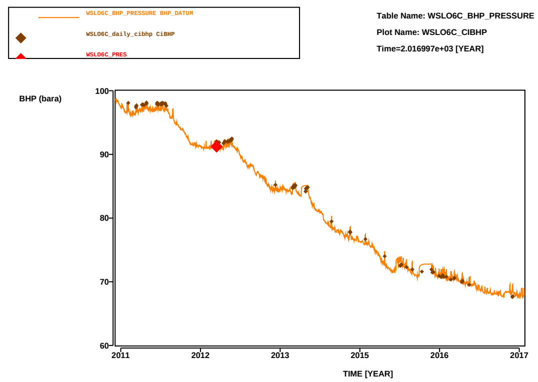

Creation date: Thu 09/02/2017 16:09
Runfile: GRO_2016_ED_v60.run

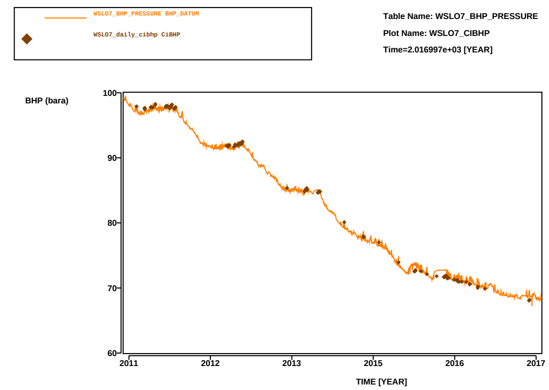

Creation date: Thu 09/02/2017 16:09
Runfile: GRO_2016_ED_v60.run

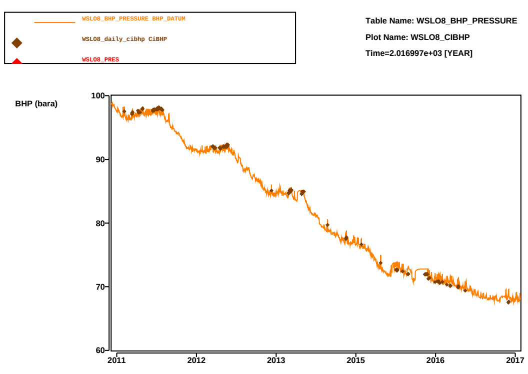

Creation date: Thu 09/02/2017 16:09
Runfile: GRO_2016_ED_v60.run

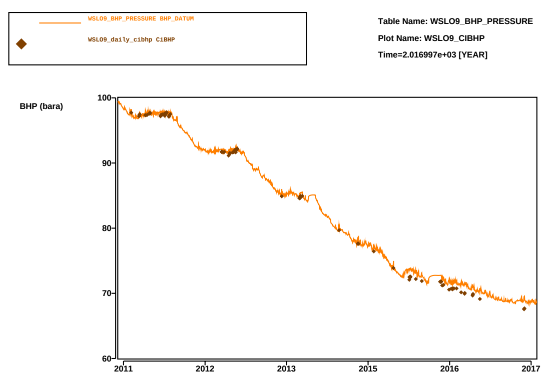

Creation date: Thu 09/02/2017 16:09
Runfile: GRO_2016_ED_v60.run

Table Name: WSPI1_BHP_PRESSURE
Plot Name: WSPI1_CIBHP
Time=2.016997e+03 [YEAR]

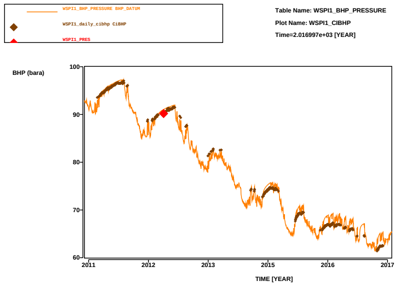

Creation date: Thu 09/02/2017 16:09
Runfile: GRO_2016_ED_v60.run

Table Name: WSPI2_BHP_PRESSURE
Plot Name: WSPI2_CIBHP
Time=2.016997e+03 [YEAR]

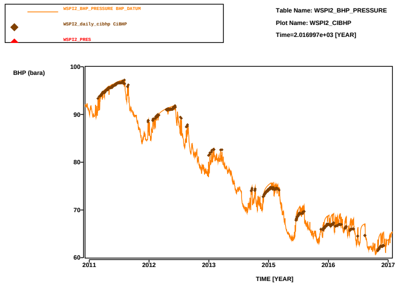

Creation date: Thu 09/02/2017 16:09
Runfile: GRO_2016_ED_v60.run

Table Name: WSPI3_BHP_PRESSURE
Plot Name: WSPI3_CIBHP
Time=2.016997e+03 [YEAR]

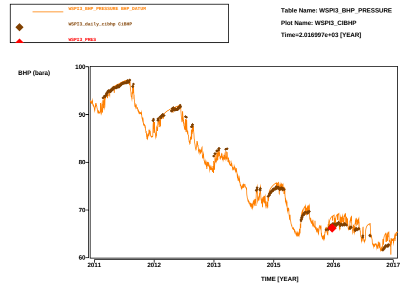

Creation date: Thu 09/02/2017 16:09
Runfile: GRO_2016_ED_v60.run

Table Name: WSPI4_BHP_PRESSURE
Plot Name: WSPI4_CIBHP
Time=2.016997e+03 [YEAR]

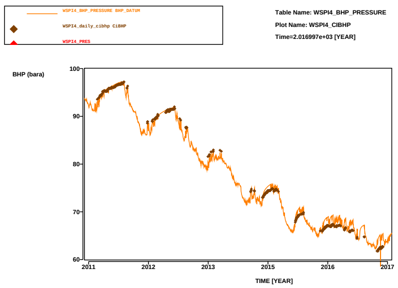

Creation date: Thu 09/02/2017 16:09
Runfile: GRO_2016_ED_v60.run

Table Name: WSPI5_BHP_PRESSURE
Plot Name: WSPI5_CIBHP
Time=2.016997e+03 [YEAR]

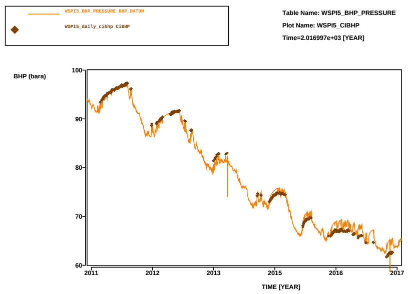

Creation date: Thu 09/02/2017 16:09
Runfile: GRO_2016_ED_v60.run

Table Name: WSPI6_BHP_PRESSURE
Plot Name: WSPI6_CIBHP
Time=2.016997e+03 [YEAR]

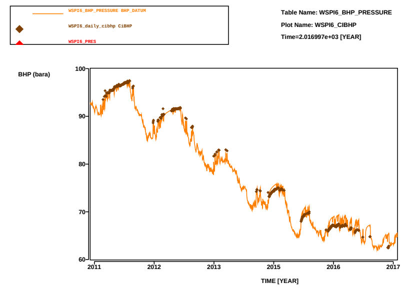

Creation date: Thu 09/02/2017 16:09
Runfile: GRO_2016_ED_v60.run

Table Name: WSPI7_BHP_PRESSURE
Plot Name: WSPI7_CIBHP
Time=2.016997e+03 [YEAR]

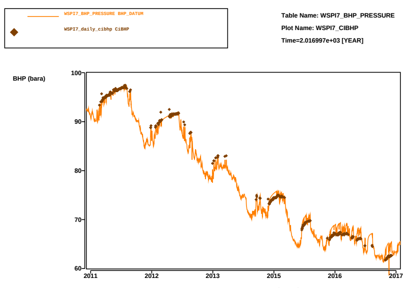

Creation date: Thu 09/02/2017 16:09
Runfile: GRO_2016_ED_v60.run

Table Name: WSPI8_BHP_PRESSURE
Plot Name: WSPI8_CIBHP
Time=2.016997e+03 [YEAR]

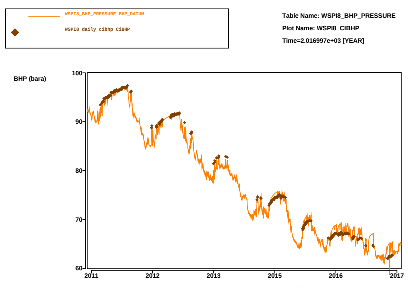

Creation date: Thu 09/02/2017 16:09
Runfile: GRO_2016_ED_v60.run

Table Name: WSPI9_BHP_PRESSURE
Plot Name: WSPI9_CIBHP
Time=2.016997e+03 [YEAR]

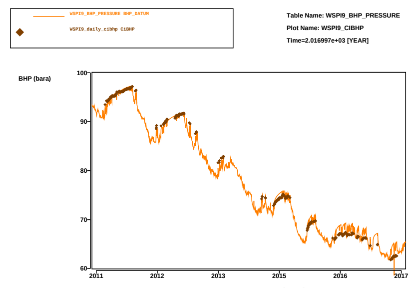

Creation date: Thu 09/02/2017 16:09
Runfile: GRO_2016_ED_v60.run

Table Name: WSPI10_BHP_PRESSURE
Plot Name: WSPI10_CIBHP
Time=2.016997e+03 [YEAR]

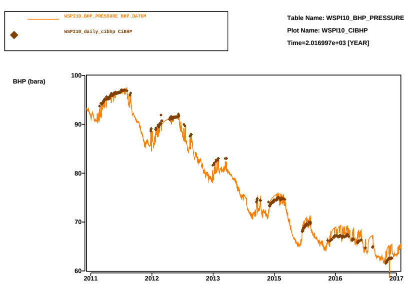

Creation date: Thu 09/02/2017 16:09
Runfile: GRO_2016_ED_v60.run

WSPI201_BHP_PRESSURE BHP_DATUM
WSPI201_daily_cibhp CIBHP
WSPI201_PRES

Table Name: WSPI201_BHP_PRESSURE
Plot Name: WSPI201_CIBHP
Time=2.016997e+03 [YEAR]

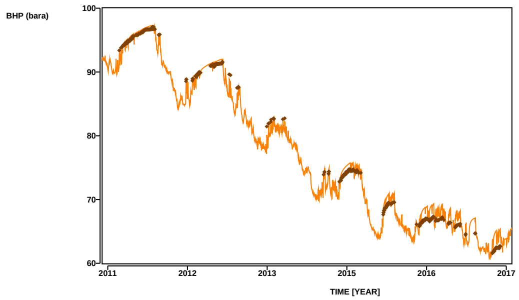

Creation date: Thu 09/02/2017 16:09
Runfile: GRO_2016_ED_v60.run

WSPI202_BHP_PRESSURE BHP_DATUM
WSPI202_daily_cibhp CIBHP
WSPI202_PRES

Table Name: WSPI202_BHP_PRESSURE
Plot Name: WSPI202_CIBHP
Time=2.016997e+03 [YEAR]

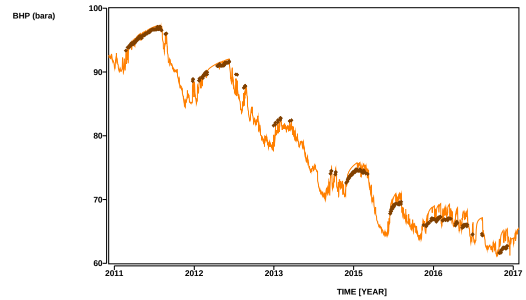

Creation date: Thu 09/02/2017 16:09
Runfile: GRO_2016_ED_v60.run

WSPI203_BHP_PRESSURE BHP_DATUM
WSPI203_daily_cibhp CIBHP

Table Name: WSPI203_BHP_PRESSURE
Plot Name: WSPI203_CIBHP
Time=2.016997e+03 [YEAR]

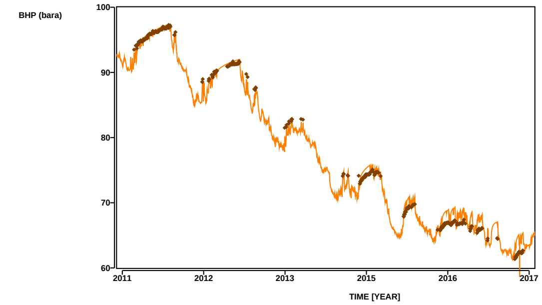

Creation date: Thu 09/02/2017 16:09
Runfile: GRO_2016_ED_v60.run

WSPI204_BHP_PRESSURE BHP_DATUM
WSPI204_daily_cibhp CIBHP

Table Name: WSPI204_BHP_PRESSURE
Plot Name: WSPI204_CIBHP
Time=2.016997e+03 [YEAR]

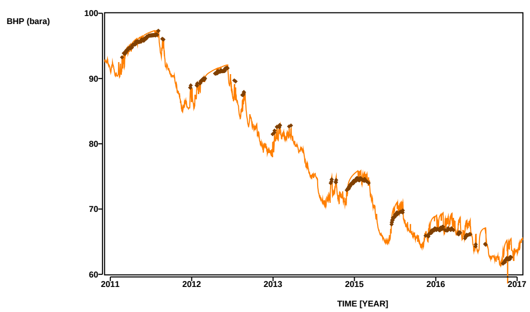

Creation date: Thu 09/02/2017 16:09
Runfile: GRO_2016_ED_v60.run

WSPI205_BHP_PRESSURE BHP_DATUM
WSPI205_daily_cibhp CIBHP

Table Name: WSPI205_BHP_PRESSURE
Plot Name: WSPI205_CIBHP
Time=2.016997e+03 [YEAR]

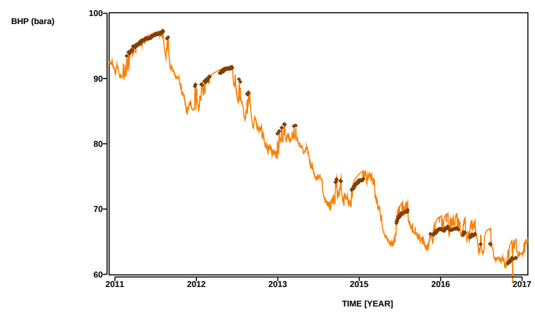

Creation date: Thu 09/02/2017 16:09
Runfile: GRO_2016_ED_v60.run

WSPI206_BHP_PRESSURE BHP_DATUM
WSPI206_daily_cibhp CIBHP
WSPI206_PRES

Table Name: WSPI206_BHP_PRESSURE
Plot Name: WSPI206_CIBHP
Time=2.016997e+03 [YEAR]

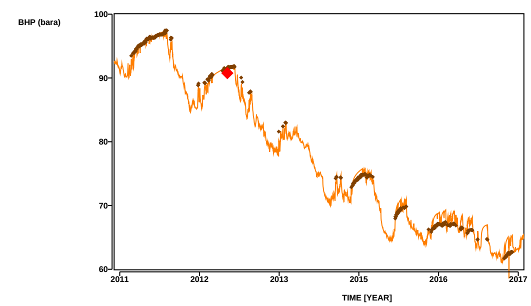

Creation date: Thu 09/02/2017 16:09
Runfile: GRO_2016_ED_v60.run

WSPI207_BHP_PRESSURE BHP_DATUM
WSPI207_daily_cibhp CIBHP

Table Name: WSPI207_BHP_PRESSURE
Plot Name: WSPI207_CIBHP
Time=2.016997e+03 [YEAR]

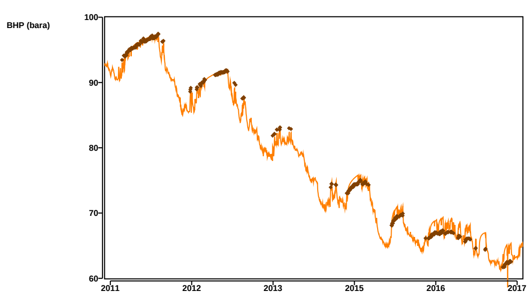

Creation date: Thu 09/02/2017 16:09
Runfile: GRO_2016_ED_v60.run

WSPI208_BHP_PRESSURE BHP_DATUM
WSPI208_daily_cibhp CIBHP

Table Name: WSPI208_BHP_PRESSURE
Plot Name: WSPI208_CIBHP
Time=2.016997e+03 [YEAR]

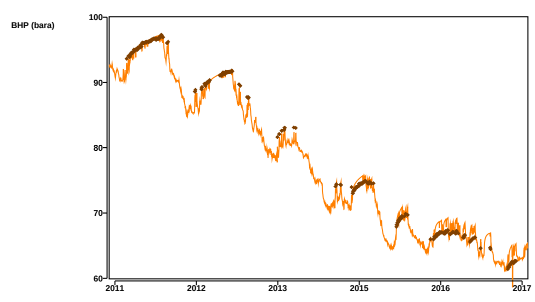

Creation date: Thu 09/02/2017 16:09
Runfile: GRO_2016_ED_v60.run

WSPI209_BHP_PRESSURE BHP_DATUM
WSPI209_daily_cibhp CIBHP

Table Name: WSPI209_BHP_PRESSURE
Plot Name: WSPI209_CIBHP
Time=2.016997e+03 [YEAR]

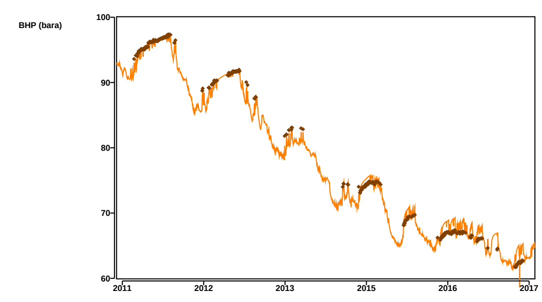

Creation date: Thu 09/02/2017 16:09
Runfile: GRO_2016_ED_v60.run

WSZW1_BHP_PRESSURE BHP_DATUM
WSZW1_daily_cibhp CiBHP

Table Name: WSZW1_BHP_PRESSURE
Plot Name: WSZW1_CIBHP
Time=2.016997e+03 [YEAR]

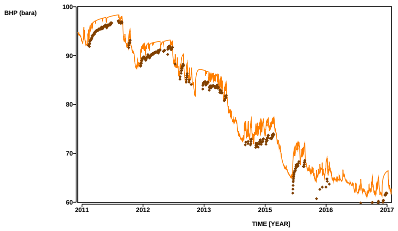

Creation date: Thu 09/02/2017 16:09
Runfile: GRO_2016_ED_v60.run

WSZW2_BHP_PRESSURE BHP_DATUM
WSZW2_daily_cibhp CiBHP
WSZW2_PRES

Table Name: WSZW2_BHP_PRESSURE
Plot Name: WSZW2_CIBHP
Time=2.016997e+03 [YEAR]

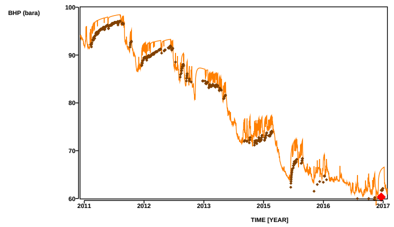

Creation date: Thu 09/02/2017 16:09
Runfile: GRO_2016_ED_v60.run

WSZW3A_BHP_PRESSURE BHP_DATUM
WSZW3A_daily_cibhp CiBHP

Table Name: WSZW3A_BHP_PRESSURE
Plot Name: WSZW3A_CIBHP
Time=2.016997e+03 [YEAR]

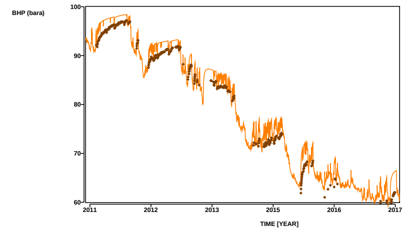

Creation date: Thu 09/02/2017 16:09
Runfile: GRO_2016_ED_v60.run

WSZW4_BHP_PRESSURE BHP_DATUM
WSZW4_daily_cibhp CiBHP
WSZW4_PRES

Table Name: WSZW4_BHP_PRESSURE
Plot Name: WSZW4_CIBHP
Time=2.016997e+03 [YEAR]

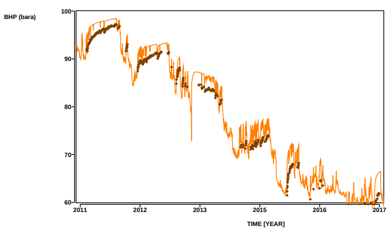

Creation date: Thu 09/02/2017 16:09
Runfile: GRO_2016_ED_v60.run

WSZW5B_BHP_PRESSURE BHP_DATUM
WSZW5B_daily_cibhp CiBHP

Table Name: WSZW5B_BHP_PRESSURE
Plot Name: WSZW5B_CIBHP
Time=2.016997e+03 [YEAR]

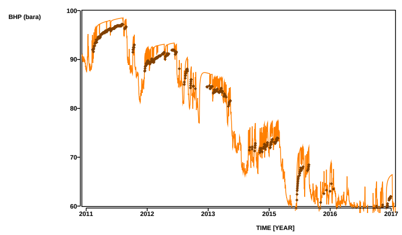

Creation date: Thu 09/02/2017 16:09
Runfile: GRO_2016_ED_v60.run

WSZW6_BHP_PRESSURE BHP_DATUM
WSZW6_daily_cibhp CiBHP
WSZW6_PRES

Table Name: WSZW6_BHP_PRESSURE
Plot Name: WSZW6_CIBHP
Time=2.016997e+03 [YEAR]

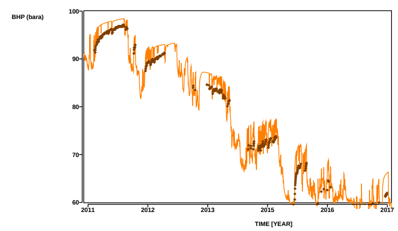

Creation date: Thu 09/02/2017 16:09
Runfile: GRO_2016_ED_v60.run

WSZW7_BHP_PRESSURE BHP_DATUM
WSZW7_daily_cibhp CiBHP

Table Name: WSZW7_BHP_PRESSURE
Plot Name: WSZW7_CIBHP
Time=2.016997e+03 [YEAR]

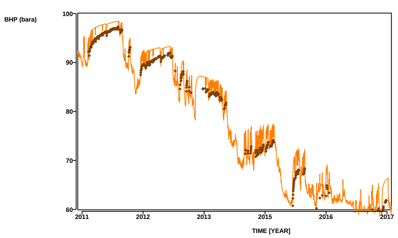

Creation date: Thu 09/02/2017 16:09
Runfile: GRO_2016_ED_v60.run

WSZW8_BHP_PRESSURE BHP_DATUM
WSZW8_daily_cibhp CiBHP

Table Name: WSZW8_BHP_PRESSURE
Plot Name: WSZW8_CIBHP
Time=2.016997e+03 [YEAR]

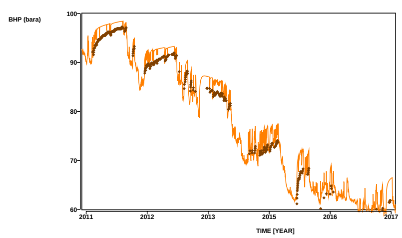

Creation date: Thu 09/02/2017 16:09
Runfile: GRO_2016_ED_v60.run

WSZW9_BHP_PRESSURE BHP_DATUM
WSZW9_daily_cibhp CiBHP

Table Name: WSZW9_BHP_PRESSURE
Plot Name: WSZW9_CIBHP
Time=2.016997e+03 [YEAR]

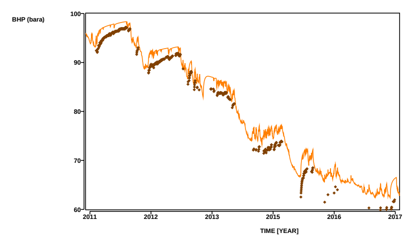

Creation date: Thu 09/02/2017 16:09
Runfile: GRO_2016_ED_v60.run

WSZW10_BHP_PRESSURE BHP_DATUM
WSZW10_daily_cibhp CiBHP

Table Name: WSZW10_BHP_PRESSURE
Plot Name: WSZW10_CIBHP
Time=2.016997e+03 [YEAR]

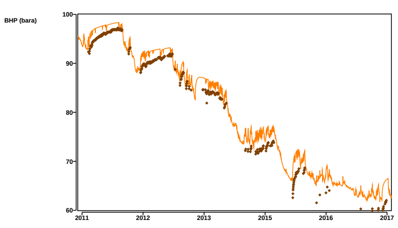

Creation date: Thu 09/02/2017 16:09
Runfile: GRO_2016_ED_v60.run

WSZW201_BHP_PRESSURE BHP_DATUM
WSZW201_daily_cibhp CiBHP
WSZW201_PRES

Table Name: WSZW201_BHP_PRESSURE
Plot Name: WSZW201_CIBHP
Time=2.016997e+03 [YEAR]

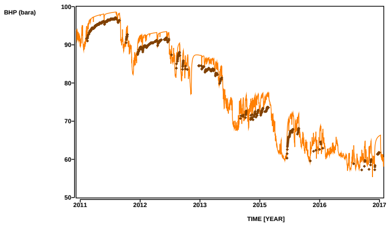

Creation date: Thu 09/02/2017 16:09
Runfile: GRO_2016_ED_v60.run

WSZW202_BHP_PRESSURE BHP_DATUM
WSZW202_daily_cibhp CiBHP
WSZW202_PRES

Table Name: WSZW202_BHP_PRESSURE
Plot Name: WSZW202_CIBHP
Time=2.016997e+03 [YEAR]

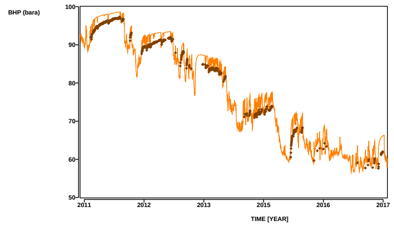

Creation date: Thu 09/02/2017 16:09
Runfile: GRO_2016_ED_v60.run

WSZW203_BHP_PRESSURE BHP_DATUM
WSZW203_daily_cibhp CiBHP

Table Name: WSZW203_BHP_PRESSURE
Plot Name: WSZW203_CIBHP
Time=2.016997e+03 [YEAR]

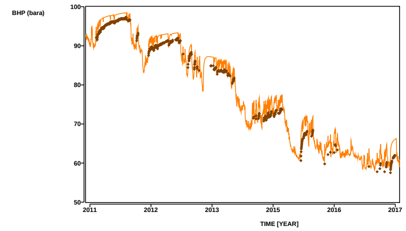

Creation date: Thu 09/02/2017 16:09
Runfile: GRO_2016_ED_v60.run

WSZW204C_BHP_PRESSURE BHP_DATUM
WSZW204C_daily_cibhp CiBHP
WSZW204C_PRES

Table Name: WSZW204C_BHP_PRESSURE
Plot Name: WSZW204C_CIBHP
Time=2.016997e+03 [YEAR]

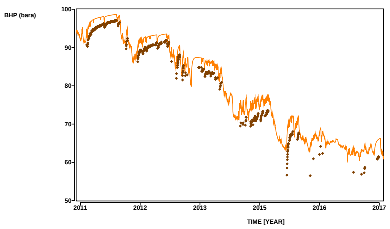

Creation date: Thu 09/02/2017 16:09
Runfile: GRO_2016_ED_v60.run

WSZW205_BHP_PRESSURE BHP_DATUM
WSZW205_daily_cibhp CiBHP

Table Name: WSZW205_BHP_PRESSURE
Plot Name: WSZW205_CIBHP
Time=2.016997e+03 [YEAR]

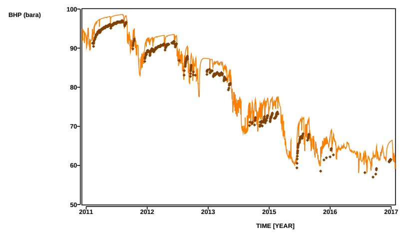

Creation date: Thu 09/02/2017 16:09
Runfile: GRO_2016_ED_v60.run

WSZW206_BHP_PRESSURE BHP_DATUM
WSZW206_daily_cibhp CiBHP

Table Name: WSZW206_BHP_PRESSURE
Plot Name: WSZW206_CIBHP
Time=2.016997e+03 [YEAR]

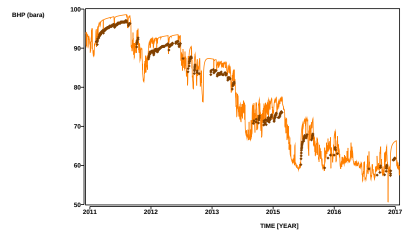

Creation date: Thu 09/02/2017 16:09
Runfile: GRO_2016_ED_v60.run

WSZW207_BHP_PRESSURE BHP_DATUM
WSZW207_daily_cibhp CiBHP

Table Name: WSZW207_BHP_PRESSURE
Plot Name: WSZW207_CIBHP
Time=2.016997e+03 [YEAR]

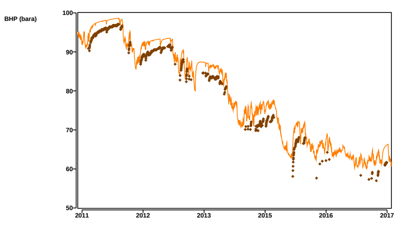

Creation date: Thu 09/02/2017 16:09
Runfile: GRO_2016_ED_v60.run

WSZW208_BHP_PRESSURE BHP_DATUM
WSZW208_daily_cibhp CiBHP

Table Name: WSZW208_BHP_PRESSURE
Plot Name: WSZW208_CIBHP
Time=2.016997e+03 [YEAR]

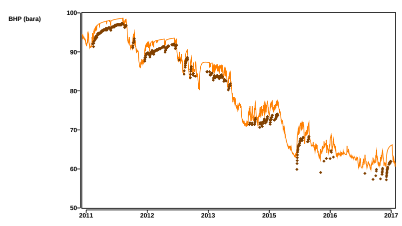

Creation date: Thu 09/02/2017 16:09
Runfile: GRO_2016_ED_v60.run

WSZW209_BHP_PRESSURE BHP_DATUM
WSZW209_daily_cibhp CiBHP
WSZW209_PRES

Table Name: WSZW209_BHP_PRESSURE
Plot Name: WSZW209_CIBHP
Time=2.016997e+03 [YEAR]

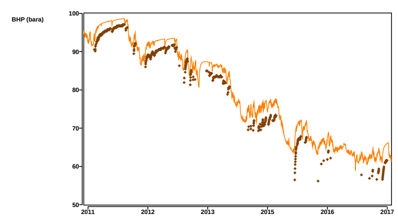

Creation date: Thu 09/02/2017 16:09
Runfile: GRO_2016_ED_v60.run

WSZW210_BHP_PRESSURE BHP_DATUM
WSZW210_daily_cibhp CiBHP

Table Name: WSZW210_BHP_PRESSURE
Plot Name: WSZW210_CIBHP
Time=2.016997e+03 [YEAR]

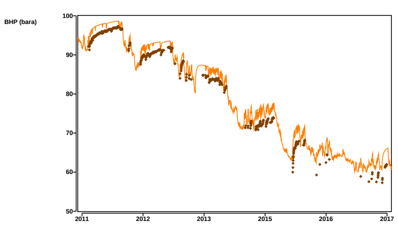

Creation date: Thu 09/02/2017 16:09
Runfile: GRO_2016_ED_v60.run

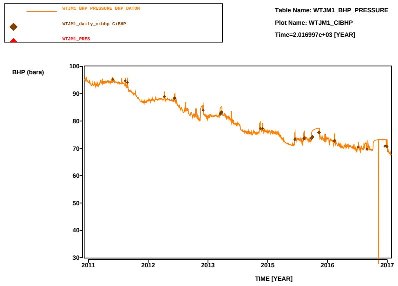

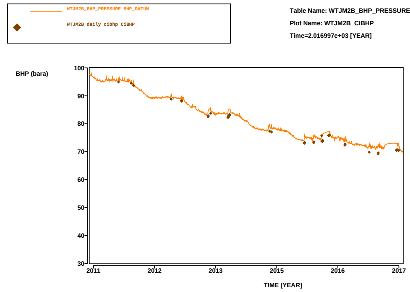

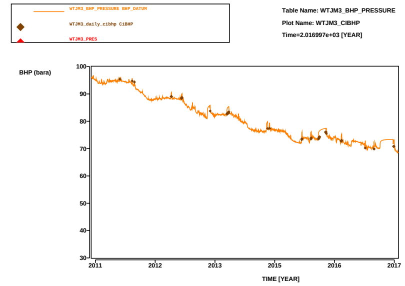

Creation date: Thu 09/02/2017 16:09
Runfile: GRO_2016_ED_v60.run

Creation date: Thu 09/02/2017 16:09
Runfile: GRO_2016_ED_v60.run

Creation date: Thu 09/02/2017 16:09
Runfile: GRO_2016_ED_v60.run

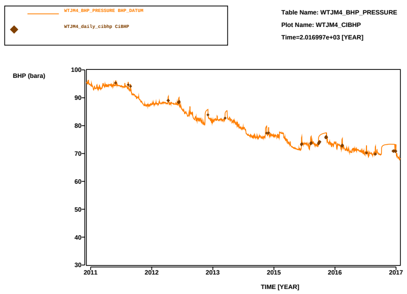

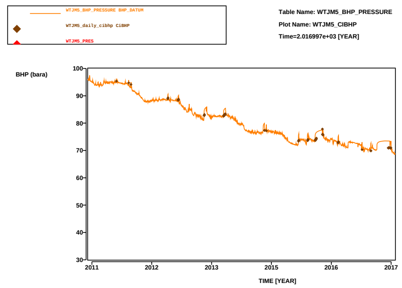

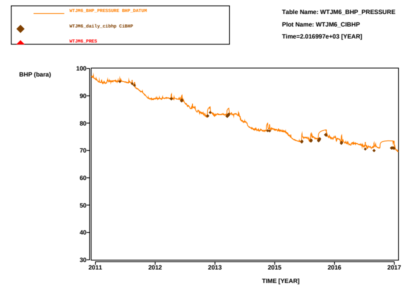

Creation date: Thu 09/02/2017 16:09
Runfile: GRO_2016_ED_v60.run

Creation date: Thu 09/02/2017 16:09
Runfile: GRO_2016_ED_v60.run

Creation date: Thu 09/02/2017 16:09
Runfile: GRO_2016_ED_v60.run

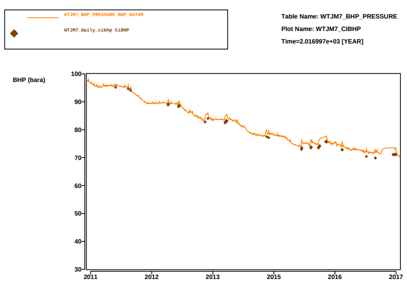

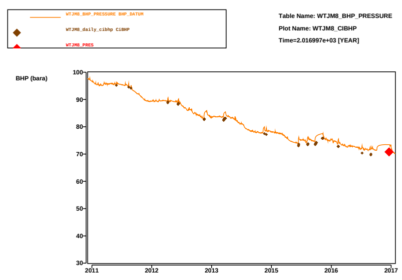

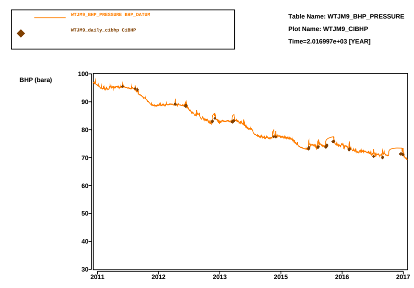

Creation date: Thu 09/02/2017 16:09
Runfile: GRO_2016_ED_v60.run

Creation date: Thu 09/02/2017 16:09
Runfile: GRO_2016_ED_v60.run

Creation date: Thu 09/02/2017 16:09
Runfile: GRO_2016_ED_v60.run

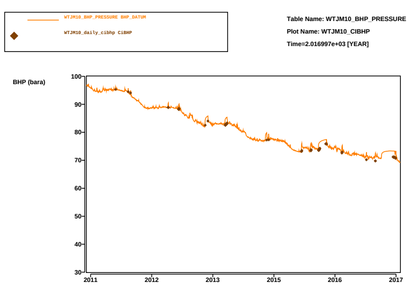

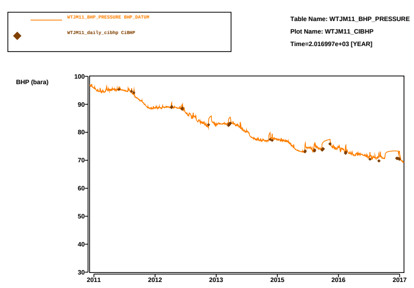

Creation date: Thu 09/02/2017 16:09

Creation date: Thu 09/02/2017 16:09

Runfile: GRO_2016_ED_v60.run

Runfile: GRO_2016_ED_v60.run

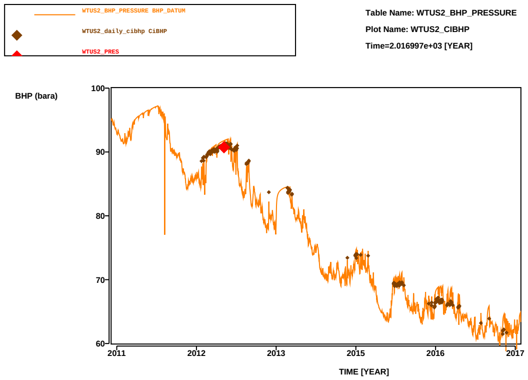

Creation date: Thu 09/02/2017 16:09
Runfile: GRO_2016_ED_v60.run

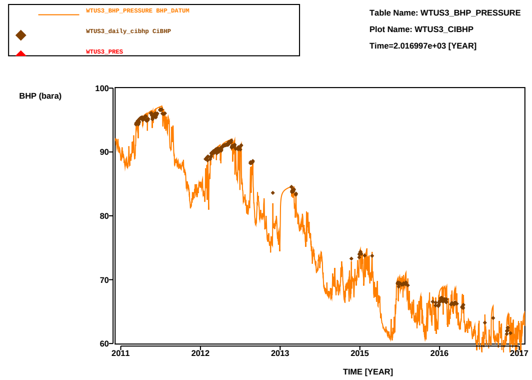

Creation date: Thu 09/02/2017 16:09
Runfile: GRO_2016_ED_v60.run

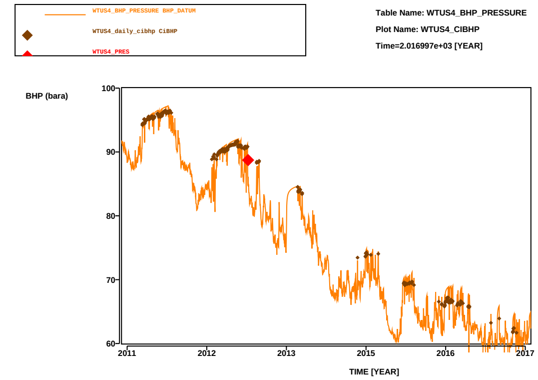

Creation date: Thu 09/02/2017 16:09
Runfile: GRO_2016_ED_v60.run

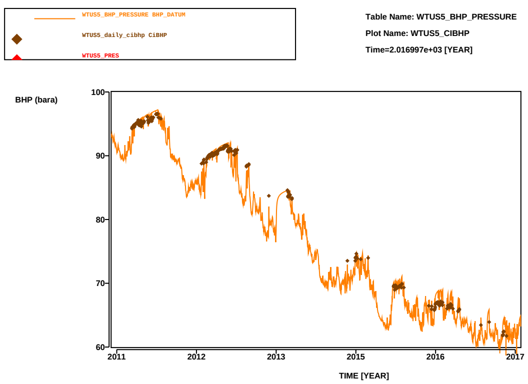

Creation date: Thu 09/02/2017 16:09
Runfile: GRO_2016_ED_v60.run

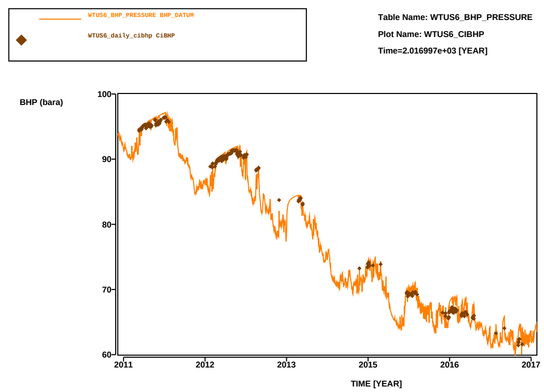

Creation date: Thu 09/02/2017 16:09
Runfile: GRO_2016_ED_v60.run

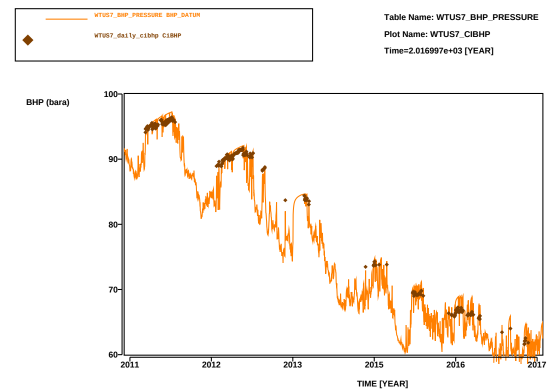

Creation date: Thu 09/02/2017 16:09
Runfile: GRO_2016_ED_v60.run

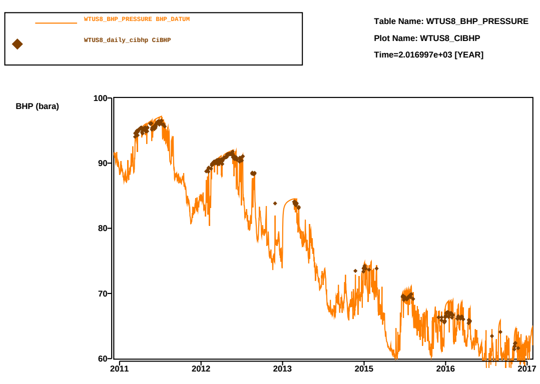

Creation date: Thu 09/02/2017 16:09
Runfile: GRO_2016_ED_v60.run

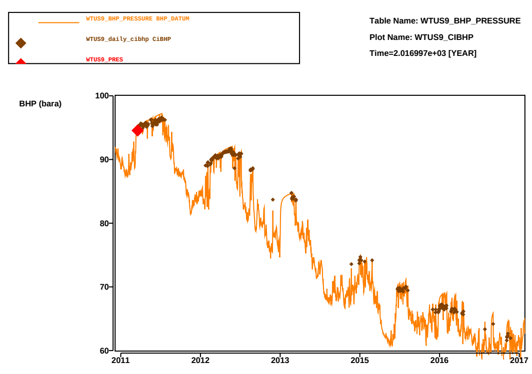

Creation date: Thu 09/02/2017 16:09
Runfile: GRO_2016_ED_v60.run

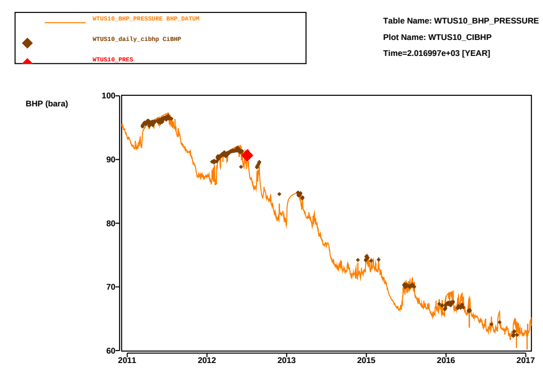

Creation date: Thu 09/02/2017 16:09
Runfile: GRO_2016_ED_v60.run

Table Name: WZND1_BHP_PRESSURE
Plot Name: WZND1_CIBHP
Time=2.016997e+03 [YEAR]

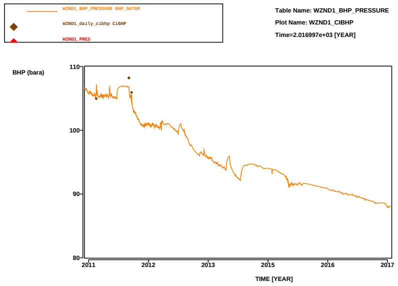

Creation date: Thu 09/02/2017 16:09
Runfile: GRO_2016_ED_v60.run

Table Name: WZND2A_BHP_PRESSURE
Plot Name: WZND2A_CIBHP
Time=2.016997e+03 [YEAR]

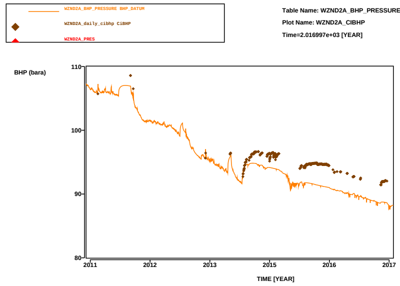

Creation date: Thu 09/02/2017 16:09
Runfile: GRO_2016_ED_v60.run

Table Name: WZND3_BHP_PRESSURE
Plot Name: WZND3_CIBHP
Time=2.016997e+03 [YEAR]

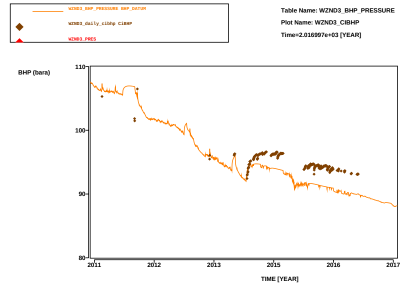

Creation date: Thu 09/02/2017 16:09
Runfile: GRO_2016_ED_v60.run

Table Name: WZND4_BHP_PRESSURE
Plot Name: WZND4_CIBHP
Time=2.016997e+03 [YEAR]

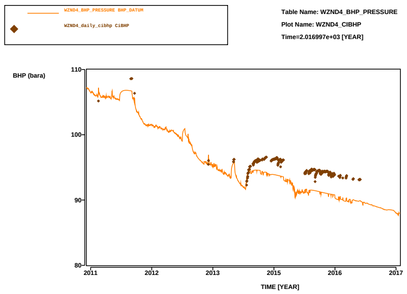

Creation date: Thu 09/02/2017 16:09
Runfile: GRO_2016_ED_v60.run

Table Name: WZND5_BHP_PRESSURE
Plot Name: WZND5_CIBHP
Time=2.016997e+03 [YEAR]

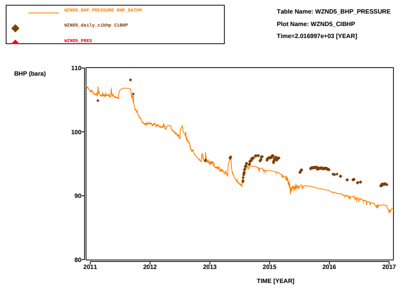

Creation date: Thu 09/02/2017 16:09
Runfile: GRO_2016_ED_v60.run

Table Name: WZND6A_BHP_PRESSURE
Plot Name: WZND6A_CIBHP
Time=2.016997e+03 [YEAR]

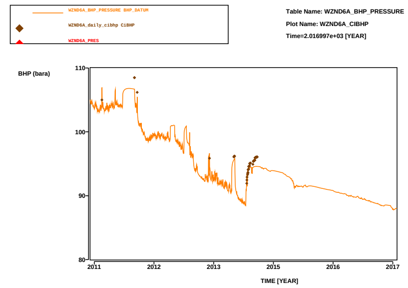

Creation date: Thu 09/02/2017 16:09
Runfile: GRO_2016_ED_v60.run

Table Name: WZND7_BHP_PRESSURE
Plot Name: WZND7_CIBHP
Time=2.016997e+03 [YEAR]

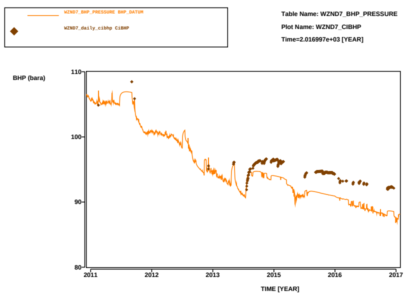

Creation date: Thu 09/02/2017 16:09
Runfile: GRO_2016_ED_v60.run

Table Name: WZND9A_BHP_PRESSURE
Plot Name: WZND9A_CIBHP
Time=2.016997e+03 [YEAR]

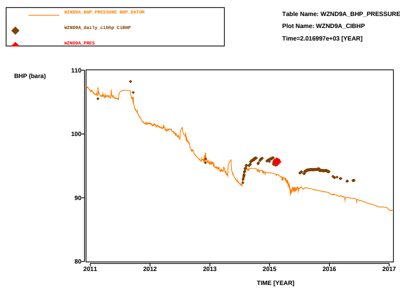

Creation date: Thu 09/02/2017 16:09
Runfile: GRO_2016_ED_v60.run

Table Name: WZND10_BHP_PRESSURE
Plot Name: WZND10_CIBHP
Time=2.016997e+03 [YEAR]

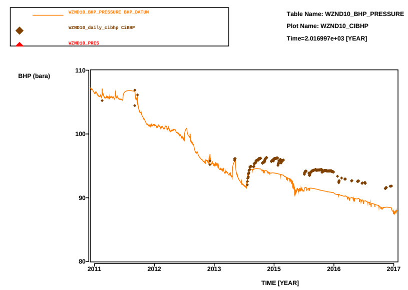

Creation date: Thu 09/02/2017 16:09
Runfile: GRO_2016_ED_v60.run

Table Name: WZND12B_BHP_PRESSURE
Plot Name: WZND12B_CIBHP
Time=2.016997e+03 [YEAR]

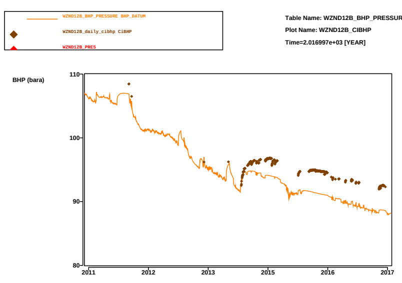

Creation date: Thu 09/02/2017 16:09

Runfile: GRO_2016_ED_v60.run

Table Name: WZPD1_BHP_PRESSURE
Plot Name: WZPD1_CIBHP
Time=2.016997e+03 [YEAR]

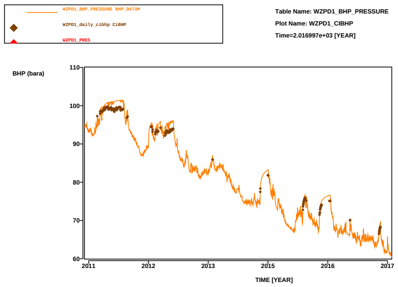

Table Name: WZPD2_BHP_PRESSURE
Plot Name: WZPD2_CIBHP
Time=2.016997e+03 [YEAR]

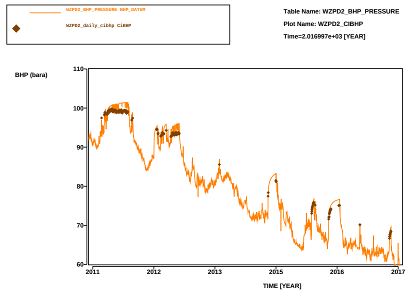

Table Name: WZPD3C_BHP_PRESSURE
Plot Name: WZPD3C_CIBHP
Time=2.016997e+03 [YEAR]

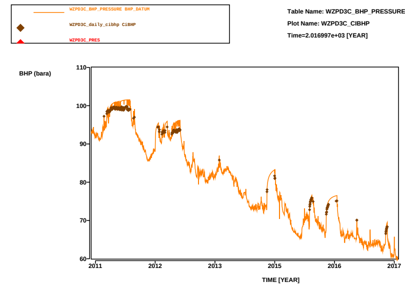

Table Name: WZPD4_BHP_PRESSURE
Plot Name: WZPD4_CIBHP
Time=2.016997e+03 [YEAR]

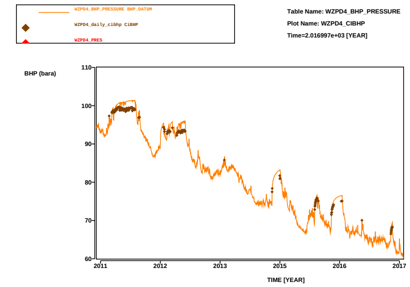

Creation date: Thu 09/02/2017 16:09
Runfile: GRO_2016_ED_v60.run

Creation date: Thu 09/02/2017 16:09
Runfile: GRO_2016_ED_v60.run

Creation date: Thu 09/02/2017 16:09
Runfile: GRO_2016_ED_v60.run

Creation date: Thu 09/02/2017 16:09
Runfile: GRO_2016_ED_v60.run

Table Name: WZPD5_BHP_PRESSURE
Plot Name: WZPD5_CIBHP
Time=2.016997e+03 [YEAR]

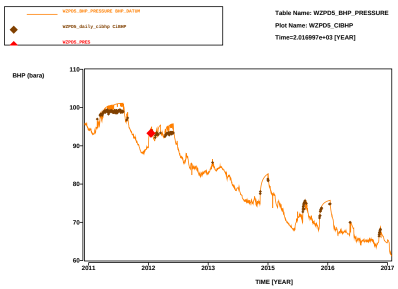

Table Name: WZPD6_BHP_PRESSURE
Plot Name: WZPD6_CIBHP
Time=2.016997e+03 [YEAR]

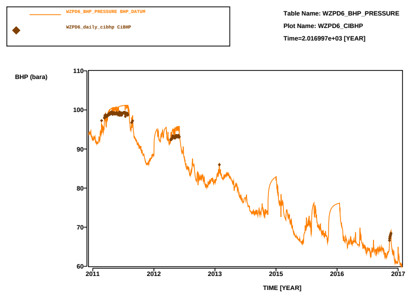

Table Name: WZPD7_BHP_PRESSURE
Plot Name: WZPD7_CIBHP
Time=2.016997e+03 [YEAR]

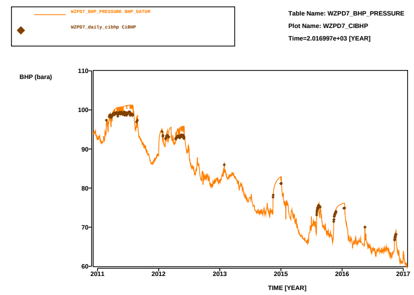

Table Name: WZPD8_BHP_PRESSURE
Plot Name: WZPD8_CIBHP
Time=2.016997e+03 [YEAR]

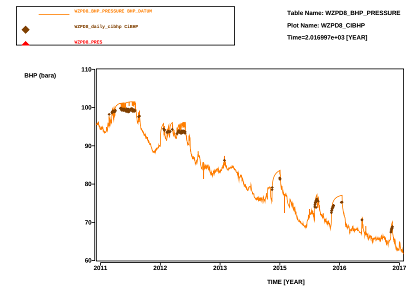

Creation date: Thu 09/02/2017 16:09
Runfile: GRO_2016_ED_v60.run

Creation date: Thu 09/02/2017 16:09
Runfile: GRO_2016_ED_v60.run

Creation date: Thu 09/02/2017 16:09
Runfile: GRO_2016_ED_v60.run

Creation date: Thu 09/02/2017 16:09
Runfile: GRO_2016_ED_v60.run

Table Name: WZPD9_BHP_PRESSURE
Plot Name: WZPD9_CIBHP
Time=2.016997e+03 [YEAR]

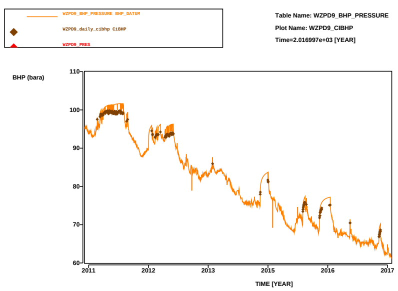

Table Name: WZPD10_BHP_PRESSURE
Plot Name: WZPD10_CIBHP
Time=2.016997e+03 [YEAR]

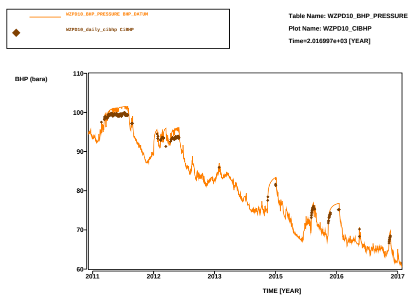

Table Name: WZPD11_BHP_PRESSURE
Plot Name: WZPD11_CIBHP
Time=2.016997e+03 [YEAR]

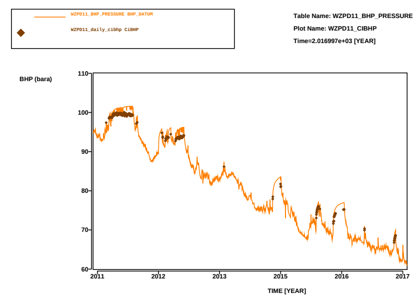

Table Name: WZPD12A_BHP_PRESSURE
Plot Name: WZPD12A_CIBHP
Time=2.016997e+03 [YEAR]

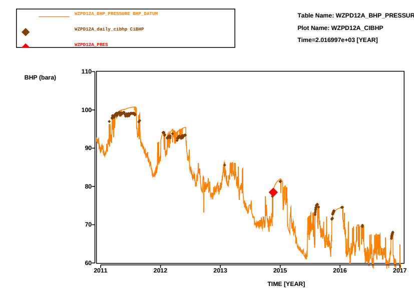

Creation date: Thu 09/02/2017 16:09
Runfile: GRO_2016_ED_v60.run

Creation date: Thu 09/02/2017 16:09
Runfile: GRO_2016_ED_v60.run

Creation date: Thu 09/02/2017 16:09
Runfile: GRO_2016_ED_v60.run

Creation date: Thu 09/02/2017 16:09
Runfile: GRO_2016_ED_v60.run

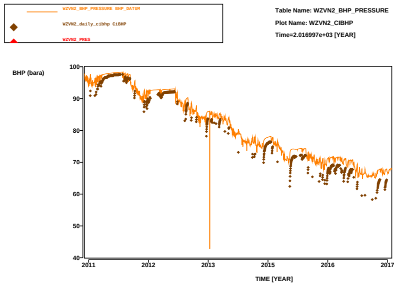

Creation date: Thu 09/02/2017 16:09
Runfile: GRO_2016_ED_v60.run

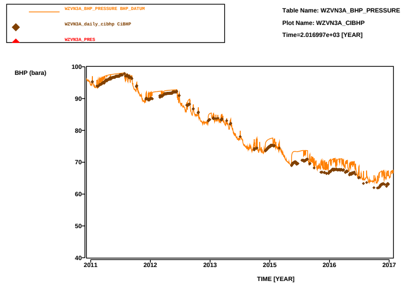

Creation date: Thu 09/02/2017 16:09
Runfile: GRO_2016_ED_v60.run

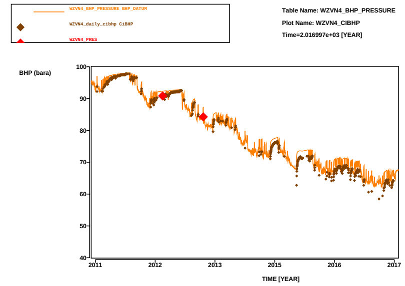

Creation date: Thu 09/02/2017 16:09
Runfile: GRO_2016_ED_v60.run

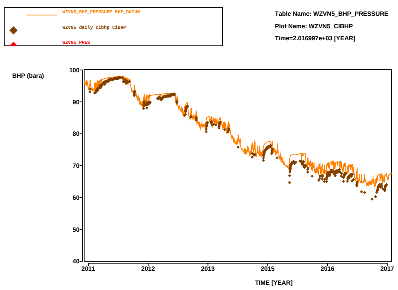

Creation date: Thu 09/02/2017 16:09
Runfile: GRO_2016_ED_v60.run

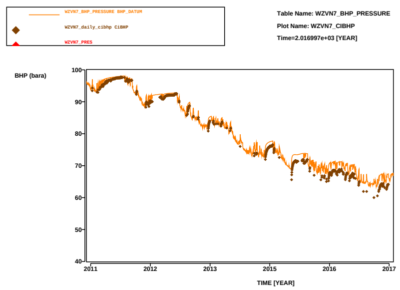

Creation date: Thu 09/02/2017 16:09
Runfile: GRO_2016_ED_v60.run

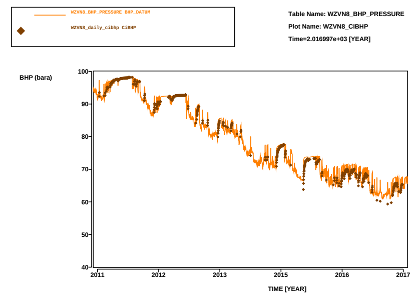

Creation date: Thu 09/02/2017 16:09
Runfile: GRO_2016_ED_v60.run

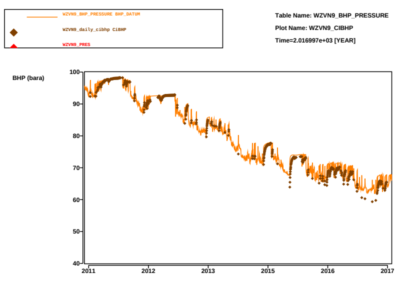

Creation date: Thu 09/02/2017 16:09
Runfile: GRO_2016_ED_v60.run

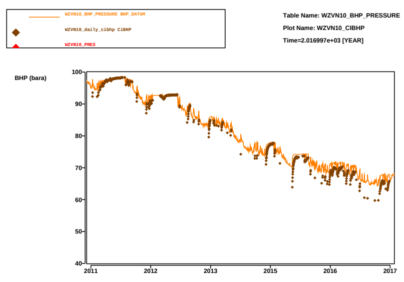

Creation date: Thu 09/02/2017 16:09
Runfile: GRO_2016_ED_v60.run

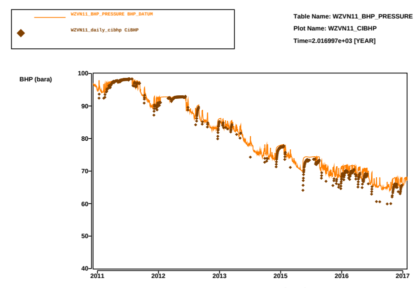

Creation date: Thu 09/02/2017 16:09
Runfile: GRO_2016_ED_v60.run

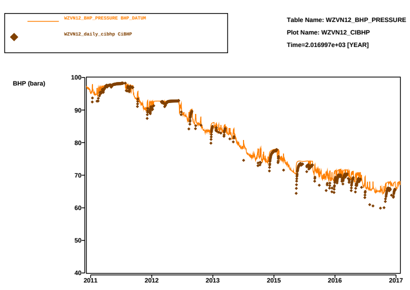

Creation date: Thu 09/02/2017 16:09

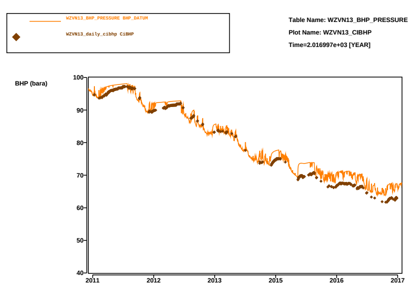

Creation date: Thu 09/02/2017 16:09

Runfile: GRO_2016_ED_v60.run

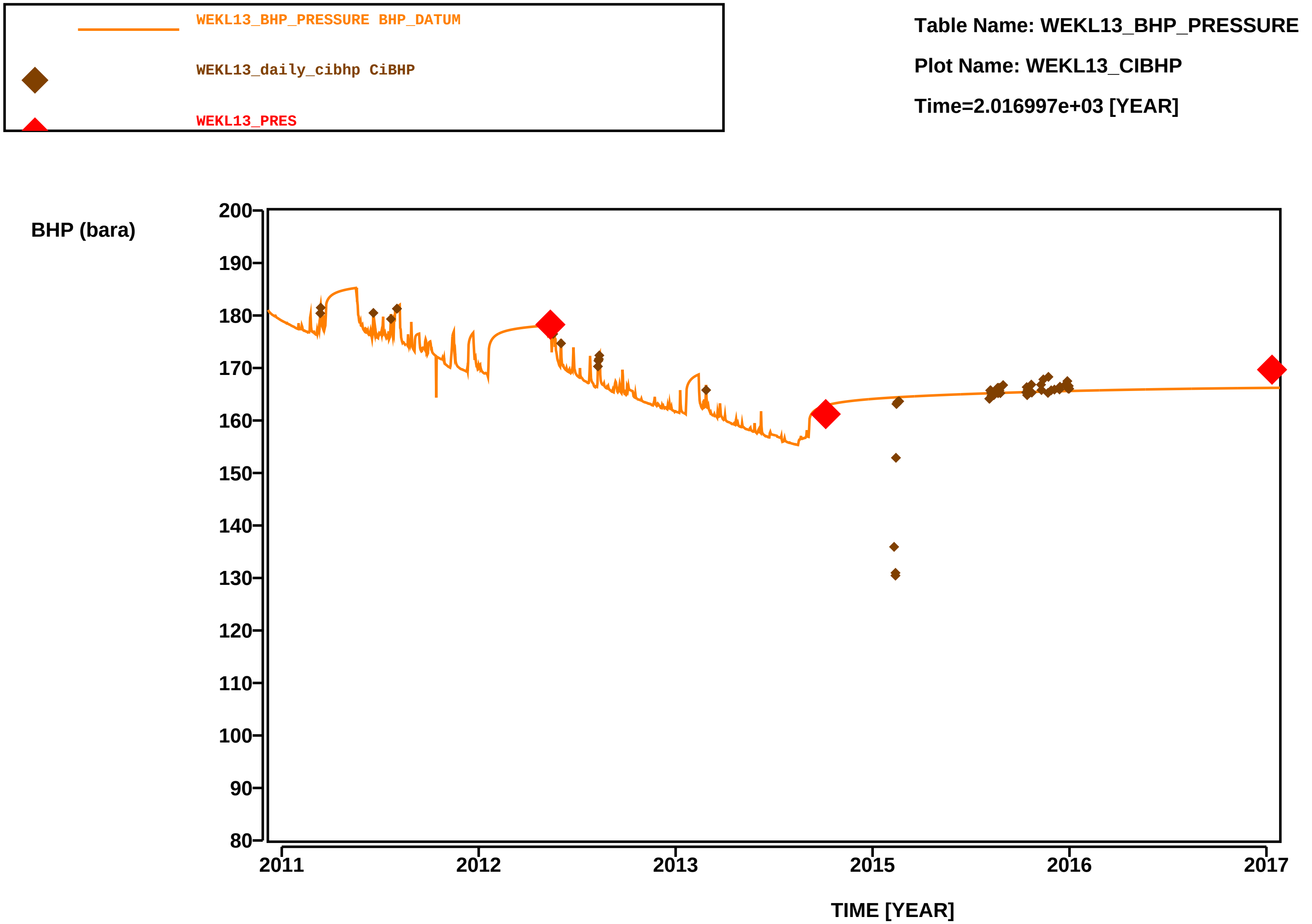

Creation date: Thu 09/02/2017 16:09
Runfile: GRO_2016_ED_v60.run

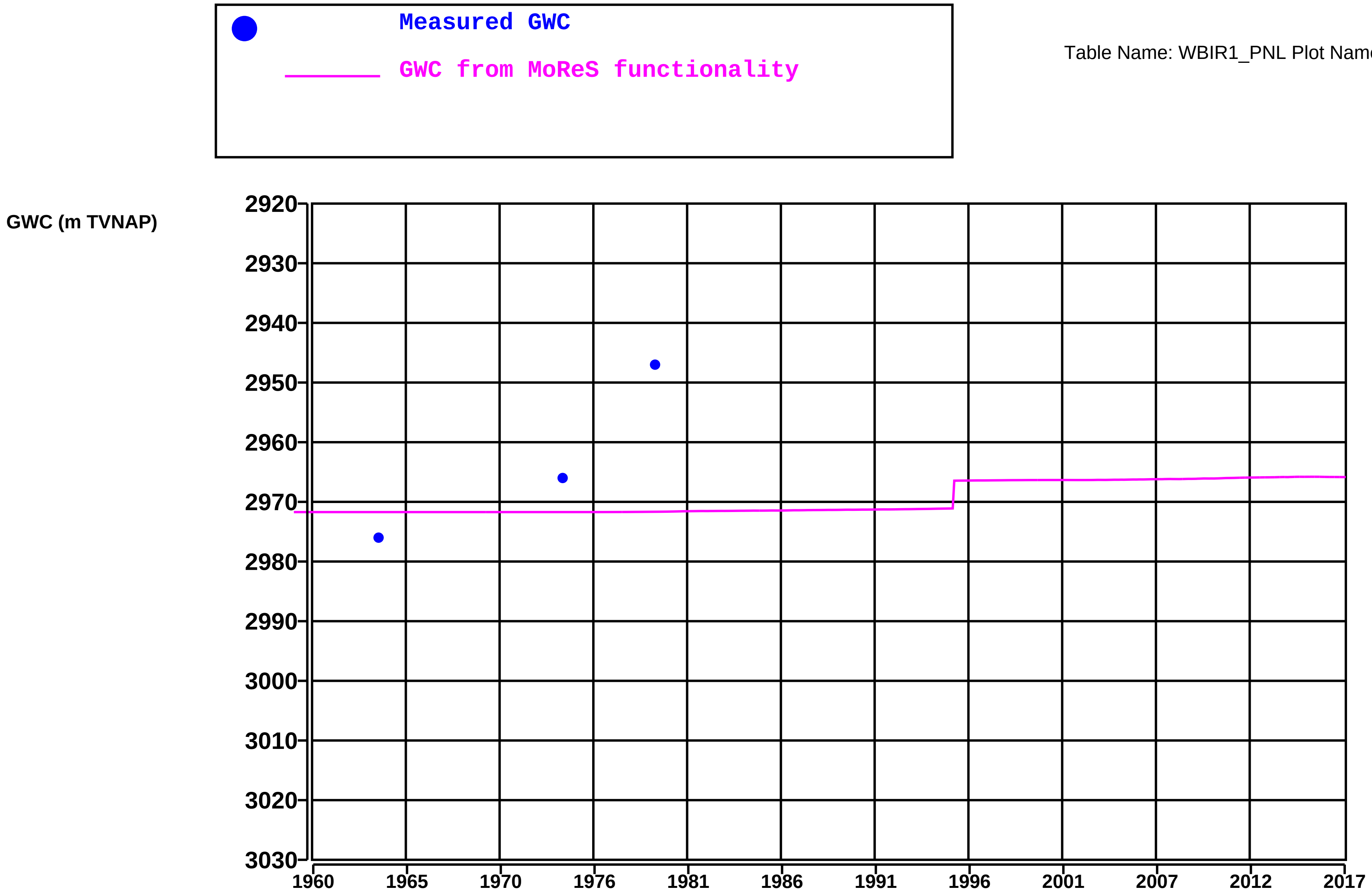

Table Name: WBIR1_PNL Plot Name: PN

Creation date: Thu 09/02/2017 16:08
Runfile: GRO_2016_ED_v60.run

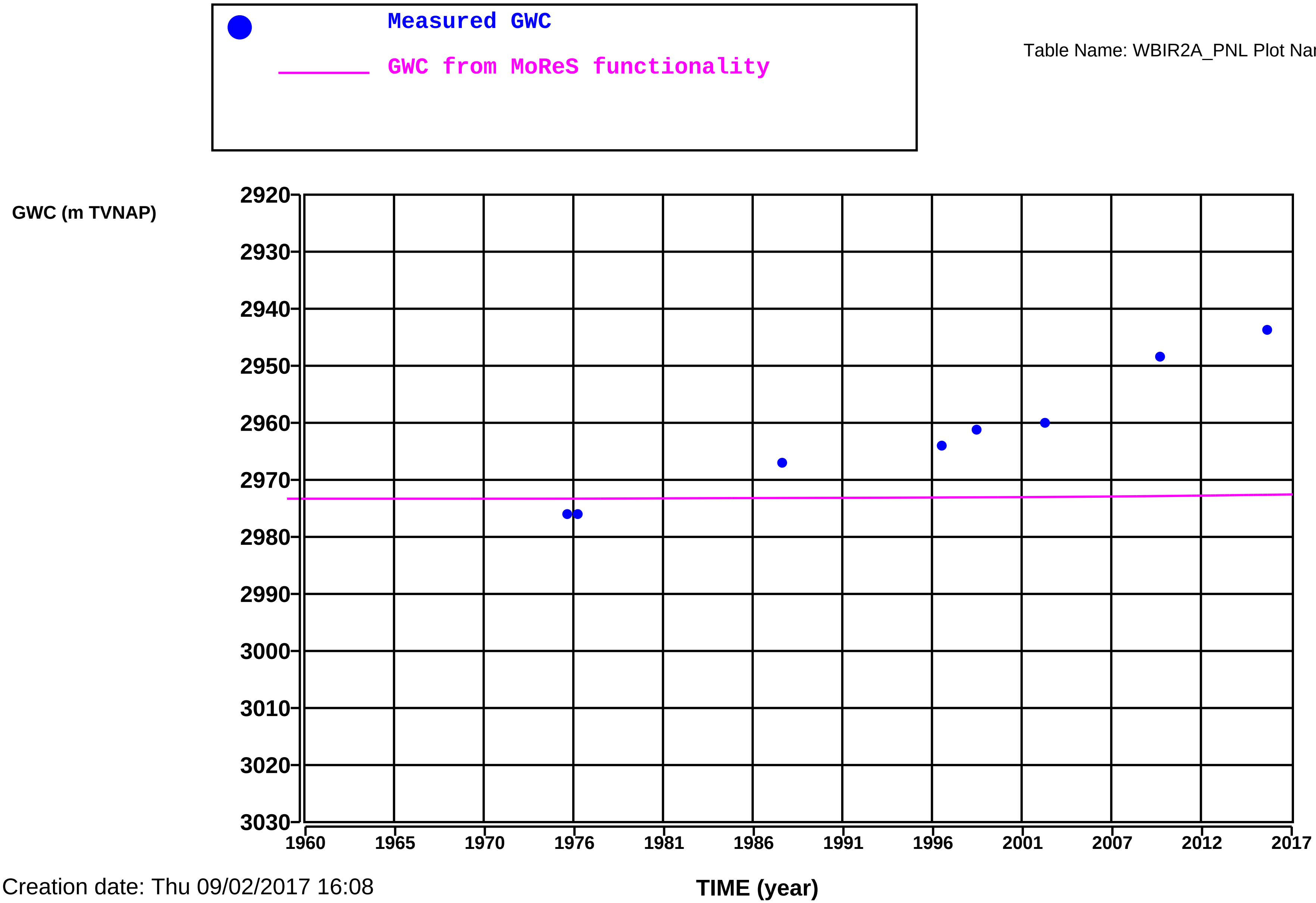

Table Name: WBIR2A_PNL Plot Name: P

Creation date: Thu 09/02/2017 16:08
Runfile: GRO_2016_ED_v60.run

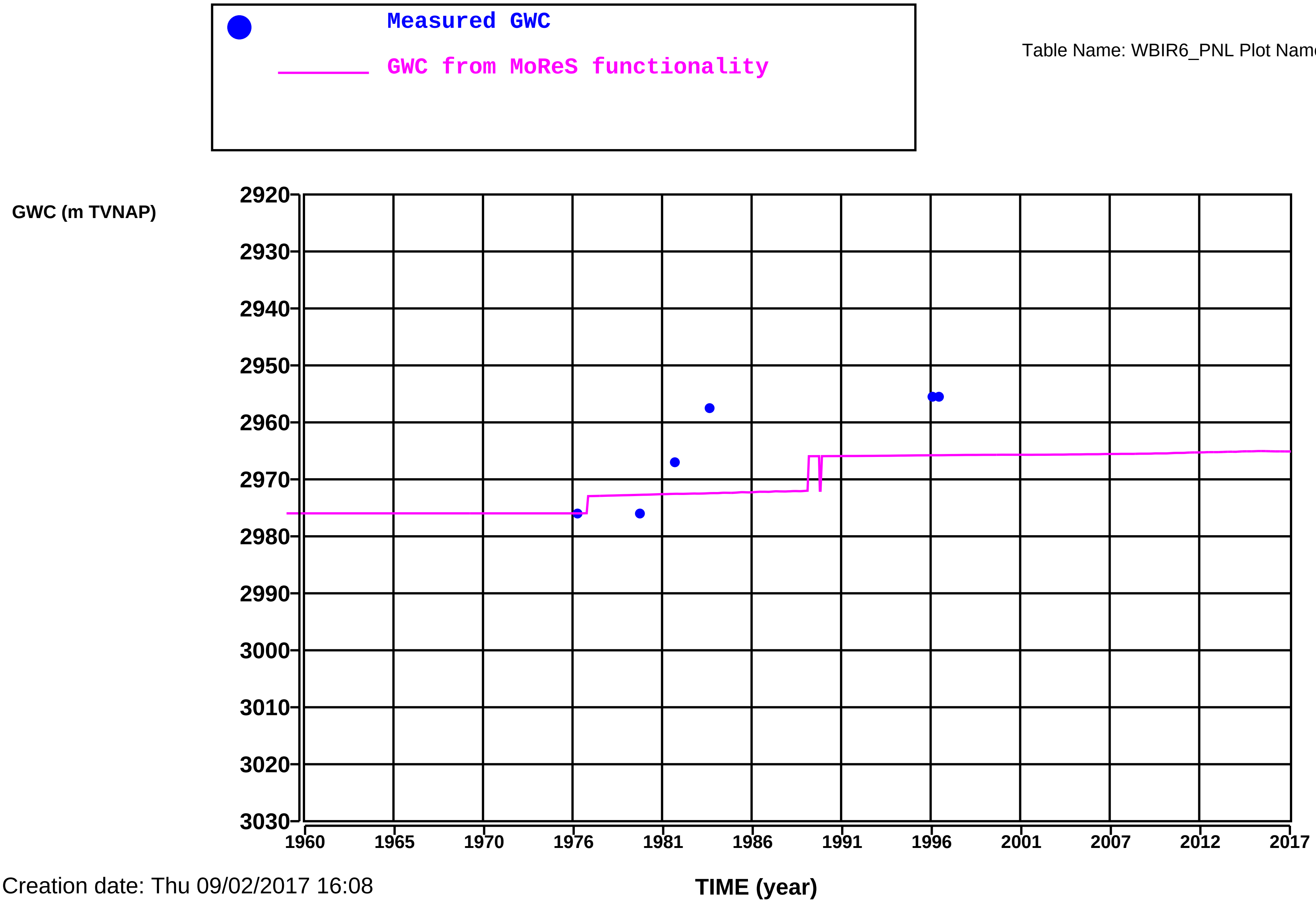

Table Name: WBIR6_PNL Plot Name: PN

Creation date: Thu 09/02/2017 16:08
Runfile: GRO_2016_ED_v60.run

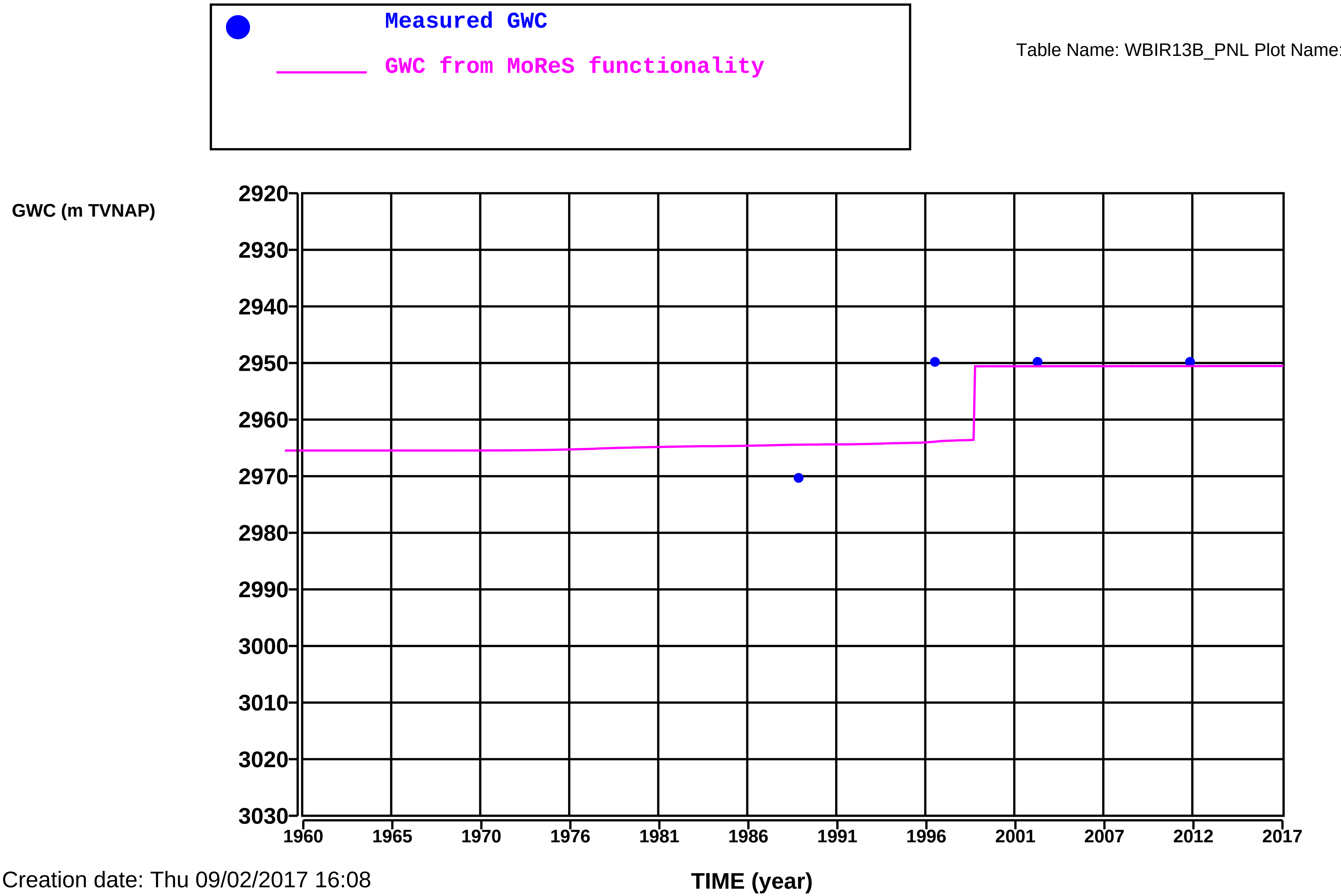

Creation date: Thu 09/02/2017 16:08
Runfile: GRO_2016_ED_v60.run

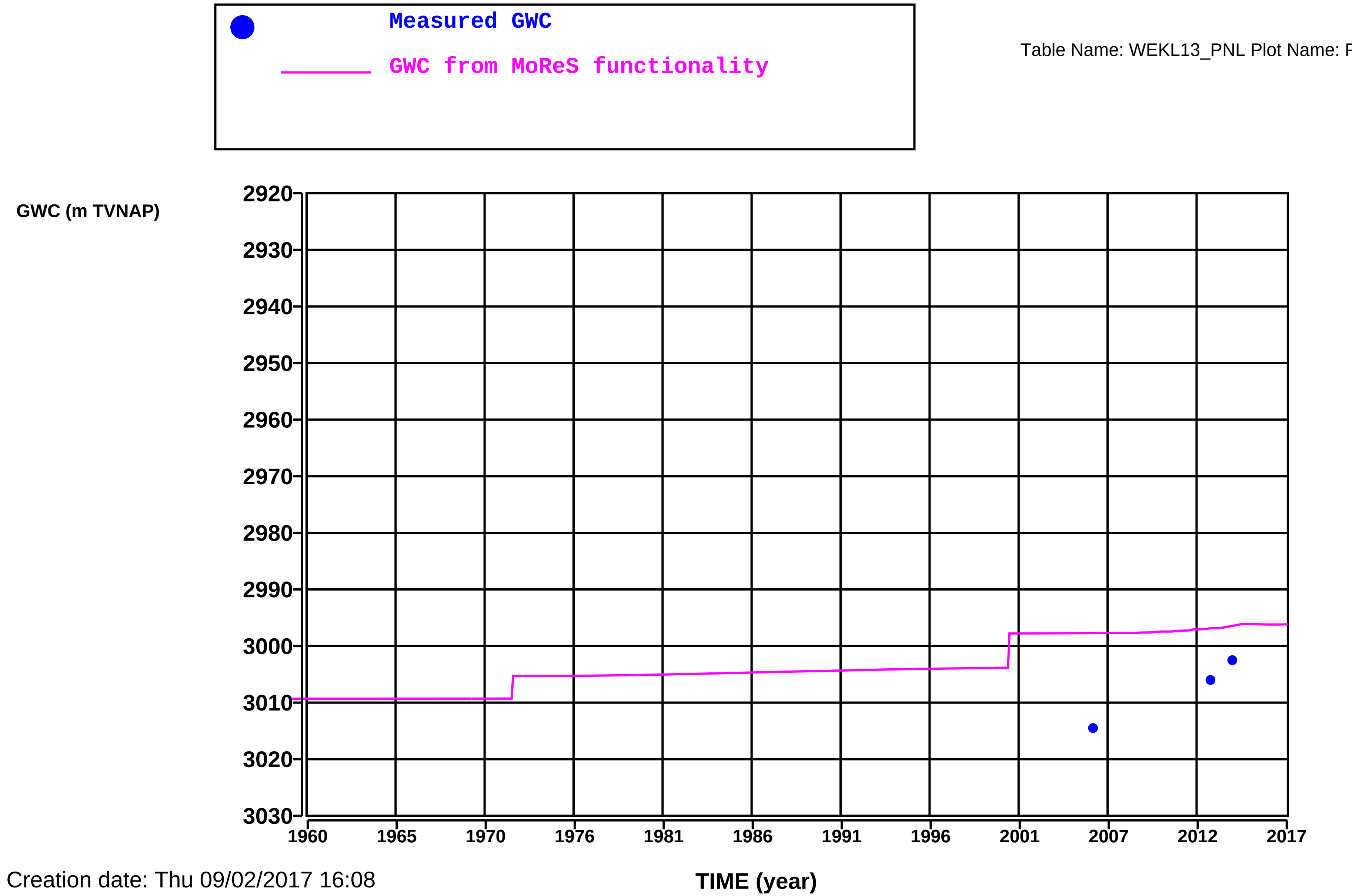

Creation date: Thu 09/02/2017 16:08
Runfile: GRO_2016_ED_v60.run

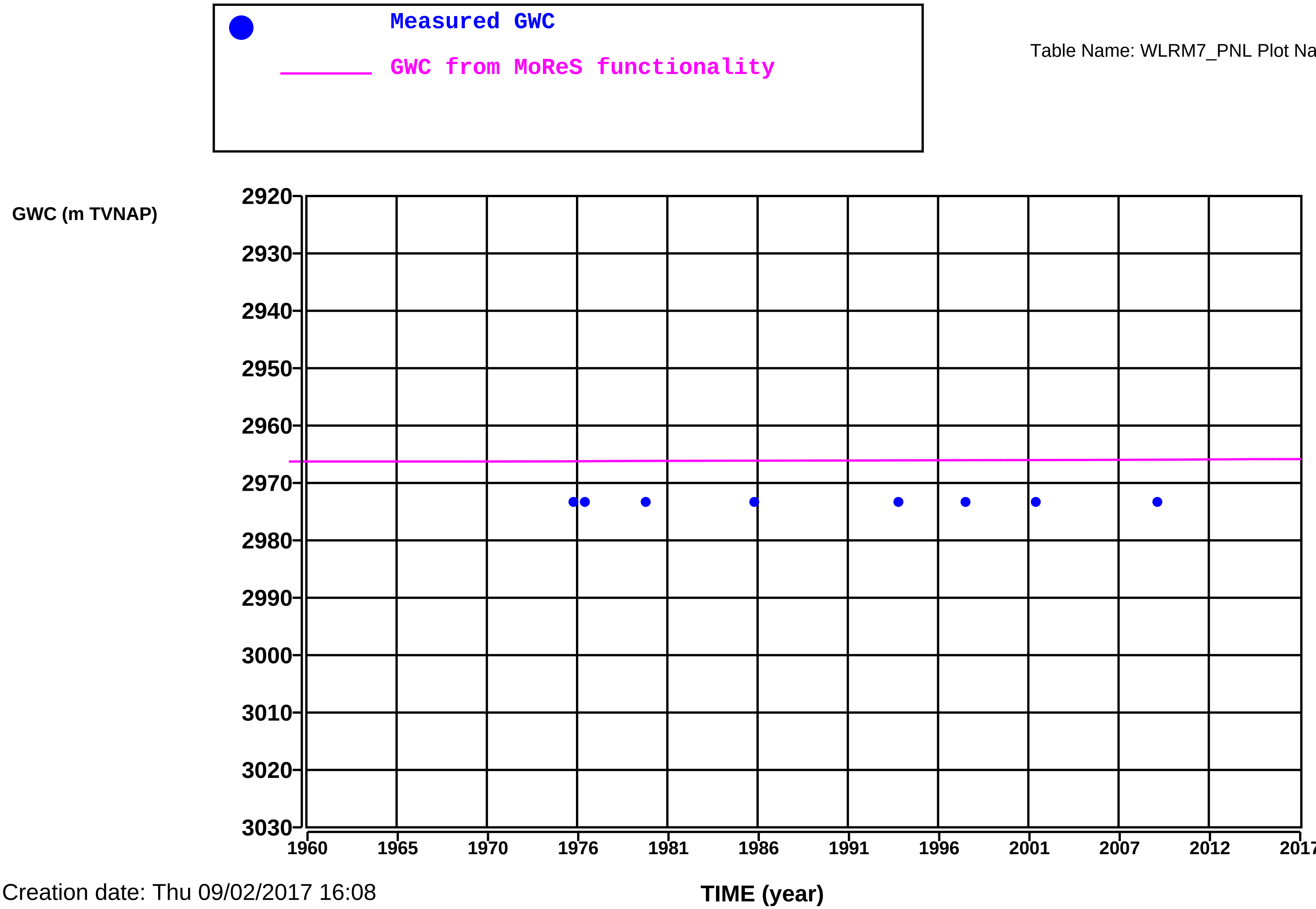

Table Name: WLRM7_PNL Plot Name: P

Creation date: Thu 09/02/2017 16:08
Runfile: GRO_2016_ED_v60.run

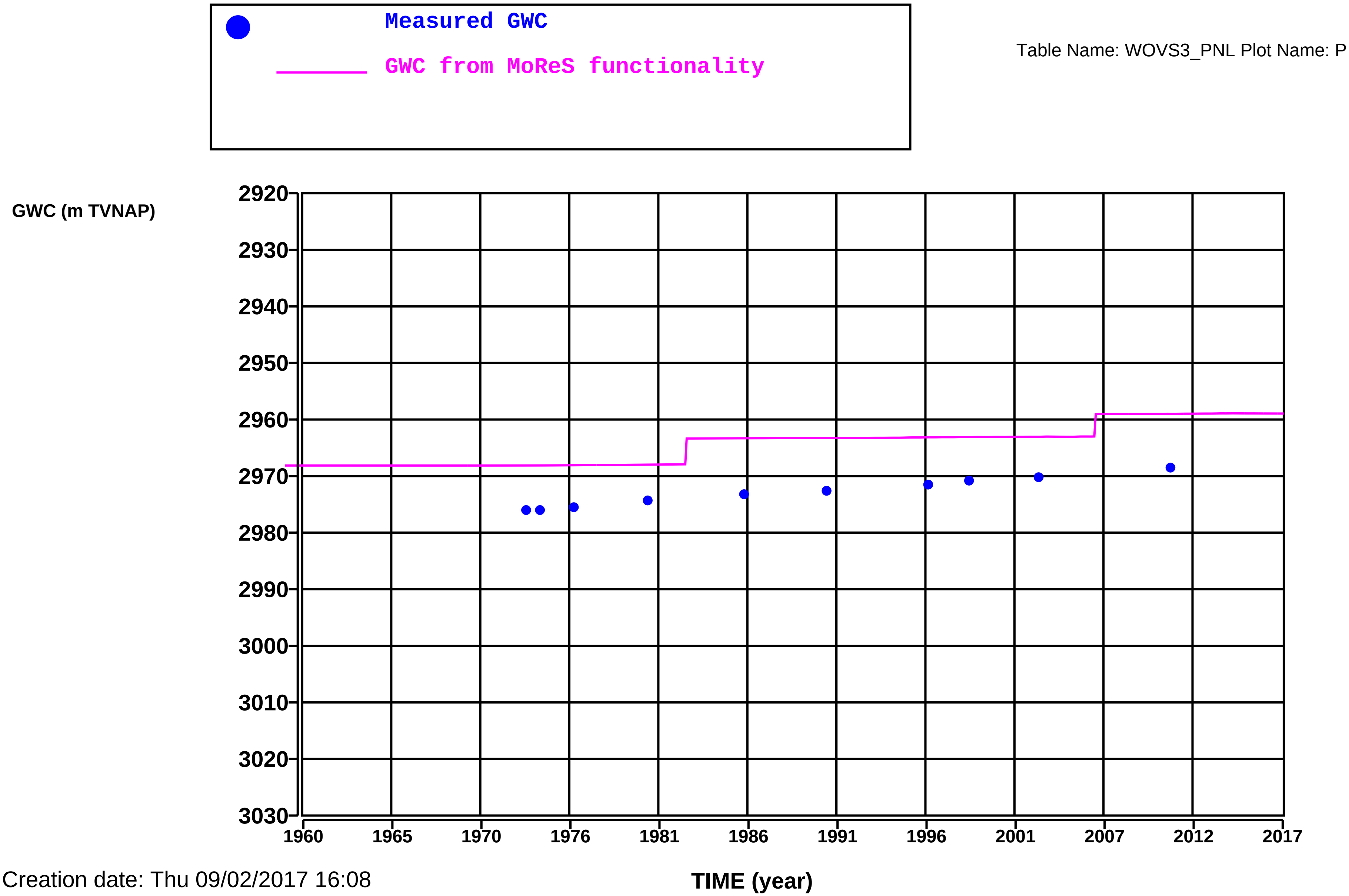

Creation date: Thu 09/02/2017 16:08
Runfile: GRO_2016_ED_v60.run

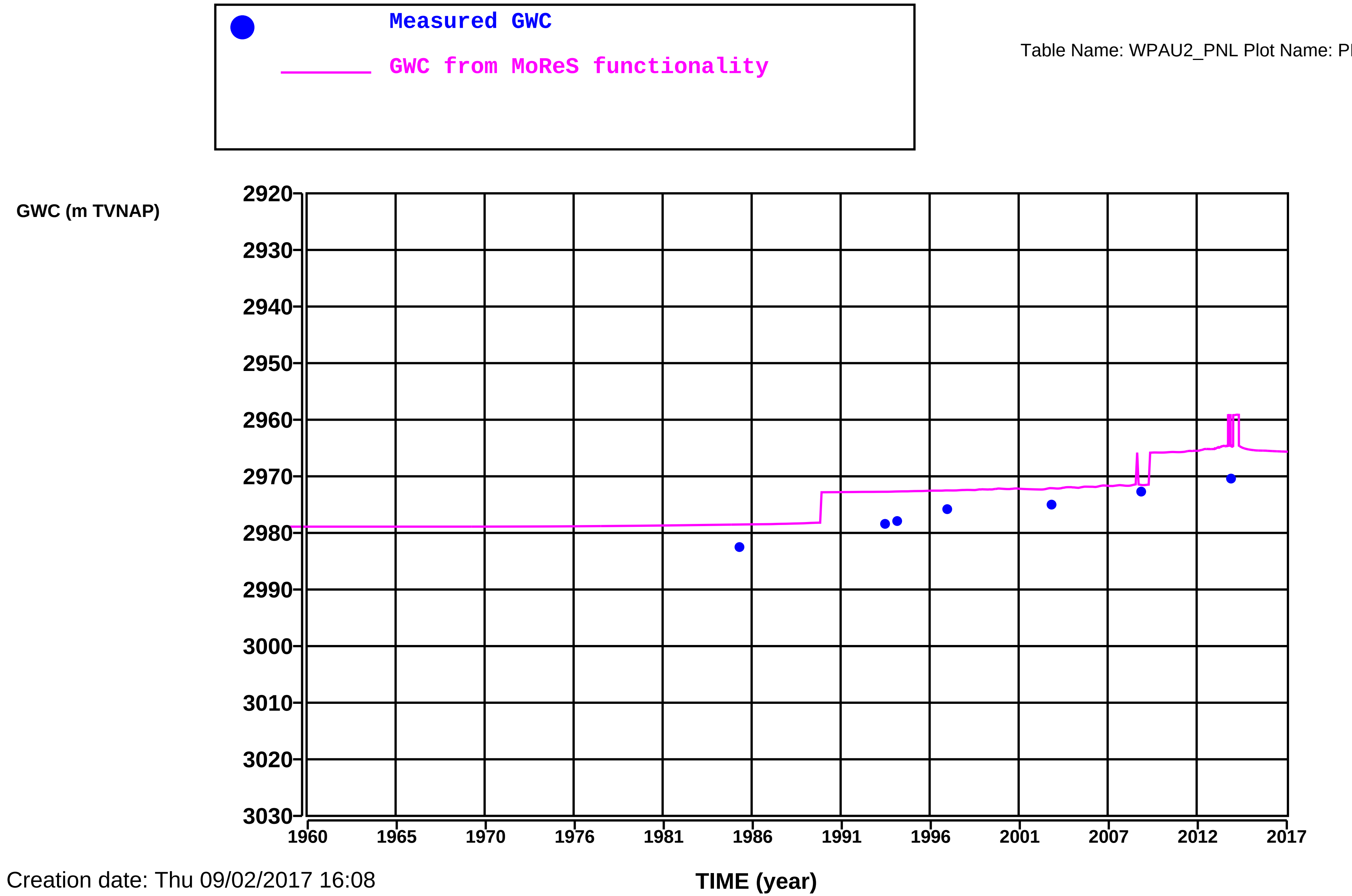

Creation date: Thu 09/02/2017 16:08
Runfile: GRO_2016_ED_v60.run

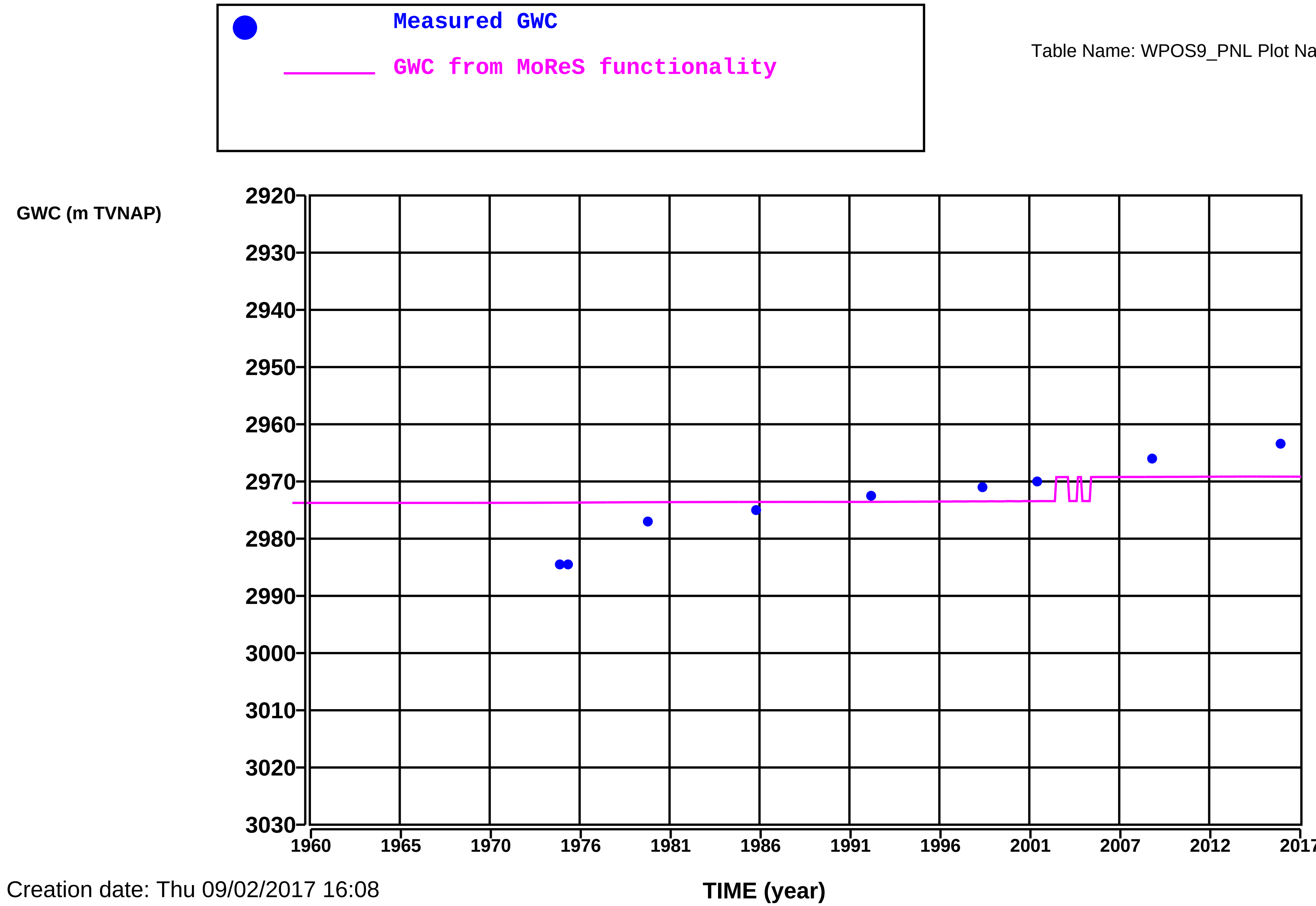

Table Name: WPOS9_PNL Plot Name: P

Creation date: Thu 09/02/2017 16:08
Runfile: GRO_2016_ED_v60.run

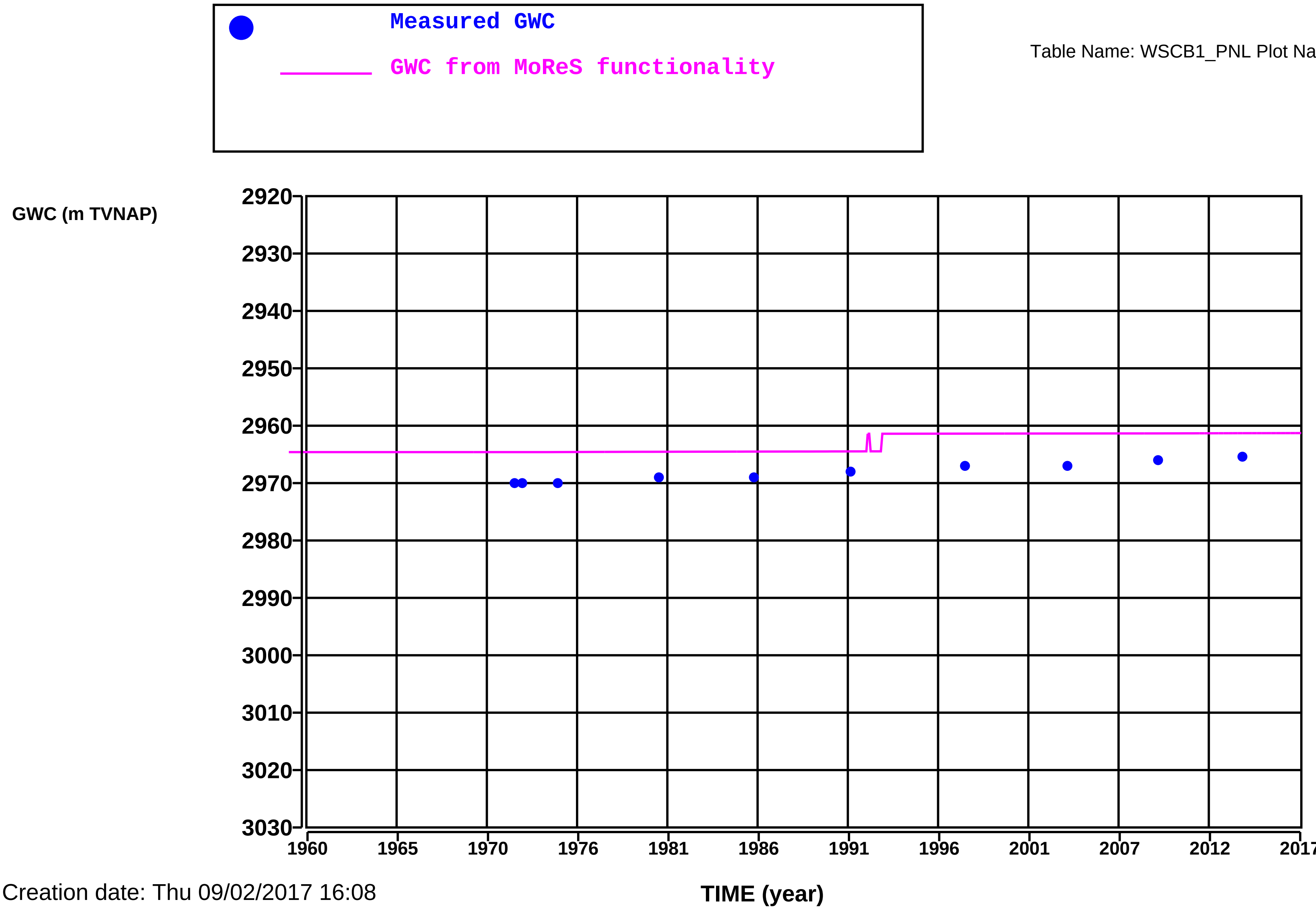

Table Name: WSCB1_PNL Plot Name: Pl

Creation date: Thu 09/02/2017 16:08
Runfile: GRO_2016_ED_v60.run

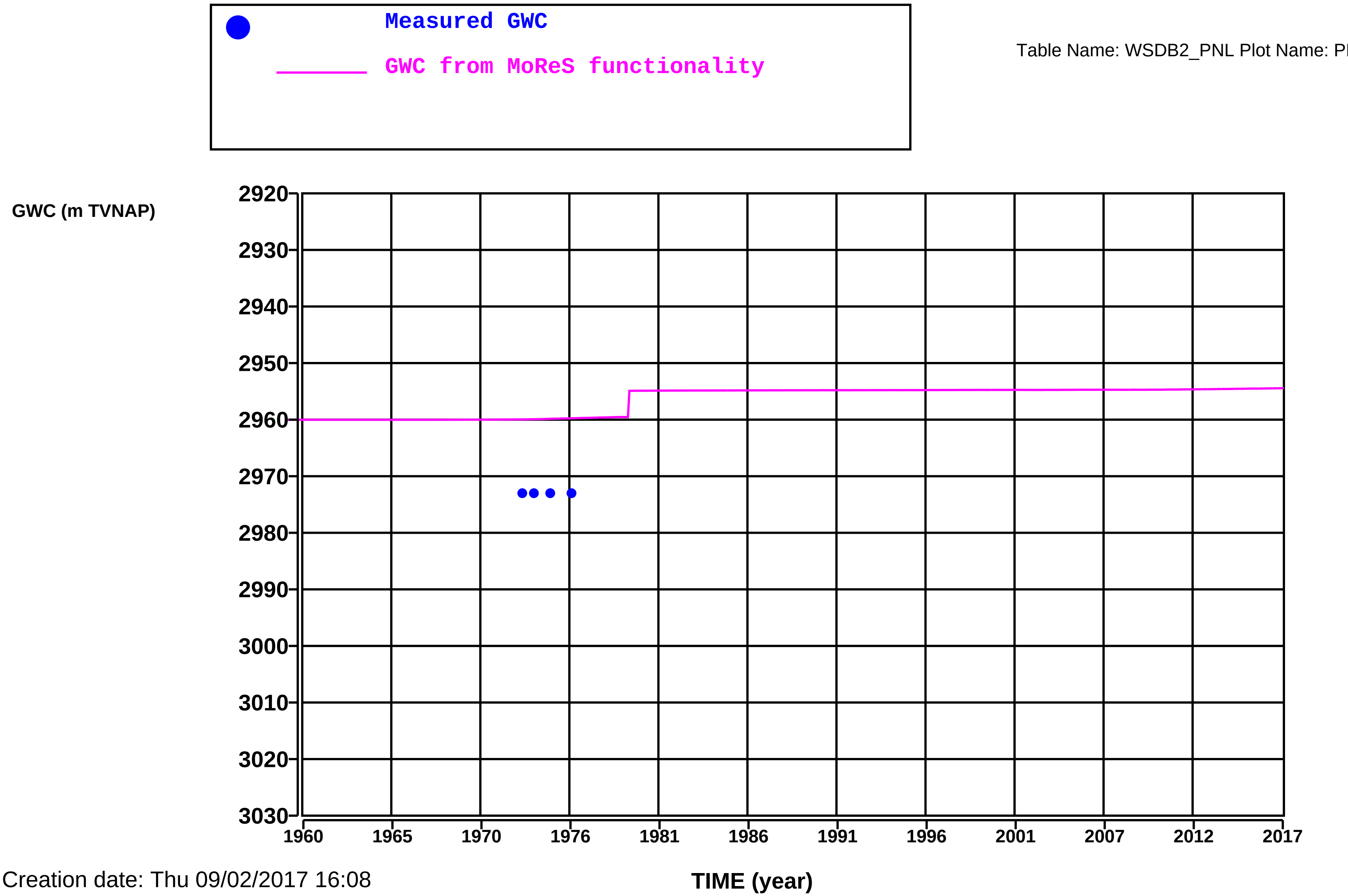

Creation date: Thu 09/02/2017 16:08
Runfile: GRO_2016_ED_v60.run

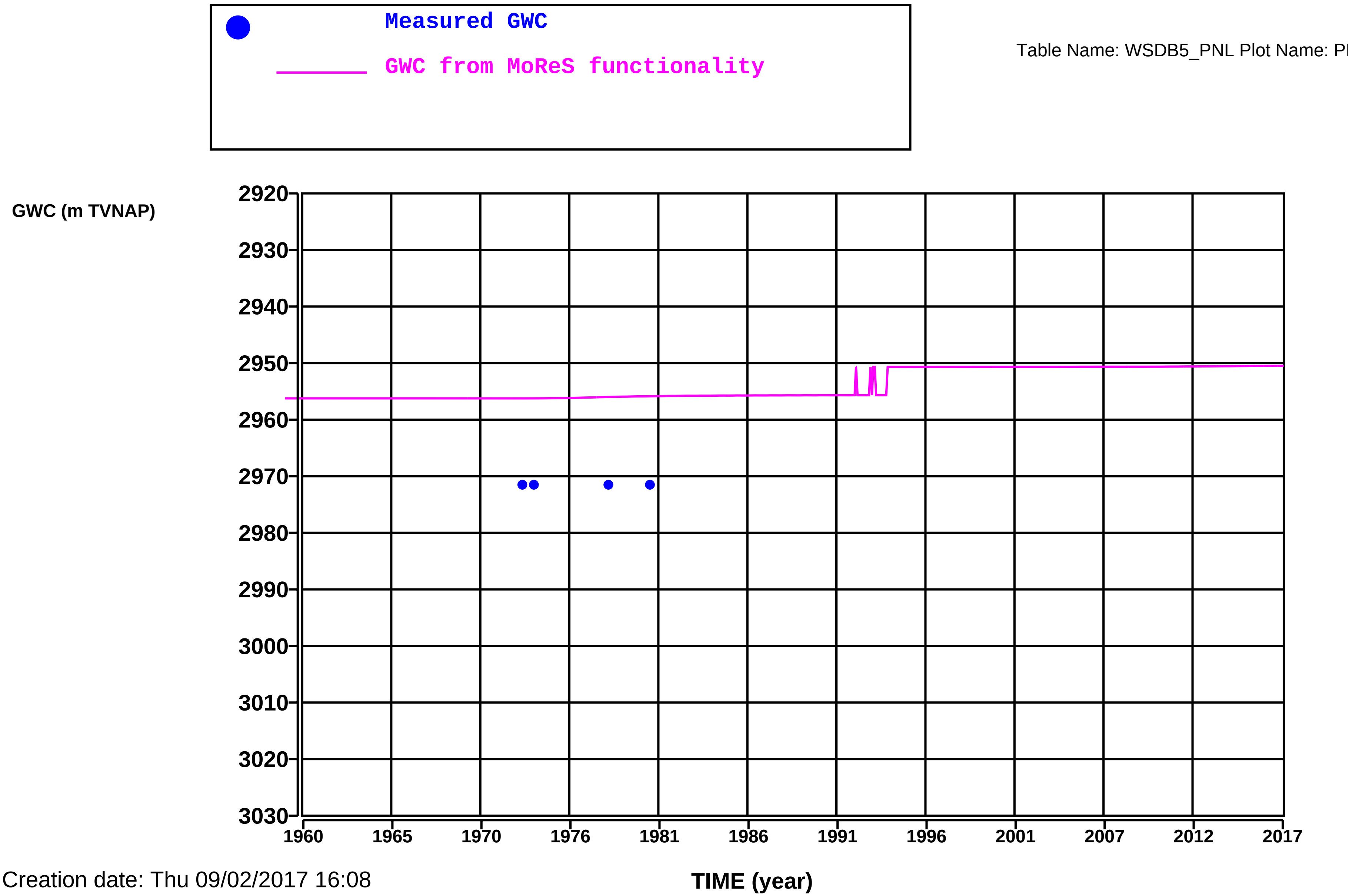

Creation date: Thu 09/02/2017 16:08
Runfile: GRO_2016_ED_v60.run

Table Name: WSDB7_PNL Plot Name: Pl

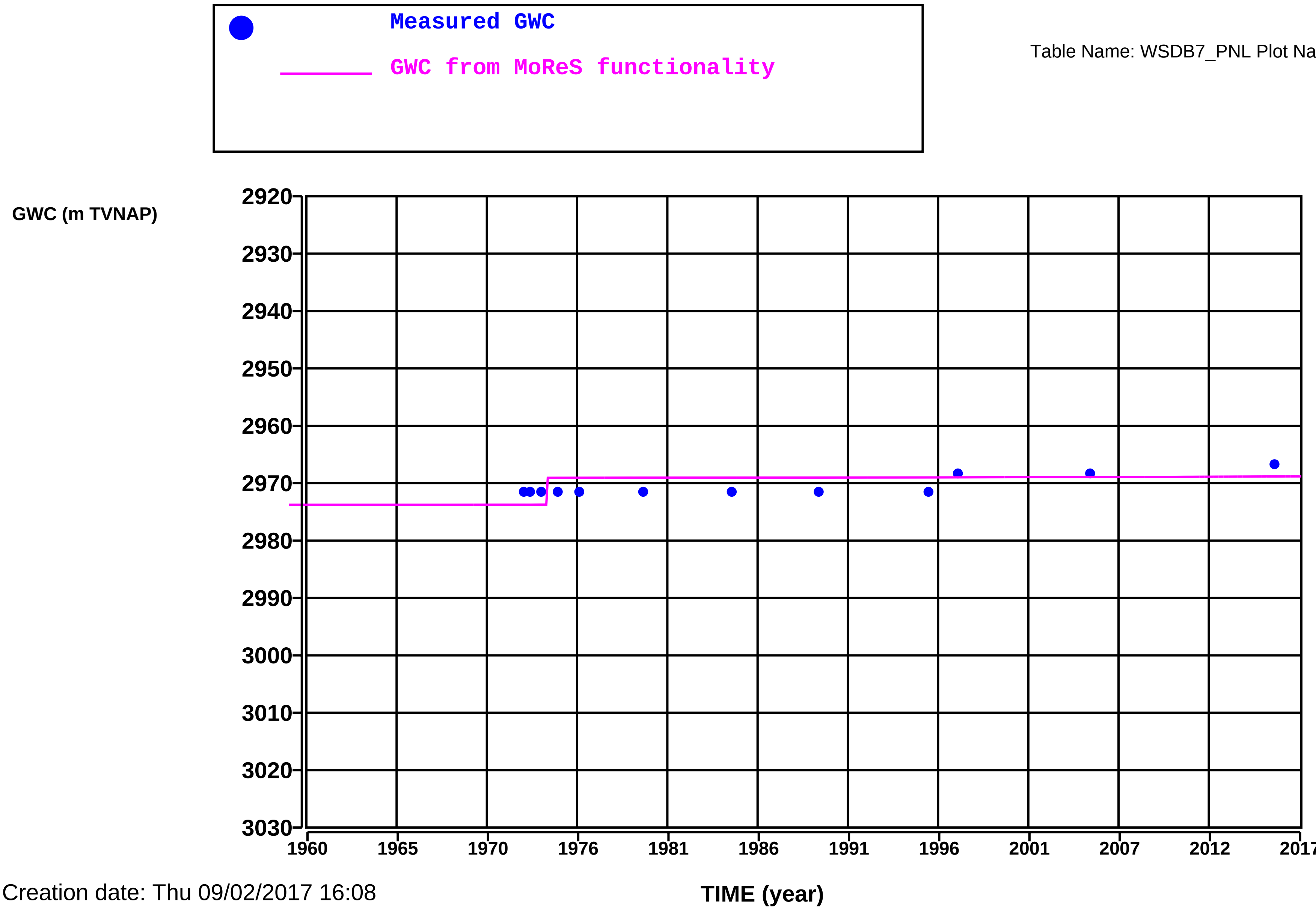

Creation date: Thu 09/02/2017 16:08
Runfile: GRO_2016_ED_v60.run

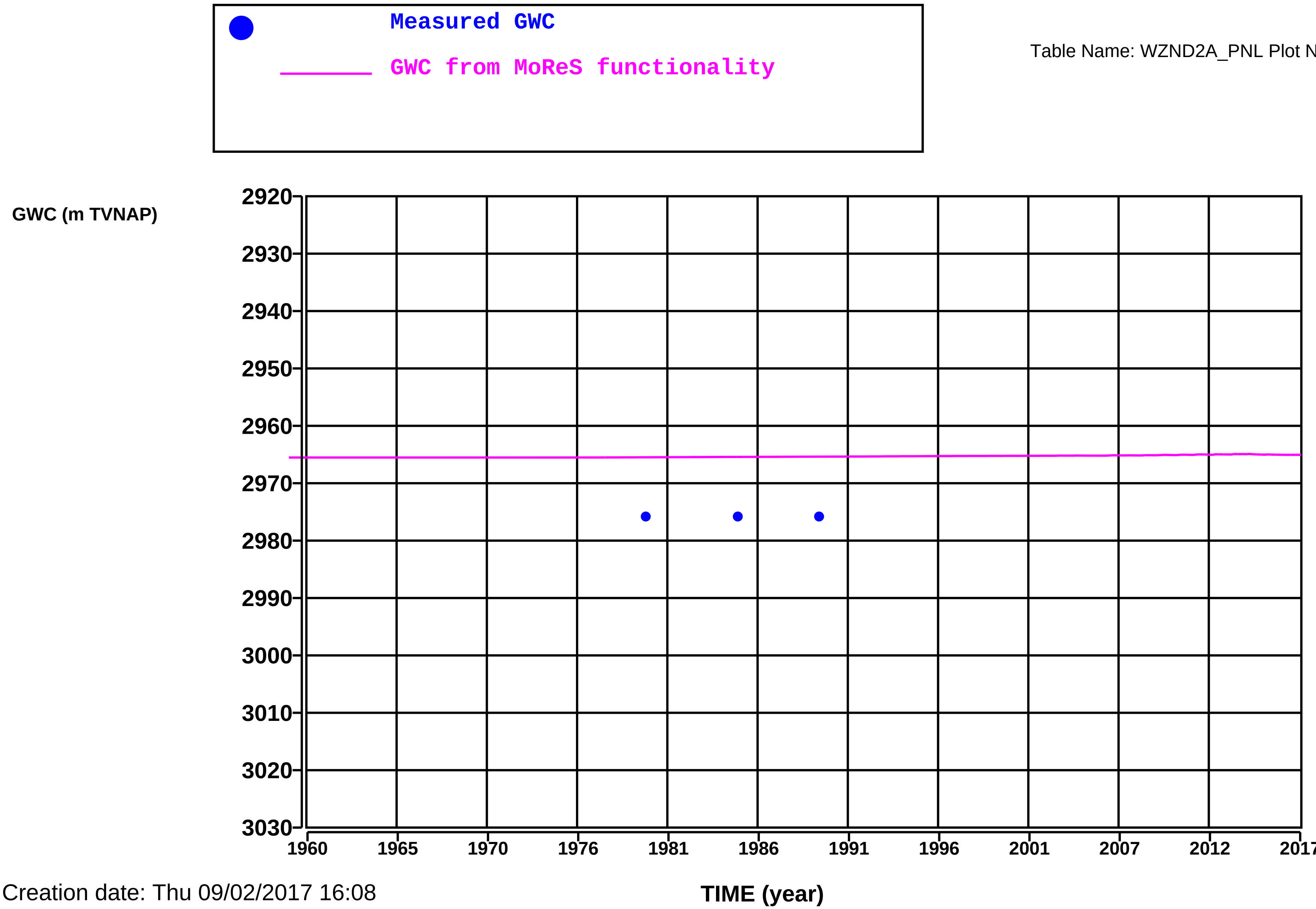

Table Name: WZND2A_PNL Plot Name: I

Creation date: Thu 09/02/2017 16:08
Runfile: GRO_2016_ED_v60.run

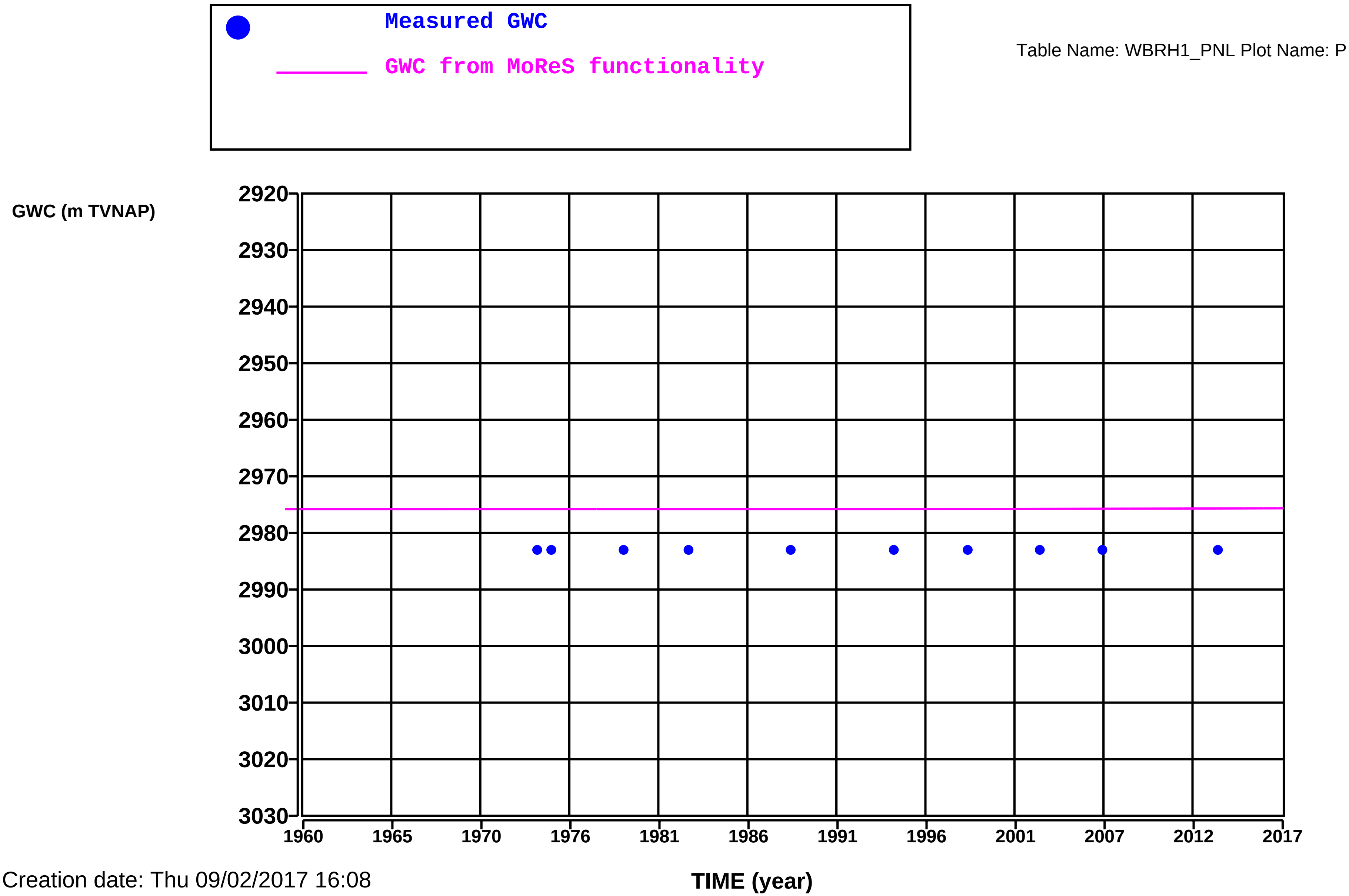

Creation date: Thu 09/02/2017 16:08
Runfile: GRO_2016_ED_v60.run

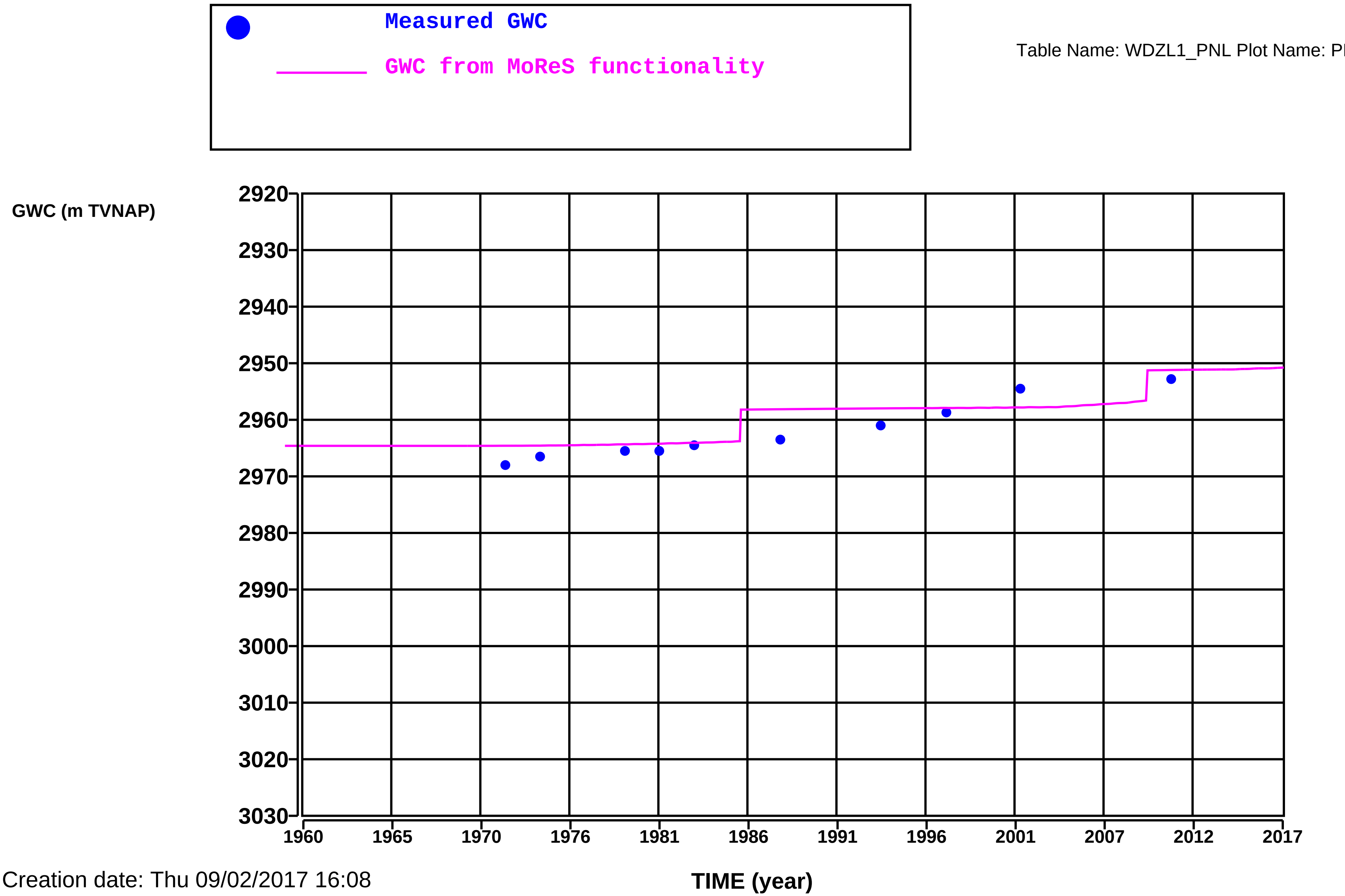

Creation date: Thu 09/02/2017 16:08
Runfile: GRO_2016_ED_v60.run

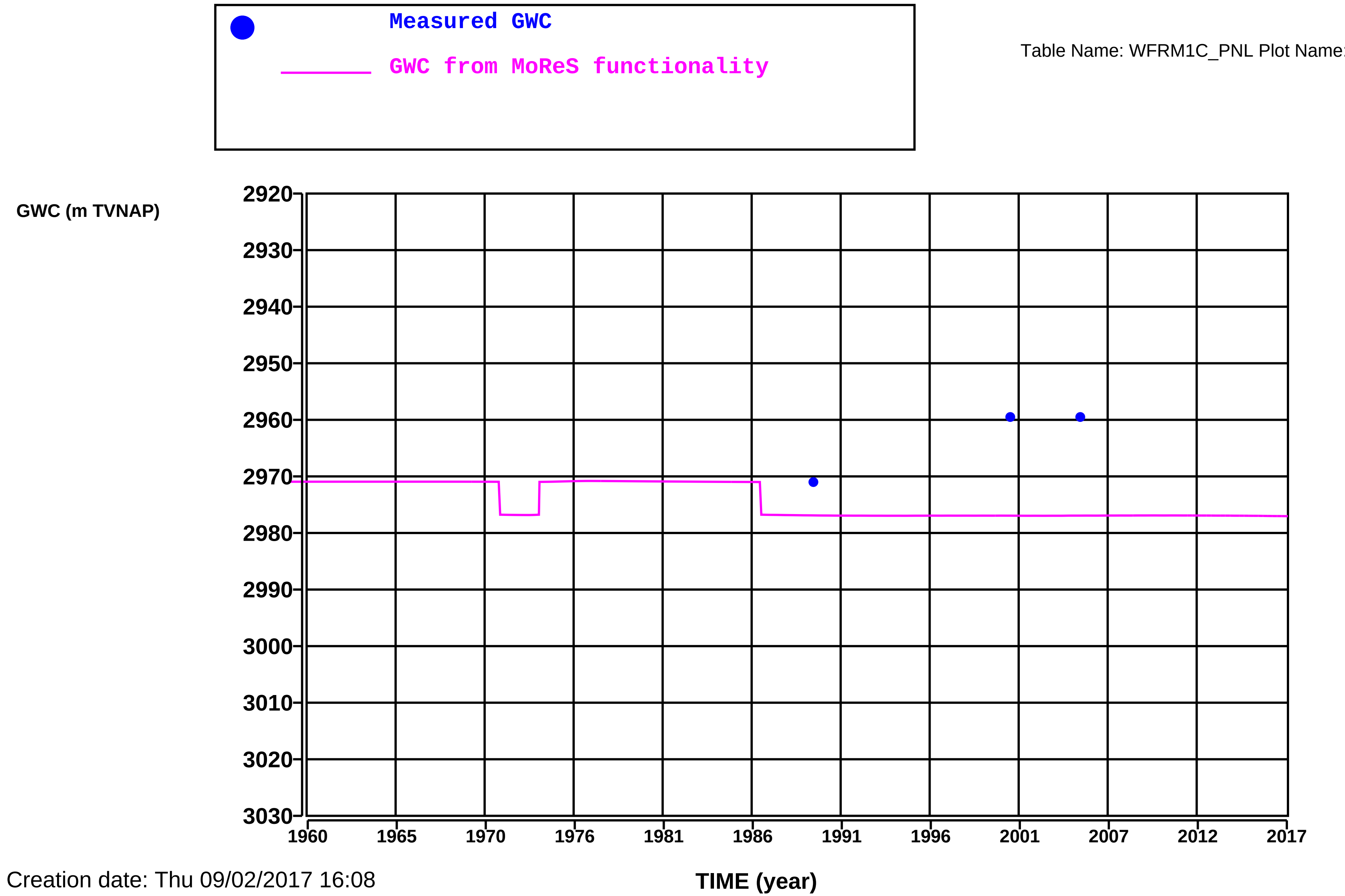

Creation date: Thu 09/02/2017 16:08
Runfile: GRO_2016_ED_v60.run

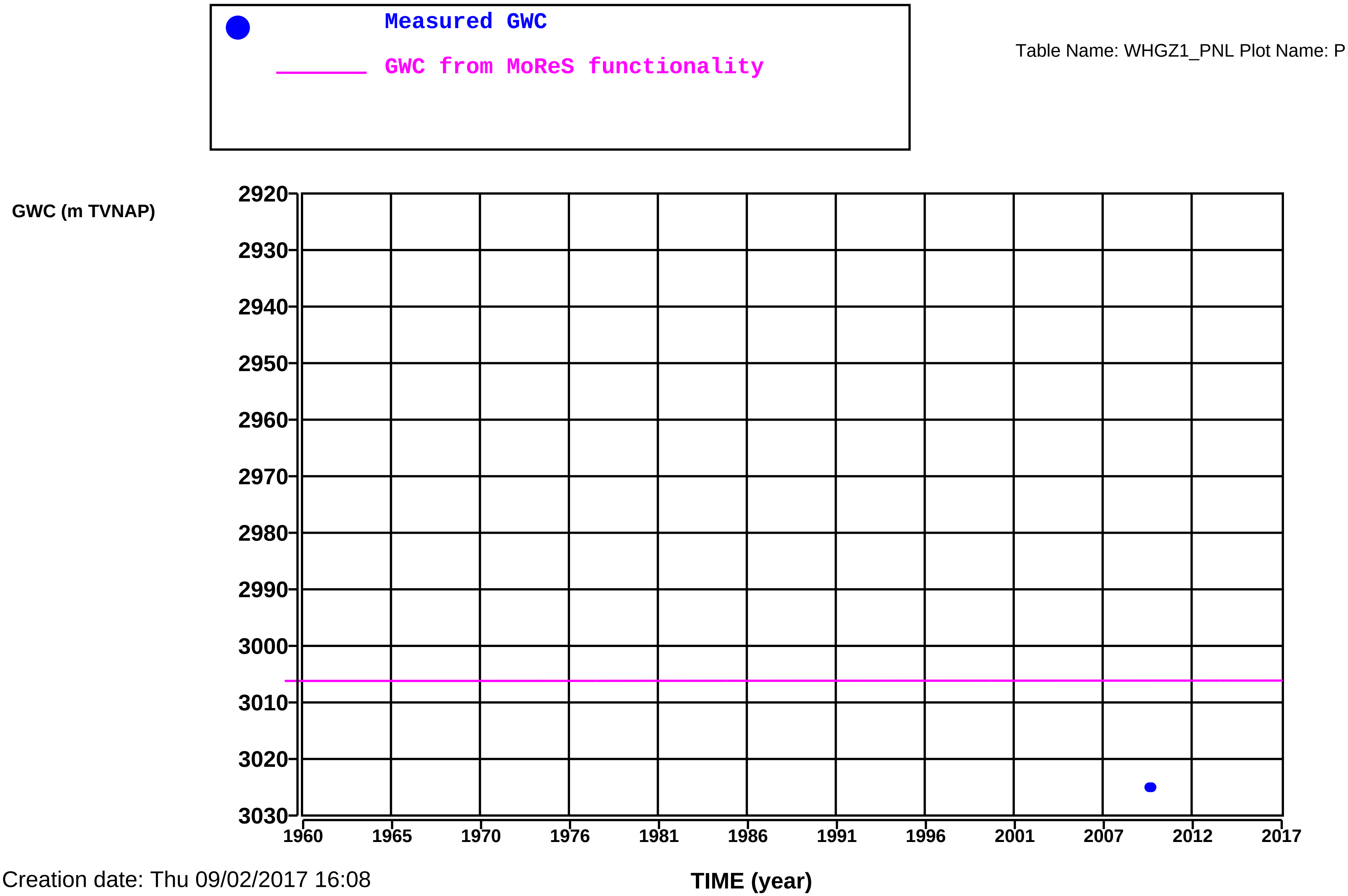

Creation date: Thu 09/02/2017 16:08
Runfile: GRO_2016_ED_v60.run

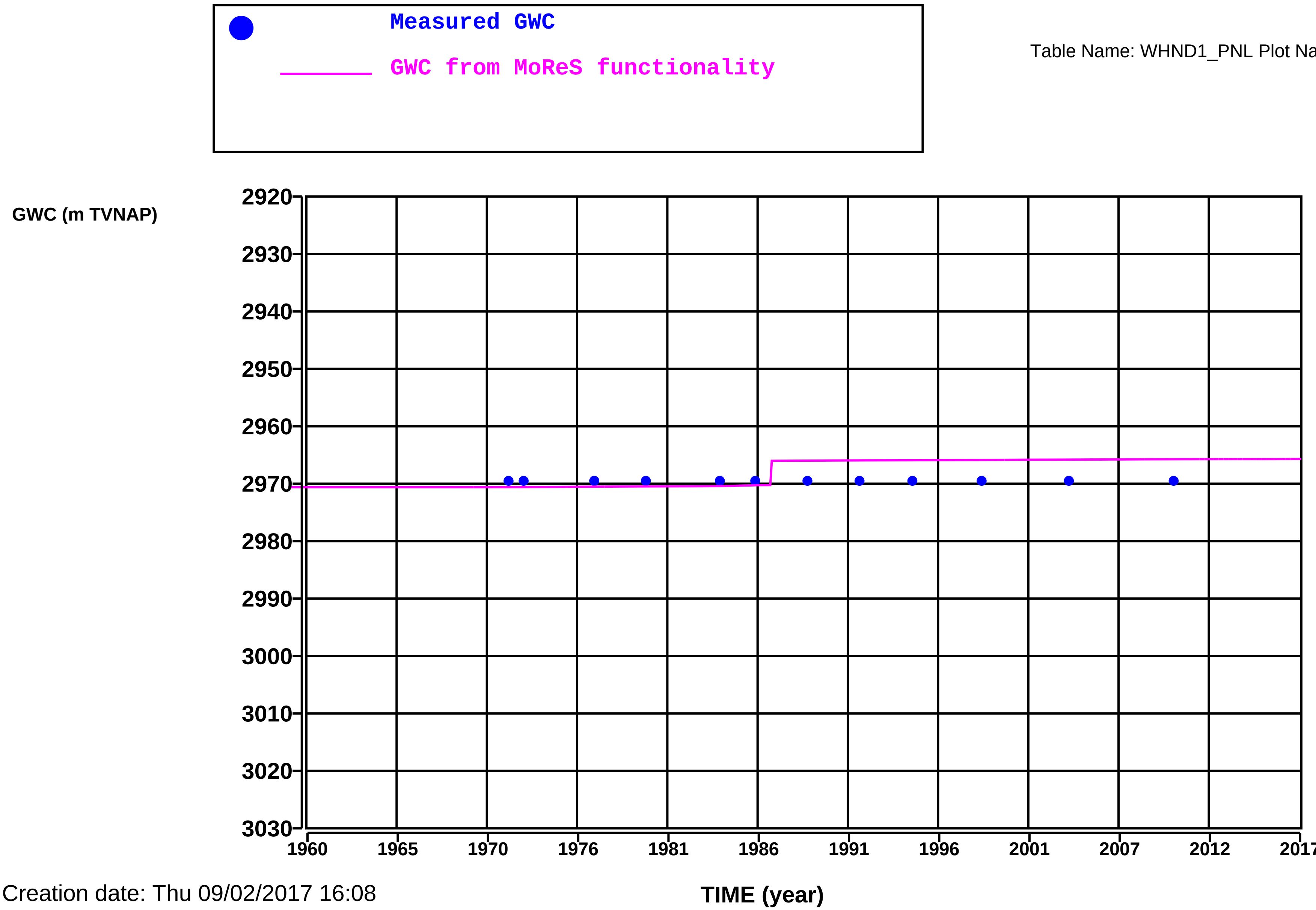

Table Name: WHND1_PNL Plot Name: P

Creation date: Thu 09/02/2017 16:08
Runfile: GRO_2016_ED_v60.run

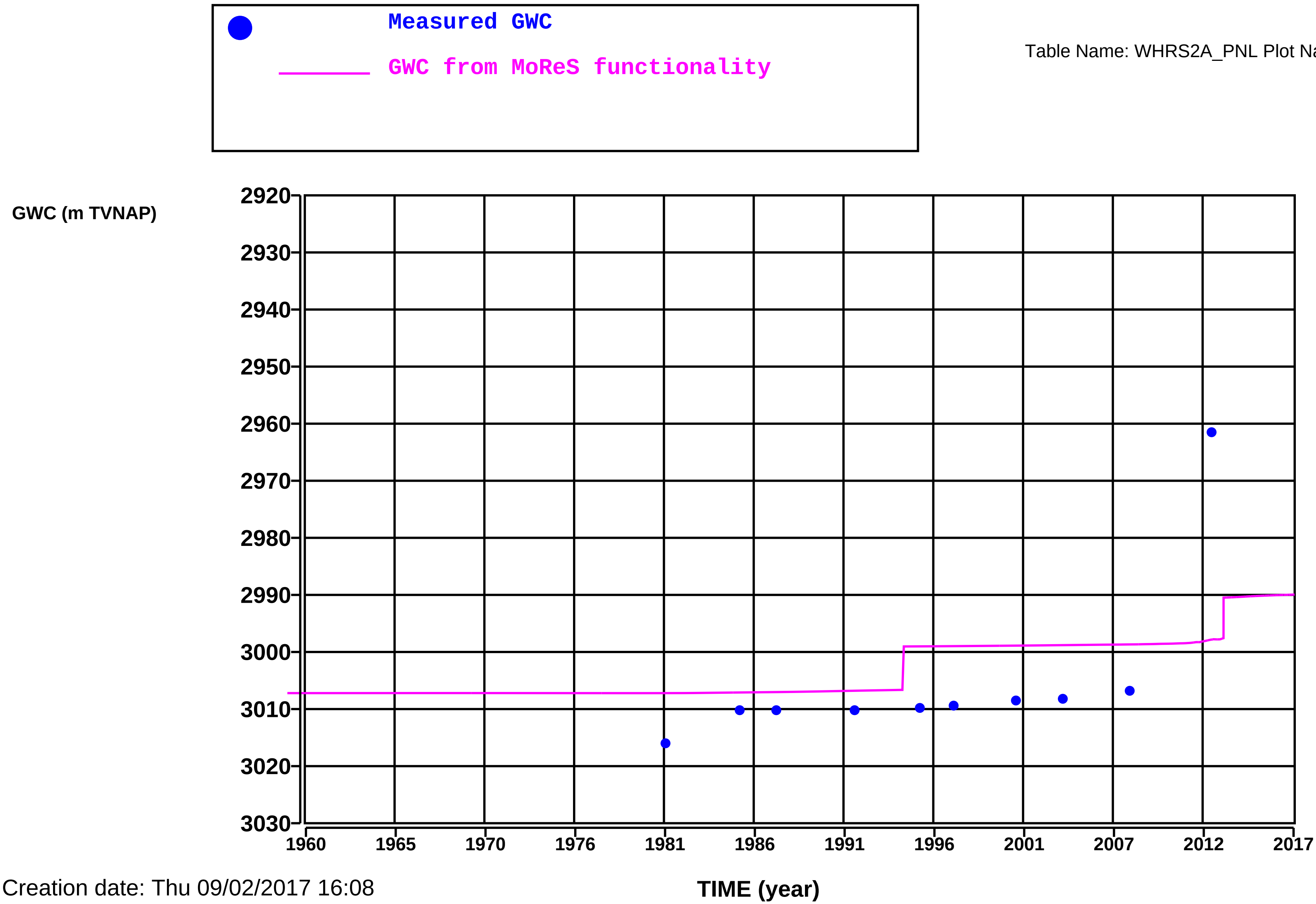

Table Name: WHRS2A_PNL Plot Name:

Creation date: Thu 09/02/2017 16:08
Runfile: GRO_2016_ED_v60.run

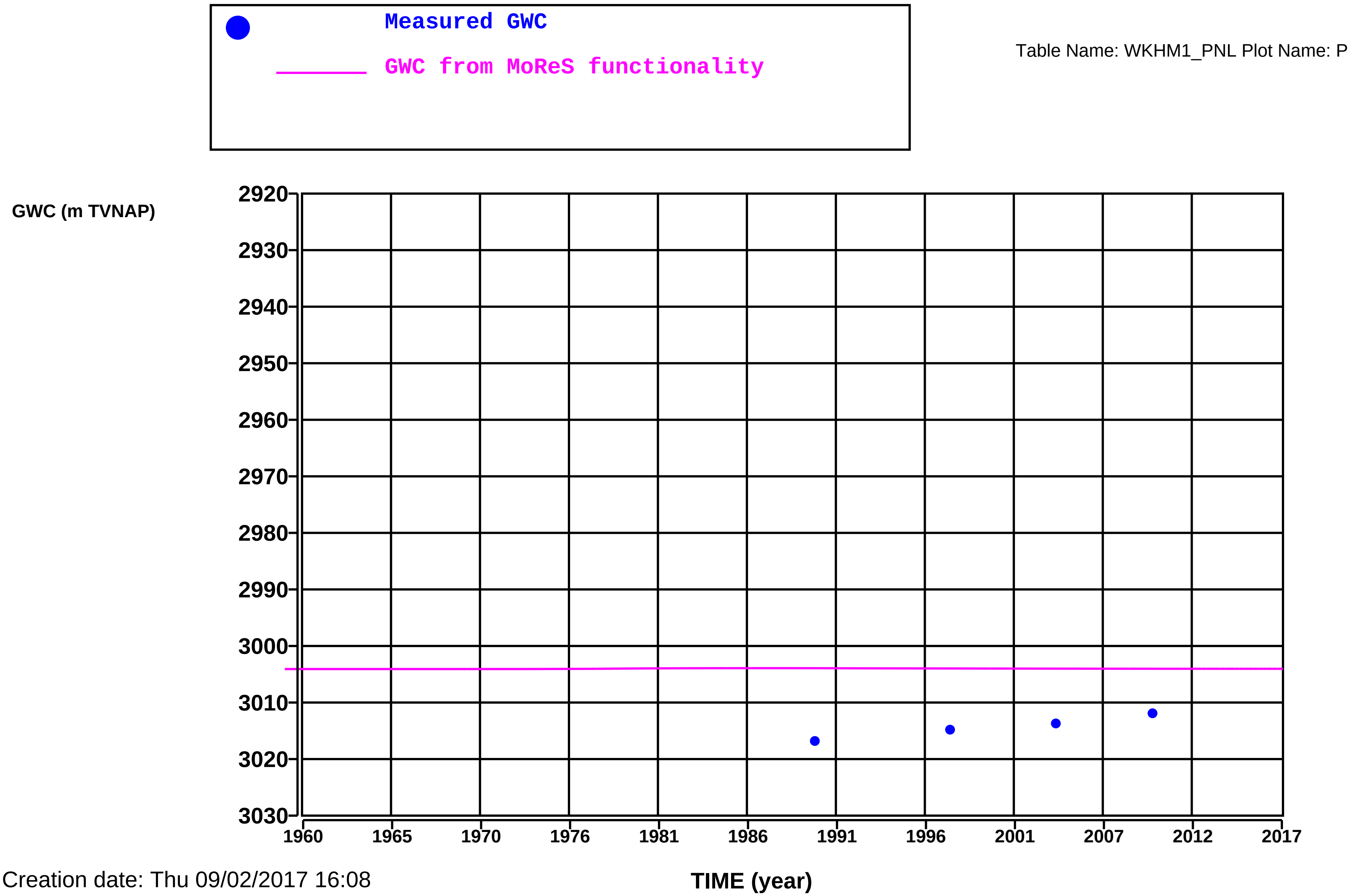

Creation date: Thu 09/02/2017 16:08
Runfile: GRO_2016_ED_v60.run

Table Name: WODP1_PNL Plot Name: P

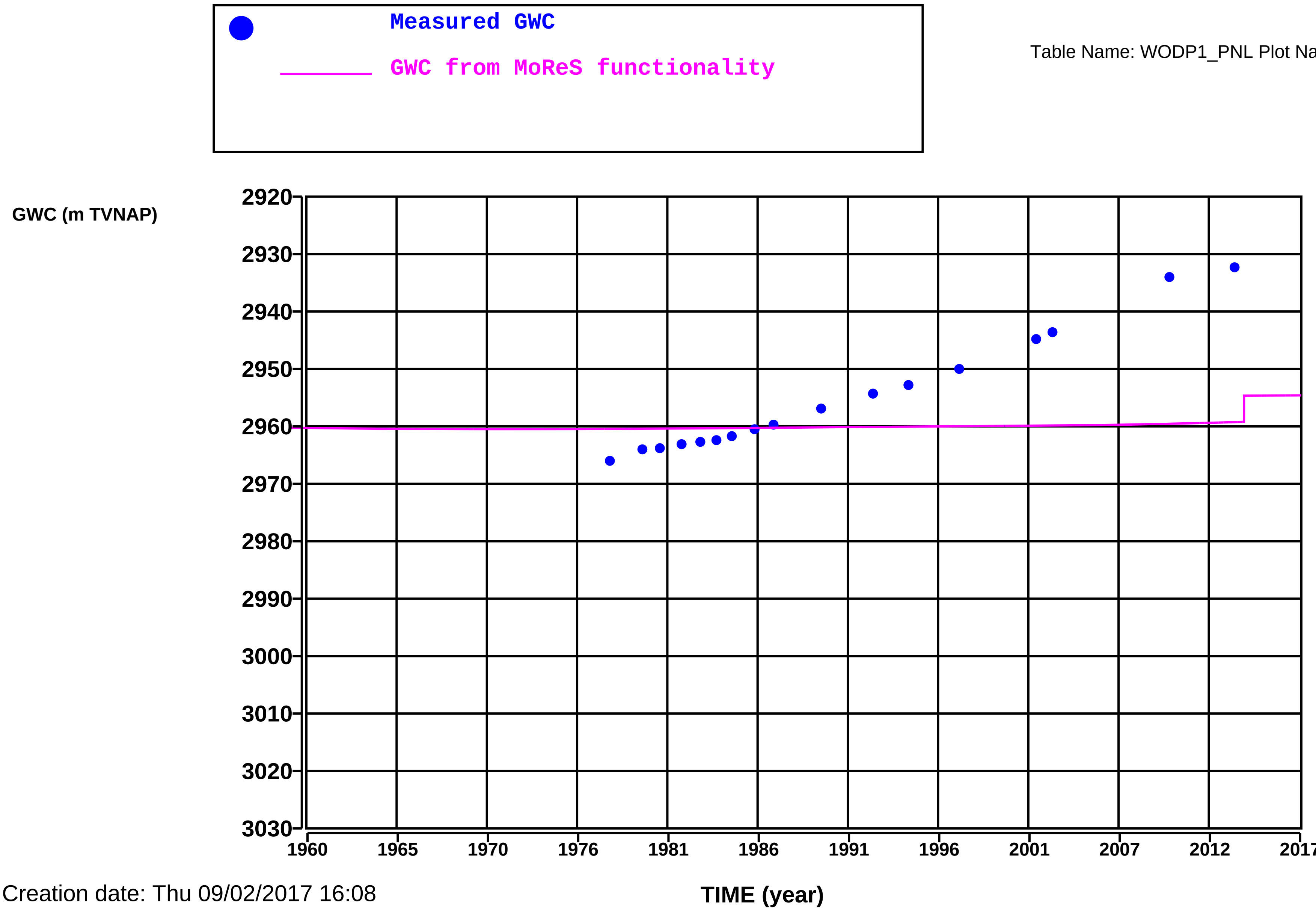

Creation date: Thu 09/02/2017 16:08
Runfile: GRO_2016_ED_v60.run

Table Name: WOLD1_PNL Plot Name: Pl

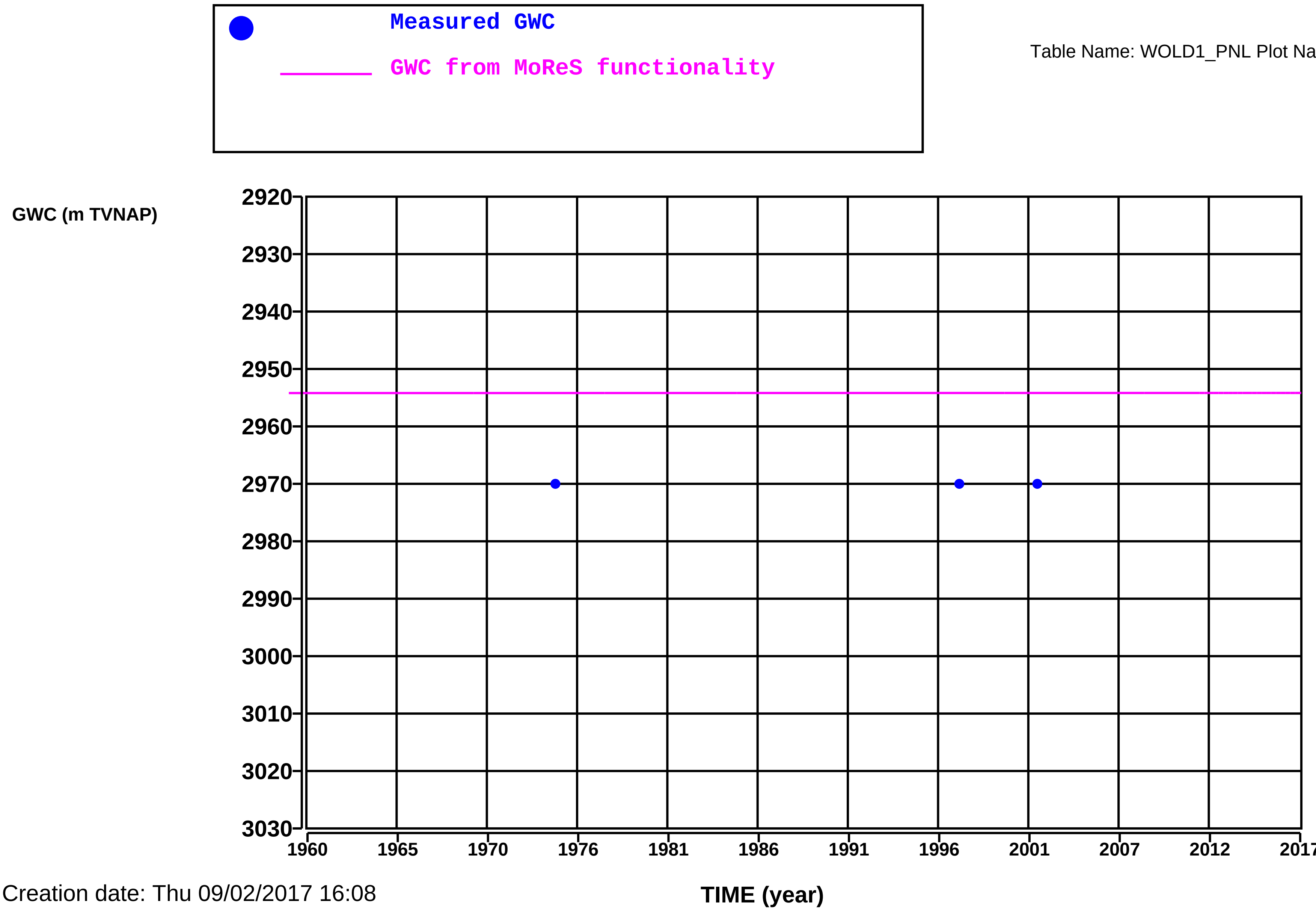

Creation date: Thu 09/02/2017 16:08
Runfile: GRO_2016_ED_v60.run

Table Name: WSDM1_PNL Plot Name: P

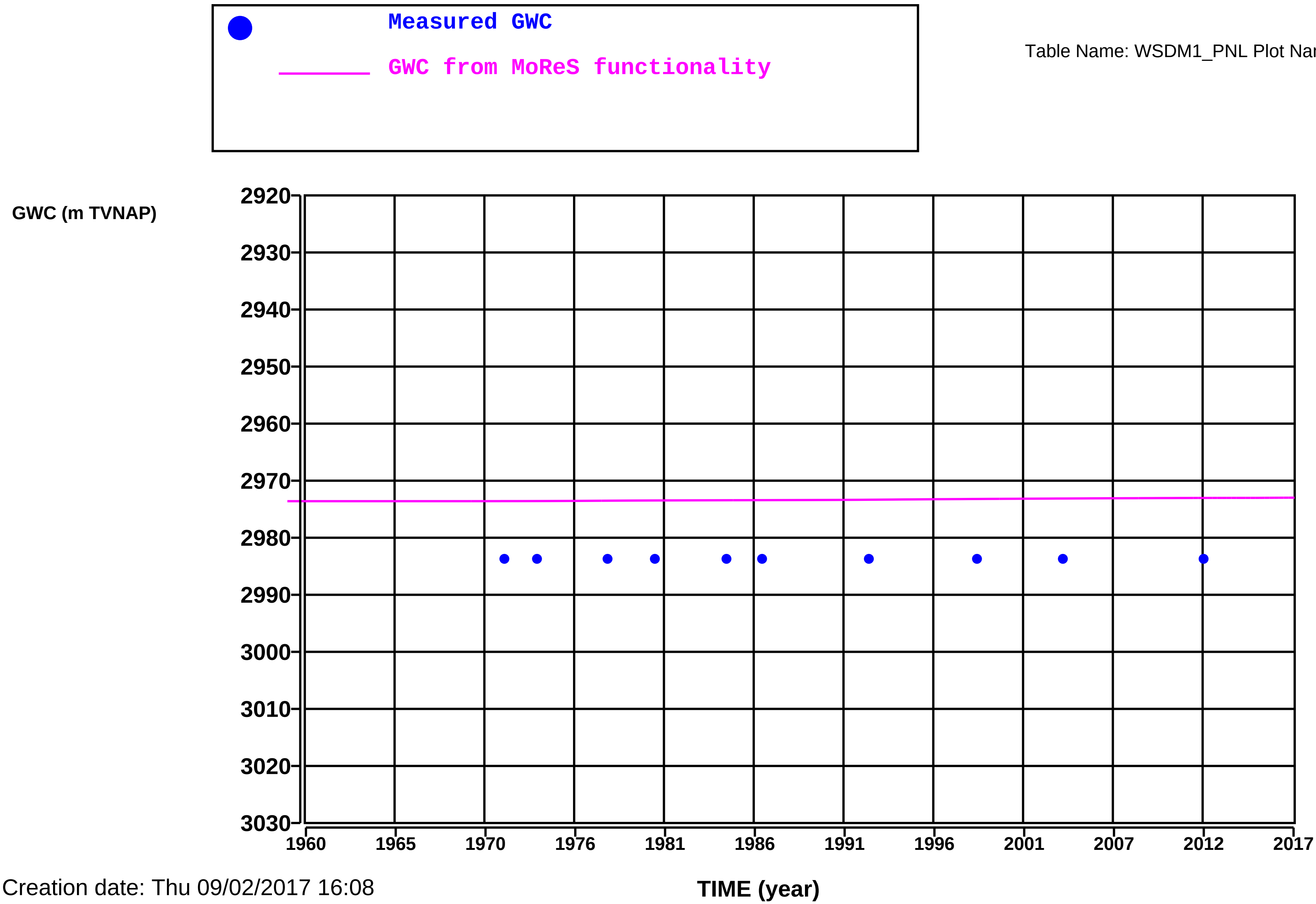

Creation date: Thu 09/02/2017 16:08
Runfile: GRO_2016_ED_v60.run

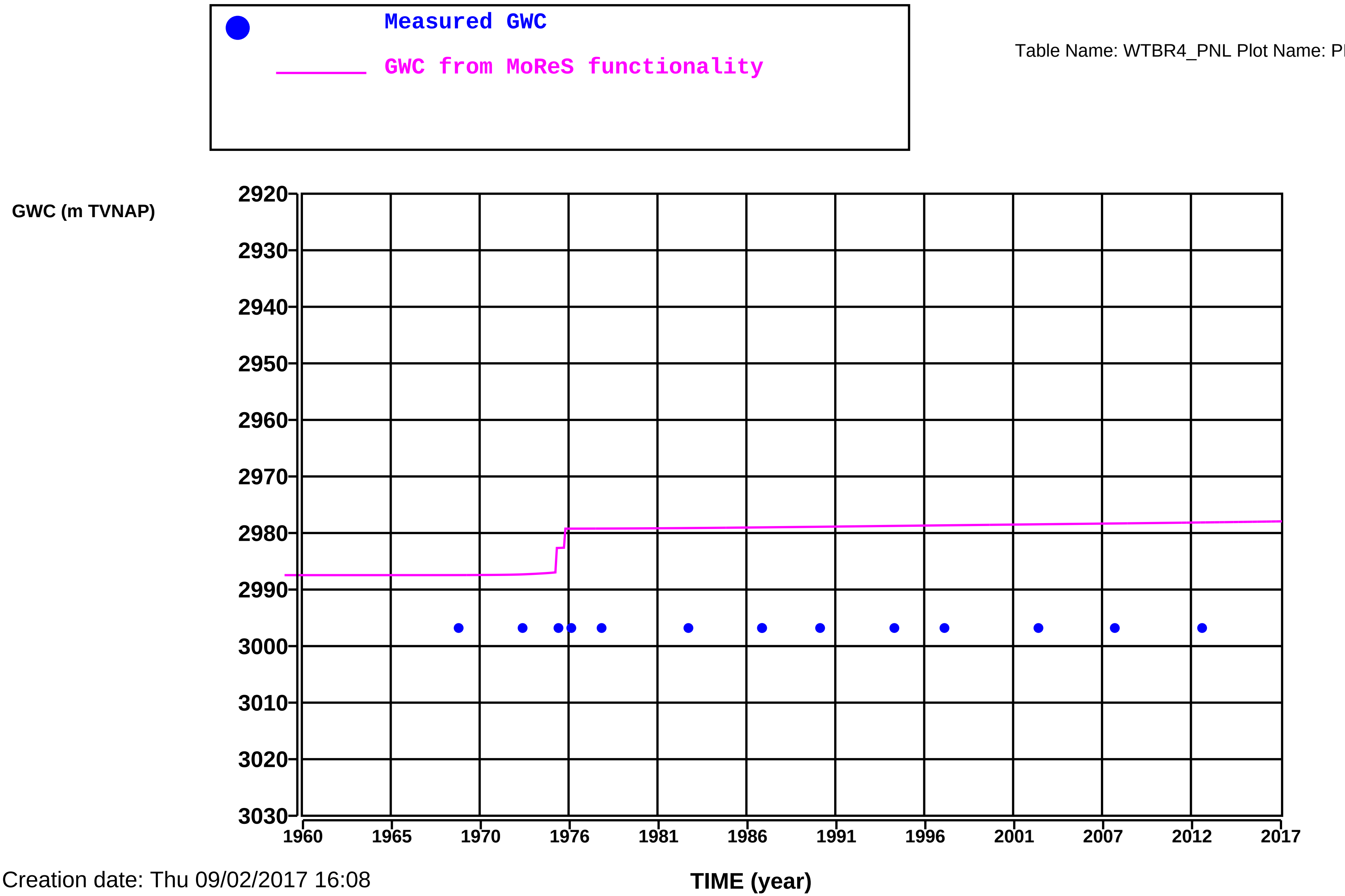

Creation date: Thu 09/02/2017 16:08
Runfile: GRO_2016_ED_v60.run

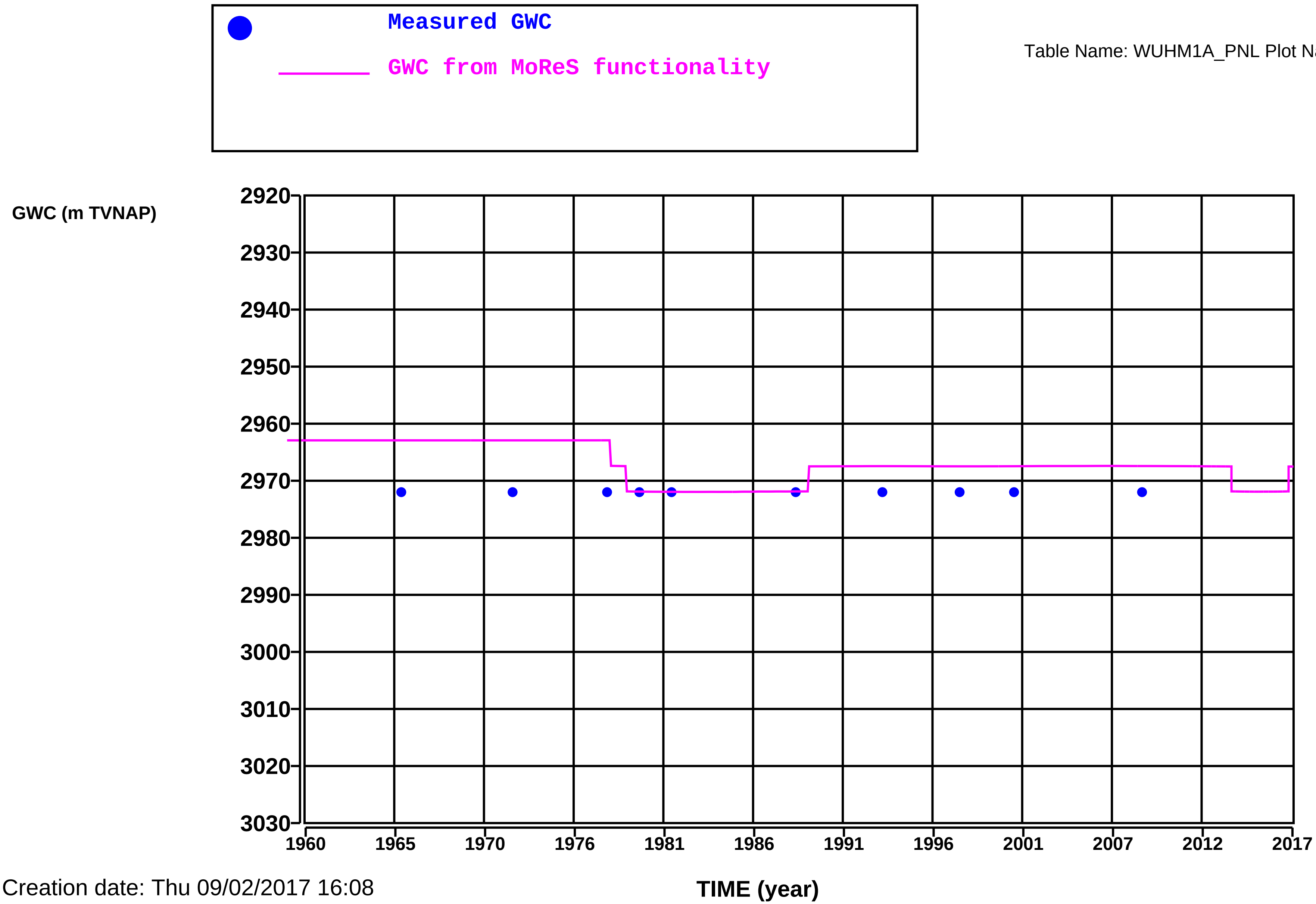

Table Name: WUHM1A_PNL Plot Name:

Creation date: Thu 09/02/2017 16:08
Runfile: GRO_2016_ED_v60.run

Table Name: WUHZ1_PNL Plot Name: Pl

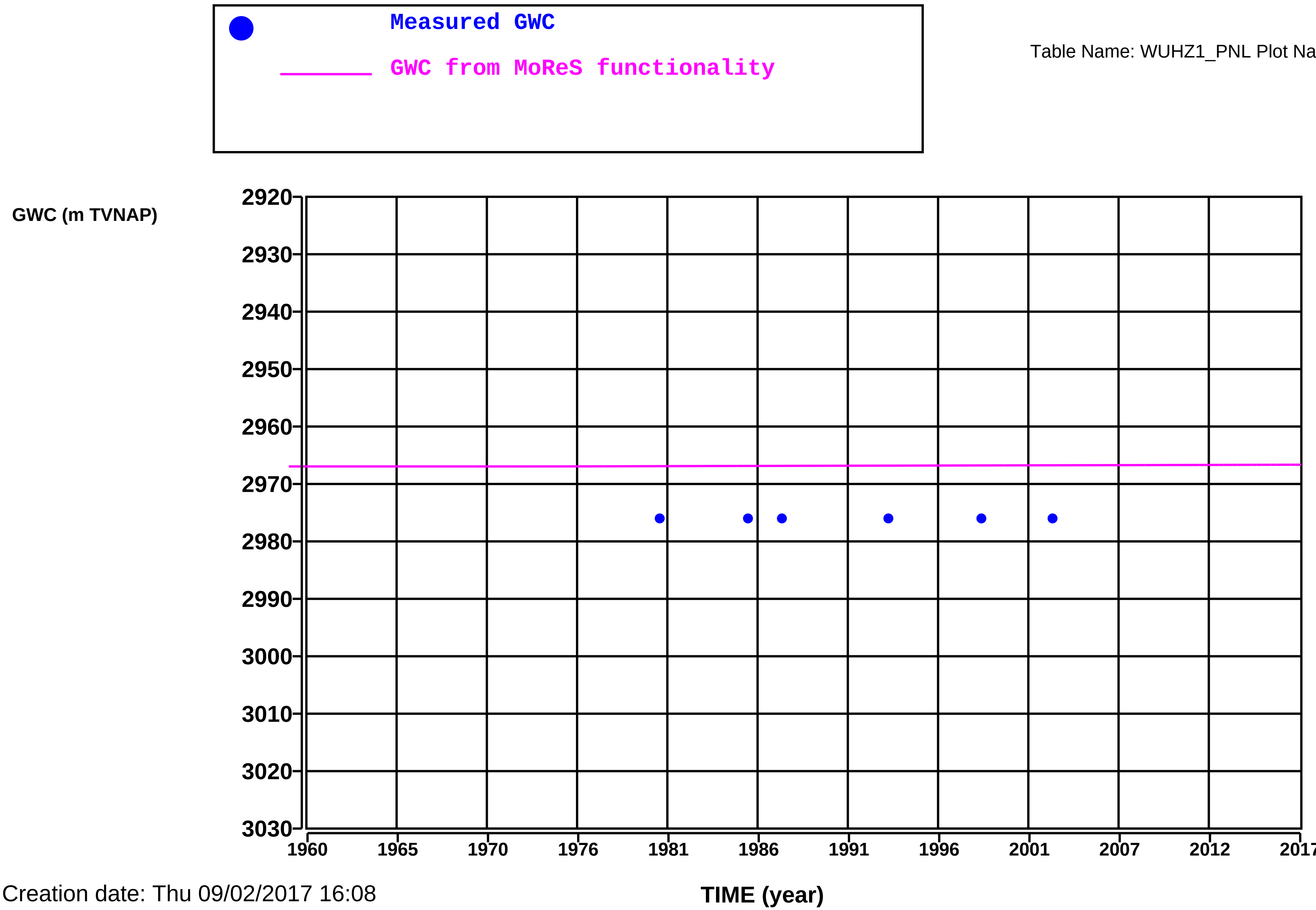

Creation date: Thu 09/02/2017 16:08
Runfile: GRO_2016_ED_v60.run

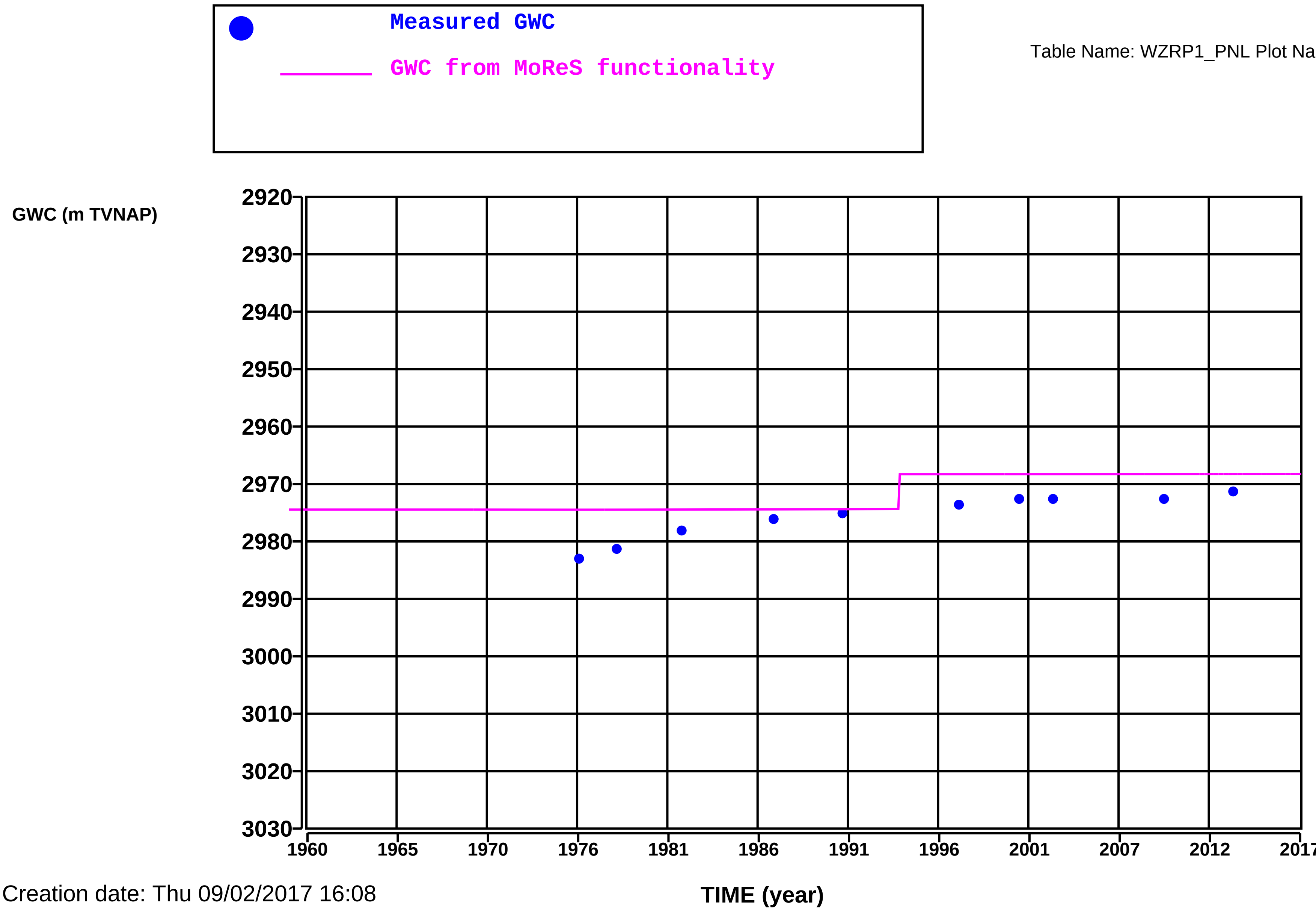

Table Name: WZRP1_PNL Plot Name: PI

Creation date: Thu 09/02/2017 16:08
Runfile: GRO_2016_ED_v60.run

Table Name: WZWD2A_PNL Plot Name:

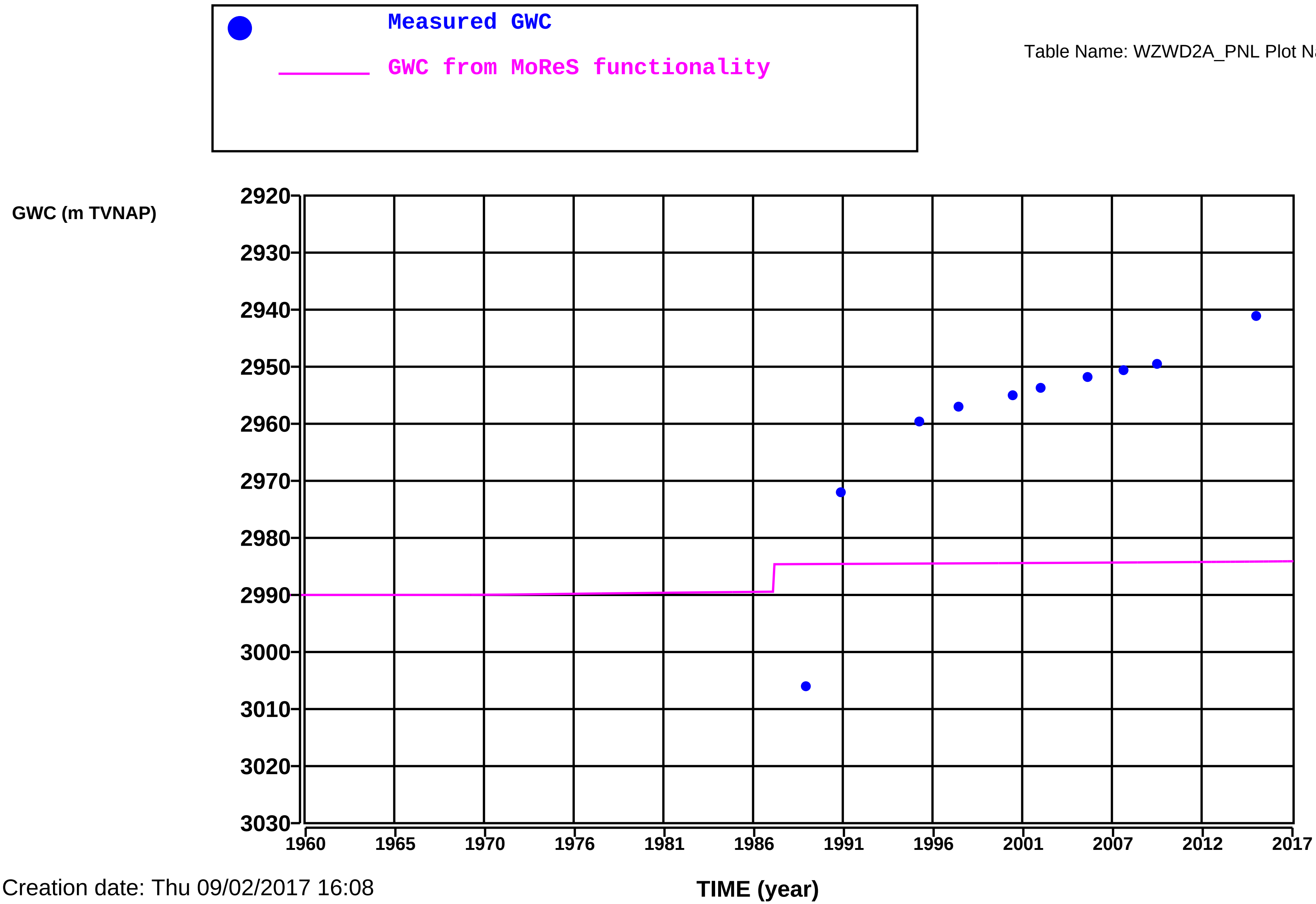

Creation date: Thu 09/02/2017 16:08
Runfile: GRO_2016_ED_v60.run

Table Name: WBDM1_PNL Plot Name: P

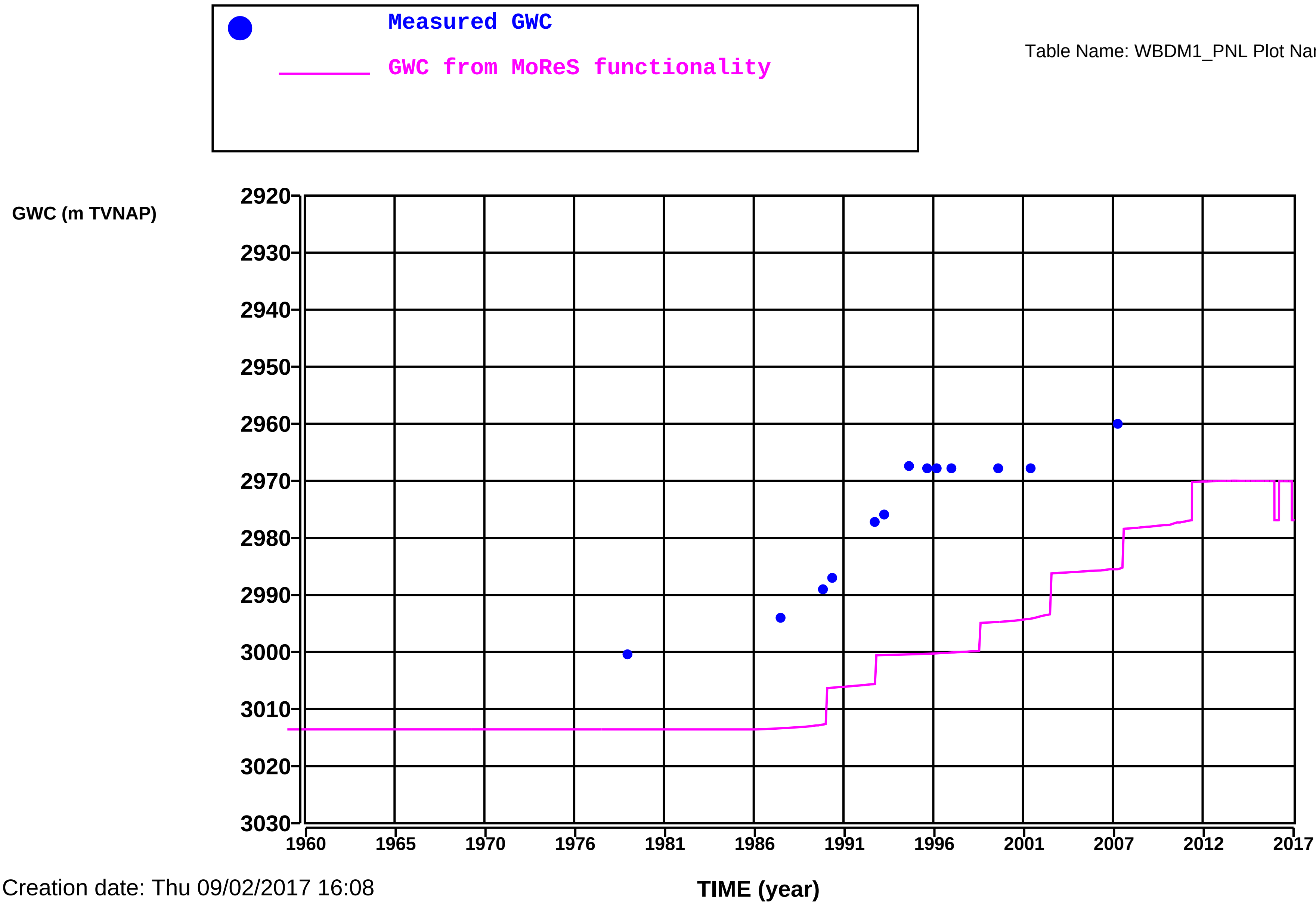

Creation date: Thu 09/02/2017 16:08
Runfile: GRO_2016_ED_v60.run

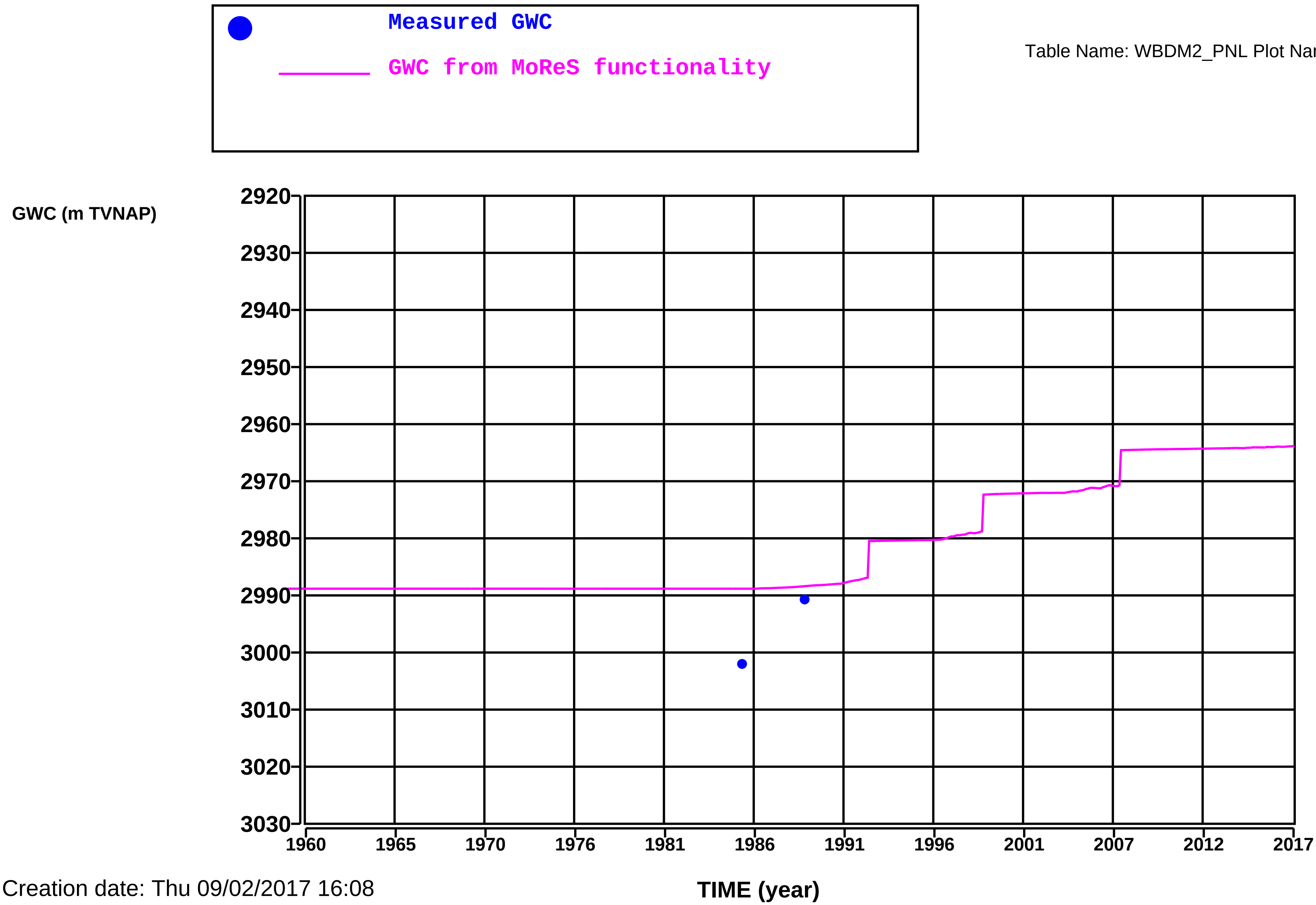

Table Name: WBDM2_PNL Plot Name: P

Creation date: Thu 09/02/2017 16:08
Runfile: GRO_2016_ED_v60.run

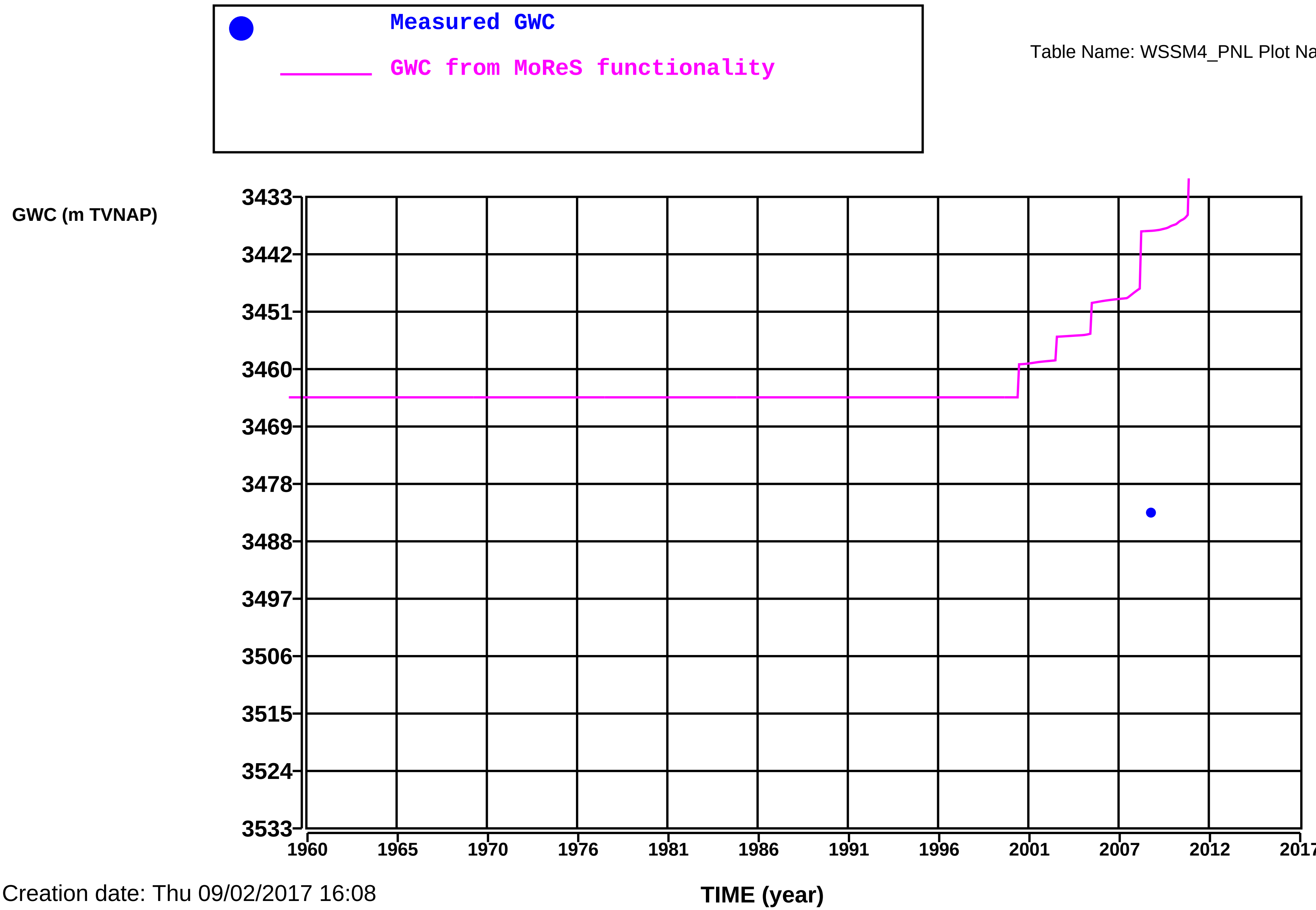

Table Name: WSSM4_PNL Plot Name: P

Creation date: Thu 09/02/2017 16:08
Runfile: GRO_2016_ED_v60.run

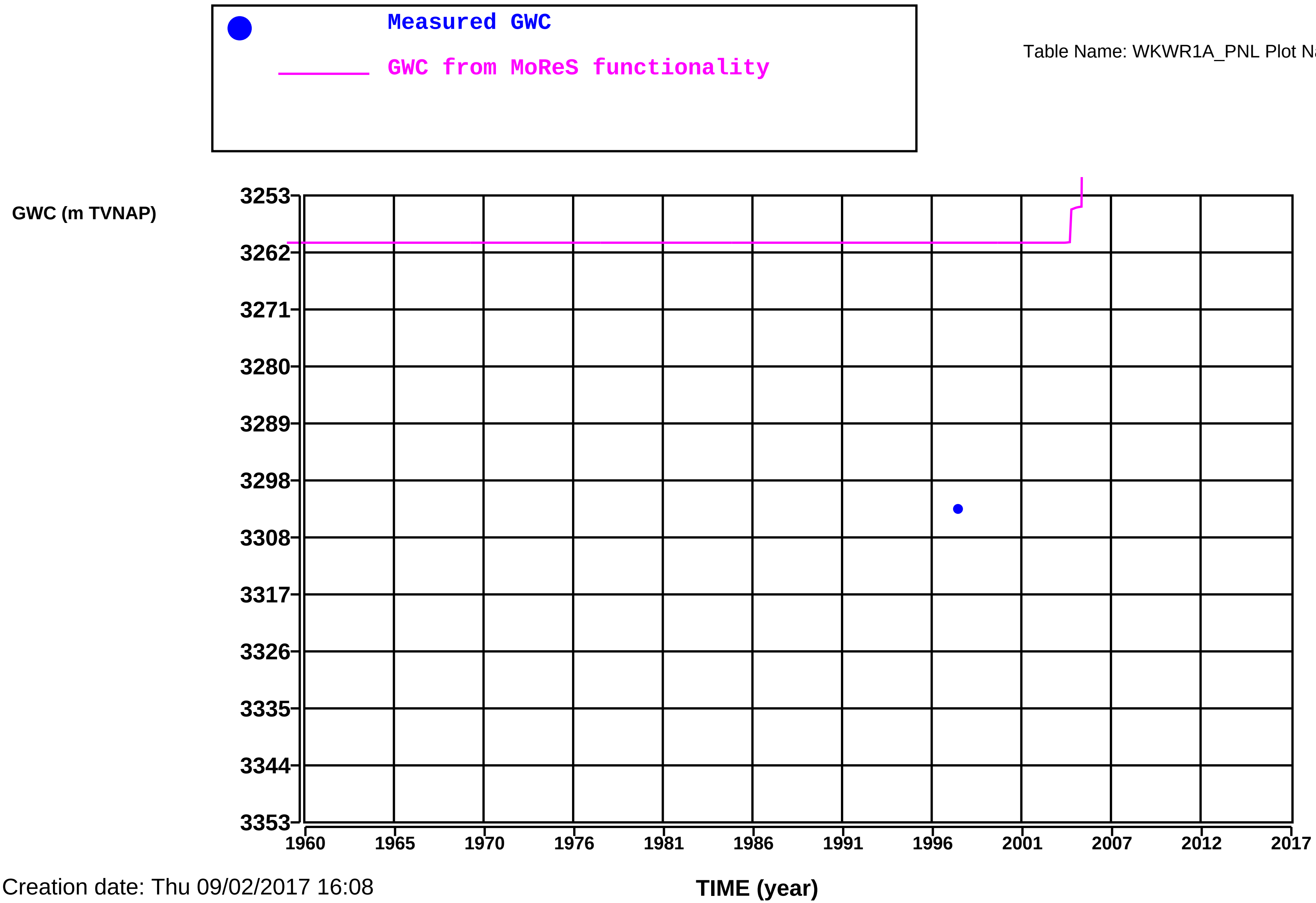

Table Name: WKWR1A_PNL Plot Name:

Creation date: Thu 09/02/2017 16:08
Runfile: GRO_2016_ED_v60.run

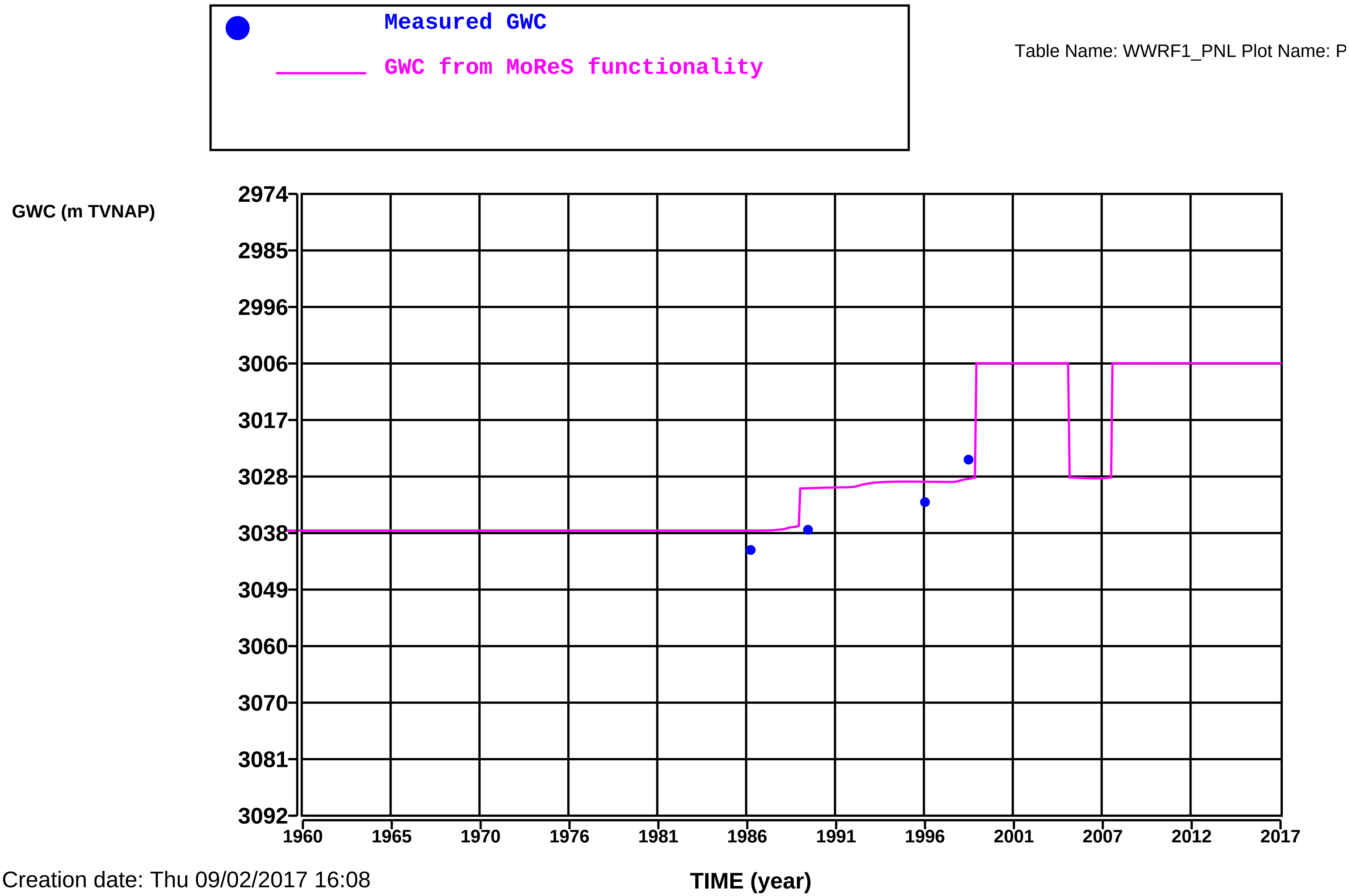

Creation date: Thu 09/02/2017 16:08
Runfile: GRO_2016_ED_v60.run

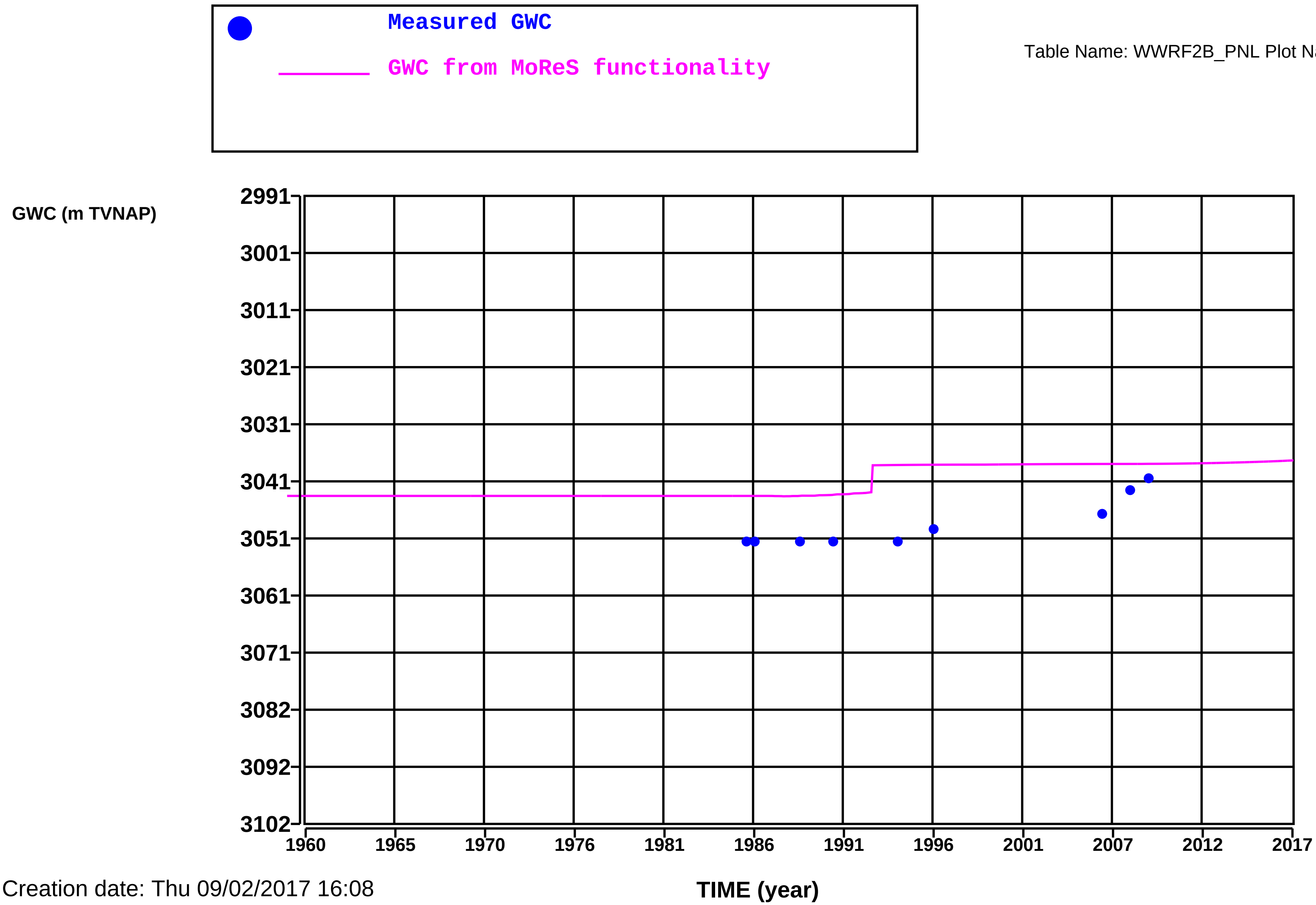

Table Name: WWRF2B_PNL Plot Name:

Creation date: Thu 09/02/2017 16:08
Runfile: GRO_2016_ED_v60.run